Historical Unrest at Large Calderas of the World

Volume 2

U.S. GEOLOGICAL SURVEY BULLETIN 1855

COVER

Long Valley Caldera and Mono–Inyo chain of domes and craters, viewed from the southeast. Unrest since 1979, including earthquakes along and near the caldera's southern boundary and uplift of the caldera floor and resurgent dome, heightened concern about a possible strong earthquake or volcanic eruption and stimulated this review of unrest at calderas around the world. (From Tau Rho Alpha, Roy A. Bailey, Kenneth R. Lajoie, and Malcolm M. Clark, 1983, Physiographic diagrams of Long Valley, Mono and Inyo Counties, California: U.S. Geological Survey Miscellaneous Field Investigations Map MF–1659, sheet 1 of 2.)

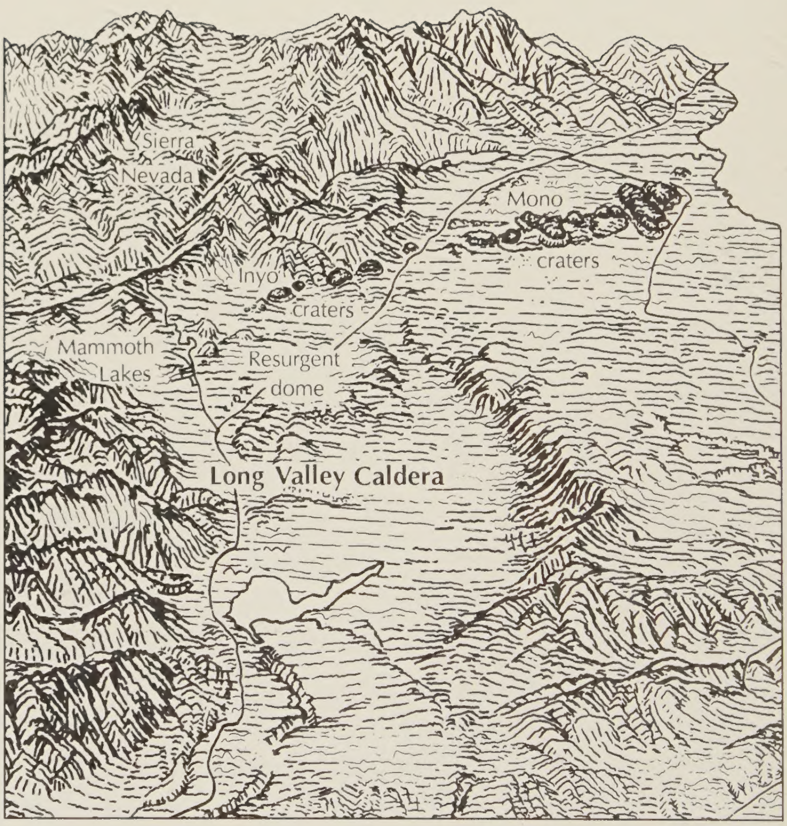

Historical Unrest at Large Calderas of the World

By CHRISTOPHER G. NEWHALL and DANIEL DZURISIN

Volume 2

U.S. GEOLOGICAL SURVEY BULLETIN 1855

DEPARTMENT OF THE INTERIOR
DONALD PAUL HODEL, Secretary

U.S. GEOLOGICAL SURVEY
Dallas L. Peck, Director

Library of Congress Catalog Number 88-600541

UNITED STATES GOVERNMENT PRINTING OFFICE, WASHINGTON : 1988

For sale by the
Books and Open-File Reports Section
U.S. Geological Survey
Federal Center, Box 25425
Denver, CO 80225

CONTENTS

Volume 1.

Volume 2.

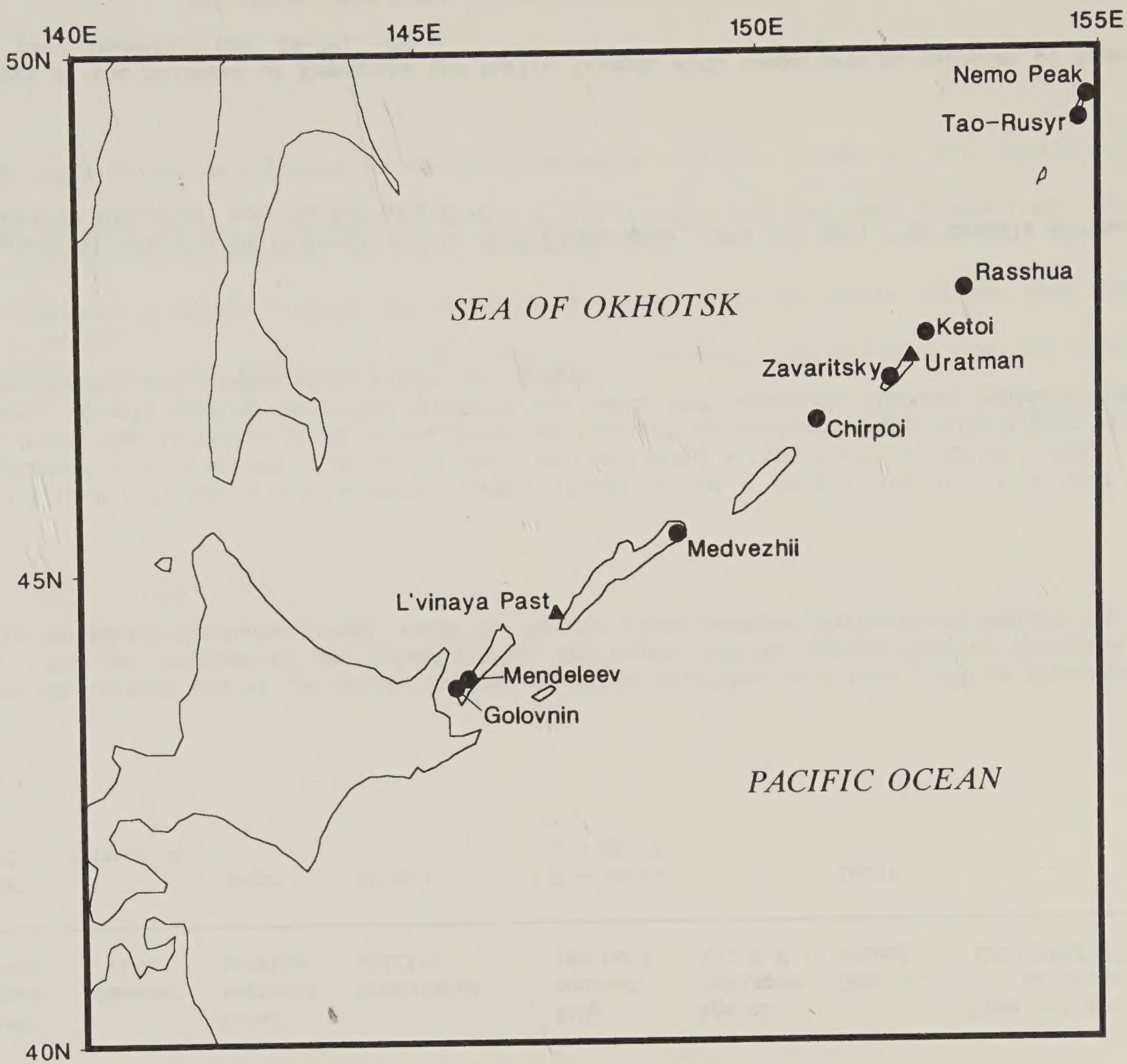

Figure 9. Locations of large, Quaternary restless calderas (solid circles) and nonrestless calderas (triangles) in Region 9.

GOLOVNIN

CAVW number (active vent)	Latitude Longitude (degrees)	Diameter (km)	Local tectonic setting	Precaldera edifice	SiO_2 content (wt pct)	Age of collapse (yr B.P.)	Date of unrest	Type and duration of unrest ESTU STHF MGTF H Te	Eruption type
09-00-01 (Golovnin)	43.82N 145.53E	7 (inner, 4)	Compr	Strato	R = 58-65 C = 66-72		1848?	---- ---- ---- - --	ex

TECTONIC SETTING

Golovnin lies near the western end of the Kurile island arc, which stretches more than 1,200 km from Hokkaido in the west to Kamchatka in the east. The arc consists of two island chains, the Lesser and the Greater Kuriles (Gorshkov, 1970). The Kurile island arc is related to the Kurile-Kamchatka Trench, where the Pacific plate subducts northwestward beneath the Eurasian plate.

GEOLOGIC HISTORY

Golovnin (figs. 9.1.1, 9.1.2) has a 4-km-diameter summit crater within a larger ring structure that might be a caldera (Gorshkov, 1970) or, alternatively, a series of extrusive domes emplaced along a ring fracture (Erlich, 1986). The southwest part of the inner caldera is a bench that is raised 70-80 meters above the floor of the northern (lake-filled) part of the caldera. On the edge of the uplifted part, steeply dipping lacustrine sediments and radial and concentric fissures indicate resurgent doming (Erlich, 1986). Postcaldera andesite and dacite domes occur within the caldera.

HISTORICAL ACTIVITY

The only known historical eruption of Golovnin was in 1848 (Gushchenko, 1979, p. 239). No details of the eruption are known. The caldera contains numerous fumaroles, some as hot as 100 °C.

REFERENCES

Erlich, E., 1986, Geology of the calderas of Kamchatka and Kurile Islands with comparison to calderas of Japan and the Aleutians, Alaska: U.S. Geol. Surv. Open-File Rep. 86-291, 300 p.

GOLOVNIN (continued)

REFERENCES (continued)

Gorshkov, G.S., 1958, Catalogue of active volcanoes of the world including solfatara fields, Pt. VII, Kurile Islands: Naples, IAVCEI, 99 p.

----- 1970, Volcanism and the upper mantle: Investigations in the Kurile Volcanic Arc: New York, Plenum Press, 385 p.

Gushchenko, I.I., 1979, Eruptions of volcanoes of the world, a catalog: Acad. Sci. USSR Far Eastern Sci. Center, Moscow, Nauka Publ., 474 p.

Markhinin, E.K., 1959, Volcanoes of Kunashir Island, <u>in</u> Volcanism of Kamchatka and the Kurile Islands: Akad. Nauk USSR, Trudy Lab. Vulkanol., no. 17, p. 64-115.

Ostapenko, V.F., Fedorchenko, V.I., and Shilov, V.N., 1967, Pumices, ignimbrites, and rhyolite from the Great Kurile arc: Bull. Volcanol., v. 30, p. 81-92.

Figure 9.1.1. Perspective drawing looking northwestward at Golovnin Caldera and caldera lake, from Markhinin (1959). 1, east dome; 2, west dome; 3, lava dome; 4, outer dome; 5, steep dome; 6, "turtle" structure with solfatara area; 7, unnamed solfatara area; 8, warm part of the lake; 9, Mt. Golovnin.

Figure 9.1.2. Sketch showing structure of Golovnin Caldera, from Gorshkov (1958). Cross in circle, solfatara.

MENDELEEV

CAVW number (active vent)	Latitude Longitude (degrees)	Diameter (km)	Local tectonic setting	Precaldera edifice	SiO_2 content (wt pct)	Age of collapse (yr B.P.)	Date of unrest	Type and duration of unrest ESTU STHF MGTF H Te	Eruption type
09-00-02 (Mendeleev)	43.90N 145.70E	6 (inner, 3)	"on 2 volcano-tectonic lines"	Strato (2 or more)	R = 53-66 C = 67?	pre-Würm inter-stadial	1880	---- ---- ---- - --	pex
							1900?	---- ---- ---- - --	pex
							1988	xx-- ---- ---x - --	none

TECTONIC SETTING

Mendeleev lies along the western part of the Kurile island arc (Gorshkov, 1970; see section on TECTONIC SETTING of Golovnin Caldera).

GEOLOGIC HISTORY

The precaldera edifice is a stratovolcano with dominantly andesitic and basaltic andesite products (figs. 9.2.1, 9.2.2). The caldera formed after eruption of dacitic magma, perhaps shortly before the Würm interstadial (that is, before about 39,000 yr B.P.) (Erlich, 1986). A new cone of basalt and basaltic andesite then formed during the interstadial. A "directed blast" (debris avalanche?) breached the west side of the new cone, and a dacite dome formed in its crater. Goriachy Pliazk geothermal field is located on the east flank of the Mendeleev complex, outside the caldera (Erlich, 1986).

HISTORICAL ACTIVITY

An eruption in 1880 was reportedly of gas and included weak explosions (Gorshkov, 1970). When Milne (1886) visited Mendeleev in 1880(?), he found a number of trees that had been killed by solfataric activity and thus inferred that activity to have been "not long in existence."

In hot springs at the base of Mendeleev Volcano, Cl, SO_4, and CO_2 increased by 10, 3, and 11 percent, respectively, from 1965 to 1966, during a period when seismic activity at Kunashir Island also increased (Markhinin and Bozhkova, 1975). NH_4 and HBO_2 increased 70 and 55 percent, respectively, in the same springs over the same time period. No measurements for subsequent years were reported.

MENDELEEV

HISTORICAL ACTIVITY (continued)

A summit earthquake swarm with focal depths of less than 10 km was recorded on 4-5 May 1987. The temperature at 74-m-depth in a geothermal bore hole 10 km from the summit of Mendeleev was found on 25-28 September 1987 to be 4 °C higher than in 1986. Temperatures increased 4-5 °C in hot springs on the east and south flanks, but fumaroles in the same area showed essentially no variation from 1986. Soviet geologists reported that the earthquakes seemed to be caused by exploitation of geothermal wells, used for heat production (Smithsonian Institution, 1988).

REFERENCES

Erlich, E., 1986, Geology of the calderas of Kamchatka and Kurile Islands with comparison to calderas of Japan and the Aleutians, Alaska: U.S. Geol. Surv. Open-File Rep. 86-291, 300 p.

Gorshkov, G.S., 1958, Catalogue of active volcanoes of the world including solfatara fields, Pt. VII, Kurile Islands: Naples, IAVCEI, 99 p.

----- 1970, Volcanism and the upper mantle: Investigations in the Kurile Volcanic Arc: New York, Plenum Press, 385 p.

Markhinin, E.K., and Bozhkova, L.I., 1975, Dependence of the chemical composition of thermal water upon seismic activity: Bull. Volcanol., v. 39, p. 104-111.

Milne, J., 1886, The volcanoes of Japan: Trans. Seismol. Soc. Japan, v. 9, pt. II, 184 p.

Smithsonian Institution, Scientific Event Alert Network (SEAN), 1988, Mendeleev volcano: SEAN Bull., v. 13, no. 1, p. 8 (information from G.S. Steinberg).

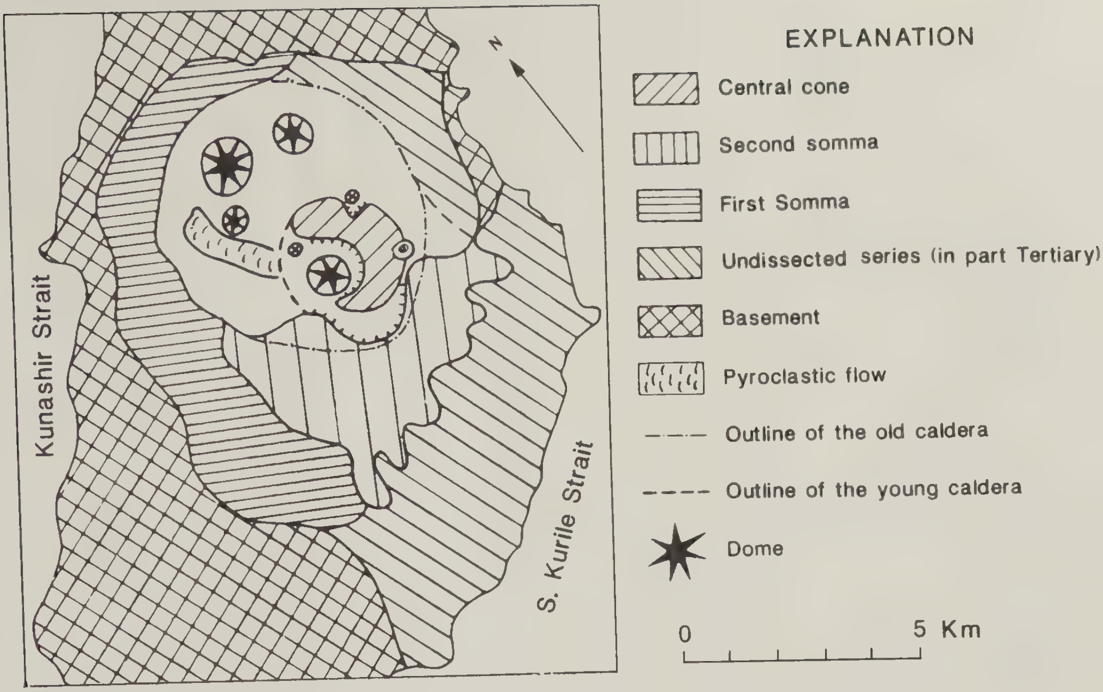

Figure 9.2.1. Sketch of structure of Mendeleev Volcano, from Gorshkov (1970).

Figure 9.2.2. Sketch showing structure of Mendeleev Volcano, from Gorshkov (1958). Cross in circle, solfatara.

PART 3: HISTORICAL UNREST AT LARGE QUATERNARY CALDERAS (continued)
See inside back cover for explanation and abbreviations

MEDVEZHII

CAVW number (active vent)	Latitude Longitude (degrees)	Diameter (km)	Local tectonic setting	Precaldera edifice	SiO_2 content (wt pct)	Age of collapse (yr B.P.)	Date of unrest	Type and duration of unrest ESTU STHF MGTF H Te	Eruption type
09-00-10 (Kudriavy)	45.38N 148.80E	8	Compr	Strato	R = 49-55 C = 63-67	pre-glacial	1778 or 1779	---- ---- ---- - --	ex
							1883	---- ---- ---- - --	ex,lf
							1946	---- ---- ---- - --	pex
							1958	---- ---- ---? - --	unknown

TECTONIC SETTING

Medvezhii (figs. 9.3.1, 9.3.2) lies along the Kurile island arc (Gorshkov, 1970; see section on TECTONIC SETTING of Golovnin Caldera).

GEOLOGIC HISTORY

Most precaldera and postcaldera eruptions have been of basalt and andesite; the caldera-forming eruption was of dacite. Some postcaldera cones and domes occur along an E-W line through the caldera (Erlich, 1986). Ostapenko (1969) likened the precaldera edifice of Medvezhii to that of Hawaiian volcanoes.

HISTORICAL ACTIVITY

Explosions occurred in the summit crater of Kudriavy in 1778 or 1779, and in May-June 1883 (Gorshkov, 1958). Intense solfataric activity persists in the summit crater and at Kudriavy cone (Smithsonian Institution, 1981; Erlich, 1986).

REFERENCES

Erlich, E., 1986, Geology of the calderas of Kamchatka and Kurile Islands with comparison to calderas of Japan and the Aleutians, Alaska: U.S. Geol. Surv. Open-File Rep. 86-291, 300 p.

Gorshkov, G.S., 1958, Catalogue of active volcanoes of the world including solfatara fields, Pt. VII, Kurile Islands: Naples, IAVCEI, 99 p.

----- 1970, Volcanism and the upper mantle: Investigations in the Kurile Volcanic Arc: New York, Plenum Press, 385 p.

MEDVEZHII (continued)

REFERENCES (continued)

Ostapenko, V.F., 1967, Welded tuff of Medvezhya caldera (Iturup Island), Kurile Islands: Dokl. Akad. Sci. USSR, v. 174, no. 4, p. 941-944.

----- 1969, About the character of previous eruptions of Medvezhiy zone (Iturup Island), in Volcanism and Izverzhenia: Moscow, Nauka Press, p. 122-126.

----- 1970, Morphology and structure of caldera-volcano Medvezhiy (Iturup Island, Kuriles): Izv. Sakhalin Div. of Geogr. Soc. USSR, iss. 1, p. 99-108.

Ostapenko, V.F., Fedorchenko, V.I., and Shilov, V.N., 1967, Pumices, ignimbrites, and rhyolite from the Great Kurile arc: Bull. Volcanol., v. 30, p. 81-92.

Smithsonian Institution, Scientific Event Alert Network (SEAN), 1981, Kudriavy Cone: SEAN Bull., v. 6, no. 12, p. 8 (information from G.S. Steinberg).

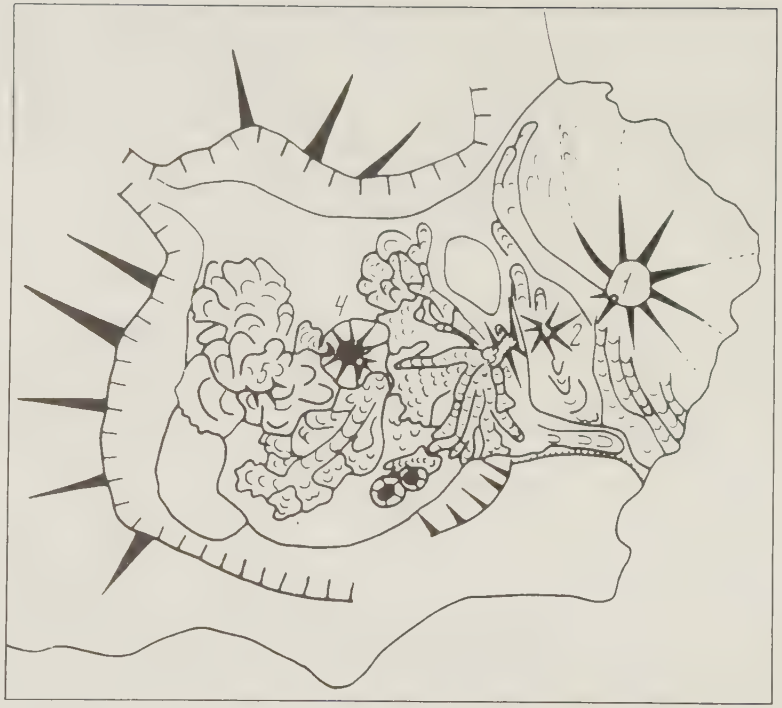

EXPLANATION

Young lava flows
Cone with crater
Dome
1) Medvezhii Cone
2) Srednii Cone
3) Kudryavyi Cone
4) Men'shoi Brat Dome
5) Effusive dome

Figure 9.3.1. Sketch of structure of Medvezhii Caldera, from Gorshkov (1970).

Figure 9.3.2. Sketch showing structure of Medvezhii Caldera with its active cone Kudriavy, from Gorshkov (1958). Explanation: 1, Medvezhii cone; 2, Kudriavy cone; 3, Menshoi Brat cone with lava flows; cross in circle, solfatara.

CHIRPOI

CAVW number (active vent)	Latitude Longitude (degrees)	Diameter (km)	Local tectonic setting	Precaldera edifice	SiO_2 content (wt pct)	Age of collapse (yr B.P.)	Date of unrest	Type and duration of unrest ESTU STHF MGTF H Te	Eruption type
09-00-15 (Snow= S)	46.52N 150.88E	8-9	Southern and western parts cut by faults; compr	Ol-px basalt cone, submarine	R = 59-60 C = 68?		ca. 1712 (C)	---- ---- ---- - --	EX?
09-00-16 (Cherny= C)							between 1770 and 1810 (S)	---- ---- ---- - QU?	ex,1f
							1811 (S)	---- ---- ---- - --	ex
							1854 (?)	---- ---- ---- - --	ex
							1857 (C)	---- ---- ---- - --	Ex
							1879 (S)	---- ---- ---- - --	ex,1f
							1960 (S)	---- ---- ---- - --	ex

TECTONIC SETTING

Chirpoi lies along the Kurile island arc (Gorshkov, 1970; see section on TECTONIC SETTING of Golovnin Caldera).

GEOLOGIC HISTORY

Subaerial and submarine topography suggests that Chirpoi Island has grown within two overlapping calderas that together are 8-9 km in diameter (fig. 9.4.1). Cherny Volcano lies at the center of Chirpoi Island, and Snow Volcano is a parasitic lava cone at Cherny's southern foot (Gorshkov, 1970). Brat Chirpoev Island, southwest of Chirpoi Island, is a fragment of the precaldera edifice, an olivine-pyroxene basalt cone (Erlich, 1986); however, it might also have had recent eruptions and showed solfataric activity in the mid-18th century (Gorshkov, 1970).

HISTORICAL ACTIVITY

Snow Volcano originated sometime between a visit by Cossack Captain Chernyi in 1770 and a visit by Captain Golovnin in 1811. A major tectonic earthquake on or about 2 January 1780 devastated the islands of Ketoi, Simushir, Chirpoi, and Urup and apparently triggered an eruption of Raikoke Volcano (Perrey, 1863, p. 70). It is possible but speculative that Snow began to grow in or shortly after 1780.

CHIRPOI (continued)

REFERENCES

Erlich, E., 1986, Geology of the calderas of Kamchatka and Kurile Islands with comparison to calderas of Japan and the Aleutians, Alaska: U.S. Geol. Surv. Open-File Rep. 86-291, 300 p.

Gorshkov, G.S., 1958, Catalogue of active volcanoes of the world including solfatara fields, Pt. VII, Kurile Islands: Naples, IAVCEI, 99 p.

----- 1970, Volcanism and the upper mantle: Investigations in the Kurile Volcanic Arc: New York, Plenum Press, 385 p.

Perrey, A., 1863, Documents sur les tremblements de terre et les phénomènes volcaniques dans l'archipel des Kouriles et au Kamtschatka: Lyon, Soc. Imp. Agric. Hist. Nat. Arts, 166 p.

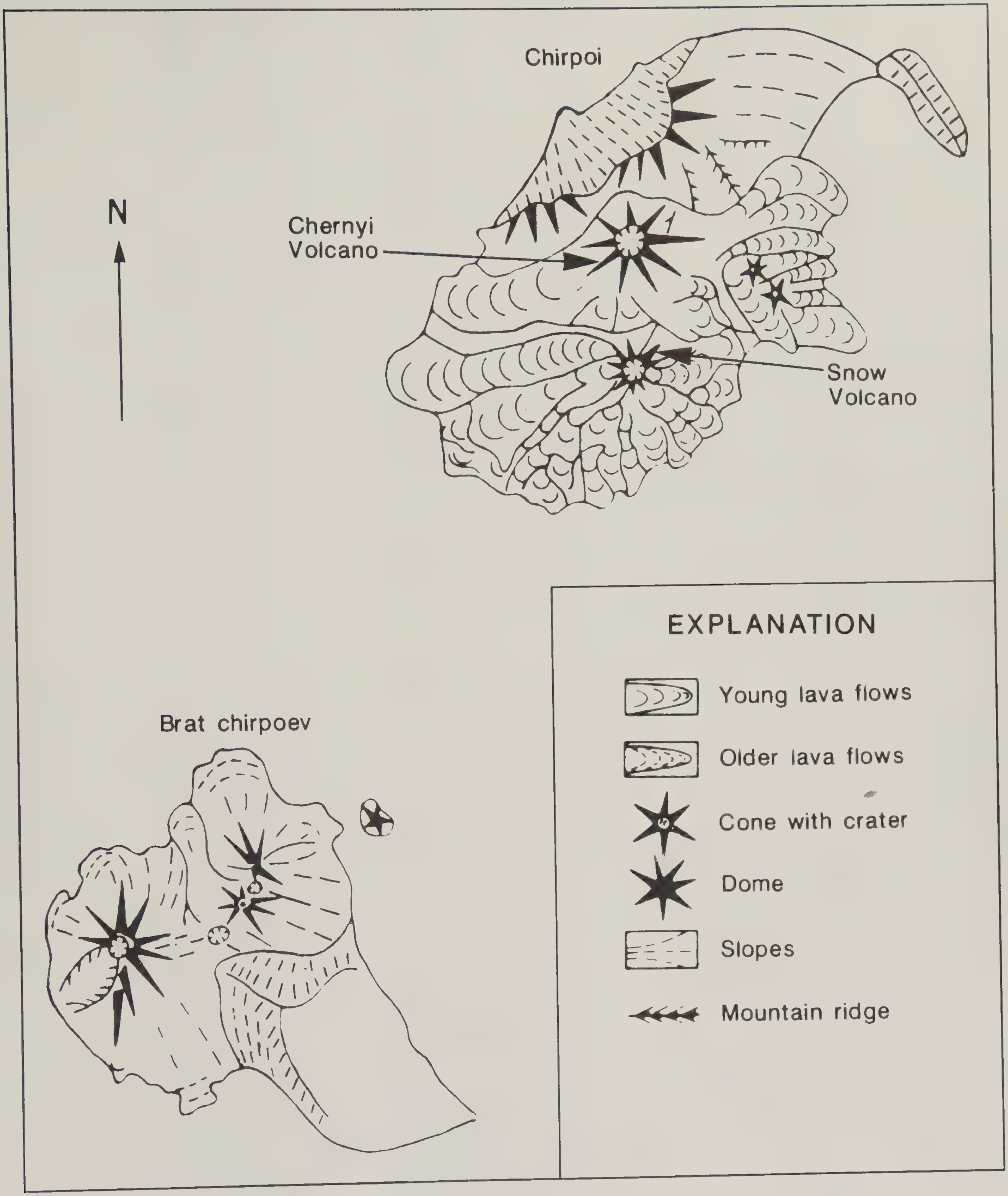

Figure 9.4.1. Sketch of structure of Chirpoi (top) and Brat Chirpoev (bottom), from Gorshkov (1970).

ZAVARITSKY

CAVW number (active vent)	Latitude Longitude (degrees)	Diameter (km)	Local tectonic setting	Precaldera edifice	SiO_2 content (wt pct)	Age of collapse (yr B.P.)	Date of unrest	Type and duration of unrest ESTU STHF MGTF H Te	Eruption type
09-00-18 (Zavaritsky)	46.92N 151.95E	10 (outer) 8 (middle) 3 (inner) (concentric)	Fault, west side of outer caldera; compr	Strato (3 generations)	R = 54-59 C = 64-72	Second caldera, inter-glacial	1916/1930	---- ---- ---- - --	ex,dm
							1957	B--- ---- Z--E E --	Ex,dm,lf

TECTONIC SETTING

Zavaritsky lies along the central part of the Kurile island arc (Gorshkov, 1970; see section on TECTONIC SETTING of Golovnin Caldera).

GEOLOGIC HISTORY

The present Zavaritsky Caldera is the smallest and innermost of three successive calderas on Zavaritsky Volcano (figs. 9.5.1-9.5.3). Steep inward dips of lacustrine sediments from an earlier, higher level of the caldera lake in the innermost caldera suggest that sliding from the walls after later explosions deepened the innermost caldera (Gorshkov, 1970, p. 153).

HISTORICAL ACTIVITY

Strong fumaroles occur and thermal springs normally discharge on the southern edge of the caldera lake. Temperature of the lake is normally 30 °C. For several months before the start of the 1957 eruption, the activity of the fumaroles and thermal springs noticeably diminished. Earthquakes were felt in Kostodhka at 2200 hr on 11 November 1957; six more shocks were felt between 0200 and 0500 hr the next day. The two strongest earthquakes occurred at 0400 hr, separated by 15-20 minutes of thunderous roaring. A moderately large eruption began on 12 November 1957. During 10-12 August 1958, the relative difference in magnetic-field strength between points inside and outside the caldera increased by 1 gamma, then decreased by 2 gammas by 18 August (Bernstein, 1960).

In a September 1981 aerial inspection, no fumarolic activity was seen (Smithsonian Institution, 1981).

ZAVARITSKY (continued)

REFERENCES

Bernstein, V.A., 1960, On the magnetic field of Zavaritsky Volcano, Simushir Island, Kurile Islands: Bull. Vulkanol. Stantsii (Kamchatka), no. 30, p. 55-68.

Erlich, E., 1986, Geology of the calderas of Kamchatka and Kurile Islands with comparison to calderas of Japan and the Aleutians, Alaska: U.S. Geol. Surv. Open-File Rep. 86-291, 300 p.

Gorshkov, G.S., 1958, Catalogue of active volcanoes of the world including solfatara fields, Pt. VII, Kurile Islands: Naples, IAVCEI, 99 p.

----- 1970, Volcanism and the upper mantle: Investigations in the Kurile Volcanic Arc: New York, Plenum Press, 385 p.

Markhinin, E.K., 1960, The eruption of Zavaritsky on Simushir Is. in the autumn of 1957: Bull. Vulkanol. Stantsii (Kamchatka), no. 29, p. 7-14.

Ostapenko, V.F., Fedorchenko, V.I., and Shilov, V.N., 1967, Pumices, ignimbrites, and rhyolite from the Great Kurile arc: Bull. Volcanol., v. 30, p. 81-92.

Smithsonian Institution, Scientific Event Alert Network (SEAN), 1981, Zavaritsky Caldera: SEAN Bull., v. 6, no. 12, p. 8 (information from G.S. Steinberg).

Tovarova, I.I., 1960, Fumarolic activity in the Zavaritsky caldera: Bull. Vulkanol. Stantsii (Kamchatka), no. 30, p. 50-54.

Zelenov, K.K., and Kanakina, M.A., 1962, Biriuzovoye Lake (Zavaritsky Caldera) and changing of its water chemistry as a result of the eruption in 1957: Bull. Vulkanol. Stantsii (Kamchatka), no. 32, p. 24-33.

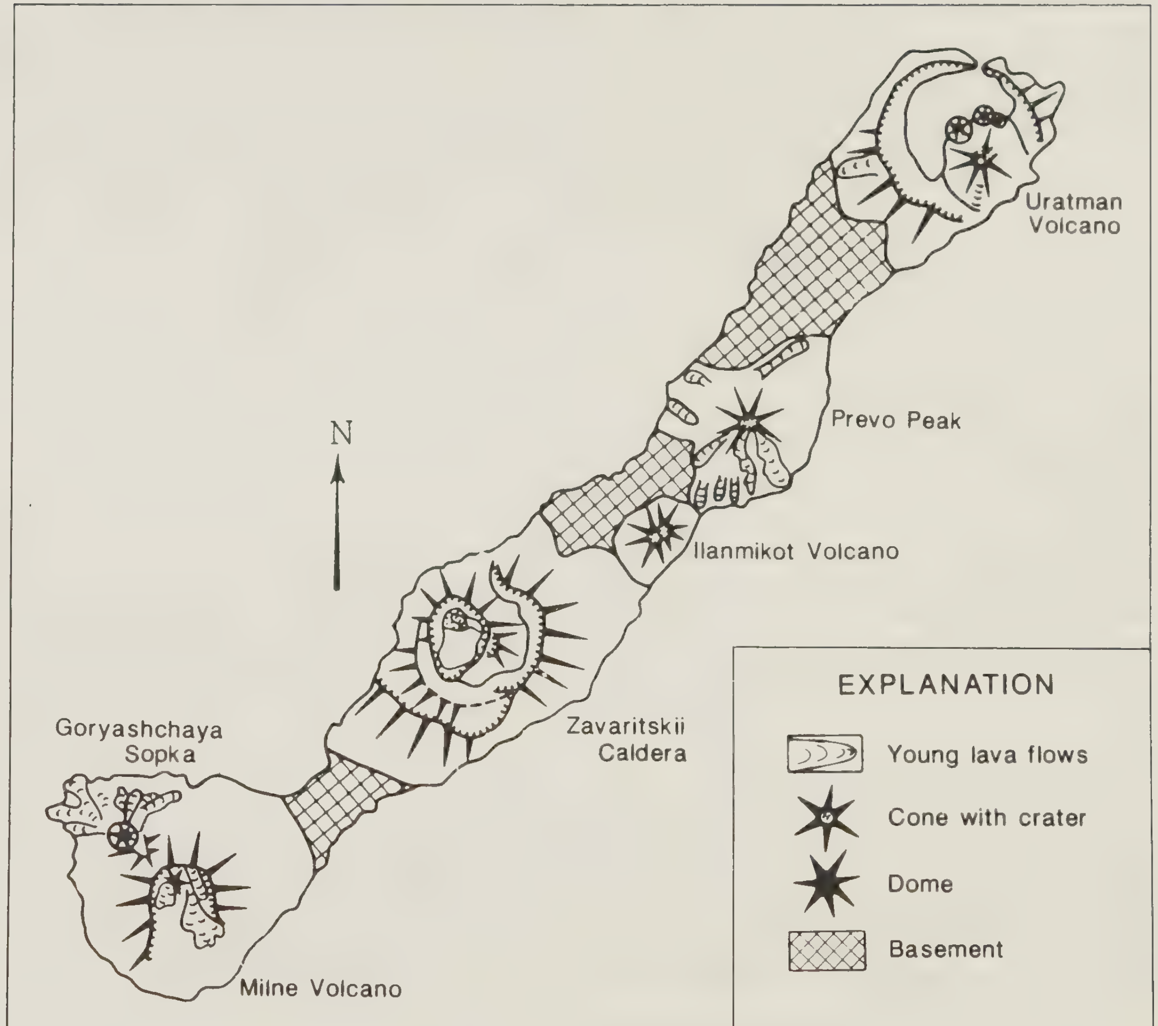

Figure 9.5.1. Sketch of distribution of volcanoes on Simushir Island, from Gorshkov (1970).

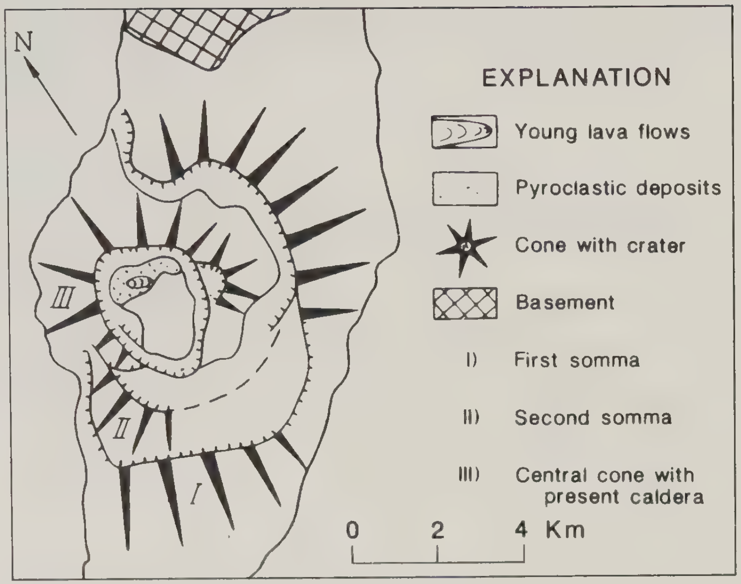

Figure 9.5.2. Sketch showing structure of Zavaritsky Caldera, from Gorshkov (1970).

Figure 9.5.3. Sketch of structure of Zavaritsky Caldera, from Gorshkov (1958): **I**, first somma; **II**, second somma; **III**, central cone with present caldera.

KETOI

CAVW number (active vent)	Latitude Longitude (degrees)	Diameter (km)	Local tectonic setting	Precaldera edifice	SiO_2 content (wt pct)	Age of collapse (yr B.P.)	Date of unrest	Type and duration of unrest ESTU STHF MGTF H Te	Eruption type
09-00-20	47.35N	5 (outer)	Compr	Shield	R= 58	pre-	1843-46	---- ---- ---- - QU?	ex,lf
(Pallas Peak)	152.48E	1.5 (inner)			C= silicic	glacial?	1924	---- ---- ---- - --	ex
							1960	---- ---- ---- - --	ex

TECTONIC SETTING

Ketoi lies along the central part of the Kurile island arc (Gorshkov, 1970; see section on TECTONIC SETTING of Golovnin Caldera).

GEOLOGIC HISTORY

Northeast-trending faults form a graben and horst that cross the northwest edge of the caldera. At least two generations of calderas are present, of which the older one is larger. Pallas Peak is a postcaldera cone on the southeastern margin of the older caldera (figs. 9.6.1, 9.6.2).

HISTORICAL ACTIVITY

Two "violent" earthquakes shook Urup Island, 1.5° of latitude (ca. 165 km) south of Ketoi, on 25 April 1843. A strong eruption of Ketoi began in July 1843, and "the whole island was on fire" (Perrey, 1863, p. 165).

In September 1981, an aerial inspection showed intense fumarolic activity on the outer north slope of the volcano (Smithsonian Institution, 1981).

REFERENCES

Erlich, E., 1986, Geology of the calderas of Kamchatka and Kurile Islands with comparison to calderas of Japan and the Aleutians, Alaska: U.S. Geol. Surv. Open-File Rep. 86-291, 300 p.

KETOI (continued)

REFERENCES (continued)

Gorshkov, G.S., 1958, Catalogue of active volcanoes of the world including solfatara fields, Pt. VII, Kurile Islands: Naples, IAVCEI, 99 p.

----- 1970, Volcanism and the upper mantle: Investigations in the Kurile Volcanic Arc: New York, Plenum Press, 385 p.

Perrey, A., 1863, Documents sur les tremblements de terre et les phénomènes volcaniques dans l'archipel des Kouriles et au Kamtschatka: Lyon, Soc. Imp. Agric. Hist. Nat. Arts, 166 p.

Smithsonian Institution, Scientific Event Alert Network (SEAN), 1981, Ketoi Caldera: SEAN Bull., v. 6, no. 12, p. 8 (information from G.S. Steinberg).

Vlasov, G.M., 1967, Kamchatka, Kuril, and Komandorskiye Islands: Geological description: Geology of the USSR, v. 31, Moscow, Izd.-vo Nedra, 827 p.

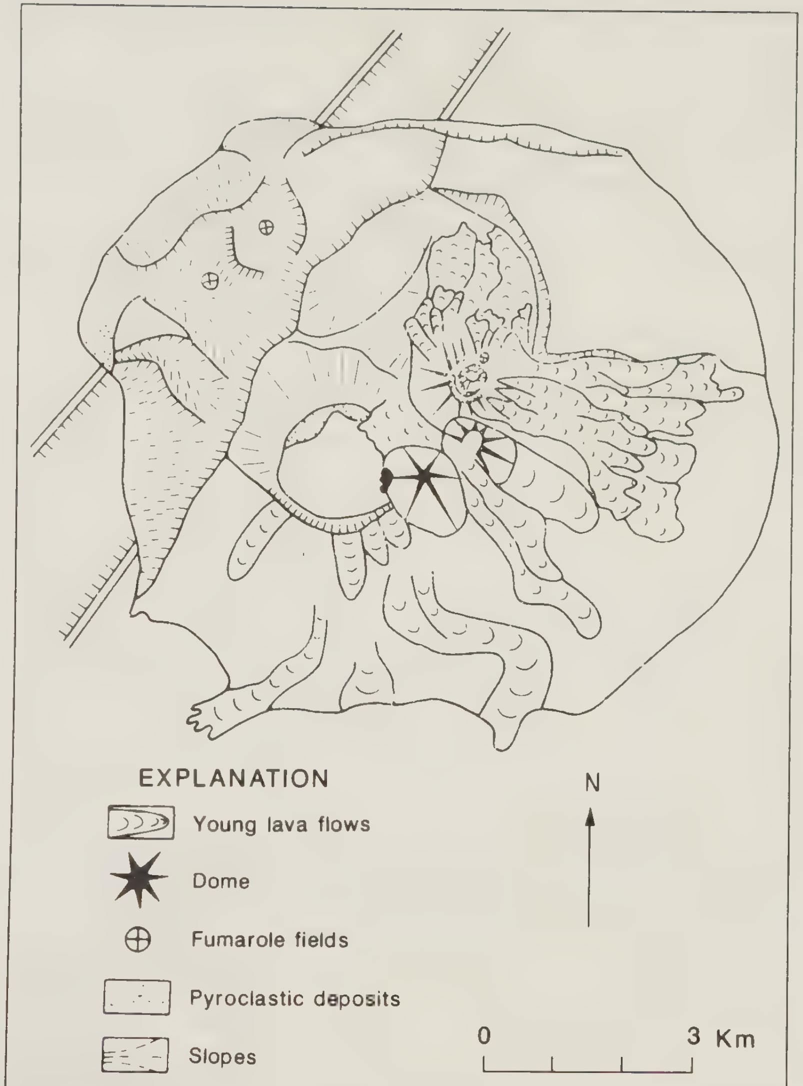

Figure 9.6.1. Sketch of structure of Ketoi Caldera, from Gorshkov (1970).

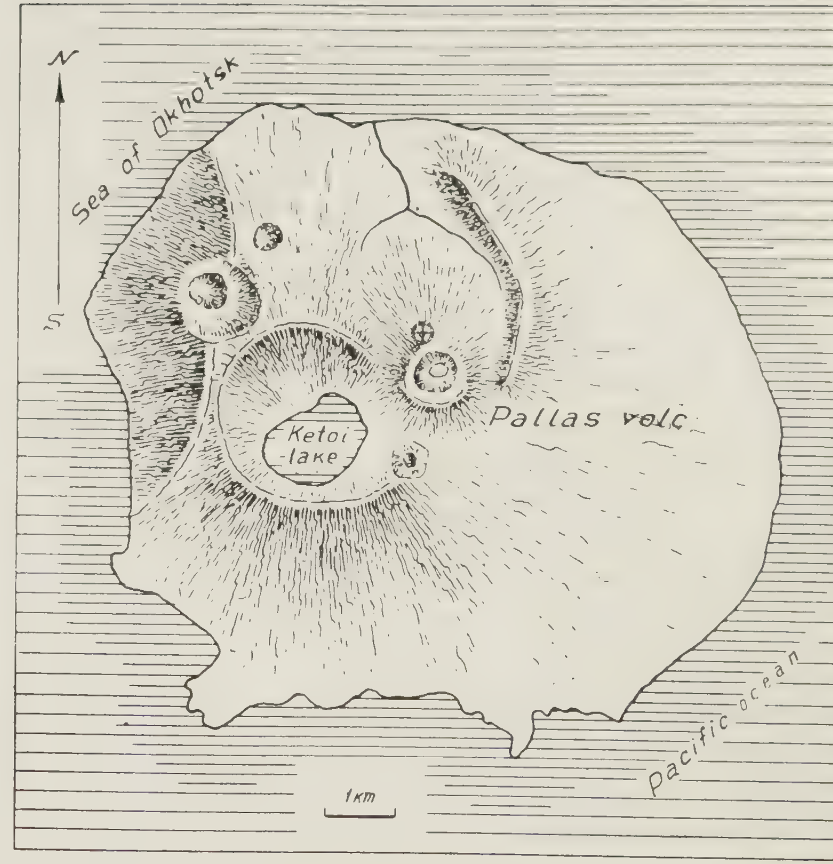

Figure 9.6.2. Sketch showing structure of Pallas Volcano and Ketoi Volcano, from Gorshkov (1958).

RASSHUA

CAVW number (active vent)	Latitude Longitude (degrees)	Diameter (km)	Local tectonic setting	Precaldera edifice	SiO_2 content (wt pct)	Age of collapse (yr B.P.)	Date of unrest	Type and duration of unrest ESTU STHF MGTF H Te	Eruption type
09-00-22	47.77N	6	Compr	Strato	R = 56±	pre-	1810?	---- ---- ---- - --	unknown
(Rasshua)	153.02E				C = ?	latest	1846	---- ---- ---- - --	Ex
						glaciation	1946	---- ---- --?C - --	none?
							1957	---- ---- --?x - --	pex?

TECTONIC SETTING

Rasshua lies along the Kurile island arc (Gorshkov, 1970; see section on TECTONIC SETTING of Golovnin Caldera).

GEOLOGIC HISTORY

Rasshua Volcano lies just north of the center of a 6-km-diameter somma (figs. 9.7.1, 9.7.2).

HISTORICAL ACTIVITY

1846: "A volcano on Rasshua smokes intensely and occasionally emits flames" (Doroshin, 1870).

1946: Steaming increased briefly on 4 November 1946, followed 3 days later by an increase in steaming at Sarichev, 28 km away, and 5 days later (on 9 November 1946) by an eruption of Sarichev.

1957: Fumarolic activity increased markedly and weak explosions occurred (Vlasov, 1967; Gorshkov, 1970).

REFERENCES

Doroshin, P., 1870, On some volcanoes, their eruptions and earthquakes in former Russian domains of America: Verhandlungen der Russisch-Kaiserlichen Mineralogischen Gesellschaft zu St. Petersburg, 2nd ser., p. 25-44.

Erlich, E., 1986, Geology of the calderas of Kamchatka and Kurile Islands with comparison to calderas of Japan and the Aleutians, Alaska: U.S. Geol. Surv. Open-File Rep. 86-291, 300 p.

RASSHUA (continued)

REFERENCES (continued)

Glavatsky, S.N., and Efremov, Yu.K., 1948, The eruption of the volcano Peak Sarichev in November 1946: Bull. Vulkanol. Stantsii (Kamchatka), no. 15, p. 8-12.

Gorshkov, G.S., 1958, Catalogue of active volcanoes of the world including solfatara fields, Pt. VII, Kurile Islands: Naples, IAVCEI, 99 p.

----- 1970, Volcanism and the upper mantle: Investigations in the Kurile Volcanic Arc: New York, Plenum Press, 385 p.

Gushchenko, I.I., 1979, Eruptions of volcanoes of the world, a catalog: Acad. Sci. USSR Far Eastern Sci. Center, Moscow, Nauka Publ., 474 p.

Vlasov, G.M., 1967, Kamchatka, Kuril, and Komandorskiye Islands: Geological description: Geology of the USSR, v. 31, Moscow, Izd.-vo Nedra, 827 p.

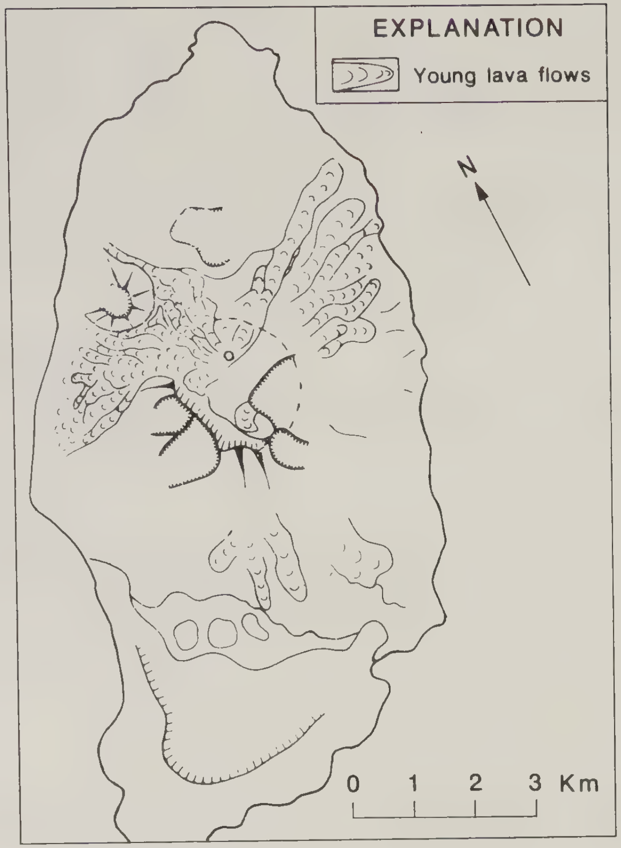

Figure 9.7.1. Sketch of structure of Rasshua Volcano, from Gorshkov (1970).

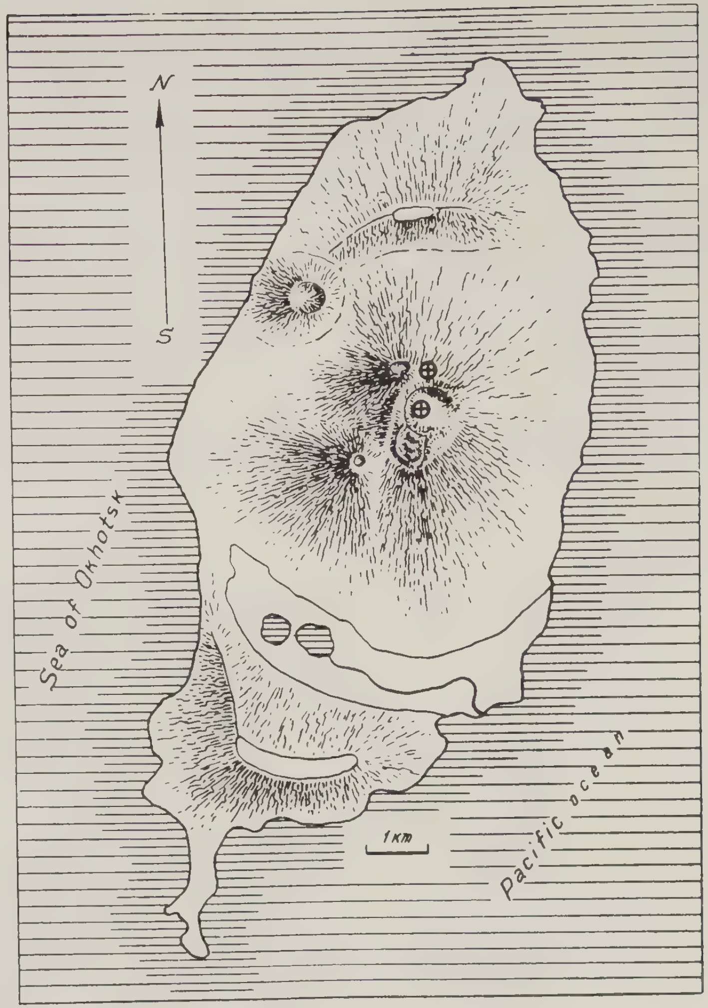

Figure 9.7.2. Sketch showing structure of Rasshua Volcano, from Gorshkov (1958).

PART 3: HISTORICAL UNREST AT LARGE QUATERNARY CALDERAS (continued)

See inside back cover for explanation and abbreviations

TAO-RUSYR

CAVW number (active vent)	Latitude Longitude (degrees)	Diameter (km)	Local tectonic setting	Precaldera edifice	SiO_2 content (wt pct)	Age of collapse (yr B.P.)	Date of unrest	Type and duration of unrest ESTU STHF MGTF H Te	Eruption type
09-00-31 (Krenitzyn Peak)	49.36N 154.71E	7.5	Inter-section of two volcano-tectonic lines	LL-strat	R = 49-64 C = 59-67	7040	1846	---- ---- ---? - --	none
							1879	---- ---- ---? - --	none
							1952	?--- ---- C--- - QU	Ex,dm

TECTONIC SETTING

Tao-Rusyr (figs. 9.8.1, 9.8.2) lies along the Kurile island arc (Gorshkov, 1970; see section on TECTONIC SETTING of Golovnin Caldera).

GEOLOGIC HISTORY

A precaldera edifice of basalt and basaltic andesite is capped by dacitic, pumiceous pyroclastic fall and flow deposits from the caldera-forming eruption. Krenitzyn Peak is an andesitic cone that grew in the caldera lake. The lake is heated from below and does not freeze over in winter.

HISTORICAL ACTIVITY

1846, 1879: Solfataric activity was noted, but it is not clear from the reports whether that was normal activity simply observed in these years or an abnormal increase in solfataric activity.

1952: An eruption occurred on 12 November 1952, from a new explosion crater on the east flank of Krenitzyn Peak. The eruption followed and may have been triggered by a strong tectonic earthquake (4 November 1952, $\underline{M}$ = 8.25, 50 km from the caldera) (Kimura, 1978). "Three days prior to the eruption, disturbances of the magnetic field were observed" (Gorshkov, 1958, p. 73). "A.A. Lettens, studying the horizontal structure of the magnetic field, detected strange behavior of a magnetic compass--a slow uneven deceleration in one direction, completely unlike normal measurements. These phenomena may have had some kind of relation and may have forewarned of the impending eruption" (Piip and Sviatlovsky, 1954). We have no details about where the disturbance was measured. Magma erupted in 1952 had an SiO_2 content of 62 percent (Gorshkov, 1954).

TAO-RUSYR (continued)

REFERENCES

Erlich, E., 1986, Geology of the calderas of Kamchatka and Kurile Islands with comparison to calderas of Japan and the Aleutians, Alaska: U.S. Geol. Surv. Open-File Rep. 86-291, 300 p.

Gorshkov, G.S., 1954, Chronology of the eruptions of the Kurile Range of volcanoes, 1713-1952: Akad. Nauk USSR, Trudy Lab. Vulkanol., no. 8, p. 58-99.

----- 1958, Catalogue of active volcanoes of the world including solfatara fields, Pt. VII, Kurile Islands: Naples, IAVCEI, 99 p.

----- 1970, Volcanism and the upper mantle: Investigations in the Kurile Volcanic Arc: New York, Plenum Press, 385 p.

Kimura, M., 1978, Significant eruptive activities related to large interplate earthquakes in the northwestern Pacific margin: Jour. Phys. Earth, v. 26 supp., p. S557-S570.

Piip, B.I., and Sviatlovsky, A.E., 1954, The eruption of Krenitzyn Peak in 1952: Bull. Vulkanol. Stantsii (Kamchatka), no. 20, p. 65-66.

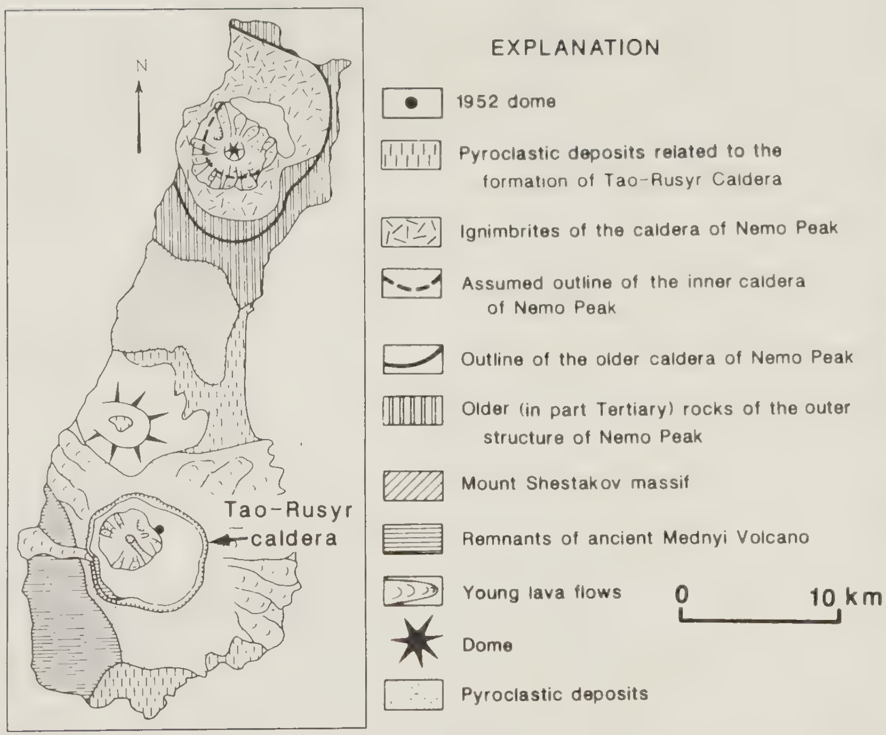

Figure 9.8.1. Sketch of structure of volcanoes of Onekotan, from Gorshkov (1970).

Figure 9.8.2. Sketch showing structure and a cross section of Krenitzyn Peak and Tao-Rusyr Caldera, from Gorshkov (1958).

NEMO PEAK

CAVW number (active vent)	Latitude Longitude (degrees)	Diameter (km)	Local tectonic setting	Precaldera edifice	SiO_2 content (wt pct)	Age of collapse (yr B.P.)	Date of unrest	Type and duration of unrest ESTU STHF MGTF H Te	Eruption type
09-00-32 (Nemo Peak)	49.57N 154.81E	11 each (older two) 5 (younger)	Two intersecting volcano-tectonic lines; compr	LL-strat	R = 54-59 C = 64	interglacial (younger); preglacial (older)	early 1700's	---- ---- ---- - --	ex
							1906	---- ---- ---- - --	ex,dm?
							1938	---- ---- ---- - --	ex

TECTONIC SETTING

Nemo Peak lies along the Kurile island arc (Gorshkov, 1970; see section on TECTONIC SETTING of Golovnin Caldera).

GEOLOGIC HISTORY

The Nemo Peak volcanic center has had repeated episodes of caldera formation. The system consists of two overlapping older calderas, each of diameter approximately 11 km, that formed in preglacial times. Then, a postcaldera cone grew on the overlapping boundaries of these two calderas until a smaller, 5-km-diameter caldera formed at its summit (figs. 9.9.1, 9.9.2). The presently active peak (Nemo Peak) grew inside the younger, smaller summit caldera.

HISTORICAL ACTIVITY

Few details are available. A young-looking dome might have formed during the eruption of 1906.

REFERENCES

Erlich, E., 1986, Geology of the calderas of Kamchatka and Kurile Islands with comparison to calderas of Japan and the Aleutians, Alaska: U.S. Geol. Surv. Open-File Rep. 86-291, 300 p.

Gorshkov, G.S., 1958, Catalogue of active volcanoes of the world including solfatara fields, Pt. VII, Kurile Islands: Naples, IAVCEI, 99 p.

----- 1970, Volcanism and the upper mantle: Investigations in the Kurile Volcanic Arc: New York, Plenum Press, 385 p.

Gushchenko, I.I., 1979, Eruptions of volcanoes of the world, a catalog: Acad. Sci. USSR Far Eastern Sci. Center, Moscow, Nauka Publ., 474 p.

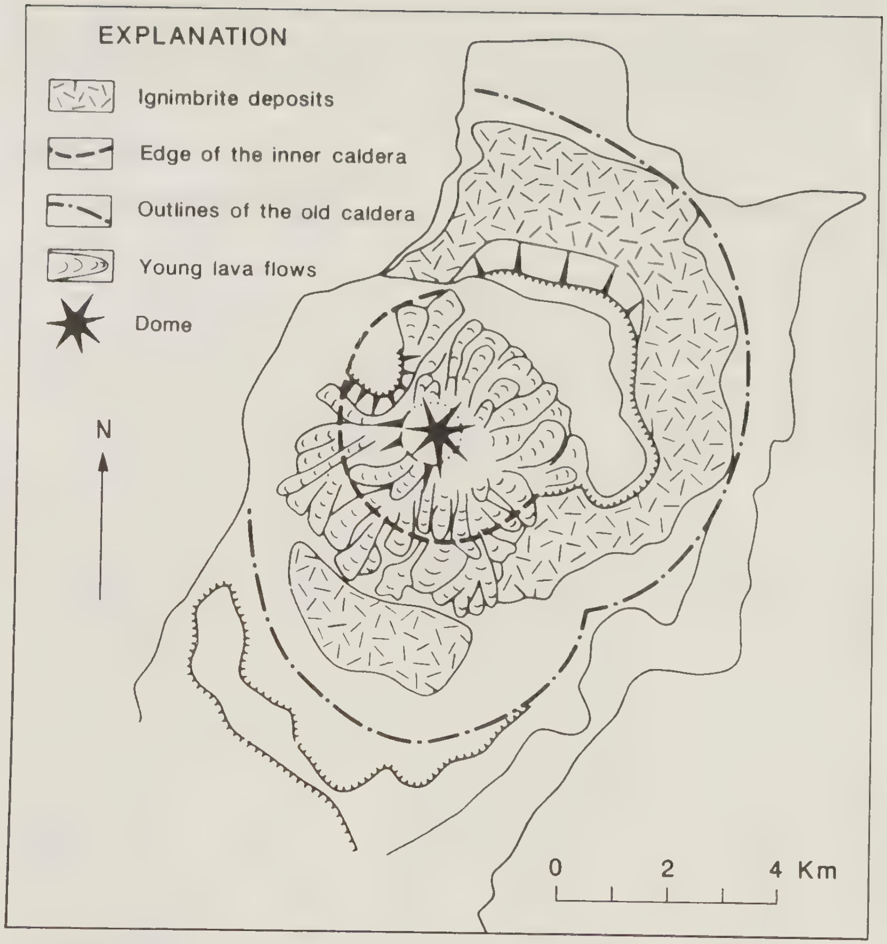

Figure 9.9.1. Sketch of structure of Nemo Peak, from Gorshkov (1970).

Figure 9.9.2. Sketch showing structure of Nemo Volcano, from Gorshkov (1958). Cross in circle, solfatara.

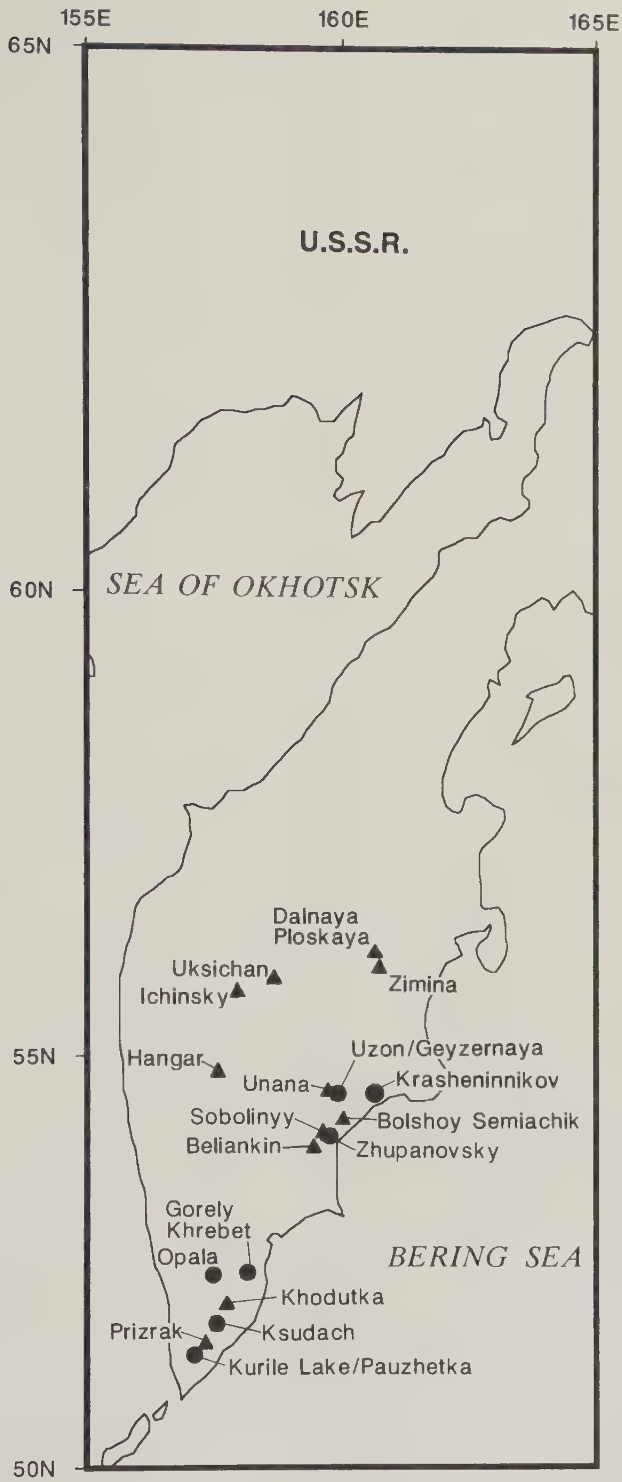

Figure 10. Locations of large, Quaternary restless calderas (solid circles) and nonrestless calderas (triangles) in part of Region 10, including Kamchatka and an adjacent part of Asian mainland (see also figure 10.8).

PART 3: HISTORICAL UNREST AT LARGE QUATERNARY CALDERAS (continued)

See inside back cover for explanation and abbreviations

KURILE LAKE/PAUZHETKA

CAVW number (active vent)	Latitude Longitude (degrees)	Diameter (km)	Local tectonic setting	Precaldera edifice	SiO_2 content (wt pct)	Age of collapse (yr B.P.)	Date of unrest	Type and duration of unrest ESTU STHF MGTF H Te	Eruption type
10-00-03 (Iliinsky)	51.45N 157.08E	20x25 (P) 10 (KL)	Inter-section of N-S graben and E-W strike-slip fault	None?	R = low 50's -63 C = d (KL); silicic (P)	8,000-8,340 (KL) 10,000-220,000 (P)	1901 1973-77+	---- ---- ---- - -- FF-- ---- ---- - --	pex, Pex none

TECTONIC SETTING

The Pauzhetka depression lies at the intersection of (a) N-S faults that form the east edge of the Kamchatka Median massif, the Golygin Mountains, with as much as 1000 m of displacement down to the east; and (b) the E-W trending Ozernovsky strike-slip fault.

GEOLOGIC HISTORY

The Pauzhetka depression is a large caldera ("volcano-tectonic depression") associated with the Golygin ignimbrite (10,000-220,000 yr B.P.) (figs. 10.1.1, 10.1.2). The presence of this ignimbrite in the Pauzhetka basin and on the Kambalny Ridge horst, as well as of lake terraces on the northeast side of Kurile Lake, suggests as much as 1000 m of resurgent doming within the recent geologic past (Beloussov, 1967). The Kurile Lake Caldera is nested within the Pauzhetka Caldera. Iliinsky is an active stratovolcano on the northeast rim of the Kurile Lake Caldera.

There has been a general migration of volcanism, including caldera-forming events, from southwest to northeast during the Quaternary. A major geothermal field has been developed in the Pauzhetka River graben - Kambalny Ridge horst area, part of the Pauzhetka depression.

Interestingly, $^{87}Sr/^{86}Sr$ ratios in ignimbrites of the Pauzhetka region (0.7023-0.7036) show little evidence of crustal contamination. Slightly higher values were found for rocks of Iliinsky Volcano (0.7054) and Cherniye Skaly Volcano (0.7054) (Erlich, 1986, Chap. 5, Table 11).

KURILE LAKE/PAUZHETKA (continued)

HISTORICAL ACTIVITY

Occasional seismic swarms, possibly seasonal in occurrence (March-April, July-August), have been reported by Levina and others (1980) (figs. 10.1.3, 10.1.4). Those in 1973 (10^{13}-10^{15} ergs of seismic energy release) were initially thought to be centered between Kambalny and Koshelev (Kirsanov and others, 1975); a more recent analysis places them along a northeast trend north of Kambalny Volcano (Levina and others, 1980). Focal mechanisms for two earthquakes suggest left-lateral strike-slip motion on a northeast-trending fault. Fumarolic activity had not changed at the conclusion of the December 1973 swarms (Kirsanov and others, 1975).

REFERENCES

Beloussov, V.I., 1967, Geological structure of the hydrothermal systems of Kamchatka: Bull. Volcanol., v. 30, p. 63-73.
Erlich, E., 1986, Geology of the calderas of Kamchatka and Kurile Islands with comparison to calderas of Japan and the Aleutians, Alaska: U.S. Geol. Surv. Open-File Rep. 86-291, 300 p.
Erlich, E.N., and Gorshkov, G.S., eds., 1979, Quaternary volcanism and tectonics in Kamchatka: Bull. Volcanol., v. 42, nos. 1-4 (spec. iss.), 298 p.
Erlich, E.N., and Melekestsev, I.V., 1972, Evolution of Quaternary volcanism and tectonics in the western part of the Pacific rim: Pacific Geol., v. 4, p. 1-22.
Erlich, E.N., Melekestsev, I.V., Tarakanovsky, A.S., and Zubin, M.I., 1972, Quaternary calderas of Kamchatka: Bull. Volcanol., v. 36, p. 222-237.
Kirsanov, I.T., Khrenov, A.P., and Vakin, Ye. A., 1975, Active volcanoes of Kamchatka and the Kurile Islands in 1973: Bull. Vulkanol. Stantsii (Kamchatka), no. 51, p. 3-18.
Kozhemyaka, N.N., 1979, Quaternary pumice, tuff-ignimbrite fields, and center of eruptions in Southern Kamchatka: Bull. Vulkanol. Stantsii (Kamchatka), no. 57, p. 26-38.
Krayevaya, T.S., Braitseva, O.A., Sheimovich, V.S., Egorova, I.A., and Lupikina, E.G., 1979, Deposits of Quaternary calderas of Kamchatka: Vulkanol. Seismol., 1979, no. 4, p. 3-11.
Krijanovsky, N., 1934, Volcanoes of Kamchatka: Bull. Geol. Soc. Am., v. 45, p. 529-550.
Leonov, V.L., 1981, Faults of the Pauzhetka volcano-tectonic structure: Vulkanol. Seismol., 1981, no. 1, p. 24-36.
Levina, V.I., Firstov, P.P., and Zobin, V.M., 1980, The seismicity of the Pauzhetka Geothermal Region in Kamchatka: Vulkanol. Seismol., 1980, no. 2, p. 81-97.
Luchitsky, I.V., ed., 1974, Development of rugged relief of Siberia: Far East: Kamchatka, Kurile, and Komandor Islands: Moscow, Nauka Press, 430 p.
Masurenkov, Yu.P., 1980a, The volcano-magma chamber-structure system (Geologic-petrologic aspect of the problem): Vulkanol. Seismol., 1980, no. 4, p. 34-49.
----- ed., 1980b, Volcanic center: structure, dynamics, and products: Karymsky structure: Moscow, Nauka Press, 299 p.
Naboko, S.I., 1954, Geysers of Pauzhetka: Bull. Vulkanol. Stantsii (Kamchatka), no. 22, p. 9-30.

Figure 10.1.1. Volcanic centers of south Kamchatka, from Kozhemyaka (1979). Details of the geology of Kurile Lake/Pauzhetka center are given in figure 10.1.2.

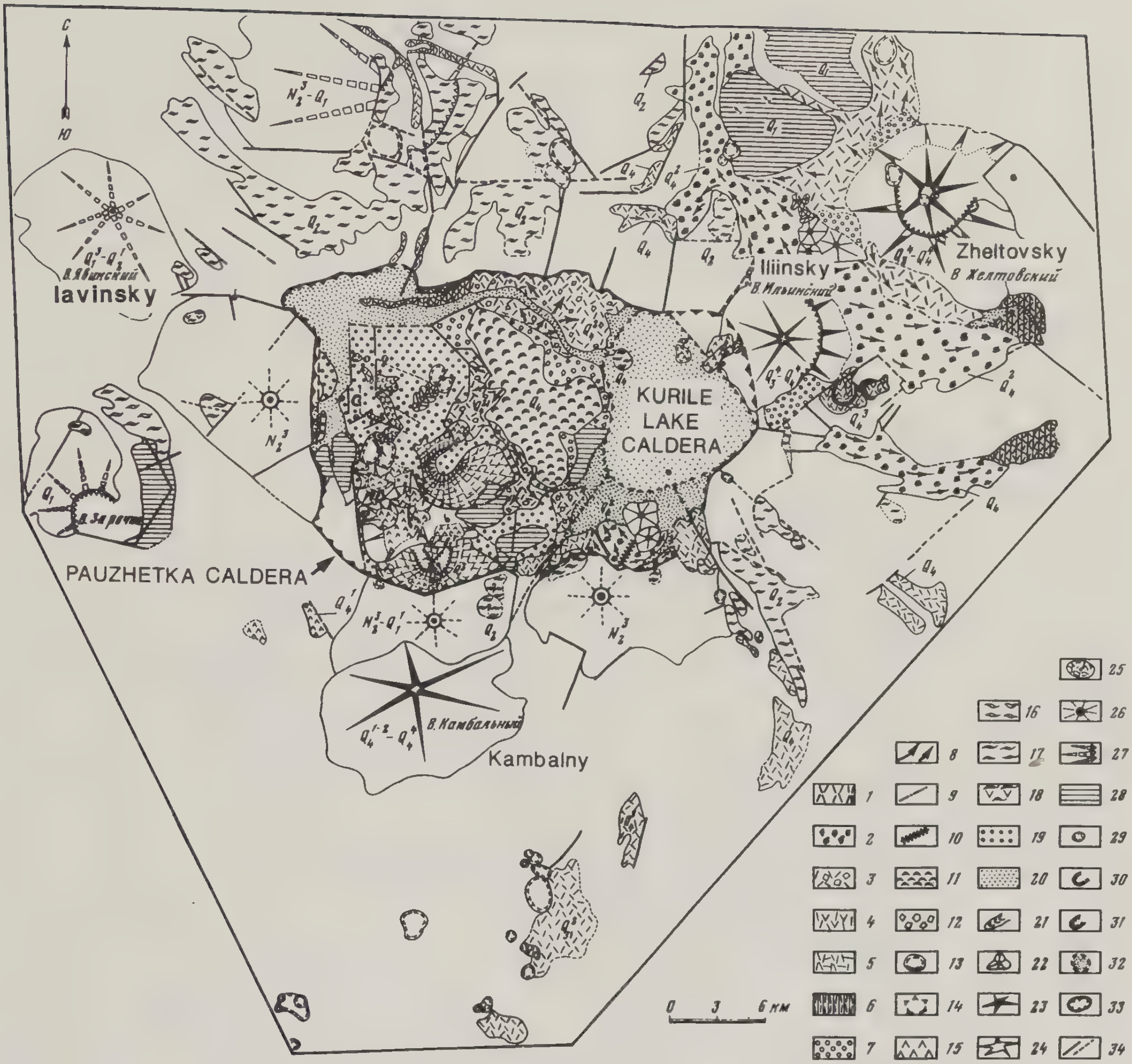

Figure 10.1.2. See next page for caption.

Figure 10.1.2. Geology of Pauzhetka volcano-tectonic depression, from Kozhemyaka (1979):

1. Pumiceous pyroclastic flow deposits from Zheltovsky Volcano -- Q_4.
2. Pumiceous pyroclastic flow deposits from Iliinsky Volcano -- Q_4.
3. Pumiceous pyroclastic flow deposits in the region of the Diky graben extrusive body - Q_4^2.
4. Modern pumice-cinder flows -- Q_4^3-Q_4^4.
5. Series of fine-grained pumiceous deposits of the fractured [unconsolidated?] type -- Q_4.
6. Reworked pumice.
7. Scoria blanket on stratovolcanoes -- Q_4.
8. Direction of pumiceous pyroclastic flows.
9. Inferred boundary between pyroclastic flows of Iliinsky and Zheltovsky volcanoes.
10. Fine-grained pumiceous deposit from a source (fissure-type) near Kirushutk -- Q_4^2.
11. Large polyphase extrusive complex of Diky graben -- Q_4.
12. Blast deposits (?) from the extrusive Diky graben complex -- Q_4.
13. Extrusive domes (cupolas) -- N_2^3.
14. Small extrusive domes -- specific extrusions of the ignimbrite tuff at Goliginsky mountain -- Q_2-Q_3.
15. Fine-grained dacitic lava.
16. Sheet of fine-grained ignimbrite tuff of dacitic composition -- Q_2-Q_3^1.
17. Platy ignimbrite tuff of liparitic dacite and liparite composition.
18. Fine-grained ignimbrite tuff of andesitic composition.
19. Thick pyroclastic tuff of the Pauzhetka sedimentary-volcanic depression -- N_2^3-Q_3^1.
20. Undifferentiated deposits of river valleys (alluvium).
21. Lava flows -- Q_3-Q_4.
22. Lava cones -- Q_3-Q_4.
23. Large conical stratovolcanoes -- Q_3^4-Q_4^4.
24. Important basaltic cones of lava volcanoes [shields?] -- Q_3.
25. Important pyroclastic strata of Kambalny Ridge -- Q_1-Q_2.
26. Important lava-shield volcanoes -- Q_1-Q_2.
27. Large, principal Pliocene volcanic centers -- N_2^3.
28. Plateau lava outliers -- Q_1.
29. Modern volcanic craters.
30. Newest explosion craters with pumice-scoria flows -- Q_4^3-Q_4^4.
31. Caldera rim volcanoes Iliinsky and Zheltovsky -- Q_4.
32. Kurile Lake volcano-tectonic depression.
33. Pauzhetka volcano-tectonic depression -- N_2^3-Q_1.
34. Tectonic shear zones -- a) known; b) hypothetical.

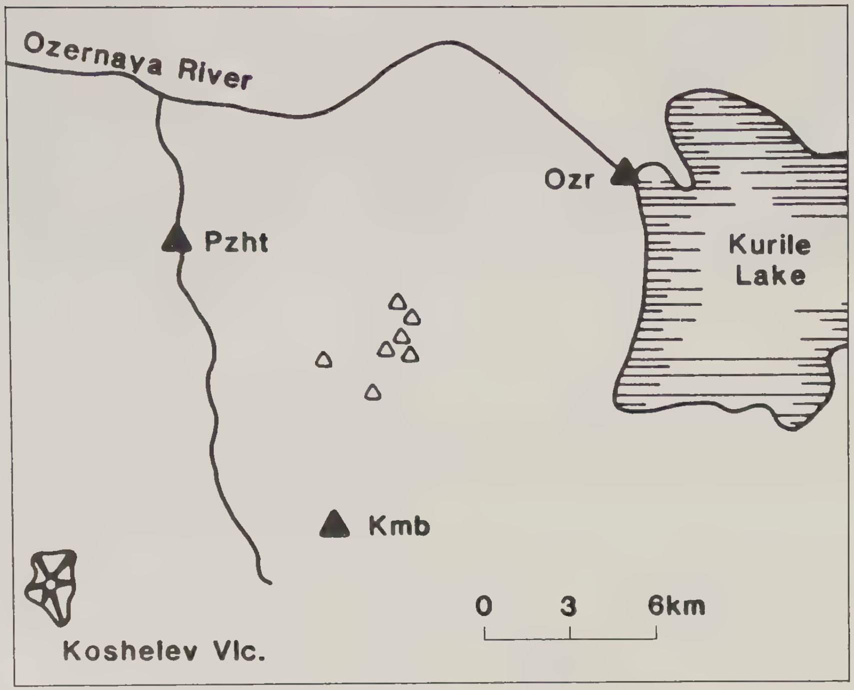

Figure 10.1.3. Epicenters of earthquakes within Pauzhetka geothermal field, from Erlich (1986) after Levina and others (1980). Solid triangles, seismic stations: Pauzhetka (Pzht), Kambalny (Kmb), and Ozernaya (Ozr). Open triangles, epicenters of earthquakes.

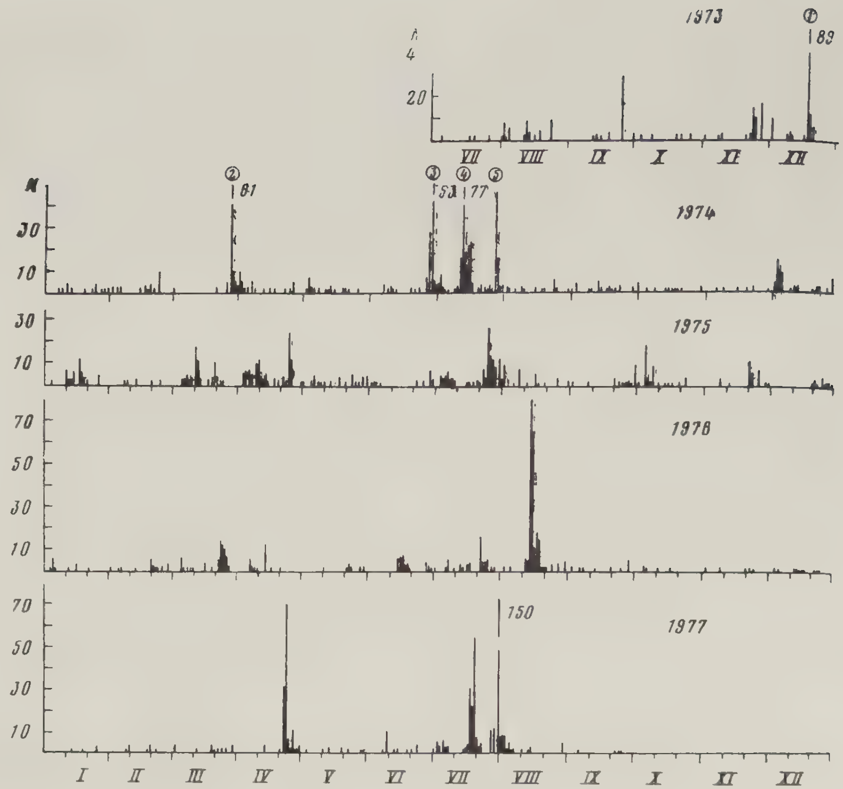

Figure 10.1.4. Daily counts of microearthquakes with energy class $\underline{K} \geq 5$, and S - P $\leq$ 2.5 sec, recorded on station Pzht in 1973-74 (detailed processing) and 1975-77 (preliminary processing), from Levina and others (1980).

PART 3: HISTORICAL UNREST AT LARGE QUATERNARY CALDERAS (continued)
See inside back cover for explanation and abbreviations

KSUDACH

CAVW number (active vent)	Latitude Longitude (degrees)	Diameter (km)	Local tectonic setting	Precaldera edifice	SiO_2 content (wt pct)	Age of collapse (yr B.P.)	Date of unrest	Type and duration of unrest ESTU STHF MGTF H Te	Eruption type
10-00-05 (Stübel cone)	51.83N 157.52E	7 x 13 (outer); 7 x 6, 4 x 5 4 x 4 4 x 4 (nested)	Inter-section of NE-trending graben and strike-slip fault	Shield	R = 60-69 C = d	>40,000 (outer); 30,000-40,000; 15,000; 8,800-3,600; 2,500-1,700 (nested)	1907	---- ---- ---- - --	EX

TECTONIC SETTING

Ksudach Caldera lies in the southern Kamchatka graben-syncline, at its intersection with a major, N45°E strike-slip fault that has offset the graben.

GEOLOGIC HISTORY

The Ksudach Caldera volcano is a shield of alternating basaltic lavas and dacitic pyroclastic deposits; this shield may have grown within a large but now poorly defined 7 km x 13 km diameter, 35-40 km^3 caldera (figs. 10.2.1-10.2.2) (Seliangin, 1987; Melekestsev and Sulerzhitsky, 1987). A 7 km x 6 km diameter main caldera and three 4-5 km diameter calderas that are nested in the north part of the 7 km x 6 km caldera all lie atop the shield. Postcaldera displacements (subsidence) and eruptions have occurred along north-northeast trending faults (Erlich, 1986). Dacitic pumice from the eruption that formed the youngest caldera is widely spread around Ksudach. A system of basaltic ring dikes that surround the rim of the youngest caldera was probably emplaced "late in the caldera-forming stage" (Erlich, 1986). At least three tephra layers are known to have originated from Stübel Cone, ca. 1650 yr B.P., ca. 700 yr B.P., and in A.D. 1907 (see below) (Melekestsev and Sulerzhitsky, 1987).

HISTORICAL ACTIVITY

More than 1 km^3 of dacitic magma was erupted in 1907 (Hulten, 1923, 1924; Piip, 1941); the silica content of compositionally banded pumice from this eruption varied from 60 to 69 percent.

KSUDACH (continued)

REFERENCES

Dubik, Yu.M., and Meniaylov, I.A., 1971, Gas-hydrothermal activity of Ksudach caldera: Bull. Vulkanol. Stantsii (Kamchatka), no. 47, p. 40-43.

Erlich, E., 1986, Geology of the calderas of Kamchatka and Kurile Islands with comparison to calderas of Japan and the Aleutians, Alaska: U.S. Geol. Surv. Open-File Rep. 86-291, 300 p.

Hulten, E., 1923, Some geographical notes on the map of South Kamchatka: Geogr. Annaler, v. 8, no. 5, 21 p.

----- 1924, Eruption of a Kamchatka volcano in 1907 and its atmospheric consequences: Geol. Foren. Forhandl., v. 46, no. 5, p. 407-417.

Melekestsev, I.V., and Sulerzhitsky, L.D., 1987, Ksudach Volcano (Kamchatka) in the last 10 thousand years: Vulkanol. Seismol., 1987, no. 4, p. 28-39.

Piip, B.I., 1941, On the intensity of the eruption of Ksudach volcano in March, 1907: Bull. Vulkanol. Stantsii (Kamchatka), no. 10, p. 12-23.

Seliangin, O.B., 1987, Geologic map of Volcano Ksudach: Vulkanol. Seismol., 1987, no. 5, p. 16-27.

Vlodavetz, V.I., and Piip, B.I., 1959, Catalogue of active volcanoes of the world including solfatara fields, Pt. VIII, Kamchatka and continental areas of Asia: Naples, IAVCEI, 110 p.

Volynets, O.N., 1979, Mixed lavas, (and) relationship of the melts forming these lavas: Bull. Volcanol., v. 42, nos. 1-4 (spec. iss.), p. 233-242.

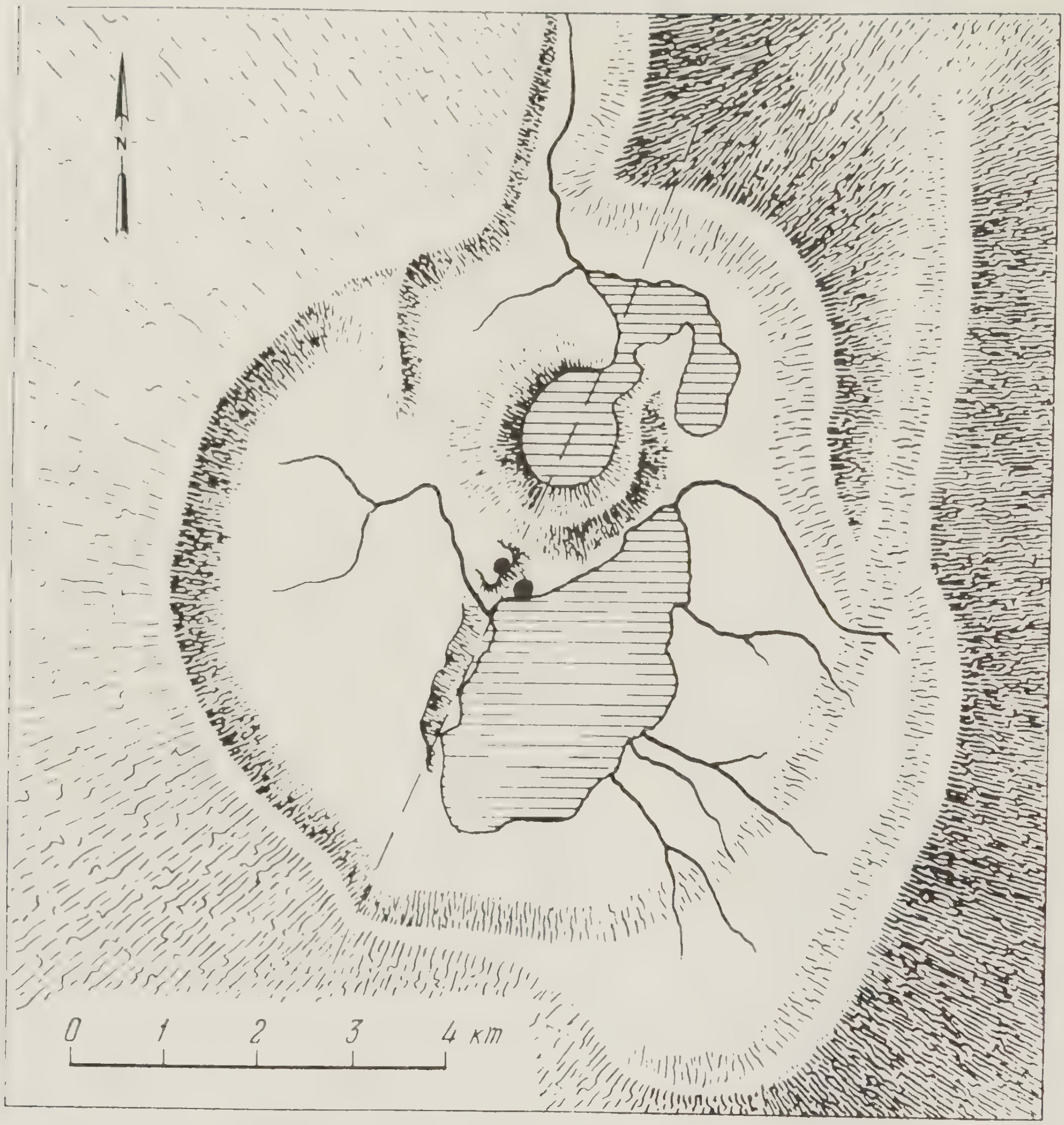

Figure 10.2.1. Sketch of top of Ksudach Volcano, from Vlovadetz and Piip (1959). Hot springs are indicated by dots, a fault by dashed line.

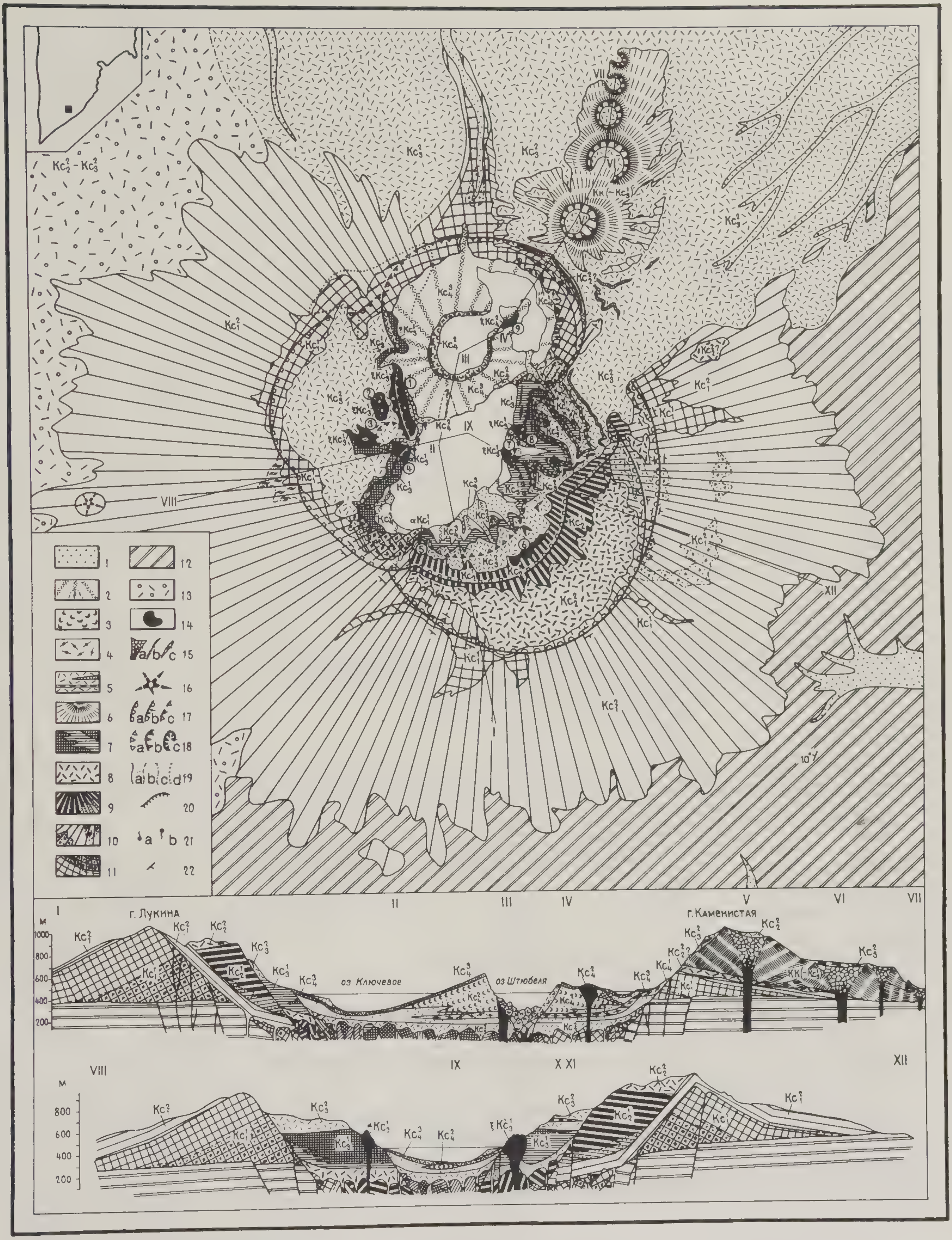

Figure 10.2.2. Geologic map of Ksudach Volcano, from Seliangin (1987). See next page for explanation.

Figure 10.2.2. Geologic map of Ksudach Volcano, from Seliangin (1987):

Kc_{1-4} -- Complexes of deposits corresponding to rhythms of volcanic activity. Most begin with phases (Kc_1^1, Kc_2^1) of basaltic-andesitic explosive-effusive volcanism, then have a break in volcanism, and conclude with phases (Kc_1^2, Kc_2^2, ...) that are explosive eruptions of mostly dacitic pumice (compositional range andesitic basalt to dacite), causing formation of great calderas and large craters.

1- alluvium.

Complex Kc_4:
2- andesitic scoria and dacitic pumices with local ignimbrite facies, blast deposits and nodules of allivalite and eucrite (olivine and augite gabbro) (Kc_4^3);
3- basaltic to andesitic lava and pyroclastic deposits of the Stübel cone, center of the most recent (1907) activity of Ksudach Volcano (Kc_4^2, complex Kc_3);
4- "early" dacitic pumice (Kc_4^1).

Complex Kc_3:
5- two horizons of pumiceous ignimbrites (the upper containing allivalite and eucrite nodules), dacite to andesite in composition (Kc_3^2);
6- complex of satellite volcanoes of the Kamenistaya Mountain (KK - Kc_3^1), basalt and basalt andesite in composition;
7- lavas of basaltic andesite to andesite composition, and sandy to gravelly volcanogenic lake deposits (closely spaced horizontal line pattern) (Kc_3^1).

Complex Kc_2:
8- andesitic and dacitic pumice (Kc_2^2);
9- lavas and pyroclastic deposits of basalt to basaltic andesite composition, and lake deposits (bold stripes in cross section) (Kc_2^1).

Complex Kc_1:
10- welded agglomerate tuffs of andesite and basaltic andesite composition (Kc_1^2);
11- tuffs of basaltic andesite, and lavas and pyroclastic rocks of basalt to andesite composition (Kc_1^1).

Basement complex:
12- sequence of basaltic lava sheets;
13- pumice deposits, undivided;
14- extrusive domes;
15- a) vents; b) dikes of basaltic andesite; c) ignimbritic dikes;
16- adventive cones;
17- boundaries of calderas of various ages: a) caldera Kc_1; b) caldera Kc_2; c) complex of calderas of the fourth generation Kc_3;
18- craters: a) destroyed and buried; b) with topographic expression; c) the most recent (Stübel crater);
19- geological contacts: a) observed; b) inferred; c) contacts between different facies of a single unit; d) boundary of recent eolian deposits;
20- faults;
21- modern geothermal manifestations: a) steam/gas; b) hot springs;
22- attitudes of layered rocks.

GORELY KHREBET

CAVW number (active vent)	Latitude Longitude (degrees)	Diameter (km)	Local tectonic setting	Precaldera edifice	SiO_2 content (wt pct)	Age of collapse (yr B.P.)	Date of unrest	Type and duration of unrest ESTU STHF MGTF H Te	Eruption type
10-00-07 (Gorely Khrebet)	52.45N 158.12E	10 x 13	WNW fracture normal to volcanic chain; compr	LL-strat	R = 51-71 (mostly b and a)	Upper Pleis- tocene	1828	---- ---- ---- - --	ex
							1832	---- ---- ---- - --	ex
							1855	---- ---- ---- - --	ex
							1869?	---- ---- ---- - --	unknown
					C = 60-66		1929-31	---- ---- ---- - --	Ex
							1947	---- ---- ---x - --	ex?
							1960-61	---- ---- --EE - --	ex
							1977-81	---- ---- --FF F --	Pex,ex
							1984-85	---- ---- ---- - --	pex

TECTONIC SETTING

Gorely Khrebet Caldera is located in the northeast corner of the southern Kamchatka graben-syncline, at the intersection of several E-W-trending "deep-seated faults" (Erlich, 1986).

GEOLOGIC HISTORY

Gorely Khrebet Caldera (figs. 10.3.1, 10.3.2) lies on the eastern margin of a large negative gravity anomaly (the Tolmachev anomaly, diameter 20-30 km, possibly representing a large buried caldera). The present volume of the upper Pleistocene ignimbrite sheet around the caldera is 120 km^3; its uneroded volume was probably greater (Luchitsky, 1974). The volume of caldera collapse was 200-250 km^3 (Erlich, 1986). Gorely Khrebet Volcano lies on an uplifted(?) area in the center of the caldera.

HISTORICAL ACTIVITY

1947: Strong solfatara activity was reported (Vlodavetz and Piip, 1959).

1960-61: Fumarolic temperatures increased, as during 1977-81 (see below). Then, after a series of minor ash eruptions (Kirsanov and others, 1964), fumarolic activity declined to a minimum during 1972-74 (Ivanov and others, 1980).

GORELY KHREBET (continued)

HISTORICAL ACTIVITY (continued)

1977-81: New fumaroles with temperatures up to 90 °C appeared in the summit crater of Gorely Khrebet in 1977 (fig. 10.3.4). During 1978-79, the number of fumaroles increased, maximum fumarole temperatures rose to 95 °C, and a warm lake formed on the crater floor. An area of hot ground appeared just west of the summit of Gorely Khrebet in 1978, and in 1979 fumarolic activity sharply increased in all craters of the massif. A green-colored lake formed in the central crater, and vigorous fumaroles became active at the base of the north wall. In August-September, gas plumes rose to heights of 500 m (Ivanov and others, 1980). Moderately large phreatic eruptions began in June 1980, and phreatomagmatic eruptions occurred in July and subsequent months. Juvenile blocks were alkali-rich basaltic andesite (Smithsonian Institution, 1980; Kirsanov and Ozerov, 1983). Earthquakes during 1980-81 occurred mainly in swarms, each lasting a few days to a few weeks (fig. 10.3.3) (Gabrilov and others, 1984).

1984-85: An eruption began on 27 December 1984. As in the 1980-81 eruption, initial phreatic activity was followed by phreatomagmatic explosions that ejected juvenile alkali-rich basaltic andesite (Kirsanov and Ozerov, 1983; Smithsonian Institution, 1985).

REFERENCES

Erlich, E., 1986, Geology of the calderas of Kamchatka and Kurile Islands with comparison to calderas of Japan and the Aleutians, Alaska: U.S. Geol. Surv. Open-File Rep. 86-291, 300 p.

Gabrilov, B.A., Gordeev, E.I., Ivanov, B.B., Ibshin, B.M., Stepanov, B.B., Farberov, A.I., Shirokov, B.A., and Yatsuk, B.B., 1984, Volcanic tremor and the Gorely Volcano earthquakes during the 1981 eruption: Vulkanol. Seismol., 1984, no. 6, p. 3-17.

Gushchenko, I.I., 1979, Eruptions of volcanoes of the world, a catalog: Acad. Sci. USSR Far Eastern Sci. Center, Moscow, Nauka Publ., 474 p.

Ivanov, B.V., Kirsanov, I.T., Chirkov, A.M., Khrenov, A.P., Andreyev, V.N., Vakin, Ye.A., and Trukhin, Yu.P., 1980, The status of the volcanoes of Kamchatka from May 1979 to January 1980: Vulkanol. Seismol., 1980, no. 3, p. 87-89.

Kirsanov, I.T., 1964, Volcanoes of southern and central Kamchatka in 1963: Bull. Vulkanol. Stantsii (Kamchatka), no. 37, p. 8-12.

----- 1967, Acid volcanism and thermal manifestations in the area of Mutnovsky and Gorely Volcanoes (southern Kamchatka): Bull. Volcanol., v. 30, p. 139-151.

----- 1981, Eruption of Gorely volcano in 1980: Vulkanol. Seismol., 1981, no. 1, p. 70-74.

Kirsanov, I.T., Ogorodov, N.V., and Chirkov, A.M., 1964, State of the Mutnovsky and Gorely volcanoes for the period from November 1960-June 1961: Bull. Vulkanol. Stantsii (Kamchatka), no. 36, p. 37-39.

Kirsanov, I.T., and Ozerov, A.Yu., 1983, Composition of products and energy effects of the eruption of Gorely Volcano, 1980-81: Vulkanol. Seismol., 1983, no. 1, p. 25-42 (English translation, Volcanol. Seismol., 1984, v. 5, p. 23-43).

Kozhemyaka, N.N., 1979, Quaternary pumice, tuff-ignimbrite fields, and center of eruptions in Southern Kamchatka: Bull. Vulkanol. Stantsii (Kamchatka), no. 57, p. 26-38.

GORELY KHREBET (continued)

REFERENCES (continued)

Luchitsky, I.V., ed., 1974, Development of rugged relief of Siberia: Far East: Kamchatka, Kurile, and Komandor Islands: Moscow, Nauka Press, 430 p.

Melekestsev, I.V., Braitseva, O.A., and Ponomareva, V.V., 1987, Dynamics of activity of Gorelyi and Mutnovskii volcanoes and volcanic hazard for adjacent areas (from tephrochronological studies): Vulkanol. Seismol., 1987, no. 3, p. 3-18.

Novograblenov, P.T., 1930, Eruption of Gorely volcano in 1929-30: Zapisky Russ. Geogr. Soc., v. 62, no. 4, p. 459-461.

Smithsonian Institution, Scientific Event Alert Network (SEAN), 1980, 1985, Gorely Khrebet: SEAN Bull., v. 5, no. 7; v. 10, no. 1 (information from Drs. Vakim and Kirsanov, and B.V. Ivanov).

Vlodavetz, V.I., and Piip, B.I., 1959, Catalogue of active volcanoes of the world including solfatara fields, Pt. VIII, Kamchatka and continental areas of Asia: Naples, IAVCEI, 110 p.

Volcanological Society of Japan, 1982, Gorely Khrebet: Bull. Volcanic Eruptions, no. 20, p. 62.

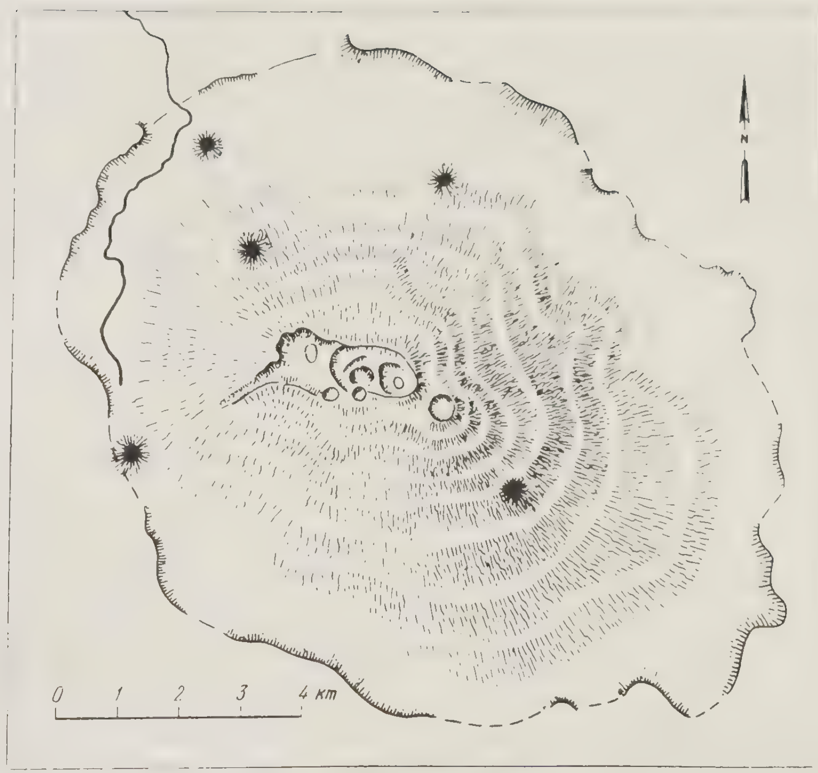

Figure 10.3.1. Sketch of caldera of Gorely Khrebet Volcano, from Vlovadetz and Piip (1959).

Figure 10.3.2. Sketch showing ash thicknesses and locations of sampling sites on flanks of Gorely Khrebet Volcano in September 1980, from Kirsanov and Ozerov (1983). Explanation: 1, caldera rim; 2, summit crater; 3, cinder cones and lava flows; 4, disposition of ash collectors and sites of cinder thickness measurements on flanks and in vicinity of volcano; 5, thickness contours at end of August - beginning of September 1980; fractions: above line, weight of ash in ash collector, below line, approximate duration of ash deposition; I, Mount Vysokaya; II, Mutnovskii station; III, Mutnovskii craters; IV, Mount Dvugorbaya; V, geologic camp Dachnye Istochniki; VI, Mount Skalistaya.

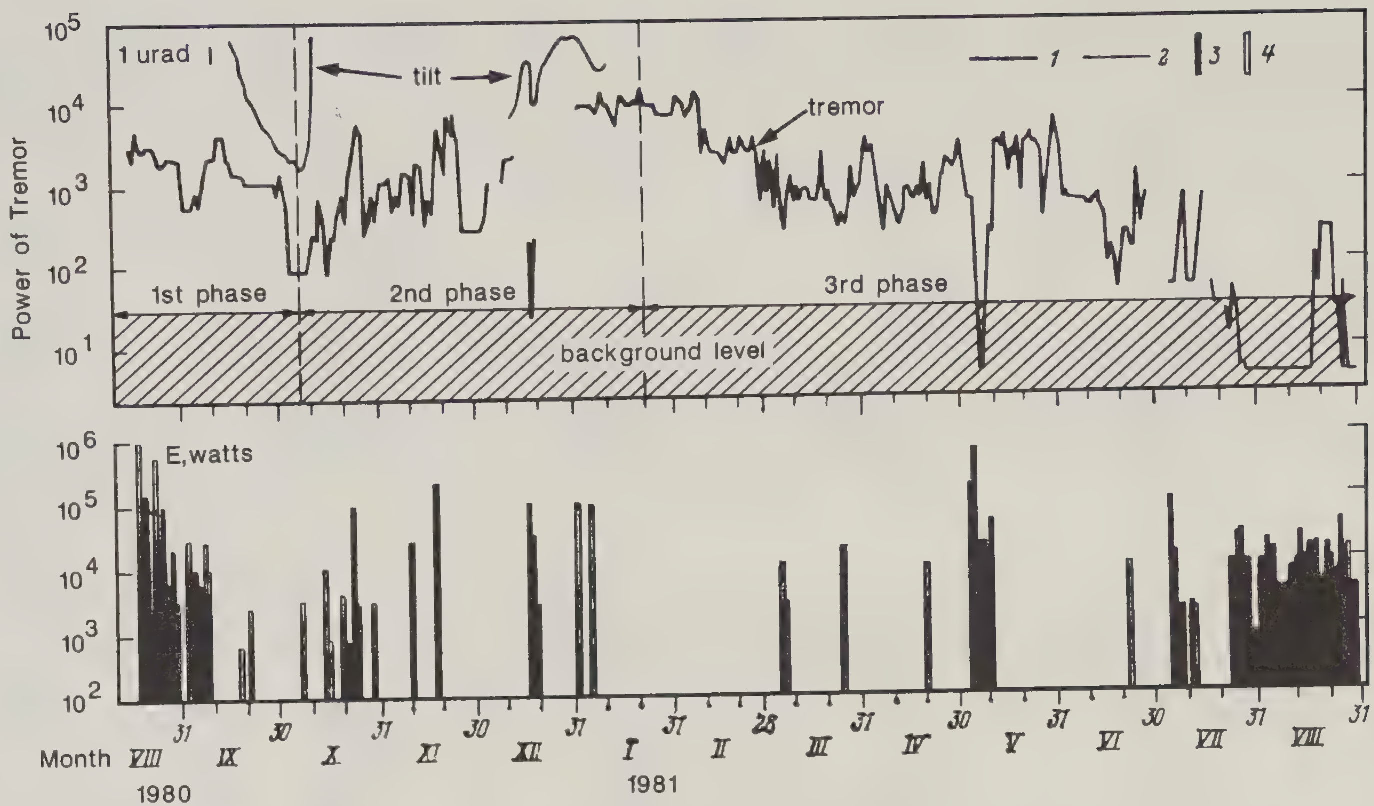

Figure 10.3.3. Graph of variability of daily averages of volcanic tremor power and earth tilt, from Gabrilov and others (1984). Top, (1) power of tremor [units=watts?]; (2) tilting motion, (small vertical bar = 1 microradian); (3) earthquakes and coseismic jumps in tilt; (4) explosion earthquakes. Bottom, daily magnitude of energy release of volcanic earthquakes, in watts.

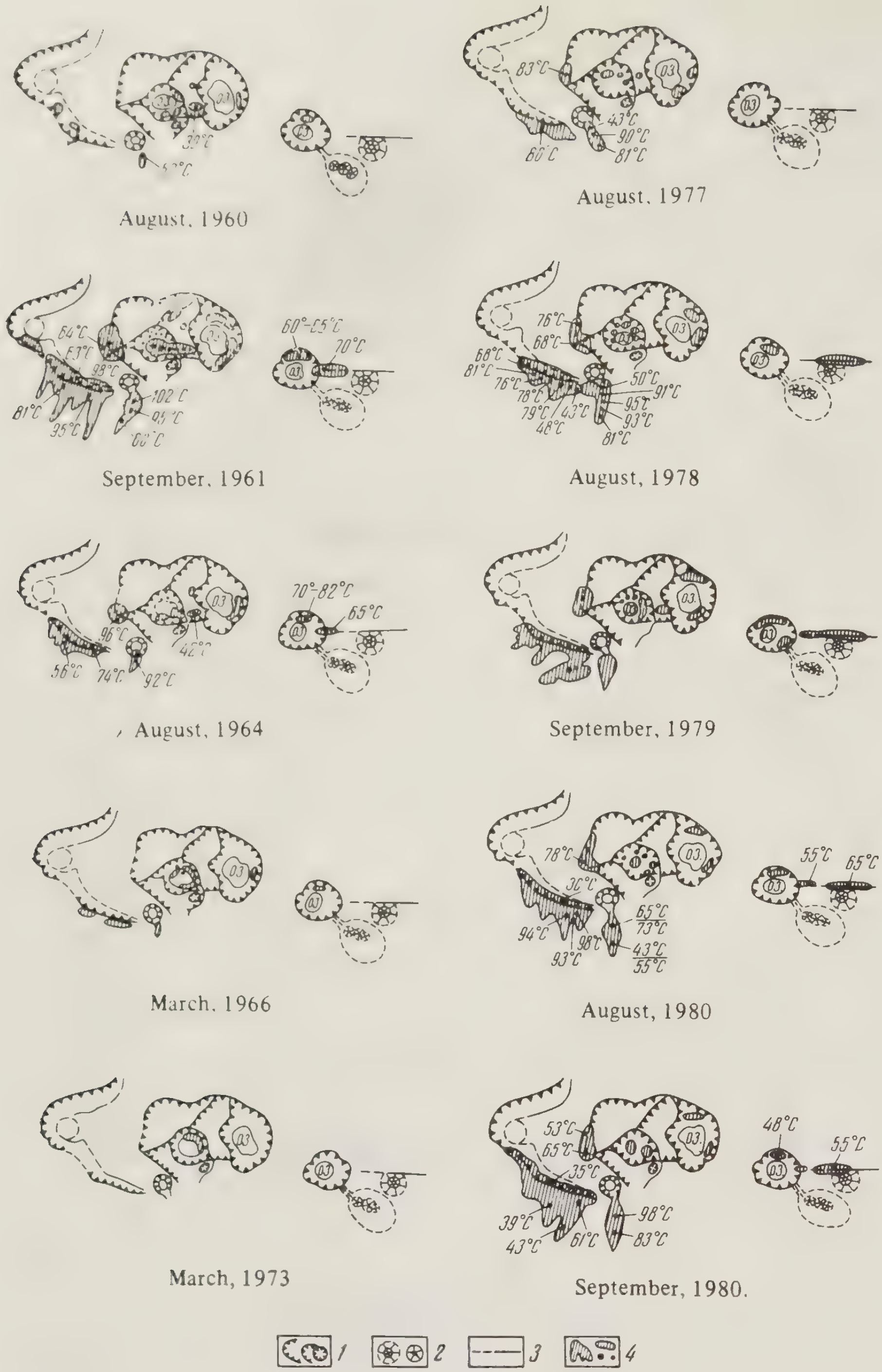

Figure 10.3.4. Changes in fumarole temperatures in summit crater of Gorely Khrebet Volcano during 1960-80, from Kirsanov and Ozerov (1983). Note that scarp at left (west) of each sketch is western rim of summit crater, not caldera. Explanation: 1, volcanic craters; 2, cinder cones; 3, fissures; 4, areas of active fumaroles, with temperatures indicated.

OPALA

CAVW number (active vent)	Latitude Longitude (degrees)	Diameter (km)	Local tectonic setting	Precaldera edifice	SiO_2 content (wt pct)	Age of collapse (yr B.P.)	Date of unrest	Type and duration of unrest ESTU STHF MGTF H Te	Eruption type
10-00-08 (Opala)	52.43N 157.45E	10 x 12	E-W faults at north end of N-S graben	Shield? LL-strat?	R = 52-66 C = silicic?	22,000	1776	---- ---- ---- - --	ex
							1827	---- ---- ---? - --	none
							1854	---- ---- ---? - --	none
							1894	---- ---- ---? - --	none

TECTONIC SETTING

Opala Caldera (figs. 10.4.1, 10.4.2) is situated in the northwest corner of the southern Kamchatka graben-syncline, where an E-W fault forms the north boundary of that graben. Opala Caldera is also located on the western margin of a strong negative regional gravity anomaly (the Tolmachev anomaly, diameter 20-30 km, possibly a buried caldera).

GEOLOGIC HISTORY

At least 90 km^3 of pumice (Erlich, 1986) was erupted about 22,000 yr B.P. (Krayevaya, 1967), forming the Opala Caldera. The postcaldera Opala stratovolcano lies on the north side of the caldera and shows a gradual evolution from basaltic to andesitic and dacitic magma (Erlich, 1986). Several postcaldera rhyolite domes lie on the east rim of the caldera. Explosions formed a 1.3 km x 2 km crater in the southeast part of the caldera about 1490 ± 90 yr B.P. (Melekestsev and others, 1967; Sheimovich and Patoka, 1979).

HISTORICAL ACTIVITY

The only known eruption in historical time (1776) was observed from Ust' Bolsheretsk, located on the western shore of Kamchatka about 100 km from Opala. Strong solfataric activity was noted in 1827, 1854, and 1894 (Vlodavetz and Piip, 1959).

REFERENCES

Erlich, E., 1986, Geology of the calderas of Kamchatka and Kurile Islands with comparison to calderas of Japan and the Aleutians, Alaska: U.S. Geol. Surv. Open-File Rep. 86-291, 300 p.

OPALA (continued)

REFERENCES (continued)

Erlich, E.N., Melekestsev, I.V., Tarakanovsky, A.S., and Zubin, M.I., 1972, Quaternary calderas of Kamchatka: Bull. Volcanol., v. 36, p. 222-237.

Kozhemyaka, N.N., 1979, Quaternary pumice, tuff-ignimbrite fields, and center of eruptions in Southern Kamchatka: Bull. Vulkanol. Stantsii (Kamchatka), no. 57, p. 26-38.

Krayevaya, T.S., 1967, New data on the age of young pumice deposits of the Kuril Lake: Probl. Kamchatka Geogr., no. 5, p. 43-56.

Luchitsky, I.V., ed., 1974, Development of rugged relief of Siberia: Far East: Kamchatka, Kurile, and Komandor Islands: Moscow, Nauka Press, 430 p.

Melekestsev, I.V., Braitseva, O.A., and Ponomareva, V.V., 1967, Dynamics of activity of Garelyi and Mutnovskii volcanoes and volcanic hazard for adjacent areas (from tephrochronological studies): Vulkanol. Seismol., 1987, no. 3, p. 3-18.

Popruzhenko, S.V., 1983, Genesis of the Opala Volcano Caldera: Vulkanol. Seismol., 1983, no. 6, p. 111-113.

Sheimovich, V.S., and Patoka, M.G., 1979, Opala Volcano and other Holocene centers of acid explosive eruptions in Southern Kamchatka: Vulkanol. Seismol., 1979, no. 5, p. 92-95.

Vlodavetz, V.I., and Piip, B.I., 1959, Catalogue of active volcanoes of the world including solfatara fields, Pt. VIII, Kamchatka and continental areas of Asia: Naples, IAVCEI, 110 p.

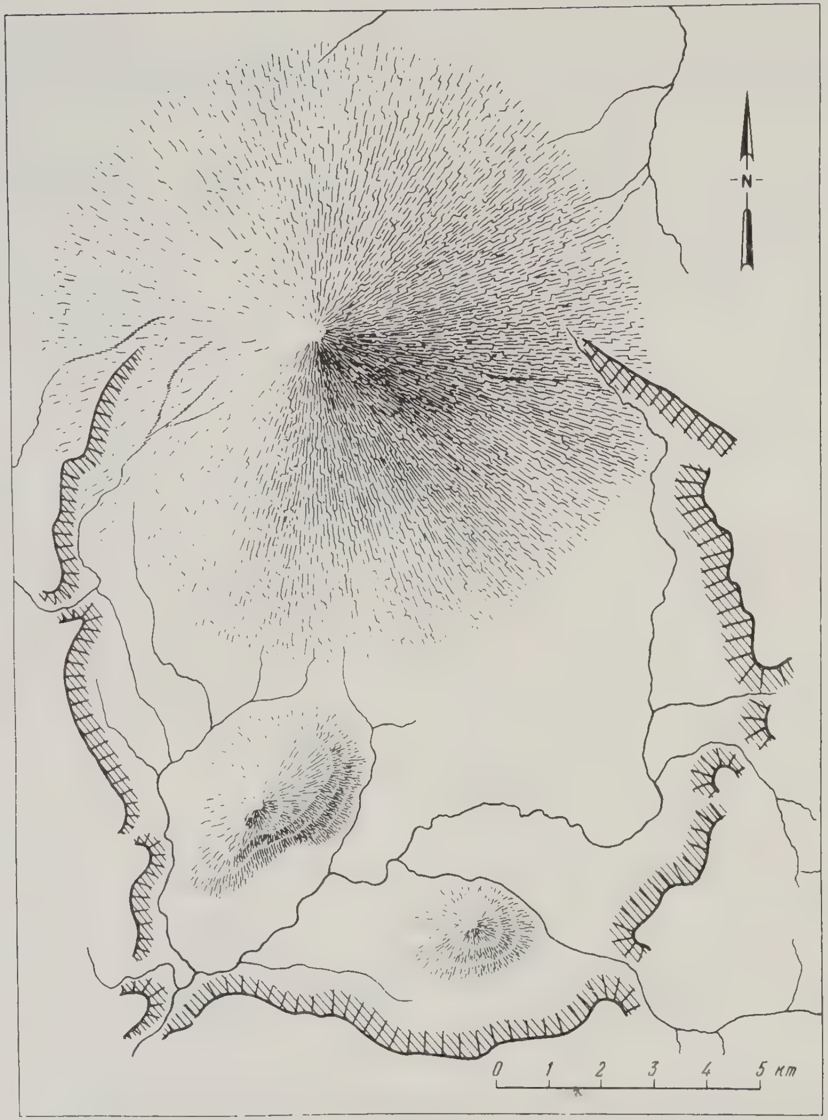

Figure 10.4.1. Sketch of caldera and cone of Opala Volcano, from Vlovadetz and Piip (1959).

I

II

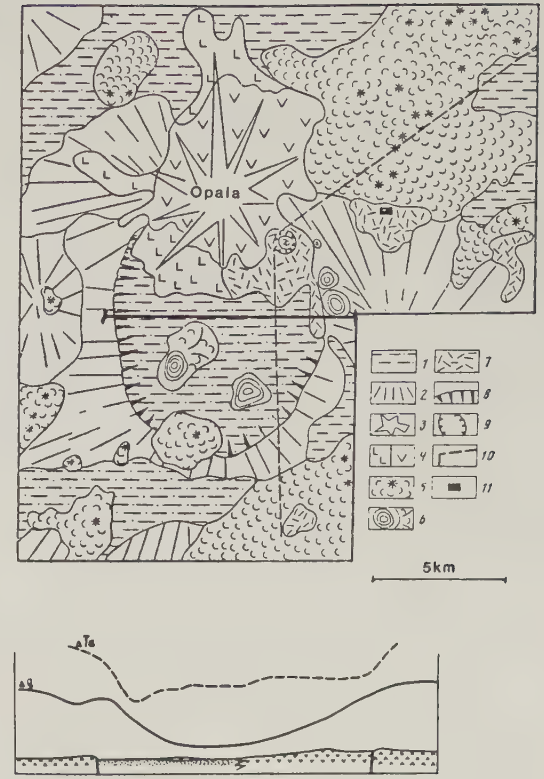

Figure 10.4.2. Geologic structure of Opala Caldera region, after Sheimovich and Patoka (1979). Explanation: I. 1, Quaternary fluvioglacial deposits; 2, lower-middle Pleistocene volcanics: basalts, andesites; 3, Holocene Opala Volcano; 4, andesite-dacite lavas of Opala Volcano; 5, Holocene basalts and scoria cones associated with areal volcanism; 6, Holocene andesitic and rhyolitic extrusive domes and associated lava flows; 7, directed blast deposits and rhyolite pyroclastic flows associated with Barany Amphitheatre crater; 8, scarps of caldera; 9, scarps of Barany Amphitheatre crater; 10, approximate boundaries of sector of spreading of pyroclastic formations of Barany Amphitheatre crater; 11, buried charcoal locality. II. Aeromagnetic (dashed) and Bouguer gravity (solid) profiles across Opala Caldera added from Erlich and others (1972).

PART 3: HISTORICAL UNREST AT LARGE QUATERNARY CALDERAS (continued)
See inside back cover for explanation and abbreviations

ZHUPANOVSKY (Z) COMPLEX

Including KARYMSKY (K), POLOVINKA (P), AKADEMII NAUK (AN), ODNOBOKY (O), STENA-SOBOLINY (SS), and MALY SEMIACHIK (MS) Calderas

CAVW number (active vent)	Latitude Longitude (degrees)	Diameter (km)	Local tectonic setting	Precaldera edifice	SiO_2 content (wt pct)	Age of collapse (yr B.P.)	Date of unrest	Type and duration of unrest ESTU STHF MGTF H Te	Eruption type
10-00-13	54.07N	Z = 40	Zone of	Shield?	K: R= a-d	8,400-	1771 (K)	---- ---- ---- - --	ex
(Karymsky)	159.60E		E-W right-		C= d	7,400	1804 (MS)	---- x--- ---- - --	Ex
	(K)	K = 5	lateral			(K)	1830 (K)	---- ---- ---- - --	ex
			strike-				1851-52(MS)	---- ---- ---- - --	ex
		P = 15	slip		P: C= a-d	mid-	1852 (K)	---- ---- ---- - --	ex
10-00-14			faulting;			Pleistocene	1854(K,MS?)	---- ---- ---- - --	ex
(Maly	54.12N	O = 4x5	compr			(P)	1908 (K)	---- ---- ---- - --	ex,LF
Semiachik)	159.88E						1911-12(K)	---- ---- ---- - --	ex
	(MS)	AN = 3x5			AN: C=	8,100	1915 (K)	---- ---- ---- - --	ex
					silicic	(AN)	1921 (K)	---- ---- ---- - --	ex
		SS = 15x21					1923 (K)	---- ---- ---- - --	ex
					MS: R= mafic	10,000-	1925 (K)	---- ---- ---- - --	ex
		MS = 6x7			C= 61-64	12,000	1929 (K)	---- ---- ---- - --	ex
						(MS)	1932-35(K)	---- ---- ---- - --	ex,lf
							1938 (K)	---- ---- ---- - --	pex
					SS: C= a-d	mid-	1940 (K)	---- ---- ---- - QU	ex
						Pleistocene	1943-47(K)	---- ---- ---- - --	ex,lf
						(SS)	1945-46(MS)	---- ---- ---- - QU	ex
							1952 (K)	---- ---- ---- - QU	ex
							1952 (MS)	---- ---- ---- - QU	ex
							1955-57(K)	?--- ---- ---- - --	ex
							1960-67(K)	E--- ---- ---- - QU	Ex,ex,lf
							1970-82(K)	YY-Y YY-- ---x E --	Ex,ex,lf,dm
							1985 (K)	---- ---- ---- - --	lf

TECTONIC SETTING

The Zhupanovsky complex lies in the eastern Kamchatka graben-syncline, in an area where that graben is crossed by a 6-8 km wide zone of E-W strike-slip faults. Earthquakes deeper than 50 km occur along these E-W faults. Parts of the Zhupanovsky complex that lie north of these faults are offset about 5 km to the east (Erlich, 1986).

ZHUPANOVSKY COMPLEX (continued)

GEOLOGIC HISTORY

A complex of several calderas lies within the large Zhupanovsky volcano-tectonic depression (figs. 10.5.1-10.5.3); terminology of calderas varies among authors. We use that of Masurenkov (1980) and Erlich (1986), who recognize the Polovinka Caldera (with Odnoboky and Akademii Nauk Calderas nested inside) and the Stena-Soboliny Caldera (with Maly Semiachik Volcano inside). The Stena-Soboliny and Polovinka Calderas may have formed about the same time--middle Pleistocene--after eruptions that together produced 280 km^3 of pyroclastic deposits. A "stable" block between the Polovinka and Stena-Soboliny Calderas contains the relatively small Karymsky and Dvor Calderas. Karymsky and Akademii Nauk are perhaps closely related, because they are separated by only 2 km and because most of the seismicity preceding eruptions in the Karymsky Caldera has been located beneath the Akademii Nauk Caldera. Karymsky Volcano is a young stratovolcano in the center of the Karymsky Caldera.

Precaldera eruptions of Maly Semiachik were of basalt and andesite; the caldera-forming eruption consisted of 6 km^3 of high-silica andesite and dacite. Recent eruptions have been of andesite and basalt. Hawaiian-like rift zones occur on the flanks of the Maly Semiachik volcanic edifice.

Major E-W strike-slip faults pass between the Polovinka and Stena-Soboliny Calderas, and much historical seismicity has occurred along these faults; other northeast- and northwest-trending faults are associated with right-lateral movement along the E-W faults.

HISTORICAL ACTIVITY

Karymsky Volcano:

Ivanov (1970) recognized two principal groups of historical eruptions of Karymsky Volcano: explosive and mixed effusive-explosive. Eruptive periods or "cycles" typically last several days to five years and are separated by reposes of 1-6 years. Most eruptions are explosive, but in 1908, 3×10^8 m^3 of dacitic lava was erupted onto the east slope of Karymsky. Magma of the 1962-65 eruption was also dacitic, with 61-63 percent SiO_2 (fig. 10.5.4) (Ivanov, 1970), and lava was again extruded in 1970 (6×10^6 m^3), 1979-82 (>5×10^6 m^3), and 1985 (small volume, as seen from U.S. Space Shuttle)(Ivanov and others, 1982; Smithsonian Institution, 1985). The total volume of tephra in 1962-65 was 0.21 km^3, and the total volume of lava for the same period was 0.06 km^3; half of the total volume was erupted in 1963 (Ivanov, 1970).

Eruptions of Karymsky are typically preceded by felt earthquakes (figs. 10.5.5-10.5.9). The November 1952 eruption followed and may have been triggered by a $\underline{M} = 8.25$ earthquake that occurred on 4 November 1952, 100-150 km from Karymsky. The April 1960 eruption followed and may have been triggered indirectly by a $\underline{M} = 8.2$ earthquake that occurred on 4 May 1959, 20 km from Karymsky.

"Not one quake was recorded from the region of Karymsky" before an eruption at 1900 hr on 10 May 1970; the first earthquake was recorded on 12 May at 0012 hr. Earthquakes increased sharply between 1200 hr on 12 May and 0400 hr on 13 May: "all quakes were

ZHUPANOVSKY COMPLEX (continued)

HISTORICAL ACTIVITY (continued)

accompanied by powerful explosions.... From 1600 hr to 0400 hr the earthquakes were so frequent that they appeared as spasmodic tremor" (Dubik and others, 1972). Frequent earthquakes occurred during July-August 1970, before dome growth in September 1970.

Earthquakes in the period 1970-73 and especially 1975, precursory to and accompanying eruptions at Karymsky Volcano, were concentrated beneath and just south of the Akademii Nauk Caldera (Firstov and others, 1977, 1978). In April and May 1975, seismicity increased 8-18 hr before eruptions and then decreased almost as sharply 2-6 hr before eruptions (fig. 10.5.9). No seismic precursor was detected before the 1976 eruption.

The area within 4 km of the summit of Karymsky Volcano subsided during 1972-81 relative to the stable block between the Karymsky and Akademii Nauk Calderas (Magus'kin and others, 1982). At a distance of 1.5 km from the crater, subsidence amounted to 3-4 cm; it was probably related to effusive activity. The volume of subsidence in a 9-year period ending in 1981 was 0.038 km^3, or 3 times the volume of lava discharged during the same period. General subsidence is interrupted occasionally by shallow-seated uplift before explosions at the volcano (figs. 10.5.11-10.5.12). Horizontal displacements of up to 5-10 cm have been noted along NW-SE faults after earthquake swarms (figs. 10.5.10, 10.5.13, 10.5.14).

A water-tube tiltmeter located 1.5 km from the crater of Karymsky Volcano was operated from 8 July to 12 September 1976, a period during which effusive activity changed to explosive activity and then back to effusive activity. Radially outward tilting began abruptly on 3 August, several days after an increase in explosion earthquakes (fig. 10.5.15). During 3-11 August, 82 arcseconds (about 410 microradians) of tilt was recorded, and an equal relaxation of that tilt occurred in the week after 11 August. During the period of inflation, explosions were frequent; then, after a series of "volcano-tectonic earthquakes," activity reverted to effusion and subsidence began (Zharinov and Firstov, 1985).

An increase in radon in thermal spring activity was noted 6-7 months before the May 1970 eruption and again before growth of the dome in September 1970 (fig. 10.5.16). The general pattern is an increase in radon 1-2 days before an increase in volcanic activity (Chirkov, 1975; Firstov and Chirkov, 1978).

Maly Semiachik Volcano:

An eruption of Maly Semiachik (fig. 10.5.17) in 1804 was the strongest historical eruption of that volcano and was accompanied by collapse of the summit (Erlich, 1986). Maly Semiachik was active again in 1851-52 and perhaps also in 1854. Additional eruptions occurred from autumn 1945 to spring 1946 and in early December 1952 (Vlodavetz and Piip, 1959). The 1952 eruption might have been a delayed response to the same $\underline{M}$=8.25 earthquake (4 November 1952) that triggered the November eruption of nearby Karymsky (see above). Local earthquakes and early melting of snow on the southern part of Maly Semiachik have preceded one or more historical eruptions (Vlodavetz and Piip, 1959).

ZHUPANOVSKY COMPLEX (continued)

REFERENCES

Braitseva, D.A., Egorova, I.A., and Sulerzhitsky, L.D., 1979, Tephrochronological study of Karymsky Volcano: Vulkanol. Seismol., 1979, no. 1, p. 48-58.

Chirkov, A.M., 1975, Radon as a possible criterion for predicting eruptions as observed at Karymsky Volcano: Bull. Volcanol., v. 39, p. 126-131.

Dubik, Yu. M., Ogorodov, N.V., Abdurakhmanor, A.I., Khrenov, A.P., Tokarev, P.I., Firstov, P.P., Shirokov, V.A., and Lemzikov, V.K., 1972, The beginning of the new eruptive cycle of activity of Karymsky Volcano in May 1970: Bull. Vulkanol. Stantsii (Kamchatka), no. 48, p. 3-20.

Erlich, E., 1986, Geology of the calderas of Kamchatka and Kurile Islands with comparison to calderas of Japan and the Aleutians, Alaska: U.S. Geol. Surv. Open-File Rep. 86-291, 300 p.

Erlich, E.N., and Gorshkov, G.S., eds., 1979, Quaternary volcanism and tectonics in Kamchatka: Bull. Volcanol., v. 42, nos. 1-4 (spec. iss.), 298 p.

Farberov, A.I., Storcheus, A.V., and Pribylov, E.S., 1984, Low-intensity seismic activity of Karymskii Volcano in August, 1978: English transl., Volcanol. Seismol., v. 5, p. 323-334.

Firstov, P.P. and Chirkov, A.M., 1978, Radon in spontaneous gas of thermal spring of Karymsky Volcano (1966-1975): Bull. Vulkanol. Stantsii (Kamchatka), no. 54, p. 35-40.

Firstov, P.P., Lemzikov, V.K., and Feofilaktov, V.D., 1978, The seismic regime of Karymsky Volcano in 1975 and several questions on the forecasting of the time of thermal eruptions: Bull. Vulkanol. Stantsii (Kamchatka), no. 54, p. 27-34.

Firstov, P.P., Lemzikov, V.K., and Rulenko, O.P., 1977, The seismic regime of Karymsky Volcano, 1970-73, in Avdeiko, G.P., ed., Volcanism and geodynamics: Acad. Sci. USSR Far Eastern Sci. Center, Inst. Volcanol., Moscow, Nauka Publ., p. 161-178.

Firstov, P.P., Tokarev, P.I., Gusev, N.A., Rulenko, O.P., and Simbirev, I.B., 1978, Dynamics of eruption and seismic regime of Karymsky Volcano in 1976: Bull. Vulkanol. Stantsii (Kamchatka), no. 55, p. 27-34.

Gorelchik, V.I., 1964, Seismological study of activity of the Karymsky volcano: Bull. Vulkanol. Stantsii (Kamchatka), no. 36, p. 3-17.

Gushchenko, I.I., 1979, Eruptions of volcanoes of the world, a catalog: Acad. Sci. USSR Far Eastern Sci. Center, Moscow, Nauka Publ., 474 p.

Ivanov, B.V., 1970, The eruption of Karymsky Volcano in 1962-1965, and the volcanoes of the Karymsky group: Moscow, Nauka Publ., 135 p.

Ivanov, B.V., Andreev, V.N., Bogoyavlenskaya, G.E., Dubik, Y.M., Kirsanov, I.T., Rulenko, O.P., Firstov, P.P., and Chirkov, A.M., 1982, The activity of volcanoes of Kamchatka and Kurile Islands in 1981: Vulkanol. Seismol., 1982, no. 4, p. 103-108.

Ivanov, B.V., Chirkov, A.M., Ozerov, A.Yu., Khrenov, A.P., Dvigabo, V.N., Razina, A.A., Ovsyannikov, A.A., Gavrilenko, G.M., and Tokarev, P., 1984, Activity of the Kamchatka and Kurile Islands volcanoes in 1983: Vulkanol. Seismol., 1984, no. 6, p. 114-122.

Khrenov, A.P., Dubik, Yu.M., Ivanov, B.V., Ovsyannikova, A.A., Pilipenko, V.P., Taran, Yu.A., Firstov, P.P., and Chirkov, A.M., 1982, Eruptive activity of Karymsky volcano for 10 years (1970-1980): Vulkanol. Seismol., 1982, no. 4, p. 29-48.

Kimura, M., 1978, Significant eruptive activities related to large interplate earthquakes in the northwestern Pacific margin: Jour. Phys. Earth, v. 26 supp., p. S557-S570.

ZHUPANOVSKY COMPLEX (continued)

REFERENCES (continued)

Kirsanov, I.T., Ogorodov, N.V., Fedorov, M.V., and Chirkov, A.M., 1964, The state of Karymsky Volcano during 1960-61, and its eruption products: Bull. Vulkanol. Stantsii (Kamchatka), no. 35, p. 3-9.

Magus'kin, M.A., Enman, V.B., Syelyeznyev, B.V., and Shkryed, V.I., 1982, Particulars on shifts of the earth's surface at Karymsky Volcano, according to geodetic and photogrammetric data during the period 1970-1981: Vulkanol. Seismol., 1982, no. 4, p. 49-64.

Masurenkov, Yu.P., ed., 1980, Volcanic center: structure, dynamics, and products. Karymsky structure: Moscow, Nauka Publ., 299 p.

Polyak, B.G., Seliangin, O.B., and Braitseva, O.A., 1979, Dynamics of Maly Semiachik volcano activity: Dokl. Akad. Nauk USSR, v. 244, no. 1, p. 175-179.

Seliangin, O.B., 1977, The evolution of the caldera complex and the rhythms and direction of the volcanic process in the Karymsky volcano group in Kamchatka, _in_ Avdeiko, G.P., ed., Volcanism and geodynamics, Moscow, Nauka Publ., p. 187-200.

Smithsonian Institution, Scientific Event Alert Network (SEAN), 1985, Karymsky Volcano: SEAN Bull., v. 10, no. 4, p. 4 (information from C.A. Wood).

Steinberg, G.S., 1966, On Maly Semiachik Caldera Volcano: Bull. Vulkanol. Stantsii (Kamchatka), no. 41, p. 29-31.

Tokarev, P.I., Firstov, P.P., and Lemzikov, V.K., 1969, Seismological investigations at Karymsky Volcano in 1966: Bull. Vulkanol. Stantsii (Kamchatka), no. 45, p. 12-21.

Vlodavetz, V.I., and Piip, B.I., 1959, Catalogue of active volcanoes of the world including solfatara fields, Pt. VIII, Kamchatka and continental areas of Asia: Naples, IAVCEI, 110 p.

Volcanological Society of Japan, 1973, 1978, Karymsky: Bull. Volcanic Eruptions, no. 11, p. 31-32; no. 16, p. 45 (information from Yu.M. Dubik).

Zharinov, I.A., and Firstov, P.P, 1985, Activity, seismic regime, and tilt of the earth's surface at Karymski Volcano during the summer of 1976: Vulkanol. Seismol., 1985, no. 2, p. 93-95.

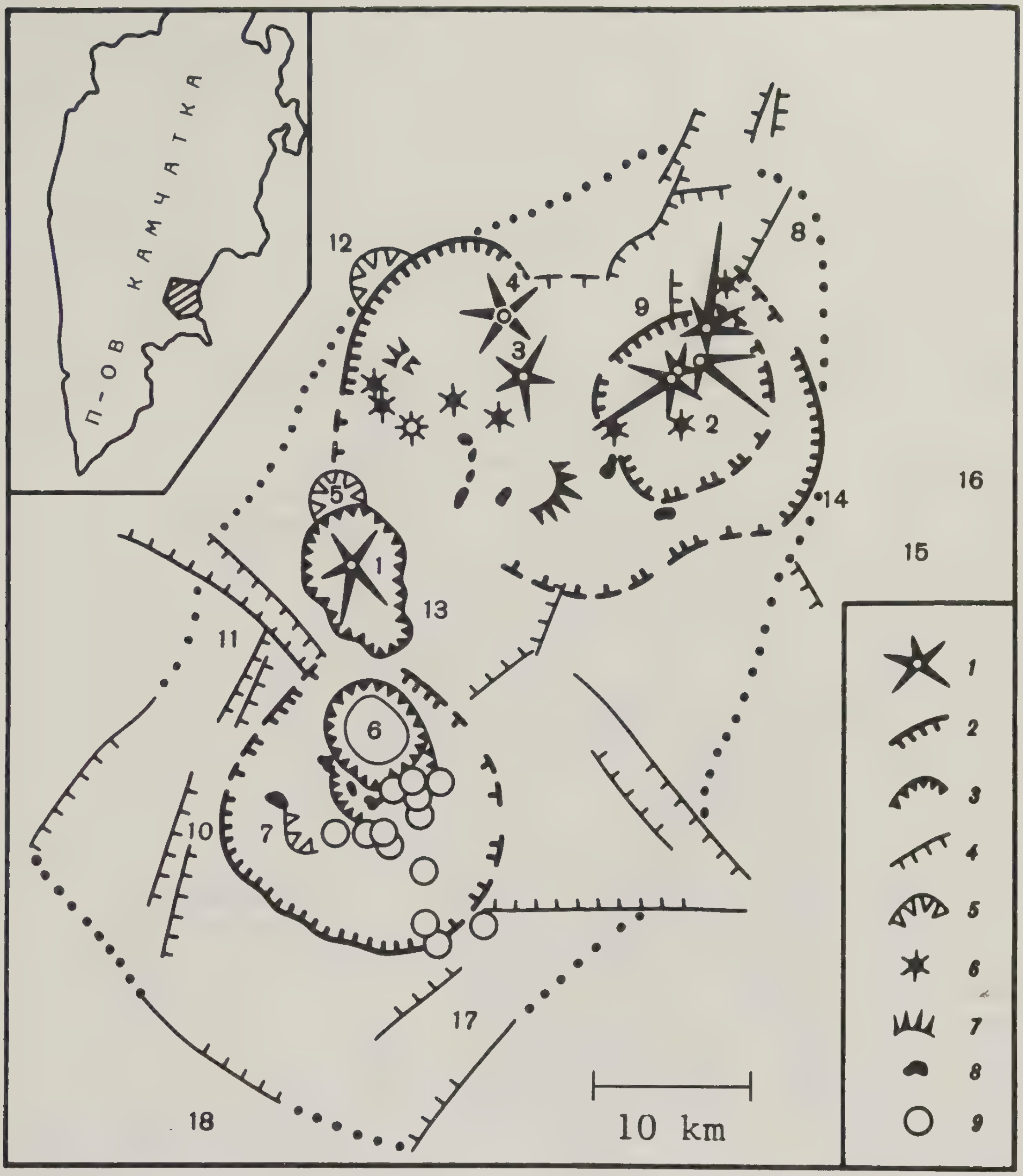

Figure 10.5.1. Volcanoes of the Karymsky complex, from Firstov and others (1978). Key to inset legend, with numbered symbols: 1, modern volcanoes; 2, caldera escarpments; 3, position of the ring fractures of ancient and young caldera groups; 4, fractures expressed in topography of displaced blocks; 5, explosion craters; 6, cinder cones and lava domes; 7, maar; 8, extrusions; 9, epicenters of volcano-tectonic earthquakes in 1975 with focal depths of 0-10 km. Key to numbers on map proper: 1, Karymsky Volcano; 2, Maly Semiachik Volcano; 3, Sukhoy; 4, Stupenchaty Bastion; 5, Dvor Caldera; 6, Akademii Nauk and Odnoboky Calderas; 7, Beliankina; 8, Drevny Karymsky; 9, Semiachik Caldera; 10, Krainy; 11, Razlaty; 12, Soboliny Caldera; 13, Berezovy; 14, Stena Caldera (Stena-Soboliny Caldera in figure 10.5.2 is a large structure encompassing both); 15, Pribezhny Iuzhy; 16, Pribezhny Severny; 17, Ditmara; 18, Zhupanovsky volcano-tectonic depression. Dotted line indicates approximate location of outer caldera rim.

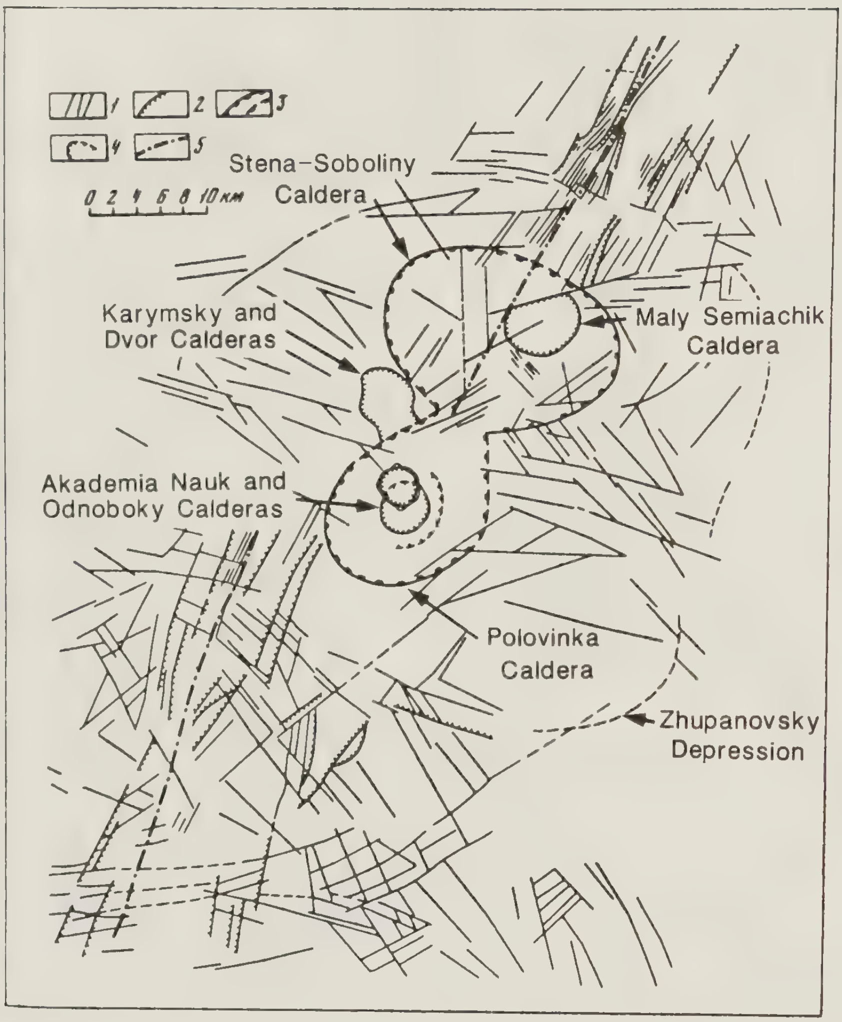

Figure 10.5.2. Structural map of Zhupanovsky volcano-tectonic depression, from Masurenkov (1980). 1, fracture without apparent displacement; 2, fracture with surface displacement; 3, mid-Pleistocene caldera fracture; 4, upper Pleistocene-Holocene caldera fracture; 5, rift axis.

Figure 10.5.3. Karymsky and neighboring calderas, from Vlodavetz and Piip (1959). Explanation: 1, crater of extinct Dvor Volcano; 2, Karymsky Volcano and its caldera; 3, Karymsky Lake and Akademii Nauk Caldera; dots, hot springs.

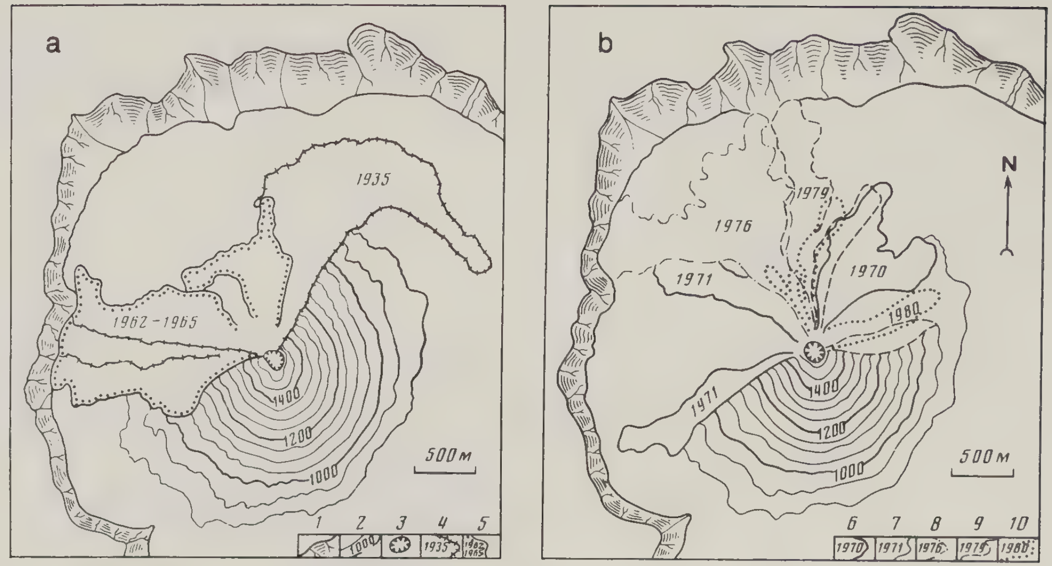

Figure 10.5.4. Lava flows at Karymsky Volcano during 1935-80, from Magus'kin and others (1982). 1, caldera boundary; 2, topographic contours, with elevations in meters; 3, volcanic crater; 4-10, margins of historical lava flows, with dates of extrusion (for example, 4= 1935; 5= 1962-65; and so forth).

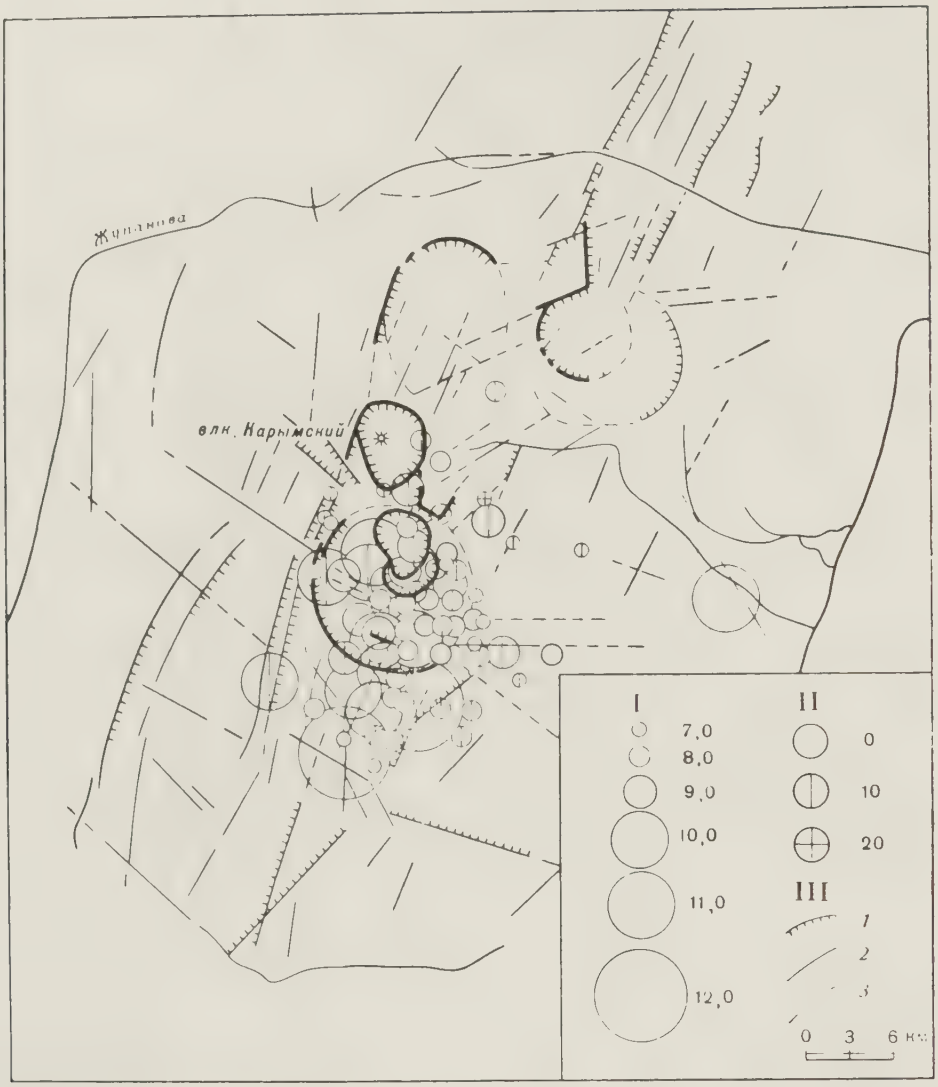

Figure 10.5.5. Epicenters near Karymsky Volcano during 1970-80, from Khrenov and others (1982). Explanation: I, energy class; II, depth (kilometers); III, faults: 1, topographic boundary; 2, minor; 3, buried and conjectured.

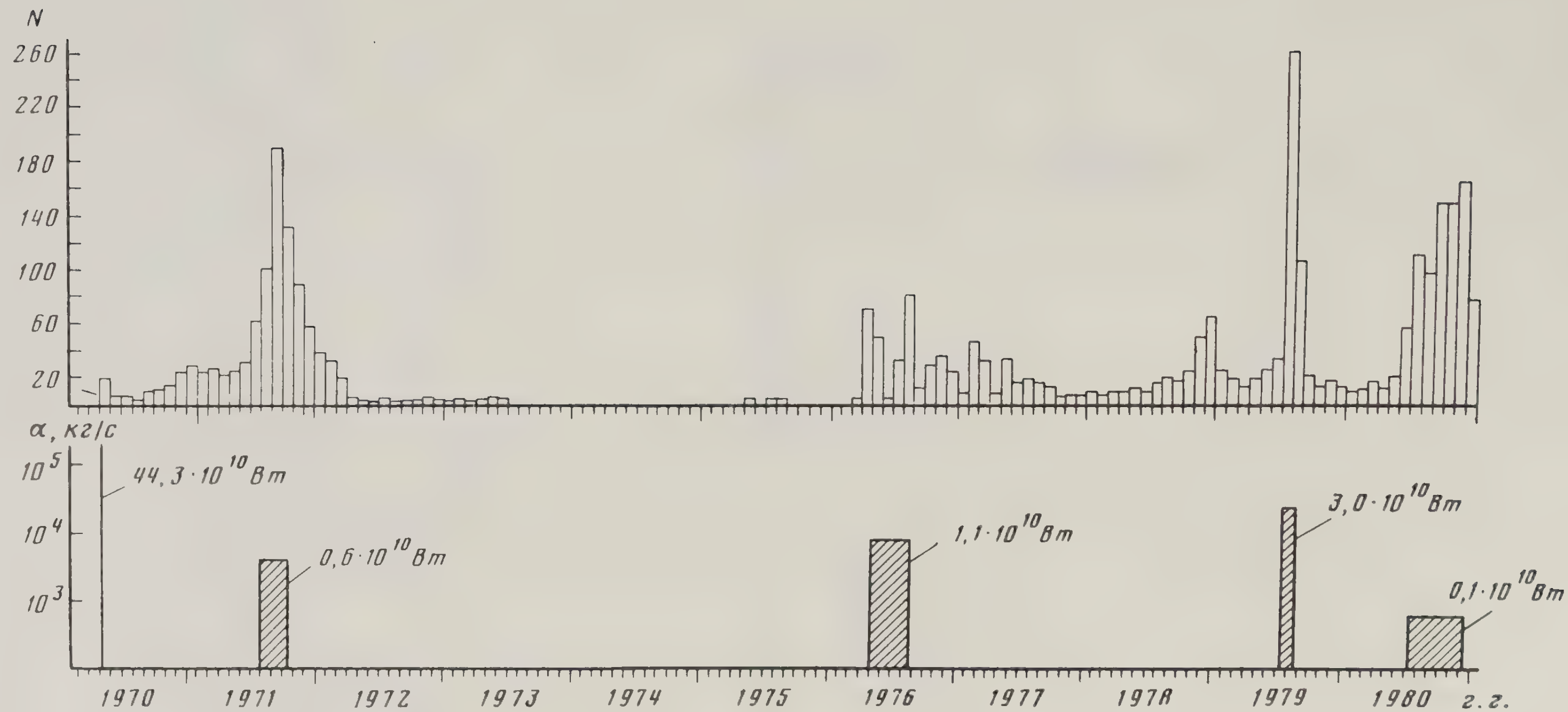

Figure 10.5.6. Monthly number of earthquakes (top) and rate of lava production (bottom) at Karymsky Volcano during 1970-80, from Khrenov and others (1982). Rate of lava production in units of kilograms per second; values beside each period of lava production are total number of kilograms(?).

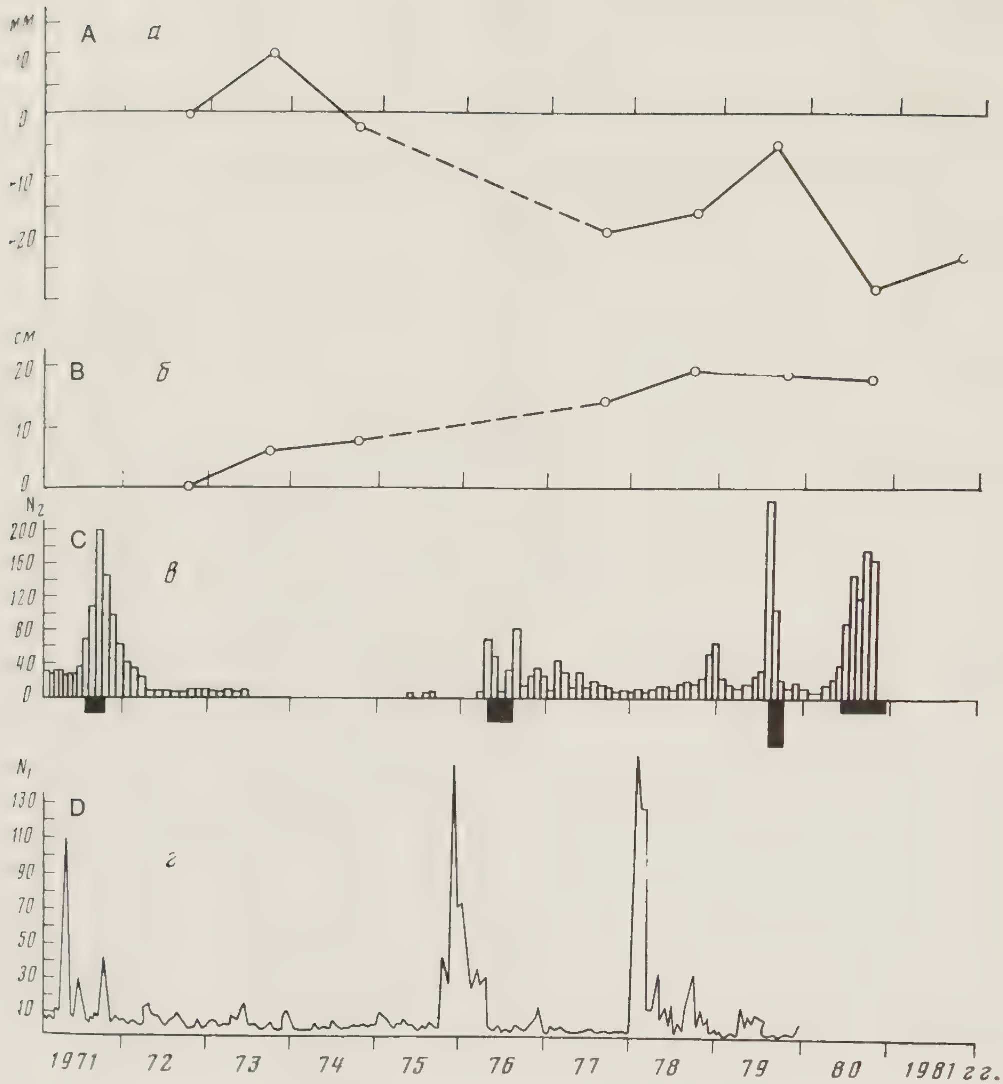

Figure 10.5.7. Activity at Karymsky Volcano from 1971 to 1981, from Magus'kin and others (1982). A, Average vertical displacement of several reference stations 1.5-1.7 km from the crater. B, Average horizontal displacement for whole area. C, Number of explosion earthquakes of energy class 5 or greater in 10-day intervals. D, Number of volcano-tectonic earthquakes of energy class $\underline{K}$ = 5 or greater for 15-day intervals. Black rectangles show times of lava outpouring; their area is proportional to volume extruded.

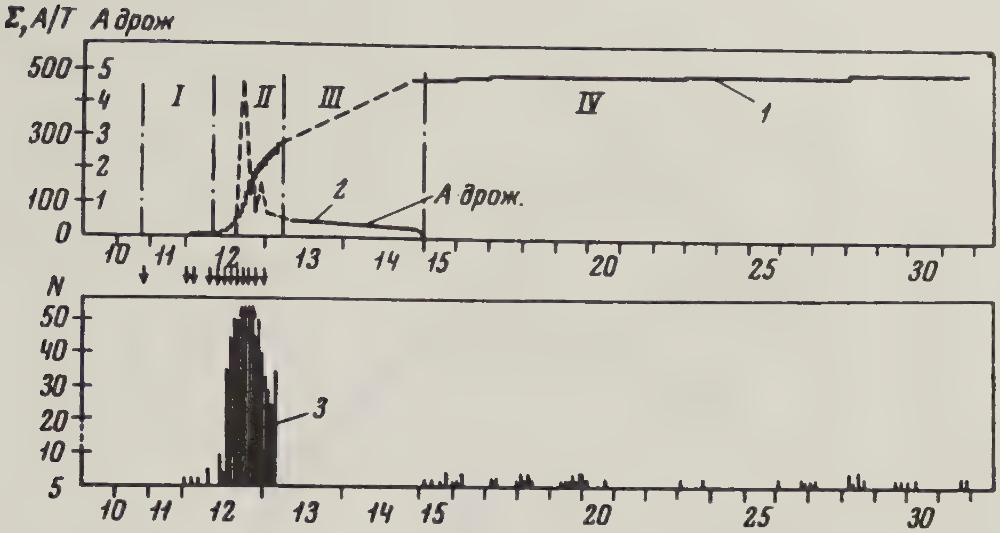

Figure 10.5.8. Seismic activity at Karymsky Volcano during May 1970, from Dubik and others (1972). Top, cumulative sum of A/T (micrometers per second), where A is maximum amplitude of surface wave and T is period: dashed line, spasmodic tremor; solid line, continuous tremor. Bottom, number of earthquakes with maximum amplitude greater than 0.5 micrometers. Arrows indicate explosions.

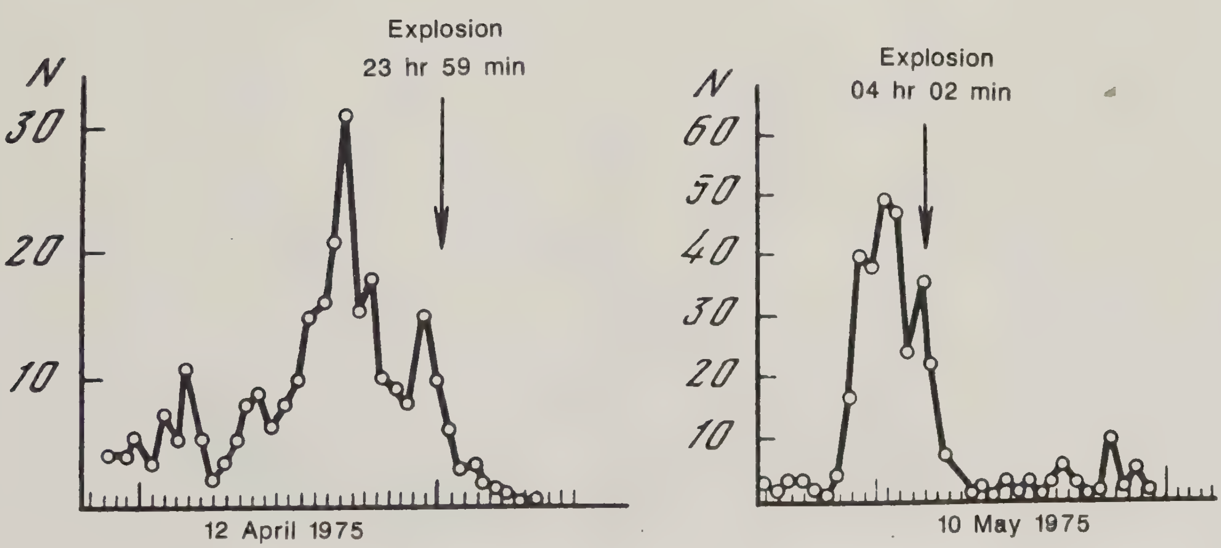

Figure 10.5.9. Hourly earthquake counts before eruptions (arrows) of Karymsky Volcano in April and May 1975, from Firstov and others (1978).

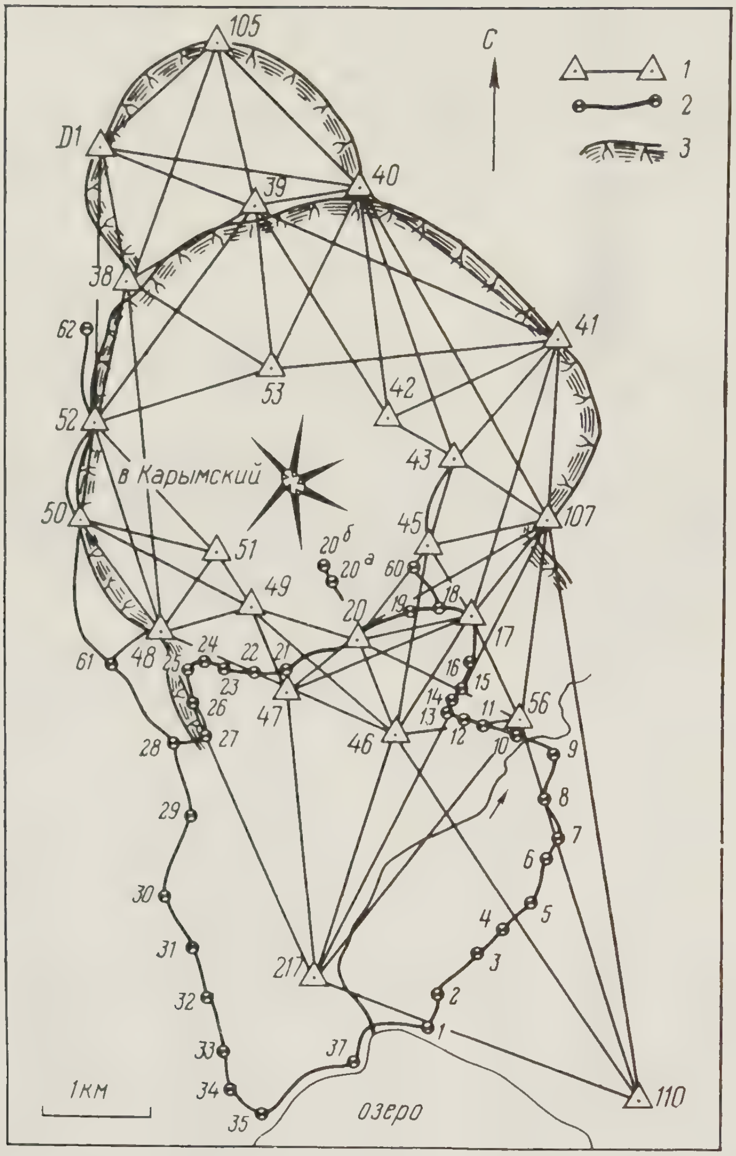

Figure 10.5.10. Geodetic networks at Karymsky Volcano, from Magus'kin and others (1982). 1, horizontal strain network; 2, leveling network; 3, crater rims. Sites 20a and 20b mark approximate location of tilt station (see figure 10.5.15).

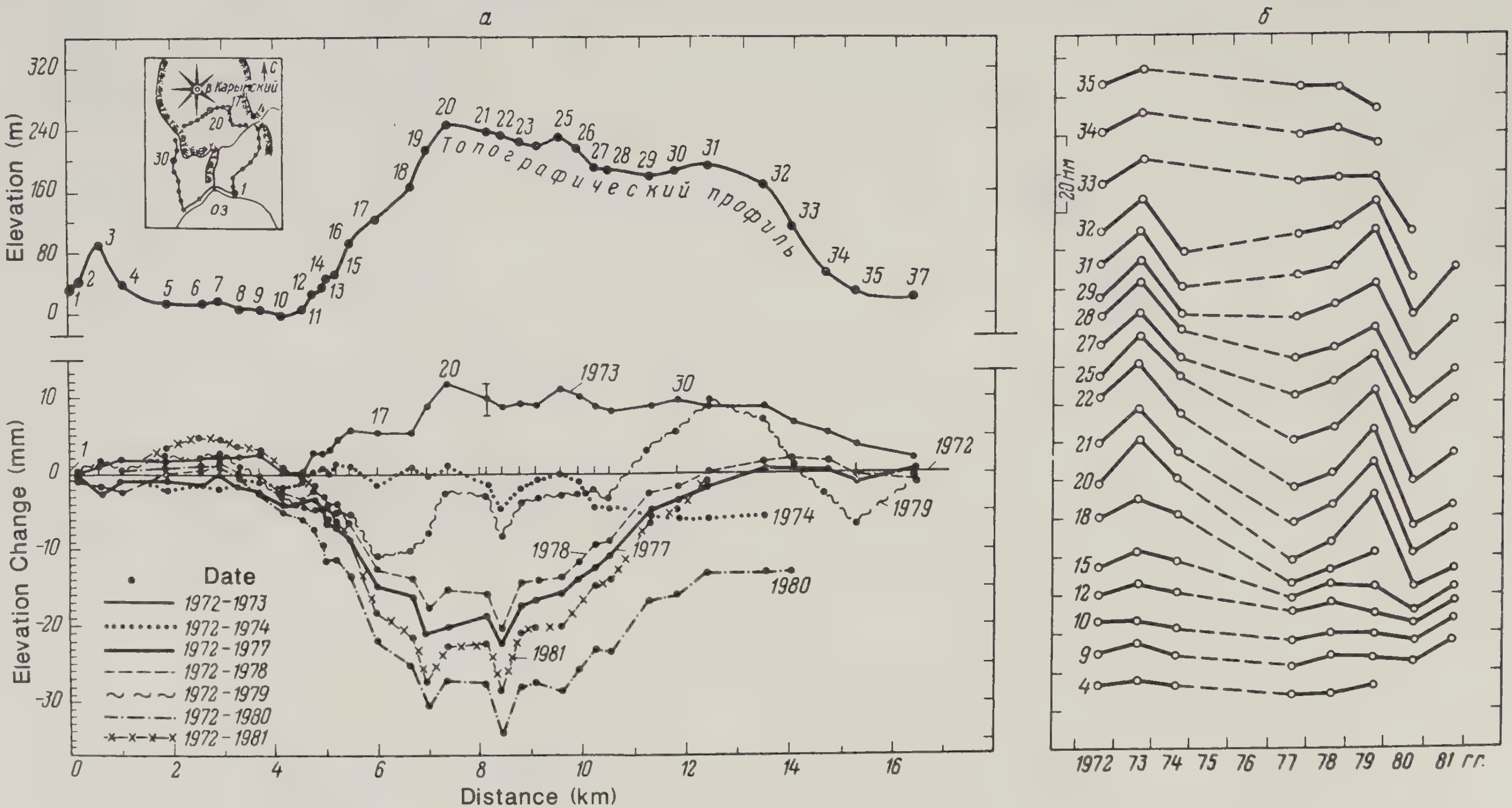

Figure 10.5.11. Elevation changes at Karymsky Volcano from 1972 to 1981, from Magus'kin and others (1982). Left, topographic profile and elevation changes measured along route shown in inset and in figure 10.5.10. Right, movements of numbered bench marks through time.

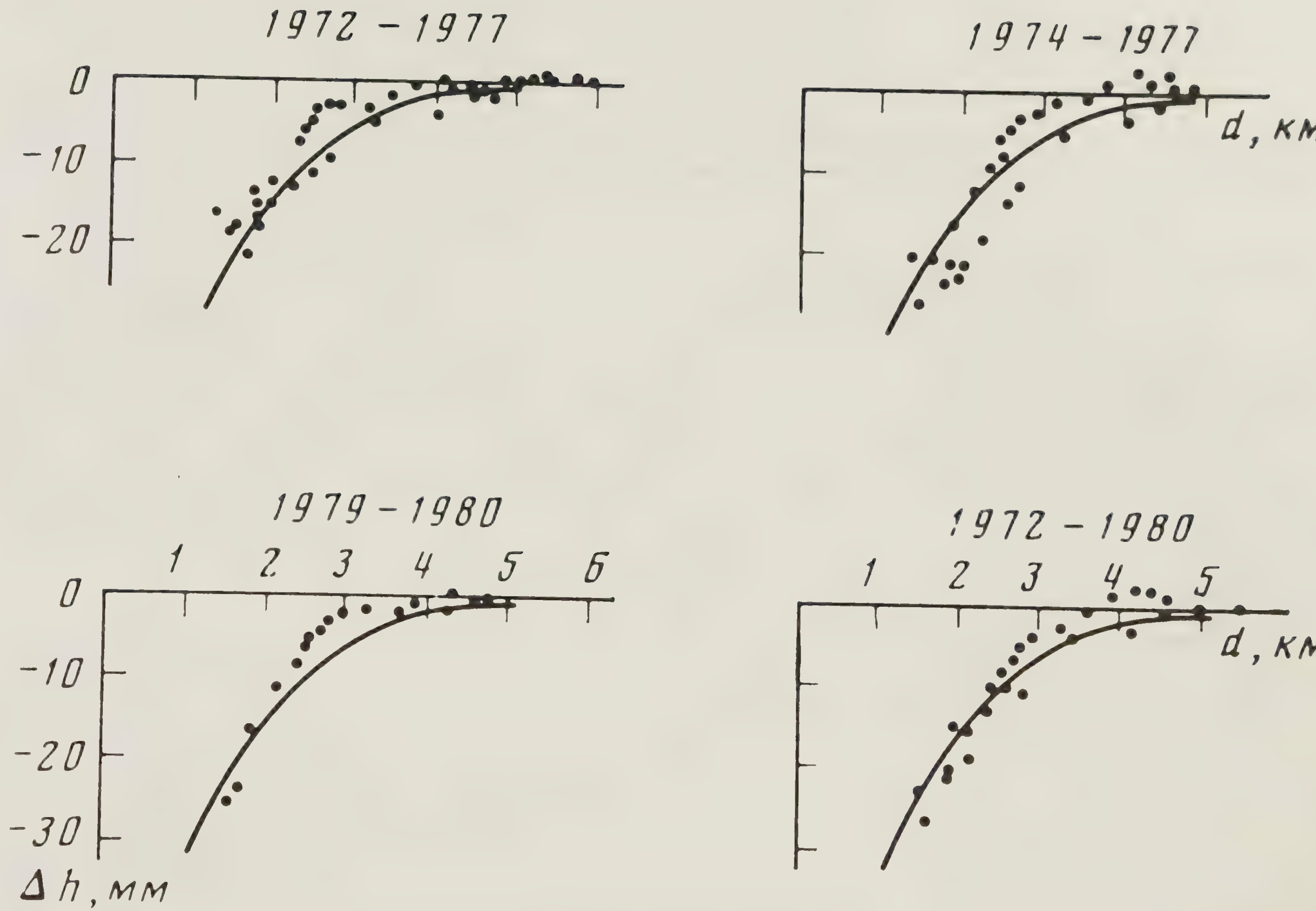

Figure 10.5.12. Subsidence profiles at Karymsky Volcano during indicated intervals, from Magus'kin and others (1982). Plot shows subsidence (ordinate) versus distance from crater of Karymsky Volcano (abscissa). Shape of profiles suggests a shallow source, possibly 1-1.5 km deep.

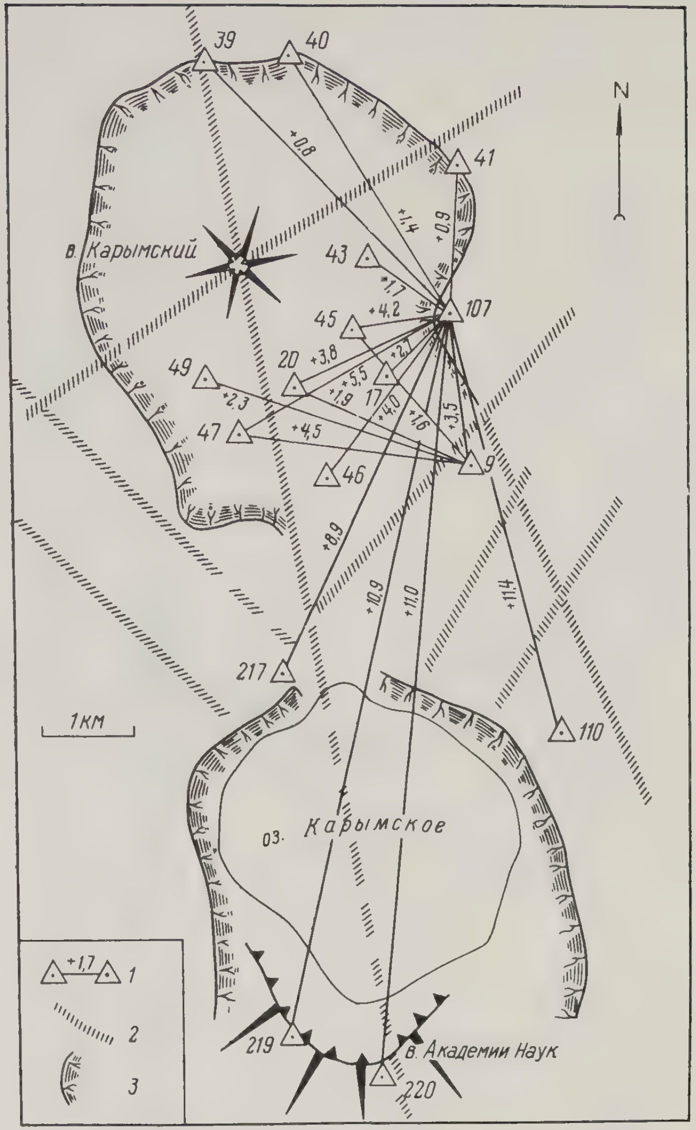

Figure 10.5.13. Horizontal distance changes at Karymsky Volcano from 1974 to 1981, from Magus'kin and others (1982). 1, endpoints of line (triangles), with change in centimeters; 2, faults; 3, crater rim.

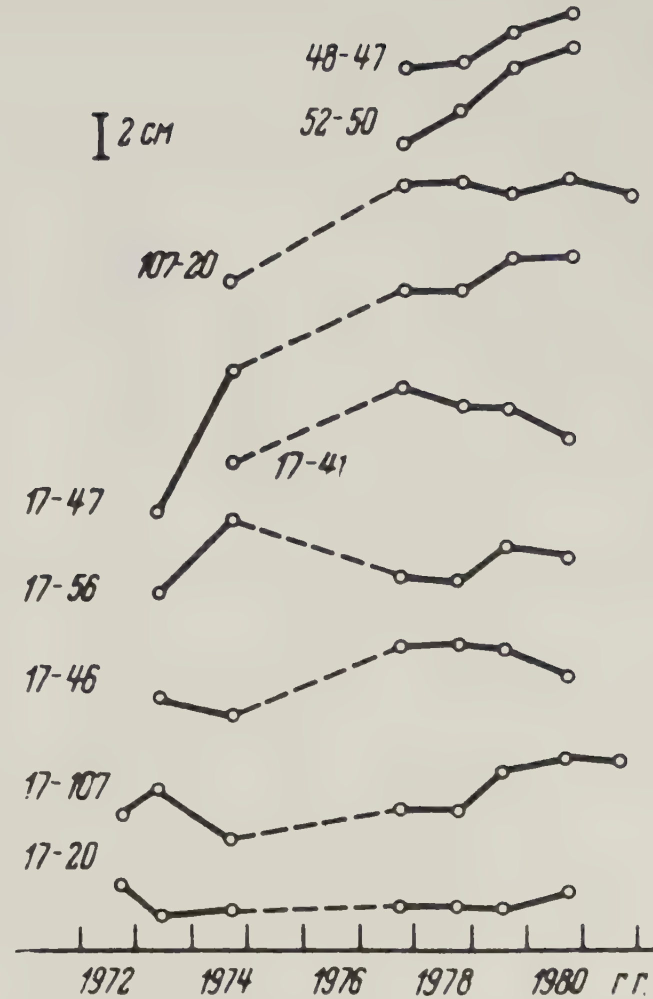

Figure 10.5.14. Horizontal distance changes as a function of time at Karymsky Volcano, from Magus'kin and others (1982). Bench-mark locations (numbers at left) are shown in figure 10.5.10.

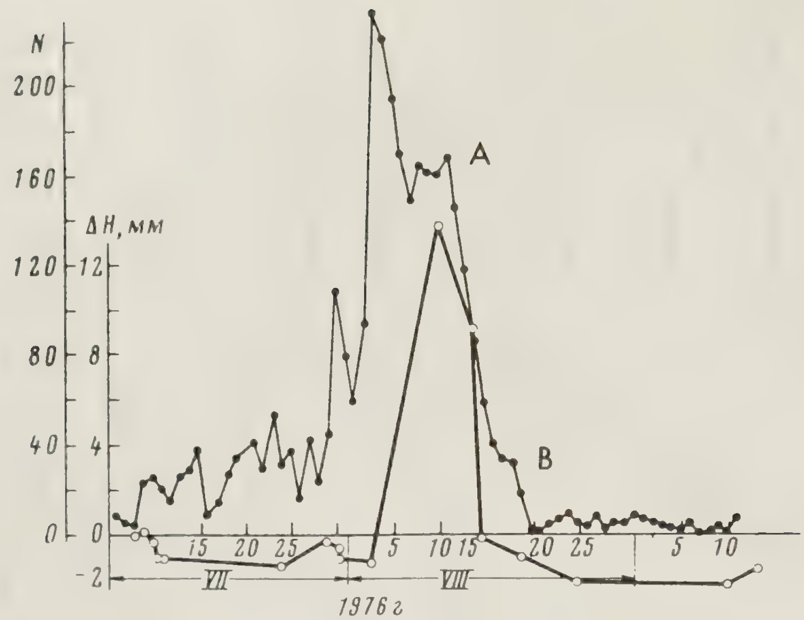

Figure 10.5.15. Activity at Karymsky Volcano during 1976, from Zharinov and Firstov (1985). A, Daily number of volcano-tectonic earthquakes at depths of 0-10 km. B, Level changes along 40-m base of radial tilt line.

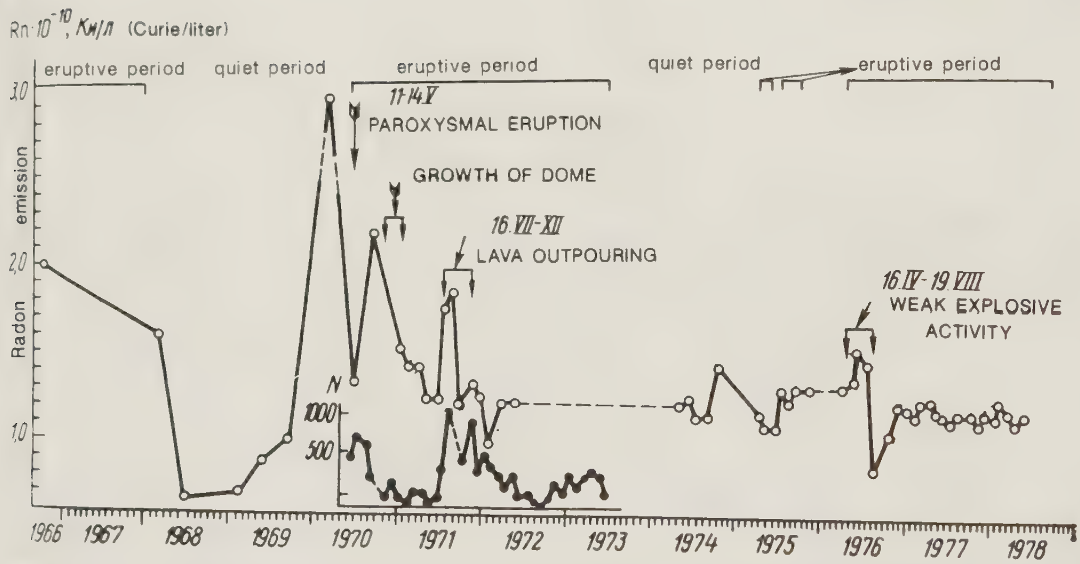

Figure 10.5.16. Radon emission and monthly number of earthquakes (inset, bottom) associated with eruptive at Karymsky Volcano during 1966-78, from Khrenov and others (1982).

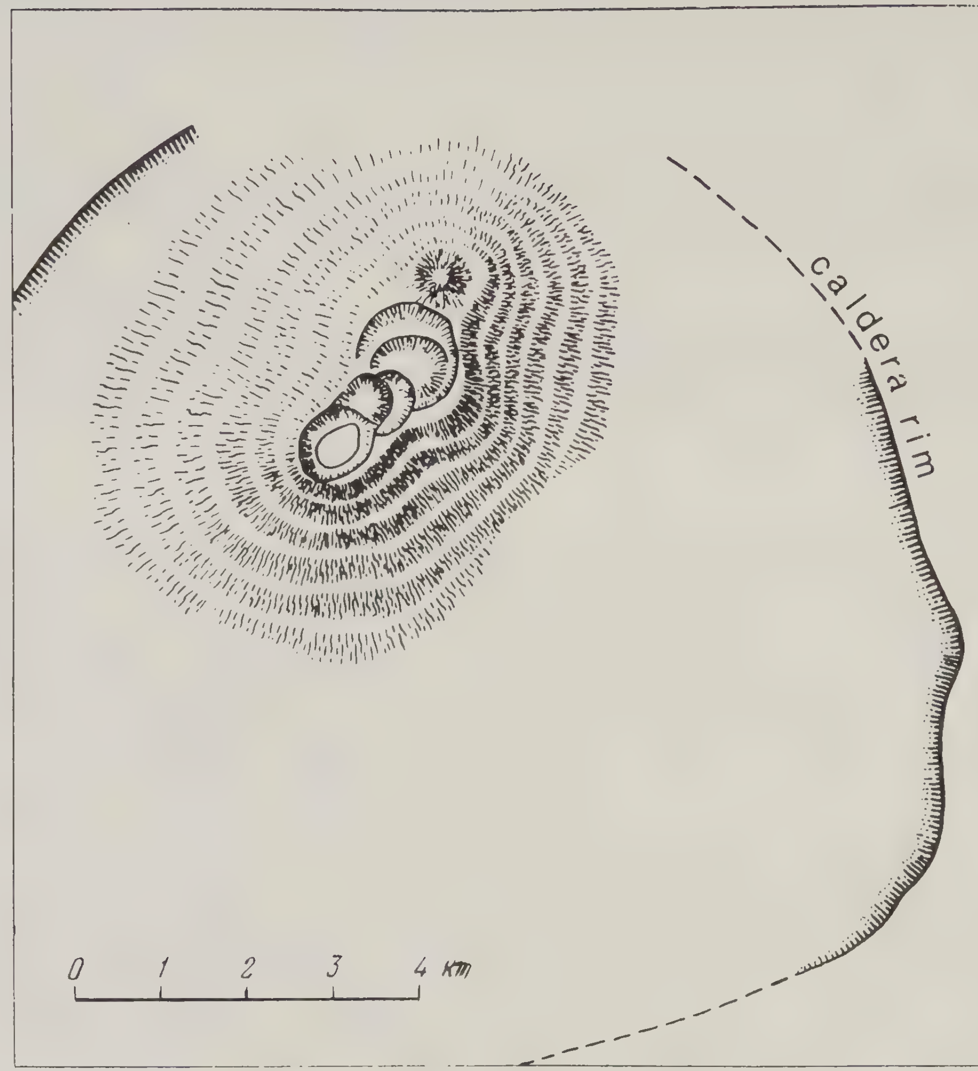

Figure 10.5.17. Sketch of Maly Semiachik Volcano and Caldera, from Vlodavetz and Piip (1959).

PART 3: HISTORICAL UNREST AT LARGE QUATERNARY CALDERAS (continued)
See inside back cover for explanation and abbreviations

UZON-GEYZERNAYA

CAVW number (active vent)	Latitude Longitude (degrees)	Diameter (km)	Local tectonic setting	Precaldera edifice	SiO_2 content (wt pct)	Age of collapse (yr B.P.)	Date of unrest	Type and duration of unrest ESTU STHF MGTF H Te	Eruption type
10-00-161 (Unana)	54.62N 159.70E	7 x 18 (Uzon and Geyzernaya combined)	Intersect. of E-W strike-slip fault zone and NNE-SSW graben	LL-strat? (Uzon)	R = 54-56+, some 65-71	mid-Pleistocene	19th cent.	---- ---- ---x - --	none
10-00-17 (Uzon)	54.53N 160.08E			Silicic edifice (Geyzernaya)	C = 68 (Uzon)		20th cent.	xx-- ---- ---x - --	none

TECTONIC SETTING

Uzon and Geyzernaya Calderas lie in the NNE-SSW-trending eastern Kamchatka graben-syncline, at its intersection with E-W faults (fig. 10.6.1). At least 3 to 5 km of left-lateral offset is apparent along the E-W faults.

GEOLOGIC HISTORY

Silicic volcanism has occurred in the Uzon area since at least the Pliocene; caldera-forming eruptions in the mid- to late Pleistocene produced a sequence of plateau-forming ignimbrites, some densely welded and others unwelded (Belousov and others, 1984; Erlich, 1986) (figs. 10.6.2-10.6.4). The Uzon and Geyzernaya basins are separate calderas, offset by 3-5 km of left-lateral movement along a major E-W fault zone that passes between the two calderas (Belousov and others, 1974; Erlich, 1986). A NNE-SSW-trending graben also passes through the Uzon-Geyzernaya area.

Together, the Uzon and Geyzernaya Calderas contain a major hydrothermal system (fig. 10.6.5). Numerous hot springs are located along northwest-trending fissures within the Uzon Caldera, just north of the main E-W fault. Other thermal features occur within and along the ring fractures of both calderas.

HISTORICAL ACTIVITY

In the middle of the 19th century, fumaroles and mud volcanoes were very active, making loud noises, and vegetation was stunted (Perrey, 1863). Similar conditions existed in 1986, so the condition described by Perrey may have been routine rather than

UZON-GEYZERNAYA (continued)

HISTORICAL ACTIVITY (continued)

anomalous. Seismic recording in this area has revealed a marked series of earthquakes along the E-W trending fault zone at a depth of 100-120 km (Naboko, 1974).

COMMENTS

The Uzon-Geyzernaya region in Kamchatka is similar in features, though not in size, to the Yellowstone region in the United States. Both occur in areas of regional crustal extension, have been sites for multiple caldera collapses, and currently exhibit vigorously active hydrothermal systems.

REFERENCES

Belousov, V.I., Grib, E.N., and Leonov, V.L., 1984, The geological setting of the hydrothermal systems in the Geysers Valley of Uzon Caldera: English translation, Volcanol. Seismol., 1984, v. 5, no. 1, p. 67-81.

Braitseva, O.A., Bogoyavlenskaya, G.E., Erlich, E.N., Pilipenko, G.F., and Karpov, G.A., 1974, Uzon-Semiachik volcanic region, in Volcanoes and hydrothermal areas of Kamchatka: Moscow, Nauka Press, p. 139-191.

Erlich, E., 1986, Geology of the calderas of Kamchatka and Kurile Islands with comparison to calderas of Japan and the Aleutians, Alaska: U.S. Geol. Surv. Open-File Rep. 86-291, 300 p.

Erlich, E.N., and Gorshkov, G.S., eds., 1979, Quaternary volcanism and tectonics in Kamchatka: Bull. Volcanol., v. 42, nos. 1-4 (spec. iss.), 298 p.

Florenskiy, I.V., and Trifonov, V.G., 1985, Recent tectonics and volcanism of the eastern volcanic zone of Kamchatka: Geotectonics, v. 19, no. 4, p. 314-320.

Naboko, S.I., 1954, Geysers of Kamchatka: Akad. Nauk USSR, Trudy Lab. Vulkanol., no. 8, p. 126-209.

----- ed., 1974, Volcanism, hydrothermal processes, and ore formation: Moscow, Nauka Press, 262 p.

Perrey, A., 1863, Documents sur les tremblements de terre et les phénomènes volcaniques dans l'archipel des Kouriles et au Kamtschatka: Lyon, Soc. Imp. Agric. Hist. Nat. Arts, 166 p.

Vlodavetz, V.I., and Piip, B.I., 1959, Catalogue of active volcanoes of the world including solfatara fields, Pt. VIII, Kamchatka and continental areas of Asia: Naples, IAVCEI, 110 p.

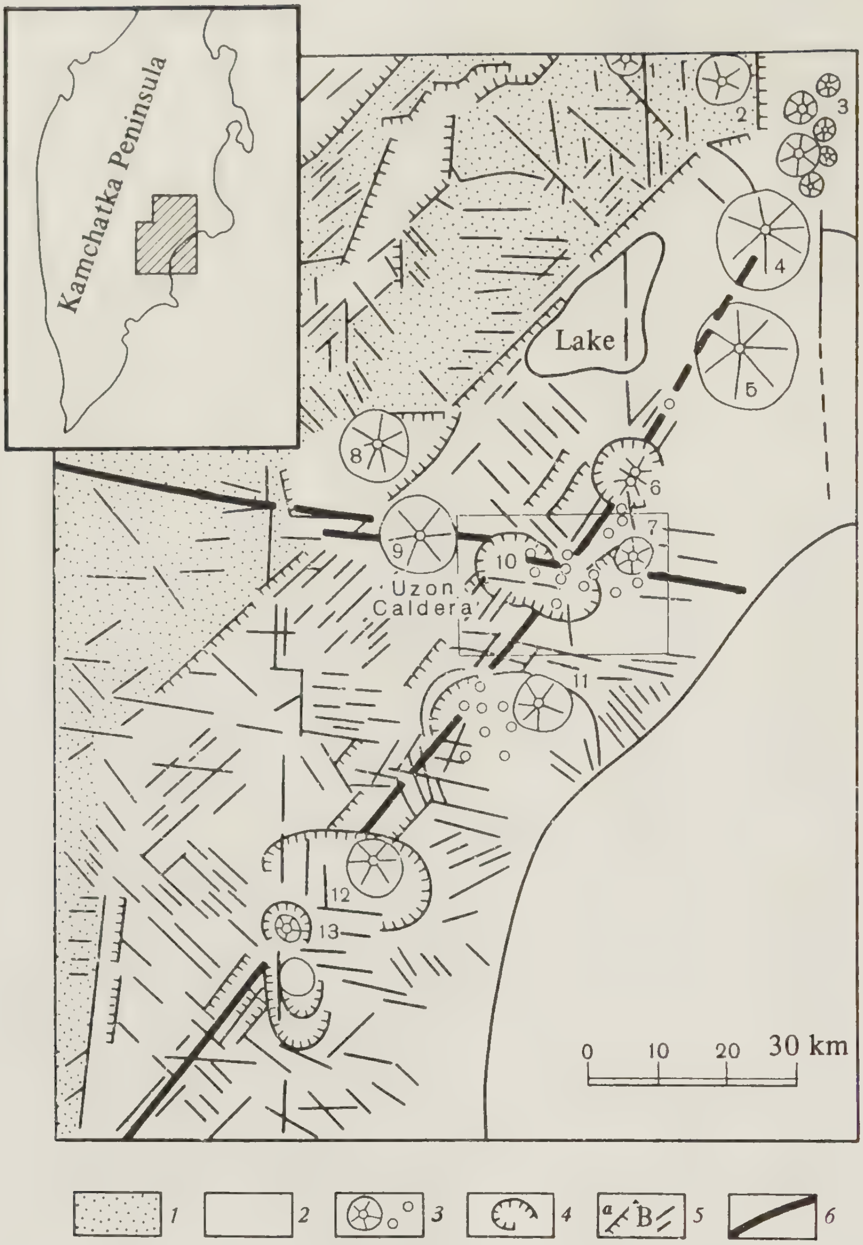

Figure 10.6.1. Structural map of eastern Kamchatka, from Belousov and others (1984). Explanation: 1, horst-anticline of Eastern Range in Kamchatka; 2, graben-syncline of eastern Kamchatka; 3, volcanoes (1, Kizimen; 2, Konradi; 3, Gamchensky ryad; 4, Shmidt's; 5, Kronotsky; 6, Krasheninnikov's; 7, Kikhpinych; 8, Unana; 9, Taunshits; 10, Uzon; 11, Greater Semyachik; 12, Lesser Semyachik; 13, Karymsky); 4, calderas and volcano-tectonic depressions; 5, faults (a, normal faults; b, cracks); 6, axial lines of northeast-trending and sublatitudinal regional fault zones intersecting Uzon-Geysernaya region. Inset, index map of the Kamchatka Peninsula showing the outline of figure 10.6.1.

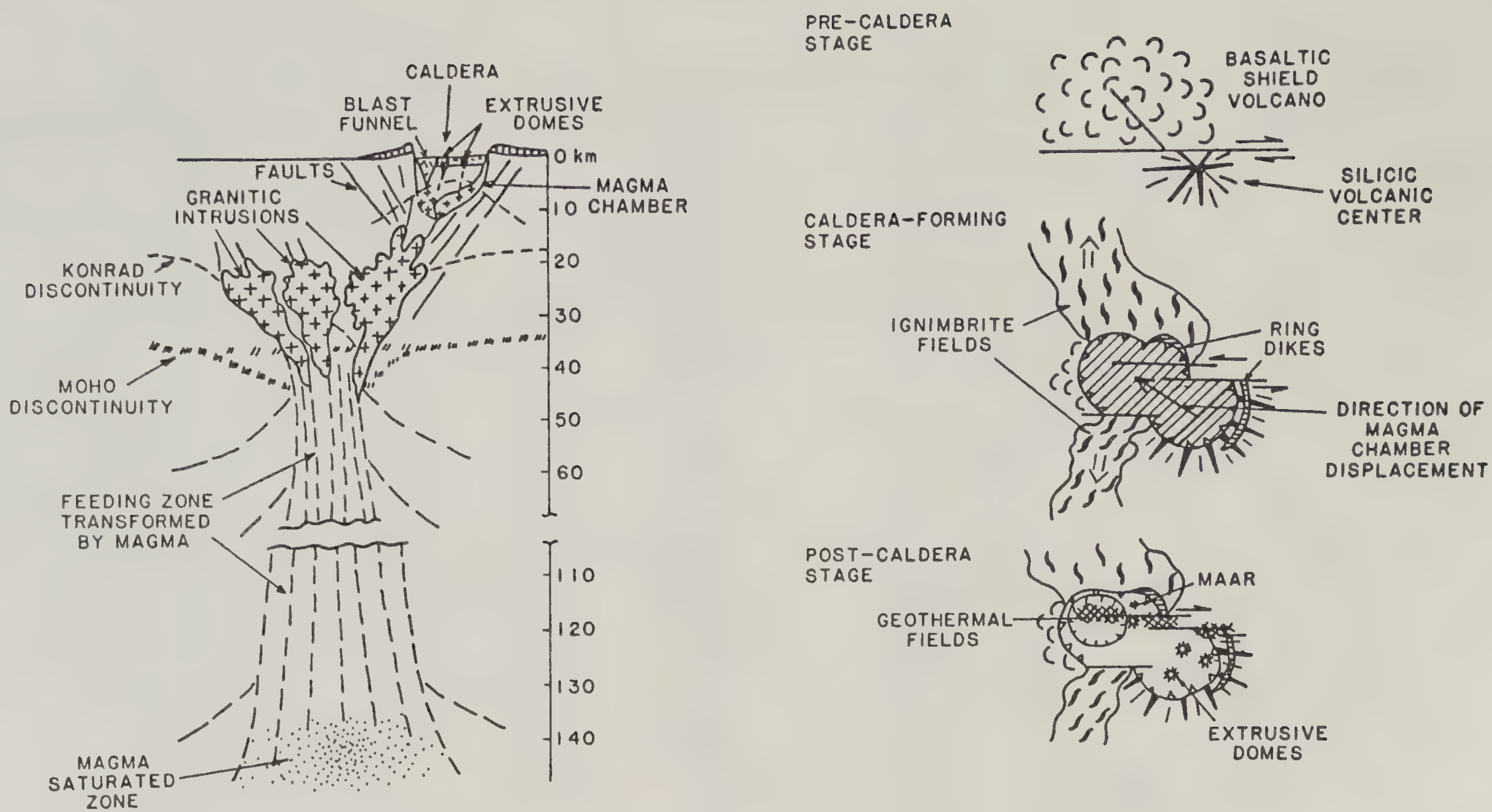

Figure 10.6.2. Model of formation of Uzon-Geyzernaya Caldera, Kamchatka, after Naboko (1974).

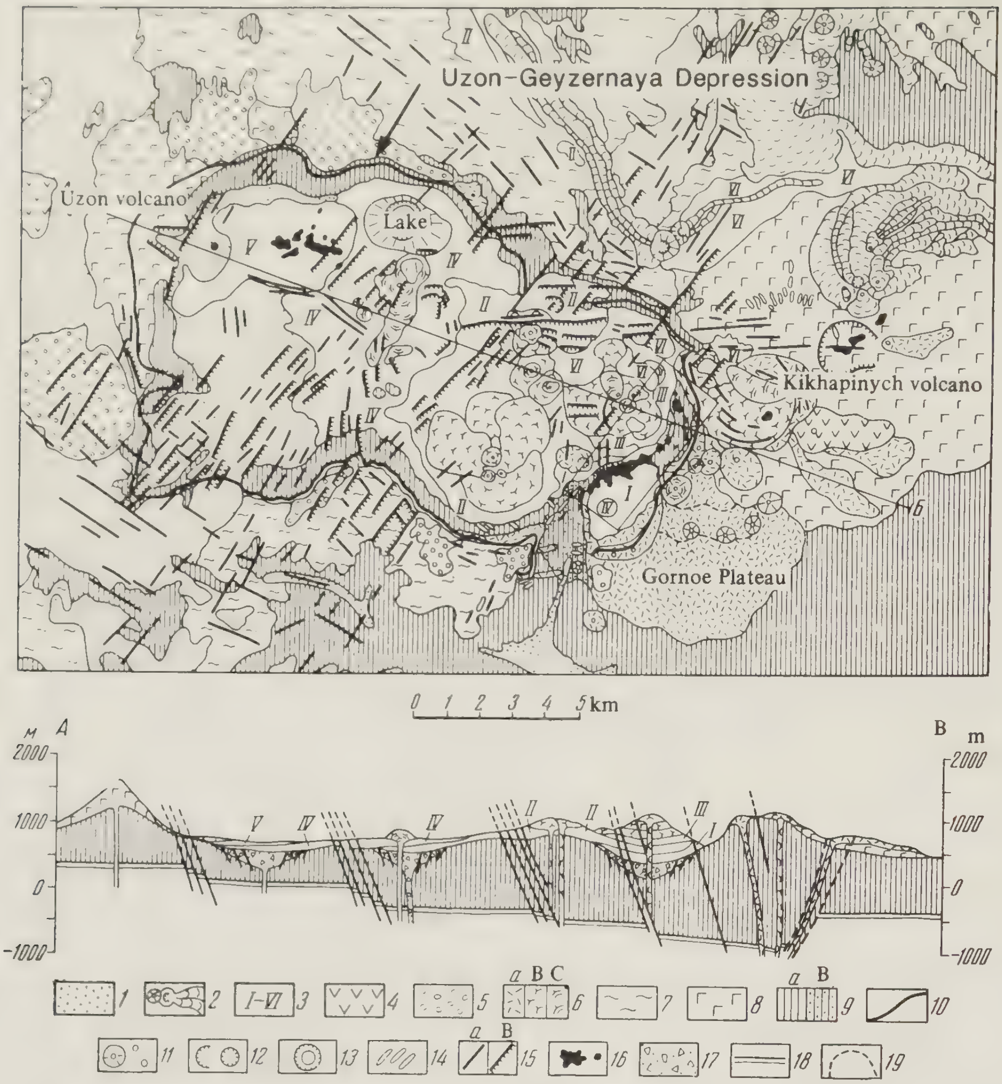

Figure 10.6.3. Schematic geologic map of Uzon-Geysernaya region, from Belousov and others (1984). Explanation: 1, alluvial, glacial, and talus-slope deposits and also cliff debris (Q4); 2, lavas and cinders of basaltic and andesite-basalt composition; 3, lacustrine sediments (members: I, Geyser; II, Pumice; III, Yellow Crags; IV, Second Lake and Southern Basin; V, Third Lake; VI, Colorado); 4, andesitic lavas; 5, explosion pumice of Uzon Caldera; 6, lavas of first (a), second (b), and third (c) cycles of Quaternary acid volcanism; 7, ignimbrite; 8, basaltic lavas; 9, Pliocene - lower Pleistocene deposits (members: a - old Lavas, Cape Tuff, Sand-Lava, Tuff-Ignimbrite, Flood Basalts; b - Estuary); 10, boundaries of erosion scarps bounding Uzon-Geysernaya depression; 11, cinder cones and other volcanic centers; 12, crater funnels; 13, maar; 14, dikes; 15, faults (a, fissures; b, normal faults); 16, areas of thermal anomalies (approximate outlines of 20 °C isotherm at 1-m depth); 17, sediments filling inferred calderas (in section); 18, tentative boundary of Pliocene - lower Pleistocene sediments (in section); 19, boundaries of separate beds and flows within identified members (markers).

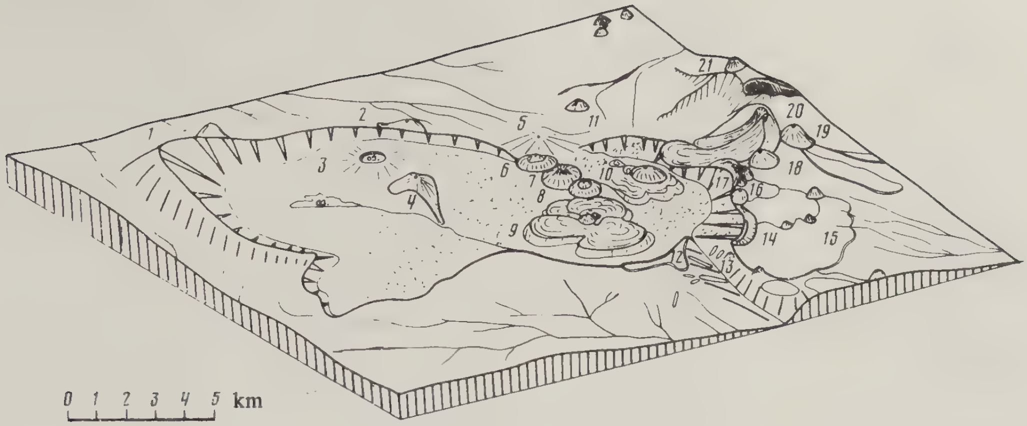

Figure 10.6.4. Block diagram of Uzon-Geysernaya region, from Belousov and others (1984). Dots indicate lacustrine sediments filling volcano-tectonic Uzon-Geysernaya depression. Explanation: 1, Mount Uzon; 2, Ozernaya extrusion; 3, maar of Lake Dal'nee; 4, Belaya extrusion; 5, pumice dome of Mount Otkrytaya, extrusions; 6, Tortik; 7, Ostanets; 8, Sestrenka; 9, Kruglaya; 10, Geyzernaya; 11, Mount Duga; 12, Shirokoe Plateau; 13, canyon of Shumnaya River, extrusions; 14, Greben; 15, Gornoe Plateau; 16, Rudich's; 17, Bortovaya; 18, First; 19, Mount Bezymyannaya; 20, Zheltaya extrusion; 21, Savich's Cone.

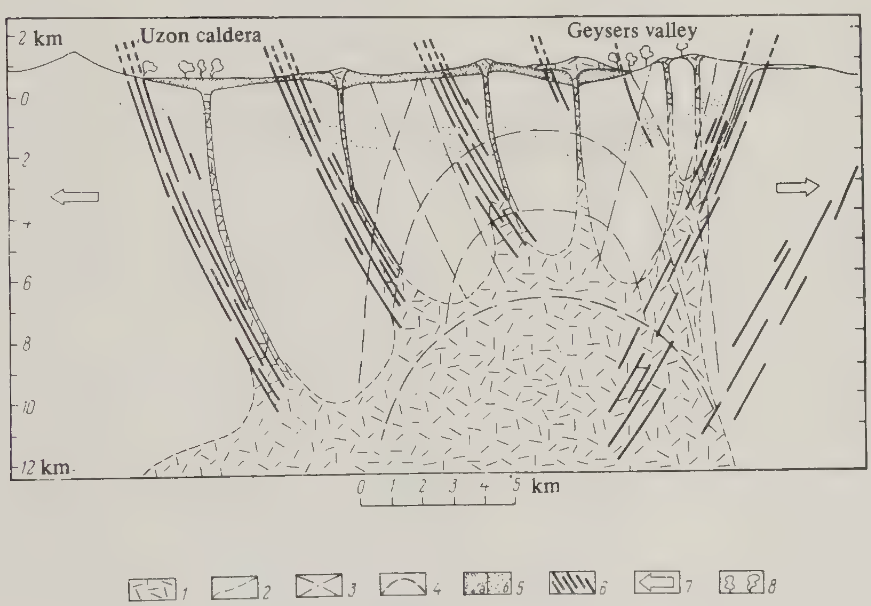

Figure 10.6.5. Schematic section showing structural control of hydrothermal system in Geysernaya Valley and Uzon Caldera, from Belousov and others (1984). Explanation: 1, area of crustal magma chamber and associated extrusions; 2, inferred boundaries of magma chamber; 3, system of ring-shaped and conical fractures above chamber, reconstructed from exposed dikes; 4, speculative upper boundary of chamber in the period of dike invasion; 5, water-bearing formations (a, upper; b, lower); 6, fault zones (arrows indicate direction of movement on faults); 7, direction of crustal extension in region; 8, manifestations of hydrothermal activity.

PART 3: HISTORICAL UNREST AT LARGE QUATERNARY CALDERAS (continued)
See inside back cover for explanation and abbreviations

KRASHENINNIKOV

CAVW number (active vent)	Latitude Longitude (degrees)	Diameter (km)	Local tectonic setting	Precaldera edifice	SiO_2 content (wt pct)	Age of collapse (yr B.P.)	Date of unrest	Type and duration of unrest ESTU STHF MGTF H Te	Eruption type
10-00-19 (Krasheninnikov)	54.62N 160.60E	9 x 11		Shield	C = d R = d,a,b	39,600	1963?	---- ---- ---x - --	none

TECTONIC SETTING

Krasheninnikov Caldera lies at the intersection of the eastern Kamchatka graben-syncline and a deep-seated, E-W fault (Erlich, 1986). In addition, a 21-km-long NNE-SSW set of fissures and small grabens cuts the caldera and localizes 15 parasitic lava vents and cinder cones (Erlich, 1986).

GEOLOGIC HISTORY

The precaldera edifice was a complex of one large stratovolcano and several smaller andesite and basalt volcanoes, extrusive domes, and scoria cones. The caldera formed ca. 39,000 yr B.P. after explosive eruption of >6 km^3 of dacitic pumice (Florensky, 1984; Erlich, 1986). Ignimbrite from this eruption overlies ignimbrite of the Uzon Caldera and is the youngest widespread pyroclastic unit in the Karymsky-Semiachinsky part of the eastern Kamchatka graben-syncline (Erlich, 1986). Krasheninnikov Volcano is a postcaldera stratocone in the center of the caldera (fig. 10.7.1). Voluminous lava flows issued from this cone 3,000 yr B.P. (Vodopadny flow), 1,500 yr B.P. (Ozerny flow), less than 600-700 yr B.P. (Yuzhny flow), and less than 400-500 yrs B.P. (Molodoy flow) (Ponomareva and Tsurupa, 1985). These flows would be described in historical accounts had they occurred in a populous area.

HISTORICAL ACTIVITY

Earthquakes occur at depths of >100 km beneath the northern margin of the caldera, possibly along a deep projection of the above-mentioned E-W fault (Erlich, 1986) or, alternatively, along the Benioff zone.

An active fumarole was discovered during aerial reconnaissance in 1963 (Steinberg, 1964). G.S. Steinberg (written commun., 1987) considers Krasheninnikov to be an active and possibly restless volcano.

KRASHENINNIKOV (continued)

REFERENCES

Erlich, E., 1986, Geology of the calderas of Kamchatka and Kurile Islands with comparison to calderas of Japan and the Aleutians, Alaska: U.S. Geol. Surv. Open-File Rep. 86-291, 300 p.

IAVCEI (International Association of Volcanology and Chemistry of the Earth's Interior), 1973, Data sheets on post-Miocene volcanoes of the world: Rome, IAVCEI.

Florensky, I.V., 1984, On the question of the age of Uzon and Krasheninnikov calderas: Vulkanol. Seismol., 1984, pt. 1, p. 102-106.

Ponomareva, V.V., and Tsurupa, A.A., 1985, Extended flows of liquid acid lava in Krasheninnikov Volcano: Vulkanol. Seismol., 1985, pt. 3, p. 85-91.

Skorokhodov, V.N., 1979, Dynamics of development of ring structures on the example of Kamchatka volcanoes Uksichan, Krasheninnikov and Maly Semiachik, in Problems of deep magmatism: Moscow, Nauka Press, p. 117-124.

Steinberg, G.S., 1964, On the activity and structure of the Krasheninnikov volcano: Bull. Vulkanol. Stantsii (Kamchatka), no. 37, p. 16-20.

Steinberg, G.S., and Rivosh, L.A., 1965, Geophysical study of the Kamchatka volcanoes: Jour. Geophys. Res., v. 70, p. 3341-3369.

Vlodavetz, V.I., and Piip, B.I., 1959, Catalogue of active volcanoes of the world including solfatara fields, Pt. VIII, Kamchatka and continental areas of Asia: Naples, IAVCEI, 110 p.

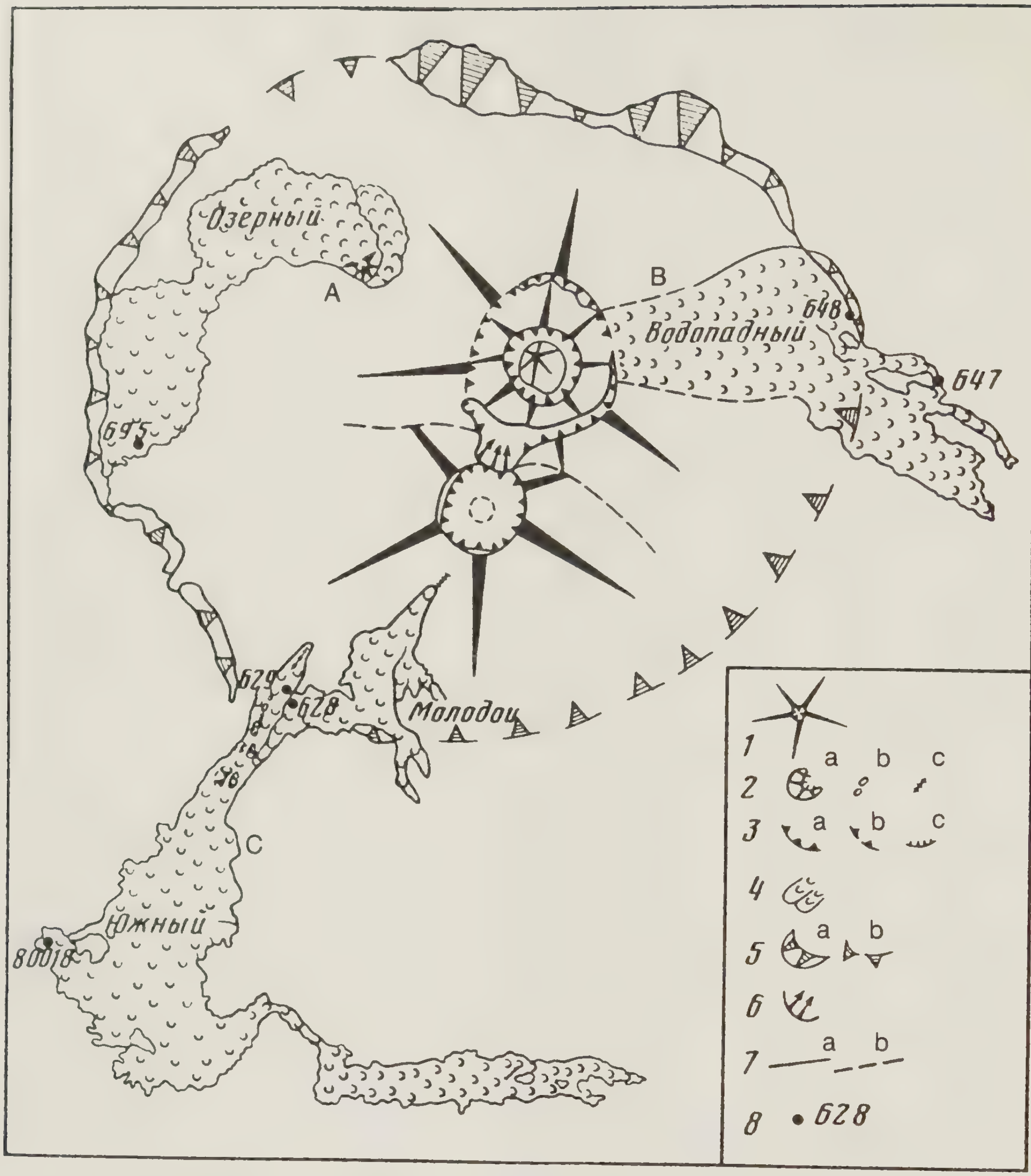

Figure 10.7.1. Geologic map of Krasheninnikov Volcano (Ponomareva and Tsurupa, 1985). A, Ozerny flow (ca. 1,500 yr B.P.); B, Vodopadny flow (ca. 3,000 yr B.P.); C, Yuzhny flow (600-700 yr B.P.); 1, stratovolcano cone; 2, Holocene eruptive vent (a, cinder cone; b, crater; c, chain of craters); 3, crater rim (a, well defined; b, inferred; c, cinder cone); 4, lava flow; 5, caldera rim (a, well defined by relief; b, inferred); 6, cirque wall; 7, fault (a, located; b, inferred); 8, lava sample location point.

Figure 10.8. Location of Tien-Chi (solid circle), a restless caldera in mainland China (Region 10).

TIEN-CHI

CAVW number (active vent)	Latitude Longitude (degrees)	Diameter (km)	Local tectonic setting	Precaldera edifice	SiO_2 content (wt pct)	Age of collapse (yr B.P.)	Date of unrest	Type and duration of unrest ESTU STHF MGTF H Te	Eruption type
10-03-02	41.98N	5	Exten?		R = 49-?	800-900	1597?	---- ---- ---- - --	unknown
(Changpaishan	128.08E				C = 71		1702?	---- ---- ---- - --	unknown
including									
= Baegdusan									
= Pai-tou-shan									
= P'aektu-san									
= Hakuto-san)									

TECTONIC SETTING/GEOLOGIC HISTORY

A large lava plateau and shield volcano on the Chinese-Korean border (Changpaishan) consists of tholeiitic to alkaline basalt flows with a cap of peralkaline silicic flows (mostly trachyte and pantellerite). A stratovolcano (or dome?)--P'aektu-san (also known as Hakuto-san)--has grown on top of the shield (fig. 10.8.1). A 5-km-wide, 850-m-deep caldera has developed at the summit of P'aektu-san (Ogura, 1969; Tomita, 1969; Whitford-Stark, 1983, 1987). A large-volume pumice deposit with a radius of 40 km is centered on the summit caldera and probably was erupted immediately before or during collapse of the caldera (Whitford-Stark, 1987). Tien-chi, a caldera lake, is 3 km x 4 km across and 375 m deep (Whitford-Stark, 1987).

This cluster of alkaline volcanoes is probably related to spreading behind the Japan arc.

HISTORICAL ACTIVITY

There are unsubstantiated reports of eruptions in 1597 and 1702 (Tomita, 1969; Ogura, 1969, p. 399).

REFERENCES

Machida, H., and Arai, F., 1983, Extensive ash falls in and around the Sea of Japan from large late Quaternary eruptions: Jour. Volcanol. Geotherm. Res., v. 18, p. 151-164.

Ogura, T., 1969, Volcanoes in Manchuria, in Ogura, T., ed., Geology and mineral resources of the Far East: Tokyo, Univ. Tokyo Press, v. 2, p. 373-413.

Tomita, T., 1969, Volcanic geology of the Cenozoic alkaline petrographic province of eastern Asia, in Ogura, T., ed., Geology and mineral resources of the Far East: Tokyo, Univ. Tokyo Press, Tokyo, v. 1, p. 139-202.

Whitford-Stark, J.L., 1983, Cenozoic volcanic and petrochemical provinces of mainland Asia: Jour. Volcanol. Geotherm. Res., v. 19, p. 193-222.

----- 1987, A survey of Cenozoic volcanism on mainland Asia: Geol. Soc. Am. Spec. Paper 213, 74 p.

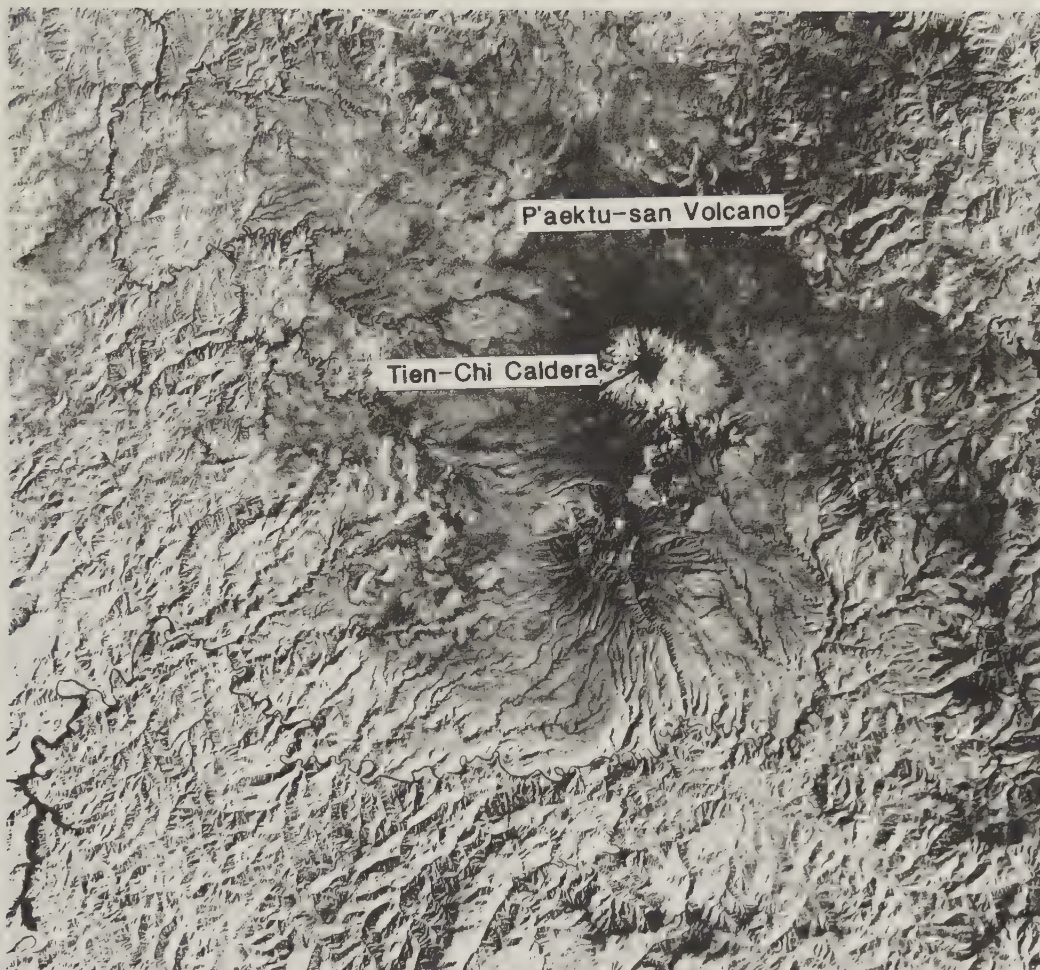

Figure 10.8.1. Landsat satellite image of P'aektu-san Volcano (northern cone) and its summit caldera, Tien-Chi (lake filled), as reproduced in Whitford-Stark (1987). Tien-Chi Caldera is approximately 5 km in diameter.

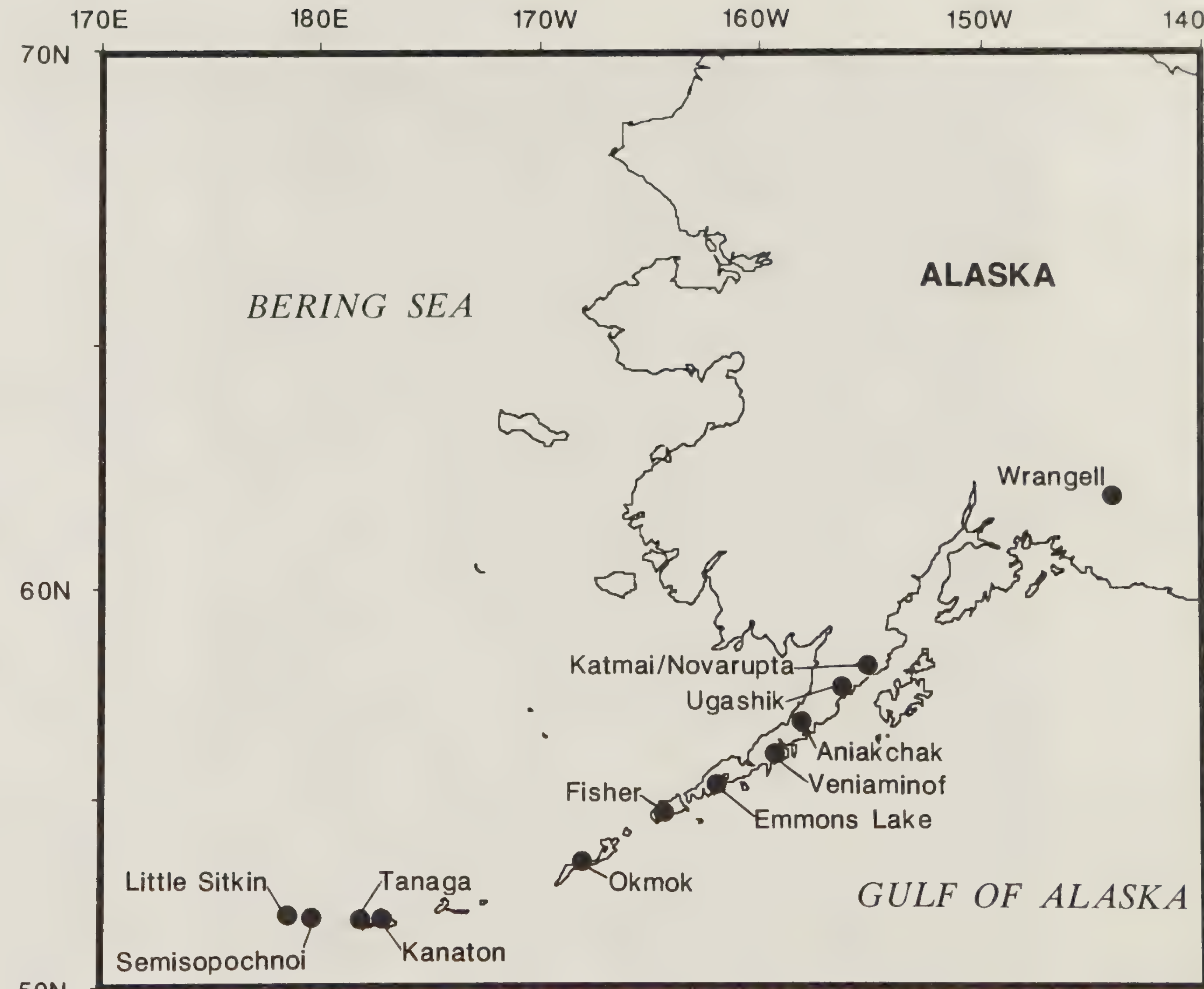

Figure 11. Locations of large, Quaternary restless calderas (solid circles) in Region 11.

LITTLE SITKIN, CALDERA ONE AND CALDERA TWO

CAVW number (active vent)	Latitude Longitude (degrees)	Diameter (km)	Local tectonic setting	Precaldera edifice	SiO_2 content (wt pct)	Age of collapse (yr B.P.)	Date of unrest	Type and duration of unrest ESTU STHF MGTF H Te	Eruption type
11-01-05 (Little Sitkin)	51.95N 178.53E	5 (outer) 3 (inner)	Compr	Strato	R = 55-69 C = 58 (One) = 60-65 (Two)		1776 1828-30	---- ---- ---- - -- ---- ---- ---- - --	unknown ex

TECTONIC SETTING

The Aleutian volcanic arc is defined by over 65 major Quaternary volcanic centers and spans 2,500 km of the Alaskan mainland and the Aleutian Islands. At least 21 of these centers have calderas (Miller and Barnes, 1976), 19 of which may have formed in the Holocene.

Little Sitkin lies near the western end of the volcanically active part of the Aleutian arc. In this part of the arc, the Pacific plate is thrust beneath the North American plate at a rate of about 8 cm/yr. A submarine scarp, the Prokhoda scarp, connects the southeast part of Little Sitkin with Semisopochnoi Island, 56 km to the southeast.

GEOLOGIC HISTORY

Caldera One formed by collapse of the summit of a large basaltic-andesitic stratovolcano (figs. 11.1.1, 11.1.2) (Snyder, 1959). A low-silica dacite tuff overlies the edifice and might be the product of the caldera-forming eruption. Voluminous dacite lava flows built a cone within Caldera One. Miarolitic andesite inclusions are abundant in these lavas. Caldera Two, largely nested within Caldera One, formed after eruption of low-silica dacite pyroclastic flows (now welded tuff). Lavas ranging in composition from andesite to rhyodacite have been erupted since formation of Caldera Two, some along a zone (fissure) trending N67°W through the center of the caldera. One very young-looking flow (undated, but perhaps only 50-100 yr old) was erupted from the central vent of Caldera Two; another was erupted from a vent along the above-mentioned fissure, just outside the west rim of Caldera One (Snyder, 1959).

HISTORICAL ACTIVITY

Young-looking lava flows were probably erupted within historical time, but the exact date of their eruption is unknown. Coats (1950) attributed a 1776 eruption with "flames" to Little Sitkin, and Dall (1870) reported "smoke" above the island during 1828-30.

LITTLE SITKIN (continued)

REFERENCES

Coats, R.R., 1950, Volcanic activity in the Aleutian arc: U.S. Geol. Surv. Bull. 974-B, p. 35-49.
Dall, W.H., 1870, Alaska and its resources: London, Sampson Low, Son, and Marston, p. 467.
Miller, T.P., and Barnes, I., 1976, Potential for geothermal energy development in Alaska, in Halbouty, M.T., Maher, J.C., and Lian, H.M., eds., Circum-Pacific energy and mineral resources: Am. Assoc. Pet. Geol. Memoir 25, p. 149-153.
Snyder, G.L., 1959, Geology of Little Sitkin Island, Alaska: U.S. Geol. Surv. Bull. 1028-H, p. 169-210.
U.S. Geological Survey, 1951, limited revisions 1983, Rat Islands topographic map, Alaska topographic series, scale 1:250,000.

Figure 11.1.1. Topographic map of Little Sitkin Island, showing approximate outline of Little Sitkin Caldera (U.S. Geological Survey, 1951).

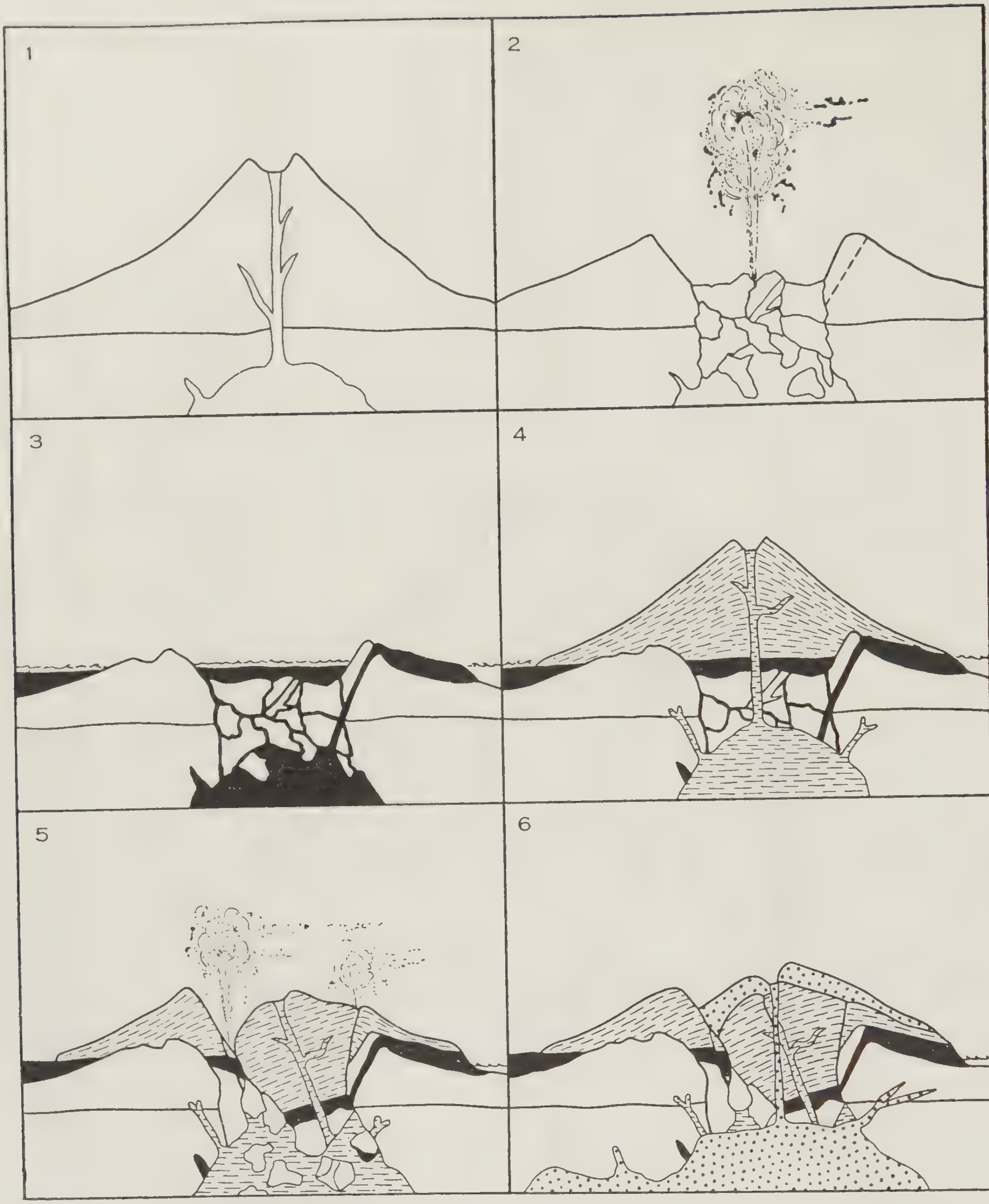

Figure 11.1.2. Schematic history of Little Sitkin Island, from Snyder (1959): 1, Erection of andesitic composite cone on platform 300 ft below sea level in late Tertiary or early Quaternary time. 2, formation of Caldera One after long period of erosion. 3, deposition of Sitkin Point formation in offshore basin and in caldera lake, and extrusion of flow sequence of East Point formation. 4, erection of high-silica dacite lava-flow cone of Double Point dacite in late Pleistocene or early Recent time. 5, formation of Caldera Two with attendant nuee ardente eruptions. 6, extrusion of low-silica dacite lava continuing to the present.

SEMISOPOCHNOI

CAVW number (active vent)	Latitude Longitude (degrees)	Diameter (km)	Local tectonic setting	Precaldera edifice	SiO_2 content (wt pct)	Age of collapse (yr B.P.)	Date of unrest	Type and duration of unrest ESTU STHF MGTF H Te	Eruption type
11-01-06	51.93N	8	Compr	Strato	R = 56-63	post-	1772?	---- ---- ---- - --	"smoke"
(Cerberus)	179.60E				C = 61-66	glacial	1790?	---- ---- ---- - --	"smoke"
							1792?	---- ---- ---- - --	"smoke"
							1830?	---- ---- ---- - --	"smoke"
							1873	---- ---- ---- - --	unknown
							1987	---- ---- ---- - --	ex

TECTONIC SETTING

Semisopochnoi Island lies near the southernmost part of the Aleutian arc. In this stretch of the arc, the Pacific plate is subducted beneath the North American plate at a rate of approximately 8 cm/yr.

GEOLOGIC HISTORY

Semisopochnoi Island (fig. 11.2.1) consists entirely of volcanic rocks and epiclastic volcanic sediments. A single, large andesitic-basaltic "shield" volcano ("Pochnoi") forms most of the present island. The central part of this edifice collapsed following eruption of a large volume of dacitic pumice. Mount Cerberus is a postcaldera stratocone, composed of basalt and basaltic andesite, that grew in the center of the caldera; Lakeshore Cone and Sugarloaf Peak are also postcaldera cones. Lava flows have nearly covered the caldera floor and have spilled onto the south flank of the precollapse edifice (Coats, 1959). One late flow from Cerberus may be less than 100 years old, because it is no more vegetated than a 40-year-old lava flow on nearby Kanaga Island (Coats, 1959).

HISTORICAL ACTIVITY

Coats (1959), citing Grewingk (1850), wrote that early explorers reported "smoke" in at least four years---1772, 1790, 1792, and 1830. Dall (1870) stated that the Semisopochnoi Islands lost their activity in 1772, but Becker (1898, p. 17) reported that a volcano on the island was again active in 1873. A plume was observed from the approximate location of Semisopochnoi on 13 April 1987, and ash-darkened snow was reported by a local pilot 11 days later (Smithsonian Institution, 1987).

SEMISOPOCHNOI (continued)

REFERENCES

Becker, G.F., 1898, Reconnaissance of the gold fields of southern Alaska, with some notes on general geology: U.S. Geol. Surv., 18th Ann. Rep., pt. 3, p. 13-24.

Coats, R.R., 1950, Volcanic activity in the Aleutian arc: U.S. Geol. Surv. Bull. 974-B, p. 35-49.

----- 1959, Geologic reconnaissance of Semisopochnoi Island, western Aleutian Islands, Alaska: U.S. Geol. Surv. Bull. 1028-O, p. 477-519.

Dall, W.H., 1870, Alaska and its resources: London, Sampson Low, Son, and Marston, p. 467.

Grewingk, C., 1850, Beitrag zur Kenntniss der orographischen und geognostischen Beschaffenheit der Nordwestküste Amerikas, mit den anliegenden Inseln: Verh. Russisch-Kaiserlichen Mineral. Gesellschaft zu St. Petersburg, 1848-49, p. 123-278.

Katsui, Y., ed., 1971, List of the world active volcanoes: Tokyo, Volcanol. Soc. Japan/IAVCEI/IUGG, 160 p.

Smith, R.L., Shaw, H.R., Luedke, R.G., and Russell, S.L., 1978, Comprehensive tables giving physical data and thermal energy estimates for young igneous systems of the United States: U.S. Geol. Surv. Open-File Rep. 78-925, 15 p. + tables.

Smithsonian Institution, Scientific Event Alert Network (SEAN), 1987, Semisopochnoi Volcano: SEAN Bull., v. 12, no. 4, p. 15 (information from J.W. Reeder, T. Miller, and W. Gould).

U.S. Geological Survey, 1951, limited revisions 1983, Rat Islands topographic map, Alaska topographic series, scale 1:250,000.

Figure 11.2.1. Topographic map of Semisopochnoi Island, showing approximate outline of Semisopochnoi Caldera (U.S. Geological Survey, 1951).

TANAGA

CAVW number (active vent)	Latitude Longitude (degrees)	Diameter (km)	Local tectonic setting	Precaldera edifice	SiO_2 content (wt pct)	Age of collapse (yr B.P.)	Date of unrest	Type and duration of unrest ESTU STHF MGTF H Te	Eruption type
11-01-08	51.88N	11	Compr	Strato	R = 52+		1763-70	---- ---- ---- - --	"active"
(Tanaga)	178.13W						1791?	---- ---- ---- - --	"smoke"
							1829	---- ---- ---- - --	ex?,"smoke"
							1914	---- ---- ---- - --	lf

TECTONIC SETTING

Tanaga Volcano and its caldera lie on the northwestern tip of Tanaga Island, near the southernmost part of the western Aleutian arc. Submarine ridges that are transverse to the arc suggest local segmentation into fault blocks. Convergence rates in this area are approximately 8 cm/yr.

GEOLOGIC SETTING

"Tanaga Volcano and its twin to the west are located within an arcuate structure, possibly a caldera. The volcano at the northwest tip of the island appears also to have been built up within a similar structure" (Fraser and Barnett, 1959). The postcaldera cone of Tanaga Volcano is unglaciated (fig. 11.3.1).

HISTORICAL ACTIVITY

No details available.

REFERENCES

Coats, R.R., 1950, Volcanic activity in the Aleutian arc: U.S. Geol. Surv. Bull. 974-B, p. 35-49.
----- 1956, Reconnaissance geology of some western Aleutian Islands, Alaska: U.S. Geol. Surv. Bull. 1028-E, p. 83-100.
Fraser, G.D., and Barnett, H.F., 1959, Geology of the Delarof and westernmost Andreanof Islands, Alaska: U.S. Geol. Surv. Bull. 1028-I, p. 211-248.
Katsui, Y., ed., 1971, List of the world active volcanoes: Tokyo, Volcanol. Soc. Japan/IAVCEI/IUGG, 160 p.
Smith, R.L., Shaw, H.R., Luedke, R.G., and Russell, S.L., 1978, Comprehensive tables giving physical data and thermal energy estimates for young igneous systems of the United States: U.S. Geol. Surv. Open-File Rep. 78-925, 15 p. + tables.
U.S. Geological Survey, 1954, limited revisions 1983, Gareloi Island topographic map, Alaska topographic series, scale 1:250,000.
----- 1957, limited revisions 1983, Adak topographic map, Alaska topographic series, scale 1:250,000.

Figure 11.3.1. Topographic map of Tanaga Island and Tanaga Volcano, showing approximate outline of Tanaga Caldera (U.S. Geological Survey, 1954, 1957).

KANATON

CAVW number (active vent)	Latitude Longitude (degrees)	Diameter (km)	Local tectonic setting	Precaldera edifice	SiO_2 content (wt pct)	Age of collapse (yr B.P.)	Date of unrest	Type and duration of unrest ESTU STHF MGTF H Te	Eruption type
11-01-11	51.93N	5.5	Compr	Strato	R = 55-60		1763?	---- ---- ---- - --	"active"
(Kanaga)	177.15W				C = 64		1768	---- ---- ---- - --	"active"
							1783-87	---- ---- ---- - --	"active"
							1790-91	---- ---- ---x - --	"smoke"
							1827-29?	---- ---- ---- - --	"smoke"
							1904	---- ---- ---- - --	lf
							1906	x--- ---- ---- - --	lf
							1933	---- ---- ---- - --	unknown
							1942	---- ---- ---- - --	unknown
							1951	---- ---- ---x - --	ex?

TECTONIC SETTING

Kanaga Volcano and the Kanaton Caldera lie on the north tip of Kanaga Island, near the southernmost part of the western Aleutian arc (figs. 11.4.1, 11.4.2). Fraser and Barnett (1959) show a major N-S fault, transverse to the arc, just west of Kanaton caldera. Convergence rates in this part of the arc are approximately 8 cm/yr.

GEOLOGIC HISTORY

An early stratovolcano (termed Mount Kanaton by Coats, 1956b) consists largely of andesitic and basaltic lava flows and tuff breccias. Collapse to form the Kanaton Caldera occurred after eruption of a dacitic tuff. The subaerial volume of that dacitic tuff is much smaller than would usually be associated with a 5.5-km-diameter caldera (Coats, 1956b), and because the northern wall of the caldera is not preserved, it is possible that this caldera formed by a very large debris avalanche rather than by collapse after a large explosive eruption. Bathymetric studies north-northwest of Kanaga would help to determine the origin of the caldera.

HISTORICAL ACTIVITY

According to a trapper who lived near Kanaga Volcano, earthquakes in May 1906 were followed by lava extrusion onto the east and west sides of the cone (Coats, 1956b). Some of the reported "smoke" from Kanaga has probably been fumarolic activity from hot

KANATON (continued)

HISTORICAL ACTIVITY (continued)

springs around the base of the volcano (Grewingk, 1850) and from conspicuous fumaroles near the summit (Coats, 1956b). Powers (1951) reported that "minor ash showers and fume emission" occurred at Kanaga and several other Aleutian volcanoes during 1951.

REFERENCES

Coats, R.R., 1950, Volcanic activity in the Aleutian arc: U.S. Geol. Surv. Bull. 974-B, p. 35-49.
----- 1952, Magmatic differentiation in Tertiary and Quaternary volcanic rocks from Adak and Kanaga Islands, Alaska: Geol. Soc. Am. Bull, v. 63, p. 485-514.
----- 1956a, Reconnaissance geology of some western Aleutian Islands, Alaska: U.S. Geol. Surv. Bull. 1028-E, p. 83-100.
----- 1956b, Geology of northern Kanaga Island, Alaska: U.S. Geol. Surv. Bull. 1028-D, p. 69-80.
Fraser, G.D., and Barnett, H.F., 1959, Geology of the Delarof and westernmost Andreanof Islands, Alaska: U.S. Geol. Surv. Bull. 1028-I, p. 211-248.
Grewingk, C., 1850, Beitrag zur Kenntniss der orographischen und geognostischen Beschaffenheit der Nordwestküste Amerikas, mit den anliegenden Inseln: Verh. Russisch-Kaiserlichen Mineral Gesellschaft zu St. Petersburg, 1848-49, p. 123-278.
Hantke, G., 1951, Uebersicht über die vulkanische tätigkeit, 1941-1947: Bull. Volcanol., v. 11, p. 161-208.
Katsui, Y., ed., 1971, List of the world active volcanoes: Tokyo, Volcanol. Soc. Japan/IAVCEI/IUGG, 160 p.
Powers, H.A., 1951, Aleutian volcanic activity: Volcano Lett., no. 514, p. 6.
Smith, R.L., Shaw, H.R., Luedke, R.G., and Russell, S.L., 1978, Comprehensive tables giving physical data and thermal energy estimates for young igneous systems of the United States: U.S. Geol. Surv. Open-File Rep. 78-925, 15 p. + tables.
U.S. Geological Survey, 1957, limited revisions 1983, Adak topographic map, Alaska topographic series, scale 1:250,000.

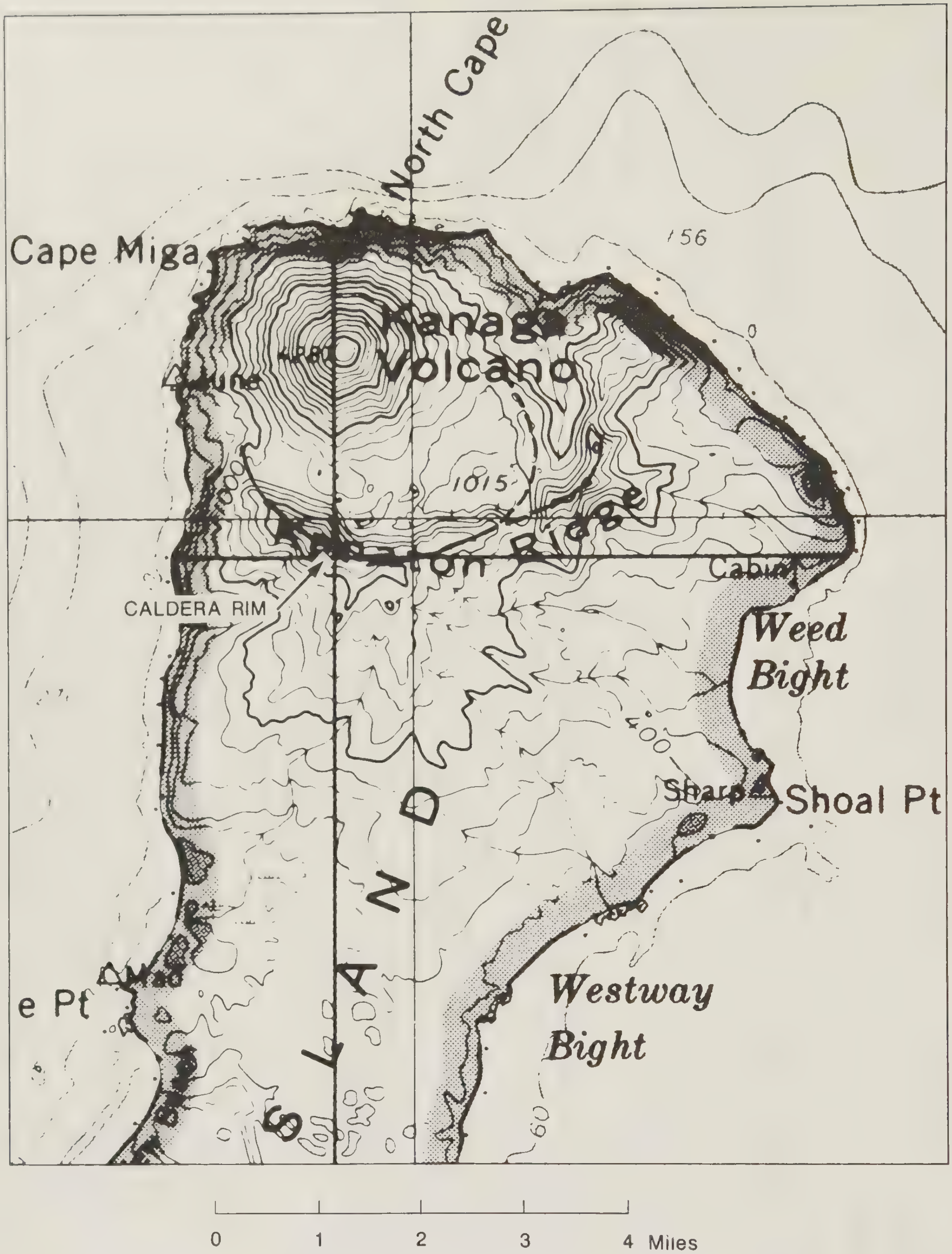

Figure 11.4.1. Topographic map of Kanaga Island, showing Kanaga Volcano and approximate outline of Kanaton Caldera (U.S. Geological Survey, 1957).

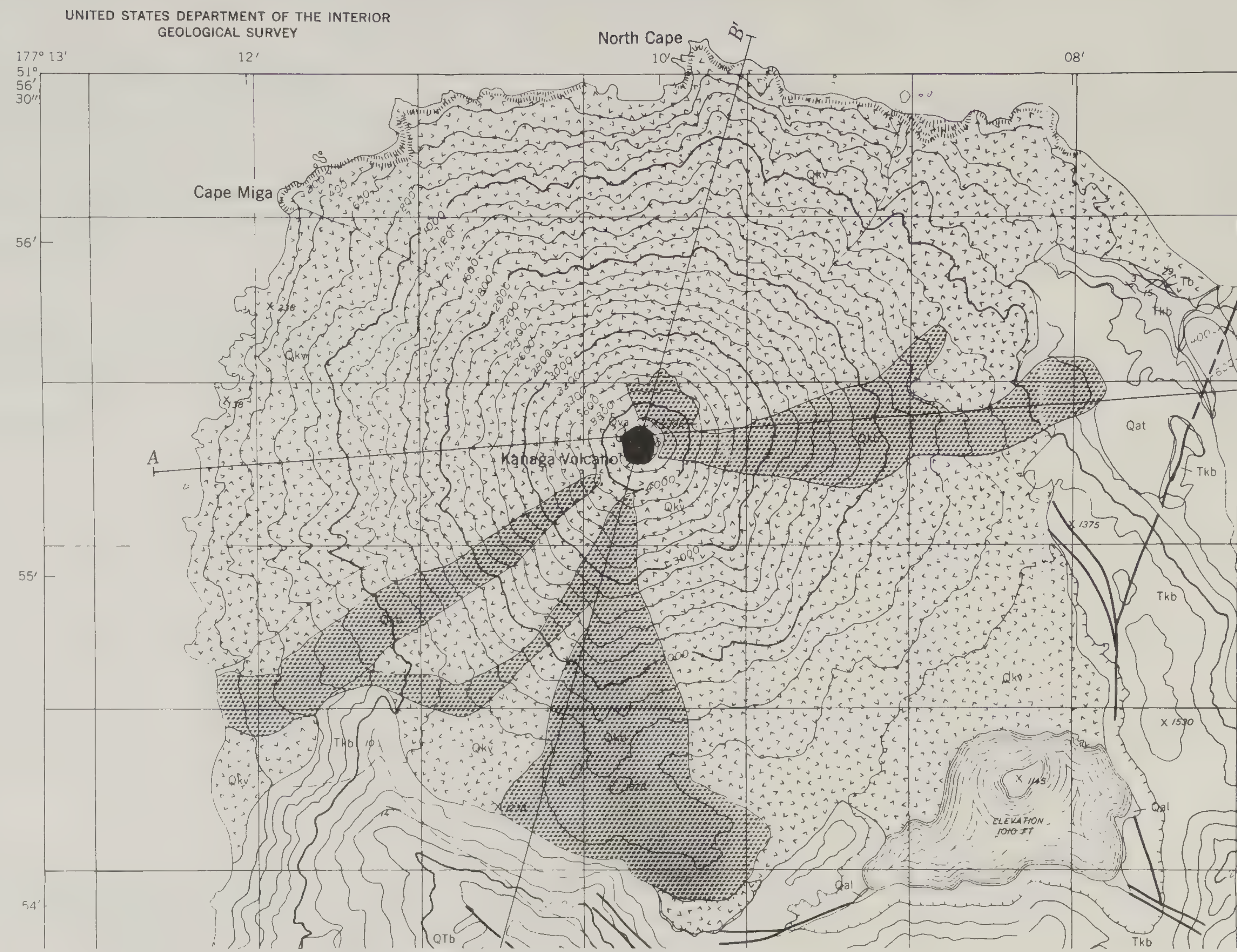

Figure 11.4.2. Recent products of Kanaga Volcano, from Coats (1956b). Stippled lava flows on volcano's flanks are historic and late prehistoric basalt flows; remainder of flanks consist of older basalt and andesite flows, scoria, and tuff breccia. See figure 11.4.1 for outline of Kanaton Caldera.

PART 3: HISTORICAL UNREST AT LARGE QUATERNARY CALDERAS (continued)
See inside back cover for explanation and abbreviations

OKMOK

CAVW number (active vent)	Latitude Longitude (degrees)	Diameter (km)	Local tectonic setting	Precaldera edifice	SiO_2 content (wt pct)	Age of collapse (yr B.P.)	Date of unrest	Type and duration of unrest ESTU STHF MGTF H Te	Eruption type
11-01-29	53.42N	10	Compr	LL-strat	R = 51-54	8,250,	1805	---- ---- ---- - --	unknown
(Okmok)	168.13W	(both			C = 54-66	<2,400	1817-20	---- ---- ---- - --	Ex
		calderas)					1824-30	---- ---- ---- - --	unknown
							1878	Y--- ---- ---- - --	unknown, + tsunami?
							1899	---- ---- ---- - --	Ex
							1931	x--- ---- ---x - --	"smoke,"lf?
							1936?	---- ---- ---- - --	"smoke"
							1938?	---- ---- ---- - --	unknown
							1943	---- ---- ---- - --	ex
							1944-45	C--- ---- ---- - --	ex,lf
							1958	---- ---- ---- - --	lf
							1960-61	---- ---- ---- - --	Ex
							1983	---- ---- ---- - --	ex
							1986-88+	---- ---- ---x - QU?	ex

TECTONIC SETTING

Okmok Caldera is on Umnak Island, where the Pacific and North American plates converge at a rate of 7-8 cm/yr. The Aleutian arc is a single arc at Umnak Island, and Quaternary volcanoes have grown over Tertiary basement; to the east from Umnak Island, non-volcanic islands lie seaward of the chain of active volcanoes.

GEOLOGICAL HISTORY

Okmok is a basaltic composite volcano with a pair of overlapping summit calderas, each with an estimated diameter of about 10 km (fig. 11.5.1). The first formed about 8,250 yr B.P. (Black, 1975; Miller and Smith, 1975, 1987), the second less than 2,400 yr B.P. (Miller and Smith, 1983, 1987). The center of second collapse is about 1.5 km southwest of the center of the first (Byers, 1959; Miller and Smith, 1983). Each caldera formed after eruption of voluminous, dominantly andesitic ash flows (the Okmok Volcanics), locally separated by a lava flow and an erosional surface. Postcaldera activity has included mostly small, intracaldera basaltic extrusions and explosions (Byers, 1959).

OKMOK (continued)

HISTORICAL ACTIVITY

1817: A large explosive eruption covered some parts of Unalaska with 15 cm of ash. Some large stones were thrown out to a distance of 50 versts (53 km), and ash reached Unimak Island.

1878: A new crater, earthquakes, and a tsunami were reported (Hantke, 1951); their relation to Okmok Caldera is unclear.

1931: On 21 March, black smoke issued from Tulik on Umnak in place of the usual white steam. Two earthquakes on 29 March were recorded on a seismograph at Dutch Harbor, on Unalaska Island. An eruption occurred on Umnak on 13 May (Jaggar, 1931).

1944-45: Bradley (1948) reported that activity began anew in 1944. Wilcox (1959) reports that on 1 June 1945, "a sharp earthquake was felt at the Umnak Island army base on the east side of the mountain. Nothing otherwise unusual was noted, and the rim of the caldera was hidden by persistent low clouds." On 4 June, pilots reported a column of dark ash, and subsequent observations showed ash ejection and a lava flow from a cinder cone in the southern part of the caldera.

1958: A new lava flow was recognized from the air.

1960-61: Explosive eruptions occurred for several months, but no new lava flow was reported (Volcanological Society of Japan, 1986).

1983: A small ash eruption was noted by a local pilot at 0900 hr on 8 July, and on satellite imagery at 1616 hr of the same day (Volcanological Society of Japan, 1986).

1986-87: A small ash eruption was seen on 18 November 1986. Then on 5 January 1987, about 13 hours after a shallow, M_s=6.6 earthquake 130 km southwest of Okmok, another small ash eruption occurred. Additional small ash eruptions occurred in January, June, July, and December 1987, and February 1988 (Smithsonian Institution, 1986, 1987, 1988).

REFERENCES

Black, R.F., 1975, Late-Quaternary geomorphic processes: effects on the ancient Aleuts of Umnak Island in the Aleutians: Arctic, v. 28, p. 159-169.
Bradley, C.C., 1948, Geologic notes on Adak Island in the Aleutian Chain: Am. Jour. Sci., v. 246, p. 214-240.
Byers, F.M., Jr., 1959, Geology of Umnak and Bogoslof Islands, Aleutian Islands, Alaska: U.S. Geol. Surv. Bull. 1028-L, p. 267-365.
----- 1961, Petrology of three volcanic suites, Umnak and Bogoslof Islands, Aleutian Islands, Alaska: Geol. Soc. Am. Bull., v. 72, p. 93-128.

OKMOK (continued)

REFERENCES (continued)

Byers, F.M., Jr., and Brannock, W.W., 1949, Volcanic activity on Umnak and Great Sitkin Islands, 1946-1948: Trans. Am. Geophys. Union, v. 30, p. 719-734.

Coats, R.R., 1950, Volcanic activity in the Aleutian arc: U.S. Geol. Surv. Bull. 974-B, p. 35-49.

Hantke, G., 1951, Uebersicht über die vulkanische tätigkeit, 1941-1947: Bull. Volcanol., v. 11, p. 161-208.

Jaggar, T.A., 1931, Difficulties of Alaskan earthquake study: Volcano Lett., no. 337, p. 1-3.

Katsui, Y., ed., 1971, List of the world active volcanoes: Tokyo, Volcanol. Soc. Japan/IAVCEI/IUGG, 160 p.

Keller, A., 1976, Okmok Caldera: Alaska Geogr., v. 4, no. 1, p. 75-83.

Miller, T.P., and Smith, R.L., 1975, Ash flows on the Alaska Peninsula: A preliminary report on their distribution, composition, and age [abs.]: Geol. Soc. Am. Abstracts with Programs, v. 7, no. 7, p. 1201.

----- 1983, Calderas of the eastern Aleutian arc [abs.]: Eos, Trans. Am. Geophys. Union, v. 64, p. 877.

----- 1987, Late Quaternary caldera-forming eruptions in the eastern Aleutian arc, Alaska: Geology, v. 15, p. 434-438.

Nye, C.J., 1983, Petrology and geochemistry of Okmok and Wrangell Volcanoes, Alaska: Univ. Calif. Santa Cruz, unpubl. Ph.D. diss.

Robinson, G.D., 1948, Exploring Aleutian volcanoes: Natl. Geogr., v. 94, no. 4, p. 509-522.

Smith, R.L., Shaw, H.R., Luedke, R.G., and Russell, S.L., 1978, Comprehensive tables giving physical data and thermal energy estimates for young igneous systems of the United States: U.S. Geol. Surv. Open-File Rep. 78-925, 15 p. + tables.

Smithsonian Institution, Scientific Event Alert Network (SEAN), 1983, 1986-88, Okmok: SEAN Bull., v. 8, no. 8; v. 11, no. 12; v. 12, nos. 1, 6, 7, 12; v. 13, no. 2 (information from J.W. Reeder).

U.S. Geological Survey, 1951a, limited revisions 1983, Umnak topographic map, Alaska topographic series, scale 1:250,000.

----- 1951b, limited revisions 1983, Unalaska topographic map, Alaska reconnaissance topographic series, scale 1:250,000.

Volcanological Society of Japan, 1986, Okmok: Bull. Volcanic Eruptions, no. 23, p. 35-36, 52-53 (information from J.W. Reeder, C.T. Madsen, and W. Gould).

Wilcox, R.E., 1959, Some effects of recent volcanic ash falls, with especial reference to Alaska: U.S. Geol. Surv. Bull. 1028-N, p. 409-476.

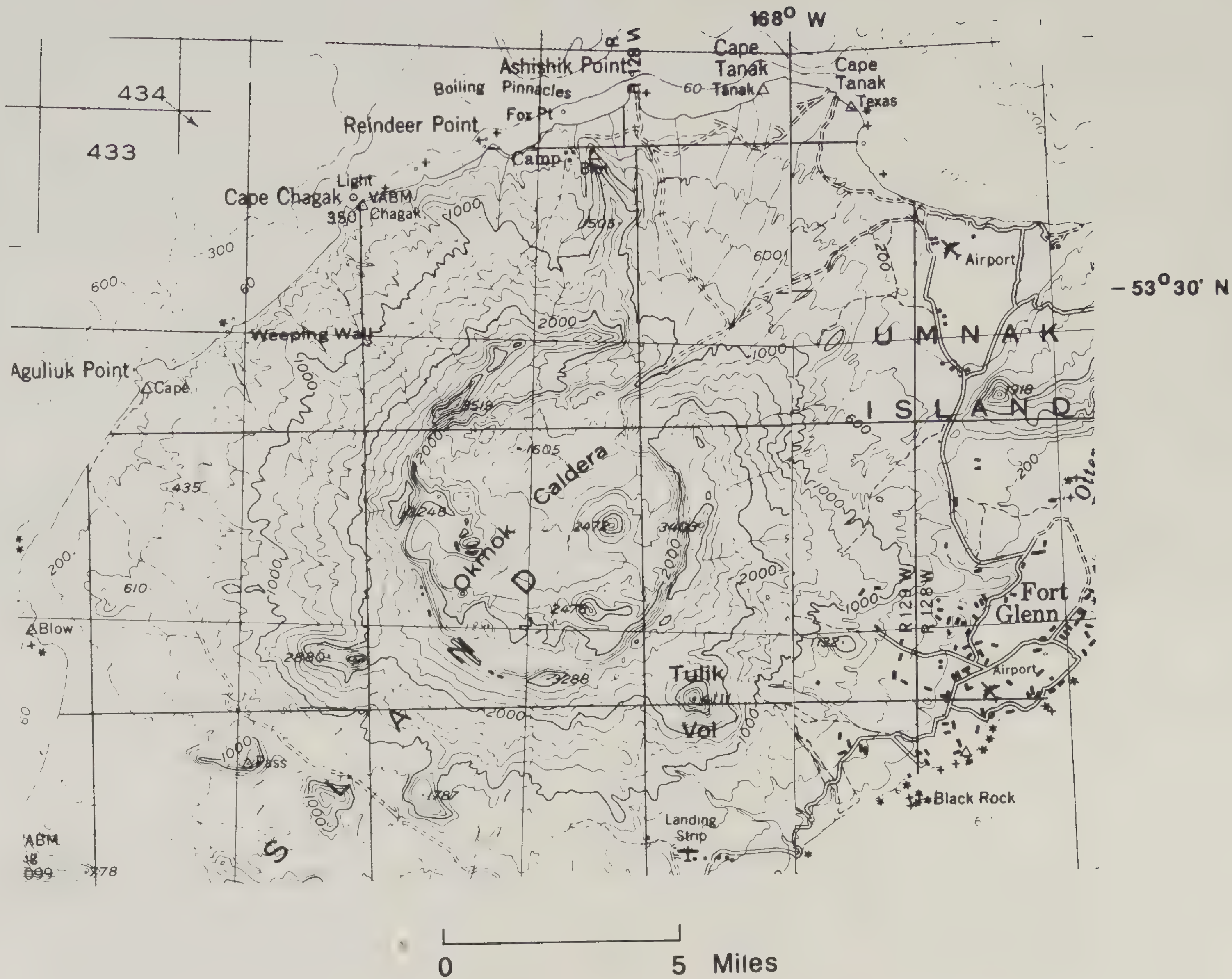

Figure 11.5.1. Topographic map of northeast Umnak Island and Okmok Caldera (U.S. Geological Survey, 1951a,b).

PART 3: HISTORICAL UNREST AT LARGE QUATERNARY CALDERAS (continued)
See inside back cover for explanation and abbreviations

FISHER

CAVW number (active vent)	Latitude Longitude (degrees)	Diameter (km)	Local tectonic setting	Precaldera edifice	SiO_2 content (wt pct)	Age of collapse (yr B.P.)	Date of unrest	Type and duration of unrest ESTU STHF MGTF H Te	Eruption type
11-01-35 (Fisher)	54.67N 164.35W	11 x 18	Compr	Strato	R = mafic? C = 67-68, minor 52-53	9,100	1795?	---- ---- ---- - --	ex
							1826-27	---- ---- ---- - --	Ex?

TECTONIC SETTING

Fisher Caldera is near the west end of Unimak Island, where the Pacific and North American plates converge at a rate of 7-8 cm/yr.

GEOLOGIC HISTORY

Fisher Caldera, one of the largest calderas in the Aleutian arc, formed about 9,100 yr B.P. by collapse of a large andesitic stratovolcano (fig. 11.6.1). Eruption of a large volume of dacitic pumice generated unusually mobile, high-velocity pyroclastic flows that climbed more than 400 m from lowlands to pass over distant ridges (Miller and Smith, 1977, 1987).

HISTORICAL ACTIVITY

Little is known of historical eruptions of Fisher Volcano. Grewingk (1850) wrote that a small volcano on the southwest side of Unimak Island exploded in 1795 and "fell in with a fearful noise." Coats (1950) attributed this to Pogromni and Isanotski, but T. Miller and J. Riehle (written commun., 1985) suggest that this eruption might have been from Fisher. Grewingk (1850) also mentioned eruptions and ashfall on the south end of Unimak Island in 1826. An active fumarole field occurs in the central part of the caldera (T.P. Miller, written commun., 1987).

REFERENCES

Coats, R.R., 1950, Volcanic activity in the Aleutian arc: U.S. Geol. Surv. Bull. 974-B, p. 35-49.
Grewingk, C., 1850, Beitrag zur Kenntniss der orographischen und geognostischen Beschaffenheit der Nordwestküste Amerikas, mit den anliegenden Inseln: Verh. Russisch-Kaiserlichen Mineral. Gesellschaft zu St. Petersburg, 1848-49, p. 123-278.
Katsui, Y., ed., 1971, List of the world active volcanoes: Tokyo, Volcanol. Soc. Japan/IAVCEI/IUGG, 160 p.
Miller, T.P., and Smith, R.L., 1977, Spectacular mobility of ash flows around Aniakchak and Fisher calderas, Alaska: Geology, v. 5, p. 173-176.
----- 1987, Late Quaternary caldera-forming eruptions in the eastern Aleutian arc, Alaska: Geology, v. 15, p. 434-438.
Smith, R.L., Shaw, H.R., Luedke, R.G., and Russell, S.L., 1978, Comprehensive tables giving physical data and thermal energy estimates for young igneous systems of the United States: U.S. Geol. Surv. Open-File Rep. 78-925, 15 p. + tables.

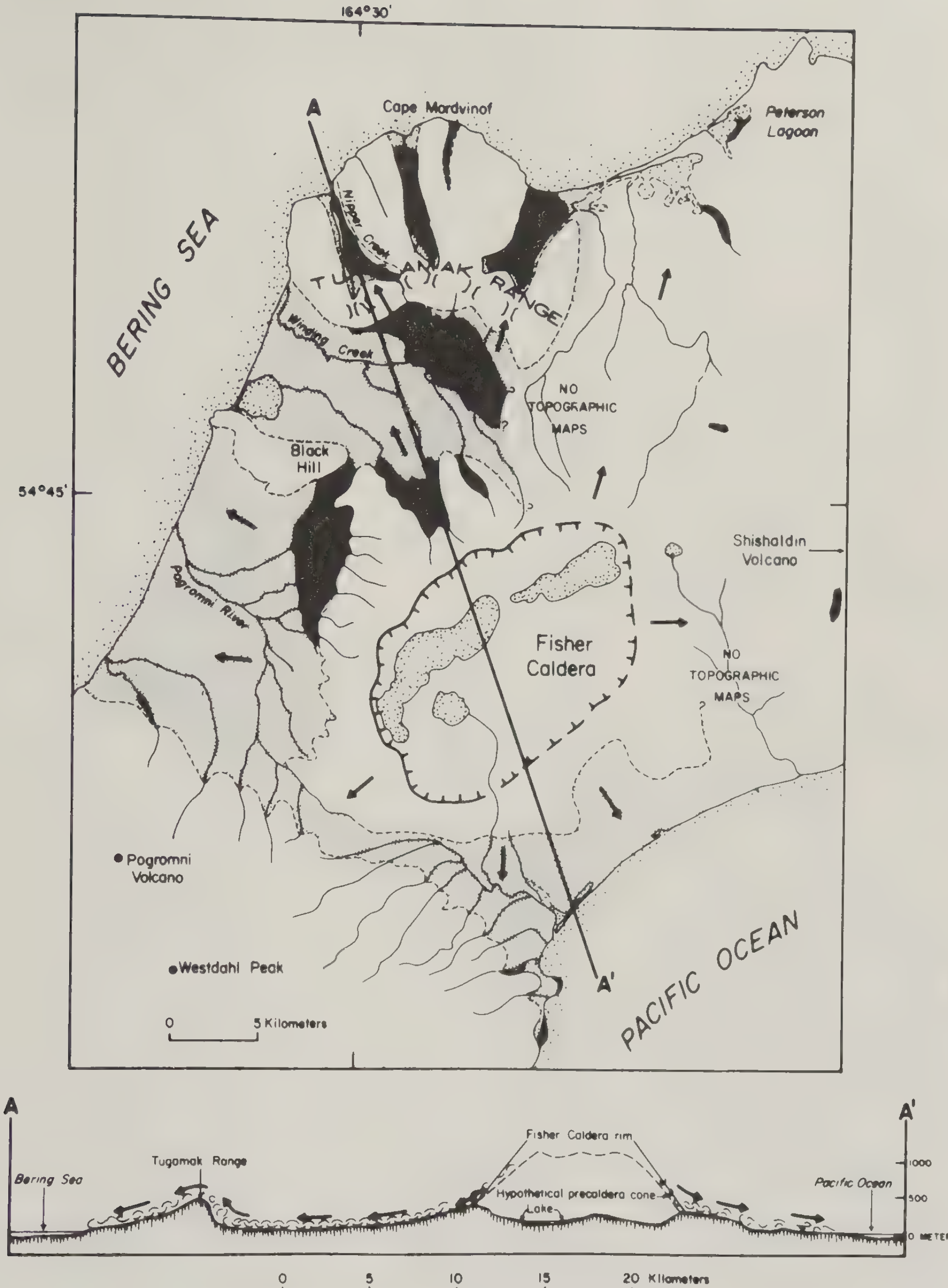

Figure 11.6.1. Fisher Caldera and distribution of ash flows from caldera-forming eruption, from Miller and Smith (1977). Outcrops, solid pattern; inferred original distribution of ash flows, shaded pattern; lakes, stippled pattern (for example, three areas on caldera floor). Arrows denote postulated flow direction of ash flows; brackets denote mountain passes. Cross section along line A-A' illustrates inferred movement of ash flows over Tugamak Range.

PART 3: HISTORICAL UNREST AT LARGE QUATERNARY CALDERAS (continued)

See inside back cover for explanation and abbreviations

EMMONS LAKE

CAVW number (active vent)	Latitude Longitude (degrees)	Diameter (km)	Local tectonic setting	Precaldera edifice	SiO_2 content (wt pct)	Age of collapse (yr B.P.)	Date of unrest	Type and duration of unrest ESTU STHF MGTF H Te	Eruption type
11-02-03	55.35N	19 x 10	Compr	Strato?	R = mafic	>10,000;	1762-86 PS?	---- ---- ---- - --	Ex,ex
(Pavlof)	162.02W				C = 72	possibly	1790	---- ---- ---- - --	unknown
						between	1817	---- ---- ---- - --	ex
11-02-04	55.45N					87,000	ca. 1825?	---- ---- ---- - --	unknown
(Pavlof	161.87W					and	1838	---- ---- ---- - --	"smoke"
Sister=PS)						105,000	1844 or 1845	---- ---- ---- - ??	ex
							1846	---- ---- ---- - --	ex,lf
							1852?	---- ---- ---- - --	"smoke"
							1866?	---- ---- ---- - UQ?	ex
							1880?	---- ---- ---- - --	unknown
							1886	---- ---- ---- - --	unknown
							1892	---- ---- ---- - --	ex
							1894	---- ---- ---- - --	ex
							1901	---- ---- ---- - --	ex
							1906-11	YY-- ---x ---- - --	"smoke",Ex
							1914	---- ---- ---- - --	ex
							1917	x--- ---- ---- - --	ex
							1922-24	---- ---- ---- - --	Ex,ex
							1929-31	---- ---- ---- - --	ex
							1936-48	---- ---- ---- - --	ex,Ex,lf?
							1950-53	---- ---- ---- - --	ex
							1958	---- ---- ---- - --	ex,lf
							1960-63	---- ---- ---- - --	ex,lf
							1966	---- ---- ---- - --	ex,lf
							1973-77+	C-Y- ---- ---- - UQ	Ex,ex,lf
							1980-83	D-Y- ---- ---- - UQ	Ex,ex,lf
							1986-88+	C-Y- ---- ---x - --	Ex,ex

EMMONS LAKE (continued)

TECTONIC SETTING

Emmons Lake Caldera, Pavlof Volcano, and Pavlof Sister Volcano lie in a particularly active part of the Aleutian arc, where the Pacific and North American plates converge at a rate of 7.5 cm/yr, and where great earthquakes ($\underline{M}$ 7.8 and greater) occur on average every 60-80 years. The most recent great earthquake in the area was in 1903, and Kelleher (1970), Sykes (1971), and Davies and others (1981) have termed this area the Shumagin seismic gap. Beavan and others (1983) and McNutt (1987) suggested that tectonic compression in the area might increase eruptive activity of Pavlof. McNutt and Beavan (1987) also noted that the larger, magmatic eruptions of Pavlof occur in the fall, including four in the period 11-15 November of different years; they tentatively attributed this fact to a seasonal, nontidal ocean loading on the North Pacific continental shelf.

A strong northeast-southwest alignment of major vents suggests control by a regional fault of the same trend.

GEOLOGIC HISTORY

The outline of the Emmons Lake Caldera is poorly known; we have sketched an approximate outline based on topography and the distribution of young vents (fig. 11.7.1). A geologic map of the caldera is in preparation (T. Miller, written commun., 1988). Kennedy and Waldron (1955) suggested that the Emmons Lake basin might be a caldera, formed "when the lavas of the Dushkin basalt were being erupted." Alternatively, Miller and Smith (1987) suggest that Emmons Lake Caldera may have been the source of the Old Crow tephra, with an estimated age of 87,000-105,000 yr B.P. and an estimated bulk volume >50 km^3. McNutt and Jacob (1986) identified a low-velocity body beneath Emmons Lake Caldera, but their station spacing was not adequate to define its size and geometry precisely. Most of the postcaldera volcanism has been basaltic.

Pavlof Volcano lies approximately 2-3 km northeast of the rim of Emmons Lake Caldera, along a northeast-trending line of vents that also includes several in the caldera and Pavlof Sister (5 km northeast of Pavlof). Asymmetry of Pavlof suggests that its vent is migrating northeastward, away from the caldera. McNutt (1987) suggests that the magma column is continuous from the surface to a depth of 100-170 km, and that the occurrence of microearthquakes below 100 km depth 8 days before to 2 days after eruptions may indicate transmission of pressure through the magma column.

HISTORICAL ACTIVITY

Frequent, intermittent eruptions occur at Pavlof, including more than 30 in the historical record and more than 20 in this century (McNutt, 1987).

EMMONS LAKE (continued)

HISTORICAL ACTIVITY (continued)

1762-86: There were reports of "signs of activity" (Dall, 1870, p. 466) and that the volcano was "active" (Charisso, cited in Perrey, 1865, p. 21). These reports probably refer to activity of Pavlof Sister, which "became active, fell in, and after a violent earthquake [ceased] its activity..." (McNutt, 1987).

1844, 1846, 1854, 1866: An unusually strong earthquake in 1844, felt at Pavlof Harbor and on nearby Kodiak Island, occurred near the time of the 1844 eruption (exact relation not known). In 1846, a 1-day eruption occurred from a fissure on the flank of the volcano. Another, lesser earthquake was felt on 16 January 1854, and an "extraordinarily strong" earthquake occurred on 25 August 1866, five months <u>after</u> an eruption on 14 March 1866 (Doroshin, 1870). Beavan and others (1983) report great earthquakes in the Shumagin gap in 1788, 1847, and possibly 1903.

1911: The most powerful historical eruption of Pavlof occurred on 6-7 December 1911; announced by earthquakes, the north flank opened, large blocks were ejected, and lava flows issued from the fissure (McNutt, 1987).

1973-present: Seismic monitoring in the Pavlof-Shumagin area began in 1973. Eruptions have been preceded by a few hours to a few weeks of emergent "B-type" and impulsive explosion earthquakes (fig. 11.7.2) that, by analogy with signals of known explosions at the surface, are all attributed to near-surface degassing. In 1974, swarms of these very shallow earthquakes occurred several days before eruptions, sometimes decreasing in number just before an eruption. Again in 1981, these events became more frequent but then decreased in number and size in the 3 days immediately before an eruption (Smithsonian Institution, 1981).

A reversal in tilt direction in the Shumagin region occurred during 1977-80. During that period, regional microseismicity was high, Pavlof did not erupt and exhibited very low seismicity, and most teleseismically recorded deep earthquakes occurred in a cluster behind Pavlof (fig. 11.7.4; McNutt, 1987). Magmatic eruptions resumed at Pavlof in November 1980. McNutt and Beavan (1981) noted a tendency for swarms to occur at Pavlof near fortnightly tidal maxima; McNutt and Beavan (1987) showed that eruptions tend to occur preferentially at times of increased sea-level deviation in the fall and winter (fig. 11.7.5).

Low-frequency and explosion earthquakes increased again at Pavlof during 11-18 July 1983--apparently accompanied by small explosions. Then in October and early November (4, 9, and 11 November), up to 40 low-frequency earthquakes per day accompanied bursts of tremor lasting several minutes to half an hour. Small explosions were recorded seismically during 11-13 November. Tremor became continuous between 1700 and 1900 hr on 14 November, reaching its greatest amplitude between midnight and 1200 hr on 15 November (fig. 11.7.3). Glow was observed at about 2330 hr, and by 1220 hr on 14 November an airline pilot reported a plume rising through clouds. After 15 November, tremor declined but continued at a low level through approximately 16 December 1983, accompanied by low frequency (B-type) earthquakes (McNutt, 1986, 1987). Several bursts of tremor from 13 min to 4 hr in duration marked the end(?) of eruptions in December 1983. After an increase in tremor (and eruptions) on 17-21 December, seismicity decreased to a background level of several tens of events per day and remained at that level as of 2 April 1984. The spectral content of tremor at

EMMONS LAKE (continued)

HISTORICAL ACTIVITY (continued)

Pavlof remained within a narrow range (0.8-3.0 Hz) during more than a decade of recording; McNutt (1986, 1988) proposed that it results from resonance of magma and gas in the conduit.

A new period of eruptions began in mid-April 1986, and continues as of the time of this writing (February 1988). Detection of eruptions depends largely on seismic monitoring of tremor and sightings by commercial airline pilots and weather satellites when weather permits.

REFERENCES

Beavan, J., Hauksson, E., McNutt, S., Bilham, R., and Jacob, K., 1983, Tilt and seismicity changes in the Shumagin seismic gap: Science, v. 222, p. 322-325.

Coats, R.R., 1950, Volcanic activity in the Aleutian arc: U.S. Geol. Surv. Bull. 974-B, p. 35-49.

Dall, W.H., 1870, Alaska and its resources: London, Sampson Low, Son, and Marston, 627 p.

Davies, J., Sykes, L., House, L., and Jacob, K., 1981, Shumagin seismic gap, Alaska Peninsula: History of great earthquakes, tectonic setting, and evidence of high seismic potential: Jour. Geophys. Res., v. 86, p. 3821-3855.

Doroshin, P., 1870, Some volcanoes, their eruptions, and earthquakes in the former Russian possessions in America: Verh. Russisch-Kaiserlichen Mineral. Gesellschaft zu St. Petersburg, 2nd ser., 1870, p. 25-44 (English translation by J.B. Kisslinger).

Grewingk, C., 1850, Beitrag zur Kenntniss der orographischen und geognostischen Beschaffenheit der Nordwestküste Amerikas, mit den anliegenden Inseln: Verh. Russisch-Kaiserlichen Mineral. Gesellschaft zu St. Petersburg, 1848-49, p. 123-278.

Katsui, Y., ed., 1971, List of the world active volcanoes: Tokyo, Volcanol. Soc. Japan/IAVCEI/IUGG, 160 p.

Kelleher, H.A., 1970, Space-time seismicity of the Alaska-Aleutian seismic zone: Jour. Geophys. Res., v. 75, p. 5745-5756.

Kennedy, G.C., and Waldron, H.H., 1955, Geology of Pavlof Volcano and vicinity, Alaska: U.S. Geol. Surv. Bull. 1028-A, 18 p.

McNutt, S.R., 1986, Observations and analysis of B-type earthquakes, explosions, and volcanic tremor at Pavlof Volcano, Alaska: Bull. Seismol. Soc. Am., v. 76, p. 153-175.

----- 1987, Eruption characteristics and cycles at Pavlof Volcano, eastern Aleutians, and their relation to regional earthquake activity: Jour. Volcanol. Geotherm. Res., v. 31, p. 239-267.

----- 1988, Volcanic tremor at Pavlof Volcano, Alaska, 1973-1986: Pure Appl. Geophys. [in press].

McNutt, S.R., and Beavan, R.J., 1981, Volcanic earthquakes at Pavlof Volcano correlated with the solid earth tide: Nature, v. 294, p. 615-618.

----- 1987, Eruptions of Pavlof Volcano and their possible modulation by ocean load and tectonic stresses: Jour. Geophys. Res., v. 92, no. B11, p. 11,509-11,523.

McNutt, S.R., and Jacob, K.H., 1986, Determination of large-scale velocity structure of the crust and upper mantle in the vicinity of Pavlof Volcano, Alaska: Jour. Geophys. Res., v. 91, no. B5, p. 5013-5022.

EMMONS LAKE (continued)

REFERENCES (continued)

Miller, T.P., and Smith, R.L., 1983, Calderas of the eastern Aleutian arc [abs.]: Eos, Trans. Am. Geophys. Union, v. 64, p. 877.

----- 1987, Late Quaternary caldera-forming eruptions in the eastern Aleutian arc, Alaska: Geology, v. 15, p. 434-438.

Perrey, A., 1865, Documents sur les tremblements de terre et les phenomenes volcaniques des îles Aleutiennes, de la peninsule d'Aljaska et de la côte NO d'Amerique. Mem. Acad. Sci. Arts Belles-Lettres, Dijon, 131 p.

Simkin, T., Siebert, L., McClelland, L., Bridge, D., Newhall, C., and Latter, J.H., 1981, Volcanoes of the world: Stroudsburg, Pa., Hutchinson Ross Publ. Co., 232 p.

Smith, R.L., Shaw, H.R., Luedke, R.G., and Russell, S.L., 1978, Comprehensive tables giving physical data and thermal energy estimates for young igneous systems of the United States: U.S. Geol. Surv. Open-File Rep. 78-925, 15 p. + tables.

Smithsonian Institution, Scientific Event Alert Network (SEAN), 1981, 1983-87, Pavlof: SEAN Bull., v. 6, no. 9, v. 8, nos. 10-12; v. 9, nos. 1, 3; v. 11, nos. 3-8, 10, 12; v. 12, nos. 1, 3, 5-8 (principal correspondents: T. Miller, E. Yount, and S. McNutt).

Sykes, L.R., 1971, Aftershock zone of great earthquakes, seismicity gaps, and earthquake prediction for Alaska and the Aleutians: Jour. Geophys. Res., v. 76, p. 8021-8041.

Volcanological Society of Japan, 1977, Pavlof: Bull. Volcanic Eruptions, no. 15, p. 41.

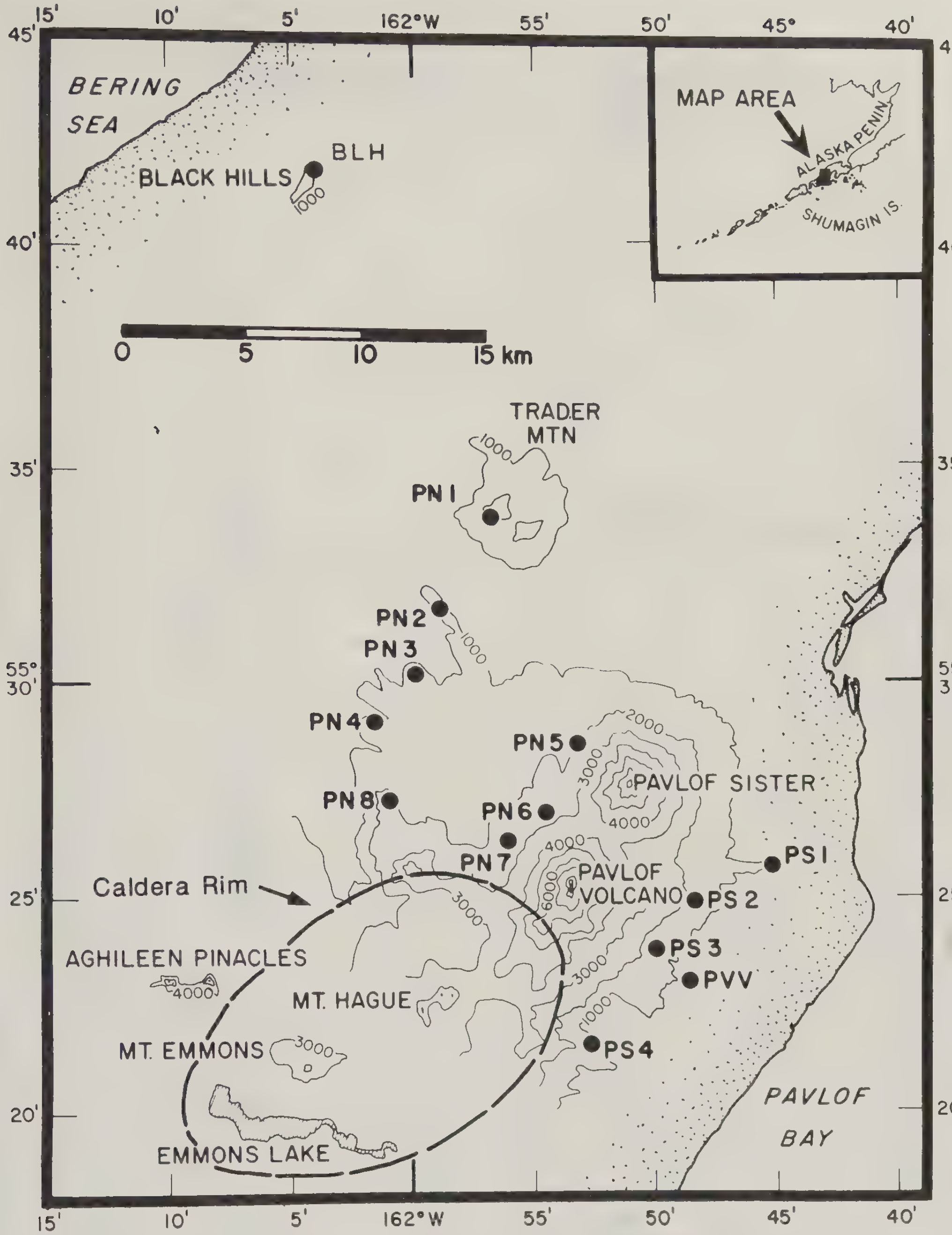

Figure 11.7.1. Sketch map showing locations of Emmons Caldera, Pavlof Volcano, and Pavlof Sister Volcano (topographic rim of Emmons Caldera added to base map of McNutt, 1987). Solid circles represent seismic stations.

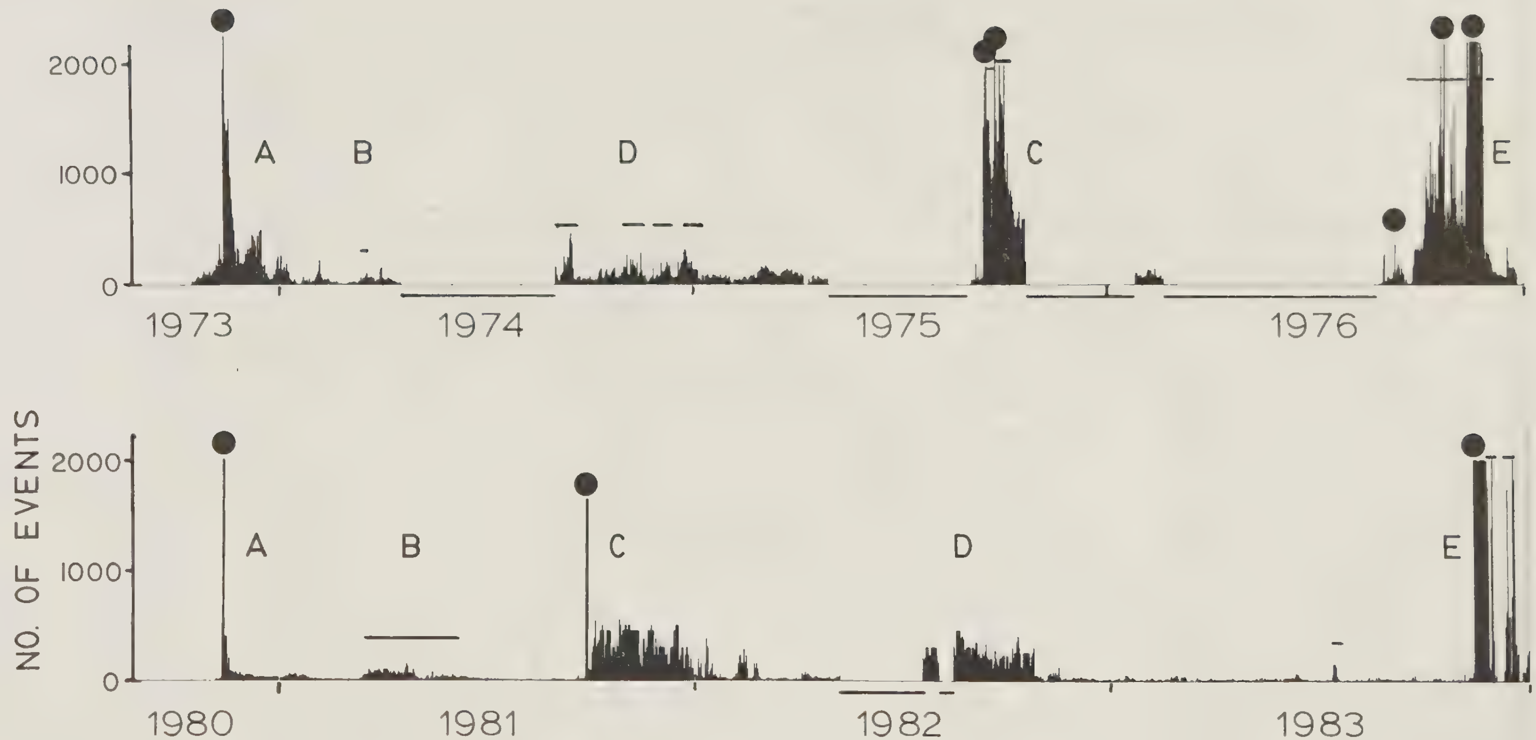

Figure 11.7.2. Number of B-type volcanic earthquakes and explosions per day at Pavlof Volcano during 1973-83, from McNutt (1987). Magmatic eruptions are indicated by solid circles, explosions by horizontal bars above data. Data gaps are indicated by horizontal bars beneath data.

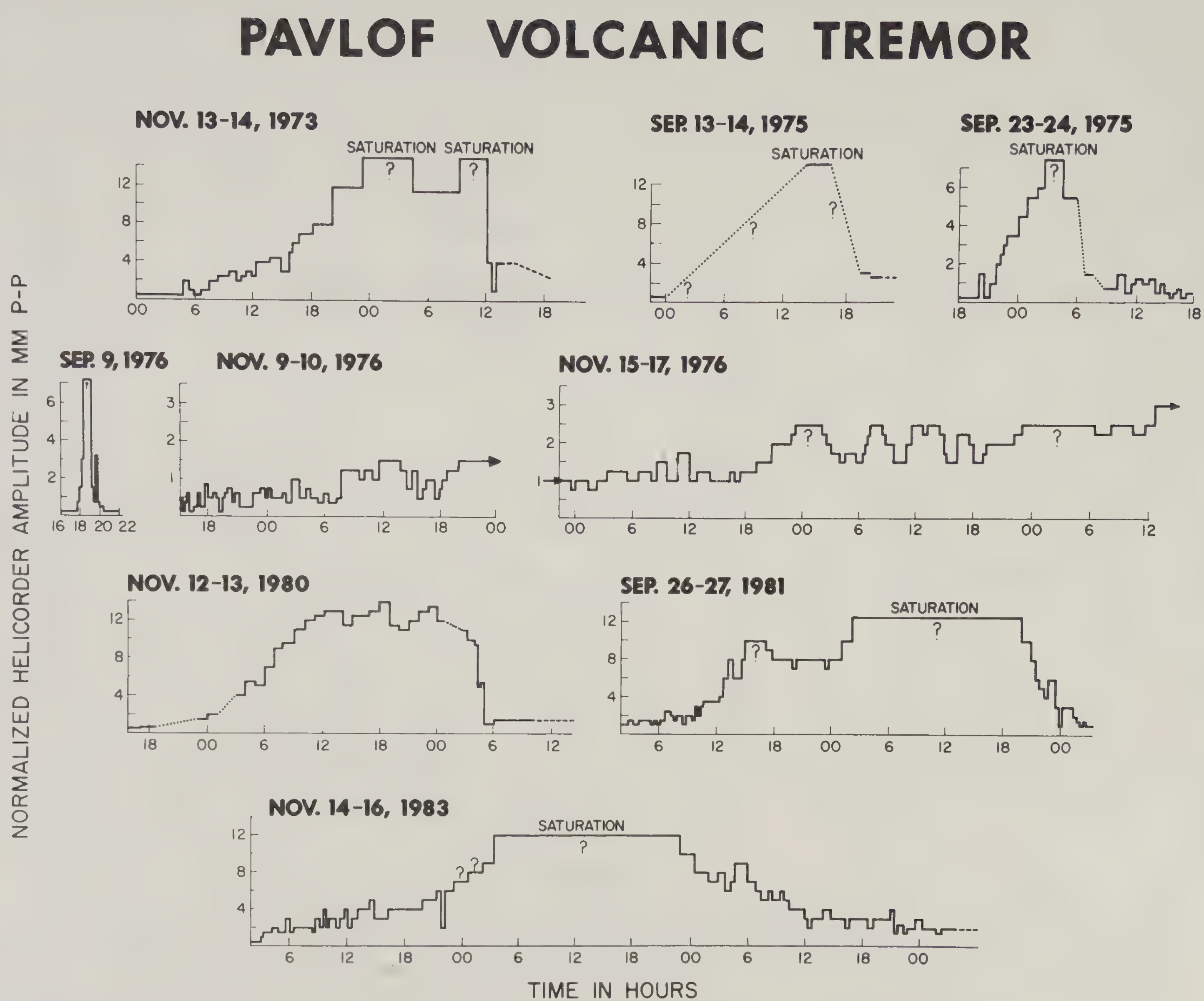

Figure 11.7.3. Tremor amplitude during magmatic eruptions at Pavlof Volcano, from McNutt (1987). Amplitudes normalized; numbers on horizontal axes, times in hours. Dotted where inferred (no seismograms available); dashed where intermittent.

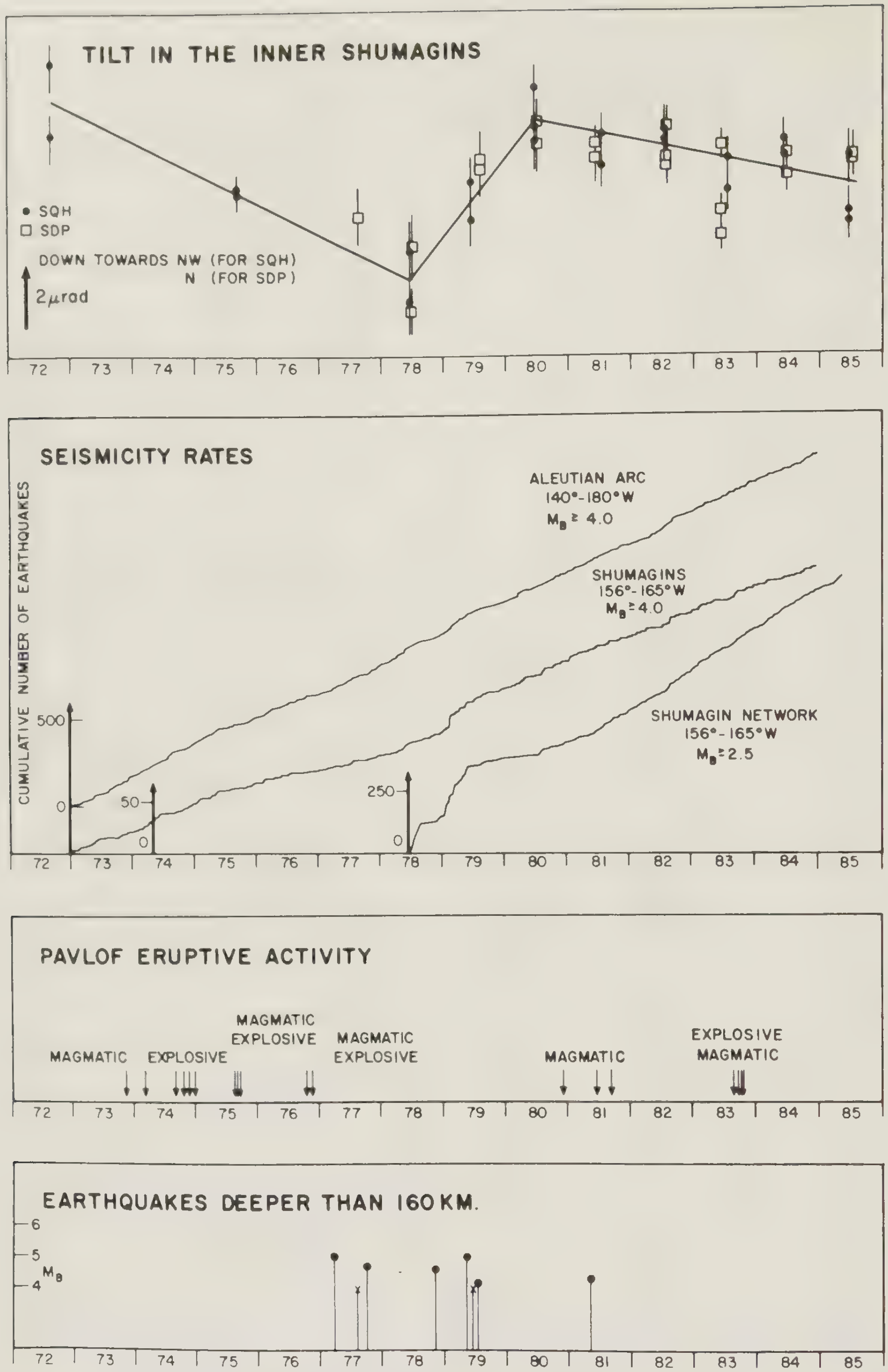

Figure 11.7.4. Tilt, seismicity rates, Pavlof eruptive activity, and deep earthquakes in the Shumagin region for time period 1972-85 (McNutt, 1987).

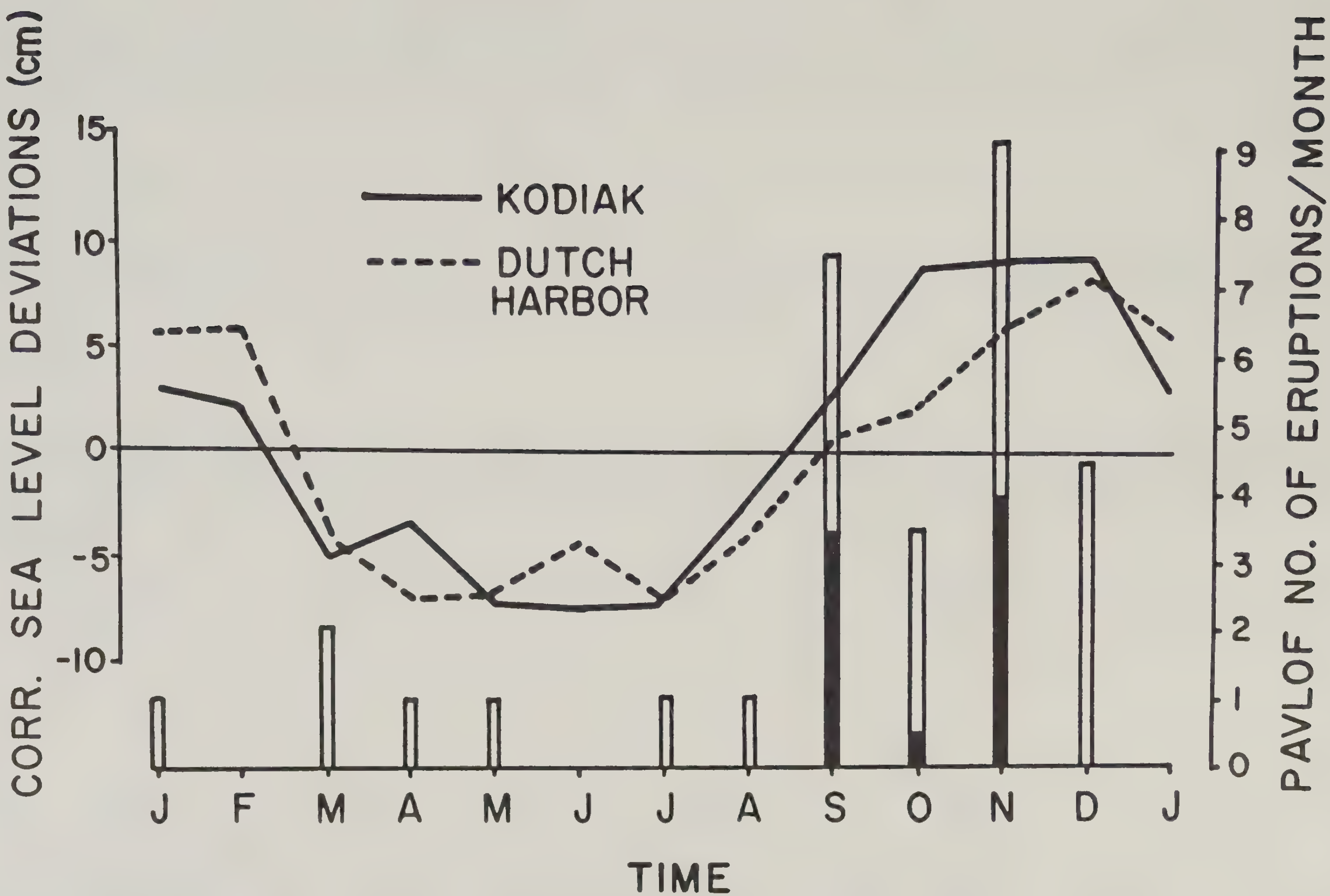

Figure 11.7.5. Deviations between monthly mean sea level and long-term mean sea level (1950-74), and number of eruptions per month at Pavlof Volcano (McNutt and Beavan, 1987). Monthly mean-sea-level data corrected for atmospheric pressure. Kodiak is about 500 km east-northeast of Pavlof; Dutch Harbor is about 350 km west-northwest of Pavlof. Histogram bars are solid for magmatic eruptions and open for explosions. Note correlation between eruptions and increased sea level in fall and winter. Copyright by the American Geophysical Union.

VENIAMINOF

CAVW number (active vent)	Latitude Longitude (degrees)	Diameter (km)	Local tectonic setting	Precaldera edifice	SiO_2 content (wt pct)	Age of collapse (yr B.P.)	Date of unrest	Type and duration of unrest ESTU STHF MGTF H Te	Eruption type
11-02-07	56.17N	10	Compr	Strato	R = 53-54	3,700	1830-39	---- ---- ---- - --	Ex?
(Veniaminof)	159.38W				C = 65		1852?	---- ---- ---? - --	"smoke"
							1874?	---- ---- ---? - --	"smoke"
							1892	---- ---- ---- - --	Ex
							1930?	---- ---- ---? - --	"smoke"
							1939	---- ---- ---- - --	ex
							1944	---- ---- ---- - --	unknown
							1956	---- ---- ---- - --	ex
							1983-84	Y-Y- ---Y ---Y - --	ex,lf
							1987	---- ---- ---- - --	ex

TECTONIC SETTING

Veniaminof Caldera is on the Alaska Peninsula, near the northeastern end of the Shumagin seismic gap (Kelleher, 1970; Sykes, 1971; Davies and others, 1981). McNutt (1987) suggests that activity of Veniaminof might be controlled in part by buildup of regional strain, as discussed below and under the Emmons Lake Caldera section.

GEOLOGIC HISTORY

The Veniaminof Caldera (figs. 11.8.1, 11.8.2) formed in the summit of a large (more than 400 km^3) basaltic-andesite stratovolcano approximately 3,700 yr B.P. (Miller and Smith, 1975, 1987). Ash flows of the caldera-forming eruption range from dacite (early) to andesite (late) (Miller and Smith, 1987). The active vent is one of several in a NW-SE-trending belt that bisects the caldera (Detterman and others, 1981; B. Yount, written commun., 1987).

HISTORICAL ACTIVITY

Early eruptions are known from reports by Grewingk (1850), Doroshin (1870), and Becker (1898). On 4 August 1838 an explosion occurred with a cracking sound and loud rumble; ash blew northeast as far as Katmai (Doroshin, 1870). The largest historical eruption was in 1892, when the skies of southwest Alaska were darkened (Becker, 1898). McNutt (1987) suggested that Veniaminof was active for a few years before and after the 1938 Shumagin earthquake, but not for 30 years before or after that period, until 1983;

VENIAMINOF (continued)

HISTORICAL ACTIVITY (continued)

therefore, the activity of Veniaminof since 1983 might foreshadow another large earthquake in this region, as might vigorous activity of Pavlof Volcano (McNutt, 1987). However, a 1944 eruption reported by Coats (1950) and an eruption in 1956 recently documented by Yount and others (1985) indicate that Veniaminof was not entirely quiet during this interval.

Before an eruption began in June 1983, the nearest seismometer was 30 km from the volcano; available reports describe seismicity only after the start of the eruption. Since June 1983, some earthquakes were felt at Perryville (25 km away) during and between eruptions. Tremor amplitude (and hence vigor of fountaining?) in early October 1983 was about half that during the June 1983 eruption. The eruption has included mild explosions, lava fountaining, lava flow(s), and growth of an intracaldera cone. Approximately 45 x 10^6 m^3 of lava was extruded from June 1983 to February 1984. Seismic activity declined in late March and early April 1984 but increased slightly in mid-April.

During field work in August 1984, occasional white vapor plumes and roaring noises lasting about 15 minutes alternated with 20-minute periods of quiet. No general increase in steaming was noted, but visibility was poor. Small earthquakes were felt during both the roaring and the quiet periods (B. Yount and T. Miller in Smithsonian Institution, 1984). A Lamont-Doherty Geological Observatory seismic station 30 km from the volcano recorded 3 events (low-frequency volcanic earthquakes and tremor) on 25 November; no events were large enough to trigger other stations, so magnitudes were less than 2.5 or 3.

Residents of Perryville were awakened by rumbling from the volcano at 0400 hr on 29 November 1984, and by 0800 hr a black ash cloud was rising from the vent. The column rose to a maximum height of 5.4 km; no incandescence was reported. Seismicity during this episode was minor compared with that at the onset of activity in June 1983.

A minor ash emission was noted on 19 March 1987 (Smithsonian Institution, 1987).

REFERENCES

Becker, G.F., 1898, Reconnaissance of the gold fields of southern Alaska, with some notes on general geology: U.S. Geol. Surv., 18th Ann. Rep., pt. 3, p. 13-24.

Coats, R.R., 1950, Volcanic activity in the Aleutian arc: U.S. Geol. Surv. Bull. 974-B, p. 35-49.

Davies, J., Sykes, L., House, L., and Jacob, K., 1981, Shumagin seismic gap, Alaska Peninsula: History of great earthquakes, tectonic setting, and evidence of high seismic potential: Jour. Geophys. Res., v. 86, p. 3821-3855.

Detterman, R.L., Miller, T.P., Yount, E., and Wilson, F., 1981, Quaternary geologic map of the Chignik and Sutwik Island quadrangles, Alaska: U.S. Geol. Surv. Misc. Invest. Ser. I-1292, 1 sheet, scale 1:250,000.

Doroshin, P., 1870, Some volcanoes, their eruptions, and earthquakes in the former Russian possessions in America: Verh. Russisch-Kaiserlichen Mineral. Gesellschaft zu St. Petersburg, 2nd ser., 1870, p. 25-44 (English translation by J.B. Kisslinger).

VENIAMINOF (continued)

REFERENCES (continued)

Grewingk, C., 1850, Beitrag zur Kenntniss der orographischen und geognostischen Beschaffenheit der Nordwestküste Amerikas, mit den anliegenden Inseln: Verh. Russisch-Kaiserlichen Mineral. Gesellschaft zu St. Petersburg, 1848-49, p. 123-278.

Kelleher, H.A., 1970, Space-time seismicity of the Alaska-Aleutian seismic zone: Jour. Geophys. Res., v. 75, p. 5745-5756.

Knappen, R.S., 1926, Geology and mineral resources of the Aniakchak district: U.S. Geol. Surv. Bull. 797, p. 161-223.

McNutt, S.R., 1987, Eruption characteristics and cycles at Pavlof Volcano, eastern Aleutians, and their relation to regional earthquake activity: Jour. Volcanol. Geotherm. Res., v. 31, p. 239-267.

Miller, T.P., and Smith, R.L., 1975, Ash flows on the Alaska Peninsula: A preliminary report on their distribution, composition, and age [abs.]: Geol. Soc. Am. Abstracts with Programs, v. 7, no. 7, p. 1201.

----- 1987, Late Quaternary caldera-forming eruptions in the eastern Aleutian arc, Alaska: Geology, v. 15, p. 434-438.

Smith, R.L., Shaw, H.R., Luedke, R.G., and Russell, S.L., 1978, Comprehensive tables giving physical data and thermal energy estimates for young igneous systems of the United States: U.S. Geol. Surv. Open-File Rep. 78-925, 15 p. + tables.

Smithsonian Institution, Scientific Event Alert Network (SEAN), 1983, 1984, 1987, Veniaminof: SEAN Bull., v. 8, nos. 5-12; v. 9, nos. 1-4, 8; v. 12, no. 3 (contributions from B. Yount, T. Miller, J. Taber, K. Hudnut, and J. Reeder).

Sykes, L.R., 1971, Aftershock zone of great earthquakes, seismicity gaps, and earthquake prediction for Alaska and the Aleutians: Jour. Geophys. Res., v. 76, p. 8021-8041.

U.S. Geological Survey, 1963, limited revisions 1983, Chignik topographic map, Alaska topographic series, scale 1:250,000.

Yount, E., and Miller, T.P., 1987, Hazard implications of the 1983-84 eruption of Mount Veniaminof, Alaska [abs.]: Alaska Geol. Soc. 1987 Geol. Hazards Symposium.

Yount, M.E., Miller, T.P., Emanuel, R.P., and Wilson, F.H., 1985, Eruption in an ice-filled caldera, Mount Veniaminof, Alaska Peninsula, in Bartsch-Winkler, S., and Reed, K.M., eds., The United States Geological Survey in Alaska: accomplishments during 1983: U.S. Geol. Surv. Circular 945, p. 59-60.

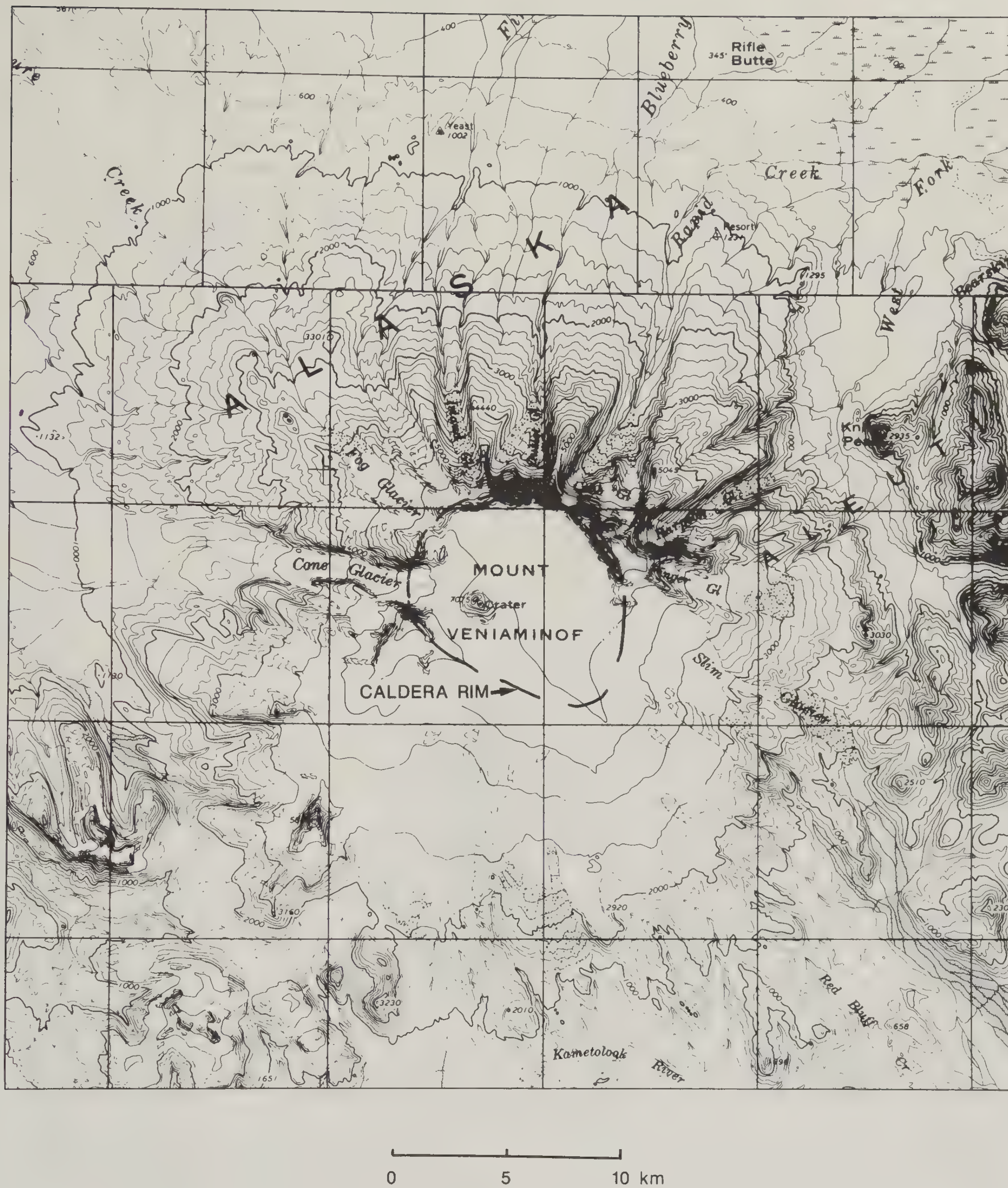

Figure 11.8.1. Topographic map showing Veniaminof Volcano and its summit caldera (U.S. Geological Survey, 1963).

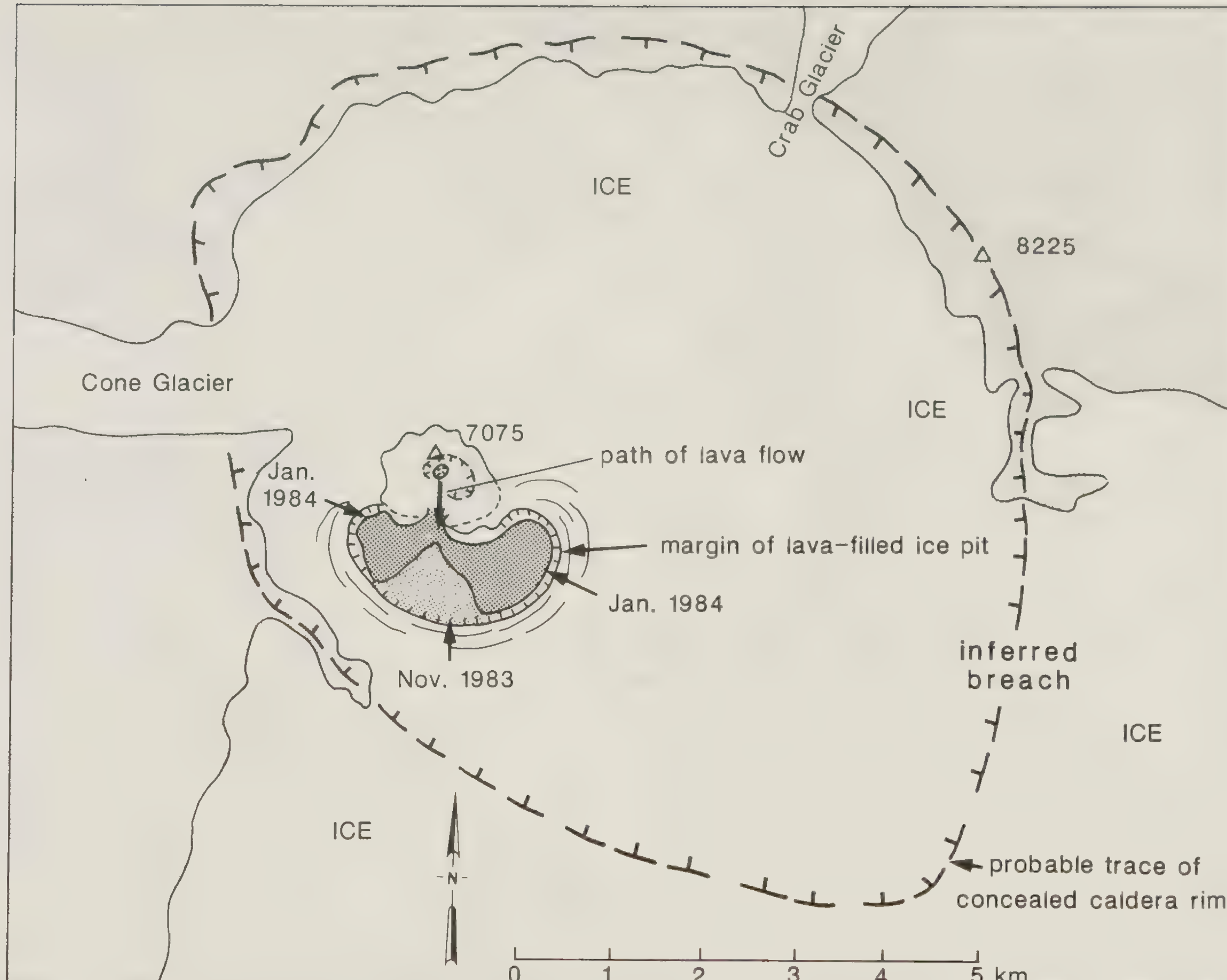

Figure 11.8.2. Sketch map of Veniaminof Caldera by Elizabeth Yount, showing eruptive activity on 15 June 1983 (Smithsonian Institution, 1983). Inferred breach in east caldera rim is after Yount and others (1985).

ANIAKCHAK

CAVW number (active vent)	Latitude Longitude (degrees)	Diameter (km)	Local tectonic setting	Precaldera edifice	SiO_2 content (wt pct)	Age of collapse (yr B.P.)	Date of unrest	Type and duration of unrest ESTU STHF MGTF H Te	Eruption type
11-02-09 (Aniakchak)	56.88N 158.15W	9.5	Compr	Strato	R = 64-66 C = 68, late andesite	3,400	1931	---- ---- ---- - --	Ex,dm

TECTONIC SETTING

Aniakchak Caldera lies along the eastern Aleutian arc, above a boundary between two subducted lithospheric segments (fig. 11.9.1) (Kienle and others, 1983). The caldera is ice free, about 10 km in diameter, and more than a kilometer deep.

GEOLOGIC HISTORY

Aniakchak Caldera (figs. 11.9.2, 11.9.3) formed in the summit of a glacially dissected andesitic stratovolcano that was built on the flank of a range of Jurassic-Tertiary basement. Ash-flow tuffs from the caldera-forming eruption extend 80 km from the caldera rim onto the Bering Sea lowlands. As at Fisher Caldera, these ash flows were extremely mobile; near Aniakchak they crossed over mountain passes that are 260 m higher than terrain closer to the volcano (Miller and Smith, 1977, 1987). The weighted mean average of three charcoal samples from the ash-flow tuff is 3,430±10 yr B.P. (Miller and Smith, 1987).

An older ash-flow tuff in isolated localities on the flanks of Aniakchak suggests the occurrence of an earlier violent eruption of unknown volume. The unit is postglacial; stratigraphic relationships constrain its age between 4,400 and 10,000 yr B.P. (Miller and Smith, 1987). No associated caldera has been identified.

Seven postcaldera cones and necks occur on the caldera floor; the largest of these (Vent Mountain) rises 670 m above the caldera floor.

HISTORICAL ACTIVITY

A series of violent explosions occurred during 1-11 May 1931 and again on 20 May; the source was apparently a cinder cone near the base of the northwest caldera wall (Jaggar, 1932). A dacitic dome was emplaced in the vent in the waning stages of the eruption.

ANIAKCHAK (continued)

REFERENCES

Coats, R.R., 1950, Volcanic activity in the Aleutian arc: U.S. Geol. Surv. Bull. 974-B, p. 35-49.

Hubbard, B.R., 1931, World inside a mountain: Aniakchak, the new volcanic wonderland of the Alaska Peninsula, is explored: Natl. Geogr., v. 60, p. 319-345.

Jaggar, T.A., 1932, Aleutian eruptions, 1930-1932: Volcano Lett., no. 375, p. 1-3.

Katsui, Y., ed., 1971, List of the world active volcanoes: Tokyo, Volcanological Soc. Japan/IAVCEI/IUGG, 160 p.

Kienle, J., Swanson, S.E., and Pulpan, H., 1983, Magmatism and subduction in the Eastern Aleutian arc, in Shimozuru, D., and Yokoyama, I., eds., Arc volcanism: physics and tectonics: Tokyo, Terra Sci. Publ., p. 191-224.

Knappen, R.S., 1926, Geology and mineral resources of the Aniakchak district: U.S. Geol. Surv. Bull. 797, p. 161-223.

Miller, T.P., and Smith, R.L., 1977, Spectacular mobility of ash flows around Aniakchak and Fisher calderas, Alaska: Geology, v. 5, p. 173-176.

----- 1987, Late Quaternary caldera-forming eruptions in the eastern Aleutian arc, Alaska: Geology, v. 15, p. 434-438.

Smith, R.L., Shaw, H.R., Luedke, R.G., and Russell, S.L., 1978, Comprehensive tables giving physical data and thermal energy estimates for young igneous systems of the United States: U.S. Geol. Surv. Open-File Rep. 78-925, 15 p. + tables.

Smith, W.R., 1925, Aniakchak Crater, Alaska Peninsula: U.S. Geol. Surv. Prof. Paper 132-J, p. 139-149.

Figure 11.9.1. Volcanoes of eastern Aleutian arc, including Aniakchak, Ugashik, and Katmai Calderas (modified from Kienle and others, 1983).

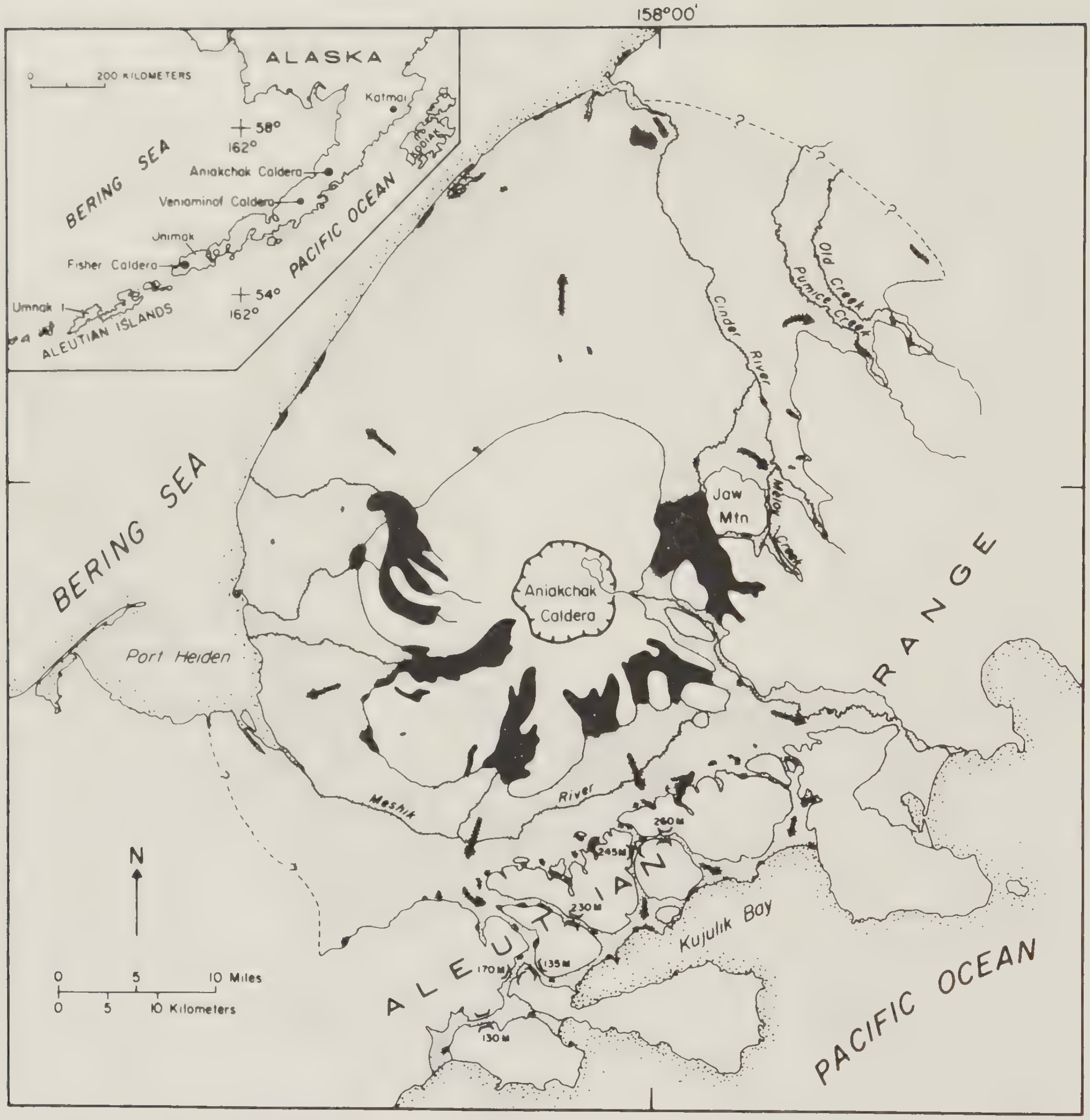

Figure 11.9.2. Aniakchak Caldera and distribution of surrounding ash flows, from Miller and Smith (1977). Outcrops shown in solid pattern; inferred original distribution of ash flows shown in shaded pattern. Arrows denote postulated flow direction of ash flows; brackets and numbers denote mountain passes and their altitudes in meters, respectively.

Figure 11.9.3. Relief map of Aniakchak Crater and vicinity, Alaska Peninsula, from Smith (1925).

PART 3: HISTORICAL UNREST AT LARGE QUATERNARY CALDERAS (continued)
See inside back cover for explanation and abbreviations

UGASHIK

CAVW number (active vent)	Latitude Longitude (degrees)	Diameter (km)	Local tectonic setting	Precaldera edifice	SiO_2 content (wt pct)	Age of collapse (yr B.P.)	Date of unrest	Type and duration of unrest ESTU STHF MGTF H Te	Eruption type
11-02-13A (Peulik=P)	57.75N 156.35W	5 x 6	Compr	Strato	R = b	40,000-171,000	1814 (P)	---- ---- ---- - --	Ex
							1852? (P)	---- ---- ---? - --	unknown
							1977 (U)	xx-- ---- ---- x --	Ex
11-02-13B (Ukinrek Maars =U)	57.83N 158.51W								

TECTONIC SETTING

Ugashik Caldera is located south of Lake Becharof on the Alaska Peninsula, on the boundary between the Semidi and Katmai segments of the Aleutian arc (fig. 11.10.1). This position astride a deep-seated cross-arc fault is thought to be favorable for formation of the caldera and back-arc maars (Kienle and others, 1983). The Ukinrek Maars lie at the intersection of this segment boundary with the NE-SW-trending Bruin Bay fault, a major regional reverse fault that dips steeply northwest with that side upthrown (Kienle and others, 1980).

GEOLOGIC HISTORY

A precaldera cone has been mostly removed by erosion, and the north rim of Ugashik Caldera has been breached by Peulik Volcano, a postglacial andesitic stratocone. Postcaldera nonglaciated silicic domes occupy the interior of the caldera (Miller and Smith, 1987). The caldera-forming eruption is tentatively assigned a late Pleistocene but pre-Holocene age, based on inferred relationships to deposits dated at about 40,000 yr B.P. and 171,000 yr B.P. (Miller and Smith, 1987).

The Ukinrek Maars (formed in 1977, 13 km north of Peulik) erupted alkali olivine basalt and are thought not to be connected to the Peulik magma plumbing system (Kienle and others, 1980).

HISTORICAL ACTIVITY

Little is known about historical eruptions of Peulik. Around 1814, "the summit of Peulik collapsed with a rumble, covering the base with enormous boulders. For about a week after this event, vapor rose from almost the entire surface of the mountain" (Doroshin, 1870).

UGASHIK (continued)

HISTORICAL ACTIVITY (continued)

In 1977, a pulse of alkali olivine basalt magma rose into water-saturated till and silicic volcanics 13 km north of Peulik. Ten days of phreatomagmatic eruptions ensued; these eruptions formed the Ukinrek Maars and spread ash north and east of the maars for at least 160 km (Kienle and others, 1980; Self and others, 1980).

COMMENTS

Ugashik Caldera is included in this compilation on the basis of Peulik's activity. The Ukinrek Maars are noted here with the Ugashik Caldera system because basaltic magma responsible for maar formation, even if not directly connected with the Ugashik magma feeder system, may have risen along a segment-boundary transverse fault connecting the two localities.

REFERENCES

Coats, R.R., 1950, Volcanic activity in the Aleutian arc: U.S. Geol. Surv. Bull. 974-B, p. 35-49.

Doroshin, P., 1870, Some volcanoes, their eruptions, and earthquakes in the former Russian possessions in America: Verh. Russisch-Kaiserlichen Mineral. Gesellschaft zu St. Petersburg, 2nd ser., 1870, p. 25-44 (English translation by J.B. Kisslinger).

Kienle, J., Kyle, P.R., Self, S., Motyka, R.J., and Lorenz, V., 1980, Ukinrek Maars, Alaska, I. April 1977 eruption sequence, petrology and tectonic setting: Jour. Volcanol. Geotherm. Res., v. 7, p. 11-37.

Kienle, J., Swanson, S.E., and Pulpan, H., 1983, Magmatism and subduction in the Eastern Aleutian arc, in Shimozuru, D., and Yokoyama, I., eds., Arc volcanism: physics and tectonics: Tokyo, Terra Sci. Publ., p. 191-224.

Miller, T.P., and Smith, R.L., 1987, Late Quaternary caldera-forming eruptions in the eastern Aleutian arc, Alaska: Geology, v. 15, p. 434-438.

Self, S., Kienle, J., and Huot, J.-P., 1980, Ukinrek Maars, Alaska, II. Deposits and formation of the 1977 craters: Jour. Volcanol. Geotherm. Res., v. 7, p. 39-65.

U.S. Geological Survey, 1963, limited revisions 1983, Ugashik topographic map, Alaska topographic series, scale 1:250,000.

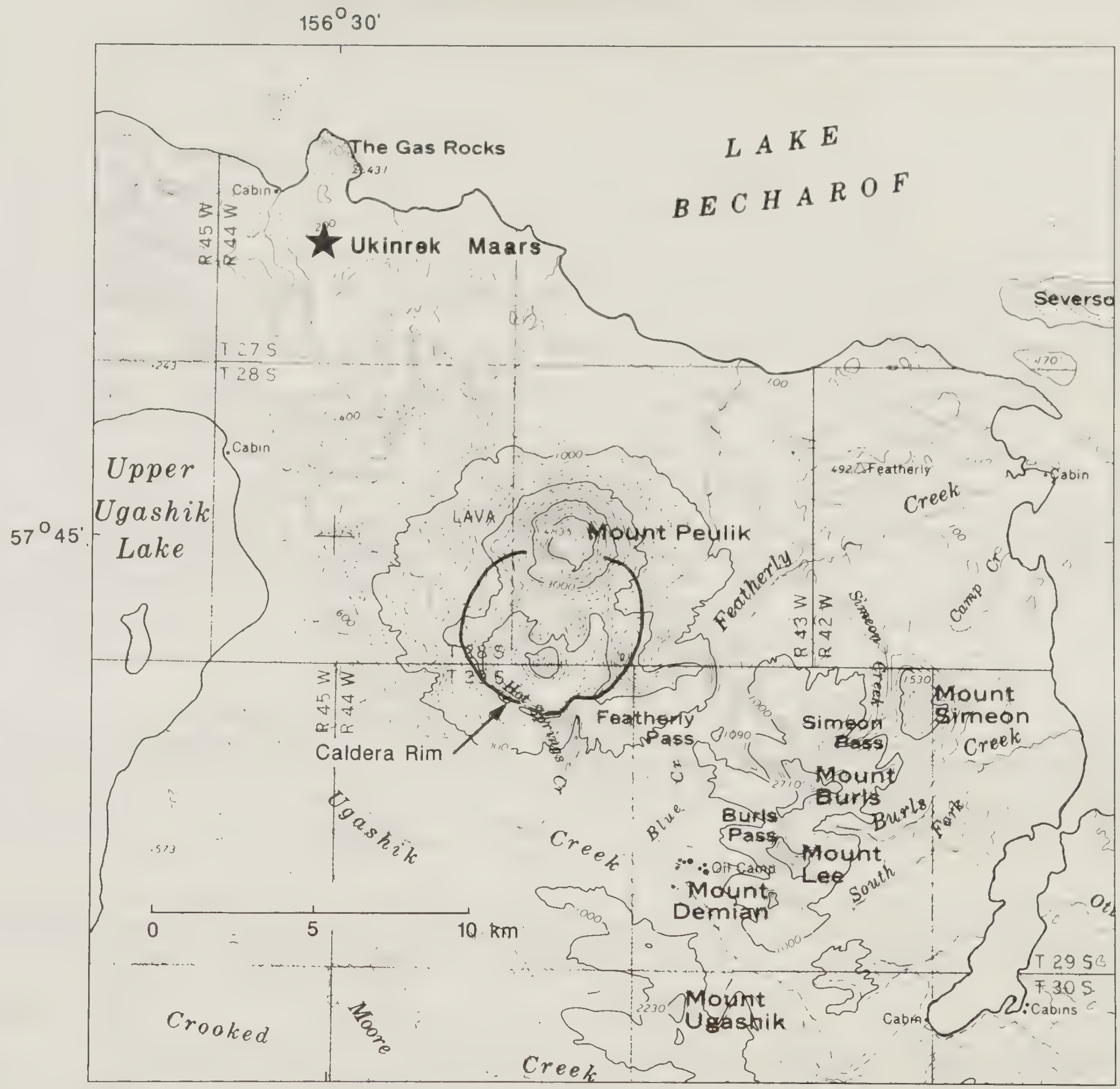

Figure 11.10.1. Topographic map showing Peulik Volcano, inferred outline of Ugashik Caldera, and approximate location of the Ukinrek Maars (star) (U.S. Geological Survey, 1963).

PART 3: HISTORICAL UNREST AT LARGE QUATERNARY CALDERAS (continued)
See inside back cover for explanation and abbreviations

KATMAI/NOVARUPTA

CAVW number (active vent)	Latitude Longitude (degrees)	Diameter (km)	Local tectonic setting	Precaldera edifice	SiO_2 content (wt pct)	Age of collapse (yr B.P.)	Date of unrest	Type and duration of unrest ESTU STHF MGTF H Te	Eruption type
11-02-16 (Novarupta)	58.27N 155.16W	2 x 3	Compr	None?	R = C= r-a	A.D. 1912	1912	C--- Z--Z ---Z - --	EX,dm
11-02-19 (Katmai)	55.27N 154.98W	3 x 4		Strato	R = none	A.D. 1912	1912	C--- Z--- ---Z - --	Pex
					C = d		1929-31?	---- ---- ---x - --	none?
11-02-17 (Griggs)	58.35N 155.12W				R = ?		1965?	---- ---- ---x - --	none
11-02-18 (Trident)	58.23N 155.12W				R = a		1912-13?	---- ---- ---- - --	ex?
							1949-68	xx-- ---- ---F - --	ex,Ex,lf
							ca. 1974-75	---- ---- ---- - --	Ex,lf
11-02-14 (Martin)	58.15N 155.38W				R = 63-64		1951?	---- ---- ---- - --	ex?
							1953?	---- ---- ---- - --	ex?
11-02-15 (Mageik)	58.20N 155.25W						1912	---- ---- ---- - --	landsl
							1927?	---- ---- ---- - --	ex?
							1929?	---- ---- ---- - --	ex?
							1936?	---- ---- ---- - --	Ex?
							1946?	---- ---- ---? - --	none?

TECTONIC SETTING

Katmai and other volcanoes of the Aleutian arc are related to subduction of the Pacific plate beneath the North American plate, at a rate of approximately 6-7 cm/yr (Kienle and Swanson, 1983; Kienle and others, 1983). Both the Pacific plate and the overlying North American plate are segmented, and volcanoes above two of three main segment breaks (Ugashik and Aniakchak) are major silicic centers; Katmai and Kaguyak lie within a segment, possibly atop more subtle discontinuities in the arc (Kienle and others, 1983).

KATMAI/NOVARUPTA (continued)

GEOLOGIC HISTORY

The Katmai group of volcanoes includes five stratovolcanoes (Mt. Katmai, Trident, Mt. Griggs, Mageik and Mt. Martin), two dacite domes (Falling Mountain and Cerberus), and Novarupta, the principal vent for the Valley of Ten Thousand Smokes (VTTS) ash flow and now largely filled with ejecta and a rhyolite-dacite dome (figs. 11.11.1-11.11.3). The sizes, shapes, and interconnections of magma bodies beneath these vents are not well known. However, the eruption at Novarupta and collapse at Mt. Katmai in 1912 and petrologic and structural relations of those vents with Trident suggest that Novarupta and Mt. Katmai are hydraulically connected via Trident at a shallow depth (Hildreth, 1987). In addition, S-wave attenuation (Kubota and Berg, 1967; Matumoto, 1971) suggests one or more large magma bodies beneath the area. Matumoto (1971) inferred three 15-km-diameter lenses of S-wave attenuation--one less than 10 km beneath the Katmai-Novarupta-Trident-Griggs area, another beneath that at 20-30 km depth, and a third at 20-30 km depth beneath Mageik and Martin (fig. 11.11.4).

A -35 mgal Bouguer gravity anomaly centered near Katmai Pass (Decker, 1963; Berg and others, 1967; Kienle, 1969; Kienle and Swanson, 1983) may reflect the same magma bodies and/or low-density fill in the Valley of Ten Thousand Smokes (fig. 11.11.5).

Hildreth (1983, 1987) inferred that rhyolitic, dacitic, and andesitic magma coexisted, perhaps in related but physically discrete parts of a magma reservoir beneath the Novarupta-Trident-Katmai area, well before the 1912 eruption.

HISTORICAL ACTIVITY

1912: The eruption of Novarupta in 1912 was the largest eruption in this century. About 15 km^3 of magma was erupted; the adjacent Valley of Ten Thousand Smokes received 11-15 km^3 of ash-flow tuff, and about 20 km^3 of airfall tephra blew to the southeast for more than 1,000 km (Griggs, 1922; Hildreth, 1983). All or nearly all products were erupted from Novarupta (Curtis, 1968; Hildreth, 1983). The summit of Mt. Katmai collapsed to form a 3 km x 4 km caldera, apparently in hydraulic response to the eruption of Novarupta. On the basis of petrologic and structural arguments, Hildreth (1987) infers that magma from Trident moved to fill a posteruption void beneath Novarupta, in turn allowing magma from Katmai to move toward Trident and allowing the Katmai summit to collapse.

Few people lived in the Katmai area before the eruption, so reports of precursors are few. A guide told Doroshin (1870) that Mt. Katmai emits smoke, "but the inhabitants of the village of Katmai were not sure of this." J.E. Spurr made a geological reconnaissance of the area in 1898. He wrote: "Extensive hot springs emerge from the Katmai side of the mountains below [Katmai] pass, and there are very frequent earthquakes and other evidences of volcanic activity. Our party itself experienced a slight earthquake just after crossing [the pass].... One of these volcanoes is said by the natives to smoke occasionally" (Spurr, 1900).

Earthquakes were felt at Katmai village, 30 km from the volcano, at least 5 days before the 1912 eruption. The intensity of these quakes increased notably on 4 and 5 June. On 4 June, frightened by these earthquakes, the people of Katmai village moved 16 km

KATMAI/NOVARUPTA (continued)

HISTORICAL ACTIVITY (continued)

down the coast to camp at Cape Kubugakli. Earthquakes were also felt at Savonoski, about 30 km northwest of Katmai, although Fenner (1925) states that one resident of Savonoski (Mr. Bob Scott) did not feel earthquakes before the eruption. Some earthquakes were felt as far away as Kanatak (94 km to the southwest), Uyak (90 km to the southeast), and Nushagak (210 km west-northwest from Katmai) (Fenner, 1925). Strong gas emission (and phreatic eruptions?) began on 5 June, and more earthquakes and explosions occurred on the morning of 6 June (Martin, 1913; Griggs, 1922; Fenner, 1925). The climactic eruption began at about 1300 hr on 6 June, and continued for 2.5 days. A particularly strong earthquake occurred at 2200 hr on 6 June, and other strong earthquakes occurred through the night of 7 June. Lesser earthquakes occurred from 8 June to 15 August, with relatively strong events on 11 June, 21 June, and 30 July (Fenner, 1925).

Griggs (1920, 1922) found that a large slide or rockfall from Falling Mountain occurred during or shortly before eruption of the Valley of Ten Thousand Smokes ash flow, and inferred from other field relations that a large rockslide from Mageik occurred at about the same time.

Both Griggs (1922) and Fenner (1925) noted fissures and faults in the Valley of Ten Thousand Smokes, concluded that magma had been erupted from these fissures, and inferred that they had therefore formed above a magma intrusion. Griggs envisioned a batholith at shallow depth and thought that all of the faults except those near Novarupta were of shallow origin. Fenner concluded that a shallow sill had fed the eruption, through many faults and fissures. In the light of current knowledge of calderas, compaction of ash-flow tuffs, relatively rapid cooling of sills, and compositional zonation of the 1912 magma, Fenner's hypothesis is probably incorrect and Grigg's single batholith is probably an oversimplification and overestimation of the size of a near-surface body.

Following Curtis (1968), Hildreth (1983) concluded that virtually all of the 1912 eruption was from the Novarupta vent; further, all of the erupted magma is closely related to other Novarupta products and unlike those of Katmai. A corollary of this conclusion is that collapse to form the Katmai Caldera was caused neither by eruption from Katmai nor by eruption of Katmai magma from Novarupta. Rather, it must have been in hydraulic response to the eruption of Novarupta, from an unknown but complex magma reservoir between the two vents (Hildreth, 1983, 1987). Curtis (1968) cites stratigraphic evidence that the summit of Mount Katmai did not collapse instantaneously, but rather collapsed slowly during the entire period of the 1912 eruption. Many of the faults around the Novarupta vent are thought to be shallow-seated compaction features within a funnel-shaped vent, rather than faults formed by collapse into an evacuated magma reservoir (Hildreth, 1983), but scarps in mountains adjacent to Novarupta are difficult to explain by compaction and may indicate some collapse.

Other volcanoes of the Katmai group have been intermittently active throughout recorded history. An eruption on 14 March 1866, "possibly from the Katmai area," caused ash to fall at Katmai Village, Afognak Island, and Pavlof Harbor, but no earthquakes or noises were reported (Doroshin, 1870). Doroshin infers that the ash came from a newly formed volcano northwest of Katmai Village, in the direction of Mt. Katmai. Snyder (1954), Muller and others (1954), Eicher and Rounsefell (1957), Decker (1963), Ward and Matumoto (1967), and Wilson and Forbes (1969) report eruptions of a new vent on the southwest flank of Trident from 1951 (or 1949?) through

KATMAI/NOVARUPTA (continued)

HISTORICAL ACTIVITY (continued)

1968. This new vent on Trident was present as a linear group of ash-emitting fumaroles by 1951, and lava extrusion began from the same fissure in 1953 (Snyder, 1954; Decker, 1963). A lava dome that was growing in the summer of 1974 was destroyed before the summer of 1975 (Volcanological Society of Japan, 1976).

Years that are followed by a question mark in the table above, for example, "1929-31?" for Katmai, refer to sightings of plumes that might be routine fumarolic emission rather than eruptions. W. Hildreth (written commun., 1987) considers them to be vapor plumes because no young erupted products are found; we accept this as likely, but note that small ash eruptions even at well-observed volcanoes leave no enduring, identifiable deposit.

During 39 days of recording with a small tripartite array in 1965, Matumoto and Ward (1967) found the primary center of earthquake activity to be 10-20 km northeast of Mt. Katmai, near Snowy Mountain (fig. 11.11.6). However, results from a 10-station network for the period from September 1987 to early March 1988 showed that the primary center of activity was a few kilometers northeast of the rim of Katmai Caldera, at depths of 0.8 to 8.5 km. The earlier results could have been in error by 10-20 km, so the 1965 activity may also have been close to Mt. Katmai (Ward and Endo, 1988). From September 1987 to early March 1988, 22 events within 80 km of the Katmai network were large enough to locate; in addition, dozens of small events per day were recorded on a station near the lower southeast flank of Mt. Katmai. Profound attenuation of seismic waves was observed during the study, but it was not possible to distinguish between site, source, and path effects. A working hypothesis is that some of the attenuation was caused by a shallow magma body beneath Mt. Katmai.

Seismicity increased slightly in the Trident-Martin area on 3-4 August 1965, and Trident may have erupted during cloudy weather during this same period (Matumoto and Ward, 1967; Ward and Matumoto, 1967). During a recording period from July 1977 to June 1981, shallow earthquakes (depths less than 5 km) were recorded in the Martin-Mageik-Trident area (Kienle and others, 1983).

COMMENTS

Areas of collapse in 1912 (Mt. Katmai summit and around Novarupta vent) are less than 5 km in diameter. However, the unusual density of stratovolcanoes in the Katmai area, the leakage of about 15 km^3 of rhyolite and dacite magma in 1912, and the "hydraulic connection" between Novarupta, Trident, and Katmai prompt us to include the Katmai/Novarupta area in this compilation as a possible future site of a large, caldera-forming eruption (see Bacon, 1985).

The size and geometry of Katmai-area magma reservoir(s) remain poorly known. Small- to moderate-size magma reservoirs may exist at shallow depth beneath each of the vents in the Katmai area, and one or more large reservoirs may exist at greater depth beneath the Katmai-Novarupta-Trident-Griggs and Mageik-Martin areas, with hydraulic interconnections. Regional studies in support of a proposed research-drilling project at Katmai should help to constrain the existence and location of crustal magma reservoirs in the area.

KATMAI/NOVARUPTA, Region 11, CAVW number 11-02-14,15,16,17,18,19

KATMAI/NOVARUPTA (continued)

REFERENCES

Bacon, C.R., 1985, Implications of silicic vent patterns for the presence of large crustal magma chambers: Jour. Geophys. Res., v. 90, no. B13, p. 11,243-11,252.

Berg, E., Kubota, S., and Kienle, J., 1967, Preliminary determination of crustal structure in the Katmai National Monument, Alaska: Bull. Seismol. Soc. Am., v. 57, no. 6, p. 1367-1392.

Curtis, G.H., 1968, The stratigraphy of the ejecta from the 1912 eruption of Mount Katmai and Novarupta, Alaska: Geol. Soc. Am. Memoir 116, p. 153-210.

Decker, R.W., 1963, Proposed volcano observatory at Katmai National Monument: A preliminary study: unpubl. rep., Hanover, N.H., Dartmouth Coll., 54 p.

Doroshin, P., 1870, Some volcanoes, their eruptions, and earthquakes in the former Russian possessions in America: Verh. Russisch-Kaiserlichen Mineral. Gesellschaft zu St. Petersburg, 2nd ser., 1870, p. 25-44 (English translation by J.B. Kisslinger).

Eicher, G.J., Jr., and Rounsefell, G.A., 1957, Effects of lake fertilization by volcanic activity on abundance of salmon: Limnology and Oceanography, v. 2, no. 2, p. 70-76.

Fenner, C.N., 1920, The Katmai region, Alaska, and the great eruption of 1912: Jour. Geol., v. 28, p. 569-606.

----- 1923, The origin and mode of emplacement of the great tuff deposit of the Valley of Ten Thousand Smokes: Natl. Geogr., Contributed Technical Papers, Katmai Ser., v. 1, p. 1-74.

----- 1925, Earth movements accompanying the Katmai eruption: Pt. I. Regional earthquakes, Pt. II. Fracturing in the Valley of Ten Thousand Smokes: Jour. Geol., v. 33, p. 116-139, 193-223.

----- 1930, Mount Katmai and Mount Mageik: Zeit. Vulkanol., v. 13, p. 1-24.

----- 1938, The phenomenon of falling Mountain: Am. Jour. Sci., v. 248, p. 593-627.

Griggs, R.F., 1920, The great Mageik landslide: Ohio Jour. Sci., v. 20, p. 325-354.

----- 1922, The Valley of Ten Thousand Smokes: Washington, D.C., Natl. Geogr. Soc., 340 p.

Hildreth, W., 1983, The compositionally zoned eruption of 1912 in the Valley of Ten Thousand Smokes, Katmai National Park, Alaska: Jour. Volcanol. Geotherm. Res., v. 18, p. 1-56.

----- 1987, New perspectives on the eruption of 1912 in the Valley of Ten Thousand Smokes, Katmai National Park, Alaska: Bull. Volcanol., v. 49, p. 680-693.

Keller, A.S., and Reiser, H.N., 1959, Geology of the Mount Katmai area, Alaska: U.S. Geol. Surv. Bull 1058-G, p. 261-298.

Kienle, J., 1969, Gravity survey in the general area of the Katmai National Monument: Fairbanks, Univ. Alaska, Ph.D. thesis, 151 p.

----- 1970, Gravity traverses in the Valley of Ten Thousand Smokes, Katmai National Monument, Alaska: Jour. Geophys. Res., v. 75, p. 6641-6649.

Kienle, J., and Swanson, S.E., 1983, Volcanism in the eastern Aleutian arc: late Quaternary and Holocene centers, tectonic setting and petrology: Jour. Volcanol. Geotherm. Res., v. 17, p. 393-432.

Kienle, J., Swanson, S.E., and Pulpan, H., 1983, Magmatism and subduction in the Eastern Aleutian arc, in Shimozuru, D., and Yokoyama, I., eds., Arc volcanism: physics and tectonics: Tokyo, Terra Sci. Publ., p. 191-224.

Kubota, S., and Berg, E., 1967, Evidence for magma in the Katmai volcanic range: Bull. Volcanol., v. 31, p. 175-214.

Martin, G.C., 1913, The recent eruption of Katmai volcano in Alaska: Natl. Geogr., v. 24, p. 131-181.

KATMAI/NOVARUPTA (continued)

REFERENCES (continued)

Matumoto, T., 1971, Seismic body waves observed in the vicinity of Mount Katmai, Alaska, and evidence for the existence of molten chambers: Geol. Soc. Am. Bull., v. 82, p. 2905-2920.

Matumoto, T., and Ward, P.L., 1967, Microearthquake study of Mount Katmai and vicinity, Alaska: Jour. Geophys. Res., v. 72, no. 10, p. 2557-2568.

Muller, E.H., Juhle, W., and Coulter, H.W., 1954, Current volcanic activity in Katmai National Monument: Science, v. 119, p. 319-321.

Smith, R.L., Shaw, H.R., Luedke, R.G., and Russell, S.L., 1978, Comprehensive tables giving physical data and thermal energy estimates for young igneous systems of the United States: U.S. Geol. Surv. Open-File Rep. 78-925, 15 p. + tables.

Snyder, G.L., 1954, Eruption of Trident Volcano, Katmai National Monument, Alaska: February-June, 1953: U.S. Geol. Surv. Circular 318, 7 p.

Spurr, J.E., 1900, A reconnaissance in southwestern Alaska in 1898: U.S. Geol. Surv., 10th Ann. Rep., pt. 7, p. 43-263.

Volcanological Society of Japan, 1976, Trident, Bull. Volcanic Eruptions, no. 14, p. 52 (information from G.E. Blinn).

Ward, P.L., and Matumoto, T., 1967, A summary of volcanic and seismic activity in Katmai National Monument, Alaska: Bull. Volcanol., v. 31, p. 107-129.

Ward, P.L., and Endo, E., 1988, A preliminary report on seismic activity in Katmai National Park, Alaska: unpubl. rep., 16 p.

Wilson, C.R., and Forbes, R.B., 1969, Infrasonic waves from Alaskan volcanic eruptions: Jour. Geophys. Res., v. 74, no. 18, p. 4511-4522.

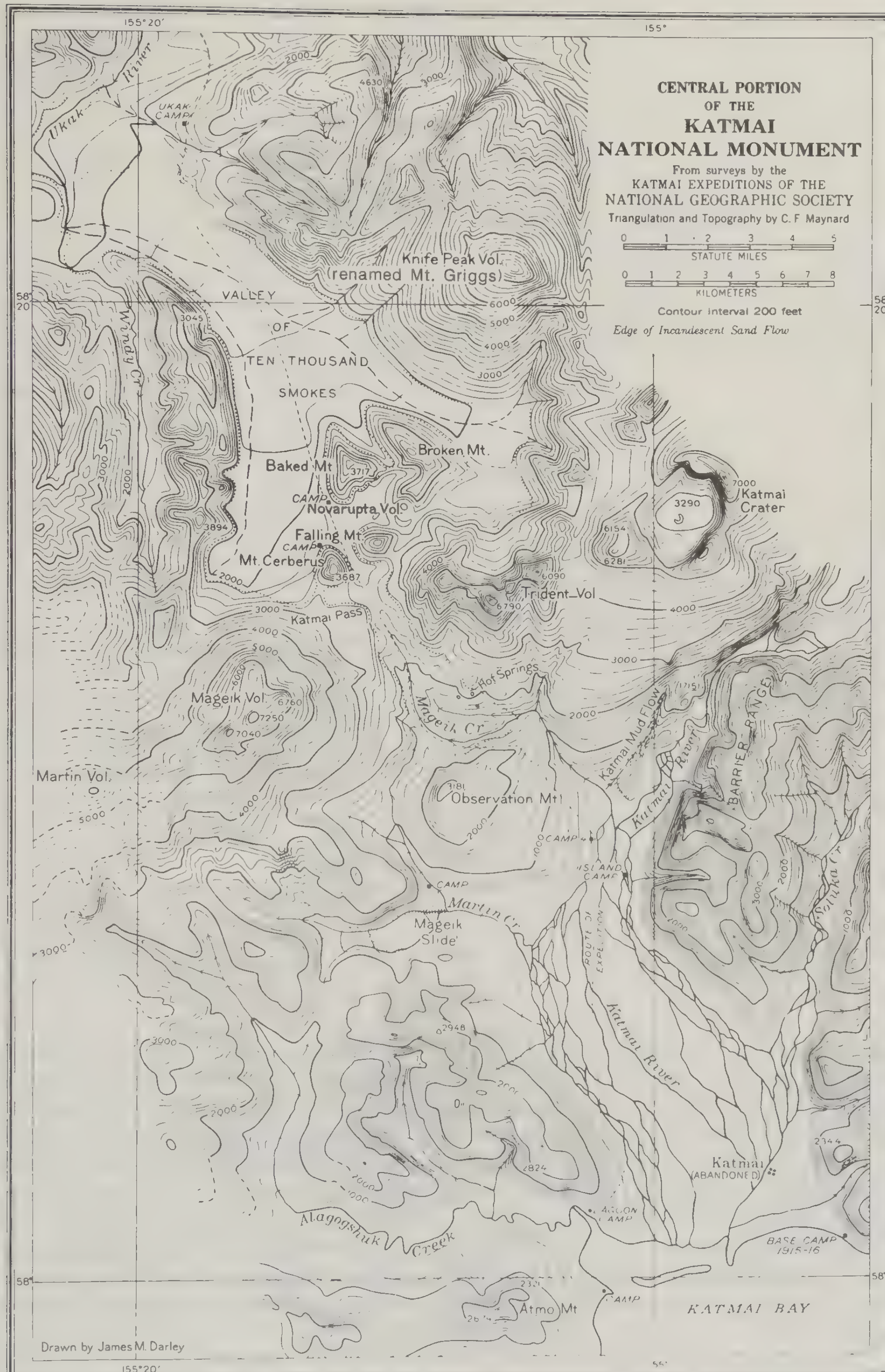

Figure 11.11.1. Topographic map of Katmai/Novarupta area, from Griggs (1922).

Figure 11.11.2. Outline map of Katmai area, from Hildreth (1987). Active andesite-dacite stratovolcanoes, Martin, Mageik, Trident, Katmai, and Griggs, surround the 1912 ash-flow sheet and a 2-km-wide vent depression within which The Turtle (T) ejecta mound and Novarupta rhyolite dome (N) were subsequently emplaced. Also near the 1912 vent are Holocene dacite domes Mount Cerberus (MC) and Falling Mountain (FM), and basement ridges Baked Mountain (BAM) and Broken Mountain (BRM). Presumed hydraulic transfer of magma from beneath Mount Katmai permitted summit collapse in 1912, forming a 600-m-deep caldera that now is occupied by a lake. VTTS, Valley of Ten Thousand Smokes. Discrete vent cones indicated by solid triangles, open craters by hachures; the 3 foundered summits of Mount Katmai (open triangles) are relocated from Griggs (1922; p. 270). The 5 Knife Creek glaciers are numbered for reference, but for clarity many other glaciers are omitted.

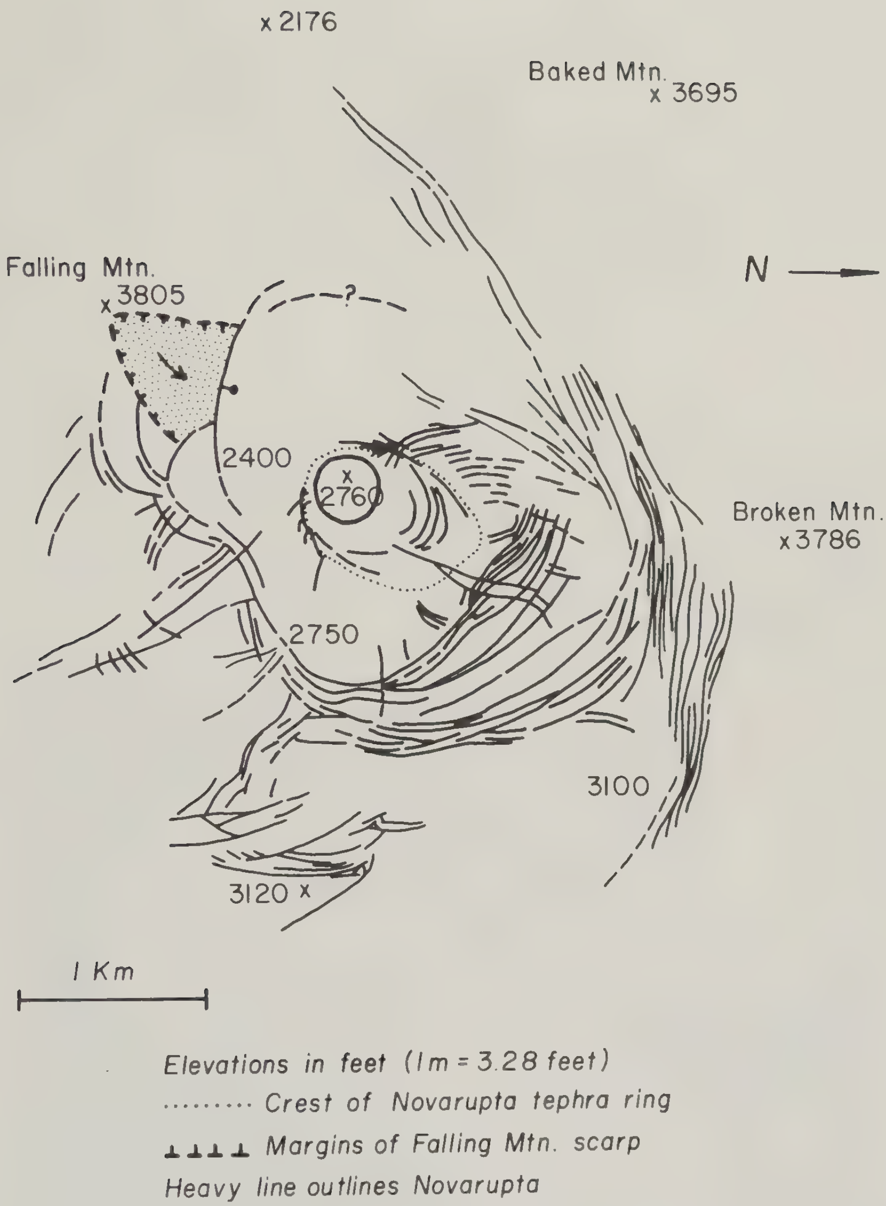

Figure 11.11.3. Fracture pattern outlining tephra-filled Novarupta Caldera, from Hildreth (1983). North is to the right.

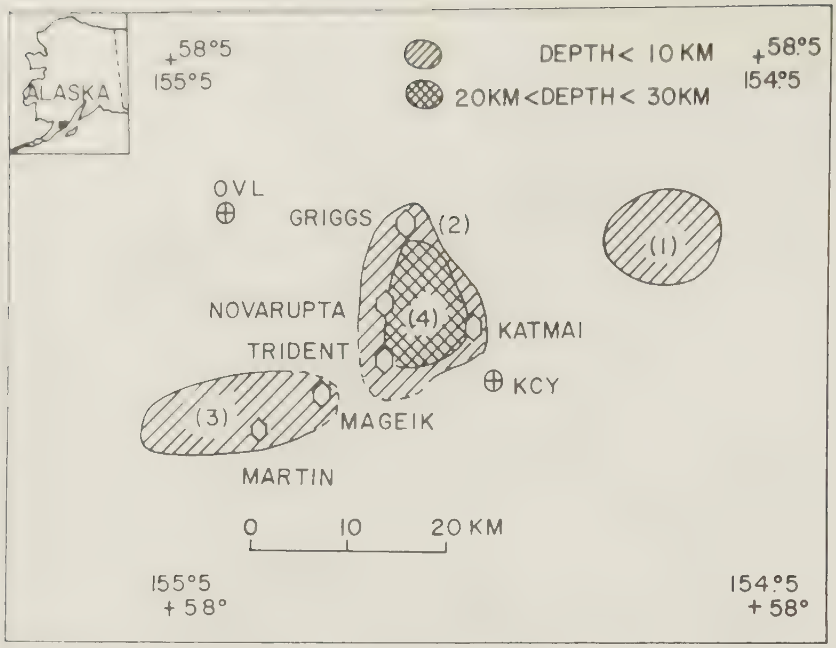

Figure 11.11.4. Magma chambers in Katmai region inferred from S-wave attenuation, from Matumoto (1971). Three chambers (1-3) may exist at shallow depths, probably less than 10 km; one chamber (4) is deeper, probably at 20-30 km depth.

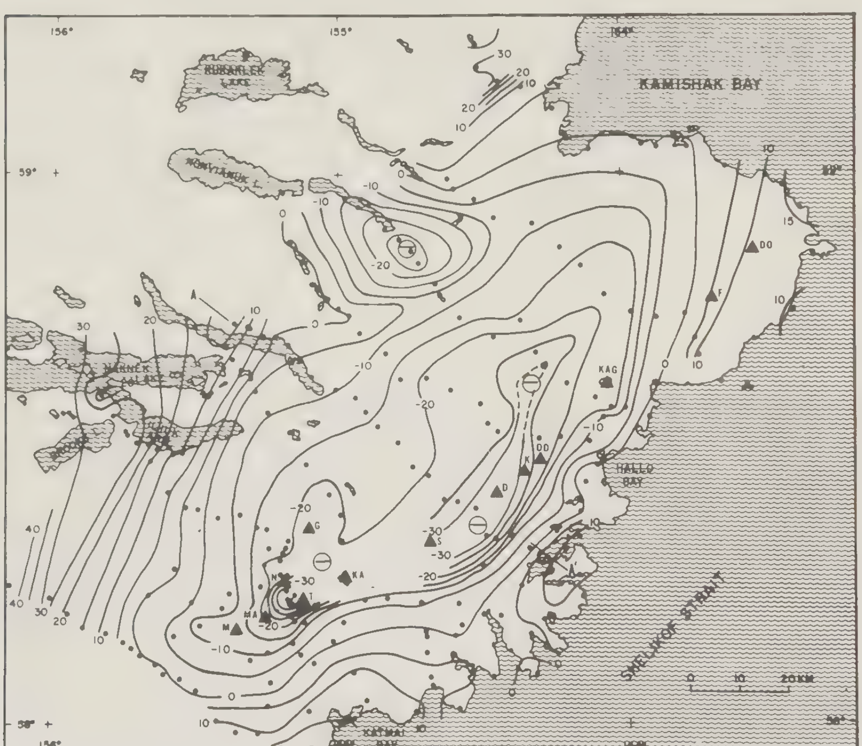

Figure 11.11.5. Bouguer gravity map of the Alaska Peninsula, from Kienle and Swanson (1983). Average crustal density of 2.67 g/cm^3 was assumed for reduction. Katmai area lies near center of gravity trough.

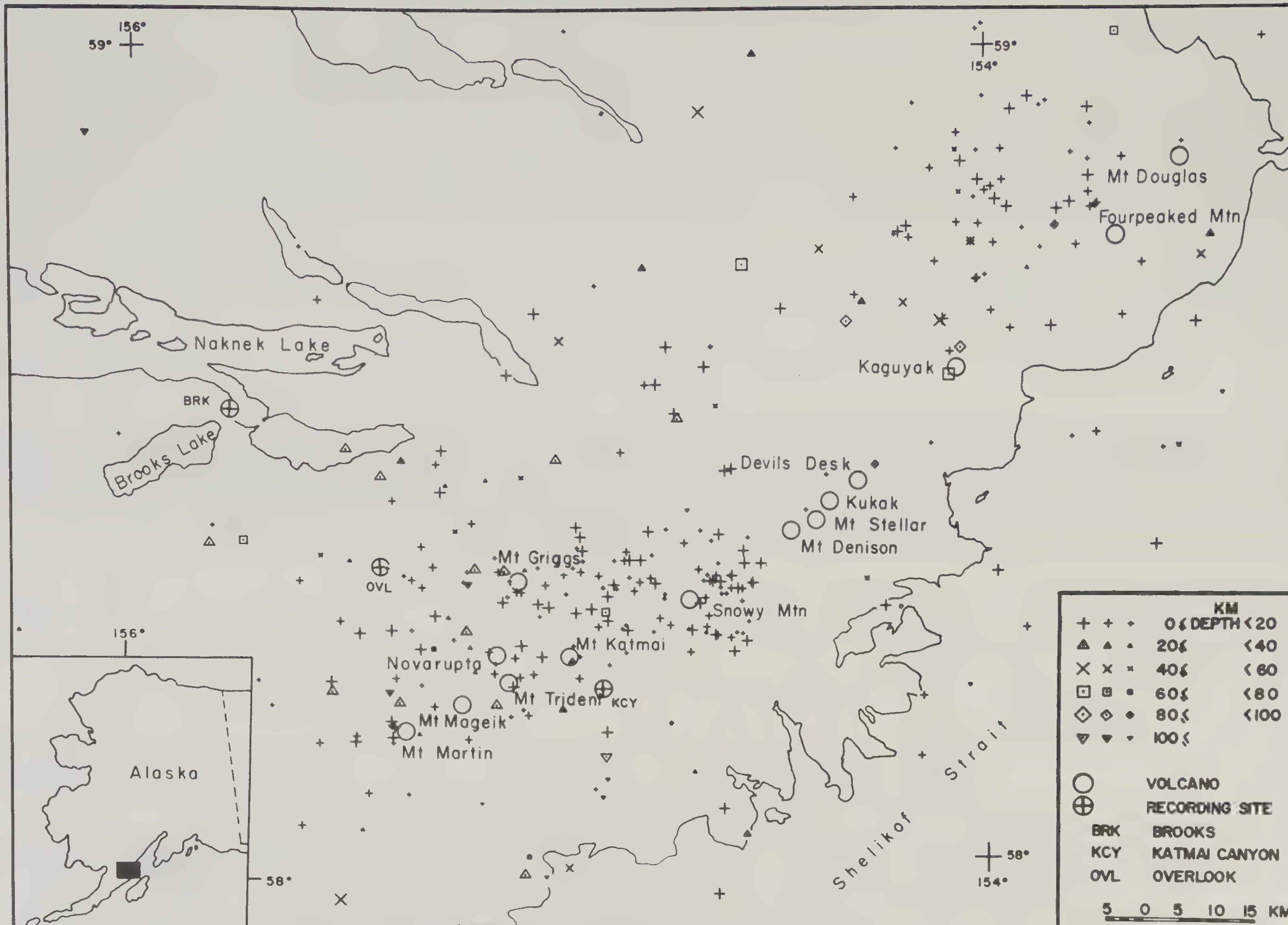

Figure 11.11.6. Seismic network and epicenters in Katmai region during summer of 1965, from Matumoto (1971). Three sizes of symbols indicate precision of hypocentral determination; larger symbol indicates more precise determination. On the basis of more accurate locations for earthquakes from September 1987 to March 1988, Ward and Endo (1988) suggest that many of the 1965 earthquakes shown near Snowy Mountain probably occurred closer to Mt. Katmai.

PART 3: HISTORICAL UNREST AT LARGE QUATERNARY CALDERAS (continued)
See inside back cover for explanation and abbreviations

WRANGELL

CAVW number (active vent)	Latitude Longitude (degrees)	Diameter (km)	Local tectonic setting	Precaldera edifice	SiO_2 content (wt pct)	Age of collapse (yr B.P.)	Date of unrest	Type and duration of unrest ESTU STHF MGTF H Te	Eruption type
11-05-02	62.00N	4 x 6		Shield	R = 58-62	late	1819?	---- ---- ---- - --	ex?
Mt. Wrangell	144.02W	(modern)			C = a?	Quaternary	1884?	---- ---- ---- - --	unknown
		15					1899	---- ---- ---x - QU?	none
		(ancestral)					1902	---- ---- ---- - --	ex
							1907	---- ---- --xx x --	none
							1965-present	xx-- ---- --xx - QU?	none yet

TECTONIC SETTING

The Wrangell Mountains are situated southeast of the main Aleutian arc, in a zone of major strike-slip faults along which narrow strips of the west coast of North America have moved northward. A triangular fragment of the continental margin (the Yakutat block) is moving with the Pacific plate and impinging on the continental block, so northeast-dipping subduction has stopped in that area. However, a weakly defined Benioff zone related to previous, northeast-dipping subduction still persists, parallel to the Wrangell chain and at an angle of about 80° to the direction of modern subduction in the Cook Inlet area (Circum-Pacific Map Project, Northeast Quadrant, 1981; Nye, 1983).

GEOLOGIC HISTORY

The Wrangell volcanoes (including Mt. Drum, Mt. Sanford, Mt. Wrangell, and Mt. Jarvis) are a group of large Pleistocene-Recent vents at the western end of the Wrangell Mountains. They are among the largest convergent margin volcanoes in the world and are thought to have grown at the unusually high rate of 30 km^3/m.y./km of arc (Nye, 1983). Mt. Wrangell itself has grown at a rate of at least several cubic kilometers per year (Nye, 1983).

On Mt. Wrangell, Benson and Motyka (1979) described an ice-filled, 1 km deep, 4 km x 6 km caldera, and an ancestral, 15-km-diameter caldera that extends northeast from Wrangell Caldera (Benson and Motyka, 1979). The age of Wrangell Caldera is unknown but is probably late Quaternary (T.P. Miller, written commun., 1987). Three postcaldera craters (North, East, and West Craters) have formed on the caldera rim (figs. 11.12.1, 11.12.2). Products of Mt. Wrangell are basaltic andesite to high-silica andesite. Some lava flows are as much as 35 km long, and the chemical compositions of one group of lava flows suggests a single zoned magma reservoir with a volume of at least a few tens of cubic kilometers (Nye, 1983).

WRANGELL (continued)

HISTORICAL ACTIVITY

Questionable eruptions occurred in 1819 and 1884 (Becker, 1898). On 3 September 1899, Mt. Wrangell steamed profusely just after a great earthquake and continued to "smoke with unusual animation for the rest of the season" (Benson and Motyka, 1979, quoting guide A.M. Powell). Crosby (1907, citing A.P. Porter) reported an increase in steaming and a warm, 2-day-long flood on 6-7 April 1907.

The best documented unrest in historical time has been from ca. 1965 to the present. Until 1965, glacial accumulation was in equilibrium with flow and basal melt, so the snow surface remained constant in altitude. Increased basal melting was first noted in 1965 and has continued, so that as of 1986 85 percent of the (pre-1965) ice in North Crater has melted (Benson and others, 1984) (fig. 11.12.3). Using the melting ice as a calorimeter, Benson and Motyka (1979) estimated that the minimum heat flow in North Crater was 1460 heat flow units (HFU), and heat flow for the caldera excluding North Crater was approximately 140 HFU.

All fumaroles were at or below the boiling temperature of water until the late 1970's, but by 1980 or 1981 some superheating was evident. By 1985, a temperature of 192 °C was measured at the edge of one fumarole. Fumarolic gases are mostly water, with CO_2 and SO_2 observed in the dry fraction. During April 1986, residents of the area reported occasional plumes rising 1 km above the summit (Benson and others, 1984; Smithsonian Institution, 1986).

COMMENTS

The cause of the current heating is not known, but Benson and Motyka (1979) and Benson and Follett (1986) speculate that it was triggered by the 1964 Prince William Sound ("Good Friday") earthquake, just as steaming of Wrangell was apparently triggered by another great earthquake in 1899 in Yakutat Bay.

REFERENCES

Becker, G.F., 1898, Reconnaissance of the gold fields of southern Alaska, with some notes on general geology: U.S. Geol. Surv., 18th Ann. Rep., pt. 3, p. 13-24.

Benson, C.S., and Follett, A.B., 1986, Applications of photogrammetry to the study of volcano-glacier interactions on Mt. Wrangell, Alaska: Photogrammetric Engineering and Remote Sensing, v. 52, no. 6, p. 813-827.

Benson, C.S., and Motyka, R.J., 1979, Glacier-volcano interactions on Mt. Wrangell, Alaska: Univ. Alaska Geophys. Inst., Ann. Rep., 1977-78, p. 1-25.

Benson, C.S., Sturm, M., Solie, D., Motyka, R., Mosely-Thompson, E., and Grootes, P., 1984, Glacier-volcano interactions, Mt. Wrangell, Alaska: Univ. Alaska Geophys. Inst., Biennial Rep., 1983-84, p. 102-104.

Circum-Pacific Map Project, Northeast Quadrant, 1981, Plate-tectonic map of the Circum-Pacific region, northeast quadrant: Tulsa, Circum-Pacific Council for Energy and Mineral Resources and the Am. Assoc. Pet. Geol., 1 sheet, scale 1,10,000,000.

WRANGELL (continued)

REFERENCES (continued)

Crosby, W.O., 1907, Volcanic activity in Alaska: Science, v. 26, p. 78.
Grewingk, C., 1850, Beitrag zur Kenntniss der orographischen und geognostischen Beschaffenheit der Nordwestküste Amerikas, mit den anliegenden Inseln: Verh. Russisch-Kaiserlichen Mineral Gesellschaft zu St. Petersburg, 1848-49, p. 123-278.
Miller, T.P., and Smith, R.L., 1975, Ash flows on the Alaska Peninsula: A preliminary report on their distribution, composition, and age [abs.]: Geol. Soc. Am. Abstracts with Programs, v. 7, no. 7, p. 1201.
Nye, C.J., 1983, Petrology and geochemistry of Okmok and Wrangell Volcanoes, Alaska: Santa Cruz, Univ. Calif., Ph.D. diss.
Smithsonian Institution, Scientific Event Alert Network (SEAN), 1986, Wrangell Volcano: SEAN Bull., v. 11, no. 4.

Figure 11.12.1. Mt. Wrangell area, showing summit caldera and approximate outline of ancestral caldera, after Benson and Motyka (1979).

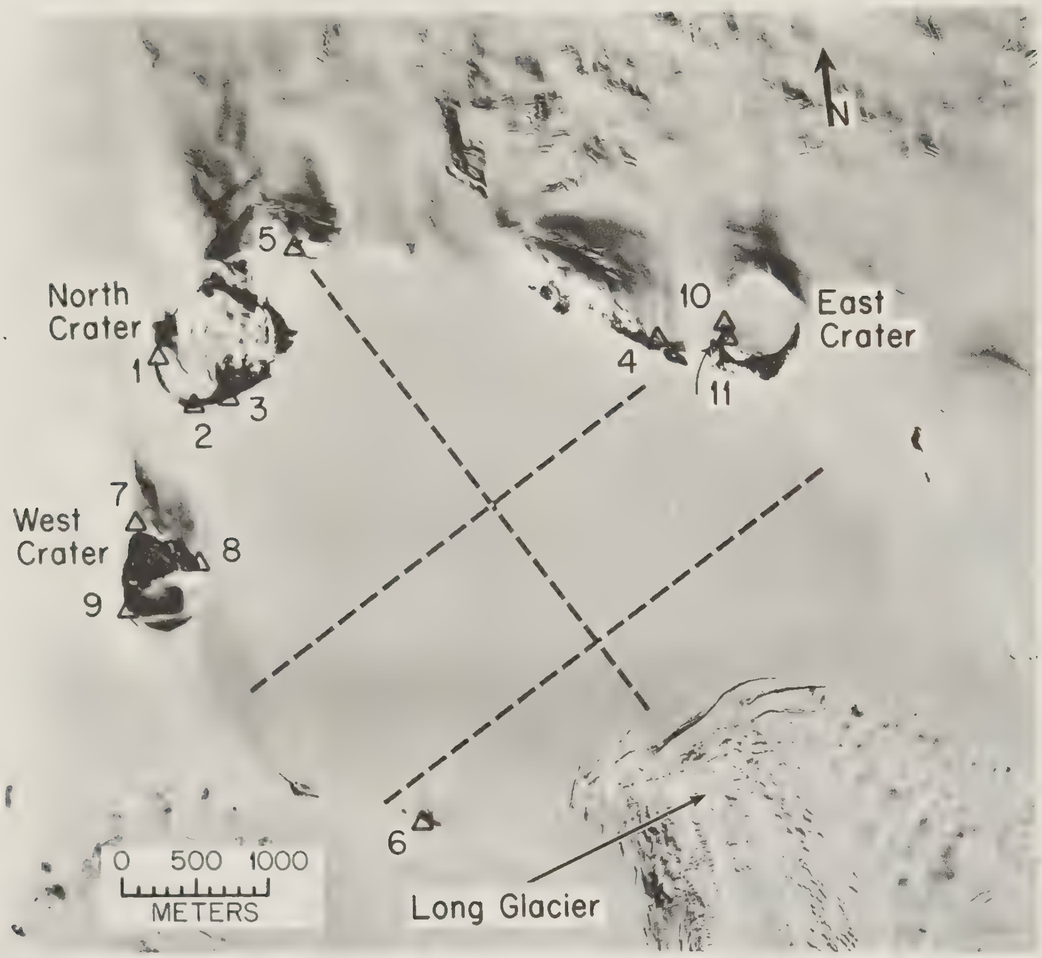

Figure 11.12.2. Summit caldera of Mt. Wrangell in 1975, after Benson and Motyka (1979). Numbers indicate control points for snow-and-ice survey; dashed lines indicate traverses for determination of ice thickness using a radio echo sounder.

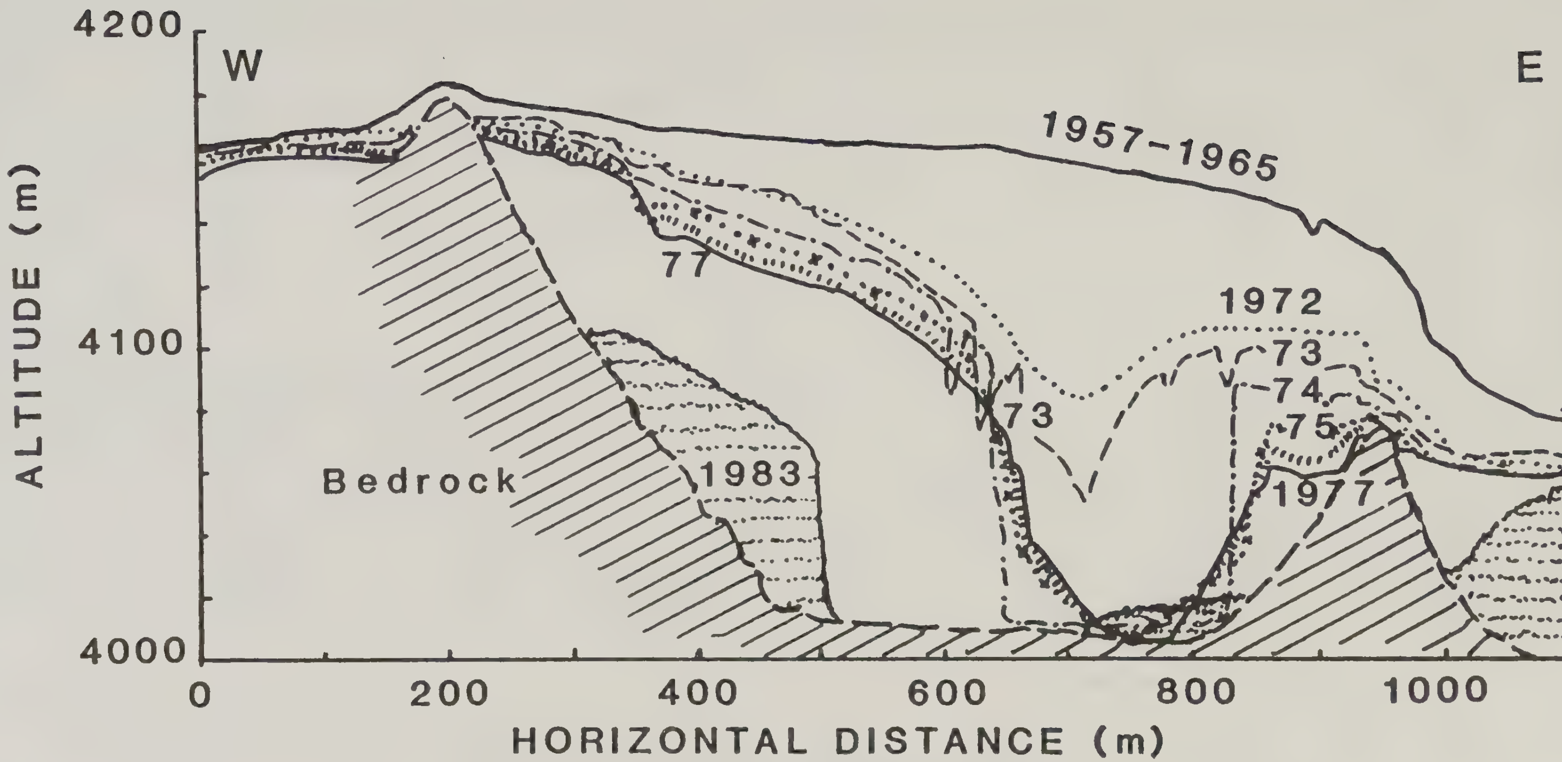

Figure 11.12.3. East-west cross section of Mt. Wrangell's North Crater, showing changes in ice volume between 1957 and 1983, after Benson and Motyka (1979).

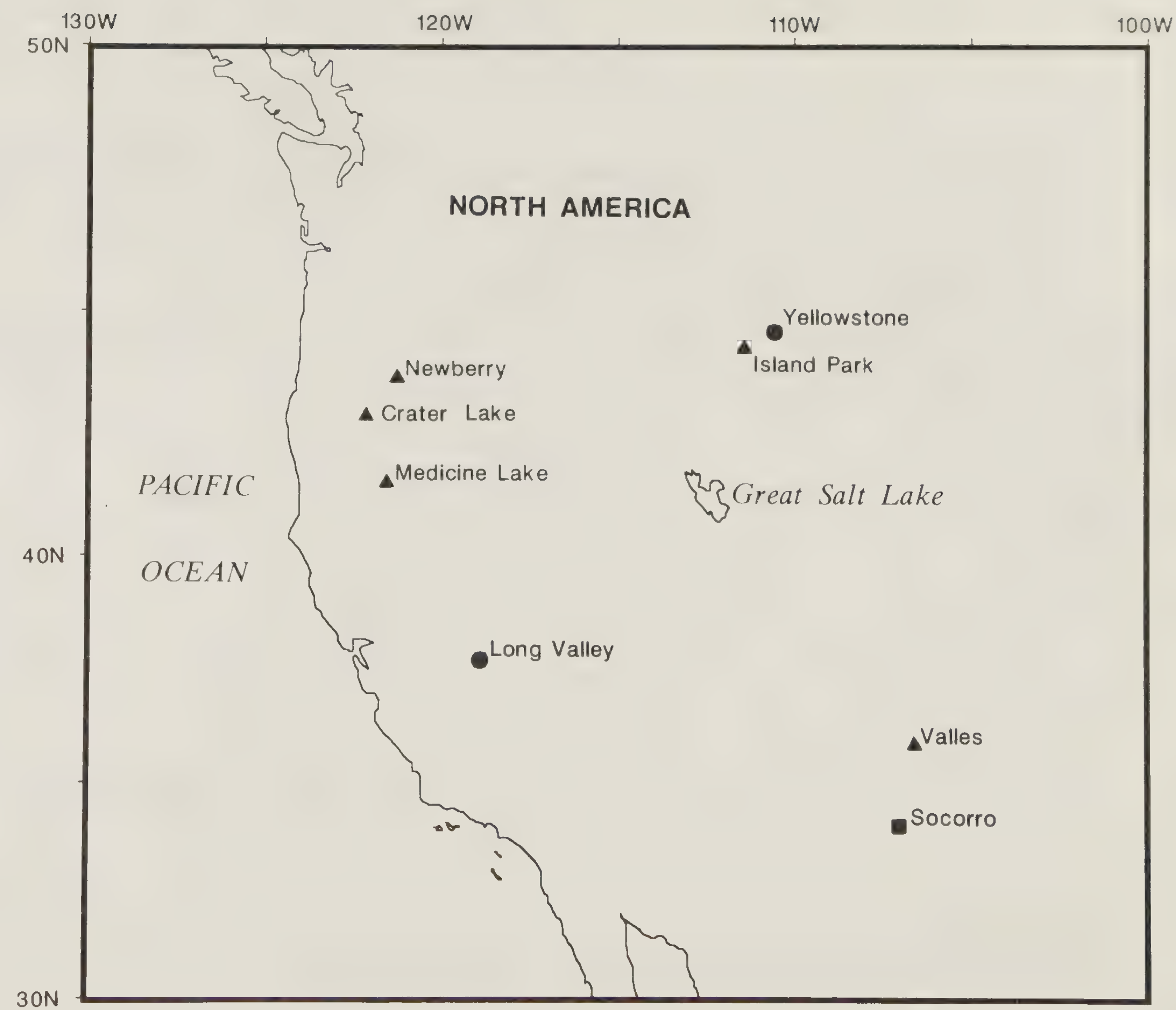

Figure 12. Locations of large, Quaternary restless calderas (solid circles), nonrestless calderas (triangles), and a restless noncaldera area (square) in Region 12.

LONG VALLEY

CAVW number (active vent)	Latitude Longitude (degrees)	Diameter (km)	Local tectonic setting	Precaldera edifice	SiO_2 content (wt pct)	Age of collapse (yr B.P.)	Date of unrest	Type and duration of unrest ESTU STHF MGTF H Te	Eruption type
12-03-08, (Mono Craters)	37.70N 118.87W	17 x 32	Exten	Domes	R = 73-74 C = 75-77	700,000	1889	x--- ---- ---- - =?	none
							1927	x--- ---- ---- - =?	none
							1941-42	x--- ---- ---- - =?	none
12-03-09 (Inyo Craters)							1978-present	FFxF -FFC FFFF F UU	none yet

TECTONIC SETTING

The Long Valley Caldera in eastern California is situated along the east edge of the Sierra Nevada tectonic block, and the western edge of the Basin and Range extensional province (figs. 12.1.1, 12.1.2). The entire region is one of high seismicity, ENE-WSW extension, and minor right-lateral strike-slip faulting. The Hilton Creek and Laurel Canyon Faults are major, recently active faults that cut the south-central part of the caldera; the Hartley Springs Fault and a set of related faults cut the northwestern part of the caldera (Pakiser, 1960; Pakiser and others, 1964; Bailey and others, 1976).

The Long Valley - Mono Craters region lies within a tectonically active zone that has produced four major earthquakes ($\underline{M}$ 6.8-8.0) since 1872, leaving three major gaps. The central gap, the White Mountains seismic gap, includes the Long Valley - Mono Craters region, and several authors have noted the potential for a major gap-filling earthquake in the coming years (Hill and others, 1985b).

GEOLOGIC HISTORY

Long Valley Caldera formed during and shortly after the Bishop tuff eruption of 700,000 yr B.P., and a resurgent dome formed shortly thereafter. Postcaldera eruptions produced moderately voluminous rhyolite domes and pyroclastic deposits, and less voluminous moat rhyolites, moat basalts, and rim quartz latites (fig. 12.1.2) (Bailey and others, 1976).

Recent eruptions in the area, from 40,000 yr B.P. to the present, have been at the Inyo domes (dominantly rhyodacitic) and the Mono domes and Mono Craters (dominantly rhyolitic) (Wood, 1977; Miller and others, 1982). The most recent eruptions in the Inyo-Mono chain occurred about 650-550 years ago, from multiple vents along nearly the full length of the Inyo chain and in the northern part of the Mono Craters chain, spanning a total distance of 40 km (Miller, 1985; Sieh and Bursick, 1986). Magmatic eruptions from the Inyo domes were followed shortly thereafter by phreatic explosions, and then by extrusion of rhyolite flows at three vents. Phreatic explosions occurred at other vents during this same period, including 12 within Long Valley Caldera (Miller, 1985). A likely

LONG VALLEY (continued)

GEOLOGIC HISTORY (continued)

explanation of this contemporaneous eruptive activity at multiple, linearly aligned vents is that a dike (or series of dikes) of silicic magma was emplaced, perhaps as part of an episode of regional crustal extension (Miller, 1985; Eichelberger and others, 1985; Fink, 1985). Recent drilling has confirmed the existence of a silicic feeder dike connecting several of the Inyo domes (Eichelberger and others, 1985). A suggestion that basaltic dike intrusion triggered these silicic eruptions 650-550 years ago (Eichelberger and others, 1987) is presently being reconsidered (J. Eichelberger, oral commun., 1988).

Seismic-refraction, heat-flow, and other studies suggest that a large body of magma exists beneath the western half of the caldera (fig. 12.1.3), overlain by an average of 1.4 km of Bishop tuff and 1 km of sedimentary and pyroclastic fill (Hill, 1976; Lachenbruch and others, 1976b; Ryall and Ryall, 1981). The fill is deepest in the northeastern and northwestern parts of the caldera. Anomalous ray paths and attenuation of S waves suggest one magma body beneath and slightly southeast of the resurgent dome, from 4.5 (mostly 7 or 8) km to at least 13 km below the surface. The same features suggest a separate cupola of magma just northwest of the resurgent dome, with its top at 5.5 km, probably connected to the central body below 8 km depth (Sanders, 1984).

A major hydrothermal system receives inflow from the west (Sierran front), and numerous hot springs occur in the center of the caldera. One of several possible models for subsurface hydrothermal reservoir temperatures (Sorey and others, 1978, model C, p. A50) has the area of highest temperatures in the southern caldera moat, just south of Casa Diablo--the area of pronounced seismicity in the current episode of unrest.

HISTORICAL ACTIVITY

1889: A $\underline{M}$=5.7 earthquake was centered just south of Long Valley Caldera (fig. 1 of Cramer and Toppozada, 1980).

1927: Seismicity increased near Long Valley.

1941-42: Seismicity increased near the south boundary of the caldera (Cramer and Toppozada, 1980; D. Hill, written commun., 1987).

1978-present: Regional seismicity in the Long Valley/Sierran front area declined during fall 1977 - summer 1978 but began to increase in 1978 and remains slightly elevated at the time of this writing (late 1987) (figs 12.1.4-12.1.7). In the Long Valley area, this increase has been in the form of recurring seismic swarms, accompanied by broad uplift of the caldera floor, and local increases in fumarolic activity. Seismic swarms began in October 1978, and four of the five largest earthquakes thus far (four $\underline{M}$=6 earthquakes) occurred during 25-27 May 1980. The first, third, and fourth of these large earthquakes occurred south of the caldera; the second occurred beneath the southern moat of the caldera, and the fifth (in 1986) occurred in Chalfant Valley, 40 km east-southeast of the caldera. Hypocentral depths of the four 1980 events were between 7 and 14 km (R. Cockerham, oral commun.; Julian

LONG VALLEY (continued)

HISTORICAL ACTIVITY (continued)

and Sipkin, 1985). Epicenters of these and other seismic events have been scattered along a roughly 30-km-long segment of a NNW-SSE-trending complex graben at the boundary between the Sierra Nevada and the Basin and Range.

The large earthquakes in 1980 were followed by at least 4 years of swarms and flurries, mostly just inside or just outside the south margin of the caldera (figs. 12.1.4-12.1.7). After May 1980, focal depths of swarms were between 2 and 11 km, with an apparent slight decrease in the mean focal depth of successive swarms, from approximately 8 km in mid-1980 to approximately 6 km in mid-1982 and between 5 and 6 km in 1983. The frequency of swarms, the numbers of earthquakes per swarm, and the energy release per swarm decreased irregularly from May 1980, increased briefly in January 1983, and have decreased since that time. Occasionally, small events in rapid succession produced "spasmodic tremor" signals. However, focal mechanisms are most consistent with ENE-WSW Basin and Range extension, with a right-lateral strike-slip component along a west-northwest-trending fault across the south margin of the caldera (Ryall and Ryall, 1983, Wallace, 1985; Hill and others, 1985a). An alternate but geologically less likely interpretation is that the focal mechanisms are compensated linear vector dipoles caused by dike intrusion along a northwest-trending fault just south of the caldera and perhaps along the southern ring fracture of the caldera (Julian, 1983; Savage and Cockerham, 1984; Julian and Sipkin, 1985; see also cautionary note by Aki, 1984). Ground fracturing during the May 1980 earthquakes was broadly consistent with E-W or NE-SW extension (Taylor and Bryant, 1980; Clark and others, 1982).

Since a swarm in July 1984, most seismicity has been outside the caldera. On 23 November 1984, a $\underline{M}_L$=5.7 earthquake occurred beneath Round Valley, 30 km southeast of Long Valley. A number of small earthquakes occurred in the Sierran block just south of the caldera in June-July 1986, and on 21 July 1986 a $\underline{M}_L$=6.4 earthquake occurred in the Chalfant Valley - White Mountains area, 40 km east-southeast of Long Valley. This foreshock-main shock sequence was followed by a typical set of aftershocks. These earthquakes, several tens of kilometers away from Long Valley, probably are not part of unrest at Long Valley, but the unrest at Long Valley might reasonably be considered part of a series of these regional earthquakes, beginning in 1978 (Ryall and Ryall, 1981, 1983).

The resurgent dome was uplifted by as much as 25 cm from 1975 (probably 1979) to October 1980, by another 8 cm by August 1982, and by yet another 7 cm by February 1983 (figs. 12.1.8-12.1.10) (Savage and Clark, 1982; Castle and others, 1984). However, by 1984 uplift had begun to slow (Hill, 1984; Hill and others, 1985a), totaling 4.5 cm from 1983 to 1984, and another 2.5 cm from 1984 to 1985 (Smithsonian Institution, 1985). The center of uplift apparently shifted several kilometers westward during 1983-85, from a site near the center of the resurgent dome to an area near the west caldera rim and the southern Inyo domes. Horizontal lines changed by as much as 45 microstrains (4.5 cm in 1 km; maximum change about 50 cm) from 1978 to mid-1982 (fig. 12.1.11), in patterns that may reflect both point-source uplift and regional extension (Savage and Clark, 1982; Denlinger and Riley, 1984). As of August 1984, extension across the south moat of the caldera and across the entire caldera continued at a rate of several microstrains per year (Estrem and others, 1985). By late 1986, rates had decreased to about 1 microstrain/yr.

Point-source models of the ground deformation suggest an inflating magma body at a depth of at least 7 km (Denlinger and Riley, 1984) or 10 km (Castle and others, 1984; Estrem and others, 1985). A model invoking two magma chambers postulates inflation of a

LONG VALLEY (continued)

HISTORICAL ACTIVITY (continued)

small reservoir at 5-km depth just east of Casa Diablo, and of a larger reservoir at 8-km depth beneath the north part of the resurgent dome (Rundle and Whitcomb, 1984). These and other models attribute inflation to injection of between 0.1 and 0.2 km^3 of magma into the Long Valley reservoir between 1975 and 1983 (Hill and others, 1985a). If one allows for uncertainties inherent in any model, all of the proposed deformation models are in reasonable agreement with the magma reservoirs postulated by Sanders (1984).

Horizontal deformation has been observed well beyond the margin of the caldera, and gravity data collected in early 1983 suggest that uplift might extend as far north as Lee Vining (Whitcomb and Rundle, 1983). However, leveling through the caldera from Tom's Place (southeast) to Lee Vining (northwest) shows no significant change in the elevation of Lee Vining relative to Tom's Place, suggesting that uplift has been confined to the caldera (Castle and others, 1984).

Magnetic field strength at sites on the southwest side of the caldera and along the Hilton Creek Fault increased systematically from 1977 to 1983, and as of May 1983 the cumulative increase was approximately 4 nT (Johnston and others, 1983). Johnston and others (1983) interpret this increase as a piezomagnetic response to increasing stresses from point-source uplift and (or) strain accumulation along the Hilton Creek Fault; they speculated that the magnetic changes will reverse if and when the stresses are relieved, as occurred at Matsushiro (see Part 4 of this compilation).

New fumaroles and vegetation kill were noted near Casa Diablo, on the south side of the resurgent dome (Casadevall and others, 1983). Hot spring pools at Hot Creek enlarged substantially in December 1982, possibly as a precursor to the January 1983 swarm (M.L. Sorey, written commun., 1983). Short-lived geysers and increased hot-spring discharge also occurred immediately after the earthquakes of May 1980 and January 1983. On at least four occasions in 1983, hydrogen gas emissions from the soil near Casa Diablo increased within a few hours or days before small earthquake swarms (K. McGee, written commun., 1983). Mercury concentrations in soils of Long Valley were significantly higher in 1982 than in a previous survey in 1975 (Varekamp and Buseck, 1984), and they were higher still in 1983 (Williams, 1985). In 1983, anomalously high radon was also found in soil gas from the area of uplift and the area of the January 1983 seismic swarm (Williams, 1985) (fig. 12.1.12).

COMMENTS

Unrest at Long Valley probably includes inflation of a residual silicic magma reservoir beneath the caldera, strain accumulation in the south moat of the caldera, and possibly heating of the shallow hydrothermal system, all in response to a regional tectonic strain event that began in 1978. Whether magma has intruded above the level of the residual magma reservoir at any time during the current unrest remains an open question. The unrest was initially considered tectonic, then magmatic or tectono-magmatic, and now certainly tectonic with shallow magma intrusion uncertain (or now, in our view, doubtful). Our doubts about shallow magma intrusion notwithstanding, caution about volcanic hazards is still required because crustal extension and a strong earthquake in the White Mountains seismic gap could trigger dike intrusion and phreatic or magmatic eruptions along the Mono Craters - Inyo domes chain (as

LONG VALLEY (continued)

COMMENTS (continued)

happened along the Mono-Inyo chain ca. 600 years ago and in the Cordón Caulle area of Chile immediately after the 1960 Chilean earthquake) (see section on Cordillera Nevada, CAVW number 15-07-14,15).

REFERENCES

Aki, K., 1984, Evidence for magma intrusion during the Mammoth Lakes earthquakes of May 1980 and implications of the absence of volcanic (harmonic) tremor: Jour. Geophys. Res., v. 89, no. B9, p. 7689-7696.

Archuleta, R.J., Cranswick, E., Mueller, C., and Spudich, P., 1982, Source parameters of the 1980 Mammoth Lakes, California, earthquake sequence: Jour. Geophys. Res., v. 87, no. B6, p. 4595-4607.

Bailey, R.A., 1982, Other potential eruption centers in California: Long-Valley-Mono Lake, Coso, and Clear Lake volcano fields, <u>in</u> Martin, R.C., and Davis, J.F., eds., Status of volcanic prediction and emergency response capabilities in volcanic hazard zones of California: Calif. Div. Mines Geol., Spec. Publ. 63, p. 17-28.

Bailey, R.A., Dalrymple, G.B., and Lanphere, M.A., 1976, Volcanism, structure and geochronology of Long Valley Caldera, Mono County, California: Jour. Geophys. Res., v. 81, p. 725-744.

Barker, J.S., and Langston, C.A., 1983, A teleseismic body-wave analysis of the May 1980 Mammoth Lakes, California, earthquakes: Bull. Seismol. Soc. Am., v. 73, p. 419-434.

Casadevall, T., Clark, M., McGee, K., Sutton, J., and Bezore, S., 1983, Monitoring hydrothermal activity at Long Valley, California [abs.]: Earthq. Notes, v. 54, no. 1, p. 76.

Castle, R.O., Estrem, J.E., and Savage, J.C., 1984, Uplift across Long Valley Caldera, California: Jour. Geophys. Res., v. 89, no. B13, p. 11,507-11,516.

Clark, M.M., Yount, J.C., Vaughan, P.R., and Zepeda, R.L., 1982, Map showing surface ruptures associated with the Mammoth Lakes, California, earthquakes of May 1980: U.S. Geol. Surv. Misc. Field Studies Map MF-1396, 1 sheet, scale 1:24,000.

Cramer, C.H., and Toppozada, T.R., 1980, A seismological study of the May 1980 and earlier earthquakes near Mammoth Lakes, California, <u>in</u> Sherburne, R.W., ed., Mammoth Lakes, California earthquakes of May 1980: Calif. Div. Mines Geol. Spec. Rep. 150, p. 91-130.

Denlinger, R.P., and Riley, F., 1984, Deformation of Long Valley Caldera, Mono County, California, from 1975 to 1982: Jour. Geophys. Res., v. 89, no. B10, p. 8303-8314.

Denlinger, R.P., Riley, F.S., Boling, J.K., and Carpenter, M.C., 1985, Deformation of Long Valley Caldera between August 1982 and August 1983: Jour. Geophys. Res., v. 90, no. B13, p. 11,199-11,209.

Dzurisin, D., Sylvester, A.G., and Cashman, K.V., 1983, Ground tilt since May 1982 at Long Valley Caldera, California [abs.]: Earthq. Notes, v. 54, no. 1, p. 75.

Eichelberger, J.C., Lysne, P.C., Miller, C.D., and Younker, L.W., 1985, Research drilling at Inyo Domes, California: 1984 results: Eos, Trans. Am. Geophys. Union, v. 66, p. 186-187.

LONG VALLEY (continued)

REFERENCES (continued)

Eichelberger, J.C., Younker, L.W., Vogel, T.A., and Miller, C.D., 1987, Coring beneath Inyo Craters, Long Valley, CA [abs.]: Eos, Trans. Am. Geophys. Union, v. 68, p. 1544.

Estrem, J.E., Lisowski, M., and Savage, J.C., 1985, Deformation in the Long Valley Caldera, California, 1983-1984: Jour. Geophys. Res., v. 90, no. B14, p. 12,683-12,690.

Fink, J.H., 1985, Geometry of silicic dikes beneath the Inyo Domes, California: Jour. Geophys. Res., v. 90, no. B13, p. 11,127-11,133.

Given, J.W., Wallace, T.C., and Kanamori, H., 1982, Teleseismic analysis of the 1980 Mammoth Lakes earthquake sequence: Bull. Seismol. Soc. Am., v. 72, p. 1093-1109.

Hermance, J.F., 1983, The Long Valley/Mono Basin volcanic complex in eastern California: Status of present knowledge and future research needs: Rev. Geophys. Space Phys., v. 21, no. 7, p. 1545-1565.

Hill, D.P., 1976, Structure of Long Valley Caldera, California, from a seismic refraction experiment: Jour. Geophys. Res., v. 81, no. 5, p. 745-753.

----- 1984, Monitoring unrest at a large silicic caldera, the Long Valley-Inyo Craters volcanic complex in east-central California: Bull. Volcanol., v. 47, no. 2, p. 371-395.

Hill, D.P., Bailey, R.A., and Ryall, A.S., 1985a, Active tectonic and magmatic processes beneath Long Valley Caldera, eastern California: An overview: Jour. Geophys. Res., v. 90, no. B13, p. 11,111-11,120.

Hill, D.P., Kissling, E., Luetgert, J.H., and Kradolfer, U., 1985b, Constraints on the upper crustal structure of the Long Valley-Mono Craters Volcanic Complex, eastern California, from seismic refraction measurements: Jour. Geophys. Res., v. 90, no. B13, p. 11,135-11,150.

Hill, D.P., Wallace, R.E., and Cockerham, R.S., 1985c, Review of evidence on the potential for major earthquakes and volcanism in the Long Valley-Mono Craters-White Mountains regions of eastern California: Earthq. Prediction Res., v. 3, p. 571-594.

Johnston, M.J.S., Mueller, R.J., Silverman, S.A., and Keller, V.G., 1983, Magnetic measurements across the Long Valley Caldera, 1972-1983: A comparison with observations and mechanisms during the Matsushiro earthquake swarm [abs.]: Earthq. Notes, v. 54, no. 1, p. 90.

Julian, B.R., 1983, Evidence for dyke intrusion earthquake mechanisms near Long Valley caldera, California: Nature, v. 303, p. 323-325.

Julian, B.R., and Sipkin, S.A., 1985, Earthquake processes in the Long Valley caldera area, California: Jour. Geophys. Res., v. 90, no. B13, p. 11,155-11,169.

Lachenbruch, A.H., Sass, J.H., Munroe, R.J., and Moses, T.H., Jr., 1976b, Geothermal setting and simple heat conduction models for the Long Valley Caldera: Jour. Geophys. Res., v. 81, no. 5, p. 769-784.

Lachenbruch, A.H., Sorey, M.L., Lewis, R.E., and Sass, J.H., 1976a, The near-surface hydrothermal regime of Long Valley Caldera: Jour Geophys. Res., v. 81, no. 5, p. 763-768.

Langbein, J., Linker, M., and Tupper, D., 1987, Analysis of two-color geodimeter measurements of deformation within the Long Valley Caldera: June 1983 to October 1985: Jour. Geophys. Res., v. 92, p. 9423-9442.

LONG VALLEY (continued)

REFERENCES (continued)

Luetgert, J.H., and Mooney, W.D., 1985, Crustal refraction profile of the Long Valley Caldera, California, from the January 1983 Mammoth Lakes earthquake swarm: Bull. Seismol. Soc. Am., v. 75, p. 211-221.

Miller, C.D., 1983, Chronology of Holocene eruptions at the Inyo volcanic chain, California [abs.]: Eos, Trans. Am. Geophys. Union, v. 64, p. 900.

----- 1985, Holocene eruptions at the Inyo volcanic chain, California: implications for possible eruptions in Long Valley caldera: Geology, v. 13, p. 14-17.

Miller, C.D., Mullineaux, D.R., Crandell, D.R., and Bailey, R.A., 1982, Potential hazards from future volcanic eruptions in the Long Valley-Mono Lake area, east-central California and southwest Nevada -- a preliminary assessment: U.S. Geol. Surv. Circular 877, 10 p.

Pakiser, L.C., 1960, Transcurrent faulting and volcanism in Owens Valley, California: Geol. Soc. Am. Bull., v. 71, p. 153-160.

Pakiser, L.C., Kane, M.F., and Jackson, W.H., 1964, Structural geology and volcanism of Owens Valley region, California--a geophysical study: U.S. Geol. Surv. Prof. Paper 438, 68 p.

Pitt, A.M., and Cockerham, R.S., 1983, Long Valley earthquake swarm: January 7, 1983 [abs.], Earthq. Notes, v. 54, no. 1, p. 73.

Rundle, J.B., Carrigan, C.R., Hardee, H.C, and Luth, W.C., 1986, Deep drilling to the magmatic environment in Long Valley Caldera: Eos, Trans. Am. Geophys. Union, v. 67, p. 490-491.

Rundle, J.B., and Hill, D.P., 1988, The geophysics of a restless caldera--Long Valley, California: Ann. Rev. Earth Planet. Sci., v. 16, p. 251-271.

Rundle, J.B., and Whitcomb, J.H., 1984, A model for deformation in Long Valley, California, 1980-1983: Jour. Geophys. Res., v. 89, no. B11, p. 9371-9380.

Ryall, A., and Ryall, F., 1981, Spatial-temporal variations in seismicity preceding the May 1980, Mammoth Lakes, California, earthquakes: Bull. Seismol. Soc. Am., v. 71, p. 747-760.

----- 1982, Propagation effects and seismicity associated with magma in Long Valley caldera, eastern California: Earthq. Notes, v. 53, no. 1, p. 46-47.

----- 1983, Spasmodic tremor and possible magma injection in Long Valley Caldera, Eastern California: Science, v. 219, p. 1432-1433.

Sanders, C.O., 1984, Location and configuration of magma bodies beneath Long Valley, California, determined from anomalous earthquake signals: Jour. Geophys. Res., v. 89, no. B10, p. 8287-8302.

Savage, J.C., and Clark, M.M., 1982, Magmatic resurgence in Long Valley Caldera, California--Possible cause of the 1980 Mammoth Lakes earthquakes: Science, v. 217, p. 531-533.

Savage, J.C., and Cockerham, R.S., 1984, Earthquake swarm in Long Valley, California, January 1983: Evidence for dike inflation: Jour. Geophys. Res., v. 89, no. B10, p. 8315-8324.

Savage, J.C., Cockerham, R.S., Estrem, J.E., and Moore, L.R., 1987, Deformation near the Long Valley Caldera, eastern California, 1982-1986: Jour. Geophys. Res., v. 92, no. B3, p. 2721-2746.

Sieh, K., and Bursick, M., 1986, Most recent eruptions of the Mono Craters, eastern central California: Jour. Geophys. Res., v. 91, no. B12, p. 12,539-12,571.

LONG VALLEY (continued)

REFERENCES (continued)

Smithsonian Institution, Scientific Event Alert Network (SEAN), 1982-85, Long Valley Caldera: SEAN Bull., v. 7, no. 12, v. 8, nos. 1, 11; v. 10, no. 10 (contributions from D. Hill, J. Savage, R. Cockerham, R.A. Bailey, F. Riley, and others).

Sorey, M.L., 1985, Evolution and present state of the hydrothermal system in Long Valley caldera: Jour. Geophys. Res., v. 90, no. B13, p. 11,219-11,228.

Sorey, M.L., Lewis, R.E., and Olmsted, F.H., 1978, The hydrothermal system of Long Valley Caldera, California: U.S. Geol. Surv. Prof. Paper 1044-A, p. A1-A60 (including preliminary geologic map of Long Valley).

Taylor, G.C., and Bryant, W.A., 1980, Surface rupture associated with the Mammoth Lakes earthquakes of 25 and 27 May, 1980, in Sherburne, R.W., ed., Mammoth Lakes, California earthquakes of May 1980: Calif. Div. Mines Geol. Spec. Rep. 150, p. 49-67.

Varekamp, J.C., and Buseck, P.R., 1984, Changing mercury anomalies in Long Valley, California: Indication for magma movement or seismic activity: Geology, v. 12, p. 283-286.

Wallace, T.E., 1985, A reexamination of the moment tensor solution of the 1980 Mammoth Lakes earthquakes: Jour. Geophys. Res., v. 90, no. B13, p. 11,171-11,176.

Whitcomb, J.H., and Rundle, J., 1983, Gravity variation in the Mammoth Lakes, Mono Lake and Owens Valley, California regions [abs.]: Earthquake Notes, v. 54, no. 1, p. 76.

Williams, S.N., 1985, Soil radon and elemental mercury distribution and relation to magmatic resurgence at Long Valley Caldera: Science, v. 229, p. 551-553.

Wood, S.H., 1977, Distribution, correlation, and radiocarbon dating of late Holocene tephra, Mono and Inyo Craters eruptions, eastern California: Geol. Soc. Am. Bull., v. 88, p. 89-95.

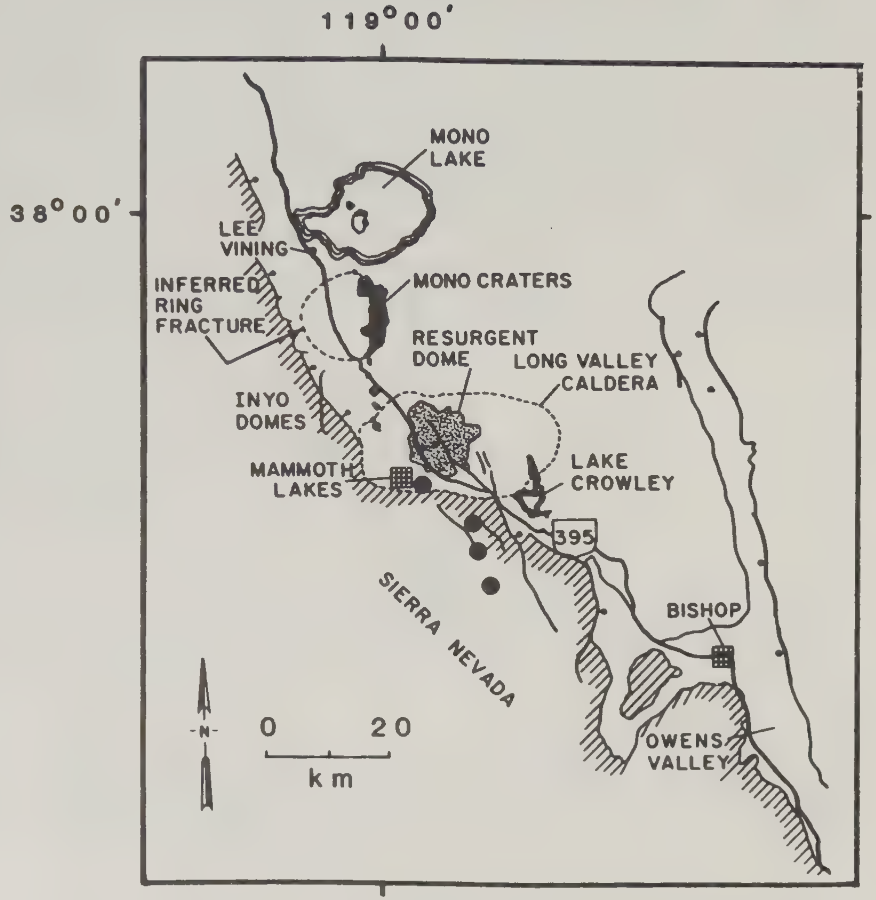

Figure 12.1.1. Generalized map of Long Valley/Mono Basin volcanic complex showing its position relative to Sierra Nevada to the west and Basin and Range province to the east (Hermance, 1983; after Bailey and others, 1976). Irregular black areas (Inyo domes, Mono Craters, and volcanic craters in Mono Lake) represent Holocene eruptive centers. Solid dots indicate epicenters of four magnitude 6 earthquakes during 25-27 May 1980. Copyright by the American Geophysical Union.

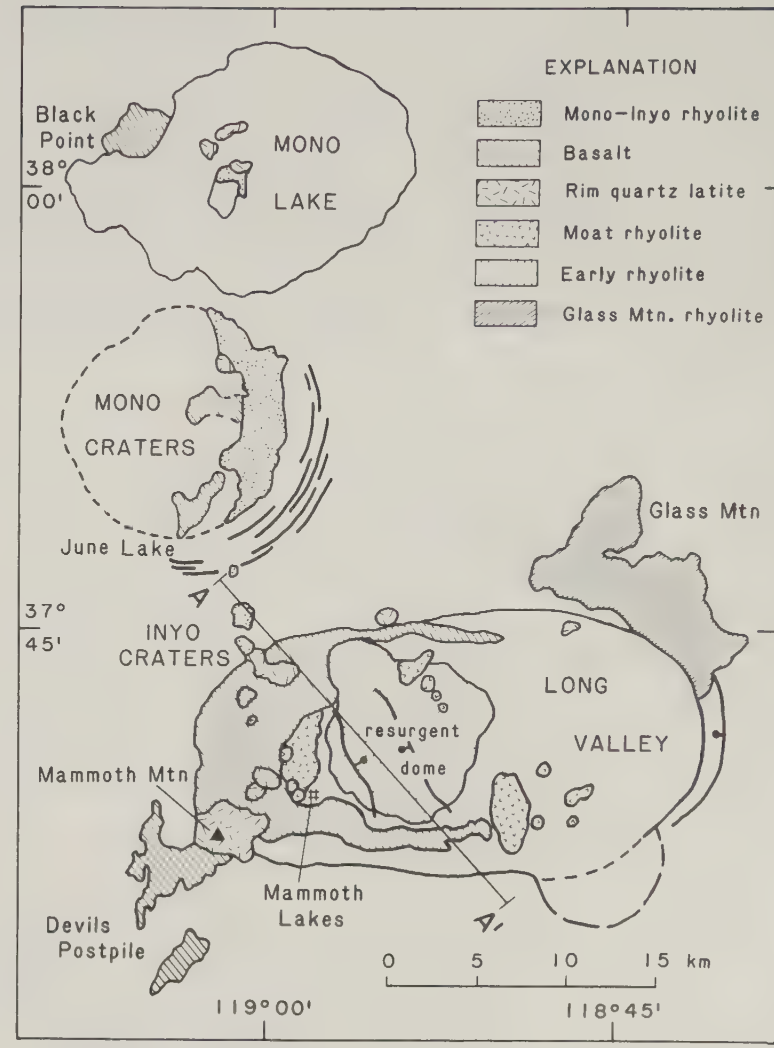

Figure 12.1.2. Generalized geologic map of Long Valley Caldera and Mono-Inyo Craters volcanic system, from Hill and others (1985c), after Bailey (1982). Line A-A' shows location of cross section in figure 12.1.3.

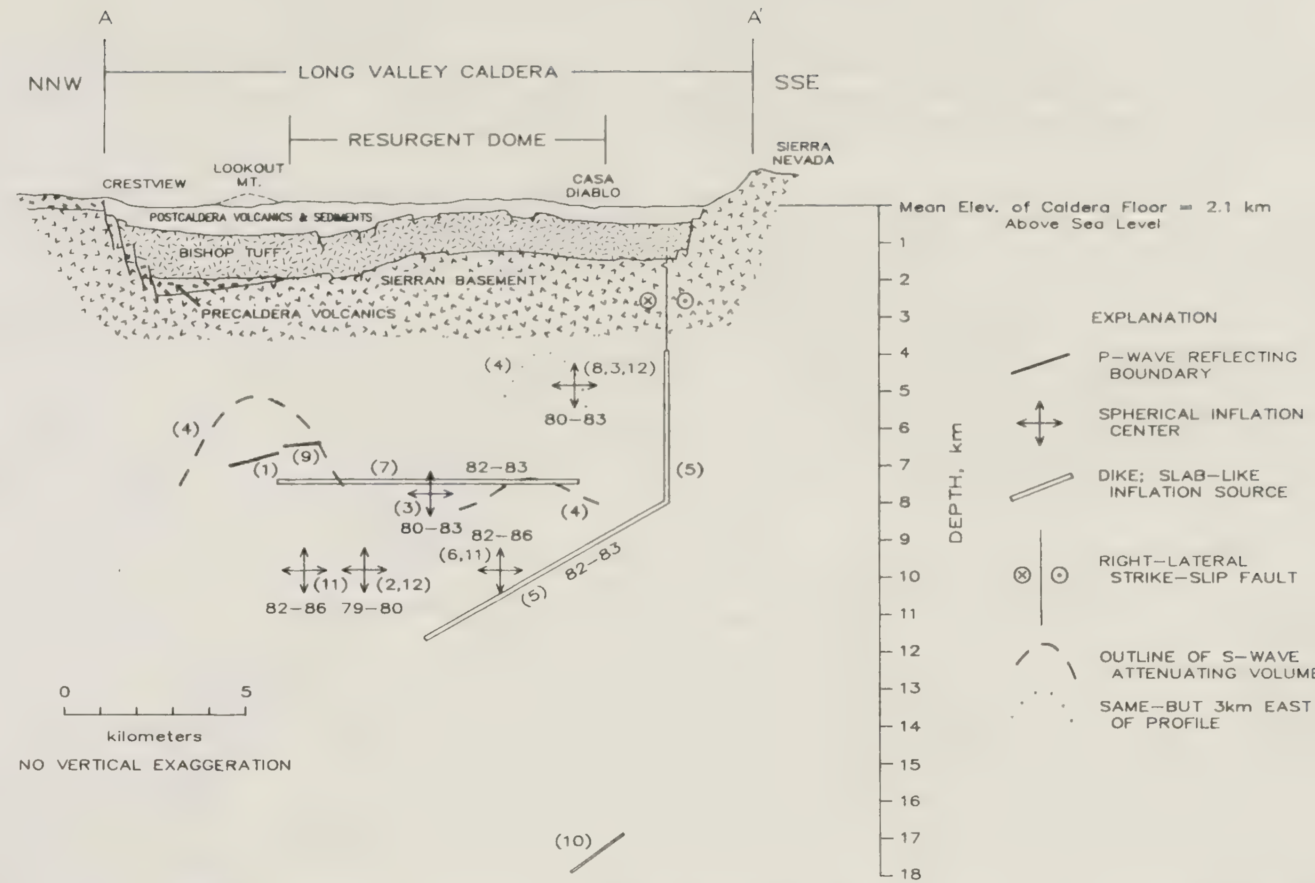

Figure 12.1.3. Vertical NW-SE section through Long Valley Caldera along line A-A' in figure 12.1.2, from Rundle and Hill (1988), after Hill and others (1985a) and Rundle and others (1986). Shallow caldera structure based on seismic-refraction results of Hill and others (1985b). Deeper structure beneath caldera shows location and geometry of inflation (dislocation) sources used to model deformation observed during years indicated (for example, 79-80), seismic P-wave reflecting boundaries, and volumes that produce anomalous S-wave attenuation. Parenthetic numbers give references: (1) Hill, 1976; (2) Savage and Clark, 1982; (3) Rundle and Whitcomb, 1984; (4) Sanders, 1984; (5) Savage and Cockerham, 1984; (7) Denlinger and Riley, 1984; (8) Denlinger and others, 1985; (9) Hill and others, 1985b; (10) Luetgert and Mooney, 1985; (11) Savage and others, 1987; (12) Langbein and others, 1987. Note that there is no seismic evidence for a large, interconnected magma reservoir at shallow depth beneath Long Valley Caldera (in contrast to the situation at Yellowstone Caldera, as shown in figures 12.2.6 and 12.2.7).

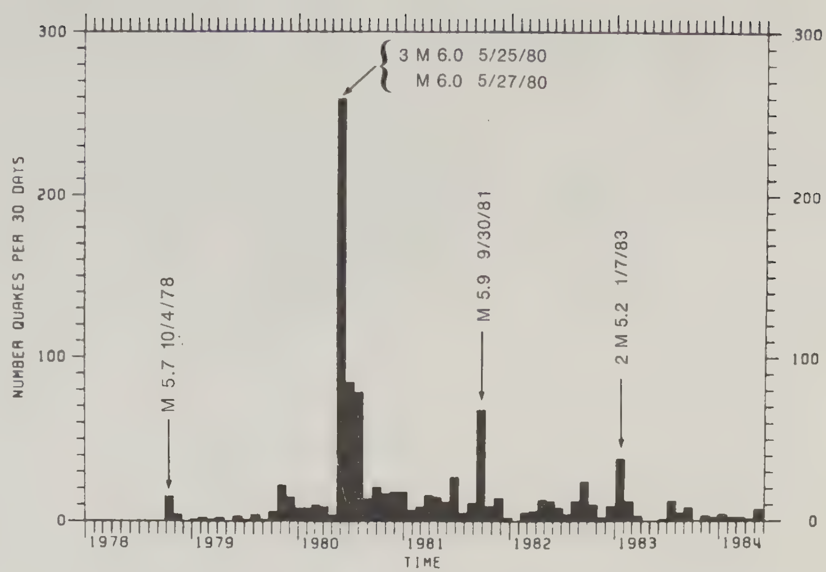

Figure 12.1.4. Temporal summary of seismic activity near Long Valley Caldera during 1978-84 in terms of occurrence rate of magnitude 3 and larger earthquakes per 30-day intervals (Hill and others, 1985c). Occurrence of principal earthquakes noted with arrows.

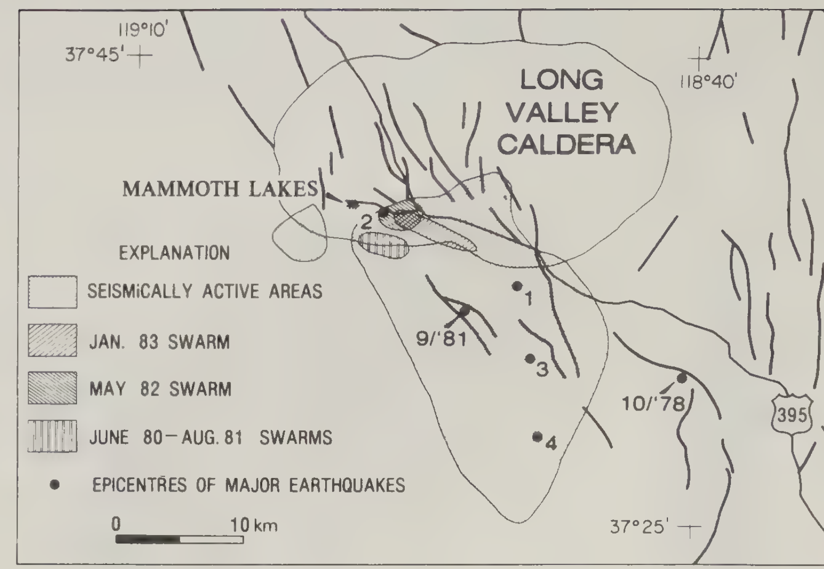

Figure 12.1.5. Map of Long Valley Caldera and vicinity, showing area of seismic activity and locations of earthquake swarms, from Julian (1983). Heavy lines, normal faults. Epicenters of four magnitude 6 earthquakes during 25-27 May 1980 are indicated with solid dots numbered in order of occurrence. Reprinted by permission from Nature; copyright 1983 by Macmillan Magazines, Ltd.

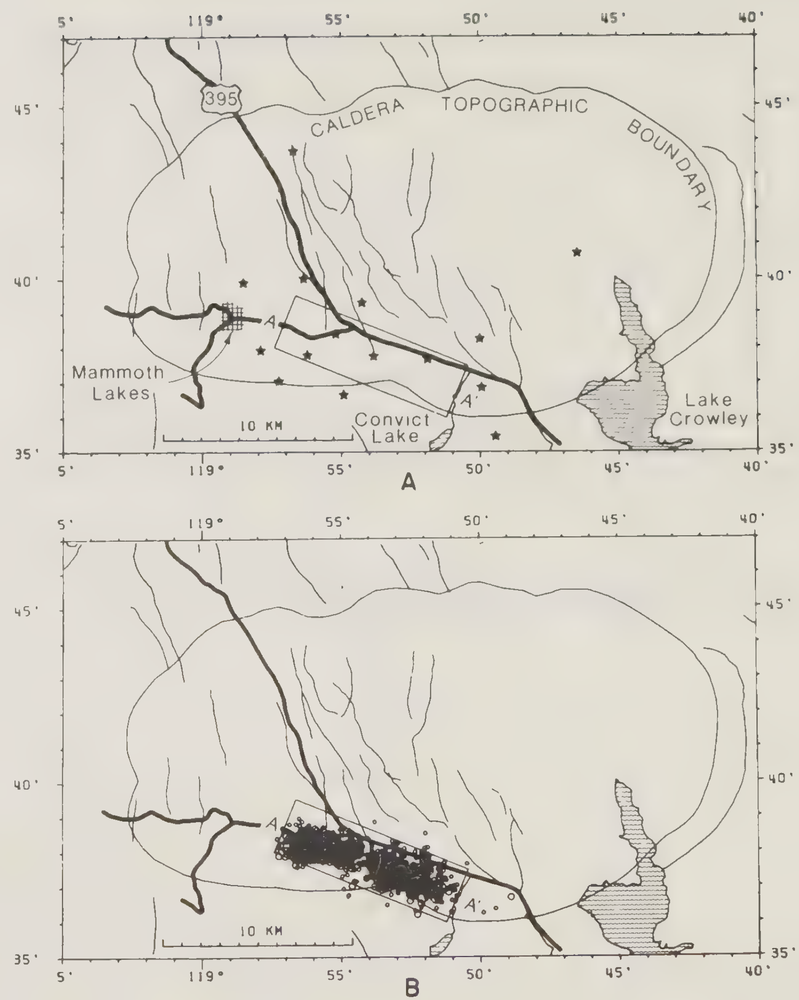

Figure 12.1.6. A, Map of Long Valley Caldera showing locations of 15 seismic stations (stars) used to locate epicenters shown below (Savage and Cockerham, 1984). B, Epicenters for 7-31 January 1983. Box encloses earthquakes plotted in cross-sectional views shown in figure 12.1.7. Outline of Long Valley Caldera and prominent faults are shown by light solid lines, principal highways by heavy lines. Copyright by the American Geophysical Union.

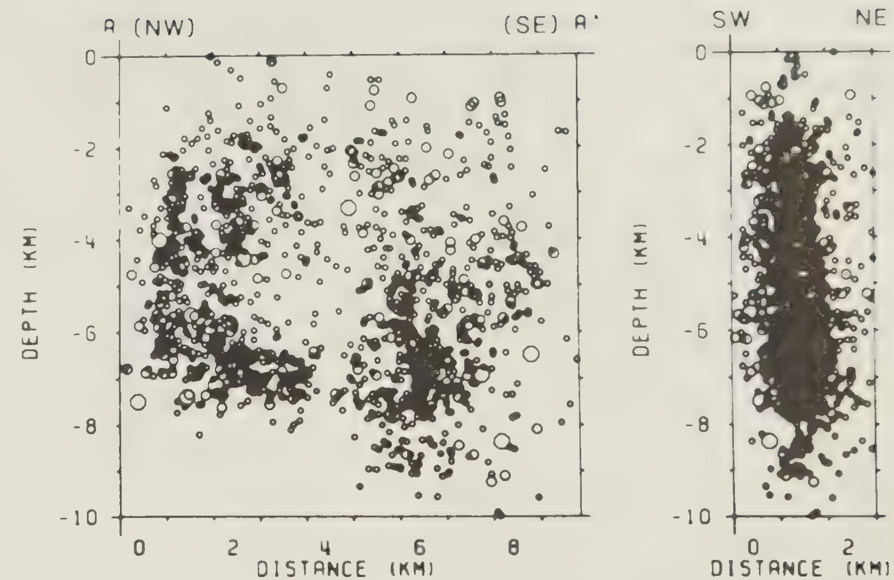

Figure 12.1.7. Projections of the hypocenters of earthquakes shown within box in figure 12.1.6 onto vertical planes striking west-northwest and south-southwest, from Savage and Cockerham (1984). Cross section A-A' is parallel to long dimension of box with A at west-northwest edge; other cross section is perpendicular to A-A'. Size of symbol is proportional to magnitude. Copyright by the American Geophysical Union.

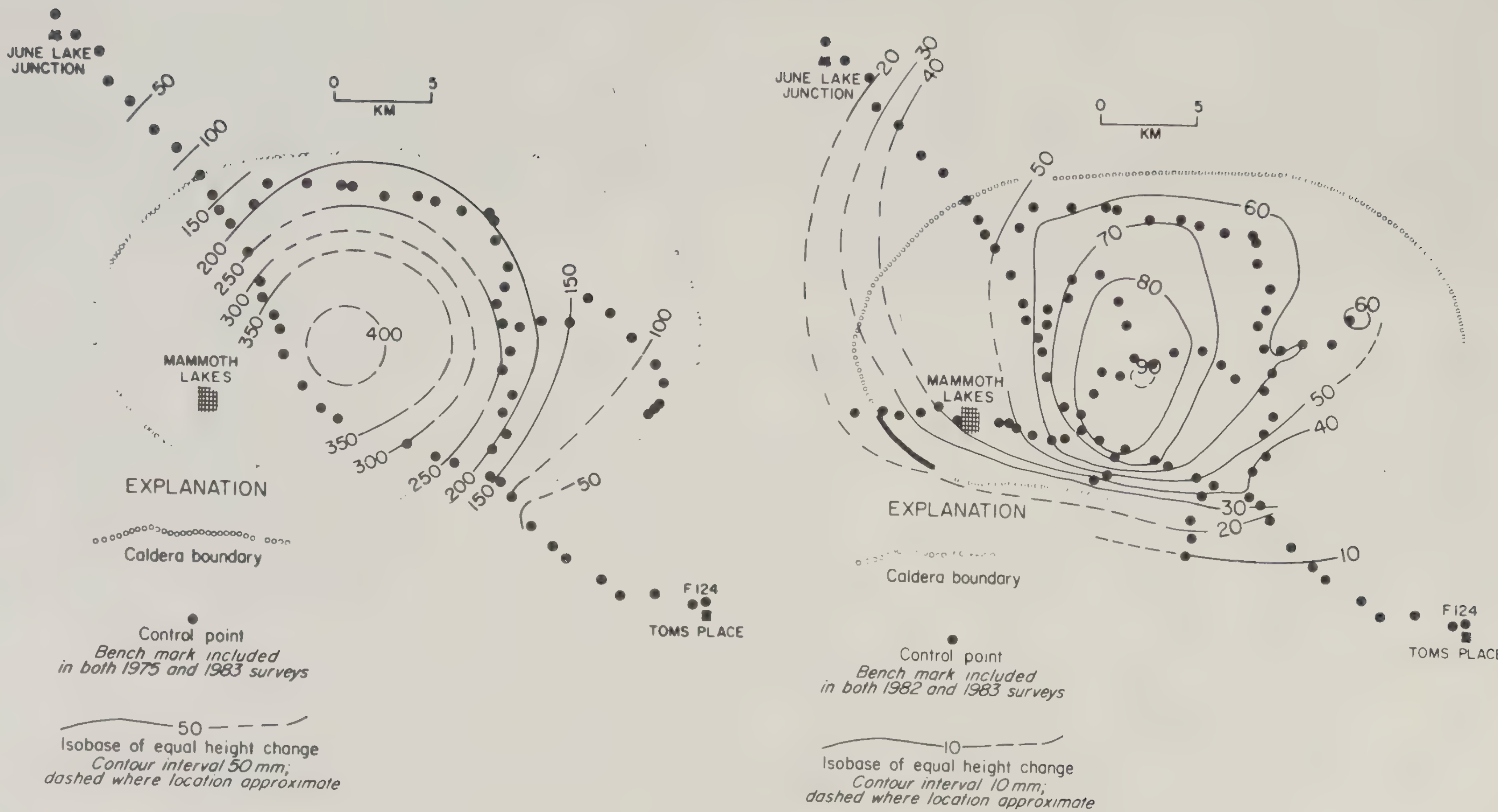

Figure 12.1.8. Uplift contours at Long Valley Caldera, 1975-83, from Castle and others (1984). Left, 1975-83; right, 1982-83. Both maps based on minimum constrained displacement adjustment with respect to bench mark F124. Copyright by the American Geophysical Union.

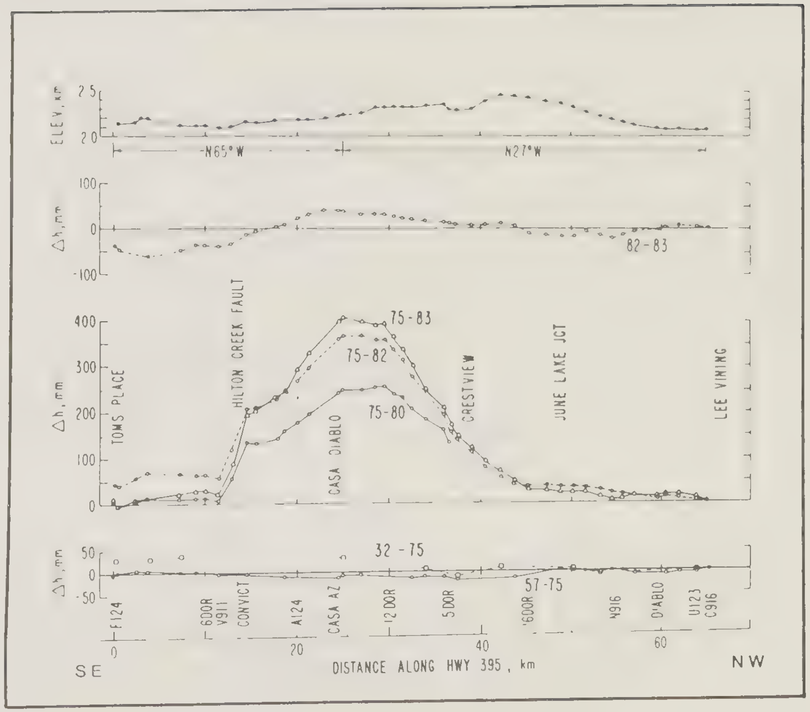

Figure 12.1.9. Elevation changes along U.S. Highway 395 across Long Valley Caldera from leveling surveys in 1932, 1957, 1975, 1980, 1982, and 1983. Note lack of appreciable deformation prior to 1975 and progressive uplift since 1980 (Hill and others, 1985c).

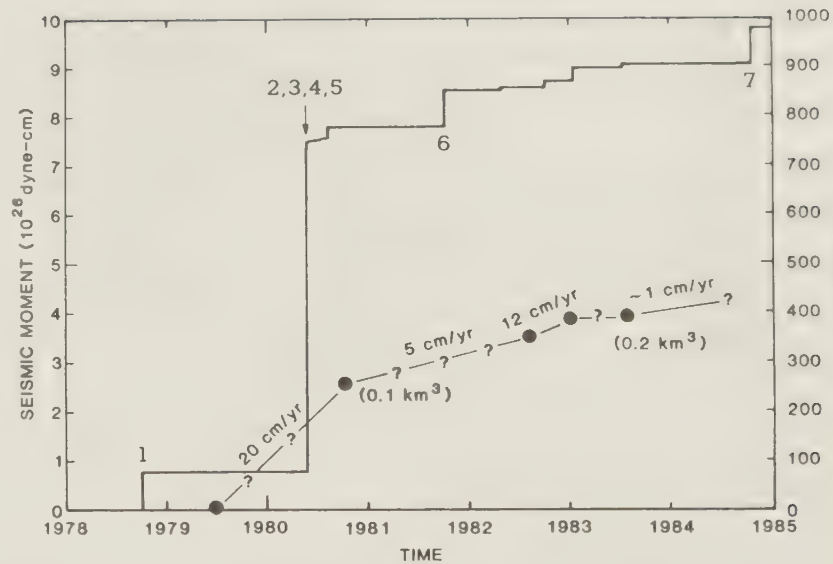

Figure 12.1.10. Summary of seismic activity and inflation of resurgent dome at Long Valley Caldera since 1978, from Hill and others (1985a). Solid line, cumulative seismic moment for earthquakes in Long Valley region from 1978 through mid-1984; solid dots, elevation history of bench mark CASA AZ near Casa Diablo Hot Springs (south part of resurgent dome). Copyright by the American Geophysical Union.

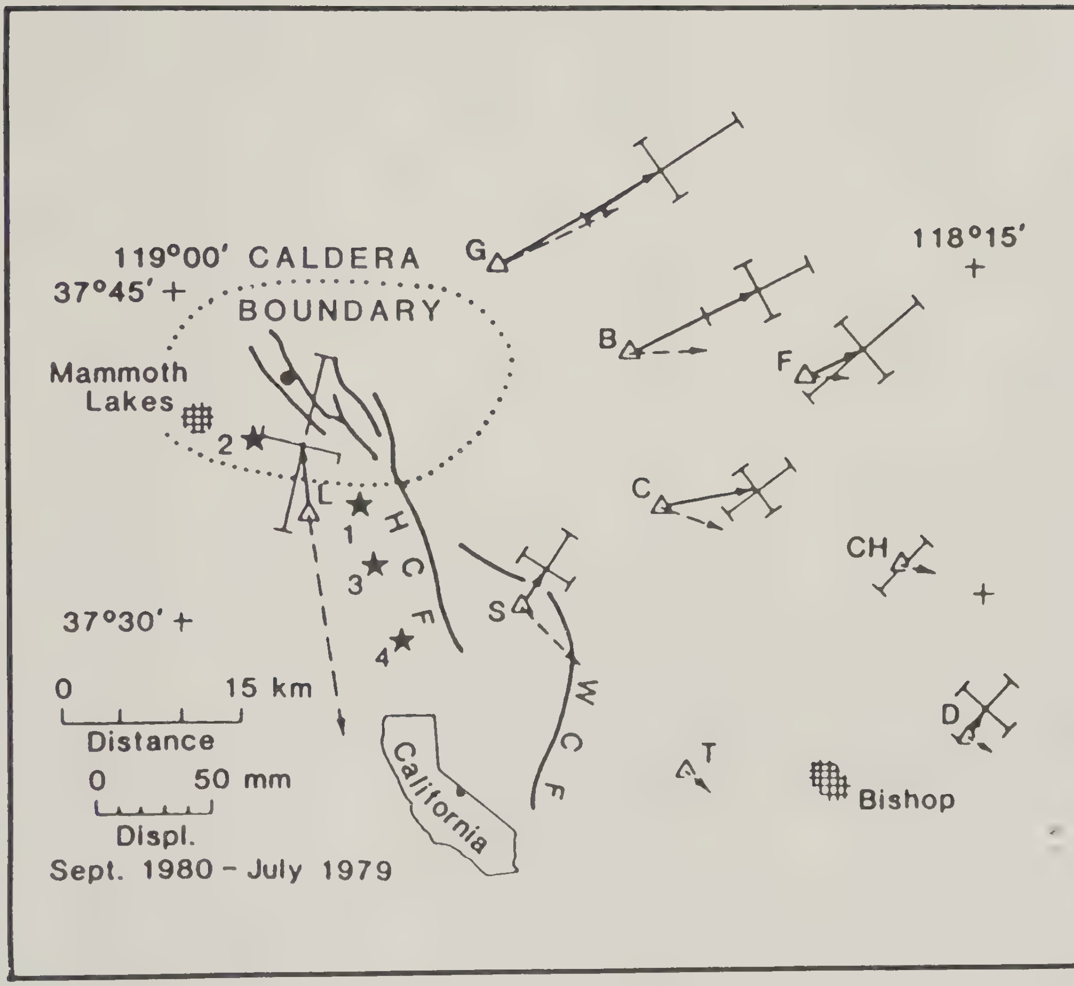

Figure 12.1.11. Horizontal displacements near Long Valley Caldera from precise trilateration surveys in July 1979 and September 1980, from Savage and Clark (1982). Solid arrows show observed displacements; dashed arrows show displacements expected from expansion of a spherical magma chamber at 11-km depth. Stars indicate epicenters of four magnitude 6 earthquakes in May 1980, in order of occurrence. Solid dot, center of resurgent dome; HCF, Hilton Creek Fault; WCF, Wheeler Crest Fault. Copyright by the American Association for the Advancement of Science.

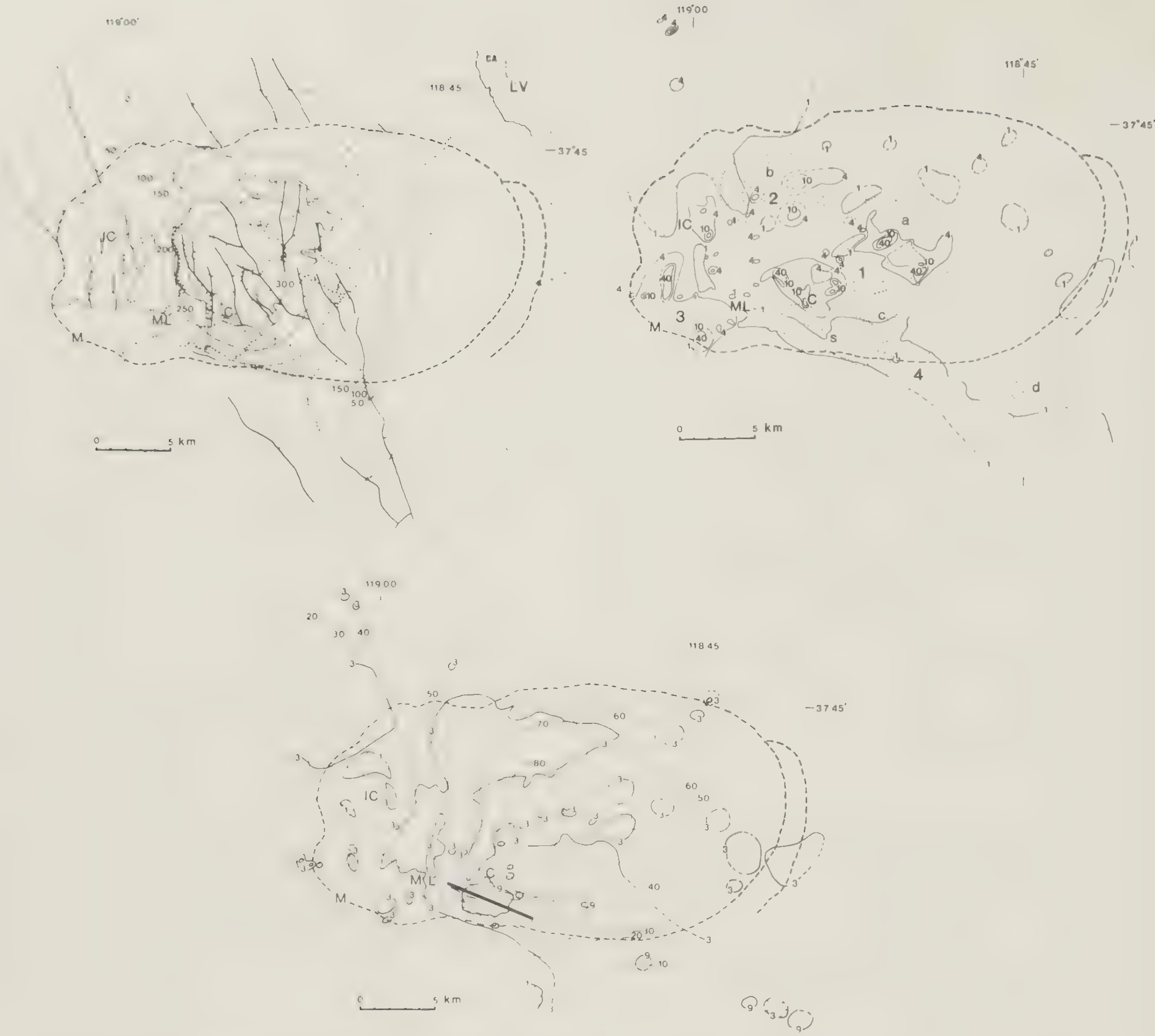

Figure 12.1.12. Top left, Long Valley Caldera (bold dashed lines) with principal faults (bold continuous lines), cumulative 1975-82 uplift in millimeters (light dashed lines), area of January 1983 seismic swarm (vertical ruling), outline of resurgent dome (light continuous line), and Hg^{O} and Rn sample sites (dots). Abbreviations: ML, city of Mammoth Lakes; IC, Inyo Craters; M, Mammoth Mountain; and C, Casa Diablo fumarole. Top right, contoured Hg^{O} anomalies (continuous lines, dashed where less certain; note irregular contour interval), magma bodies as inferred by Sanders (1984) (stippled areas a to d), and epicentral area of the January 1983 seismic swarm (hatched area labeled s). Hg^{O} contours are background (6.6 ppb), threshold (26.4 ppb), peak (66 ppb), and 264 ppb. Boldface numbers indicate broad Hg^{O} highs (areas 1 to 3) and an extensive Hg^{O} low (area 4). Bottom, contoured Rn anomalies (continuous lines, dashed where less certain), magma bodies (stippled areas), epicentral area of the January 1983 swarm (hatched), surface projection of an inferred dike (continuous heavy line), and 1982-83 uplift (light dashed lines), in millimeters. Radon contours are background (82 T/mm^2 per 30 days, threshold (246 T/mm^2 per 30 days), and peak (738 T/mm^2 per 30 days). Plots are from Williams (1985). Copyright by the American Association for the Advancement of Science.

YELLOWSTONE

CAVW number (active vent)	Latitude Longitude (degrees)	Diameter (km)	Local tectonic setting	Precaldera edifice	SiO_2 content (wt pct)	Age of collapse (yr B.P.)	Date of unrest	Type and duration of unrest ESTU STHF MGTF H Te	Eruption type
12-05-01	44.58N 110.53W	85 x 45	E-W exten with complications	None?	R = 70-77 C = 76-77	630,000	late 19th century and continuing	GG-G FG?x -GFx F QQ	none

TECTONIC SETTING

Yellowstone lies at the intersection of the Basin and Range tectonic province, dominated by E-W extension, and the eastern Snake River Plain, a linear downwarp or graben that has been a locus for basaltic volcanism since middle Miocene time (figs. 12.2.1, 12.2.2). According to one popular model, the rhyolitic Yellowstone Plateau marks the current location of a "hotspot" or melting anomaly in the upper mantle, and the basaltic Snake River Plain records the hotspot's northeastward track across the mobile North American plate (Smith and others, 1974, 1977).

Focal mechanisms (fig. 12.2.3) of a magnitude 7.5 earthquake and its aftershocks (Hebgen Lake, 1959, see below) suggested N-S extension near Hebgen Lake (about 70 km northwest of Yellowstone) and radial compression near the caldera (Ryall, 1962; Smith and others, 1974). Focal mechanisms of more recent earthquakes and geologic mapping in the caldera (Smith and others, 1977; Christiansen, 1984) suggest dominantly ENE-WSW or E-W extension.

GEOLOGIC HISTORY

Three times in the past 2 million years, large reservoirs of rhyolite magma have accumulated in the upper crust at Yellowstone, triggering cataclysmic eruptions and caldera collapses 2.0, 1.3, and 0.6 million years ago (fig. 12.2.1) (Christiansen, 1984). The first great eruption (2.0 m.y. B.P.) produced the Huckleberry Ridge Tuff (more than 2,450 km^3) and a composite caldera more than 75 km long, extending from Island Park on the west to central Yellowstone Park on the east. The second eruption (1.3 m.y. B.P.) produced the Mesa Falls Tuff (more than 280 km^3) and the Island Park Caldera west of Yellowstone Park; the third (0.6 m.y. B.P.) produced the Lava Creek Tuff (more than 1,000 km^3) and the present Yellowstone Caldera (fig. 12.2.2). Rhyolitic volcanism resumed within the Yellowstone Caldera after structural resurgence formed the Sour Creek and Mallard Lake resurgent domes. Renewed doming in the western caldera culminated with extrusion of 1,000 km^3 of intracaldera rhyolite flows between 150,000 and 75,000 yr B.P. (Christiansen, 1984).

YELLOWSTONE (continued)

GEOLOGIC HISTORY (continued)

There is abundant geophysical evidence for residual partial melt beneath Yellowstone Caldera (figs. 12.2.4-12.2.7) (Smith and others, 1974; Eaton and others, 1975; Lehman and others, 1982; Schilly and others, 1982), and the consensus among those who have studied the area is that the Yellowstone magmatic system will likely erupt again (Smith and Braile, 1983; Christiansen, 1984).

Deformed terraces along the shore of Yellowstone Lake and the Yellowstone River record a complex history of Holocene deformation that has continued to the present (fig. 12.2.8). Based on studies of the terraces, Hamilton (1985) proposed that intracaldera subsidence totaling more than 80 m occurred in stages during the early Holocene, and Meyer and Locke (1986) inferred net uplift of about 10 m in the northern Yellowstone Lake area during the late Holocene. The latter authors also cited geomorphic evidence that during the past several thousand years the lake fell to a level near the present, rose 6-7 m, fell to the present level or below, and now is rising again due to differential uplift of its outlet (see below).

Yellowstone Caldera currently contains one of the largest and most active hydrothermal systems in the world (fig. 12.2.9), and hydrothermal activity probably has been relatively constant for at least the past 10,000 years. The contemporary heat output of the Yellowstone magmatic system is 4×10^{16} cal/yr, or 5,500 MW (Fournier and Pitt, 1985; Fournier, 1986).

HISTORICAL ACTIVITY

Ferdinand V. Hayden, leader of the first scientific expedition to the Yellowstone area, reported that severe earthquakes were felt northeast of Yellowstone Lake in 1871. From that date until 1959, at least 76 earthquakes strong enough to be felt were reported in the Yellowstone Park - Hebgen Lake region. Smith and Braile (1983) report that at least seven of these exceeded magnitude 6 (fig. 12.2.10).

A magnitude 7.3 earthquake occurred in August 1959 near Hebgen Lake, 70 km northwest of Yellowstone Caldera. Most aftershocks and other earthquakes from 1959 to 1972 were just east of Hebgen Lake; a few shallow earthquakes occurred within the caldera, but none of these were in the northeast part of the caldera, where the shallowest geophysical anomalies occur. The Yellowstone Park earthquake ($\underline{M}$ 6.1) occurred on 30 June 1975 just inside the north caldera rim near Norris (Pitt and others, 1979; fig. 12.2.1).

Since 1972, many earthquakes have occurred near and within the caldera--more than can be attributed solely to an upgrading of the Yellowstone seismic network in late 1972. Events in the caldera typically occur in swarms less than 5 km deep, in contrast to events outside the caldera that are as much as 15 km deep. Many of the earthquakes occurring in the caldera are in areas of major hydrothermal activity. Swarms within the caldera include some just south of Norris Junction (1972, 1975), near the south end of Yellowstone Lake (1973), near Old Faithful (early 1978), Mud Volcano (late 1978), in West Thumb (several), and just outside the northwest caldera rim (late 1985-present). The 1985-present swarm includes 28 events larger than magnitude 3.5 from 16 October to 27 December 1985. Events of comparable size also occurred in 1986 and 1987, but the intensity of the swarm seemed to be waning as of late 1987.

YELLOWSTONE (continued)

HISTORICAL ACTIVITY (continued)

Leveling surveys in 1923 and 1975-77 detected a broad pattern of intracaldera uplift of up to 72 cm along a northeast-trending axis within Yellowstone Caldera (fig. 12.2.11) (Reilinger and others, 1977; Pelton and Smith, 1979, 1982). Annual surveys since 1983 show that the central caldera floor rose at an average rate of 15-17 mm/yr from 1976 to 1986, but that uplift stopped during 1984-85 and subsidence began during 1985-87 (Dzurisin and Yamashita, 1987 and unpubl. data) (figs. 12.2.12-12.2.14). The maximum uplift measured since the first survey in 1923 is about 86 cm near the Mud Volcano area (Dzurisin and Yamashita, 1987). No other geodetic measurements are available to determine whether the uplift occurred at a relatively constant rate between leveling surveys, or perhaps began around the time of the 1959 Hebgen Lake earthquake. However, gauging records from Yellowstone Lake suggest that tilting of the lakeshore has occurred at a relatively constant rate since 1923, with no discernible change associated with the 1959 earthquake (Hamilton, 1984). The 1923 and 1975-77 leveling surveys showed that deformation extended well beyond the caldera rim, indicating that the phenomenon is not wholly volcanic in origin. For example, doming of an 8,000 km^2 area surrounding the epicenter of the 1959 Hebgen Lake earthquake probably reflects postseismic viscoelastic relaxation of the crust in response to that earthquake (Reilinger and others, 1977; Reilinger, 1986).

Marler (1964) and Marler and White (1975) documented major changes in hydrothermal activity of the Yellowstone area as a result of the 1959 Hebgen Lake earthquake. Discharge at many hot springs increased within minutes to hours of the earthquake and in some cases was sustained for years after the earthquake. Increases in hot-spring and geyser activity were probably a result of new fractures formed in self-sealed caps that had kept water at elevated pressures, above hydrostatic pressure, and had moved boiling-point curves to abnormally high temperatures for given depths (White and others, 1975). The Yellowstone Park earthquake of 30 June 1975 also caused impressive hydrothermal changes throughout the caldera (R.A. Hutchinson, oral commun., 1987). The magnitude 7.3 Borah Peak, Idaho earthquake (250 km east-southeast of Yellowstone) on 28 October 1983 caused the average interval between eruptions at Old Faithful geyser to increase by more than 7 minutes from late October 1983 to early March 1984. The 1984 annual average interval (76.3 minutes) is the longest known in more than 115 years of observation (R.A. Hutchinson, written commun., 1985). Starting in April 1984, the average interval between eruptions started to decline toward its pre-earthquake value of 69.2 minutes. Then about 10 days after a small earthquake swarm beneath the Pitchstone Plateau (25 km south of Old Faithful) on 6 June 1987, the interval suddenly increased from 70.1 minutes to 75.7 minutes, apparently as a delayed response to the swarm (R.A. Hutchinson, written commun., 1988).

Hydrothermal changes in 1959, 1975, and 1983 followed large earthquakes, not vice versa. However, the relation between subsequent seismic swarms and hydrothermal changes has not been as clear, and hydrothermal activity may have influenced recent seismicity. Increased seismicity at Mud Volcano in 1978 preceded an increase in thermal activity there, but increased thermal activity in the Norris geyser basin in 1972 (and on several previous occasions) preceded seismic activity. At Norris, Trimble and Smith (1975) suggest that high fluid pressure and temperature reduce rock strength and induce earthquake swarms; Pitt and Hutchinson (1982) grant that this is plausible, but they note that thermal changes in the Norris basin are related to annual fluctuation of the water table and are only sometimes followed or accompanied by earthquakes.

YELLOWSTONE (continued)

COMMENTS

Yellowstone Caldera is the largest caldera in this compilation and is unique for several other reasons. The Yellowstone region has produced three caldera-forming eruptions in the past 2 million years, two of those among the largest eruptions known to have occurred on Earth (each more than 1,000 km^3). Yellowstone's hydrothermal system is among the largest and most active in the world, and its historical seismicity and uplift are comparable to those at the most active calderas in this compilation. In spite of this, the implications of historical unrest at Yellowstone for short-term tectonic and volcanic hazards are not well understood. For example, it is not known whether recent unrest is typical of quiescent periods or precursory to the next major earthquake or eruption. It is also not clear whether the Yellowstone magmatic system is in the waning stage of its third volcanic cycle that climaxed 630,000 years ago or in the early stage of a fourth cycle.

Possible causes of historical uplift at Yellowstone include (1) inflation owing to basaltic intrusions into the upper crust beneath the caldera (Pelton and Smith, 1979, 1982), (2) pressurization of a deep hydrothermal system by accumulation of magmatic fluids that are released during cooling and crystallization of a silicic magma body (Fournier, 1986), and (3) increased compressive strain that upwarps the hot and mechanically weak crust beneath the caldera (Meertens and Levine, 1985; Meertens, 1987). Over geological time scales, Yellowstone's vigorous hydrothermal system must derive its heat ultimately from basaltic intrusions, because the system's current heat flux would result in complete crystallization and cooling of about 10^4 km^3 of rhyolite in 10^5 years (Fournier, 1986). Stated differently, a 3-km-thick lens of rhyolite beneath the entire caldera would have completely cooled since the last magmatic eruption 75,000 yr B.P. unless there was additional heat input from basaltic intrusions sometime during that period. However, there is no compelling evidence that basalt has intruded beneath the caldera during historical time, because the current heat flux could be supplied entirely by heat derived from cooling of already crystalline rocks, or from crystallization of rhyolitic magma (Fournier, 1986). Evidence for the release of magmatic fluids from beneath the caldera includes high $^3He/^4He$ ratios and high chloride concentrations in hydrothermal waters (Fournier and Pitt, 1985). It is possible that both magmatic inflation and cooling/crystallization are occurring simultaneously, the first near the base of the silicic reservoir and the second at higher levels within the reservoir. With regard to the third mechanism listed above, Meertens and Levine (1985) and Meertens (1987) suggested that, although Yellowstone lies in zone of regional tectonic extension, compressive strain beneath the caldera could be a consequence either of magmatic inflation beneath the Hebgen Lake region or of subsurface movements during or after the 1959 $\underline{M} = 7.3$ Hebgen Lake earthquake.

Processes that might account for subsidence include (1) deflation owing to withdrawal of magma from beneath the caldera, most likely by lateral intrusion of basalt from beneath the silicic magma reservoir into preexisting zones of weakness along the caldera rim, (2) depressurization of the deep hydrothermal system caused by rupturing of an impermeable cap and upward migration of hydrothermal fluids, and (3) regional tectonic extension. The only suggestion that magma might have moved laterally from beneath the caldera since the onset of subsidence is a prolonged swarm of earthquakes just outside the northwest caldera rim that began in October 1985. However, that swarm occurred in the vicinity of the Hebgen Lake fault zone and probably was primarily tectonic in origin (R.B. Smith, oral commun., 1988). Measurements of total chloride flux from within the caldera show no definite increase during the period of subsidence, but an increase of 10 to 15 percent could have gone undetected (R. Fournier, oral commun., 1988).

YELLOWSTONE (continued)

COMMENTS (continued)

There is no evidence from precise trilateration measurements for unusual crustal extension in the Yellowstone region since the onset of subsidence: strain rates have been relatively linear during 1972-87 in the Hebgen Lake area, and only small movements that were consistent with the observed subsidence occurred during 1984-87 in the northeast part of Yellowstone Caldera (J.C. Savage, written commun., 1988).

REFERENCES

Christiansen, R.L., 1984, Yellowstone magmatic evolution: its bearing on understanding large-volume explosive volcanism, in Boyd, F.R., ed., Explosive volcanism: Inception, evolution, and hazards: National Research Council Studies in Geophysics, Washington, D.C., National Academy Press, p. 84-95.

----- 1988, The Quaternary and Pliocene Yellowstone Plateau volcanic field of Wyoming, Idaho, and Montana: U.S. Geol. Surv. Prof. Paper 729 [in press].

Dzurisin, D., and Yamashita, K.M., 1987, Vertical surface displacement at Yellowstone Caldera, Wyoming, 1976-1986: Jour. Geophys. Res., v. 92, no. B13, p. 13,753-13,766.

Eaton, G.P., Christiansen, R.L., Iyer, H.M., Pitt, A.M., Mabey, D.R., Blank, H.R., Jr., Zietz, I., and Gettings, M.E., 1975, Magma beneath Yellowstone National Park: Science, v. 188, p. 787-796.

Fournier, R.O., 1986, Hydrothermal activity in relation to late Holocene dynamics in the Yellowstone caldera: Proceedings, Science in the National Parks Conference, Colorado State University, Fort Collins, Colorado, July 1986.

Fournier, R.O., and Pitt, A.M., 1985, The Yellowstone magmatic-hydrothermal system, in Stone, Claudia, ed., Geothermal resources Council 1985 International Symposium on Geothermal Energy, Transactions: Int. Vol., p. 319-327.

Hamilton, W.L., 1984, Applying lake level gaging records to the investigation of uplift within the Yellowstone caldera, Yellowstone National Park [abs.]: Eos, Trans. Am. Geophys. Union, v. 65, p. 192-193.

----- 1985, Deformation models for interpreting warped Holocene terraces of Yellowstone Lake and the Yellowstone River at the Yellowstone caldera, Wyoming [abs.]: Eos, Trans. Am. Geophys. Union, v. 66, no. 46, p. 853.

Iyer, H.M., Evans, J.R., Zandt, G., Stewart, R.M., Cookley, J.M., and Roloff, J.N., 1981, A deep low velocity body under the Yellowstone caldera, Wyoming; Delineation using teleseismic P-wave residuals and tectonic interpretations: Summary: Geol. Soc. Am. Bull., v. 92, p. 792-798.

Lehman, J.A., Smith, R.B., Schilly, M.M., and Braile, L.W., 1982, Upper crustal structure of Yellowstone from seismic and gravity observations: Jour. Geophys. Res., v. 87, no. B4, p. 2713-2730.

Marler, G.D., 1964, Effects of the Hebgen Lake earthquake of August 17, 1959 on the hot springs of the Firehole Geyser basins, Yellowstone National Park: Geol. Soc. Am. Bull., v. 86, p. 749-759.

Marler, G.D., and White, D.E., 1975, Seismic geyser and its bearing on the evolution of geyser and hot springs of Yellowstone National Park: Geol. Soc. Am. Bull., v. 86, p. 749-759.

Meyer, G.A., and Locke, W.W., 1986, Origin and deformation of Holocene shoreline terraces, Yellowstone Lake, Wyoming: Geology, v. 14, p. 699-702.

YELLOWSTONE (continued)

REFERENCES (continued)

Meertens, C.M., 1987, Tilt tides and tectonics at Yellowstone National Park: Boulder, Univ. of Colorado, Ph.D. thesis, 236 p.

Meertens, C., and Levine, J., 1985, Compressive tectonic strain as a possible mechanism for long-term vertical deformation of the Yellowstone caldera: Eos, Trans. Am. Geophys. Union, v. 66, no. 46, p. 853.

Muffler, L.J.P., White, D.E., and Truesdell, A.H., 1971, Hydrothermal explosive craters in Yellowstone National Park: Geol. Soc. Am. Bull., v. 82, p. 723-740.

Nicholls, H.R., and Rinehart, J.S., 1967, Geophysical study on geyser action in Yellowstone National Park: Jour. Geophys. Res., v. 72, p. 4651-4663.

Pelton, J.R., and Smith, R.B., 1979, Recent crustal uplift in Yellowstone National Park: Science, v. 206, p. 1179-1182.

----- 1982, Contemporary vertical surface displacements in Yellowstone National Park: Jour. Geophys. Res., v. 87, p. 2745-2761.

Pitt, A.M., and Hutchinson, R.A., 1982, Hydrothermal changes related to earthquake activity at Mud Volcano, Yellowstone National Park, Wyoming: Jour. Geophys. Res., v. 87, p. 2762-2766.

Pitt, A.M., Weaver, C.S., and Spence, W., 1979, The Yellowstone Park earthquake of June 30, 1975: Bull. Seismol. Soc. Am., v.69, no. 1, p. 187-205.

Reilinger, R.E., 1986, Evidence for postseismic viscoelastic relaxation following the 1959 $\underline{M}$ = 7.5 Hebgen Lake, Montana earthquake, Jour. Geophys. Res., v. 91, no. B9, p. 9488-9494.

Reilinger, R.E., Citron, G.P., and Brown, L.D., 1977, Recent vertical crustal movements from precise leveling data in southwestern Montana, western Yellowstone National Park, and the Snake River Plain: Jour. Geophys. Res., v. 82, p. 5349-5359.

Ryall, A., 1962, The Hebgen Lake, Montana, earthquake of August 18, 1959: P-waves: Bull. Seismol. Soc. Am., v. 52, p. 235-271.

Schilly, M.M., Smith, R.B., Braile, L.W., and Ansorge, J., 1982, The 1978 Yellowstone-Eastern Snake River Plain seismic profiling experiment: data and upper crustal structure of the Yellowstone region, Jour. Geophys. Res., v. 87, no. B4, p. 2692-2704.

Smith, R.B., and Braile, L.W., 1983, Crustal structure and evolution of an explosive silicic volcanic system at Yellowstone National Park, in Boyd, F.R., ed., Explosive volcanism: Inception, evolution, and hazards: National Research Council Studies in Geophysics, Washington, D.C., National Academy Press, p. 96-109.

Smith, R.B., and Christiansen, R.L., 1980, Yellowstone Park as a window on the Earth's interior: Sci. Am., v. 242, p. 104-117.

Smith, R.B., Shuey, R.T., Freidline, R.O., Otis, R.M., and Alley, L.B., 1974, Yellowstone hot spot: new magnetic and seismic evidence: Geology, v. 2, p. 451-455.

Smith, R.B., Shuey, R.T., Pelton, J.R., and Bailey, J.P., 1977, Yellowstone hot spot: contemporary tectonics and crustal properties from earthquake and aeromagnetic data, Jour. Geophys. Res., v. 82, p. 3665-3676.

Trimble, A.B., and Smith, R.B., 1975, Seismicity and contemporary tectonics of the Hebgen Lake-Yellowstone Park region: Jour. Geophys. Res., v. 80, p. 733-741.

White, D.E., Fournier, R.O., Muffler, L.J.P., and Truesdell, A.H., 1975, Physical results of research drilling in thermal areas of Yellowstone National Park, Wyoming: U.S. Geol. Surv. Prof. Paper 892, 70 p.

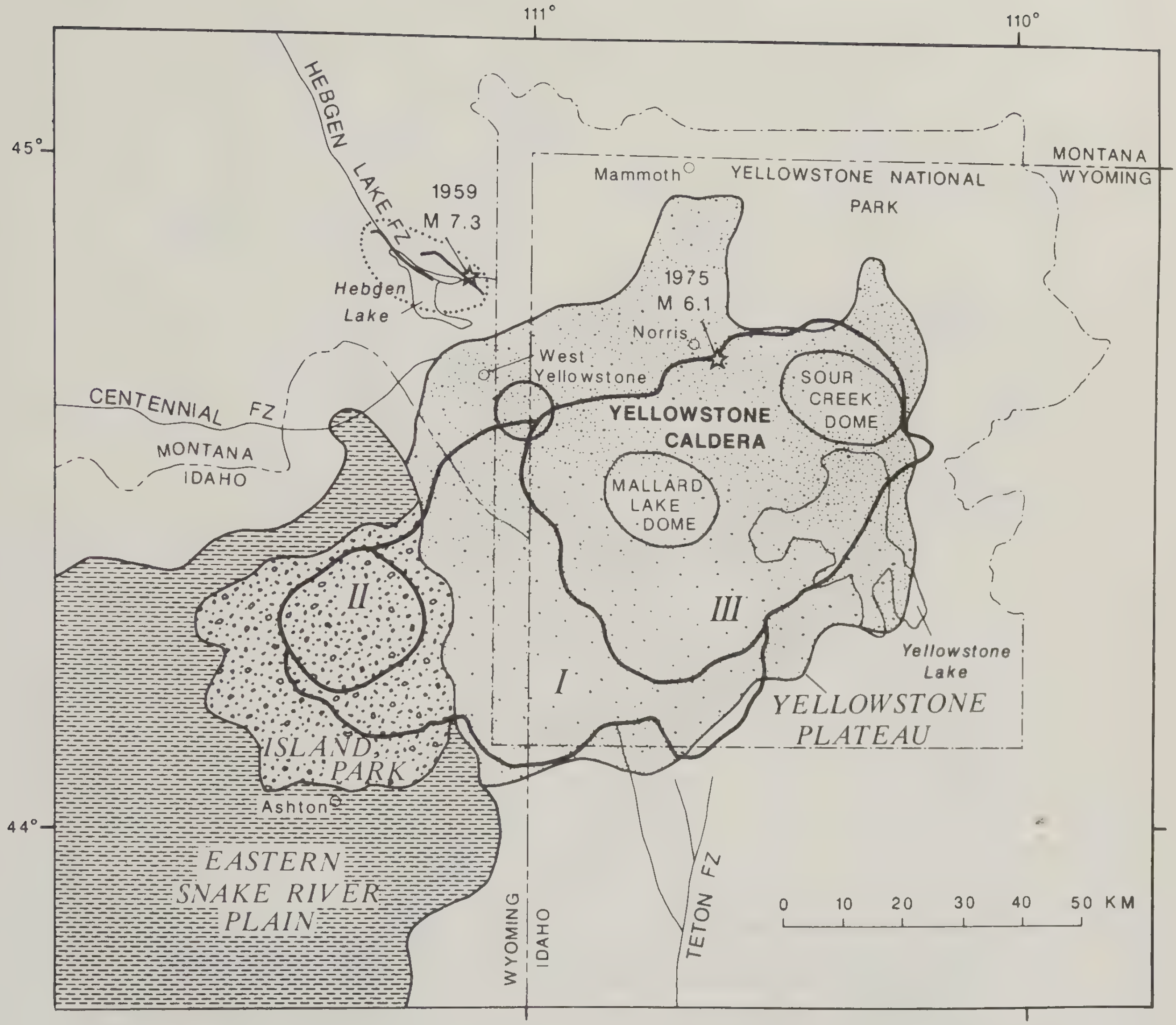

Figure 12.2.1. Yellowstone Plateau volcanic field, after Christiansen (1984). Rhyolitic Yellowstone Plateau lies along northeastward extension of basaltic Snake River Plain. Also shown are the Mallard Lake and Sour Creek resurgent domes, approximate outlines of three large calderas that formed in the past 2 million years (I, II, and III in order of formation), epicenters (stars) of the 1959 Hebgen Lake earthquake ($\underline{M}$ 7.3) and 1975 Yellowstone Park earthquake ($\underline{M}$ 6.1), and outline of Yellowstone National Park (irregular broken line). Reprinted with permission of National Academy Press, Washington, D.C.

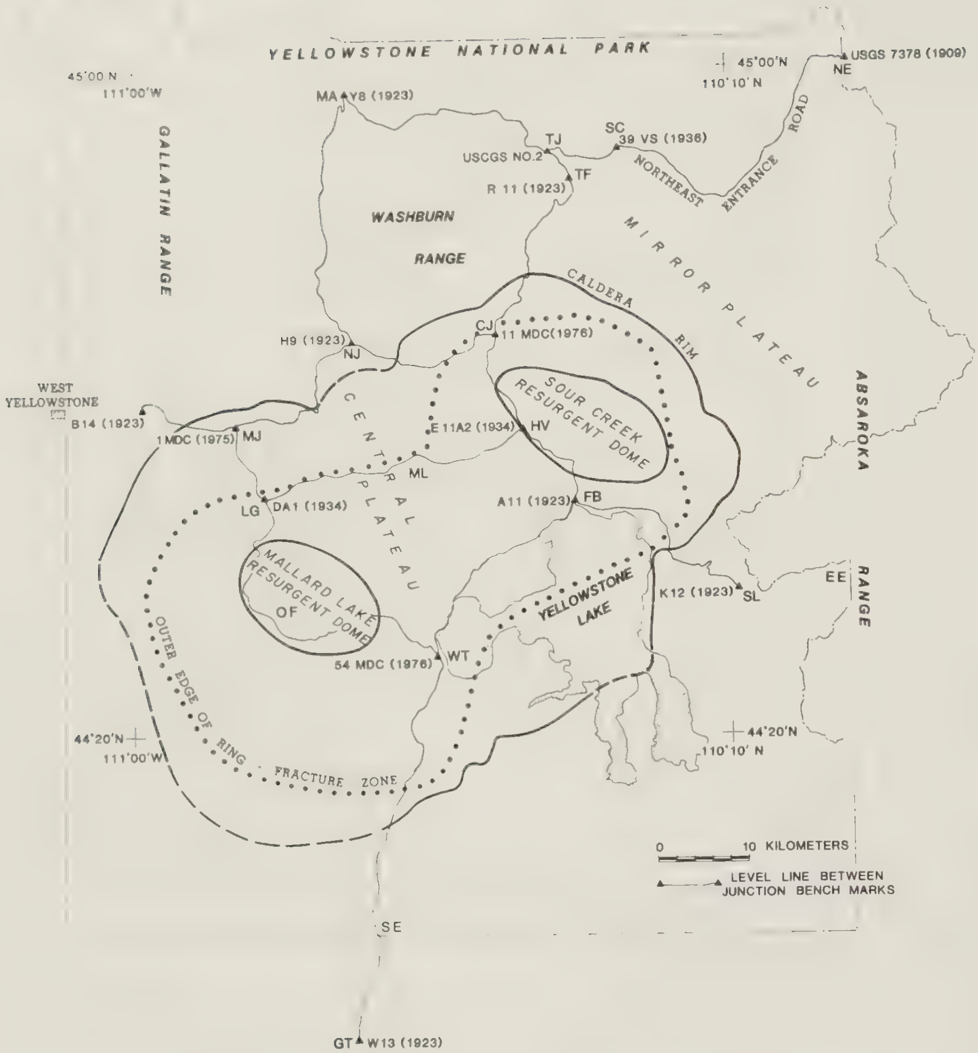

Figure 12.2.2. Yellowstone National Park (irregular broken line) and Yellowstone Caldera (topographic rim, heavy line; ring fracture, dotted line), from Pelton and Smith (1982). Also shown are Mallard Lake and Sour Creek resurgent domes, Yellowstone Lake, and leveling routes for surveys in 1923 and 1975-77 (fine lines). MA, Mammoth Hot Springs; TJ, Tower Junction; TF, Tower Falls; SC, Slough Creek turnoff; NE, Northeast Entrance; SL, Sylvan Lake; GT, Grand Teton National Park entrance; SE, South Entrance; WT, West Thumb; OF, Old Faithful; LG, Lower Geyser Basin; MJ, Madison Junction; NJ, Norris Junction; CJ, Canyon Junction; HV, Hayden Valley; ML, Mary Lake; FB, Fishing Bridge; EE, East Entrance. Lake Butte is near bench mark K12 (1923); Lewis Lake is near ring fracture south of WT (see figures 12.2.11 - 12.2.14 for leveling results). Copyright by the American Geophysical Union.

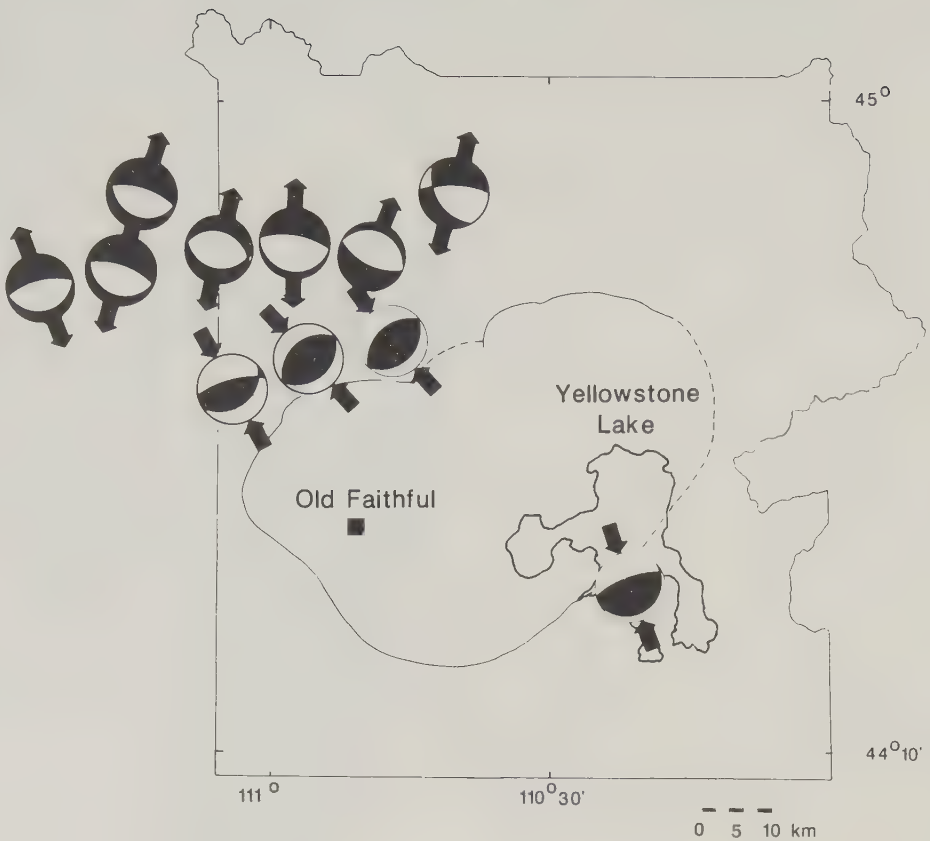

Figure 12.2.3. Fault-plane solutions for earthquakes in Hebgen Lake and Yellowstone regions, from Smith and others (1974). Upper hemisphere, equal-area stereographic nets. Dark quadrants, compression; light quadrants, dilatation. Inward arrows, P-axes; outward arrows, T-axes.

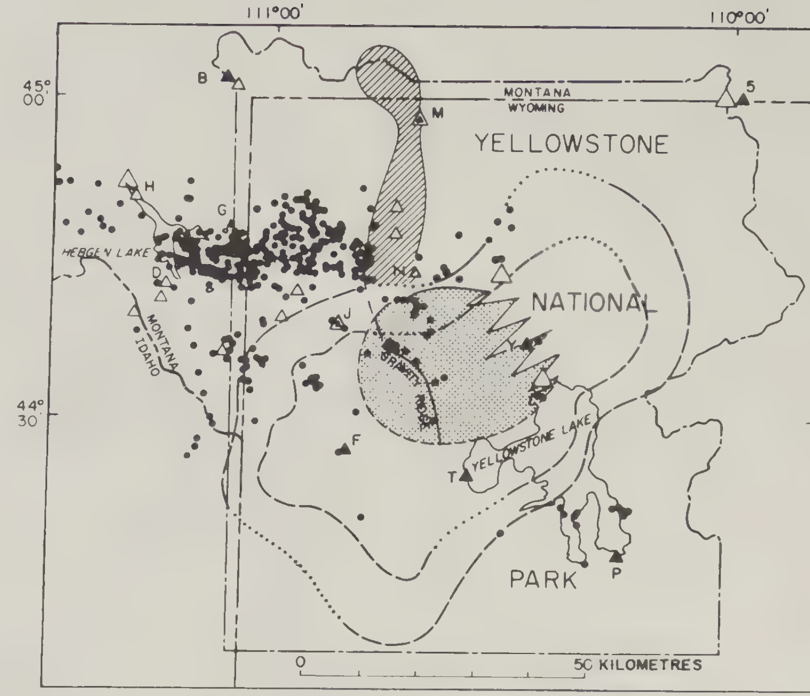

Figure 12.2.4. Seismicity and seismic attenuation in Yellowstone Plateau region, from Eaton and others (1975). Triangles identified by letters indicate seismograph stations operated from 1963 to 1975. Circles denote earthquake epicenters. Stippled area defines a zone of observed attenuation for compressional seismic waves from local earthquakes; shear waves are absent on some records for paths through this zone. Dashed curves denote top and bottom of local gravity gradient; dotted curves mark interrupted portions. Cross-ruling defines Norris-Mammoth corridor. Copyright by the American Association for the Advancement of Science.

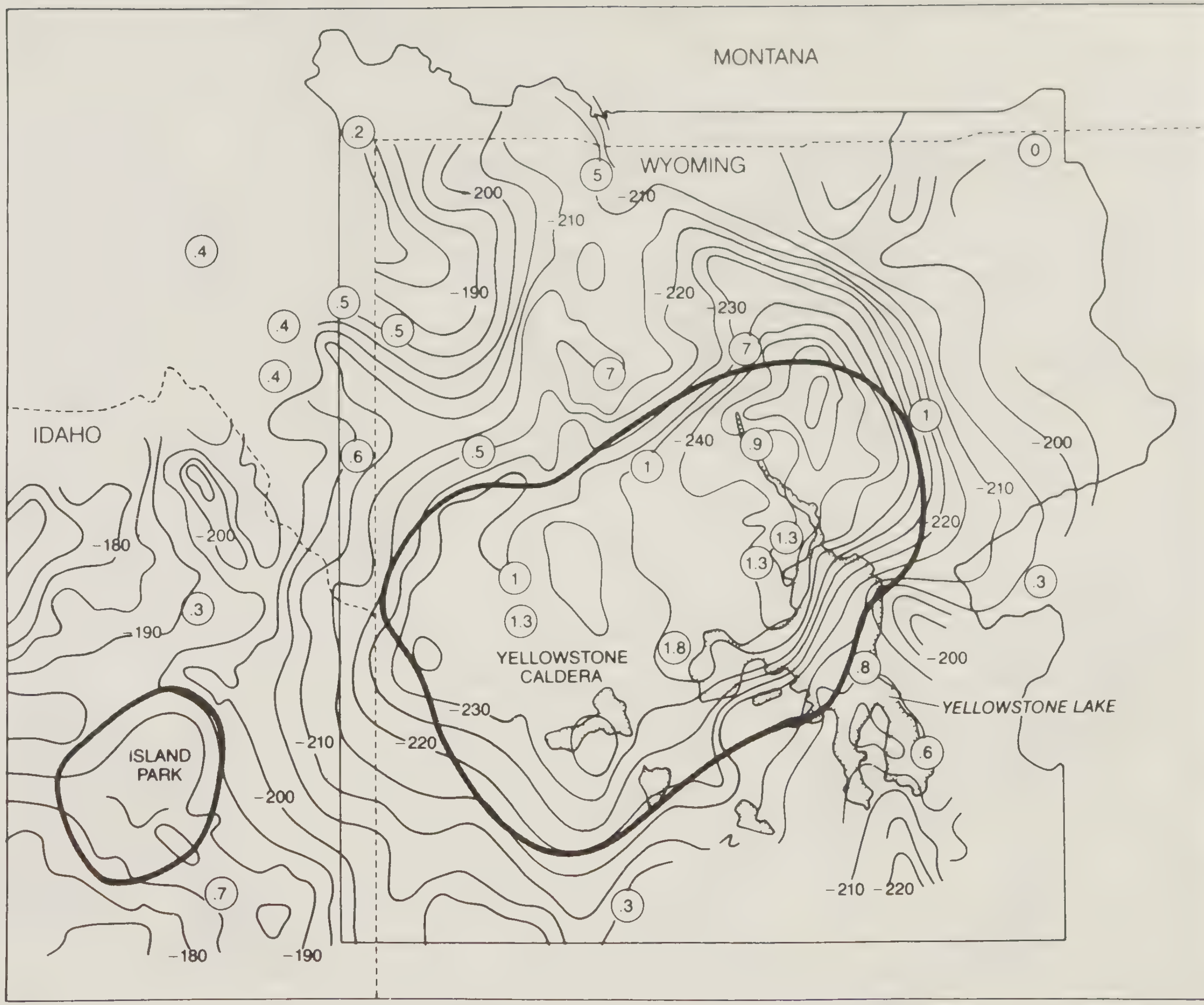

Figure 12.2.5. Bouguer gravity anomaly map and average P-wave delays in Yellowstone region, from Smith and Braile (1983). Contour interval, 5 milligals. Open circles, locations of seismograph stations that recorded teleseismic P-wave delays. Average delays are shown within circles in seconds. P-wave delays were normalized to seismograph station in northeast corner of Yellowstone National Park. Reprinted with permission of National Academy Press, Washington, D.C.

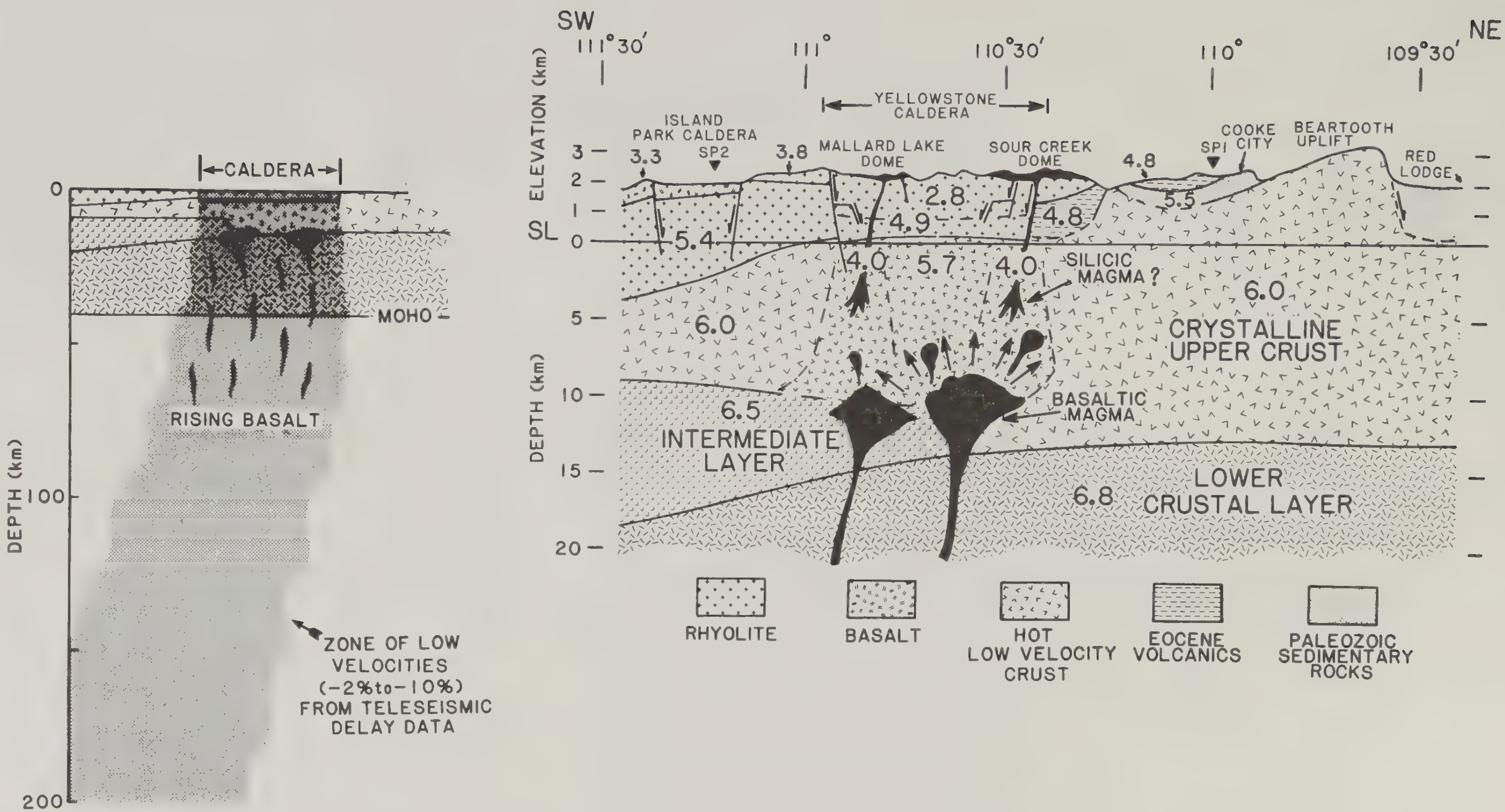

Figure 12.2.6. Idealized NE-SW geologic-seismic velocity model for crustal structure of Yellowstone - Island Park - Snake River Plain region, from Smith and Braile (1983). P-wave velocities are given in kilometers per second; low velocities in lower crust and upper mantle inferred from teleseismic delay studies (Iyer and others, 1981). Basaltic melt rising into crust from upper mantle provides thermal energy required to maintain silicic magma reservoir and active hydrothermal system in upper crust. Reprinted with permission of the National Academy Press, Washington, D.C.

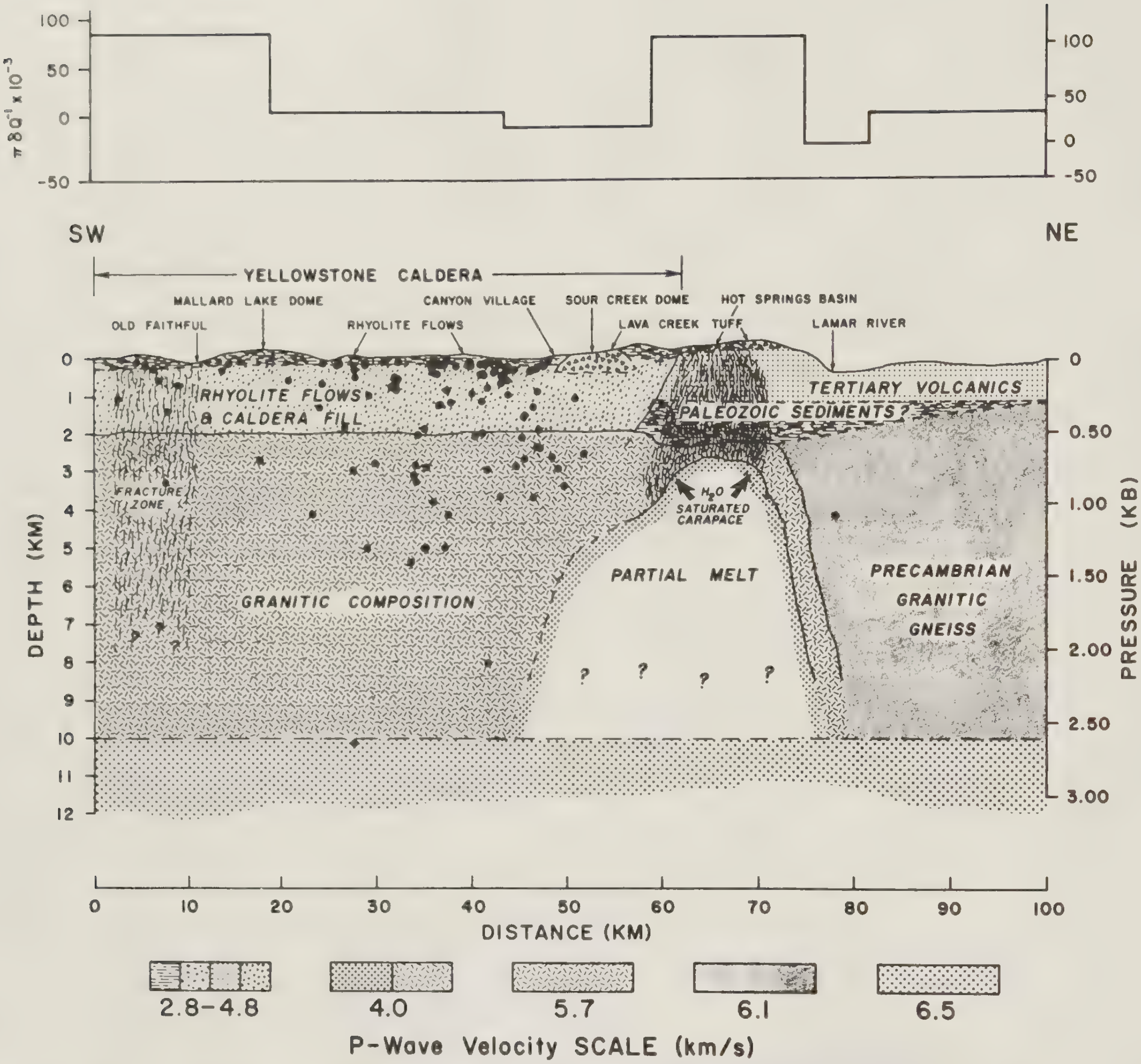

Figure 12.2.7. Relative P_g seismic attenuation (top) and generalized upper-crustal cross section (bottom) oriented SW-NE, parallel to axis of Yellowstone Caldera, from Smith and Braile (1983). Note in upper plot that apparent-Q is high over a low-velocity body beneath northeast caldera rim (inferred to be partial melt) and also over southwest caldera rim (inferred to be an area of fracturing and strong hydrothermal activity). Lowest P-wave velocities occur within caldera fill. Focal depths (black dots) were projected from outside low-velocity body. Reprinted with permission of the National Academy Press, Washington, D.C.

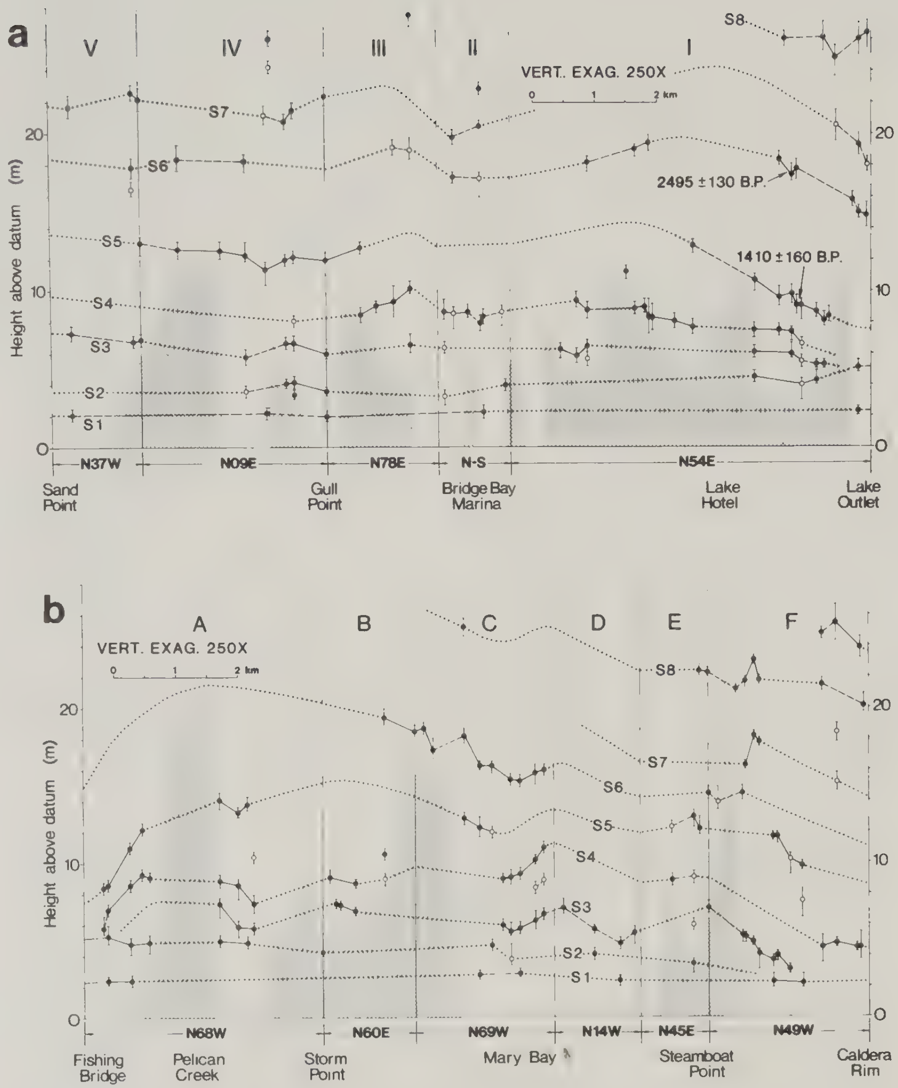

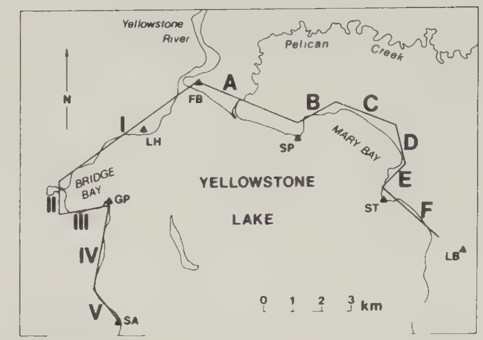

Figure 12.2.8. Deformed shoreline features at Yellowstone Lake, from Meyer and Locke (1986). Solid circles, good terrace morphology; open circles, probable shoreline; S1-S8, tentative shoreline correlations; patterned areas, area of modern wave-cut cliff or lateral stream erosion. (a), Northwest shore; (b), northeast shore.

Figure 12.2.9. Sketch map of Yellowstone Caldera and its main thermal features, from Christiansen (1984). Stars, intracaldera rhyolite vents; irregular black areas, thermal areas. Contours of heat flow shown in Yellowstone Lake in units of milliwatts per square meter. Reprinted with permission of the National Academy Press, Washington, D.C.

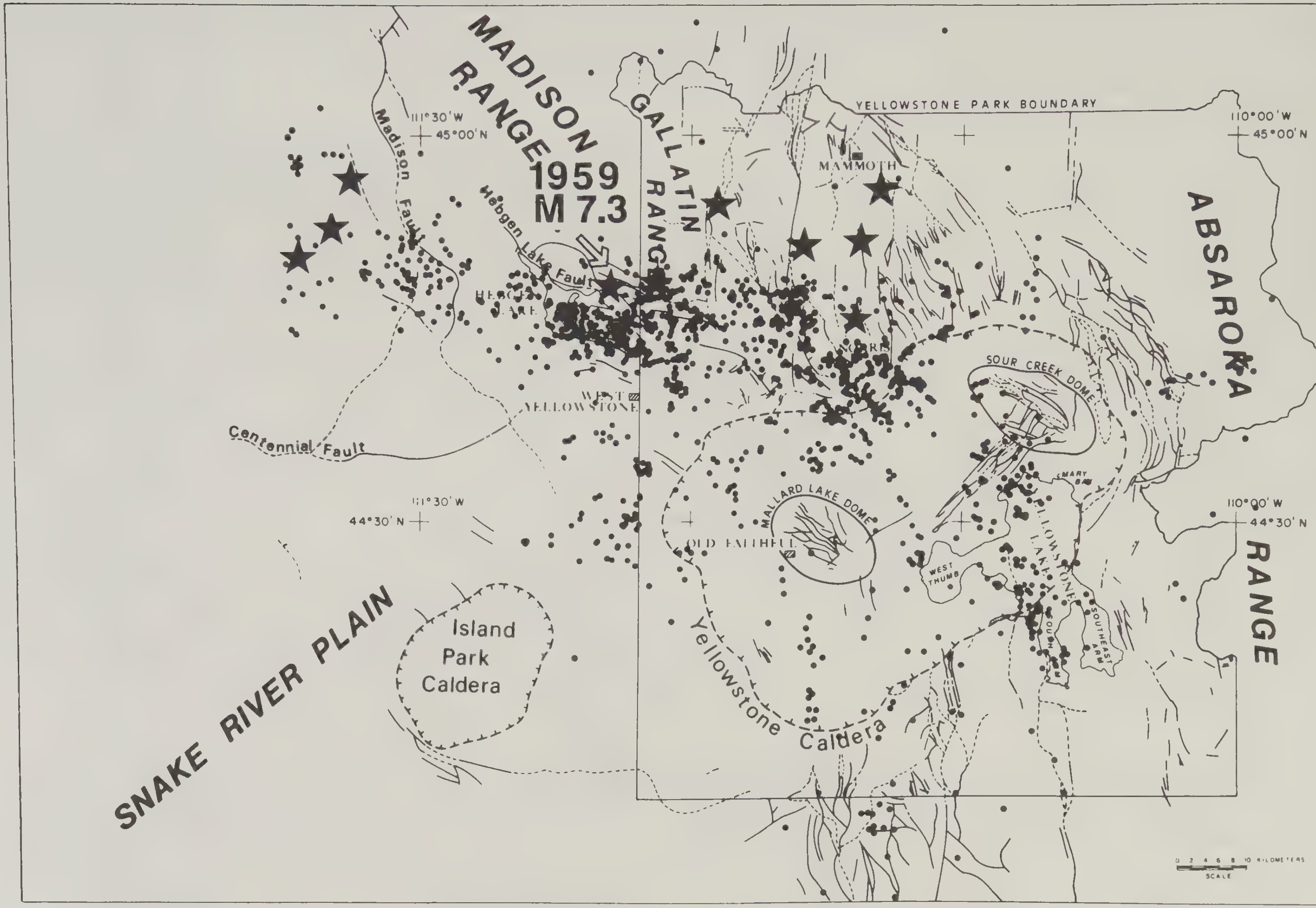

Figure 12.2.10. Earthquake distribution in Yellowstone - Hebgen Lake region from 1971 to 1979, from Smith and Braile (1983). Large stars correspond to epicenters of historical earthquakes larger than magnitude 6. The epicenter of the Yellowstone Park earthquake of 30 June 1975, which is shown just inside the north caldera rim near Norris in figure 12.2.1, is not shown here because estimates of its magnitude ranged from 5.7 to 6.1. Reprinted with permission of the National Academy Press, Washington, D.C.

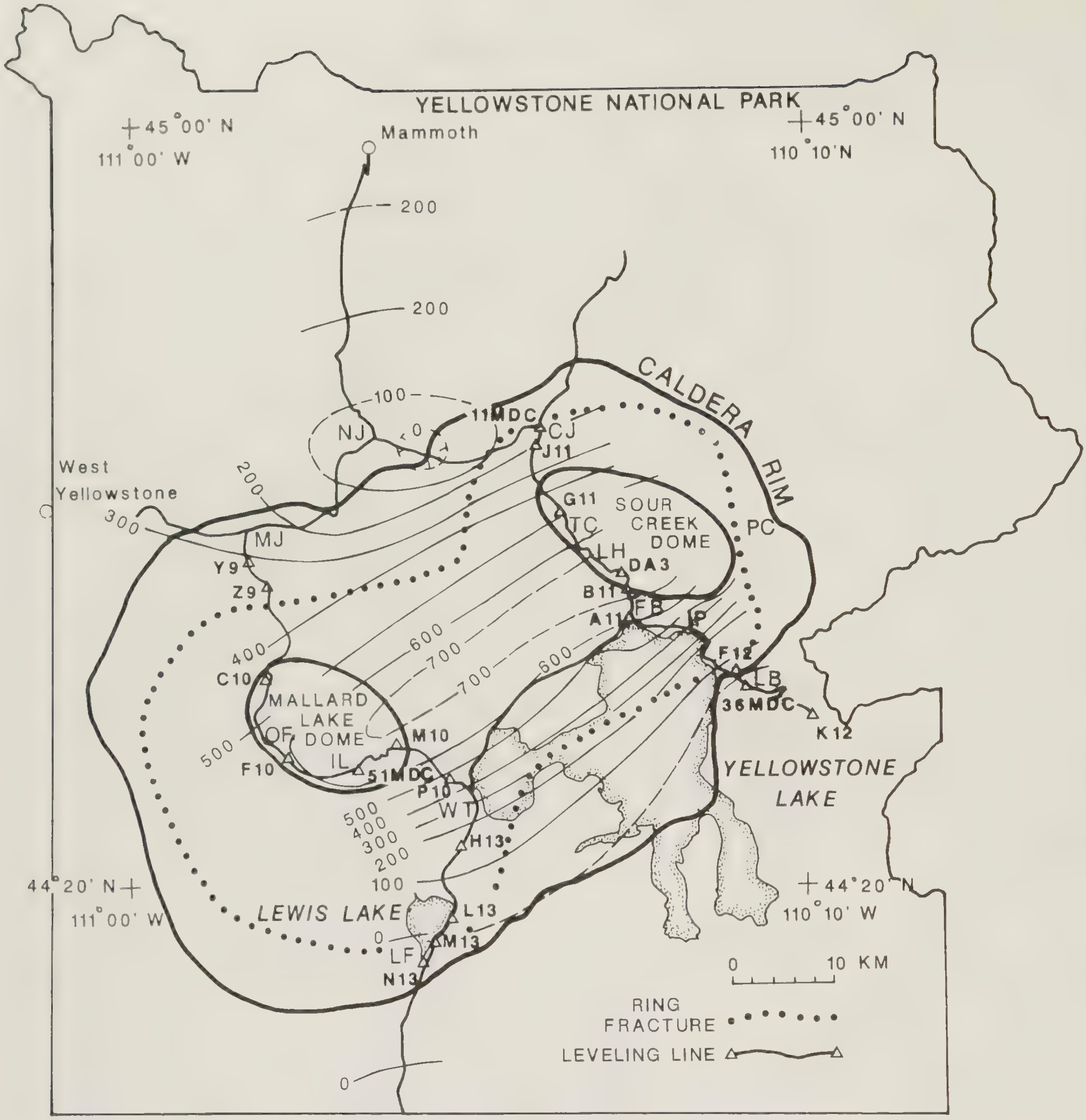

Figure 12.2.11. Contours of uplift at Yellowstone Caldera for the interval 1923-76, from Pelton and Smith (1982). Contour interval is 100 mm. Letter-number designations (for example, Z9, F10, DA3) indicate bench marks. MJ, Madison Junction; OF, Old Faithful; IL, Isa Lake; WT, West Thumb; LF, Lewis Falls; NJ, Norris Junction; CJ, Canyon Junction; TC, Trout Creek; LH, LeHardys Rapids; FB, Fishing Bridge; LB, Lake Butte. See figures 12.2.12 - 12.2.14 for 1983-86 leveling results between Lewis Falls and Madison Junction, and between Lake Butte and Canyon Junction. Copyright by the American Geophysical Union.

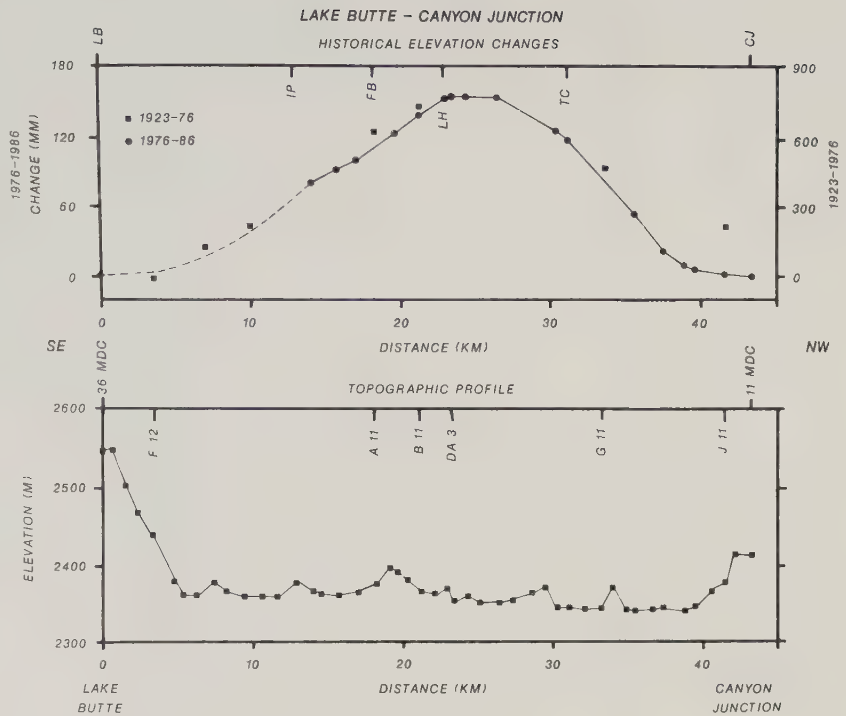

Figure 12.2.12. Historical elevation changes (top) and topography (bottom) along a line from Lake Butte to Canyon Junction (see figures 12.2.2, 12.2.11), from Dzurisin and Yamashita (1987). Copyright by the American Geophysical Union.

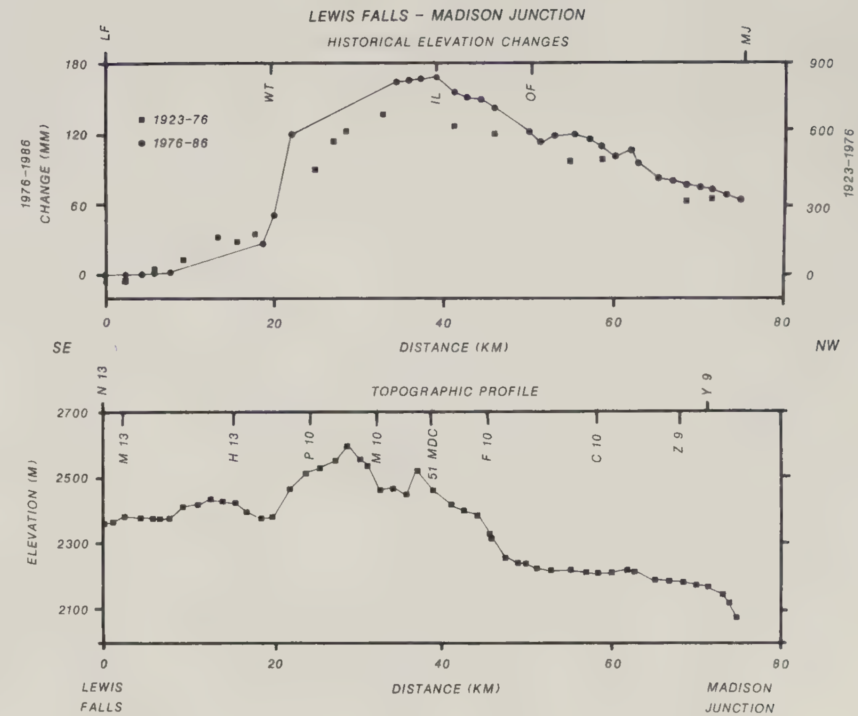

Figure 12.2.13. Historical elevation changes (top) and topography (bottom) along a line from Lewis Lake to Madison Junction (see figures 12.2.2, 12.2.11), from Dzurisin and Yamashita (1987). Copyright by the American Geophysical Union.

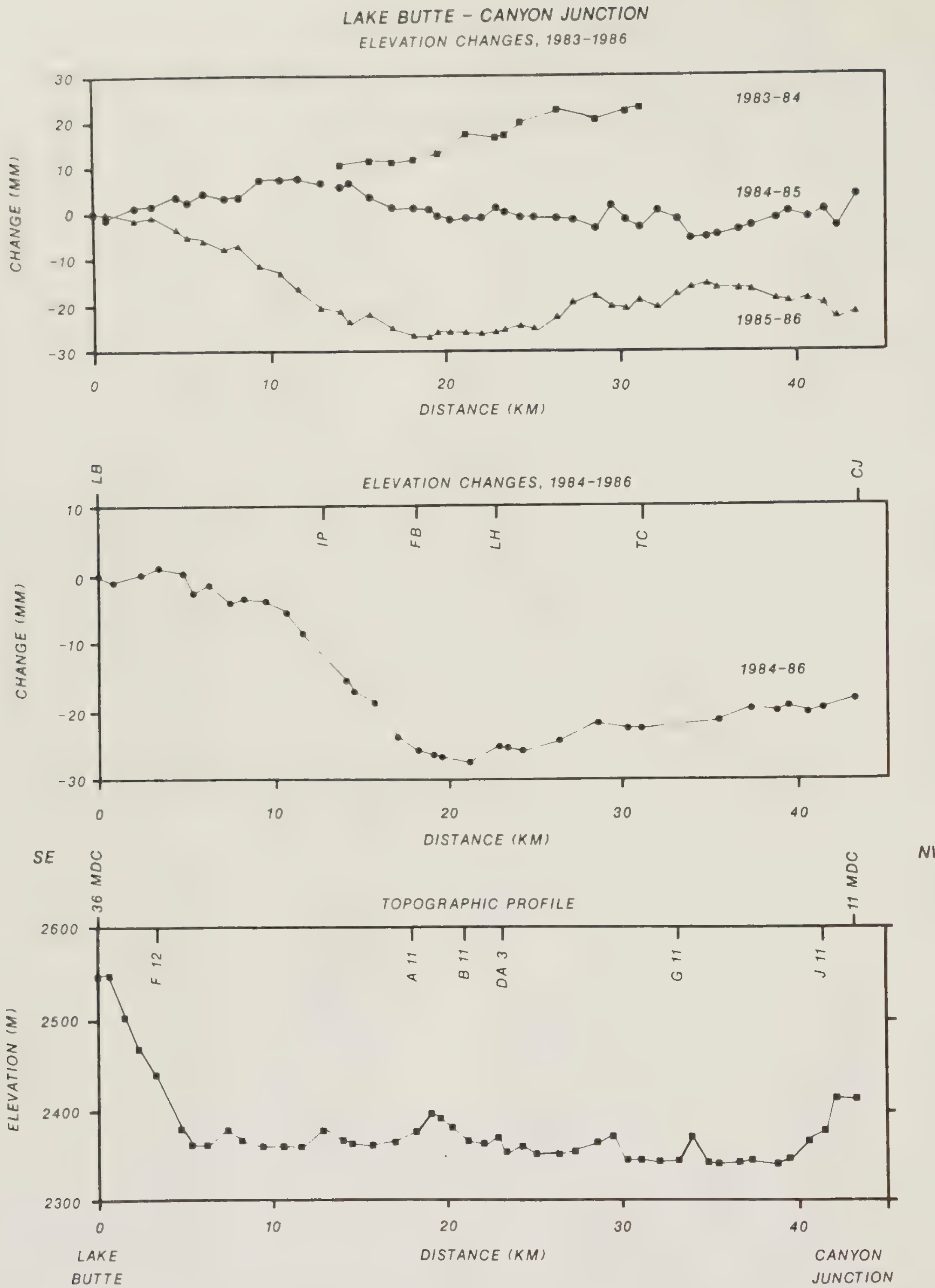

Figure 12.2.14. Annual elevation changes since 1983 along a line from Lake Butte to Canyon Junction (see figures 12.2.2, 12.2.11), from Dzurisin and Yamashita (1987). Copyright by the American Geophysical Union.

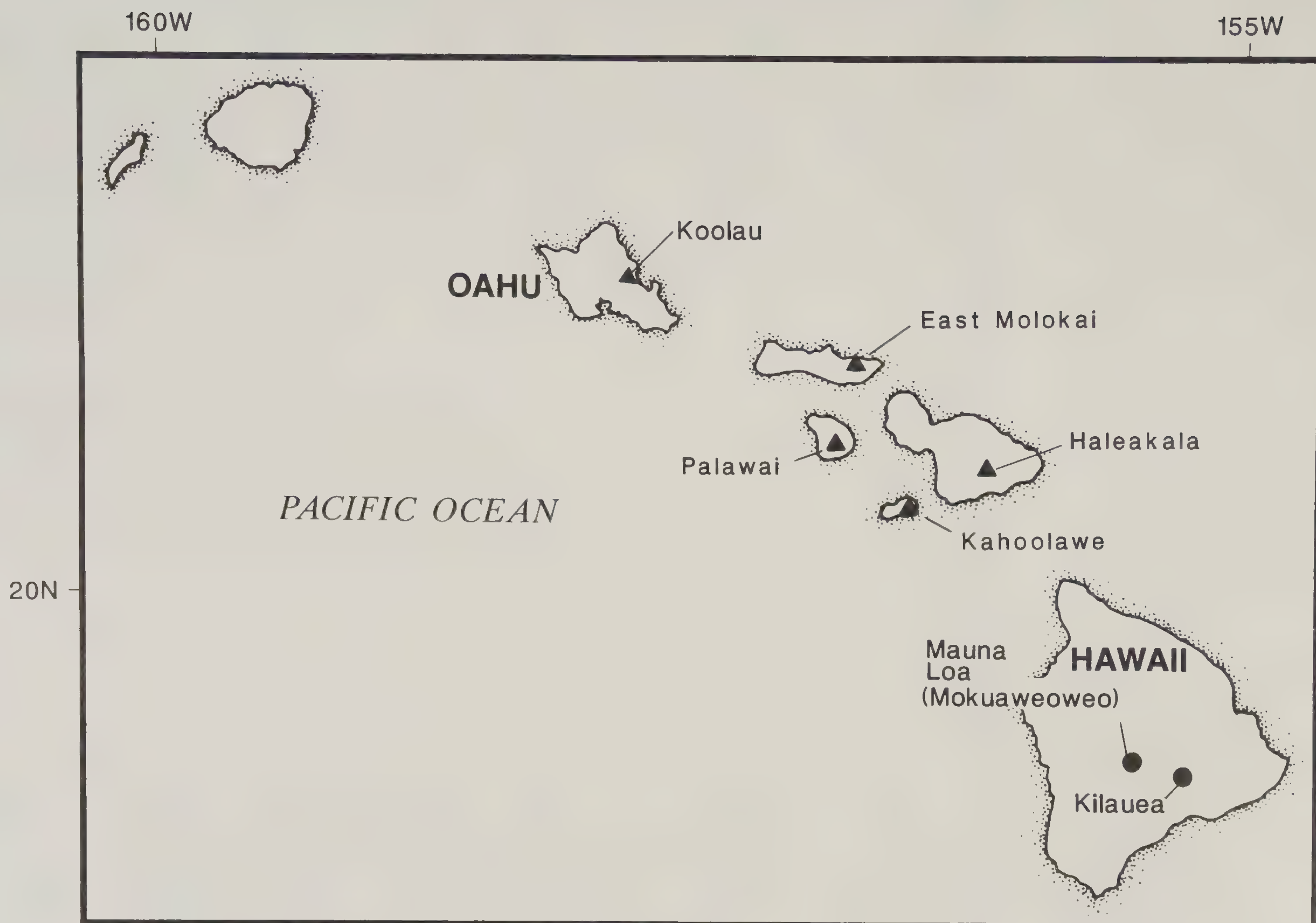

Figure 13. Locations of large, Quaternary restless calderas (solid circles) and nonrestless calderas (triangles) in Region 13.

PART 3: HISTORICAL UNREST AT LARGE QUATERNARY CALDERAS (continued)
See inside back cover for explanation and abbreviations

KILAUEA

CAVW number (active vent)	Latitude Longitude (degrees)	Diameter (km)	Local tectonic setting	Precaldera edifice	SiO_2 content (wt pct)	Age of collapse (yr B.P.)	Date of unrest	Type and duration of unrest ESTU STHF MGTF H Te	Eruption type
13-02-01	19.42N	8 (outer)	Hotspot	Shield	R = 47-51	ca. 1500	1750(?)	---- ---- ---- - --	lf
(Kilauea)	155.29W	4 (inner)			C = 47-51	200-250	1790(?)	---- x--- ---- - --	lf,P-Ex
							1823	---- x--- ---- - --	lf
							1832	---- x--- ---- - --	lf
							1840	---- x--- ---- - --	lf
							1868	---- x--- ---- - UU	lf
							1877	---- ---- ---- - --	lf
							1884	---- ---- ---- - --	sub lf?
							1885	---- ---- ---- - --	lf,ll
							1886	---- x--- ---- - --	sub lf?
							1891	---- x--- ---- - --	none?
							Mar 1894	---- ---- ---- - --	lf
							Jul 1894	---- x--- ---- - --	lf
							1916	---- x--- ---- - --	none?
							1918	---- ---- ---- - --	lf
							Feb 1919	---- ---- ---- - --	lf,ll
							Dec 1919	---- x--- ---- - --	lf,ll
							1921	---- ---- ---- - --	lf
							1922	---- x--- ---- - --	lf
							1923	---- x--- ---- - --	lf
							May 1924	EED- ED-D ---- - --	pex
							Jul 1924	---- ---- ---- - --	lf
							1927	x-B- ---- ---- - --	lf,ll
							Feb 1929	B-x- -E-- ---- - --	lf,ll
							Jul 1929	x-B- -x-- ---- - --	lf
							1930	CBA- -C-- ---- - --	lf
							1931	D-Y- -E-- ---- - --	lf
							1934	B-B- -B-x ---- - --	lf
							Nov 1944	D--D xD-- ---- - --	none
							1950	x--E xE-x ---- - --	none
							1952	D--- -C-- ---- - --	lf,ll
							1954	EBB- -E-- ---- - --	lf

KILAUEA, Region 13, CAVW number 13-02-01

KILAUEA (continued)

CAVW number (active vent)	Latitude Longitude (degrees)	Diameter (km)	Local tectonic setting	Precaldera edifice	SiO_2 content (wt pct)	Age of collapse (yr B.P.)	Date of unrest	Type and duration of unrest ESTU STHF MGTF H Te	Eruption type
(continued from previous page)							1955	ECx- -C-x ---- - --	lf,cc
							1959	ECB- -E-- ---D - --	lf,cc
							1960	DCB- BD-B ---- - --	lf,cc
							Feb 1961	EBB- -E-- ---- - --	lf
							Mar 1961	D-Y- -D-- ---- - --	lf
							Jul 1961	D-Y- -E-- ---- - --	lf,ll
							Sep 1961	DBB- BE-Y ---- - --	lf
							1962	CBB- YE-- ---- - --	lf,ll
							May 1963	CxC- xD-x ---- - --	none
							Jul 1963	CCxx xC-x ---- - --	none
							Aug 1963	DDD- -E-x ---- - UU	lf,ll
							Oct 1963	B-B- BB-- ---- - --	lf
							Mar 1965	D-B- YEY- ---- - --	lf,ll
							Aug 1965	CC-- xD-- ---- - --	none
							Dec 1965	BBB- YE-Y ---- - --	lf
							1967-68	A-BF YFEY ---- - --	lf,ll
							Aug 1968	DCYx YDxx ---- - --	lf
							Oct 1968	BYBY YEx- ---x - --	lf
							1969-71	CYYE YEEY --YY - --	lf,ll
							1972-74	EYDY YEYY Y-YY - UU	lf,ll
							1975	DYY- YYxx -x-- - UU	lf
							Jun 1976	BB-- BBx- ---- - --	none
							Jul 1976	BB-- BB-- ---- - --	none
							Aug 1976	NN-x DDx- ---- - --	none
							Feb 1977	CBB- BBxx xx-- - --	none
							Sep 1977	BBB- BBxx -x-- - --	lf,cc
							May 1979	BB-- BB-- ---- - --	none
							Aug 1979	BBN- BB-- ---- - --	none
							Nov 1979	CCYY YDxx ---x - --	lf

KILAUEA (continued)

CAVW number (active vent)	Latitude Longitude (degrees)	Diameter (km)	Local tectonic setting	Precaldera edifice	SiO_2 content (wt pct)	Age of collapse (yr B.P.)	Date of unrest	Type and duration of unrest ESTU STHF MGTF H Te	Eruption type
(continued from previous page)							Mar 1980	CCY- YY-Y ---Y - --	lf (minor)
							Aug 1980	BB-x BB-- ---x - --	none
							Oct 1980	CBx- BB-- ---x - --	none
							Nov 1980	BB-- BB-- ---x - --	none
							Jan 1981	EE-- DDx- ---- - --	none
							Jun 1981	BBBx -B-- ---- - --	none
							Aug 1981	CCCx xCxx --xx - --	none
							Apr 1982	BBBY -BxY ---x - --	lf
							Jun 1982	CCC- CCxx ---C - --	none
							Sep 1982	BBBB -BxY ---Y - --	lf
							Dec 1982	BBN- BB-- --x- - --	none
							Jan 1983-88+	BBYY YYYY -xxx x --	lf,cc,ll

TECTONIC SETTING

Kilauea is one of five basaltic shield volcanoes that comprise the Island of Hawaii at the southeast end of the Hawaiian archipelago (figs. 13.1.1-13.1.3). The island marks the current location of the Hawaiian "hotspot" or melting anomaly in the upper mantle; northwestward migration of the Pacific plate relative to the hotspot has produced the Hawaiian-Emperor chain of volcanic islands and seamounts that stretches from Hawaii northwestward to the junction of the Kurile and Aleutian Trenches (Clague and Dalrymple, 1987).

Kohala and Mauna Kea volcanoes are the most mature on the Island of Hawaii; both have passed through a tholeiitic shield-building stage into an alkalic stage, and both have been dormant throughout historical time. Hualalai Volcano has erupted alkalic basalts repeatedly in the last 500 years, most recently in 1800-1801 (Moore and others, 1987). Mauna Loa and Kilauea Volcanoes have erupted tholeiitic basalts frequently during the 19th and 20th centuries and, with Loihi seamount off the southeast coast of Hawaii, form the current locus of hotspot volcanism along the Hawaiian-Emperor chain.

GEOLOGIC HISTORY

Kilauea has grown to its current summit elevation of 1,240 m above sea level through repeated extrusions of fluid basalt from its summit region and two prominent rift zones (figs. 13.1.3-13.1.6). Magma derived from a zone of partial melting in the upper

KILAUEA (continued)

GEOLOGIC HISTORY (continued)

mantle usually is stored in a shallow crustal reservoir 3-5 km beneath the summit region before being intruded into the volcanic edifice or extruded onto its surface. Explosive eruptions are rare at Kilauea, mainly because the basaltic magmas are very fluid. The few notable explosive eruptions have been phreatic or phreatomagmatic (for example, in 1790 and 1924) (Christiansen, 1979; Decker and Christiansen, 1984). The eruption of 1924 (relatively small, phreatic) occurred during a period of rapid subsidence of the summit region and notably of the Halemaumau lava lake; subsidence may have allowed ground water to enter the conduit area and "fuel" the phreatic explosions (Jaggar and Finch, 1924; Macdonald and Abbott, 1970). A similar mechanism may apply to large phreatomagmatic eruptions of Kilauea: catastrophic draining of the shallow magma reservoir during large flank eruptions or intrusions may trigger rapid summit subsidence, phreatomagmatic explosions, and caldera collapse (Peterson and Moore, 1987).

Two summit calderas have been identified at Kilauea--a prominent, 3 km x 5 km diameter caldera nested within an older, 8-km-diameter caldera that is largely filled by subsequent lava flows (figs. 13.1.4, 13.1.5) (Holcomb, 1980, 1987). Halemaumau is a small pit crater on the floor of the inner, modern caldera. Many historical eruptions have occurred both within the summit caldera and along rift zones that extend southwestward and eastward from the caldera. The main body of Kilauea is built on, and episodically slides away from, the much larger edifice of Mauna Loa. Such movements occur in response to gravitational and intrusive stresses (the latter induced by repeated forceful intrusions into the rift zones), causing major earthquakes (magnitude 7+) and ground displacements (many meters) (Fiske and Jackson, 1972; Swanson and others, 1976; Duffield and others, 1982).

During a magnitude 7.2 earthquake near Kalapana on the southeast coast of Hawaii in November 1975, parts of Kilauea's south flank moved as much as 3.5 m downward and 8 m seaward (figs. 13.1.8, 13.1.9); subsidence and horizontal movement were concentrated within the Hilina fault system (location shown in fig. 13.1.3). Historical geodetic measurements show that points between the summit area and the Hilina fault system moved progressively upward and southward in the years preceding the 1975 earthquake, suggesting that the earthquake was caused by gravitational slumping in response to accumulation of compressive strain during repeated intrusions into the east rift zone (figs. 13.1.7) (Lipman and others, 1985).

Similar ground movements probably occurred during large earthquakes at Kilauea in 1823 and 1868. Ellis (1963, p. 195; reprint of 1827 edition) reported that in 1823, "the ground, after being agitated some minutes with a violent tumultuous motion, suddenly burst open, for several miles in extent, in a direction from north by east, to south by west, and emitted, in various places at the same instant, a considerable quantity of smoke and luminous vapor, but none of the people were injured by it." After the earthquake, water in a well that was split by a crack became brackish, and the average water level in the well increased from about 0.5 m to nearly 1 m (suggesting at least 0.5 m of subsidence). Similarly, Brigham (1909, p. 481-482) reported that soon after the large earthquake at Kilauea in 1868, an area near the boat landing at Keauhou "appeared to have sunk, and the sea was flowing a fathom deep where houses formerly stood."

The modern Kilauea Caldera formed in the late 18th century, probably during the eruption(s) responsible for the Keanakakoi Ash, a widespread phreatomagmatic tephra in the Kilauea summit region that has been dated from oral accounts as having been deposited in

KILAUEA (continued)

GEOLOGIC HISTORY (continued)

about A.D. 1790 (Christiansen, 1979; Decker and Christiansen, 1984). The Uwekahuna Ash is an older, more widespread tephra that was deposited in at least two episodes of phreatomagmatic eruptions 1,000 to 2,200 years ago, possibly during earlier caldera-forming episodes (Dzurisin and Casadevall, 1986; Lockwood and Rubin, 1986).

Petrologic studies of Kilauea's eruptive products lead to the following conclusions concerning the petrogenesis of Kilauea lavas and the structure and dynamics of the magma plumbing system beneath the volcano (Wright and Fiske, 1971):

1. The chemical composition of magma erupted at the summit of Kilauea varies with the date of the eruption. Lavas erupted before 1750, during the eighteenth and nineteenth centuries, and in the twentieth century form groups that can be distinguished chemically.

2. During late prehistoric time, pockets of differentiated magma were formed within the rift zones by separation of the liquid remaining after partial crystallization of bodies of summit magma.

3. Lava from some eruptions has the composition of the liquid fraction as it is generated within the rift. Lava compositions of other eruptions are best explained by mixing of magma supplied from a central reservoir beneath the Kilauea summit with differentiated liquid in the rift.

4. The fact that components of "summit composition" appear in rift eruptions <u>before</u> they appear undiluted at the summit suggests that the central reservoir is vertically zoned. Rift eruptions are fed from lower levels, where younger magma is available; summit eruptions are fed from the relatively older magma above.

5. The unique and uniform composition of lava of each successive summit eruption suggests that summit eruptions end when all of the magma of one composition has been erupted. Magma erupted from the upper levels of the reservoir during one cycle is continually replaced from below by younger magma of different composition.

HISTORICAL ACTIVITY

Because unrest at Kilauea is essentially continuous, we have listed only the dates of eruptions and intrusions in the table above. Intrusions are usually characterized by rapid summit deflation, earthquake swarms along a rift zone, and inflation or ground cracking along that rift zone. Eruptions are defined to begin with the arrival of magma at the surface and to end when tremor at the vent ceases for at least several days.

KILAUEA (continued)

HISTORICAL ACTIVITY (continued)

Most historical eruptions of Kilauea until 1924 occurred in the inner summit caldera; from 1823 to 1894 and from 1907 to 1924, a lava lake was active almost continuously on the caldera floor or in Halemaumau, and eruptions along the rift zones were infrequent and shortlived. Flank eruptions in 1823, 1832, 1840, and 1868 were accompanied by pistonlike sinking of the caldera floor as magma drained from the summit area into the rift zones. The 1868 eruption was triggered by a magnitude 7.5 earthquake near the southern tip of Hawaii on 2 April, which also caused a tsunami and mudslide responsible for 79 deaths. The earthquake was preceded by a small eruption at the summit of Mauna Loa on 27 March, followed by a larger outbreak along Mauna Loa's southwest rift zone starting on 7 April. Phreatic explosions and collapse at Halemaumau in 1924 marked a change in the style of activity, and most eruptions since 1955 have been along the rift zones (Macdonald and Abbott, 1970; Peterson and others, 1976; Macdonald and others, 1983; Holcomb, 1987). Volumes of erupted lava are typically between 10^6 and 10^8 m^3 (Klein, 1982).

Seismicity and ground deformation at Kilauea are closely linked to the movement of magma into a shallow reservoir beneath the summit and into the rift zones (Klein and others, 1987). Infrequent deep earthquakes hint at supply of magma into the shallow magma storage system from depth (Eaton and Murata, 1960; Eaton and others, 1987; Klein and others, 1987) (figs. 13.1.10-13.1.12); more commonly, shallow earthquakes reflect inflation of the summit reservoir and the leading edge of a rift-zone intrusion (as in 1959 along the east rift zone; Eaton and Murata, 1960) (figs. 13.1.13-13.1.17). The hypocenters of historical earthquakes define in remarkable detail the magma conduit system beneath Kilauea, from a source of partial melting in the upper mantle through a near-vertical pipe to a shallow crustal reservoir and into the rift zones (figs. 13.1.12, 13.1.18) (Ryan and others, 1981). Earthquake swarms are common as magma intrudes the rift zones (fig. 13.1.19); swarms that are not clearly attributable to movement of magma (for example, ones in which regional tectonic stress release is modified to swarm activity in fractured and (or) high-pore-pressure environments) are not common at Kilauea. Inflation and deflation of the summit region are directly linked to filling and draining of the summit reservoir (Eaton and Murata, 1960; Fiske and Kinoshita, 1969; Ryan and others, 1983) (figs. 13.1.20-13.1.23). Ground deformation along the rift zones, including surface rupture, is directly attributable to intrusion along the rifts (Swanson and others, 1976; Pollard and others, 1983) (figs. 13.1.24, 13.1.25). In detail, the ground surface is uplifted along two ridges parallel to an intruding dike; these ridges move closer together as the dike nears the surface (Pollard and others, 1983). This pattern, combined with the distribution of earthquakes, can provide good indications of the depth of an intrusion and of any upward movement of the intrusion that might culminate in an eruption.

Tremor is often a short-term precursor to eruptions--beginning minutes to a few hours before the start of fountaining; a further, sharp increase in tremor accompanies the start of fountaining (figs. 13.1.34 and 13.1.35). Most eruptions are preceded by slow inflation of the summit area for a period of a few weeks to many months and are accompanied by rapid deflation of the summit (fig. 13.1.26). Typically, summit deflation begins a few hours (or occasionally as much as several days) before a flank eruption begins and is thus another, though less reliable, short-term precursor of eruptions. Many phases of the 1983-present eruption (see below) along the east rift zone have been preceded by several hours to several days of low-level activity at the Puu Oo vent, including a rise in the level of lava within that vent.

KILAUEA (continued)

HISTORICAL ACTIVITY (continued)

The magnitude of ground deformation before and after an eruption varies greatly in proportion to the size, depth, and shape of the source of the deformation. Typical deformation precursors to an eruption are several tens to several hundreds of microradians of inflationary tilt at the Hawaiian Volcano Observatory on the inner caldera rim (figs. 13.1.20, 13.1.21, 13.1.26), several centimeters to a few tens of centimeters of uplift and horizontal extension of the summit region (figs. 13.1.20, 13.1.21, 13.1.27, 13.1.28), and several tens of centimeters to a meter or more of outward displacement of points at and several kilometers outside the caldera rim. Contours of uplift are skewed toward one of the rifts if the magma migrates into that rift (figs. 13.1.24, 13.1.25).

The flux of SO_2 gas from Kilauea's summit area has been monitored regularly since June 1979. The average daily emission rate from 1979 to 1982 was 170 ± 70 t/d (metric tonnes/day); during 1983-84, the rate increased to 260 ± 90 t/d (Casadevall and others, 1987) (fig. 13.1.29). The increase coincided with the start of the long-lived Puu Oo eruption along Kilauea's east rift zone in January 1983. Casadevall and others (1987) found no evidence of precursory increases in SO_2 emission before eruptions during 1979-84, and indeed Gerlach (1986) has calculated that magmas at Kilauea will reach very close to the surface before "precursory" degassing of sulfur gases will be noticeable. Recent monitoring of the net flux of several magmatic gases including H_2, SO_2, and H_2S has yielded promising results (fig. 13.1.30); the flux of such gases may be an indirect reflection of strain and microfracturing before shallow magma movements within Kilauea (McGee and others, 1987). Occasionally, anomalous steaming or tree kill occurs during shallow intrusions or eruptions.

Although varied in detail, unrest at Kilauea follows a general pattern that is well illustrated by two recent periods of sustained activity along the east rift zone: Mauna Ulu during 1969-71 (Swanson and others, 1979) and 1972-74 (Tilling and others, 1987), and the Puu Oo area from 1983 to the present (December 1987) (Wolfe and others, 1987). In both cases, early fountaining episodes were preceded by slow inflation of the summit area for weeks or months and accompanied by rapid summit deflation and earthquakes at the summit and along the rift zone (figs. 13.1.31-13.1.39). Later episodes were characterized by progressively less seismicity and ground deformation until a quasi-steady state was established in which magma reached the extrusion sites continuously through well-developed conduit systems along the rift zone (fig. 13.1.40). Gravity, leveling, and trilateration data show that magma was stored elastically in the summit reservoir between fountaining episodes at Puu Oo during 1984-85 (fig. 13.1.41), but that at other times horizontal extension of the volcanic edifice owing to seaward movement of its south flank decreases lateral support of the fluid magma reservoir, thus lowering the pressure in the reservoir and allowing more magma to be injected without vertical uplift (Johnson, 1987).

Dzurisin (1980) and Klein (1982) noted that eruptions can be triggered by relatively small external disturbances such as fortnightly earth tides. Klein writes: "One useful concept considers the summit reservoir as a tank with drain valves for the rift zones and summit fissures. Forces small in comparison with the total magmatic pressures or tectonic strains can control flow by opening or partially opening the valves." Shimozuru (1987) reviewed earlier work on fortnightly tidal triggering of Hawaiian eruptions and showed that semidiurnal fluctuations in the level of the Halemaumau lava lake during 1919 were well correlated with solid-Earth tides.

KILAUEA (continued)

HISTORICAL ACTIVITY (continued)

Many intrusions at Kilauea do not culminate in eruptions (see listings of intrusions in Klein, 1982; Klein and others, 1987). Swanson (1972) concluded that about half of all magma supplied to Kilauea from depth is emplaced as intrusions and not erupted; Dzurisin and others (1984) concluded that from 1956 to 1983, about 35 percent of the total magma supply was extruded, 55 percent was intruded into the east rift zone, and 10 percent was intruded into the southwest rift zone.

COMMENTS

Kilauea is one of the most intensely studied volcanoes on Earth. The Hawaiian Volcano Observatory (HVO), perched on the northwest rim of Kilauea Caldera, was established in 1912 and recently commemorated its 75th anniversary. Numerous observations made by HVO staff through the years suggest the presence of a long-lived magma storage reservoir beneath the summit region. In fact, shallow magma reservoirs probably migrate upward within the volcanic edifice throughout much of the growth cycle of Hawaiian shields, giving rise to repeated episodes of caldera collapse and refilling (Decker, 1987). Most historical unrest at Kilauea can be linked directly to magma movements within the volcanic system, either upward from a zone of magma generation in the upper mantle or laterally within the volcanic edifice. Even large "tectonic" earthquakes such as those in 1868 and 1975 are probably triggered in large part by magmatic intrusions into Kilauea's rift zones.

REFERENCES

Brigham, W.T., 1909, The Volcanoes of Kilauea and Mauna Loa on the Island of Hawaii, their variously recorded history to the present time, Memoirs of the Bernice Pauahi Bishop Museum, v. 2, no. 4: Honolulu, Bishop Museum Press.

Casadevall, T.J., Stokes, J.B., Greenland, L.P., Malinconico, L.L., Casadevall, J.R., and Furukawa, B.T., 1987, SO_2 and CO_2 emission rates at Kilauea volcano, 1979-1984, in Decker, R.W., Wright, T.L., and Stauffer, P.H., eds., Volcanism in Hawaii, U.S. Geol. Surv. Prof. Paper 1350, v. 1, p. 771-780.

Christiansen, R.L., 1979, Explosive eruption of Kilauea Volcano in 1790 [abs.]: IAVCEI Hawaii Symp. on Intraplate Volcanism and Submarine Volcanism, Hilo, July 16-22, 1979.

Clague, D. A., and Dalrymple, G. B., 1987, The Hawaiian-Emperor volcanic chain, Part I, Geologic evolution, in Decker, R.W., Wright, T.L., and Stauffer, P.H., eds., Volcanism in Hawaii, U.S. Geol. Surv. Prof. Paper 1350, v. 1, p. 5-54.

Decker, R.W., 1987, Dynamics of Hawaiian volcanoes: An overview, in Decker, R.W., Wright, T.L., and Stauffer, P.H., eds., Volcanism in Hawaii, U.S. Geol. Surv. Prof. Paper 1350, v. 2, p. 997-1018.

Decker, R.W., and Christiansen, R.L., 1984, Explosive eruptions of Kilauea Volcano, Hawaii, in Boyd, F.R., ed., Explosive volcanism: Inception, evolution, and hazards: National Research Council in Geophysics, Washington, D.C., National Academy Press, p. 122-132.

KILAUEA (continued)

REFERENCES (continued)

Decker, R.W., Hill, D.P., and Wright, T.L., 1966, Deformation measurements on Kilauea Volcano, Hawaii: Bull. Volcanol., v. 29, p. 721-732.

Decker, R.W., and Kinoshita, W.T., 1971, Geodetic measurements, in The surveillance and prediction of volcanic activity: Paris, UNESCO, p. 47-74.

de St. Ours, P., 1982, Structural map of the summit area of Kilauea Volcano, Hawaii: U.S. Geol. Surv. Misc. Field Studies Map MF-1368, scale 1:24,000.

Duffield, W.A., Christiansen, R.L., Koyanagi, R.Y., and Peterson, D.W., 1982, Storage, migration and eruption of magma at Kilauea Volcano, Hawaii, 1971-1972: Jour. Volcanol. Geotherm. Res., v. 13, p. 273-307.

Duffield, W.A., Jackson, D.B., and Swanson, D.A., 1976, The shallow, forceful intrusion of magma and related ground deformation at Kilauea Volcano, May 15-16, 1970, in Gonzales Ferran, O., ed., Proc. Symp. on Andean and Antarctic Volcanology Problems: Rome, IAVCEI, p. 577-597.

Dvorak, J.J., and Okamura, A.T., 1987, A hydraulic model to explain variations in summit tilt rate at Kilauea and Mauna Loa volcanoes, in Decker, R.W., Wright, T.L., and Stauffer, P.H., eds., Volcanism in Hawaii, U.S. Geol. Surv. Prof. Paper 1350, v. 2, p. 1281-1296.

Dzurisin, D., 1980, Influence of fortnightly earth tides at Kilauea Volcano, Hawaii: Geophys. Res. Lett., v. 7, p. 925-928.

Dzurisin, D., Anderson, L.A., Eaton, G.P., Koyanagi, R.Y., Lipman, P.W., Lockwood, J.P., Okamura, R.T., Puniwai, G.S., Sako, M.K., and Yamashita, K.M., 1980, Geophysical observations of Kilauea Volcano, Hawaii, 2., Constraints on the magma supply during November 1975-September 1977: Jour. Volcanol. Geotherm. Res., v. 7, p. 241-269.

Dzurisin, D., and Casadevall, T.J., 1986, Stratigraphy and chemistry of the Uwekahuna Ash: product of prehistoric phreatomagmatic eruptions of Kilauea volcano, Hawaii [abs.]: Abstracts, Int. Volcanol. Congr., New Zealand, February 1986, p. 100.

Dzurisin, D., Koyanagi, R.Y., and English, T.T., 1984, Magma supply and storage at Kilauea volcano, Hawaii, 1956-1983: Jour. Volcanol. Geotherm. Res., v. 21, p. 177-206.

Eaton, J.P., and Murata, K.J., 1960, How volcanoes grow: Science, v. 132, p. 925-938.

Eaton, J.P., Richter, D.H., and Krivoy, H.L., 1987, Cycling of magma between the summit reservoir and Kilauea Iki lava lake during the 1959 eruption of Kilauea volcano, in Decker, R.W., Wright, T.L., and Stauffer, P.H., eds., Volcanism in Hawaii, U.S. Geol. Surv. Prof. Paper 1350, v. 2, p. 1307-1335.

Ellis, William, 1963 (reprint of 1827 edition), Journal of William Ellis, Narrative of a tour of Hawaii, with remarks on the history, traditions, manners, customs, and language of the inhabitants of the Sandwich Islands: Honolulu, Advertiser Publ. Co., Ltd., 342 p.

Fiske, R.S., and Jackson, E.D., 1972, Orientation and growth of Hawaiian volcanic rifts: the effect of regional structure and gravitational stresses: Proc. Roy. Soc. London, Ser. A, v. 329, p. 299-326.

Fiske, R.S., and Kinoshita, W.T., 1969, Inflation of Kilauea Volcano prior to its 1967-1968 eruption: Science, v. 165, p. 341-349.

Gerlach, T.M., 1986, Exsolution of H_2O, CO_2, and S during eruptive episodes at Kilauea Volcano, Hawaii: Jour. Geophys. Res., v. 91, no. B12, p. 12,177-12,185.

Greenland, L.P., Rose, W.I., and Stokes, J.B., 1985, An estimate of gas emissions and magmatic gas content from Kilauea Volcano: Geochimica et Cosmochimica Acta, v. 49, p. 125-129.

KILAUEA (continued)

REFERENCES (continued)

Holcomb, R.T., 1980, Kilauea Volcano: Chronology and morphology of the surficial lava flows: Stanford, Calif., Stanford Univ., Ph.D. diss., 321 p.

Holcomb, R.T., 1987, Eruptive history and long-term behavior of Kilauea volcano, in Decker, R.W., Wright, T.L., and Stauffer, P.H., eds., Volcanism in Hawaii, U.S. Geol. Surv. Prof. Paper 1350, v. 1, p. 261-350.

Jaggar, T.A., and Finch, R.H., 1924, The explosive eruption of Kilauea in Hawaii, 1924: Am. Jour. Sci., v. 8, p. 353-374.

Johnson, D.J., 1987, Elastic and inelastic magma storage at Kilauea volcano, in Decker, R.W., Wright, T.L., and Stauffer, P.H., eds., Volcanism in Hawaii, U.S. Geol. Surv. Prof. Paper 1350, v. 2, p. 1297-1306.

Kinoshita, W.T., Swanson, D.A., and Jackson, D.B., 1974, The measurement of crustal deformation related to volcanic activity at Kilauea Volcano, Hawaii, in Civetta, L., Gasparini, P., Luongo, G., and Rapolla, A., eds., Physical volcanology: Amsterdam, Elsevier, p. 87-115.

Klein, F.W., 1982, Patterns of historical eruptions at Hawaiian volcanoes: Jour. Volcanol. Geotherm. Res., v. 12, p. 1-35.

Klein, F.W., Koyanagi, R.Y., Nakata, J.S., and Tanigawa, W.R., 1987, The seismicity of Kilauea's magma system, in Decker, R.W., Wright, T.L., and Stauffer, P.H., eds., Volcanism in Hawaii, U.S. Geol. Surv. Prof. Paper 1350, v. 2, p. 1019-1185.

Koyanagi, R.Y., Chouet, B., and Aki, K., 1987, Origin of volcanic tremor in Hawaii, Part I, Data from the Hawaiian Volcano Observatory 1969-1985, in Decker, R.W., Wright, T.L., and Stauffer, P.H., eds., Volcanism in Hawaii, U.S. Geol. Surv. Prof. Paper 1350, v. 2, p. 1221-1257.

Lipman, P.W., Lockwood, J.P., Okamura, R.T., Swanson, D.A., and Yamashita, K.M., 1985, Ground deformation associated with the 1975 magnitude-7.2 earthquake and resulting changes in activity of Kilauea volcano, Hawaii: U.S. Geol. Surv. Prof. Paper 1276, 45 p.

Lockwood, J.P., and Rubin, M., 1986, Distribution and age of the Uwekahuna Ash, Kilauea volcano, Hawaii [abs.]: Abstracts, Int. Volcanol. Congr., New Zealand, February 1986, p. 112.

Macdonald, G.A., 1955, Catalogue of active volcanoes of the world including solfataric fields, pt. III, Hawaiian Islands: Naples, IAVCEI, 37 p.

----- 1972, Volcanoes: Englewood Cliffs, N.J., Prentice-Hall, Inc., 510 p.

Macdonald, G.A., and Abbott, A.T., 1970, Volcanoes in the sea: Honolulu, Univ. Hawaii Press, 441 p.

Macdonald, G.A., Abbott, A.T., and Peterson, F.L., 1983, Volcanoes in the sea (2nd ed.): Honolulu, Univ. Hawaii Press, 517 p.

McGee, K.A., Sutton, A.J., and Sato, M., 1987, Use of satellite telemetry for monitoring active volcanoes, with a case study of a gas-emission event at Kilauea volcano, December 1982, in Decker, R.W., Wright, T.L., and Stauffer, P.H., eds., Volcanism in Hawaii, U.S. Geol. Surv. Prof. Paper 1350, v. 1, p. 821-825.

Moore, R.B., Clague, D.A., Rubin, M., and Bohrson, W.A., 1987, Hualalai volcano: a preliminary summary of geologic, petrologic, and geophysical data, in Decker, R.W., Wright, T.L., and Stauffer, P.H., eds., Volcanism in Hawaii, U.S. Geol. Surv. Prof. Paper 1350, v. 1, p. 571-585.

Peterson, D.W., Christiansen, R.L., Duffield, W.A., Holcomb, R.T., and Tilling, R.I., 1976, Recent activity of Kilauea Volcano, Hawaii, in Gonzales Ferran, O., ed., Proc. Symp. on Andean and Antarctic Volcanology Problems: Rome, IAVCEI, p. 646-656.

Peterson, D.W., and Moore, R.B., 1987, Geologic history and evolution of geologic concepts, Island of Hawaii, in Decker, R.W., Wright, T.L., and Stauffer, P.H., eds., Volcanism in Hawaii, U.S. Geol. Surv. Prof. Paper 1350, v. 1, p. 149-189.

KILAUEA (continued)

REFERENCES (continued)

Pollard, D.D., Delaney, P.T., Duffield, W.A., Endo, E.T., and Okamura, A.T., 1983, Surface deformation in volcanic rift zones: Tectonophysics, v. 94, p. 541-584.

Ryan, M.P., Blevins, J.Y.K., Okamura, A.T., and Koyanagi, R.Y., 1983, Magma reservoir subsidence mechanics: theoretical summary and application to Kilauea Volcano, Hawaii: Jour. Geophys. Res., v. 88, p. 4147-4181.

Ryan, M.P., Koyanagi, R.Y., and Fiske, R.S., 1981, Modeling the three-dimensional structure of macroscopic magma transport systems, Application to Kilauea Volcano, Hawaii: Jour. Geophys. Res., v. 86, p. 7111-7129.

Shimozuru, D., 1987, Tidal effects on Hawaiian volcanism, in Decker, R.W., Wright, T.L., and Stauffer, P.H., eds., Volcanism in Hawaii, U.S. Geol. Surv. Prof. Paper 1350, v. 2, p. 1337-1343.

Swanson, D.A., 1972, Magma supply rates at Kilauea Volcano, 1952-1971: Science, v. 175, p. 169-170.

Swanson, D.A., and Christiansen, R.L., 1973, Tragic base surge at Kilauea volcano: Geology, v. 1, p. 83-86.

Swanson, D.A., Duffield, W.A., and Fiske, R.S., 1976, Displacement of the south flank of Kilauea Volcano: the result of forceful intrusion of magma into the rift zones: U.S. Geol. Surv. Prof. Paper 963, 39 p.

Swanson, D.A., Duffield, W.A., Jackson, D.B., and Peterson, D.W., 1979, Chronological narrative of the 1969-71 Mauna Ulu eruption of Kilauea Volcano, Hawaii: U.S. Geol. Surv. Prof. Paper 1056, 55 p.

Tilling, R.I., Christiansen R.L., Duffield, W.A., Endo, E.T., Holcomb, R.T., Koyanagi, R.Y., Peterson, D.W., and Unger, J.D., 1987, The 1972-1974 Mauna Ulu eruption, Kilauea Volcano: An example of quasi-steady-state magma transfer, in Decker, R.W., Wright, T.L., and Stauffer, P.H., eds., Volcanism in Hawaii, U.S. Geol. Surv. Prof. Paper 1350, v. 1, p. 405-469.

Wolfe, E.W., Garcia, M.O., Jackson, D.B., Koyanagi, R.Y., Neal, C.A., and Okamura, A.T., 1987, The Puu Oo eruption of Kilauea Volcano, episodes 1-20, January 3, 1983 to June 8, 1984, in Decker, R.W., Wright, T.L., and Stauffer, P.H., eds., Volcanism in Hawaii, U.S. Geol. Surv. Prof. Paper 1350, v. 1, p. 471-508.

Wright, T.L., 1971, Chemistry of Kilauea and Mauna Loa lava in space and time: U.S. Geol. Surv. Prof. Paper 735, 40 p.

Wright, T.L., and Fiske, R.S., 1971, Origin of the differentiated and hybrid lavas of Kilauea Volcano, Hawaii: Jour. Petrol., v. 12, no. 1, p. 1-65.

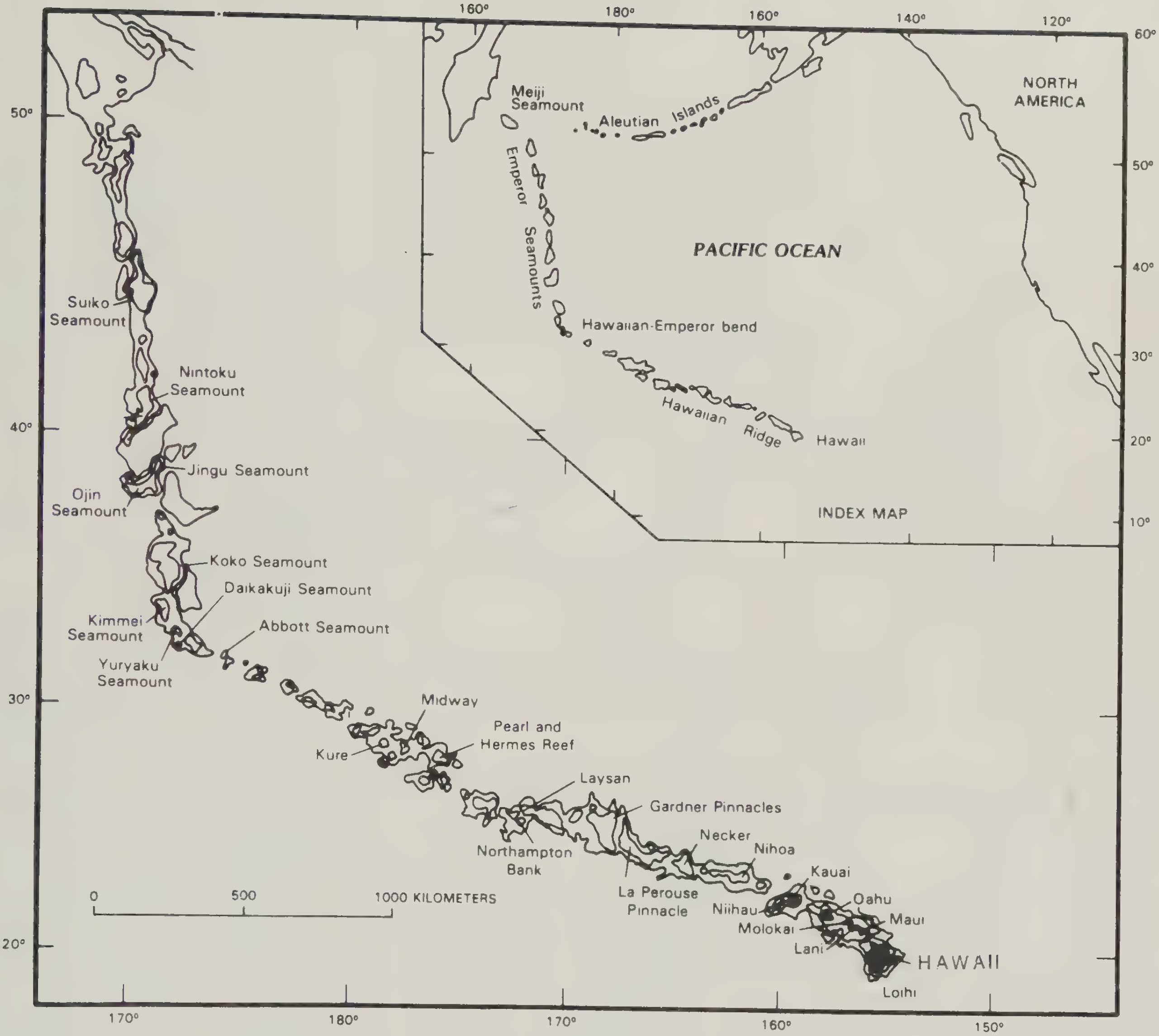

Figure 13.1.1. Bathymetry of the Hawaiian-Emperor volcanic chain, from Clague and Dalrymple (1987). Contours at 1-km and 2-km depths are shown in area of chain only. Inset shows location of chain (outlined by 2-km depth contour) in central North Pacific.

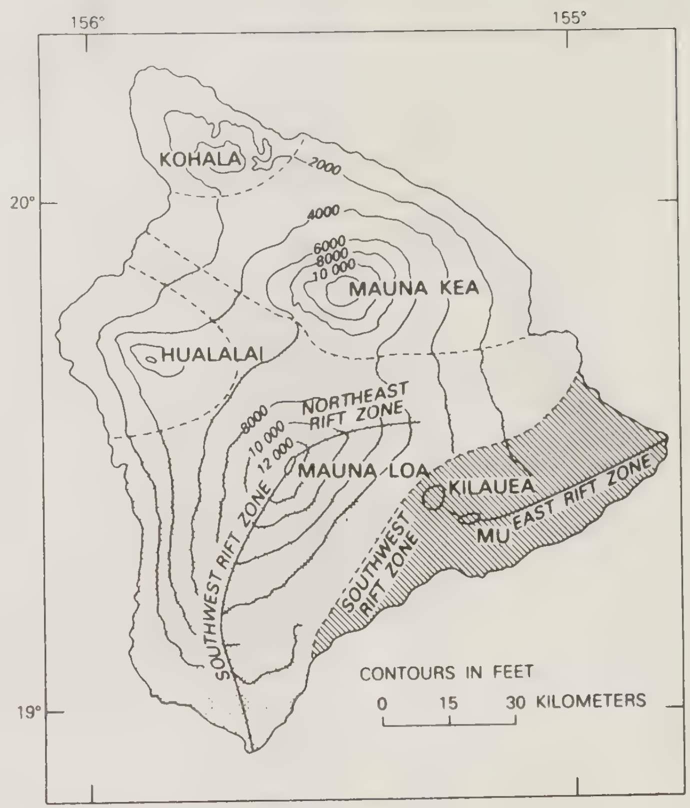

Figure 13.1.2. Index map showing the five volcanoes that make up Island of Hawaii and the rift zones of Kilauea and Mauna Loa Volcanoes, from Wright (1971). MU, site of the 1969-74 Mauna Ulu eruptions along Kilauea's upper east rift zone.

Figure 13.1.3. Kilauea Volcano, from Tilling and others (1987), showing summit caldera, rift zones, and principal fault systems; locations of the Hawaiian Volcano Observatory (HVO) and Uwekahuna vault (UWE) are also shown. Inset shows volcanoes making up the Island of Hawaii: KO, Kohala; MK, Mauna Kea; H, Hualalai; ML, Mauna Loa; and K, Kilauea. Mauna Ulu eruption site (1969-74) is along upper east rift zone; Puu Oo eruption site (1983-present) is along middle east rift zone (sites indicated by solid triangles). Mauna Iki (1919-20), Heiheiahulu (1750?), and Kane Nui o Hamo (prehistoric) are older volcanic shields along rift zones.

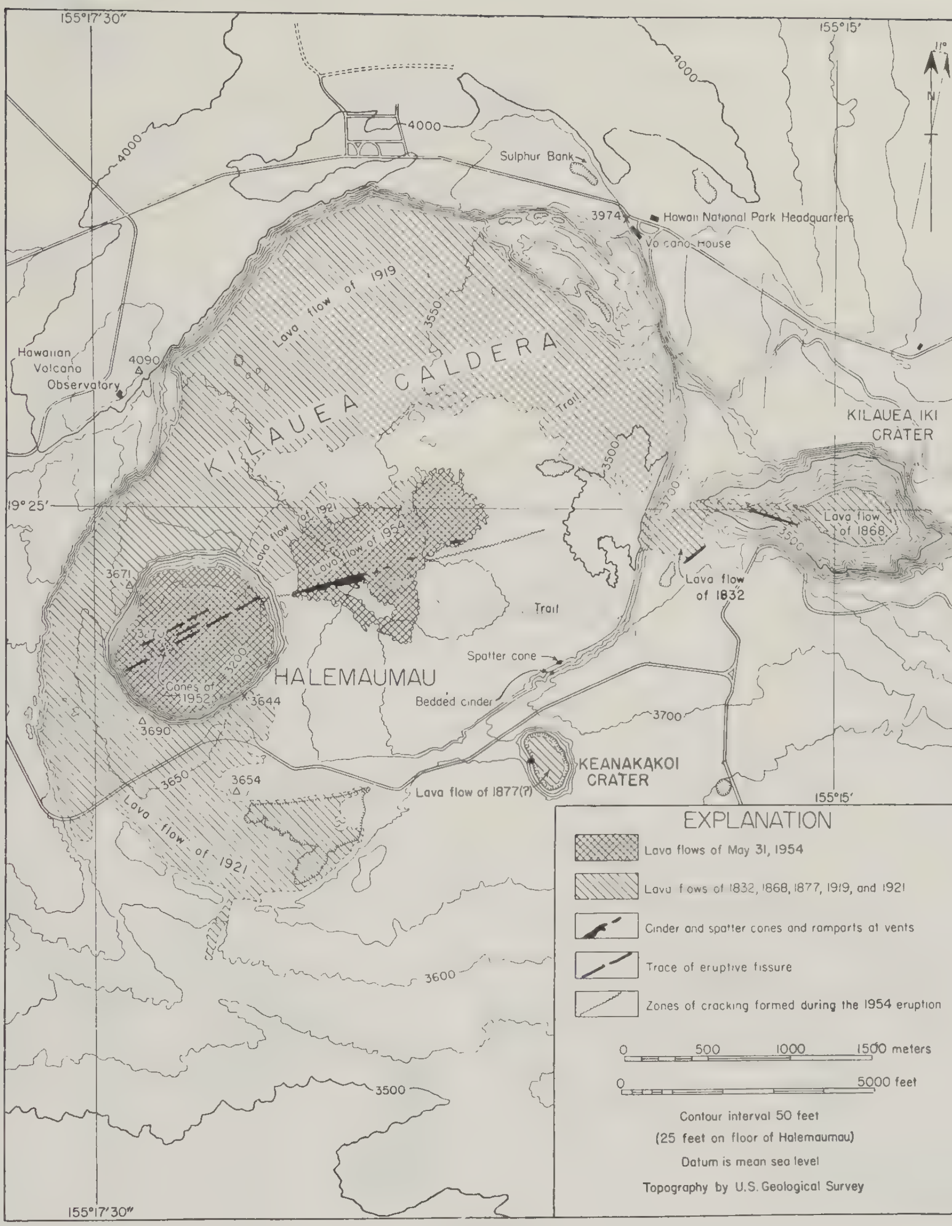

Figure 13.1.4. Topographic map of summit area of Kilauea Volcano, showing outline of Kilauea Caldera, Halemaumau (an inner pit crater), and recent lava flows (Macdonald, 1955).

Figure 13.1.5. Historical eruptions and property development on Kilauea Volcano, from Holcomb (1987). A, stratigraphy of Kilauea, showing outlines of current caldera ("Kilauea Caldera") and an earlier, mostly buried caldera ("Powers Caldera"), plus historical lava flows erupted before 1954. B, Property subdivisions, developed mostly after 1950. C, Lava flows erupted during 1955-84.

Figure 13.1.6. Series of maps summarizing Kilauea's eruption history during the last 1,500 years, from Holcomb (1987).

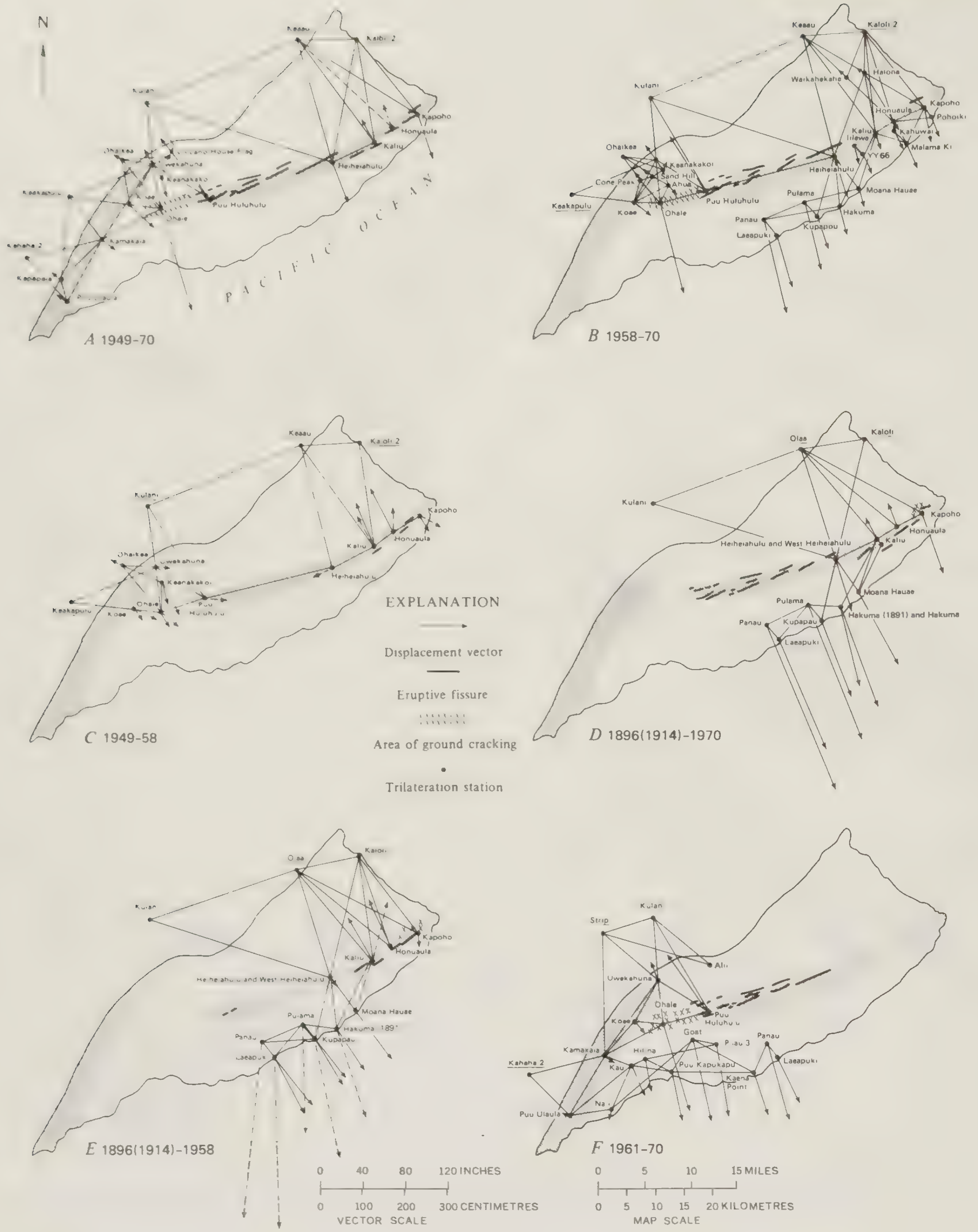

Figure 13.1.7. Horizontal ground displacements (arrows) at Kilauea Volcano derived from comparison of 1896 (1914), 1949, 1958, and 1961 triangulation surveys with 1970 trilateration survey (Swanson and others, 1976). Base stations considered stable are underlined; rift zones are shaded. Locations of rift eruptions and major episodes of ground cracking that occurred during a given survey are indicated.

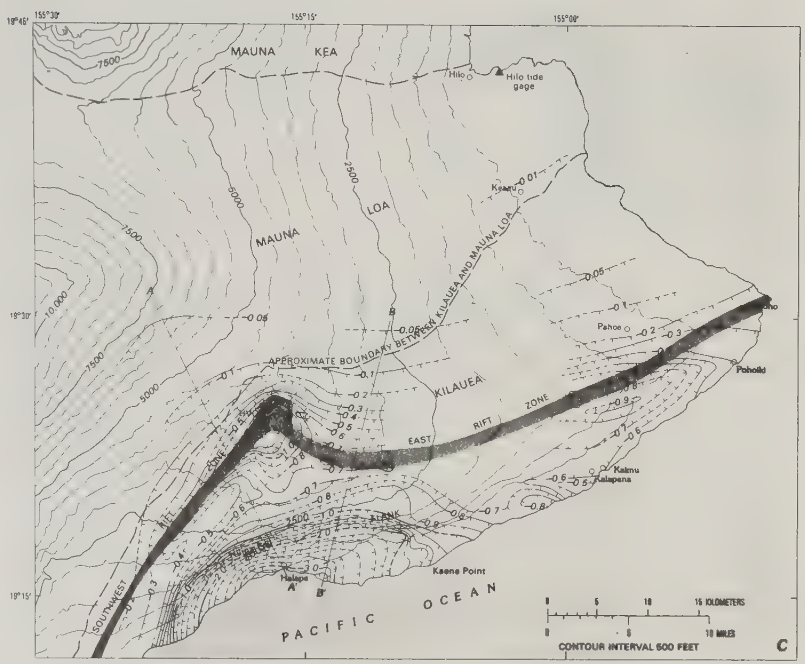

Figure 13.1.8. Interpreted contours of elevation changes associated with the November 1975 M 7.2 Kalapana earthquake, from Lipman and others (1985). Summit caldera and rift zones indicated by shaded pattern. Contour interval is 0.1 m, with supplemental 0.01- and 0.05-m contours; alternate contours omitted for values larger than -1.0 m. Hachures show direction of relative movement.

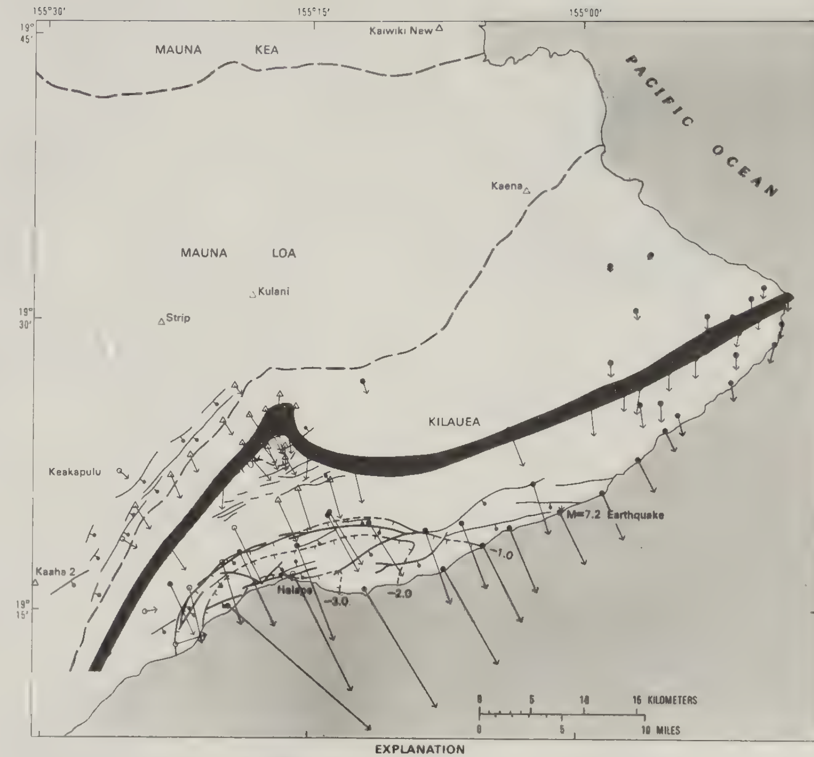

Figure 13.1.9. Interpretation of displacements associated with the November 1975 M 7.2 Kalapana earthquake, from Lipman and others (1985). Summit caldera and rift zones indicated by shaded pattern. Arrow tails at geodetic stations; lengths of arrows indicate amounts of displacement.

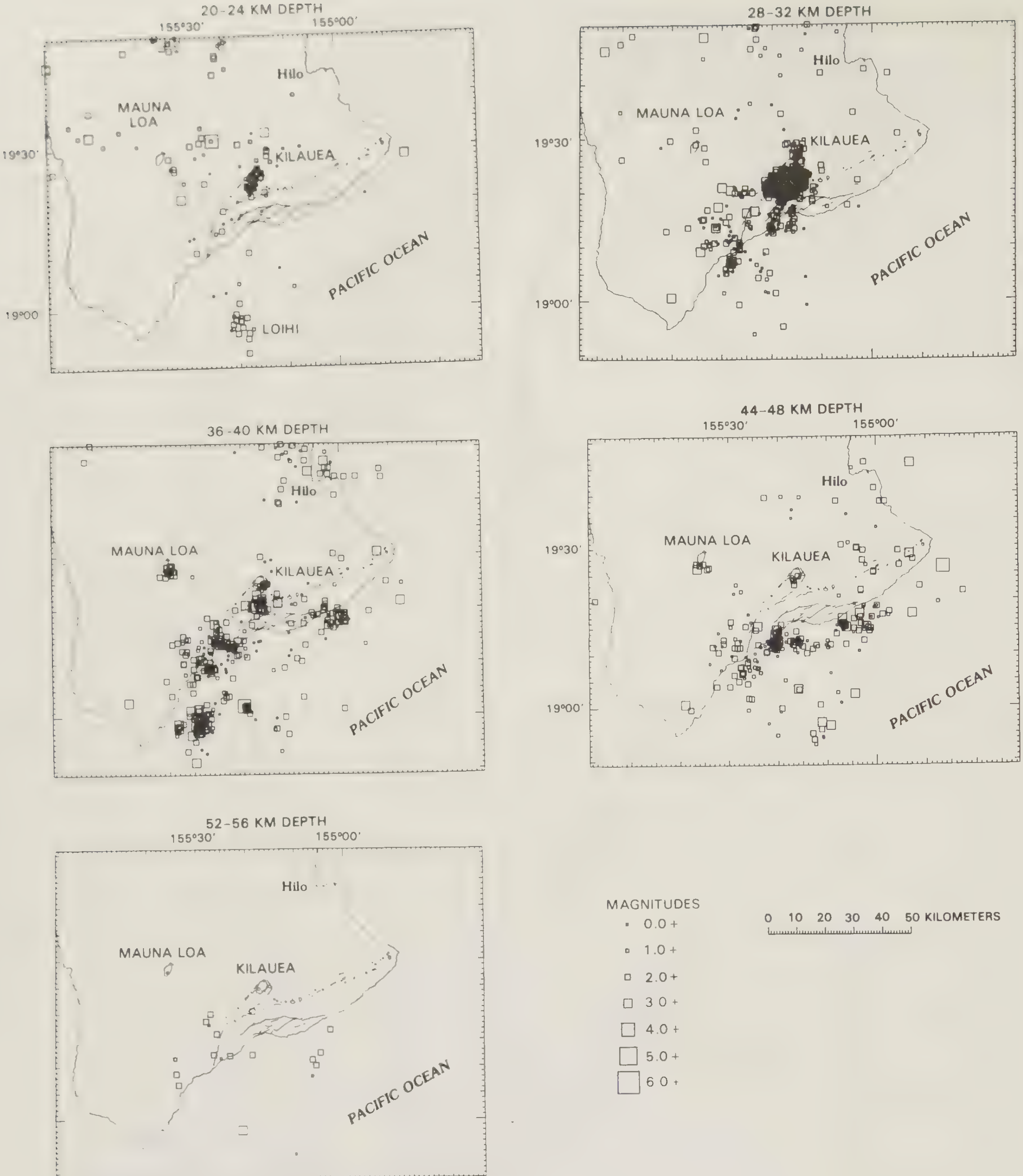

Figure 13.1.10. Selected depth slices from 20 to 60 km showing hypocenters of south Hawaii earthquakes, 1970-83, from Klein and others (1987). Note that magma conduit beneath summit caldera is nearly vertical, relatively narrow from 15- to 25-km depth, and more diffuse from 25- to 40-km depth (see also figure 13.1.11).

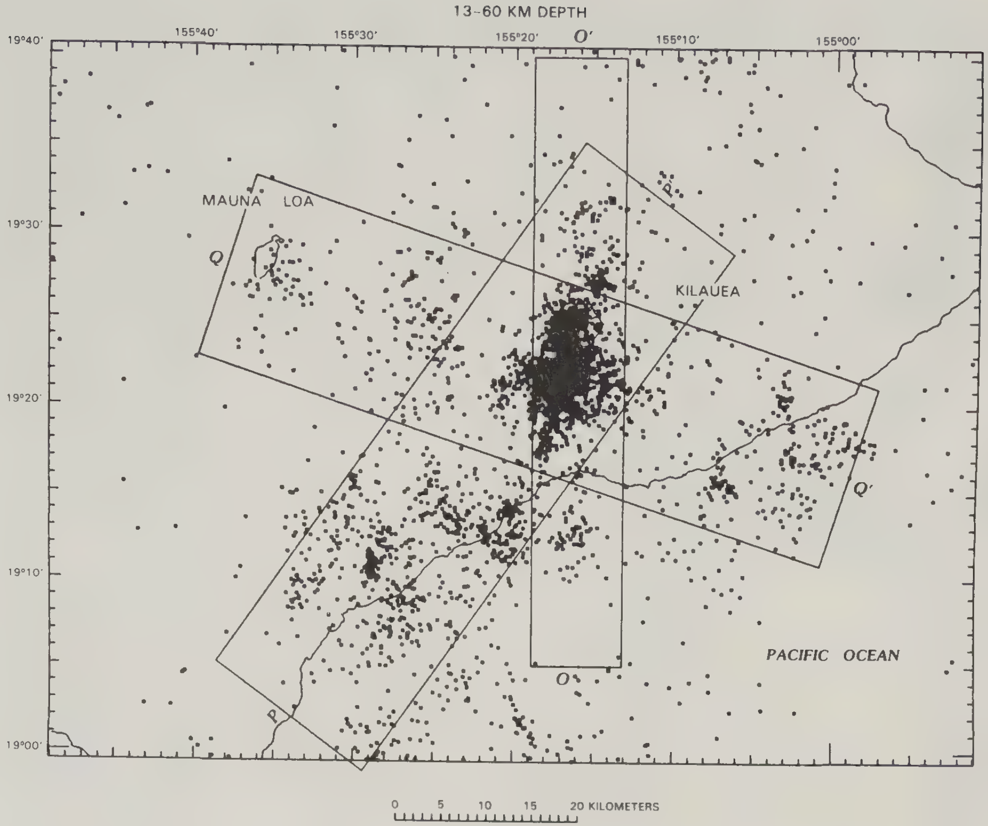

Figure 13.1.11. Above, Locations of 1970-83 earthquakes from 13- to 60-km depth beneath south Hawaii, from Klein and others (1987). Cross sections O-O' through Q-Q' are shown in figure 13.1.12. Only earthquakes within rectangular areas are plotted on sections. Although events above 13 km are plotted on sections, they are omitted from this map for clarity. All three sections include Kilauea's vertical magma conduit. Faults, fissures, and pit craters are shown in figure 13.1.3.

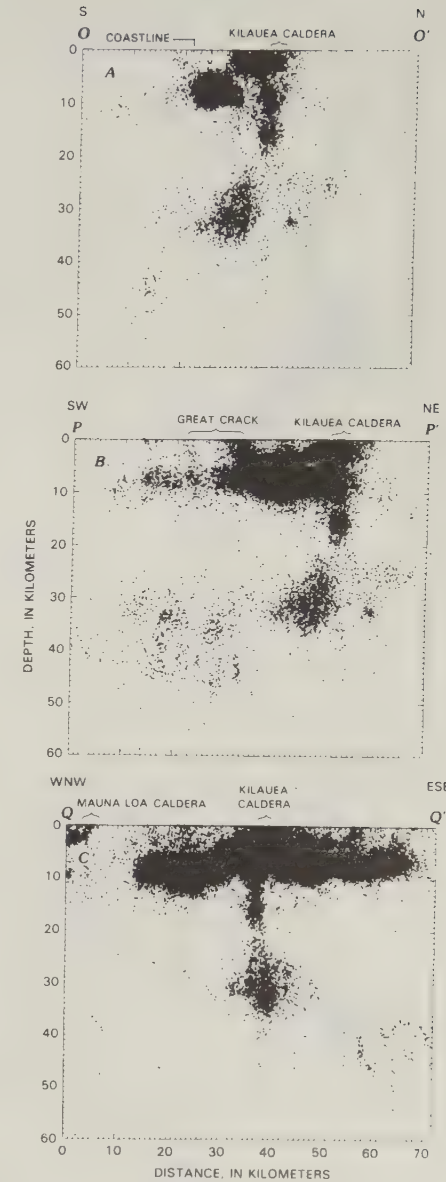

Figure 13.1.12. Right, Cross sections through Kilauea taken from surface to deepest seismicity at 60 km, from Klein and others (1987). Events during 1970-83 within areas of rectangles on previous figure are projected onto sections.

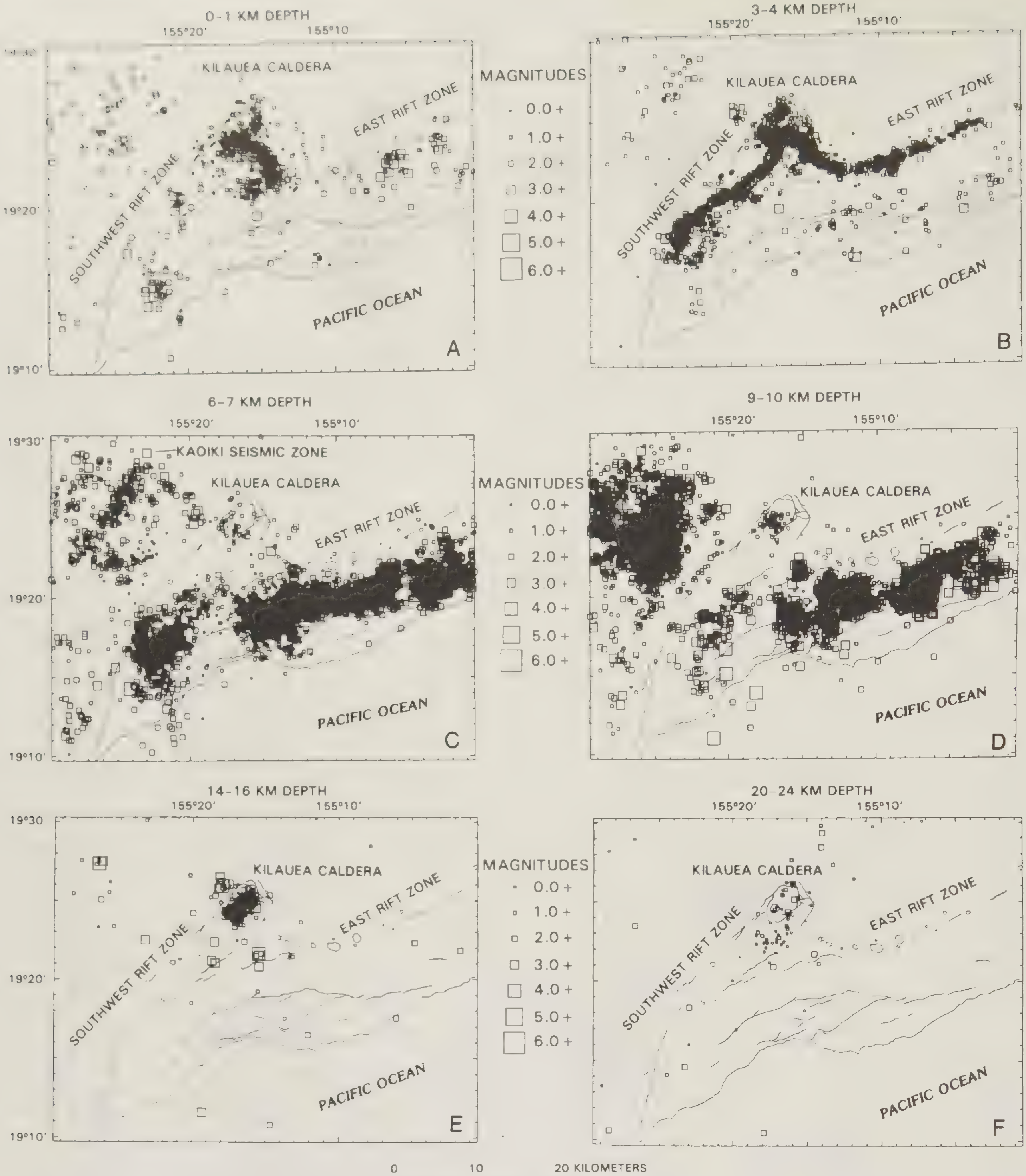

Figure 13.1.13. Selected depth slices from 0 to 24 km showing hypocenters of Kilauea earthquakes, 1970-83, from Klein and others (1987). Earthquake symbols are squares whose size depends on magnitude. Faults, fissures, and pit craters are shown in figure 13.1.3. From 0 to 2 km depth, most earthquakes occur in carapace rocks above summit magma chamber. From 2 to 4 km depth, earthquakes occur primarily in summit area and along two prominent rift zones. Kilauea's south flank and Kaoiki seismic zone between Kilauea and Mauna Loa are most active areas from 6 to 12 km depth; magma conduit beneath caldera is well defined by earthquakes from 14- to 40-km depth (see also figures 13.1.11, 13.1.12, and 13.1.14).

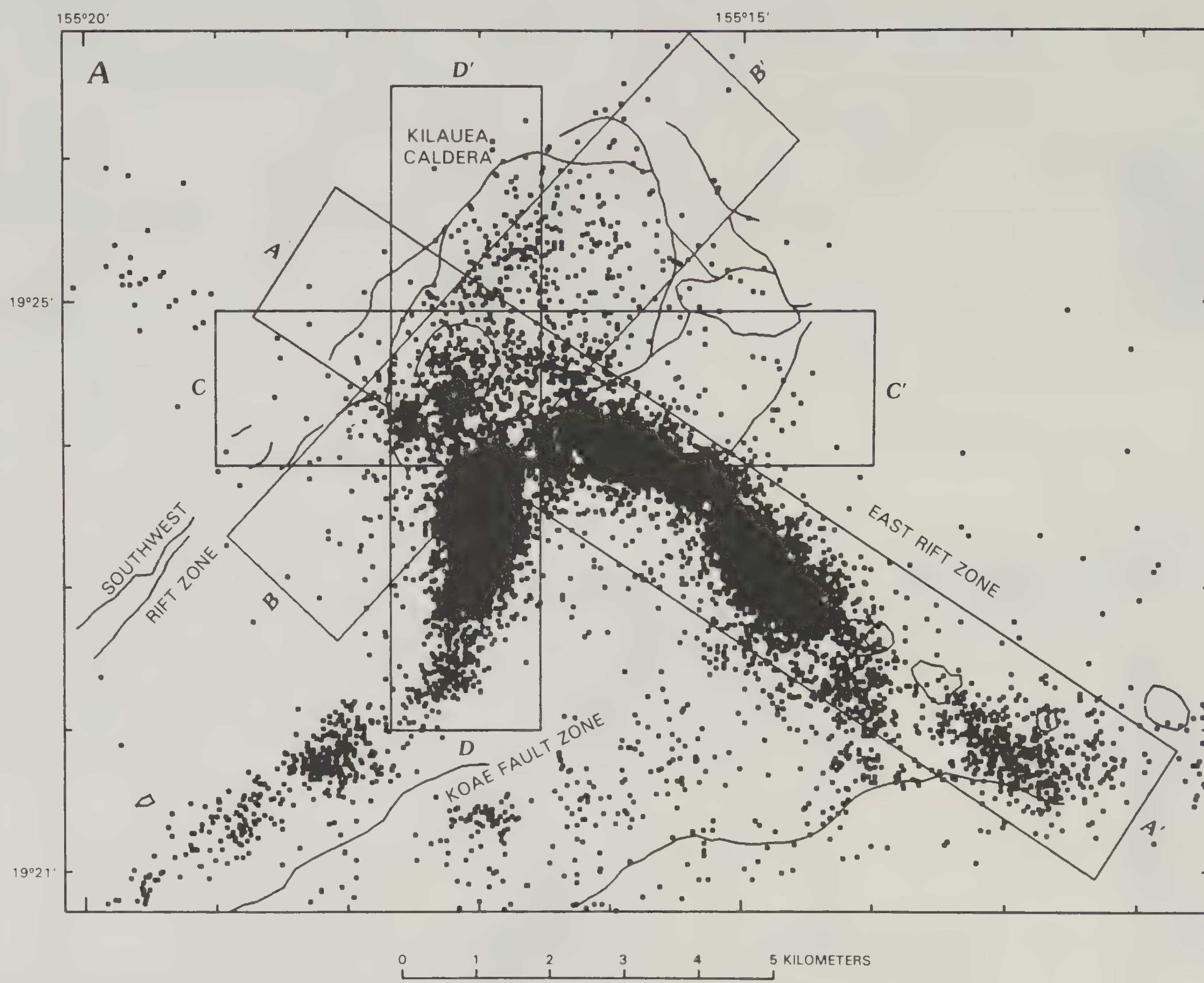

Figure 13.1.14. Epicenters of shallow 1970-83 earthquakes near Kilauea Caldera, from Klein and others (1987). Cross sections (rectangles) cross over buried magma reservoir. Note that sections in figure 13.1.15 extend to 12-km depth, but epicenters are shown here only for events in upper 5 km for clarity.

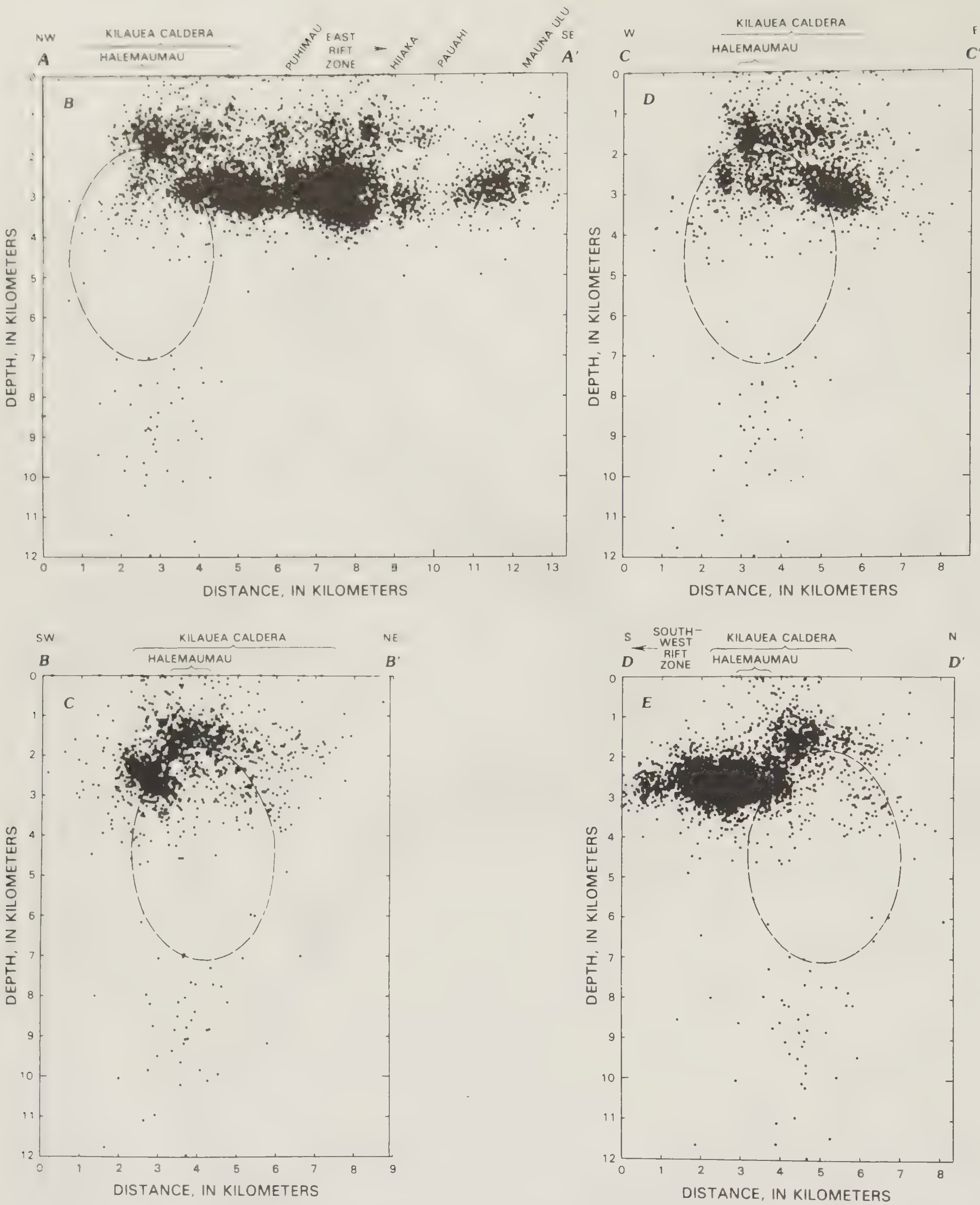

Figure 13.1.15. Cross sections of 1970-83 earthquakes shown in figure 13.1.14, from Klein and others (1987). Position of magma reservoir is approximated by dashed oval. Horizontal and vertical error of all hypocenters plotted is 1 km or less.

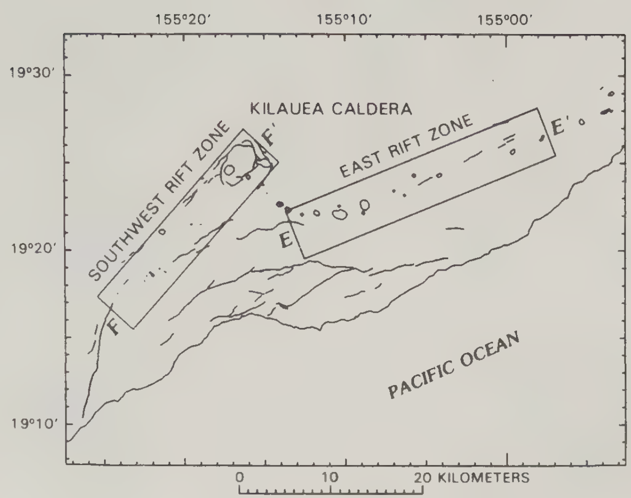

Figure 13.1.16. Areas included in longitudinal cross sections of rift zones (shown in figure 13.1.17), from Klein and others (1987). Only earthquakes within rectangles are plotted in the sections.

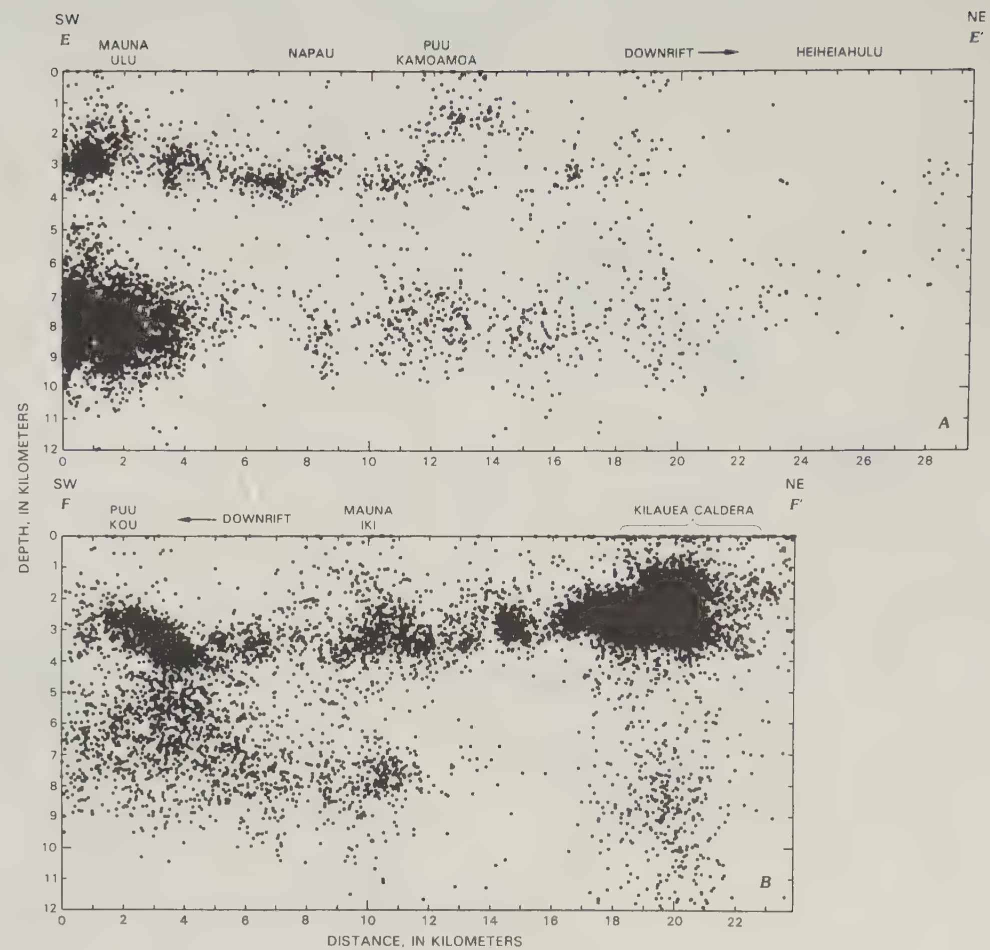

Figure 13.1.17. Longitudinal cross sections of earthquakes below east rift zone (A) and southwest rift zone (B), from Klein and others (1987). Positions and areas of sections are shown in figure 13.1.16. Main magma conduits (outlined by subhorizontal bands of seismicity) are at about 3-km depth.

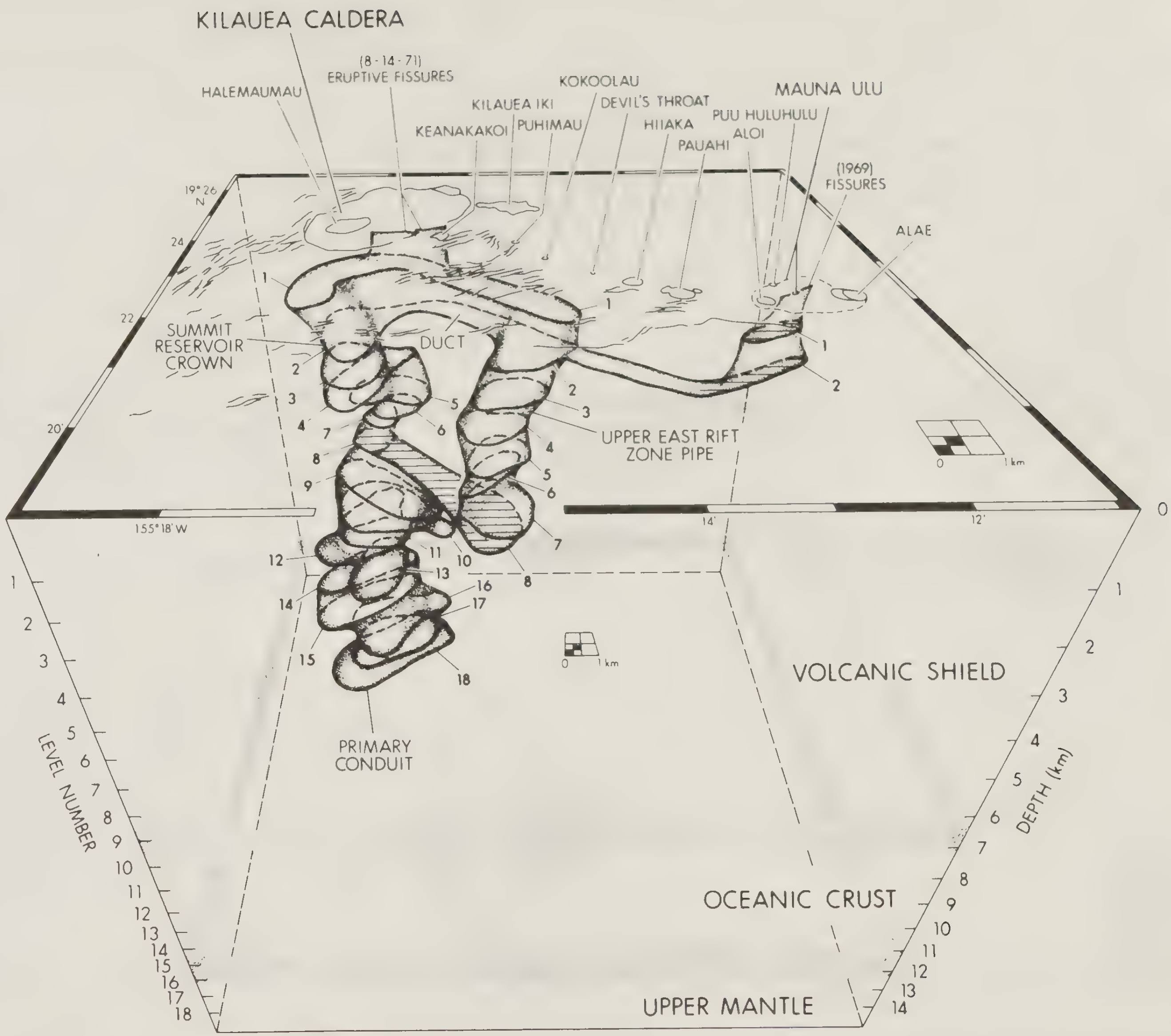

Figure 13.1.18. Perspective view northward and downward into interior of Kilauea Volcano, from Ryan and others (1981). Magma conduits are defined by zones of earthquake hypocenters that surround them over periods of several years. Numbers on magma conduits represent horizontal sections (slices) at depths corresponding to level-number scale on left side. Copyright by the American Geophysical Union.

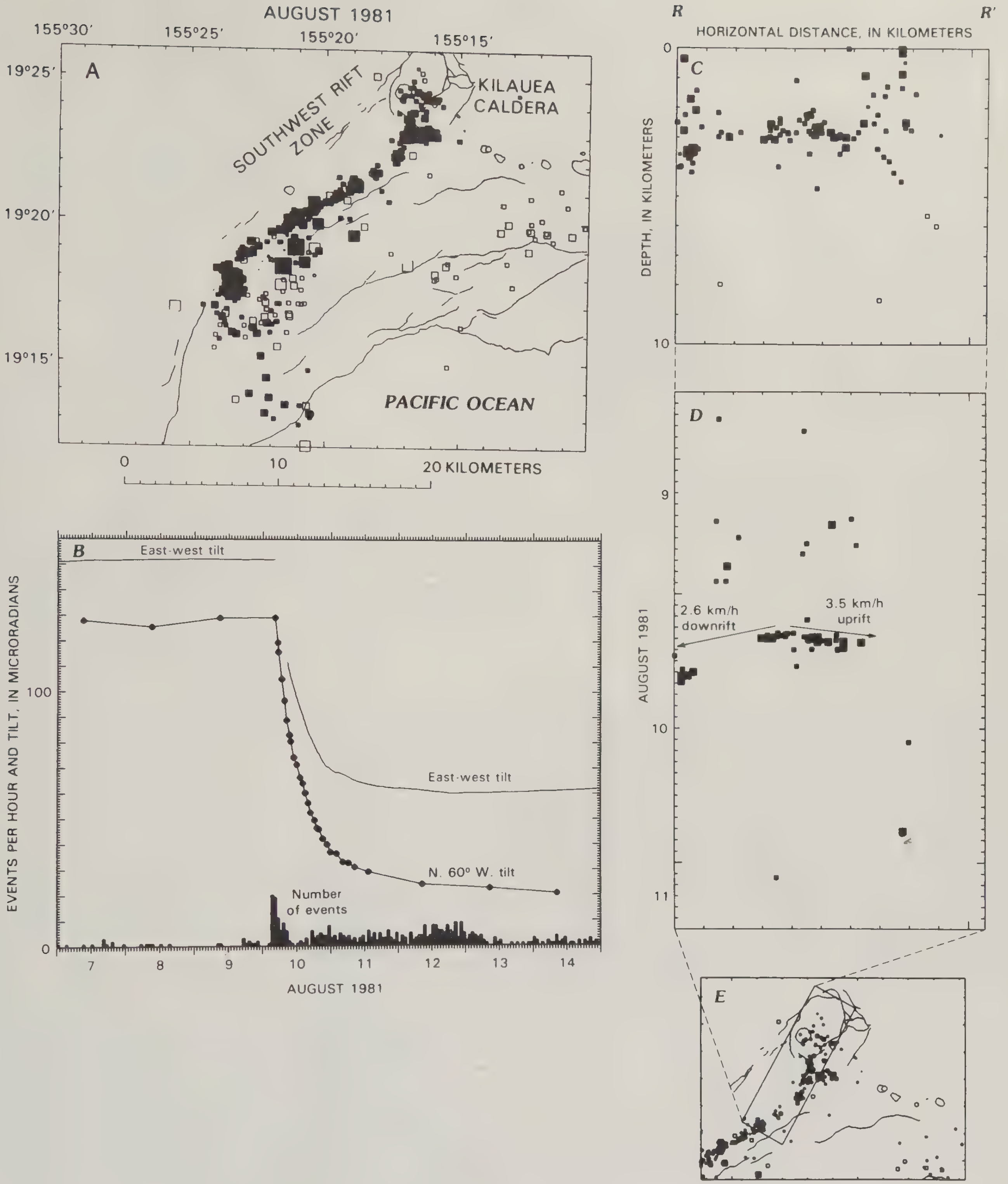

Figure 13.1.19. Seismicity and ground tilt during an intrusion into Kilauea's southwest rift zone on 10 August 1981, from Klein and others (1987). Map and cross section include earthquakes beginning on 9 August 1981. Solid lines in D indicate average lateral migration rates of earthquakes (uprift and downrift) during intrusion.

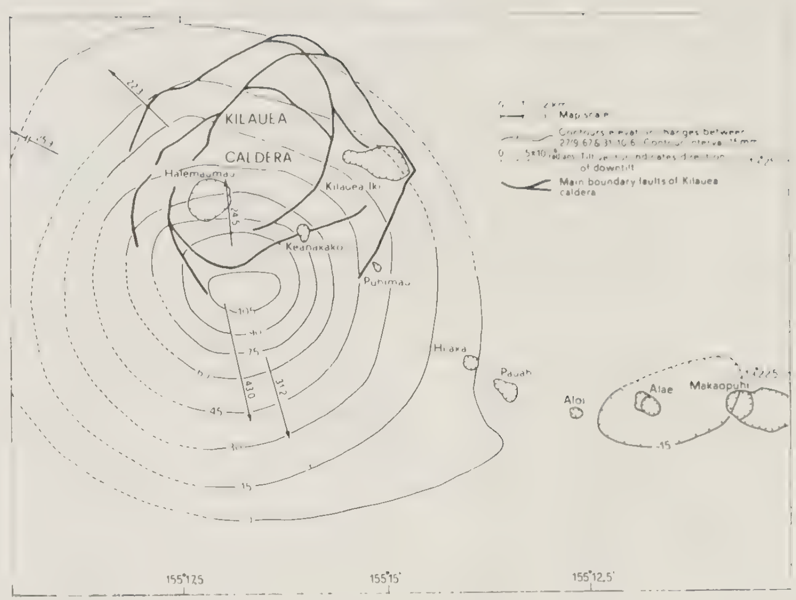

Figure 13.1.20. Contour map of vertical displacements from 27 September to 31 October 1967, from Kinoshita and others (1974). More than 100 mm of inflation during that interval was followed by a lava-lake eruption at Halemaumau from 5 November 1967 to 13 July 1968.

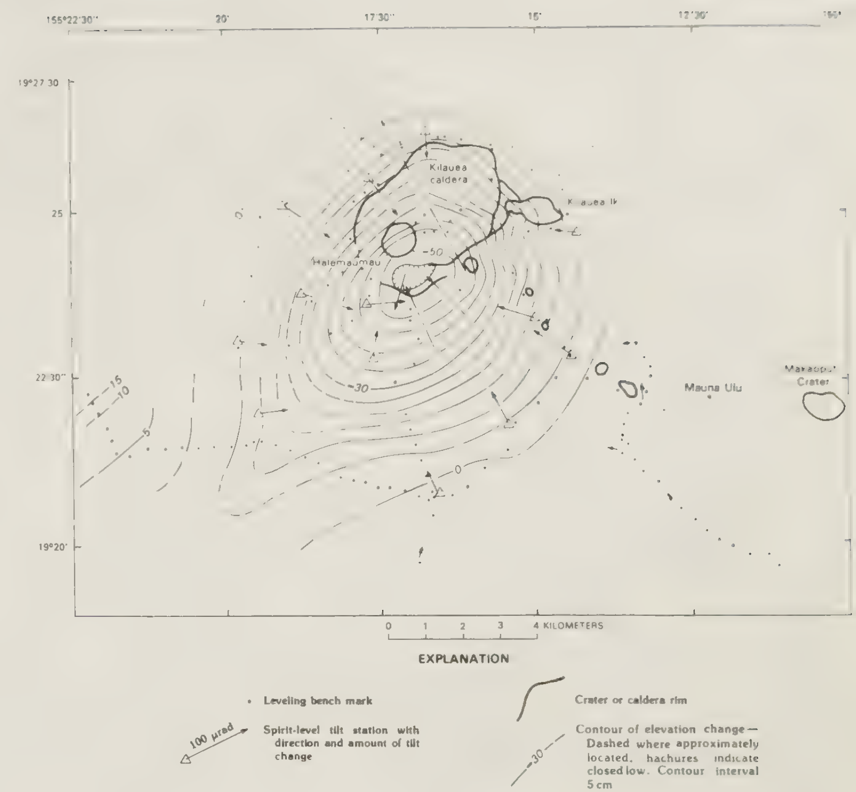

Figure 13.1.21. Subsidence and tilt in Kilauea summit region from 27 September - 5 October 1982 to 7-11 February 1983 (Wolfe and others, 1987). Contours show relative elevation change in centimeters.

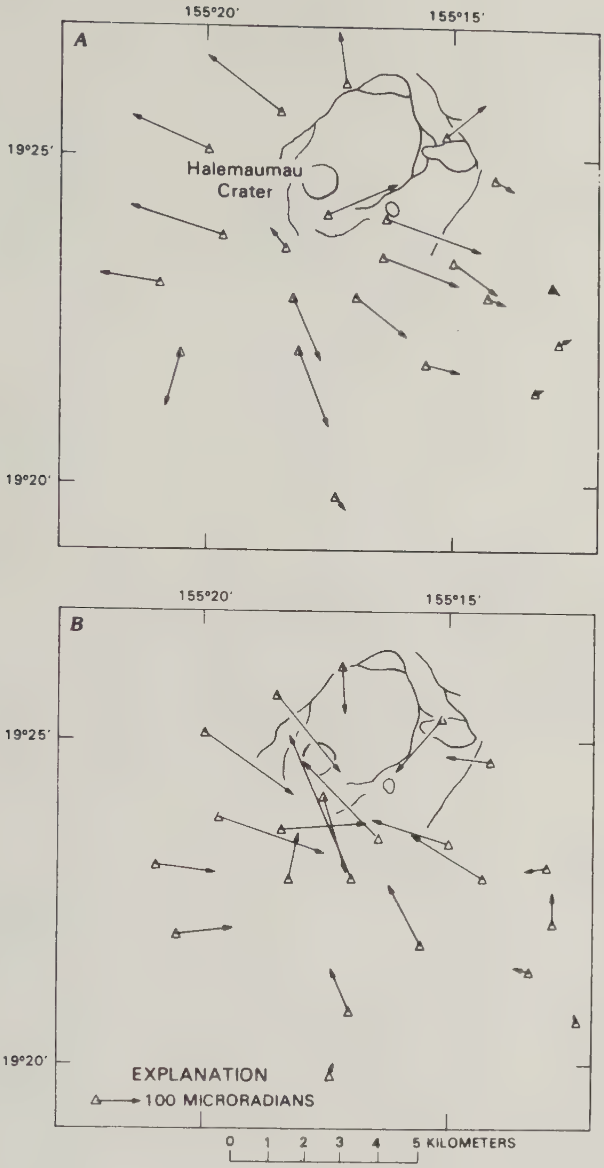

Figure 13.1.22. Tilt vectors measured in Kilauea summit region, from Dvorak and Okamura (1987). A, Uplift of 12-14 August 1981 to 3 March - 5 April 1982. B, Subsidence of 27 September - 14 October 1982 to 2-11 February 1983. Vectors were determined by measuring changes in relative elevation along 40-m-long triangles. Station locations shown by open triangles; tilt vectors point in direction of downward deflection of surface. General radial pattern of tilt vectors indicates that the most active part of summit magma reservoir lies beneath southern part of caldera (see also figure 13.1.23).

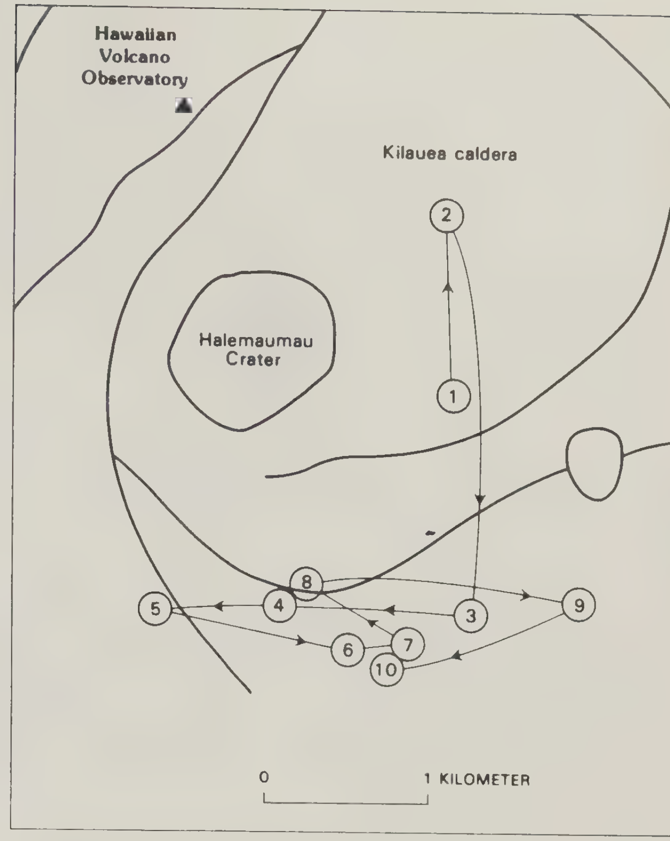

Figure 13.1.23. Lateral shift of apex of uplift of inflating bulge at Kilauea summit, modified from Fiske and Kinoshita (1969). Leveling surveys demonstrate shifting center of uplift: (1) January-July 1966; (2) July-October 1966; (3) October 1966 - January 1967; (4) January-February 1967; (5) during February 1967; (6) February-May 1967; (7) May-June 1967; (8) June-July 1967; (9) July-September 1967; (10) September-October 1967. Total uplift of the 10-km-wide bulge at its apex from January 1966 to October 1967 was approximately 70 cm; summit eruption of Kilauea began in November 1967. Copyright by the American Association for the Advancement of Science.

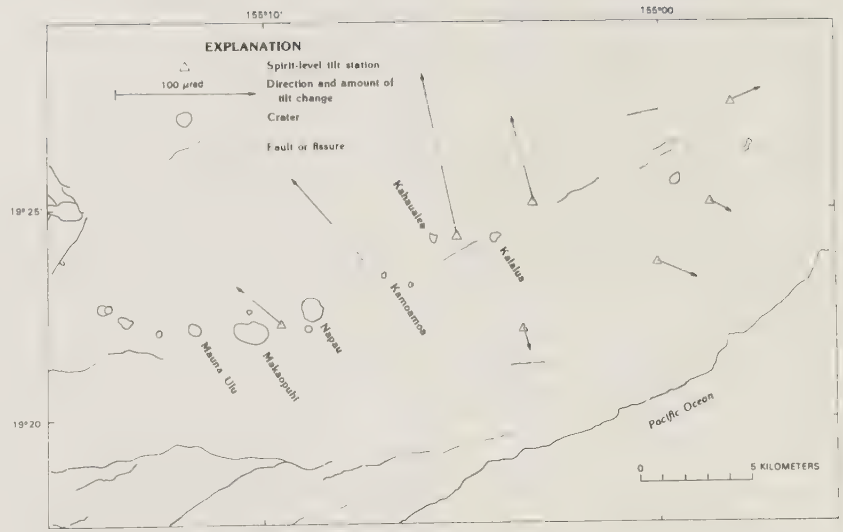

Figure 13.1.24. Tilt changes along east rift zone from spirit-level measurements, January 1978 to March 1981 (Wolfe and others, 1987). Inflation of rift zone occurred during a series of intrusions into rift following the September 1977 eruption. It culminated in a long-lived eruption on middle east rift zone that began in January 1983.

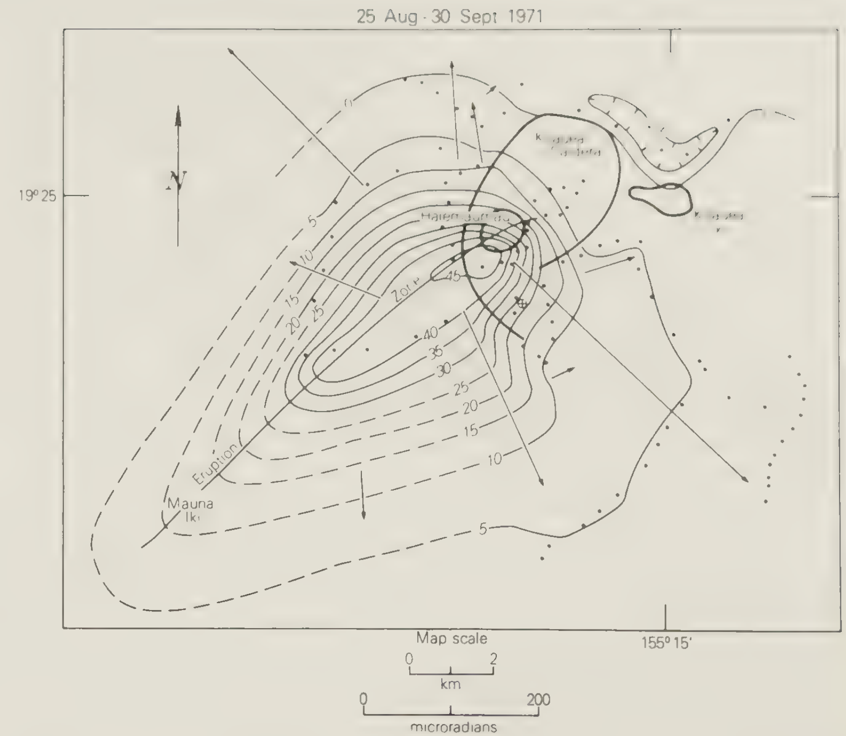

Figure 13.1.25. Vertical ground-displacement contours (in centimeters) and ground-tilt vectors for the period 25 August to 30 September 1971 (Duffield and others, 1982). Bench marks shown as dots; preeruption center of ground tilt shown as circle with cross. Zone of eruptive and noneruptive fissures generalized as solid line.

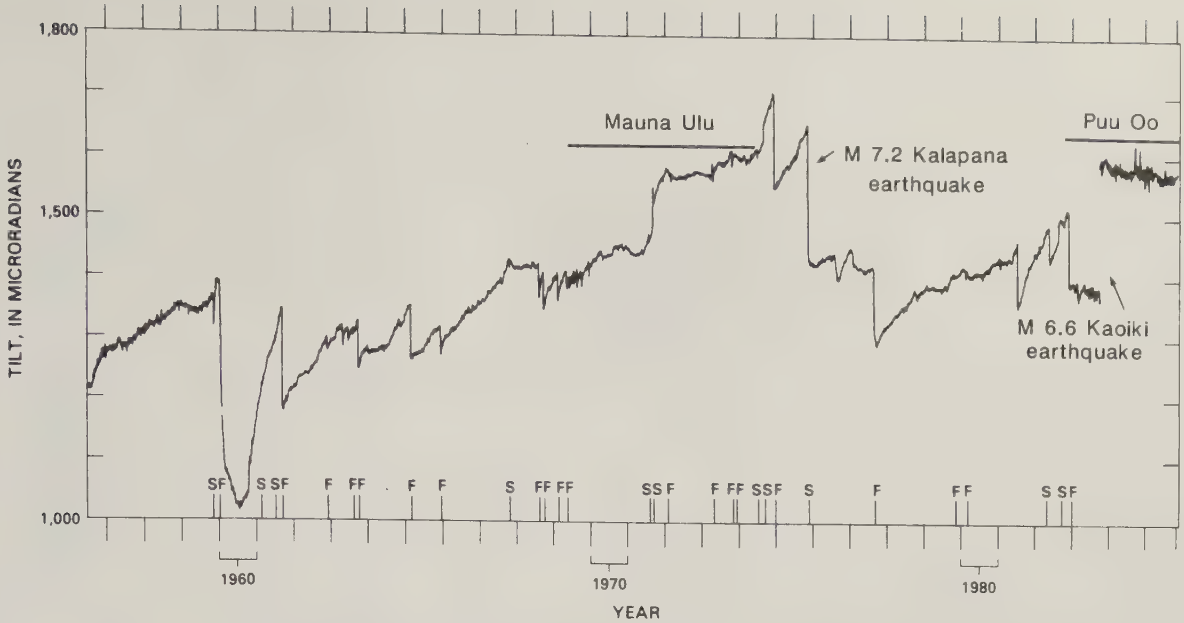

Figure 13.1.26. Radial tilt at Uwekahuna vault (see figure 13.1.3) on northwest rim of Kilauea Caldera for the period 1956-85, from Decker (1987). Increasing tilt (radially outward) indicates inflation of summit region; decreasing tilt indicates deflation. Magma added slowly to shallow reservoir system from depth between eruptions (slow inflation) is removed rapidly during flank eruptions and intrusions (sudden deflation). Vertical lines indicate eruptions; S, summit eruptions; F, flank eruptions. Offset in November 1983 caused by M 6.6 earthquake.

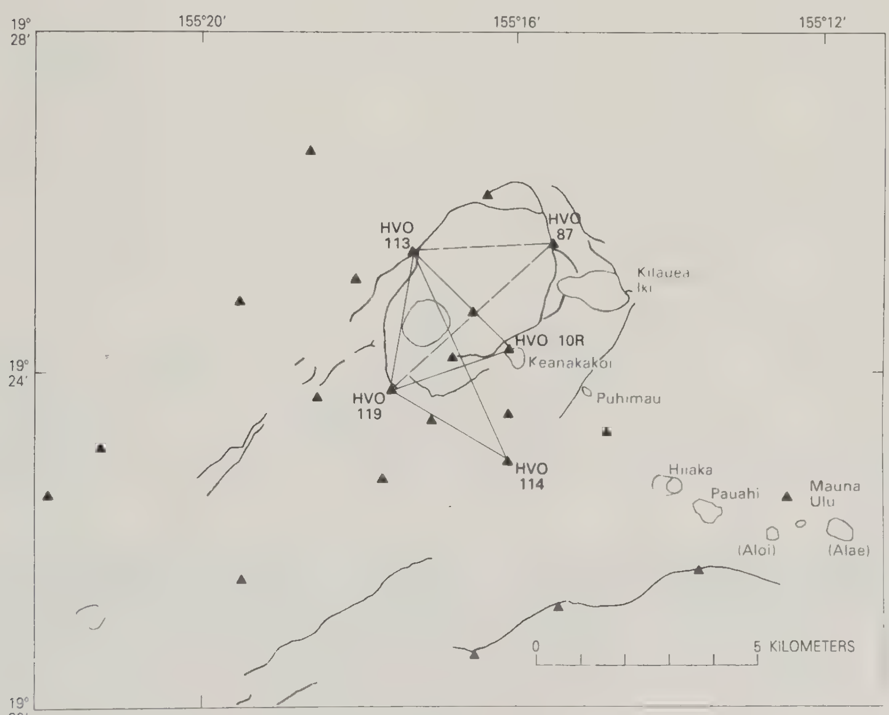

Figure 13.1.27. Location of electronic distance measurement (EDM) bench marks of Kilauea summit trilateration network, from Tilling and others (1987). Solid lines are measured more frequently than dashed lines (see figure 13.1.28).

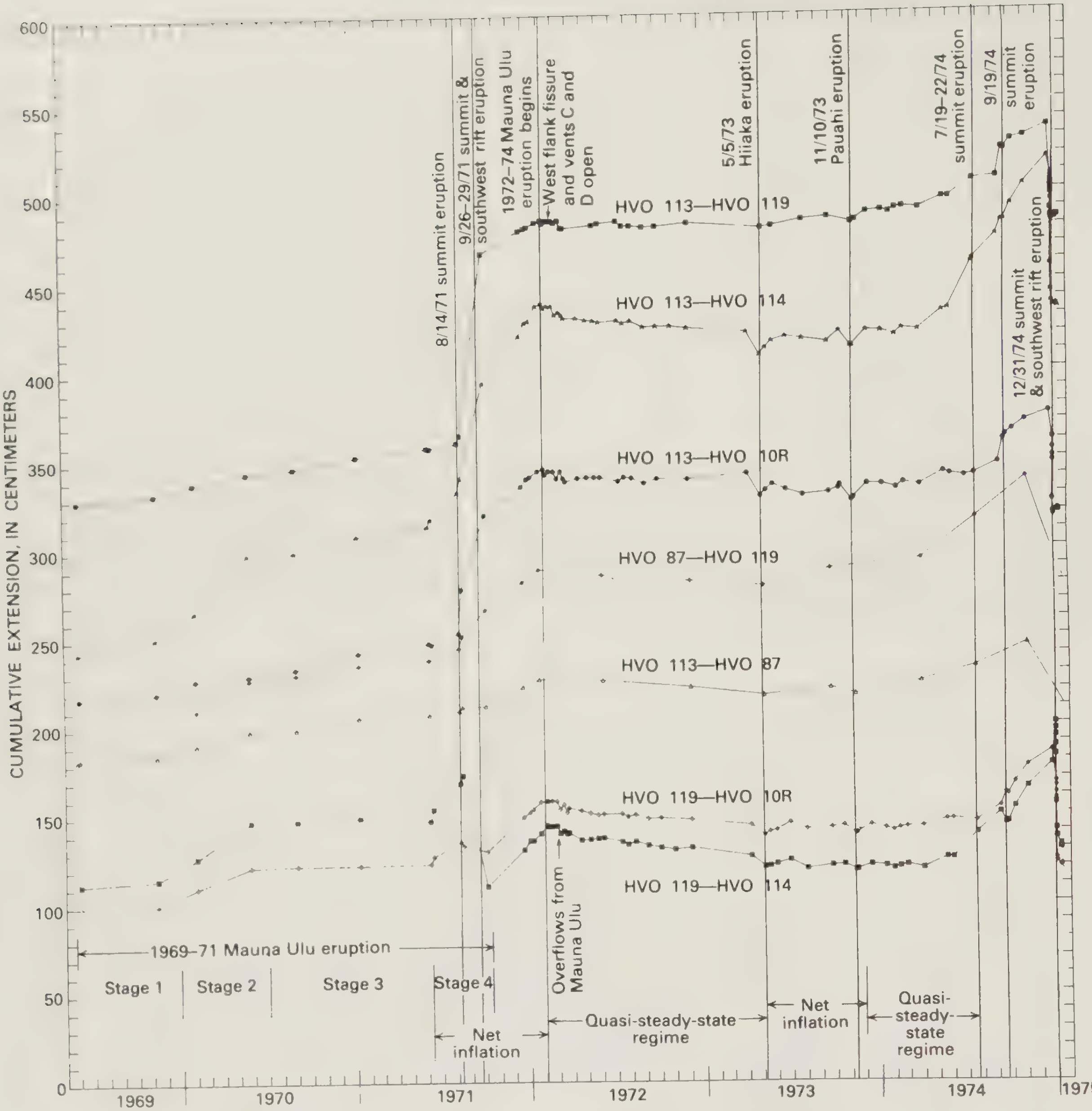

Figure 13.1.28. Variations of distances between electronic distance measurement (EDM) bench marks (figure 13.1.27) between May 1969 and January 1975, from Tilling and others (1987). Starting value for each cumulative extension curve is arbitrary. Frequency of measurements during 1969-71 was about the same as during 1972-75, but not all data are plotted here.

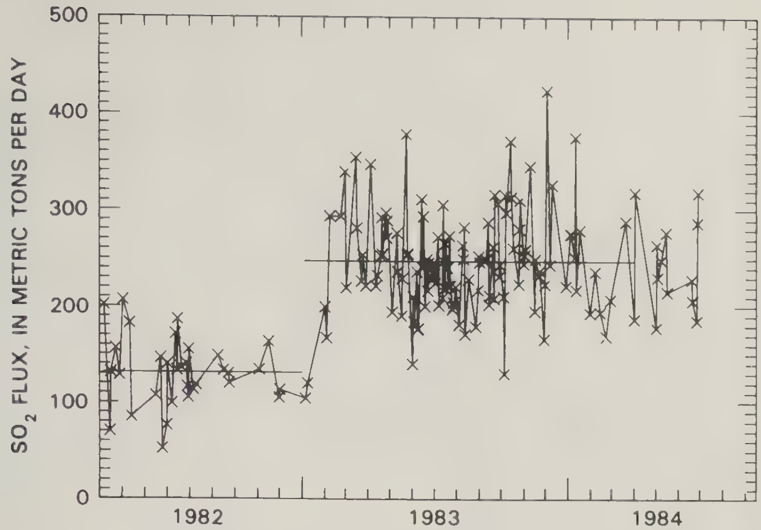

Figure 13.1.29. Total sulfur dioxide (SO_2) flux from Kilauea summit fumaroles, April 1982 through June 1984, based on ground measurements (Wolfe and others, 1987; modified from Greenland and others, 1985). Horizontal lines show change in average flux after start of Puu Oo eruption on middle east rift zone in January 1983.

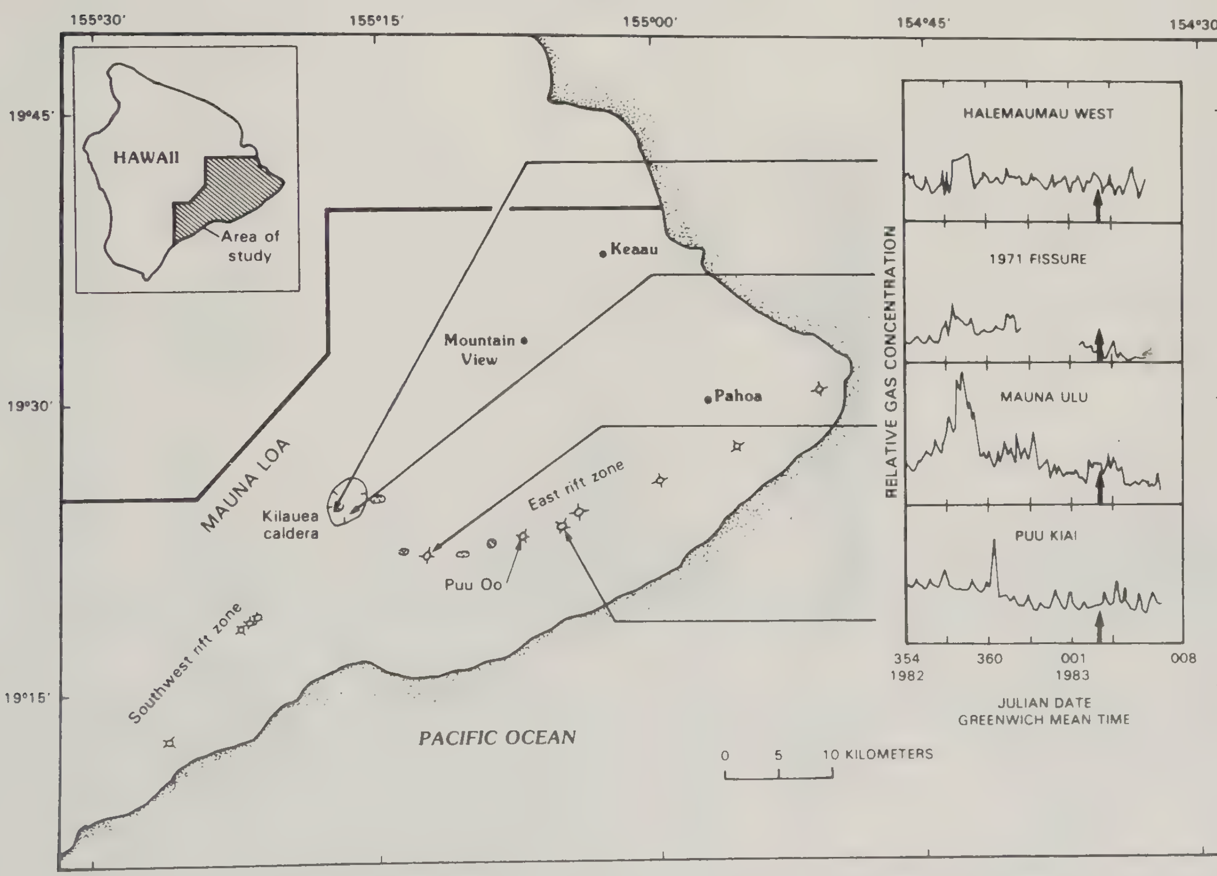

Figure 13.1.30. Results from satellite-telemetered gas-monitoring stations at Kilauea for late December 1982 through early January 1983, from McGee and others (1987). Increased gas emission in late December was detected simultaneously by two summit stations (Halemaumau West and 1971 Fissure) and upper east rift station (Mauna Ulu). Vertical arrow marks onset of eruptive activity at Puu Oo.

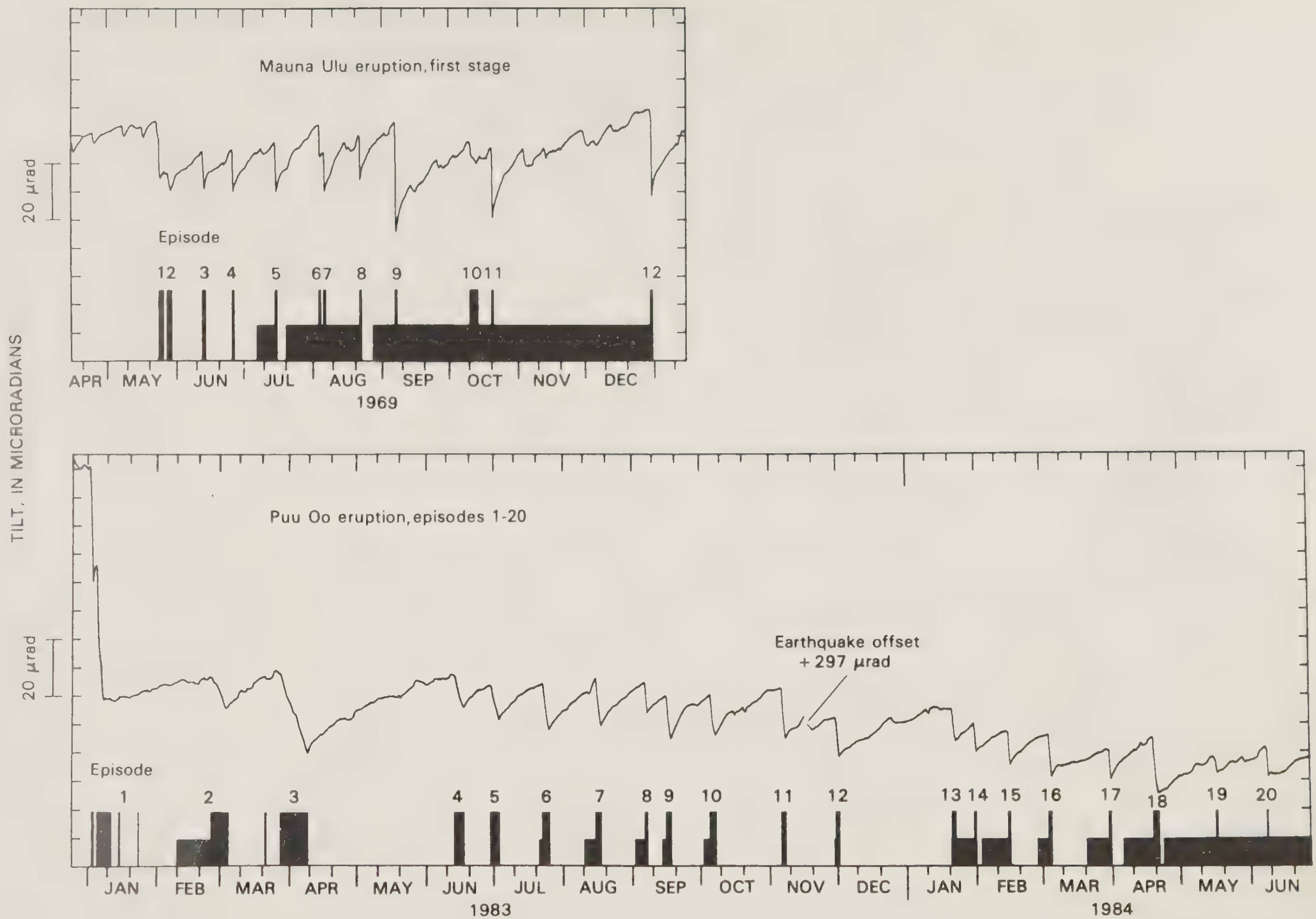

Figure 13.1.31. East-west tilt at Kilauea summit (measured at Uwekahuna vault; see figure 13.1.3), episodes of high lava fountaining (full-height bars), and periods of observed low-level eruptive activity (half-height bars) during first stage of the 1969-71 Mauna Ulu eruption (top) and during fountaining episodes 1-20 of the 1983-present Puu Oo eruption (bottom), from Wolfe and others (1987).

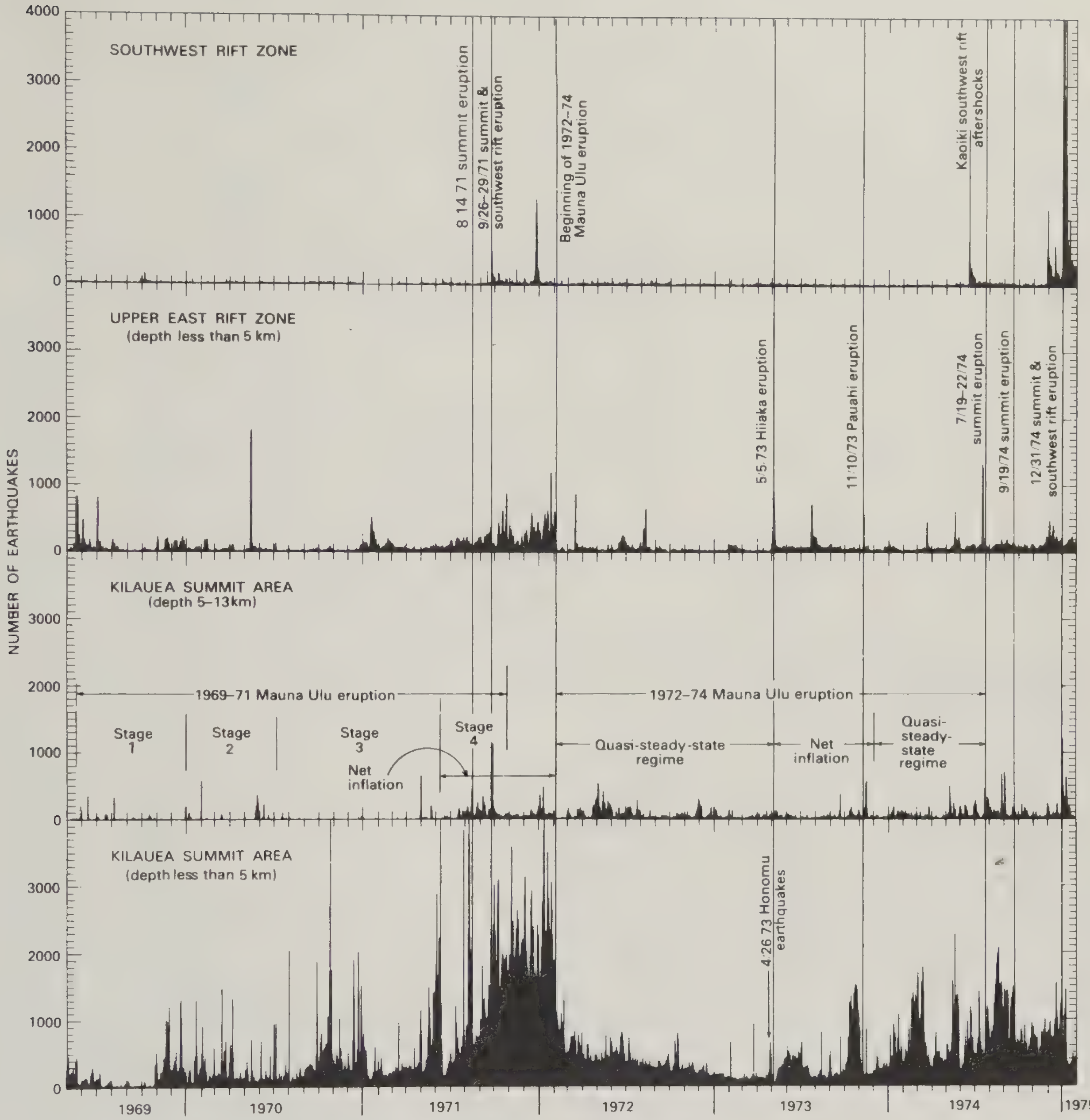

Figure 13.1.32. Numbers of earthquakes in summit area (shallow and crustal depth), in upper east rift zone, and in southwest rift zone of Kilauea from May 1969 to January 1975, from Tilling and others (1987). All events are counted, whether or not hypocenters are well determined; counts for southwest-rift earthquakes include those in Kaoiki fault system.

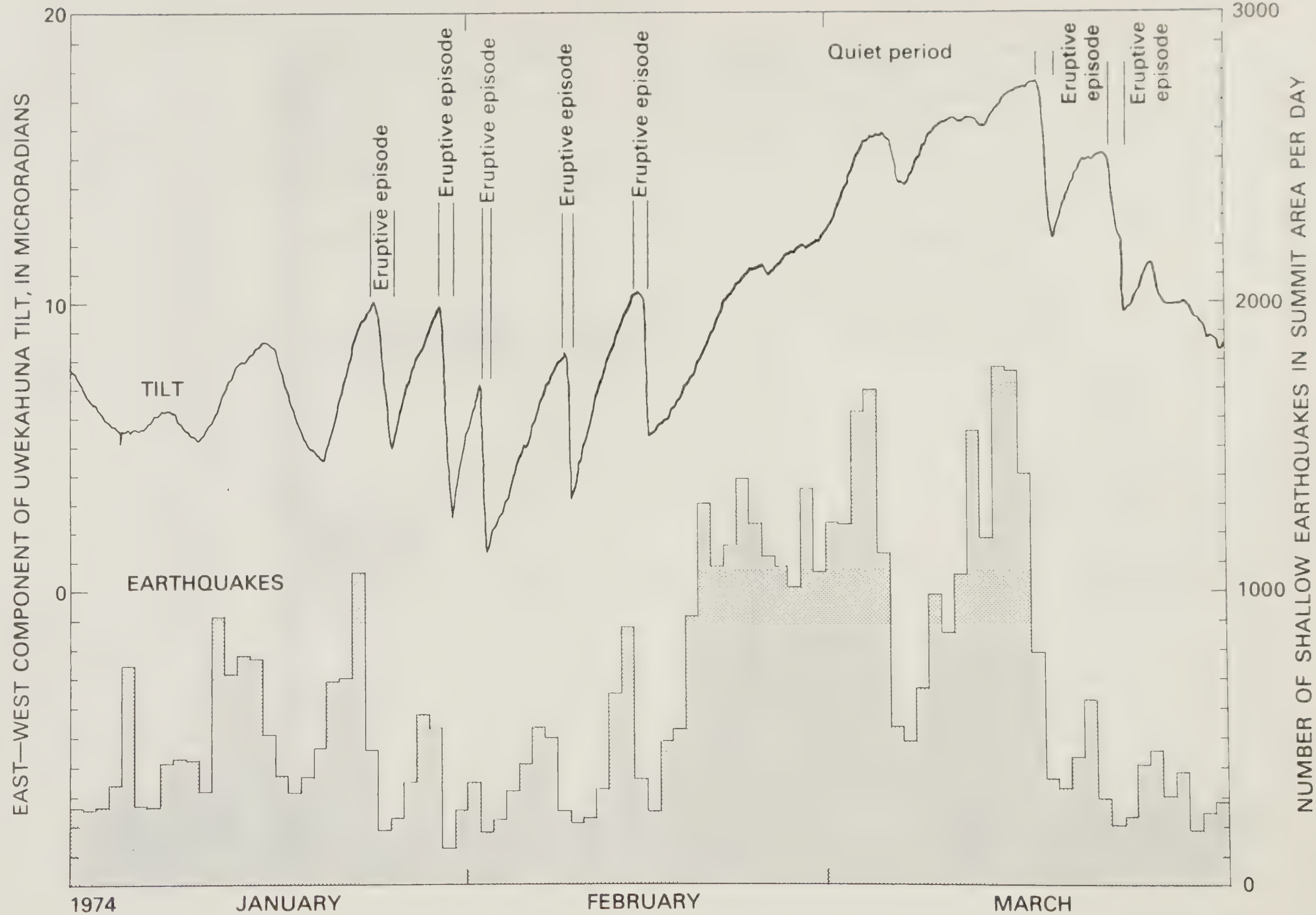

Figure 13.1.33. Correlation of eruptive episodes at Mauna Ulu during January-March 1974, characterized by vigorous fountaining and voluminous overflows, with variations in Uwekahuna tilt and daily number of shallow (depth less than 5 km) summit earthquakes (Tilling and others, 1987).

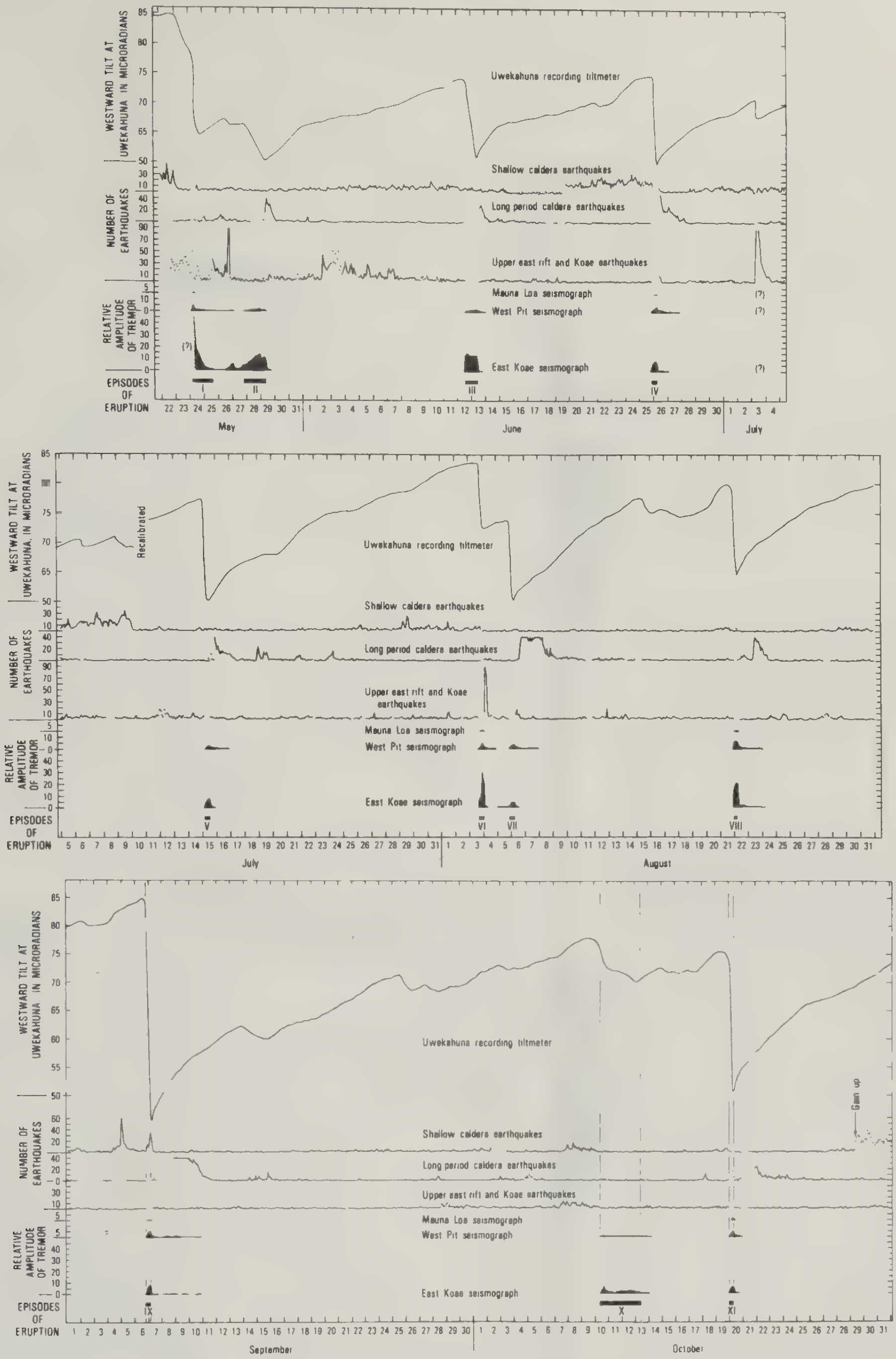

Figure 13.1.34. Summit tilt, shallow earthquakes, relative amplitude of tremor, and episodes of extrusion for first stage of Mauna Ulu eruption, May-October 1969 (Koyanagi and others, 1987). Tilt at 2-hr intervals from Uwekahuna tiltmeter (E-W) near northwest rim of Kilauea Caldera (see figure 13.1.3). Earthquake counts at 2-hr intervals from selected local stations (detection threshold about magnitude 0.1). Amplitude of tremor from adjusted hourly readings of smoked-paper records, plotted in relative units above background at three stations: Mauna Loa (MLO), 25 km from eruption site; West Pit (WPT), 11 km from eruption site; and East Koae (EKO), 5 km from eruption site. Times of major eruptive episodes shown by horizontal bars labeled with sequence numbers.

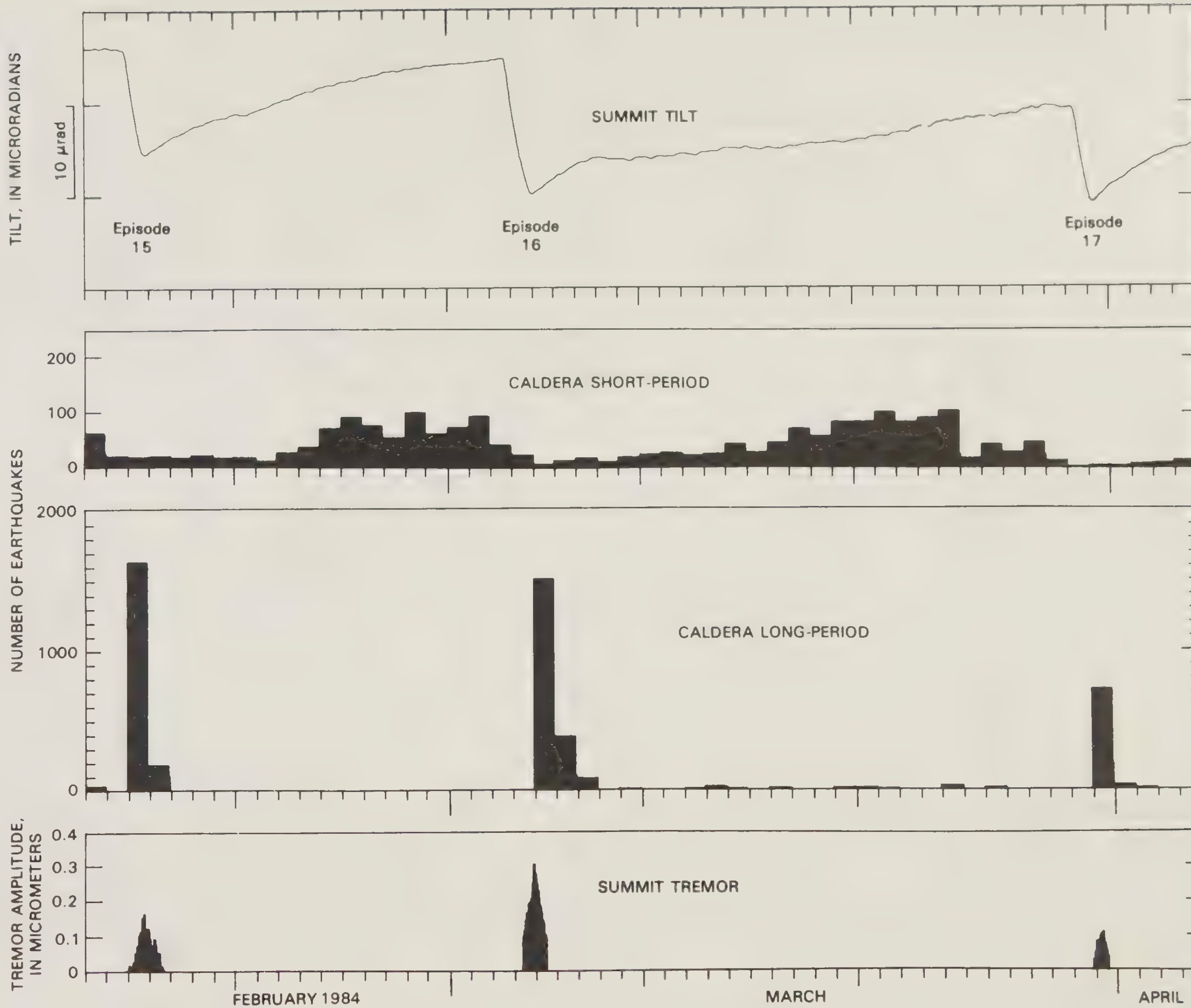

Figure 13.1.35. East-west summit tilt, daily frequency of short-period caldera earthquakes, and amplitude of shallow harmonic tremor beneath Kilauea Caldera for episodes 15-17 of Puu Oo eruption, from Wolfe and others (1987).

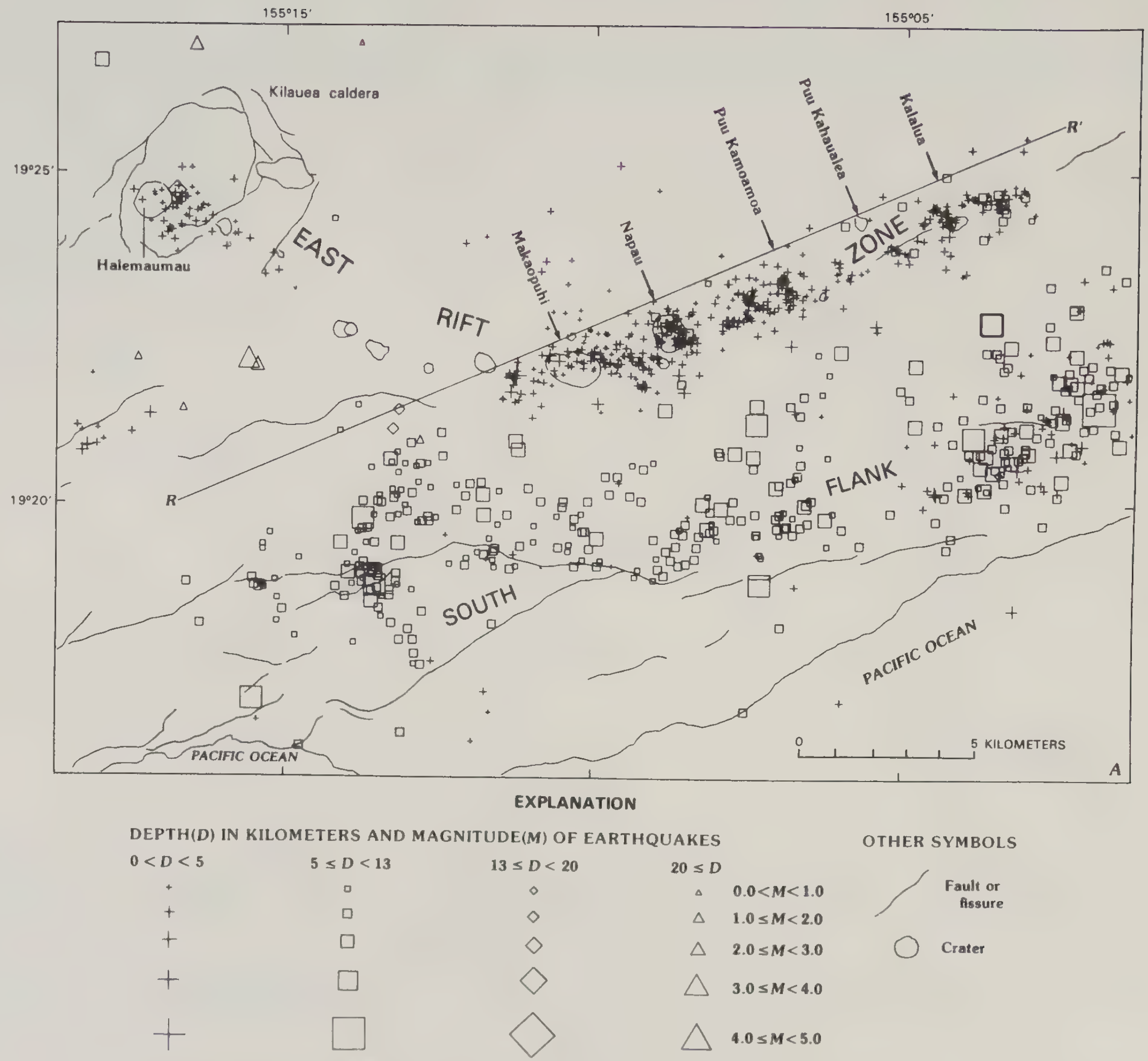

Figure 13.1.36. Located earthquakes at Kilauea during January 1983, from Wolfe and others (1987). A vertical cross section along line R-R′ is shown in figure 13.1.37.

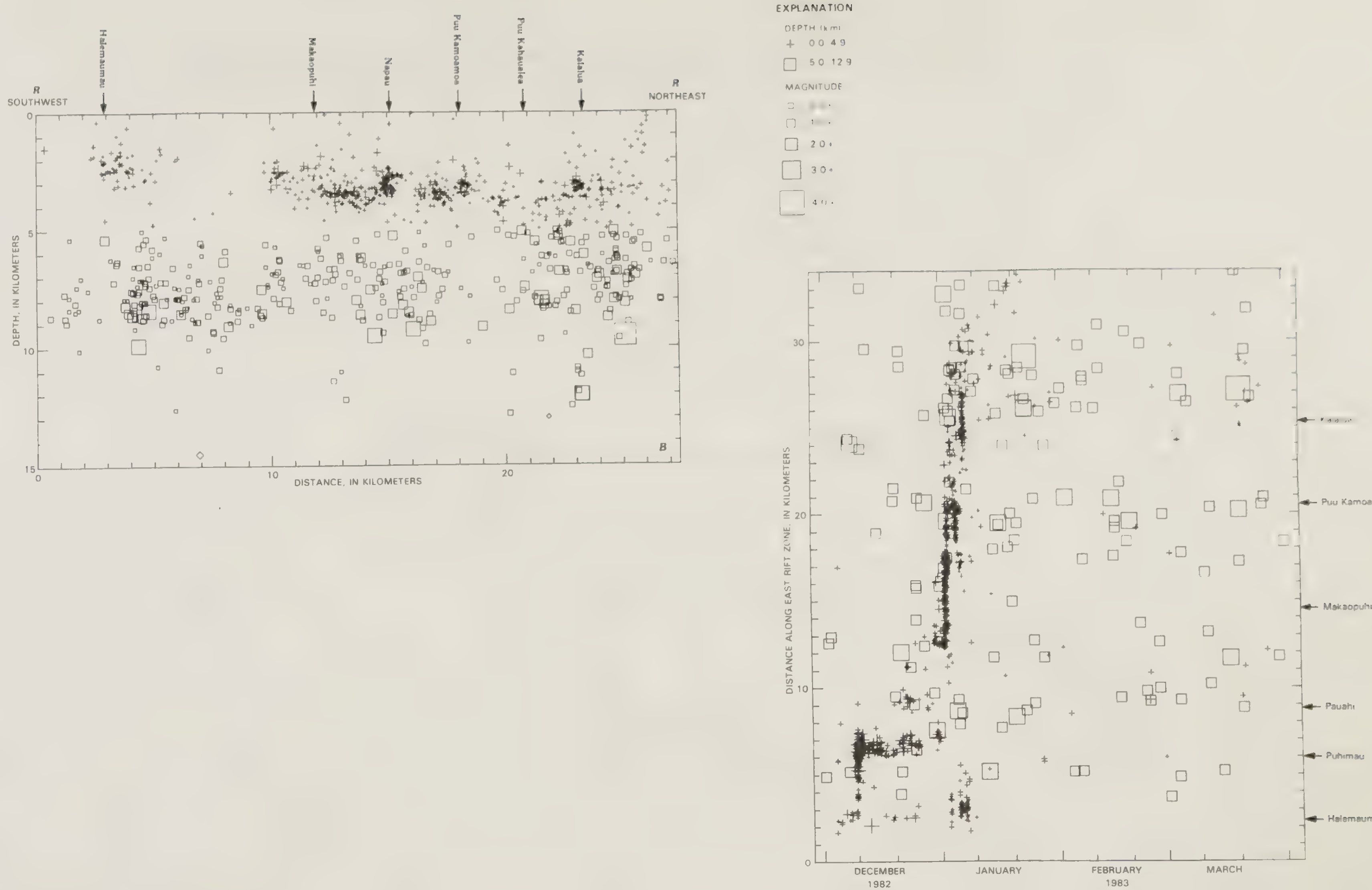

Figure 13.1.37. Depth-distance distribution (left) of earthquakes shown in figure 13.1.36, projected onto line R-R'. Space-time diagram (right) of Kilauea earthquakes, December 1982 to March 1983, with epicenters projected onto an east-west line. Both plots are from Wolfe and others (1987).

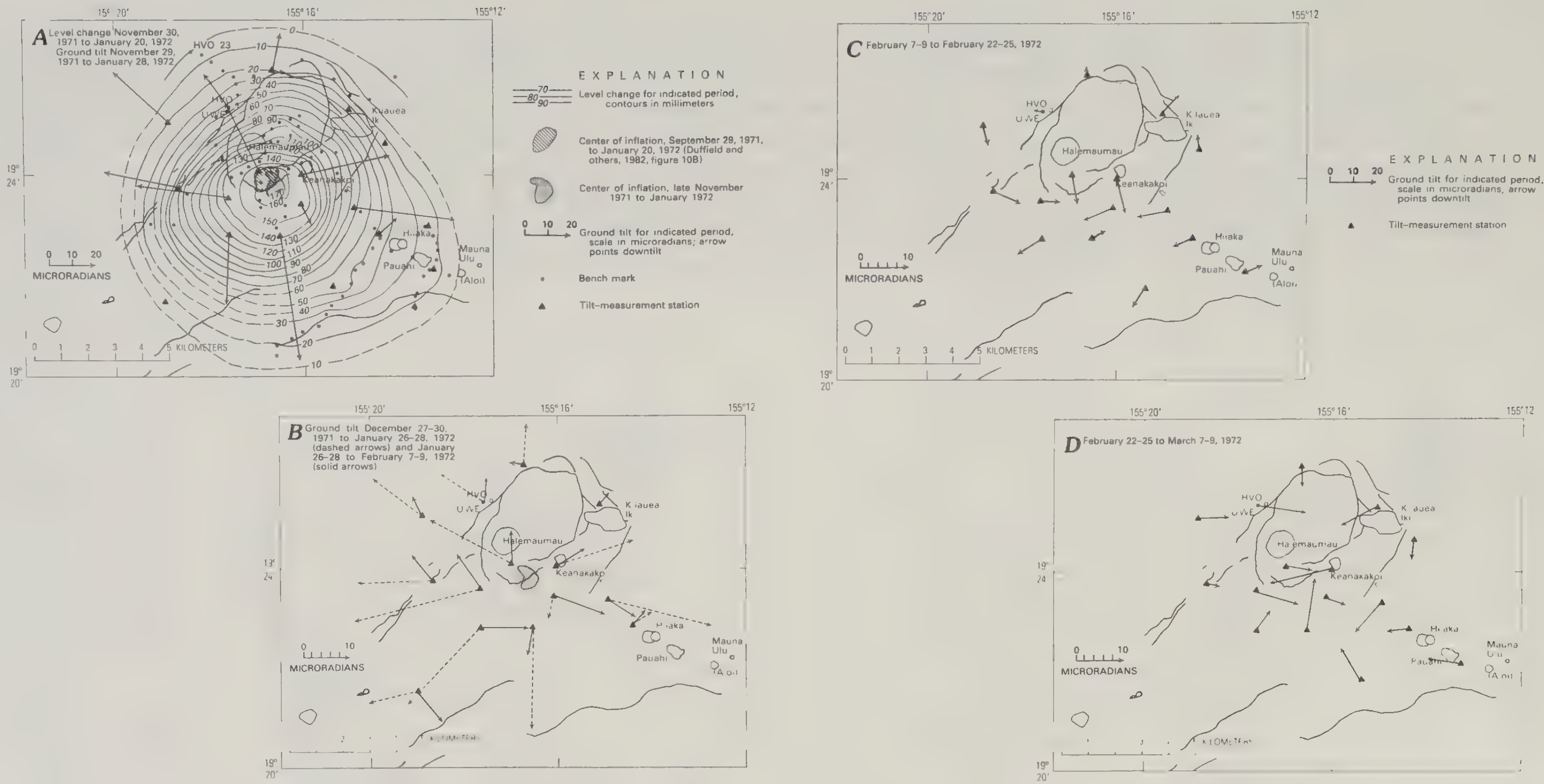

Figure 13.1.38. Results of leveling and tilt surveys on Kilauea before and during first two months of 1972-74 Mauna Ulu eruption, from Tilling and others (1987). Vector UWE calculated from E-W and N-S components of Uwekahuna tiltmeter. Contours of leveling data referenced to bench mark HVO 23, assumed to be stable. A, Level changes and ground tilt for the period November 1971 - January 1972. Inflation center defined for this 2-month period is virtually coincident with that obtained by Duffield and others (1982) for the 4-month period building toward the 1972-1974 Mauna Ulu eruption. B, Tilt changes for periods spanning the final month of preeruption inflation (dashed vectors) and first days of the eruption beginning on 3 February 1972 (solid vectors). C, Tilt changes from 7-9 February 1972 to 22-25 February 1972. D, Tilt changes from 22-25 February 1972 to 7-9 March 1972.

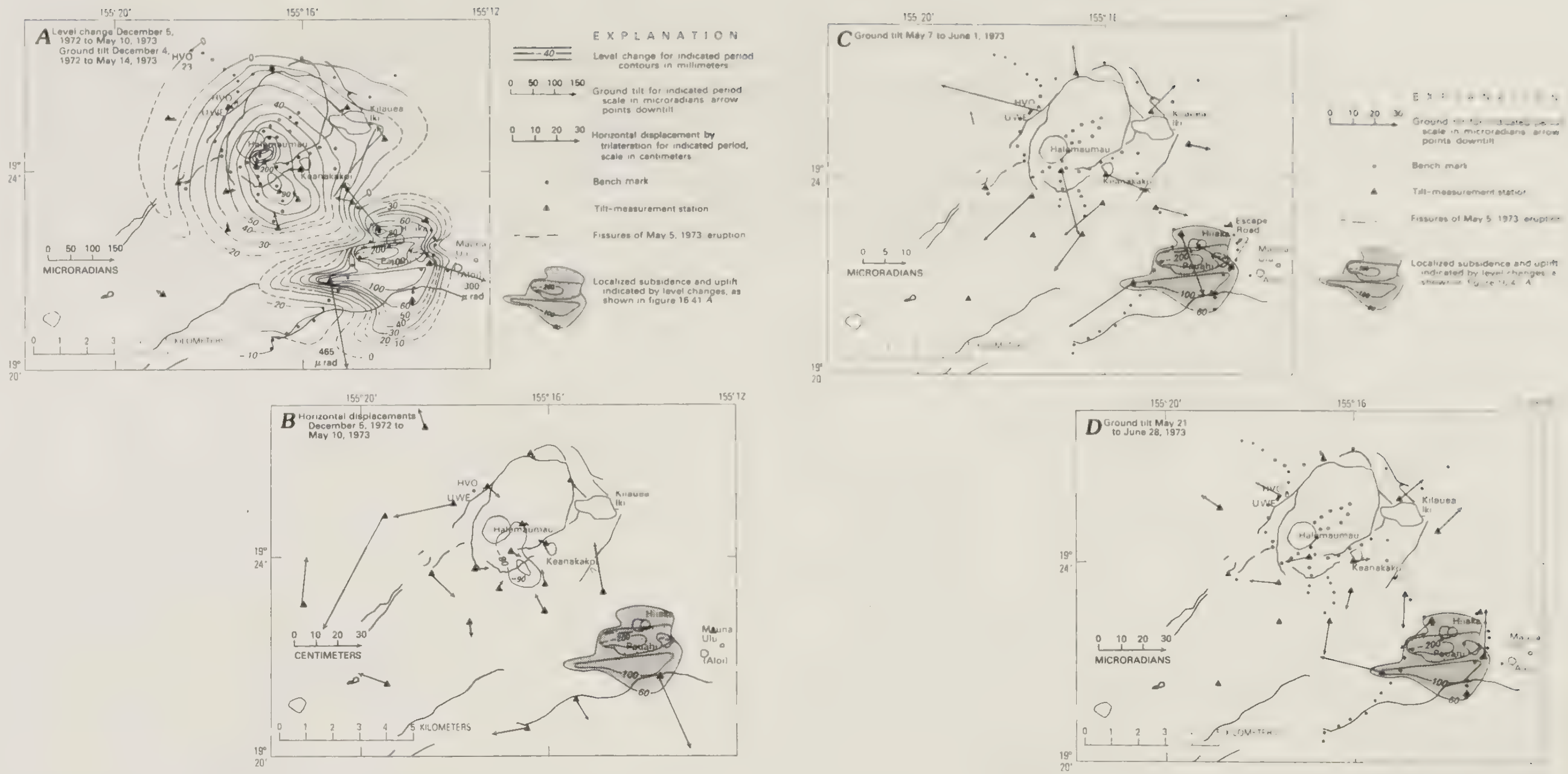

Figure 13.1.39. Results of leveling, tilt, and trilateration surveys from December 1972 to June 1973, from Tilling and others (1987). Vector UWE calculated from E-W and N-S components of Uwekahuna tiltmeter. Contours of leveling data referenced to bench mark HVO 23, assumed to be stable. A, Changes in elevation and tilt from December 1972 to May 1973, showing effect of the 5 May 1973 Pauahi-Hiiaka eruption and intrusion into eastern end of Koae fault system. B, Horizontal displacements from trilateration surveys between December 1972 and May 1973. Also shown are areas of localized subsidence and uplift determined from leveling data (A). C, Tilt changes between 7 May 1973 and 1 June 1973, showing relatively small changes (note change in vector scale from A) that generally reflect summit inflation following 5 May eruption. D, Tilt changes between 21 May 1973 and 28 June 1973; this period included the 9 June partial draining of lava lake at Mauna Ulu. Effect of draining and associated intrusion is apparently masked by net inflation.

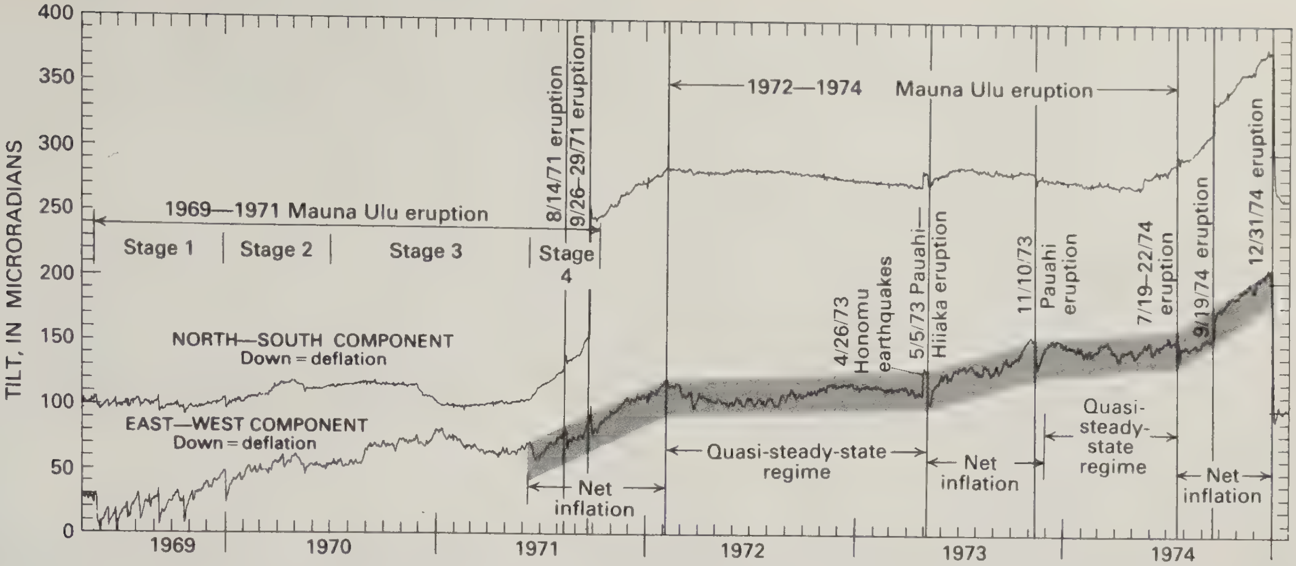

Figure 13.1.40. Variation in Kilauea summit tilt for the period May 1969 - January 1975 as measured by short-base water-tube tiltmeter at Uwekahuna vault (figure 13.1.3), from Tilling and others (1987). Microradian scale arbitrary, with value on 1 May 1969 taken as zero. Magnitude 6.2 Honomu earthquake (26 April 1973) caused an 18-microradian offset of E-W component of tilt. Tilt record for 1972-74 Mauna Ulu eruption is characterized by two distinctive plateaulike segments ("quasi-steady-state regime") separated by a period of net inflation.

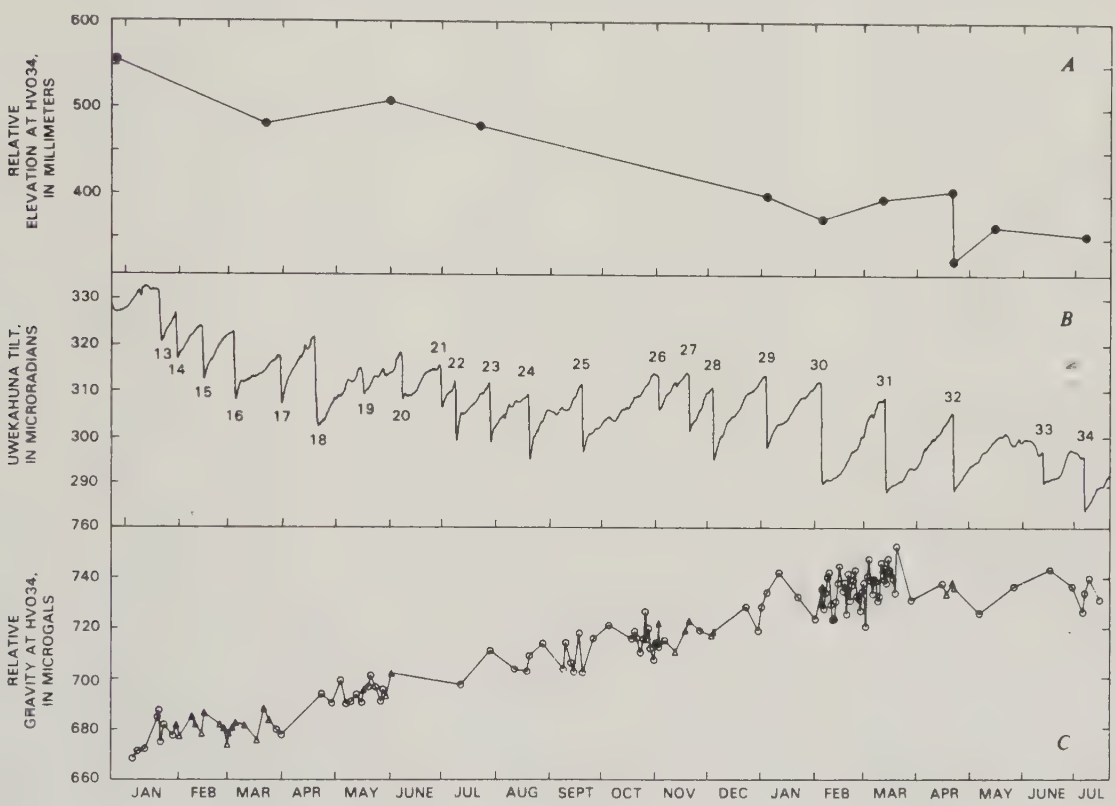

Figure 13.1.41. Relative elevation and gravity at bench mark HVO 34 (south part of Kilauea Caldera) and of E-W tilt at Uwekahuna, from Johnson (1987). A, Relative elevation at HVO 34. B, East-west tilt at Uwekahuna; eruptive episodes at Puu Oo indicated by numbers. C, Relative gravity at HVO 34, uncorrected for elevation changes. Triangles, slightly better precision than circles.

PART 3: HISTORICAL UNREST AT LARGE QUATERNARY CALDERAS (continued)
See inside back cover for explanation and abbreviations

MAUNA LOA/MOKUAWEOWEO

CAVW number (active vent)	Latitude Longitude (degrees)	Diameter (km)	Local tectonic setting	Precaldera edifice	SiO_2 content (wt pct)	Age of collapse (yr B.P.)	Date of unrest	Type and duration of unrest ESTU STHF MGTF H Te	Eruption type
13-02-02	19.48N	6 x 8	Hotspot	Shield	R = 48-53	< 590	1832	---- ---- ---- - --	lf
(Mauna Loa)	155.61W	(outer)			C = 48-53		1843	---- ---- ---- - --	Lf
		3 x 5					1849	---- ---- ---- - --	lf
		(inner)					1851	---- ---- ---- - --	lf
							1852	---- ---- ---- - --	lf
							1855	---- ---- ---- - --	lf
							1859	---- ---- ---- - --	LF
							1865	---- ---- ---- - --	lf
							1868	---- ---- ---- - UU	lf
							1870	---- ---- ---- - --	lf
							1871	---- ---- ---- - --	lf
							1872	---- ---- ---- - --	lf
							1873	---- ---- ---- - --	lf
							1875	---- ---- ---- - --	lf
							1876	---- ---- ---- - --	lf
							1877	---- ---- ---- - --	lf
							1880	---- ---- ---- - --	Lf
							1887	---- ---- ---- - --	Lf
							1892	---- ---- ---- - --	lf
							1896	---- ---- ---- - --	lf
							1899	---- ---- ---- - --	lf
							1903	---- ---- ---- - --	lf
							1907	---- ---- ---- - --	lf
							1914	---- ---- ---- - --	lf
							1916	---- ---- ---- - --	lf
							1919	---- ---- ---- - --	Lf
							1926	E-B- -E-- ---- - --	lf
							1933	--Y- ---- ---Y - --	lf
							1935	B-Y- ---Y ---Y - --	lf
							1940	E-Y- -E-- ---Y - --	lf
							1942	E-Y- ---Y ---Y - --	lf
							1943	D-Y- ---- ---D - --	lf

MAUNA LOA/MOKUAWEOWEO (continued)

CAVW number (active vent)	Latitude Longitude (degrees)	Diameter (km)	Local tectonic setting	Precaldera edifice	SiO_2 content (wt pct)	Age of collapse (yr B.P.)	Date of unrest	Type and duration of unrest ESTU STHF MGTF H Te	Eruption type
(continued from previous page)									
							1949	Y-Y- -E-Y ---E - --	lf,cc
							1950	D-Y- -E-Y ---E - --	LF
							1975	FEYE YEEY ---Y - --	lf
							1984	FFYF YFFY -xEE - UU	Lf

TECTONIC SETTING

Mauna Loa is one of five basaltic shield volcanoes that comprise the Island of Hawaii at the southeast end of the Hawaiian archipelago (fig. 13.2.1). Mauna Loa and Kilauea have erupted tholeiitic basalts frequently during historical time and, with Loihi seamount off the southeast coast of Hawaii, form the current locus of volcanism along the Hawaiian-Emperor chain. (See section on Kilauea Caldera, CAVW number 13-02-01).

GEOLOGIC HISTORY

Mauna Loa, which rises nearly 9 km above the isostatically depressed floor of the central Pacific (to 4,167 m above sea level), is the largest active volcano on Earth; its volume has been estimated at about 40,000 km^3 (Macdonald, 1972, p. 258), but that volume is probably too high because older, separate volcanoes are likely buried at depth (Lockwood and Lipman, 1987). Mauna Loa's lavas cover about 5,125 km^2 of the Island of Hawaii and approximately 4,000 km^2 of its submarine slopes.

Lavas of known historical age cover 13 percent of Mauna Loa's surface; they were erupted at an average rate of 45×10^6 m^3/yr from 1843 to 1876 but at less than half that rate since 1877 (fig. 13.2.3). This change coincides with an abrupt change in lava chemistry and may be related to effects of the magnitude 7.6 earthquake in April 1868 (see below). The average historical production rate is higher than average rates for the preceding 650 years, from shortly before the formation of Mokuaweoweo Caldera until the start of historical records in 1843. The preceding period of about 750 years was characterized by voluminous overflows from a summit lava lake. More than one-half of Mauna Loa has been buried by flows during the past 1,500 years, and almost 90 percent has been buried within the last 4,000 years (Lockwood and Lipman, 1987).

Mokuaweoweo Caldera is the younger and smaller of two calderas at the summit of Mauna Loa (Holcomb, 1980) (fig. 13.2.2). Major rift zones radiate southwestward and northeastward from Mokuaweoweo (fig. 13.2.1); most eruptions occur in Mokuaweoweo or along the rift zones (Lockwood and Lipman, 1987).

MAUNA LOA/MOKUAWEOWEO (continued)

HISTORICAL ACTIVITY

Except for a hiatus from 1950 to 1975, Mauna Loa has been continually restless, so we have listed only the dates of eruptions in the table above. Eruptions are defined to begin with the arrival of magma at the surface and to end when tremor at the vent ceases for at least several days.

Several historical eruptions have followed a pattern in which a summit eruption was followed by another summit eruption 2 to 3 years later, then by a flank eruption starting 1 to 4 days later (Lockwood and others, 1976; Lockwood and others, 1987, p. 544). The pattern seems clear for selected eruptions but is not statistically convincing if all historical eruptions are considered (Klein, 1982). Volumes of erupted lava typically are more than at Kilauea, often more than 10^8 m^3 (Lockwood and Lipman, 1987).

Relatively strong earthquakes occur every few years beneath the flanks of Mauna Loa, generally along arcuate fault zones that seem to bound large blocks of the shield that are shouldered aside by intrusions along the rift zones (figs. 13.2.4, 13.2.5). One particularly severe earthquake on 2 April 1868 ($\underline{M}$ 7.5) was preceded by a short summit eruption at Mauna Loa on 27 March and followed by a major flank eruption starting on 7 April (Wood, 1914; Macdonald and others, 1983; Endo, 1985). The most recent example included a large earthquake on 16 November 1983 ($\underline{M}$ 6.6, 12 km deep along the Kaoiki fault system; see fig. 13.2.16) (Koyanagi and others, 1984), followed by a major summit-flank eruption in March-April 1984 (Lockwood and others, 1985). Focal mechanisms for the earthquake and ground ruptures indicated right-lateral slip along the E-W-trending Kaoiki fault system, coupled with at least 15-20 cm of southward extension (Koyanagi and others, 1984).

In early 1974, intermediate-depth earthquakes and then shallow earthquakes increased beneath the summit area of Mauna Loa (Koyanagi and others, 1975) (figs. 13.2.6-13.2.8). Particularly intense swarms occurred in August and December 1974 and in February 1975. Most earthquakes were shallow and near the southwest rim of Mokuaweoweo Caldera; a few occurred northwest of the caldera at a depth of 5-7 km, and a few others occurred beneath the caldera at a depth of about 40 km. Geodetic measurements revealed that Mauna Loa also began to inflate during 1974 (figs. 13.2.12). Extension across the caldera amounted to more than 60 cm by mid-1975, an additional 20 cm by early 1976, and 2-5 cm/yr during 1976-83 (fig. 13.2.10). Summit tilt was on the order of several tens to almost 200 microradians during the same period. Uplift was centered near the southeast rim of Mokuaweoweo (Decker and others, 1983). Inversion of the geodetic data indicated a deformation source at 3-4 km depth, roughly coincident with an aseismic zone interpreted as a shallow magma reservoir beneath the southeast part of the summit area (fig. 13.2.14).

A small summit eruption on 5-6 July 1975 (Lockwood and others, 1987) ended the longest hiatus in eruptive activity at Mauna Loa in historical time (from 1950 to 1975). As the 1975 eruption waned, an intense swarm of earthquakes marked the progress of an intrusion into the upper northeast rift zone to a distance of 30 km from the summit (fig. 13.2.9).

Inflation continued and shallow and intermediate-depth earthquakes increased in frequency beneath Mauna Loa from 1980 to 1983, suggesting a slow but accelerating intrusion at 2-3 km depth (Decker and others, 1983). An intense swarm of intermediate-depth earthquakes (5-13 km) occurred beneath Mauna Loa's northwest flank in mid-September 1983 (figs. 13.2.6, 13.2.8). First-motion

MAUNA LOA/MOKUAWEOWEO (continued)

HISTORICAL ACTIVITY (continued)

analyses suggest that the earthquakes resulted from increasing lateral stresses generated in the summit and upper southwest rift zone, probably by intrusion of magma. On 16 November 1983, a magnitude 6.6 earthquake occurred beneath Mauna Loa's southeast flank. The earthquake generated an intense aftershock sequence that included events along Mauna Loa's upper northeast rift zone. Seismicity in that area remained high until it merged with eruptive seismicity starting on 25 March 1984. Shallow earthquakes in the summit area continued unchanged until a marked acceleration several weeks before the eruption (figs. 13.2.11, 13.2.19). The number of larger earthquakes ($\underline{M} > 1.5$) increased persistently as the eruption approached. The daily frequency of smaller earthquakes showed a more episodic increase and, in fact, decreased to below average on the day before the eruption (Lockwood and others, 1985, 1987). Continuous monitoring by electronic tiltmeters and field surveys showed that inflation continued at a steady, nonincreasing rate almost until the March 1984 outbreak (Lockwood and others, 1985).

The temperature of a fumarole along the 1975 eruptive fissure rose by 20 °C on 18 November 1983, concurrently with a brief increase in gas emission at the same site (figs. 13.2.15, 13.2.16B). These changes may have been a response to the $\underline{M}$ 6.6 Kaoiki earthquake two days earlier. Additional changes in temperature and gas emission along the 1975 fissure occurred on several occasions during December 1983 - March 1984. On 14 December 1983, an airborne observer saw an anomalous steam cloud rising to about 1 km above Mokuaweoweo, one day after an abrupt increase in temperature and gas emission along the 1975 eruptive fissure.

On 18 March 1984, a dull red glow was seen along a "crack" on the floor of Mokuaweoweo (1975 fissure?) by a hiker; on 23 March, several observers saw "steam clouds" rising above Mokuaweoweo. It is possible that the red color was a result of oxidation along the crack, and the level of steaming reflected atmospheric conditions and not changes related to the impending eruption. (Increased glow and steaming days in advance of an eruption seem unlikely, based on experience at Kilauea, but the observations cannot be refuted.) On 24 March, a day before the eruption, a professor with a geology class on the Mauna Loa summit saw "rocks and steam" being ejected from the 1975 fissure, but there was no way to alert authorities. Shallow seismicity beneath the caldera started to increase at 22:55 local time on 24 March; the onset of harmonic tremor accompanied a further increase at 23:30 (fig. 13.2.16). The earthquake swarm and tremor strengthened rapidly just before 01:00 on 25 March. Eleven earthquakes with $\underline{M}$=2.0-4.1 occurred between 00:51 and 02:10, and tiltmeters showed rapid summit inflation beginning at 01:00 (fig. 13.2.17). Magma apparently reached the surface at 01:25 that morning, based on a "strong signal" from an infrared sensor in a military satellite in Earth orbit. Eruptive fissures quickly migrated down the northeast rift zone and remained active until 15 April; a lava flow that temporarily threatened the city of Hilo stopped before doing significant damage. Phase 17 of the 1983-present Puu Oo eruption at Kilauea began on 30 March 1984, but the simultaneous eruptions did not seem to influence each other (Lockwood and others, 1987).

The amount of summit deflation accompanying the 1984 eruption was greater than the inflation since 1975, suggesting that some of the erupted magma might have been emplaced in a shallow reservoir before 1975, possibly before an electronic distance measurement (EDM) line across the caldera was first measured in 1964. Maximum subsidence during the eruption was 630 mm in the south part of the summit area. Typical electronic distance measurement lines across Mokuaweoweo contracted an average of 300 mm after initial dike-related extensions of about 600 mm, and tilt stations near the rim of Mokuaweoweo recorded 100-200 microradians of eruption-related

MAUNA LOA/MOKUAWEOWEO (continued)

HISTORICAL ACTIVITY (continued)

deflation (figs. 13.2.13, 13.2.17, 13.2.18). The summit area of Mauna Loa began to reinflate immediately after the 1984 eruption, suggesting recharge of the summit magma reservoir (Lockwood and others, 1985, 1987) (fig. 13.2.20).

COMMENTS

Mauna Loa was one of the most active volcanoes on Earth during the late 19th and early 20th centuries, but a hiatus in eruptive activity from 1950 to 1975 coincided with the development or improvement of many modern volcano-monitoring techniques. For this reason, relatively little is known about historical unrest at Mauna Loa compared with its diminutive neighbor, Kilauea (which has been intensely active since 1952). However, observations during the 1975 and 1984 Mauna Loa eruptions suggest many similarities with Kilauea, including the presence of a shallow crustal magma reservoir at 3-5 km depth. An important difference may be the relatively greater amount of magma storage along Kilauea's east rift zone, probably facilitated by dilatation across the rift zone during major south-flank subsidence events such as those in 1868 and 1975 (see section on Kilauea).

REFERENCES

Decker, R.W., Koyanagi, R.Y., Dvorak, J.J., Lockwood, J.P., Okamura, A.T., Yamashita, K.M., and Tanigawa, W.R., 1983, Seismicity and ground surface deformation of Mauna Loa Volcano, Hawaii: Eos, Trans. Am. Geophys. Union, v. 64, p. 545-547.

Endo, E.T., 1985, Seismotectonic framework for the southeast flank of Mauna Loa Volcano, Hawaii: Seattle, Univ. Washington, Ph.D. diss., 350 p.

Fiske, R.S., and Jackson, E.D., 1972, Orientation and growth of Hawaiian volcanic rifts: the effect of regional structure and gravitational stresses: Proc. Roy. Soc. London, Ser. A, v. 329, p. 299-326.

Holcomb, R.T., 1980, Kilauea Volcano: Chronology and morphology of the surficial lava flows: Stanford, Calif., Stanford Univ., Ph.D. diss., 321 p.

Klein, F.W., 1982, Patterns of historical eruptions at Hawaiian volcanoes: Jour. Volcanol. Geotherm. Res., v. 12, p. 1-35.

Koyanagi, R.Y., Endo, E.T., and Ebisu, J.S., 1975, Reawakening of Mauna Loa Volcano, Hawaii: A preliminary evaluation of seismic evidence: Geophys. Res. Lett., v. 2, p. 405-408.

Koyanagi, R.Y., Endo, E.T., Tanigawa, W.R., Nakata, J.S., Tomori, A.H., and Tamura, P.N., 1984, Kaoiki, Hawaii earthquake of November 16, 1983: A preliminary compilation of seismographic data at the Hawaiian Volcano Observatory: U.S. Geol. Surv. Open-File Rep. 84-798, 6 p.

Lockwood, J.P., Banks, N.G., English, T.T., Greenland, L.P., Jackson, D.B., Johnson, D.J., Koyanagi, R.Y., McGee, K.A., Okamura, A.T., and Rhodes, J.M., 1985, The 1984 eruption of Mauna Loa volcano, Hawaii: Eos, Trans. Am. Geophys. Union, v. 66, no. 16, p. 169-171.

Lockwood, J.P., Koyanagi, R.Y., Tilling, R.I., Holcomb, R.T., and Peterson, D.W., 1976, Mauna Loa threatening: Geotimes, v. 21, no. 6, p. 12-15.

MAUNA LOA/MOKUAWEOWEO (continued)

REFERENCES (continued)

Lockwood, J.P., and Lipman, P.W., 1987, Holocene eruptive history of Mauna Loa volcano, in R.W. Decker, T.L. Wright, and P.H. Stauffer, eds., Volcanism in Hawaii, U.S. Geol. Surv. Prof. Paper 1350, p. 509-535.
Lockwood, J.P., Dvorak, J.J., English, T.T., Koyanagi, R.Y., Okamura, A.T., Summers, M.L., and Tanigawa, W.R., 1987, Mauna Loa 1974-1984: A decade of intrusive and extrusive activity, in R.W. Decker, T.L. Wright, and P.H. Stauffer, eds., Volcanism in Hawaii, U.S. Geol. Surv. Prof. Paper 1350, p. 537-570.
Macdonald, G.A., 1972, Volcanoes: Englewood Cliffs, N.J., Prentice-Hall, Inc., 510 p.
Macdonald, G.A., and Abbott, A.T., 1970, Volcanoes in the sea: Honolulu, Univ. Hawaii Press, 441 p.
Macdonald, G.A., Abbott, A.T., and Peterson, F.L., 1983, Volcanoes in the sea (2nd ed.): Honolulu, Univ. Hawaii Press, 517 p.
Smithsonian Institution, Scientific Event Alert Network (SEAN), 1987, Mauna Loa: SEAN Bull., v. 12, no. 10.
Wood, H.O., 1914, On earthquakes of 1868 in Hawaii: Bull. Seismol. Soc. Am., v. 4, p. 169-203.

Figure 13.2.1. Island of Hawaii, showing five volcanoes (including Mauna Loa), major structural and geographic features, and bathymetry of adjacent sea (Lockwood and Lipman, 1987).

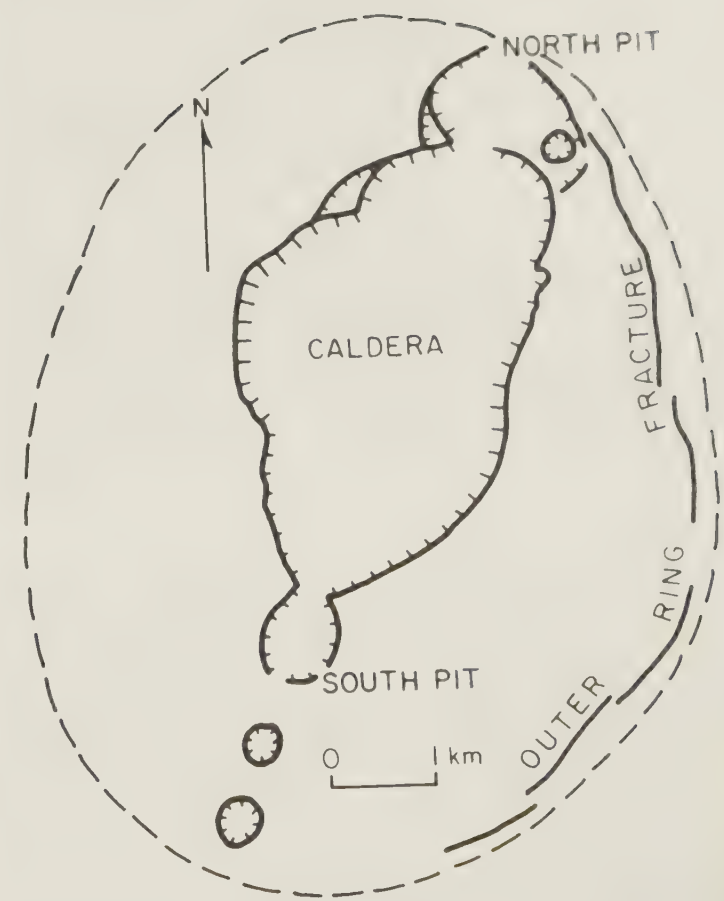

Figure 13.2.2. Outline of Mauna Loa's summit caldera and upper rift zones, from Decker and others (1983). Holcomb (1980) interprets outer ring fracture as a relic of a larger, buried caldera. Copyright by the American Geophysical Union.

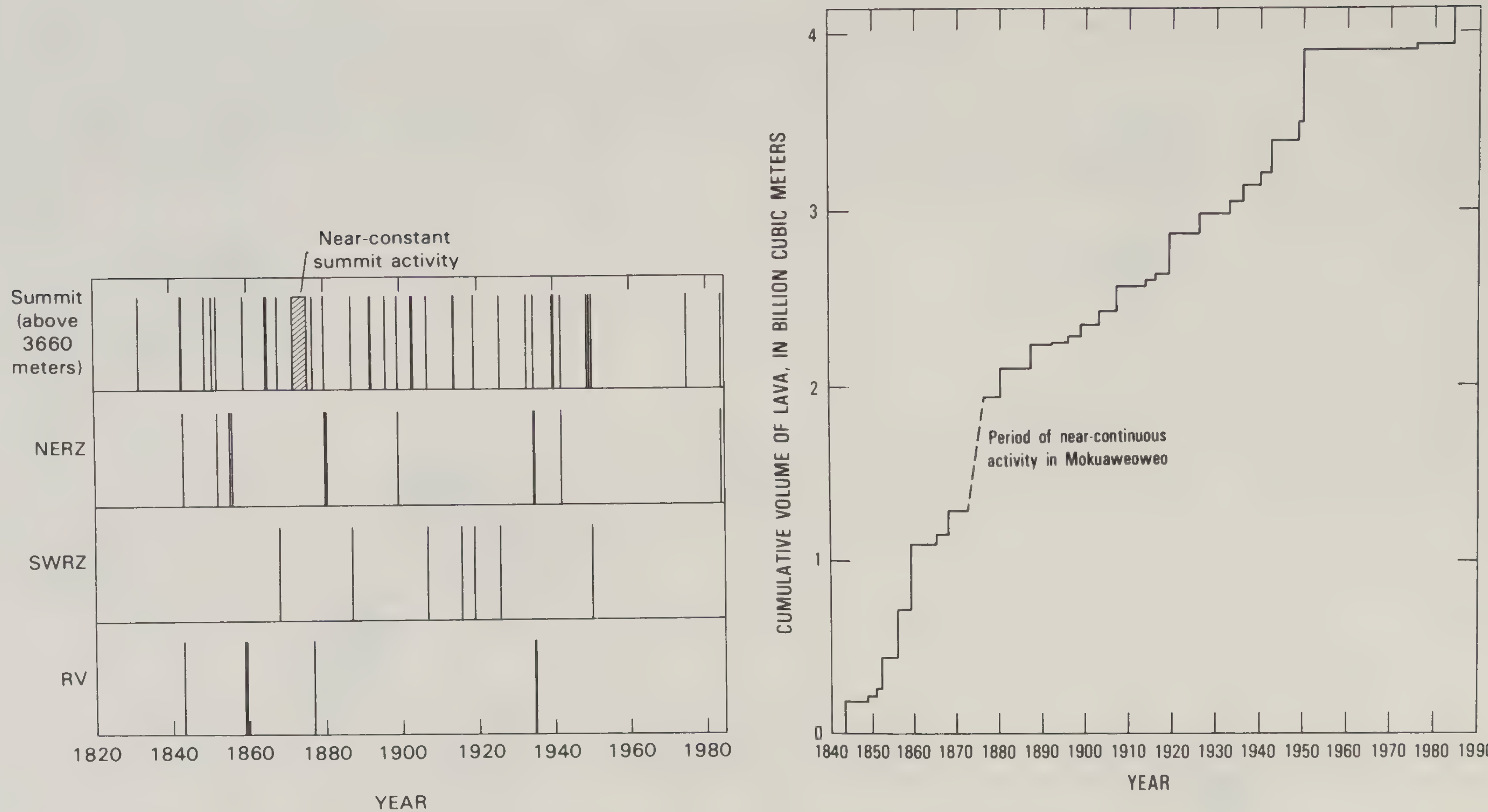

Figure 13.2.3. Chronology of historical eruptions of Mauna Loa (left), from Lockwood and Lipman (1987). NERZ, northeast rift zone; SWRZ, southwest rift zone; RV, northwest flank radial vent eruptions. Mauna Loa lava production, 1843-1984 (right), from Lockwood and Lipman (1987).

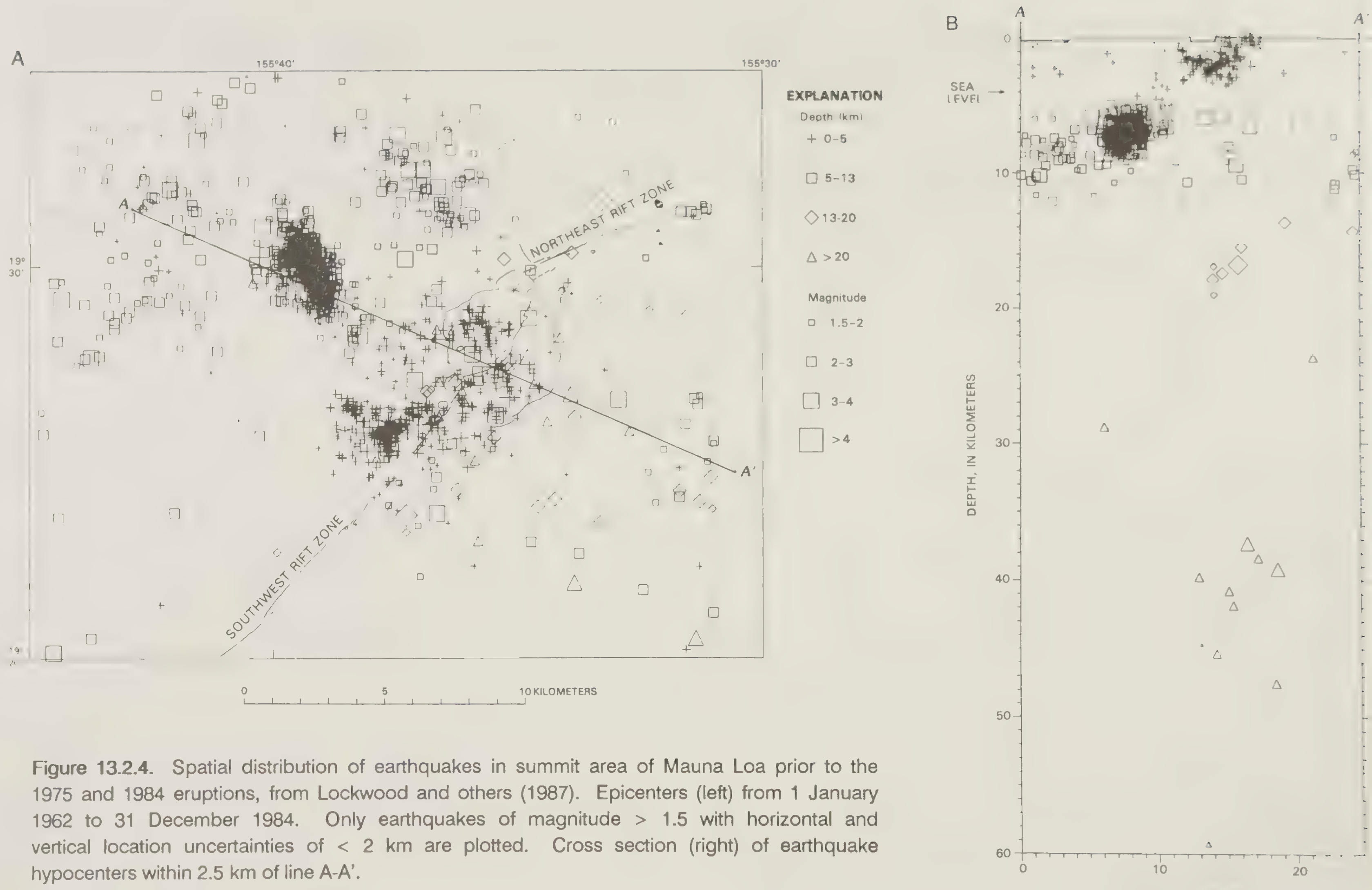

Figure 13.2.4. Spatial distribution of earthquakes in summit area of Mauna Loa prior to the 1975 and 1984 eruptions, from Lockwood and others (1987). Epicenters (left) from 1 January 1962 to 31 December 1984. Only earthquakes of magnitude > 1.5 with horizontal and vertical location uncertainties of < 2 km are plotted. Cross section (right) of earthquake hypocenters within 2.5 km of line A-A'.

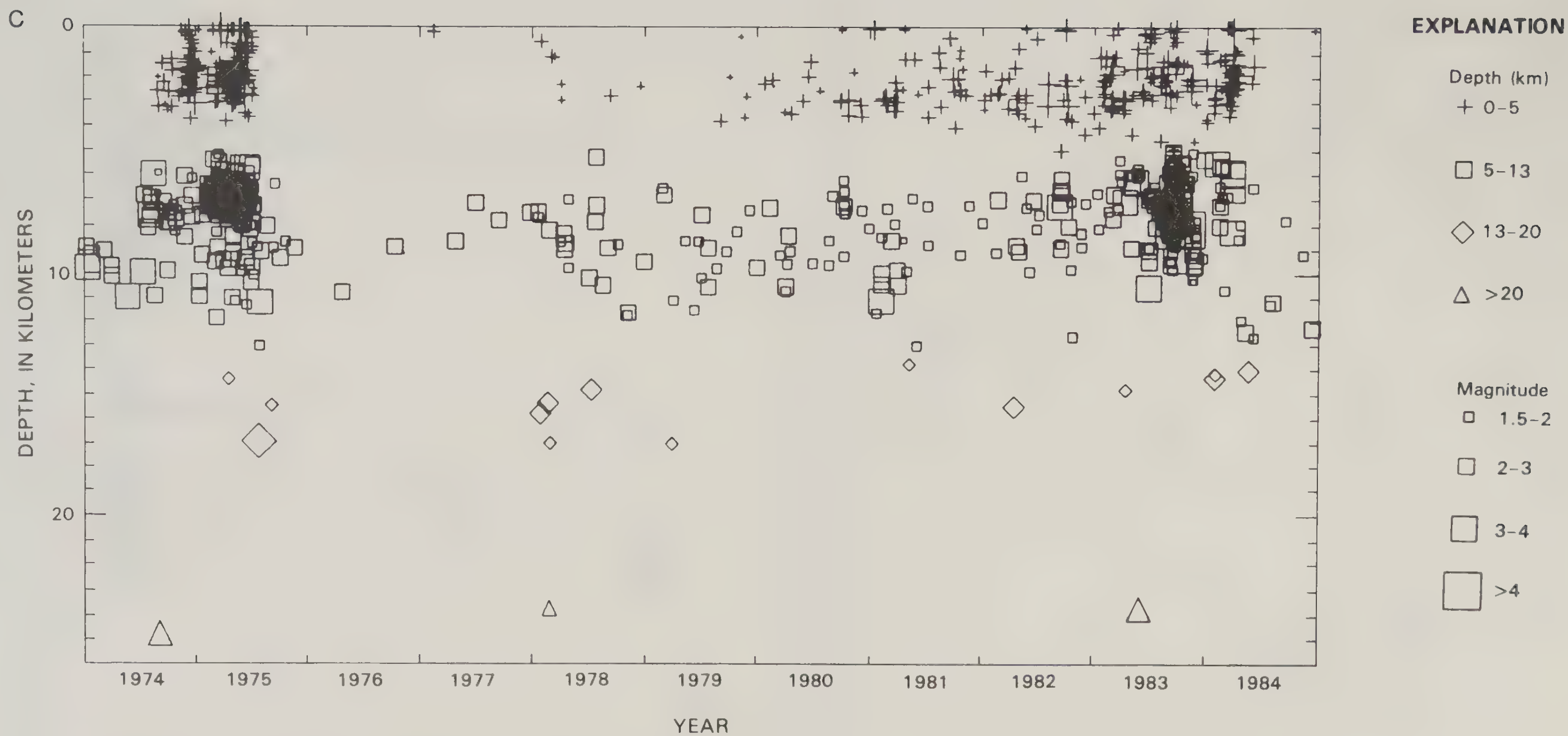

Figure 13.2.5. Depth-time plot of Mauna Loa summit earthquakes (M > 1.5) from 1 January 1974 to 31 December 1984 (Lockwood and others, 1987). Absence of earthquakes between 3- and 6-km depth suggests location of Mauna Loa's shallow magma storage reservoir.

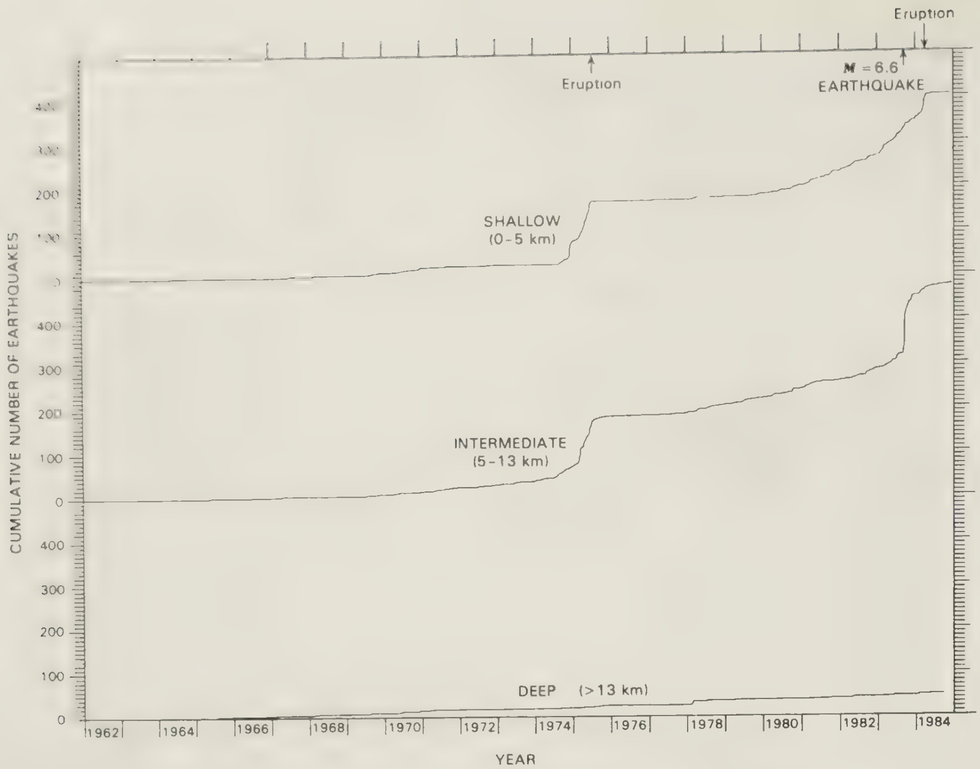

Figure 13.2.6. Earthquakes of M > 1.5 beneath Mauna Loa summit region from 1 January 1962 to 31 December 1984 (Lockwood and others, 1987). Note increase in intermediate-depth earthquakes associated with the M 6.6 earthquake of 16 November 1983.

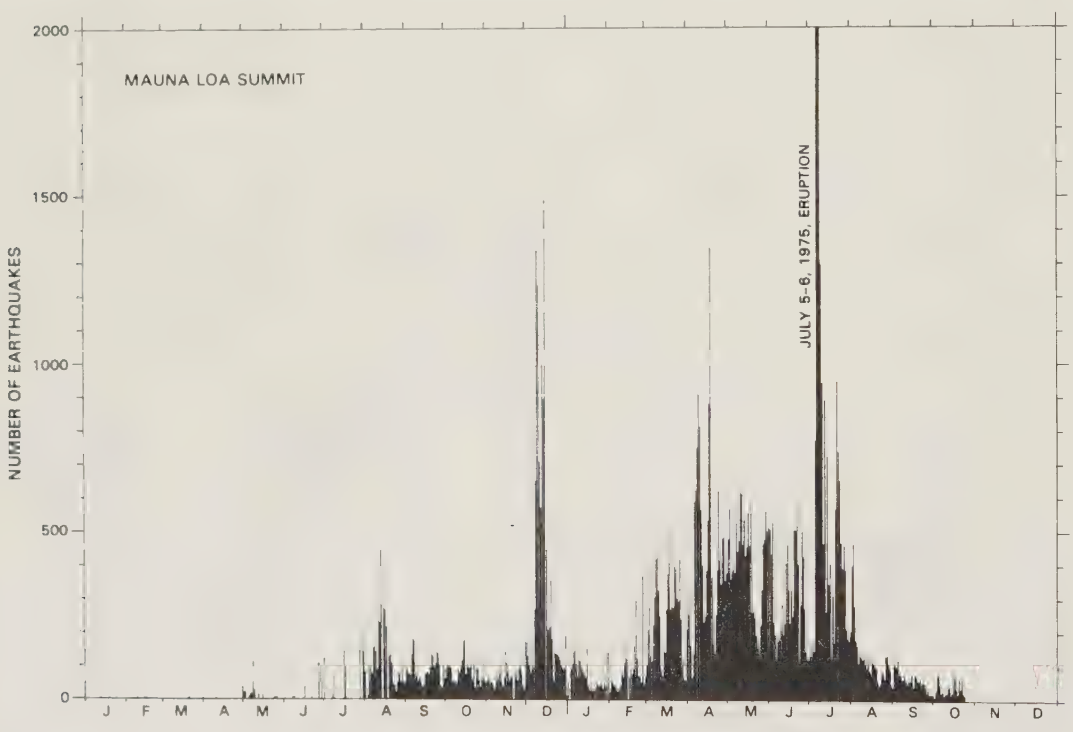

Figure 13.2.7. Daily frequency of Mauna Loa short-period earthquakes (M > 0.1), January 1974 to October 1975, from Lockwood and others (1976, 1987).

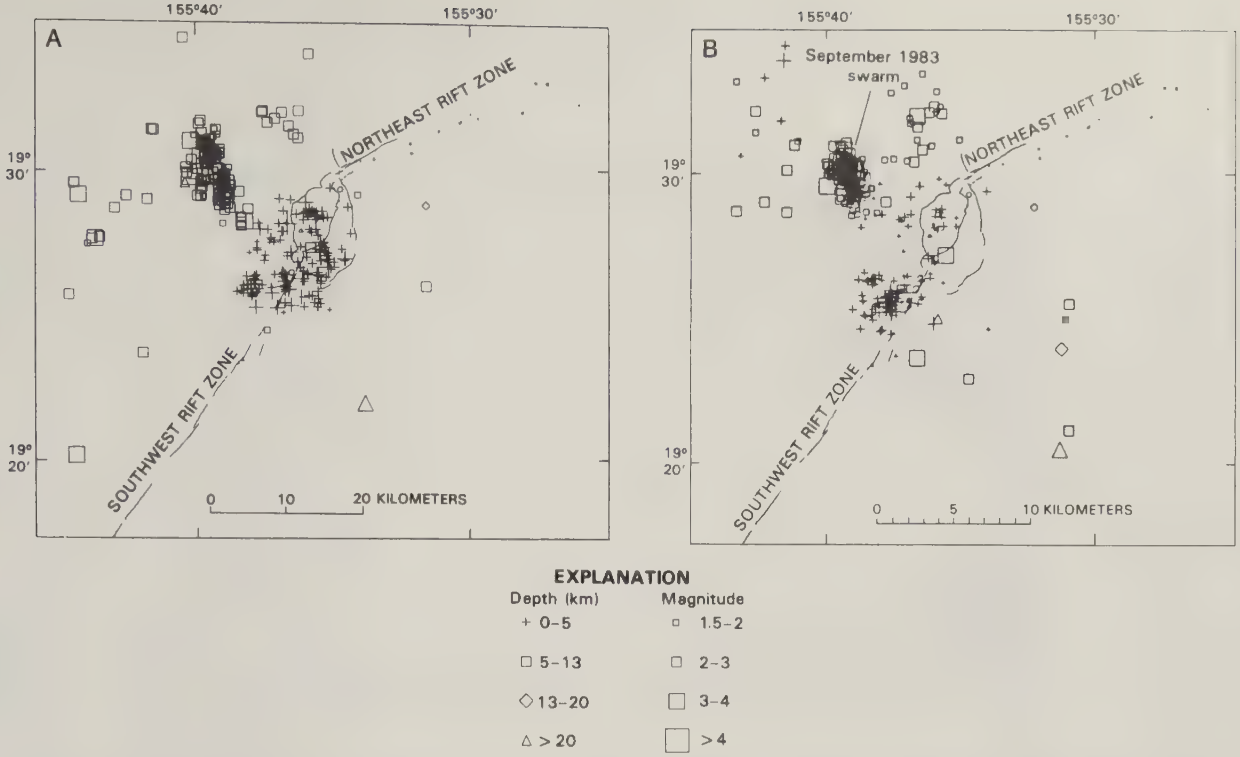

Figure 13.2.8. Earthquake foci beneath Mauna Loa summit region prior to the 1975 and 1984 eruptions, from Lockwood and others (1987). A, 1 January 1974 to 30 June 1975. B, 24 September 1982 to 24 March 1984.

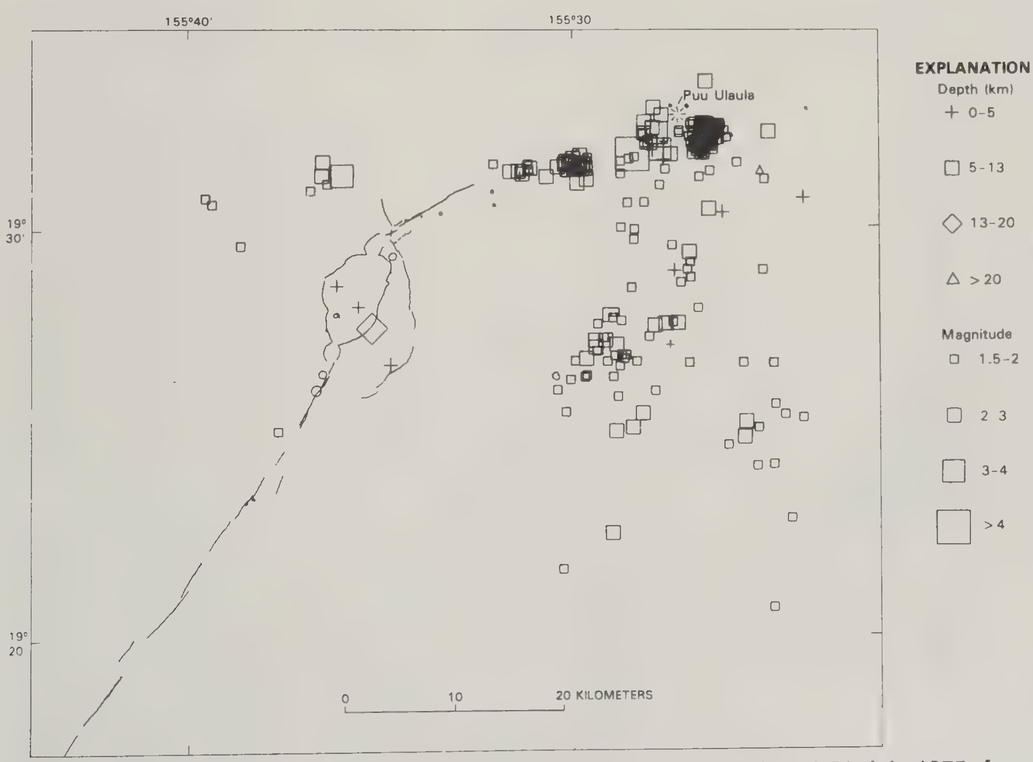

Figure 13.2.9. Earthquake foci ($\underline{M}$ > 1.5) in Mauna Loa summit region, 1-31 July 1975, from Lockwood and others (1987). Earthquakes west of 155°34′ W occurred before the 4-5 July eruption; those to east occurred mostly during 6-12 July as magma intruded from summit into upper northeast rift zone.

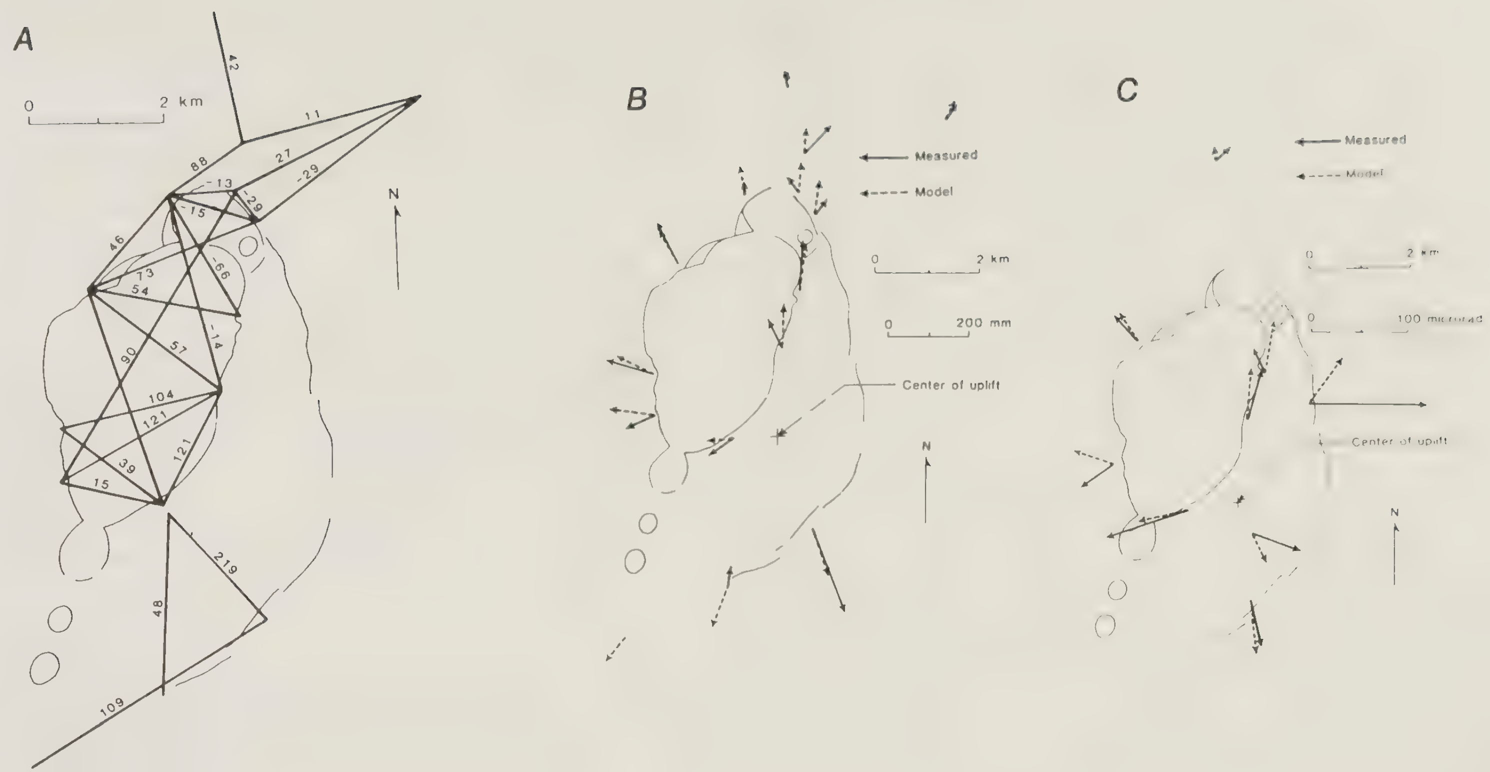

Figure 13.2.10. Horizontal displacements and tilt changes in Mauna Loa summit region from 1977 to 1981, from Decker and others (1983). A, Changes in line length (in millimeters). Positive values are extensions; negative values are contractions. Maximum measured strain is 100 microstrain on line southeast of caldera. B, Horizontal displacements (in millimeters) calculated from data in A (solid vectors) compared with those from a best-fit elastic deformation model (dashed vectors) using a point source at 3.2-km depth. C, Measured tilt vectors (solid) compared with best-fit elastic-deformation model vectors (dashed). Tilt scale shows vector amplitudes in microradians. Center of uplift is nearly identical to that determined from trilateration data in B, but source depth is 2.6 km from tilt data, compared with 3.2 km from trilateration data. Copyright by the American Geophysical Union.

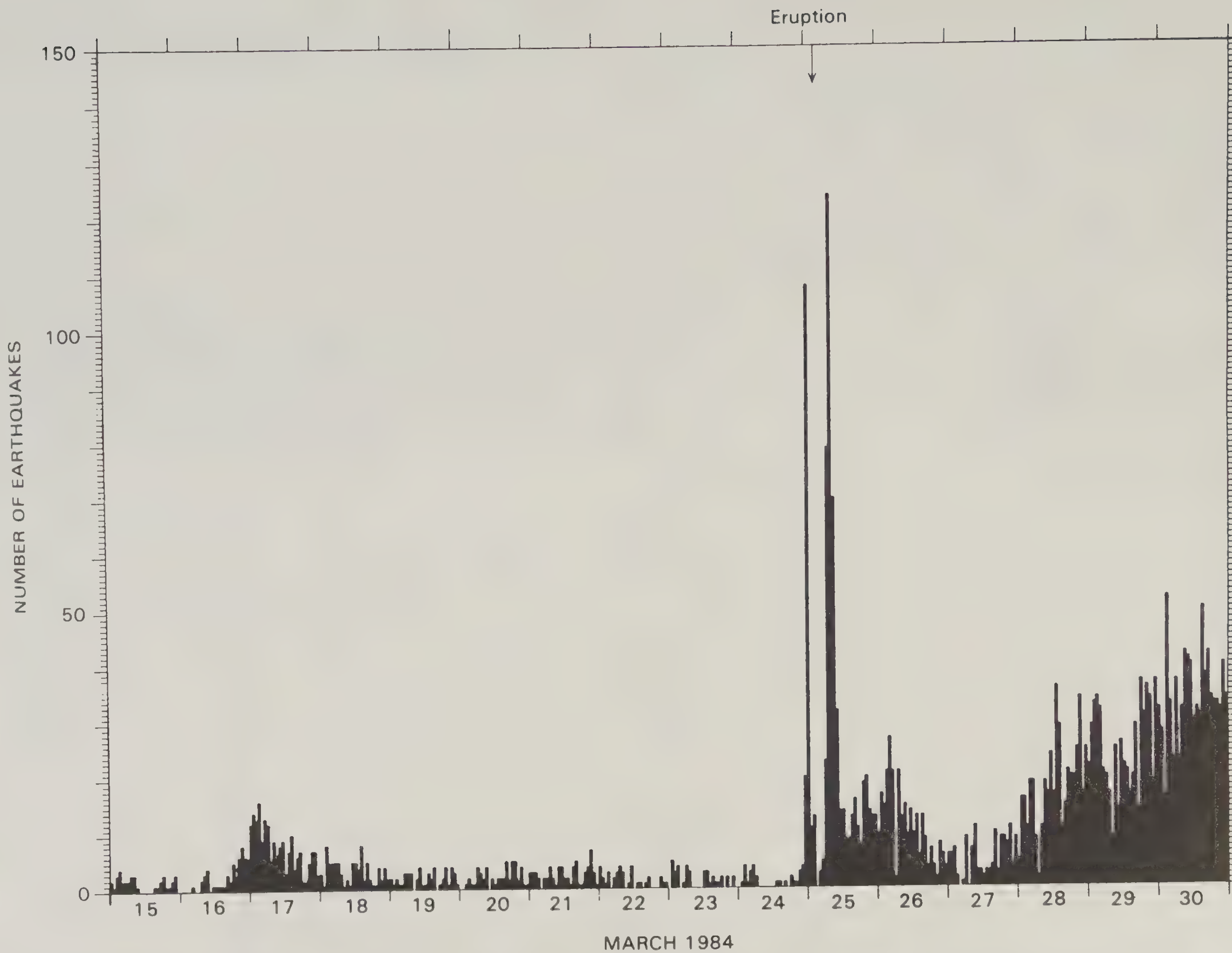

Figure 13.2.11. Hourly counts of Mauna Loa short-period summit earthquakes for the period 15-30 March 1984 (Lockwood and others, 1987). Increase in earthquake frequency after 27 March accompanied deflation of Mauna Loa summit during eruption. Low counts on morning of 25 March reflect masking by high-amplitude tremor.

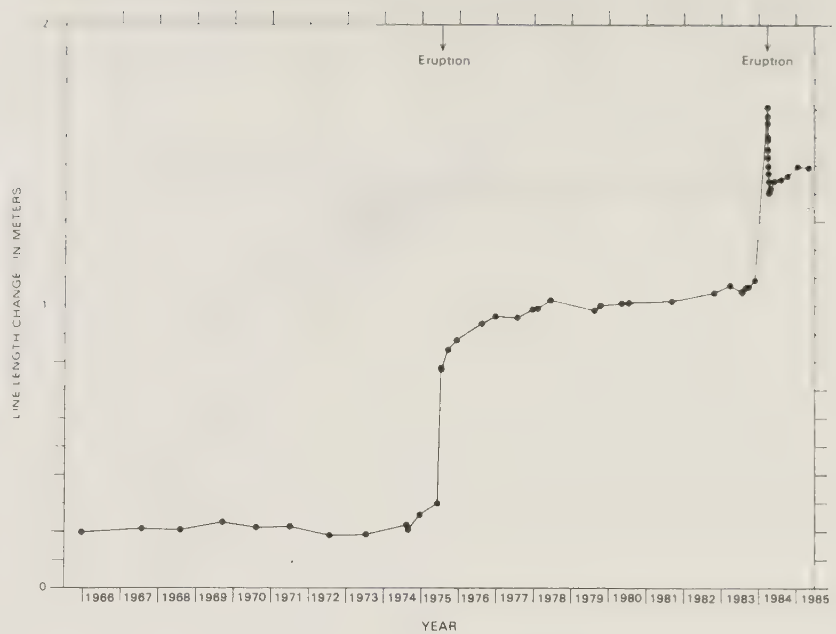

Figure 13.2.12. Horizontal extension across Mokuaweoweo Caldera, December 1965 to May 1985, as measured by trilateration surveys between stations HVO 92 and HVO 93 (see figure 13.2.16<u>B</u>). Abrupt extensions on 5 July 1975 and 25 March 1984 were associated with dike emplacement during eruptions. Reproduced from Lockwood and others (1987).

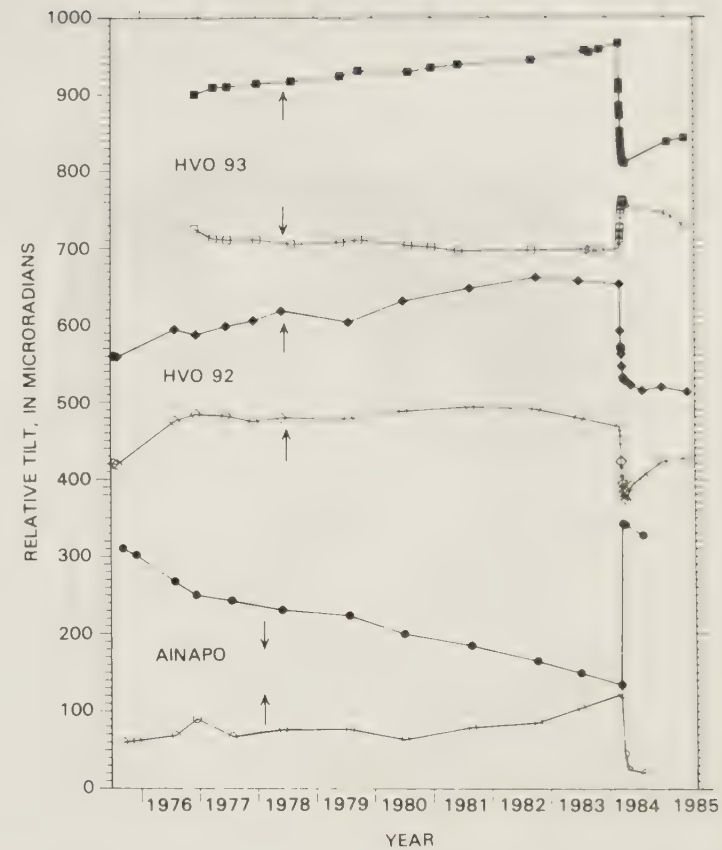

Figure 13.2.13. Spirit-level tilt changes at three Mauna Loa summit stations (see figure 13.2.16<u>B</u>), 1975 to 1985, from Lockwood and others (1987). Darkened symbols are N-S; open symbols are E-W component. Positive tilt changes indicate north or east down. Arrows show inflation direction for individual tilt components. Summit inflation is recorded at all stations prior to and after the eruption from 25 March to 15 April 1984.

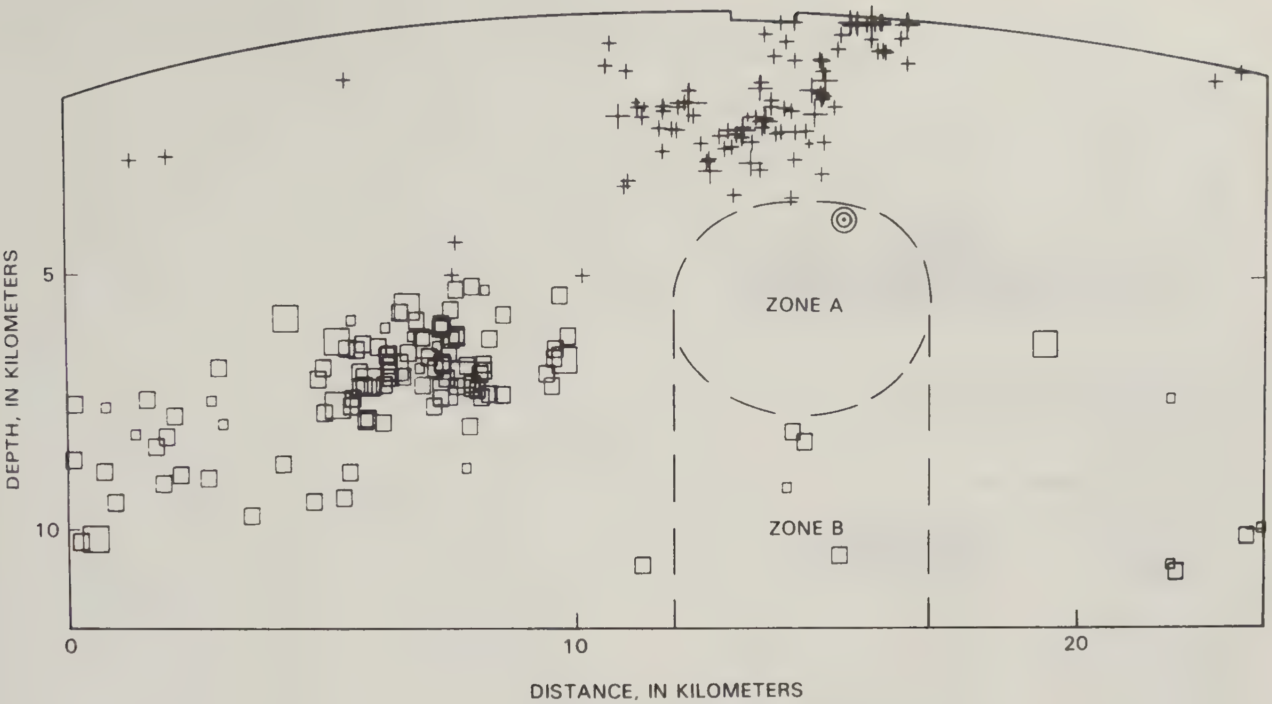

Figure 13.2.14. Approximately true-scale schematic cross section of proposed magma reservoir system beneath Mokuaweoweo, defined by aseismic zone and inversion of ground-deformation data (Lockwood and others, 1987, after Decker and others, 1983). Cross section and hypocenters same as figure 13.2.4 except earthquakes after May 1983 were omitted here. Double circle in zone A shows point-source inflation center calculated from 1977-81 deformation data.

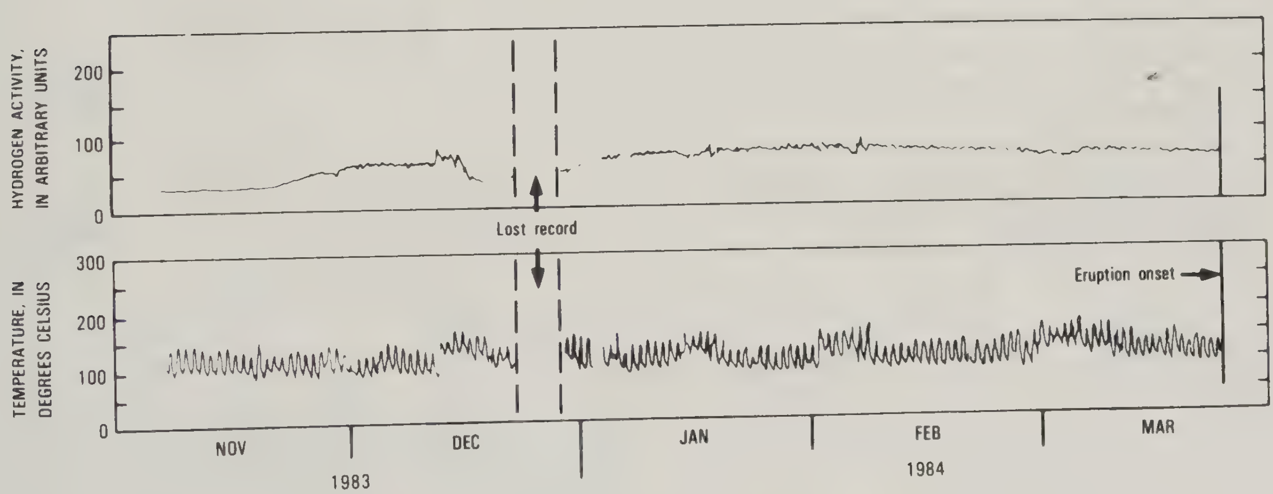

Figure 13.2.15. Variation of temperature and gas emission in a fumarole on the 1975 eruption fissure in Mokuaweoweo, between 5 November 1983 and 24 March 1984 (Lockwood and others, 1987). Large diurnal temperature variations may be caused by artificial instrumental amplification. Data from M. Sato and K. McGee, U.S. Geological Survey, in Lockwood and others (1985).

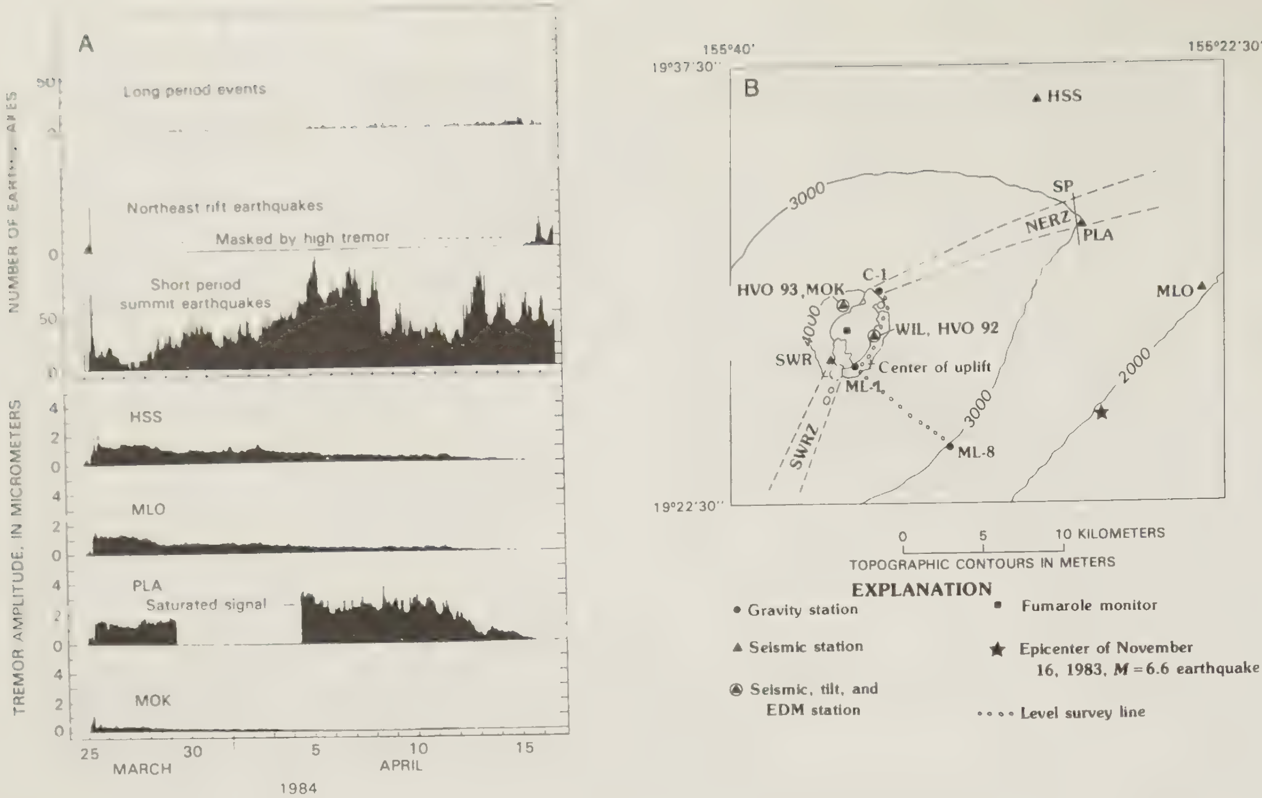

Figure 13.2.16. A (top left), Earthquake frequency (upper three plots) and tremor amplitude (lower four plots), 25 March - 16 April 1984 (Lockwood and others, 1985, 1987). Earthquakes as small as -1 magnitude were plotted when not masked by harmonic tremor. Tremor was read hourly at four seismic stations and plotted as micrometers of ground motion. Signals from station PLA were saturated until 4 April, when instrument sensitivity was lowered. B (top right), Locations of seismic stations and other monitoring sites in the Mauna Loa summit region. Note locations of fumarole monitor and epicenter of M 6.6 earthquake of 16 November 1983, both discussed in text. Copyright by the American Geophysical Union.

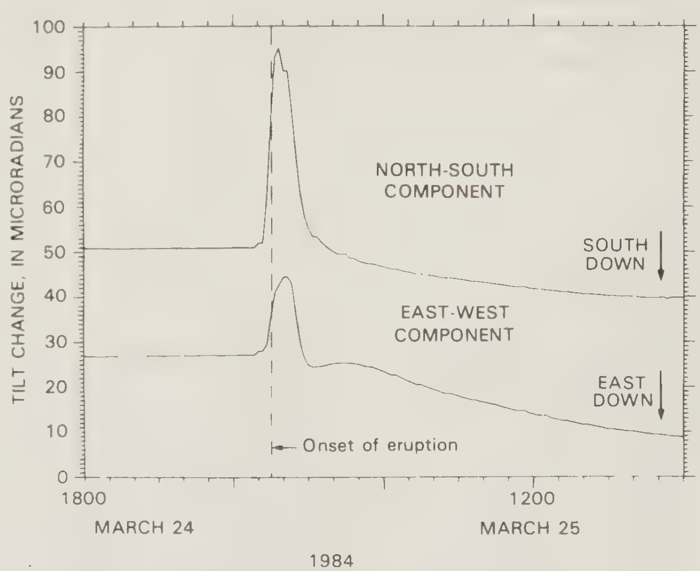

Figure 13.2.17. Bottom right, Continuously recording tiltmeter record from station MOK (see figure 13.2.16B) for a 24-hour period beginning at 1800 hr on 24 March 1984 (Lockwood and others, 1985, 1987). Positive tilt change (inflation) corresponds to downward deflection in north and west directions (that is, increasing values of both tilt components as plotted here; note different convention in figure 13.2.18). Copyright by the American Geophysical Union.

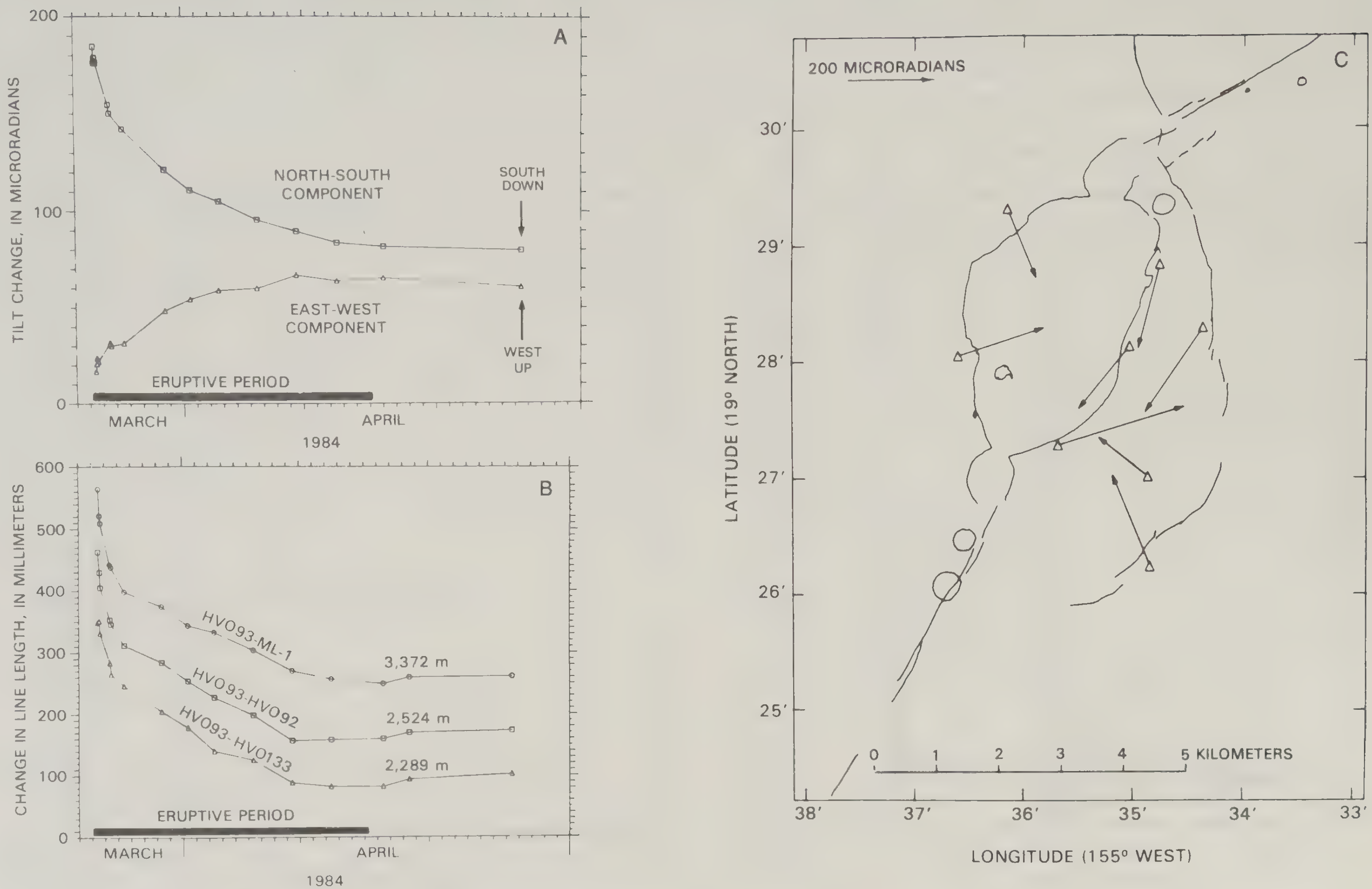

Figure 13.2.18. Tilt and horizontal-strain changes associated with the March-April 1984 eruption of Mauna Loa, from Lockwood and others (1985, 1987). A, Summit deflation curve from spirit-level tilt measurements made near station MOK (see figure 13.2.16B). A positive tilt change (inflation) corresponds to a downward deflection in north and east directions (that is, increasing value of N-S component and decreasing value of E-W component as plotted here; note different convention in figure 13.2.17). B, Summit deflation curve from measurements of horizontal distances across Mokuaweoweo Caldera. C, Net tilt changes in the Mauna Loa summit region between June 1983 and December 1984. Triangles indicate locations of stations; vectors drawn in direction of downward deflection. Copyright by the American Geophysical Union.

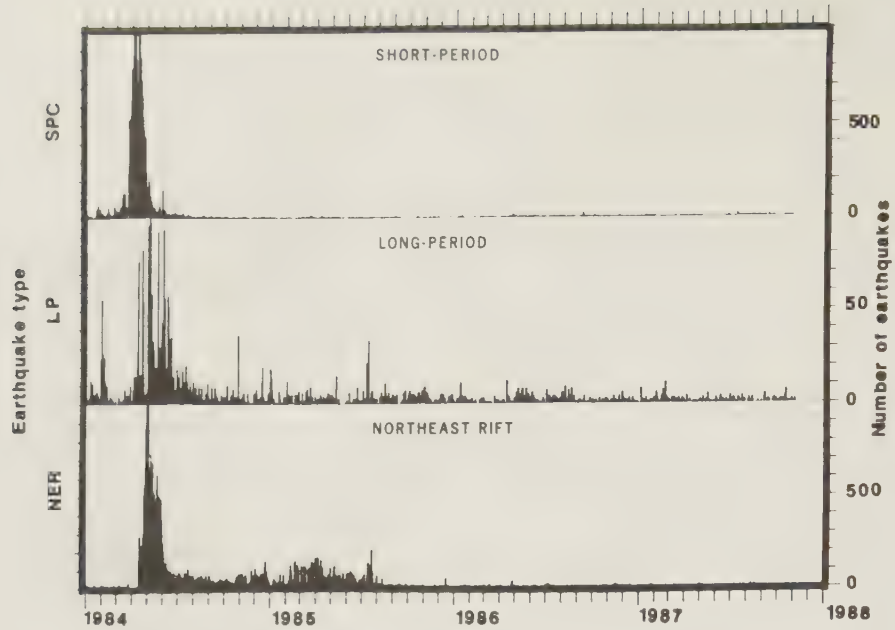

Figure 13.2.19. Daily number of recorded short-period (top) and long-period (middle) summit earthquakes, and northeast rift events (bottom) at Mauna Loa, January 1984 to 4 November 1987, from Smithsonian Institution (1987).

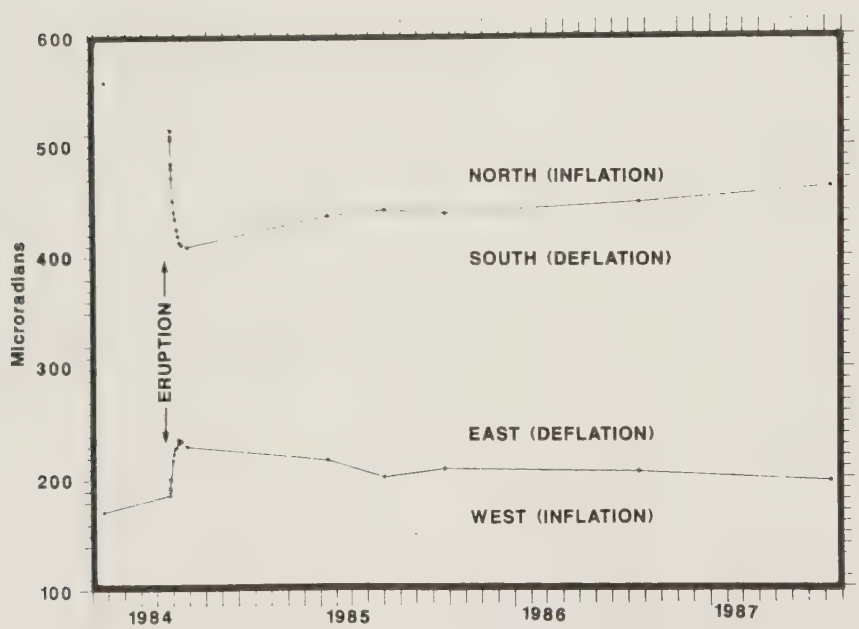

Figure 13.2.20. North-south (top) and east-west (bottom) components of summit tilt at Mauna Loa, November 1983 to August 1987, from Smithsonian Institution (1987). Note gradual reinflation since the March-April 1984 eruption.

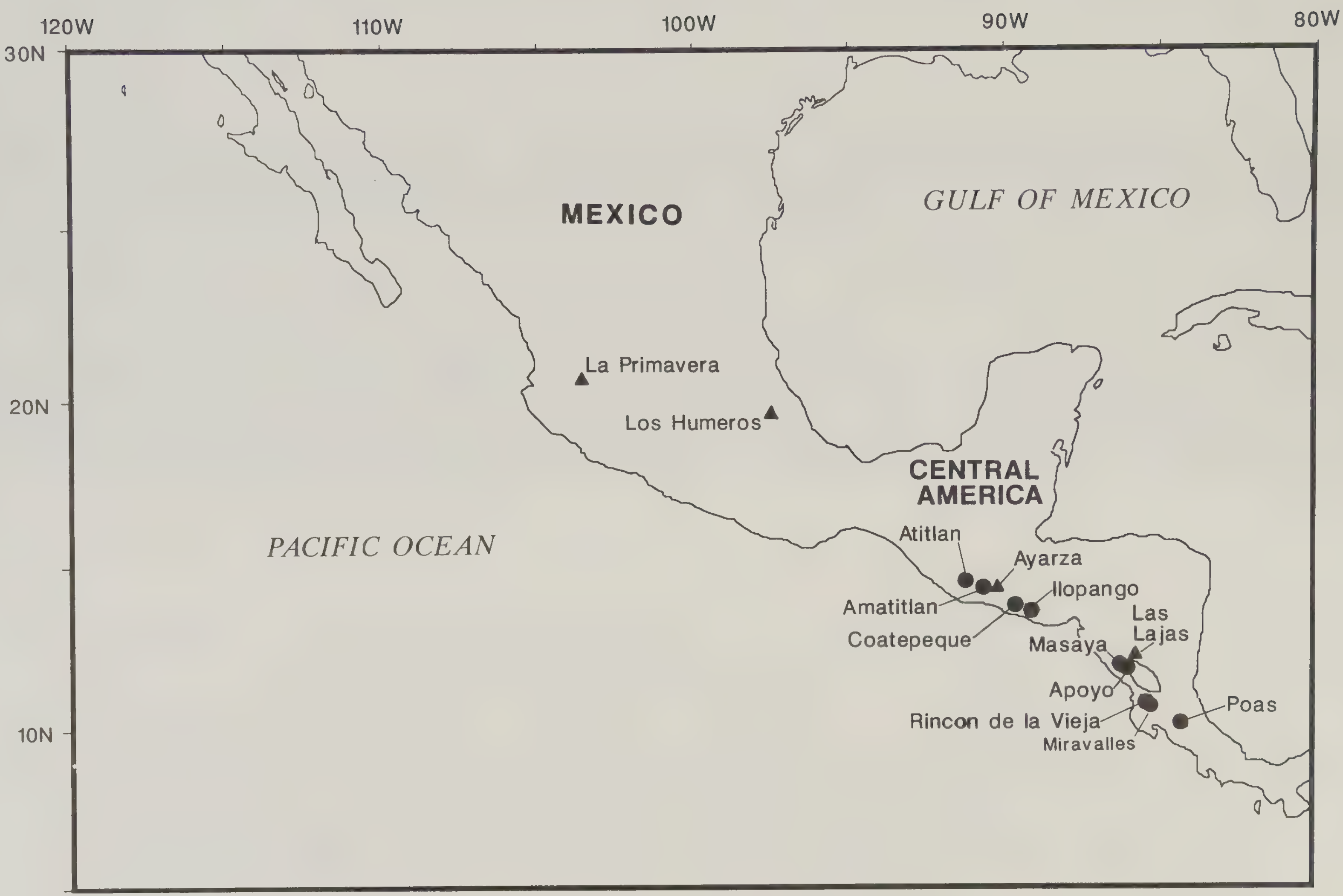

Figure 14. Locations of large, Quaternary restless calderas (solid circles) and nonrestless calderas (triangles) in Region 14.

PART 3: HISTORICAL UNREST AT LARGE QUATERNARY CALDERAS (continued)
See inside back cover for explanation and abbreviations

ATITLAN

CAVW number (active vent)	Latitude Longitude (degrees)	Diameter (km)	Local tectonic setting	Precaldera edifice	SiO_2 content (wt pct)	Age of collapse (yr B.P.)	Date of unrest	Type and duration of unrest ESTU STHF MGTF H Te	Eruption type
14-02-06 (V. Atitlán)	14.59N 91.18W	17 x 20	NW-SE right-lateral shear with N-S tension cracks	Strato (several)	R = 51-56 C = 72-76	84,000	1469	---- ---- ---- - --	ex
							1717-21	---- ---- ---- - --	"active"
							1826-28	---? ---- ---- - --	Ex,lf
							1833?	---? ---- ---- - --	ex
							1837	---? ---- ---- - --	ex
							1843?	---? ---- ---- - --	ex
							1852?-53	---? ---- ---- - --	Ex,ex
							1856?	---? ---- ---- - --	ex

TECTONIC SETTING

Volcanism in Guatemala results from subduction of the Cocos plate beneath the Caribbean plate. The modern Atitlán Caldera is thought to have formed at the intersection of a NE-SW-trending fossil boundary between the western and central Guatemala segments of Cocos-Caribbean subduction and the modern volcanic front (Newhall, 1987). Today, the principal faults of the Atitlán area are right-lateral NW-SE strike-slip faults, conjugate left-lateral NE-SW strike-slip faults, and an inferred N-S tension fracture that is defined by a N-S alignment of the modern stratovolcanoes (see below). The modern caldera is about 35 km south of the Motagua (middle) part of the boundary between the Caribbean and North American plates.

GEOLOGIC HISTORY

Three large calderas (figs. 14.1.1, 14.1.2) have formed in the Atitlán region in the past 14 m.y. (Newhall, 1987). The modern Atitlán (III) Caldera formed approximately 84,000 yr ago, shortly after an eruption of about 250 km^3 of rhyolitic magma (Koch and McLean, 1975; Hahn and others, 1979; Drexler and others, 1980; Rose and others, 1987; Newhall, 1987). Three postcaldera stratovolcanoes--V. San Pedro, V. Toliman, and V. Atitlán--have grown on or just inside the southern boundary of the caldera (Rose and others, 1980).

ATITLAN (continued)

HISTORICAL ACTIVITY

The first recorded eruption of Atitlán was in 1469 (von Seebach, 1892). The volcano "awoke" in 1717 and remained "active" until 1721 (Sapper, 1925). Other eruptions occurred as noted in the table above; the only strong eruption among these was on 3 May 1853, when ash darkened the sky around Lake Atitlán from 1100 to 1400 hr (Sapper, 1925).

Aside from the eruptions of V. Atitlán, little is known about unrest at Atitlán Caldera. Seismicity has been low during the past decade or more (White and Harlow, 1979, 1980; Harlow and White, 1980). There is a hint of relatively long-period fluctuations in lake level (fig. 14.1.3); the lake level was reportedly low in the 1820's, 10-15 m higher in the 1870's, back down to its low level in the 1920's, and high again from the 1940's to the present. Most fluctuation is a result of variation in annual rainfall or the effects of regional earthquakes on the subsurface drainage from the lake; it is not known whether any uplift and subsidence of the caldera floor is involved. Short-term changes in lake level that are attributable to rainfall may be as great as the increase of 3.3 m during the exceptionally wet year of 1933; those attributable to earthquakes may be as great as the drop of 2 m that occurred within 1 month following the Guatemala earthquake ($\underline{M}$=7.5) of 4 February 1976 (Newhall and others, 1987). Sediments of the lake floor suggest episodic, decades-long increases in sublacustrine thermal activity: alternating decades-long periods with and without annual lake overturn are interpreted as periods of relatively high and low activity of fumaroles on the caldera floor (Newhall and others, 1987).

REFERENCES

Drexler, J.W., Rose, W.I., Jr., Sparks, R.S.J., and Ledbetter, M.T., 1980, The Los Chocoyos ash, Guatemala: A major stratigraphic marker in Middle America and in three ocean basins: Quaternary Res., v. 13, p. 327-345.

Hahn, G.A., Rose, W.I., Jr., and Meyers, T., 1979, Geochemical correlation of genetically-related rhyolitic ash-flow and air-fall ashes, central and western Guatemala and the equatorial Pacific, in Chapin, C.E., and Elston, W.E., eds., Ash-flow tuffs: Geol. Soc. Am. Spec. Paper 180, p. 101-112.

Harlow, D.H., and White, R.A., 1980, Preliminary catalog of seismicity prior to the Guatemala earthquake of February 4, 1976, from the area between Guatemala City and Lake Atitlán (March 1975-February 1976): U.S. Geol. Surv. Open-File Rep. 80-60, 27 p.

Koch, A.J., and McLean, H., 1975, Pleistocene tephra and ash-flow deposits in the volcanic highlands of Guatemala: Geol. Soc. Am. Bull., v. 86, p. 529-541.

Mooser, F., Meyer-Abich, H., and McBirney, A.R., 1958, Catalogue of active volcanoes of the world including solfatara fields, Part VI, Central America: Naples, IAVCEI, 146 p.

Newhall, C.G., 1980, Geology of the Atitlán Calderas, Guatemala: Hanover, N.H., Dartmouth Coll., Ph.D. dissertation, 364 p.

----- 1987, Geology of the Lake Atitlán region, western Guatemala: Jour. Volcanol. Geotherm. Res., v. 33, p. 23-55.

Newhall, C.G., Paull, C.K., Bradbury, J.P., Higuera-Gundy, A., Poppe, L.J., Self, S., Sharpless, N. Bonar, and Ziagos, J., 1987, Recent geologic history of Lake Atitlán, a caldera lake in western Guatemala: Jour. Volcanol. Geotherm. Res., v. 33, p. 81-107.

ATITLAN (continued)

REFERENCES (continued)

Rose, W.I, Newhall, C.G., Bornhorst, T.J., and Self, S., 1987, Quaternary silicic pyroclastic deposits of Atitlán Caldera, Guatemala: Jour. Volcanol. Geotherm. Res., v. 33, p. 57-80.

Rose, W.I., Jr., Penfield, G.T., Drexler, J.W., and Larson, P.B., 1980, Geochemistry of the andesitic flank lavas of three composite cones within the Atitlán Cauldron, Guatemala: Bull. Volcanol., v. 43, p. 131-153.

Sapper, K., 1925, Los volcanes de la América Central: Halle, Max Niemeyer, 116 p.

Seebach, K., von, 1892, Ueber Vulkane Zentralamerikas: Abhandlungen der Koniglichen Gesellschaft der Wissenschaften zu Göttingen, v. 38, 251 p.

White, R.A., and Harlow, D.H., 1979, Preliminary catalog of aftershocks of the Guatemala earthquake of February 4, 1976, from the area between Guatemala City and Lake Atitlán (February-June 1976): U.S. Geol. Surv. Open-File Rep. 79-864, 63 p.

----- 1980, Preliminary catalog of seismicity from south-central Guatemala (July-December 1976): U.S. Geol. Surv. Open-File Rep. 80-83, 39 p.

Williams, H., 1960, Volcanic history of the Guatemalan highlands: Univ. Calif. Publ. Geol. Sci., v. 38, p. 1-86.

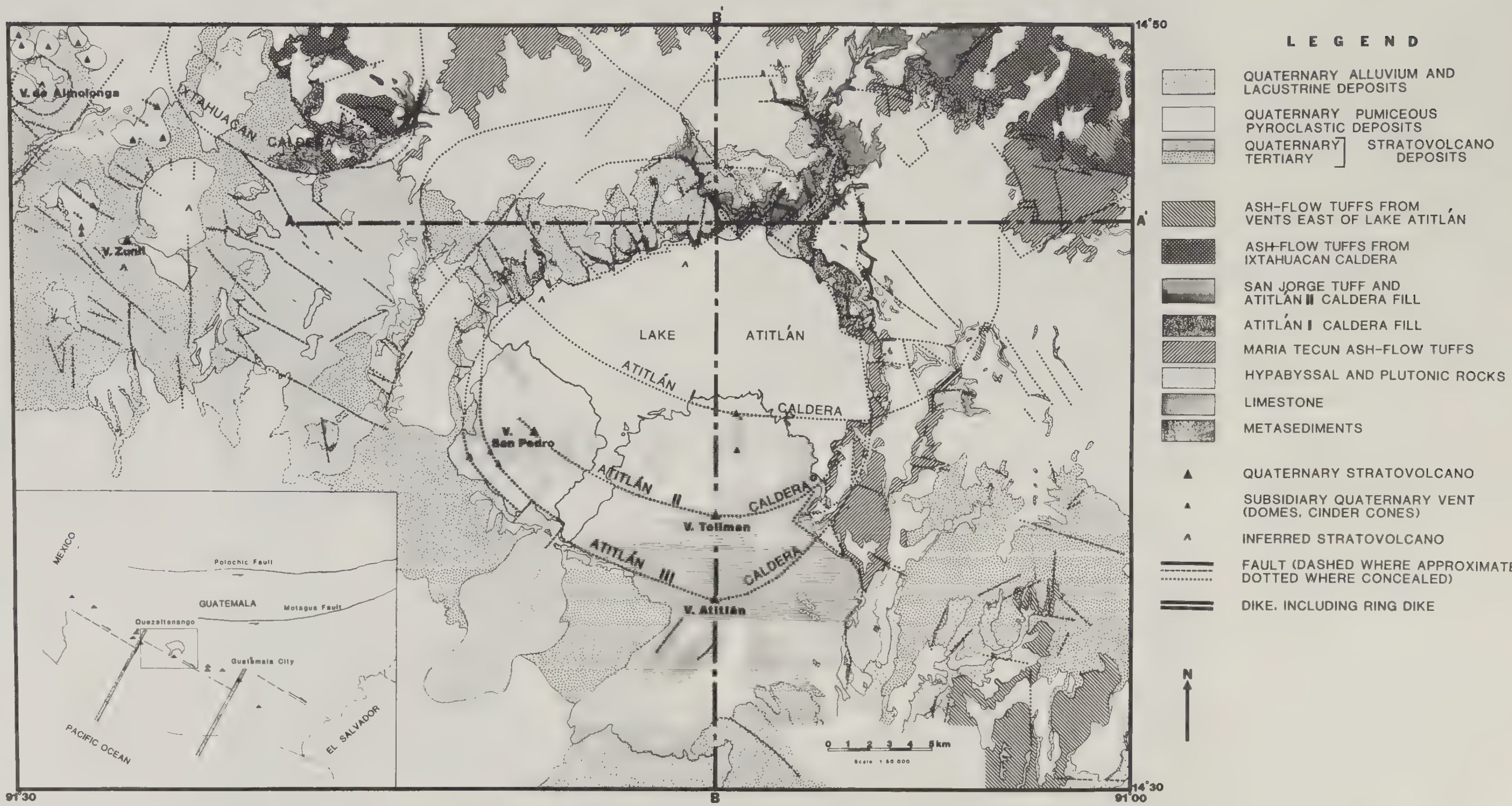

Figure 14.1.1. Geologic map of Atitlán area, showing trenchward (south-southwest) migration of successive calderas from 14 m.y. B.P. to the present, from Newhall (1987).

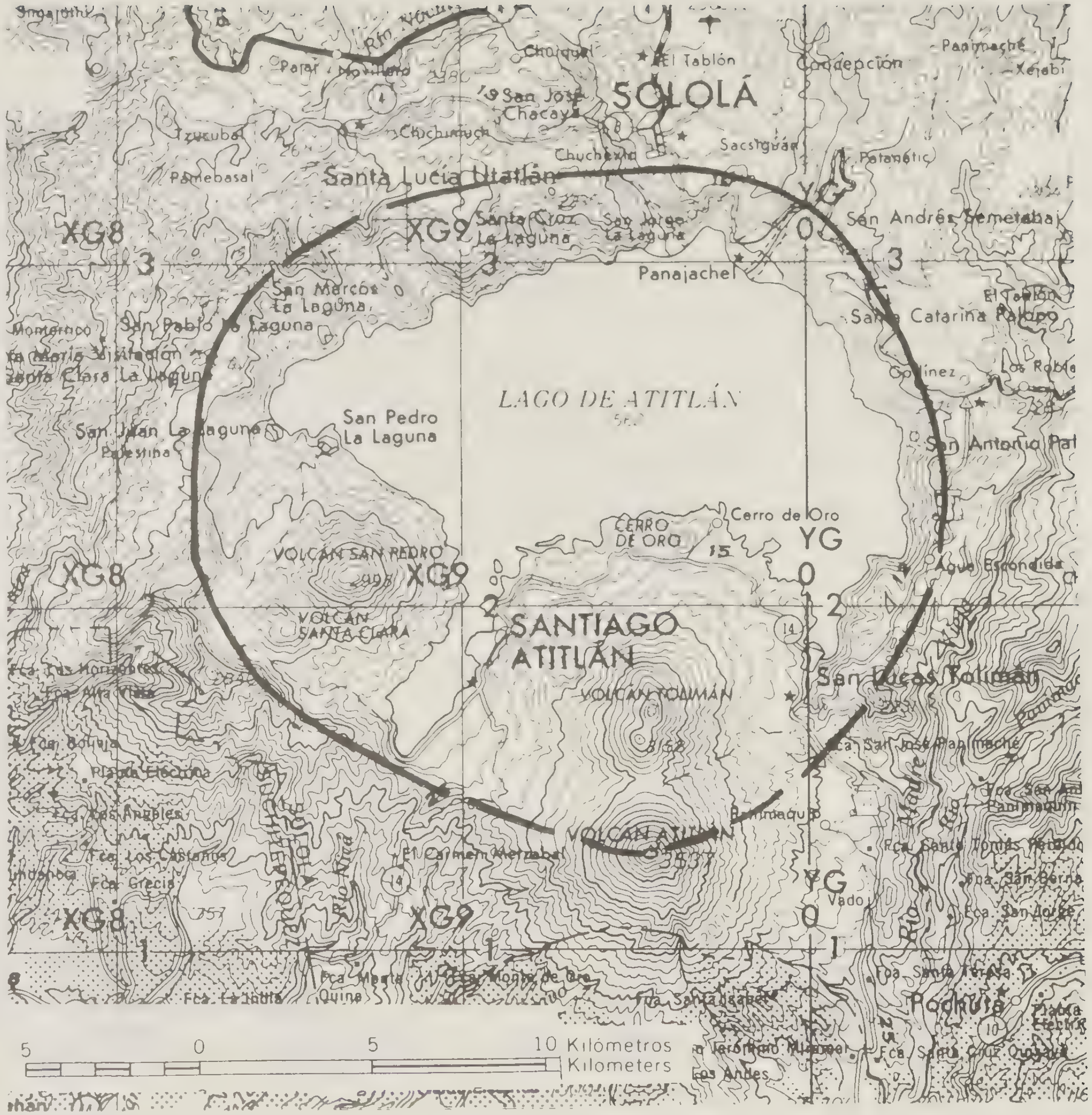

Figure 14.1.2. Topographic rim of modern, Atitlán III Caldera, and three postcaldera stratovolcanoes: V. San Pedro, V. Toliman, and V. Atitlán.

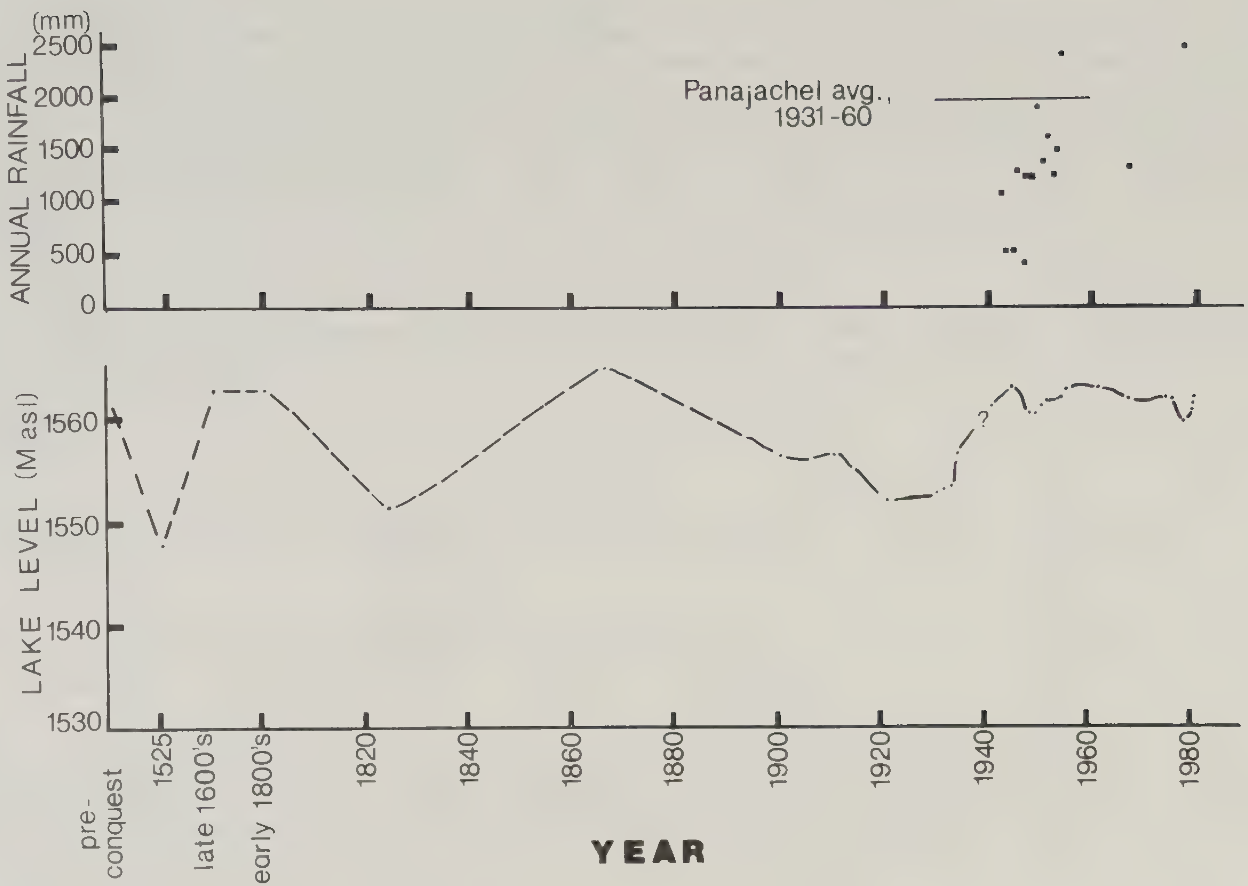

Figure 14.1.3. Annual precipitation and historical fluctuation of level of Lake Atitlán, from Newhall (1980). Annual precipitation at Panajachel (top) on northeast edge of Atitlán III Caldera. Estimate of historical fluctuations in lake level (bottom). Some of the fluctuation may be an artifact of imprecise altitude measurements. Fluctuation in lake level results from variable rainfall, earthquake-induced changes in subsurface drainage from lake, and (possibly) deformation of the caldera and its surroundings.

AMATITLAN

CAVW number (active vent)	Latitude Longitude (degrees)	Diameter (km)	Local tectonic setting	Precaldera edifice	SiO_2 content (wt pct)	Age of collapse (yr B.P.)	Date of unrest	Type and duration of unrest ESTU STHF MGTF H Te	Eruption type
14-02-11 (Pacaya)	14.38N 90.60W	14 x 16	NNE-SSW graben, transverse break in volcanic chain; intersection with WNW-ESE trend	?	R = 50-51 C = 68-75	240,000	1565	x--- ---- ---- - --	Ex,lf?
							1651	x--- ---- ---- - --	Ex
							1664-74	---- ---- ---- - --	Ex,ex
							1690-99?	---- ---- ---x - --	ex
							1775	N--- ---- ---- - --	ex,lf
							1846	---- ---- ---- - --	ex
							1891-1902	---- ---- ---x - --	none
							1961-88+	FFBx ---- -x-- - --	Ex,ex,lf

TECTONIC SETTING

Pacaya Volcano and the Amatitlán Caldera lie within a NNE-trending graben at its intersection with an ESE-WNW-trending left-lateral strike-slip fault (an extension of the Jalpatagua Fault). Pacaya and Amatitlán also lie astride the boundary between the central and eastern Guatemala segments of the Cocos-Caribbean subduction zone (Stoiber and Carr, 1973; Carr, 1976).

GEOLOGIC HISTORY

The Amatitlán area has been identified by Koch and McLean (1975) and Wunderman and Rose (1984) as the source of several voluminous silicic tephras in central Guatemala. At least nine major pyroclastic deposits, with a total volume of more than 70 km^3 (dense rock equivalent, DRE), were emplaced between about 300,000 yr and 23,000 yr B.P. (Wunderman and Rose, 1984). Wunderman and Rose (1984) inferred an Amatitlán Caldera with a resurgent dome (fig. 14.2.1). Postcaldera vents include a number of silicic domes in and around the caldera, and Pacaya Volcano, a basaltic and basaltic-andesite stratovolcano on the southern boundary of the caldera.

AMATITLAN (continued)

HISTORICAL ACTIVITY

Eruptions from Pacaya are frequent. Eruptions in 1565 and 1651, and perhaps since, were preceded or accompanied by strong earthquakes (Sapper, 1925). The most recent eruptions began in March 1983 and were continuing as of May 1987. Fumarolic activity from an area called Los Humitos, on Pacaya, began in 1891 and increased markedly in 1897 but eventually subsided without an eruption (Sapper, 1925, p. 34).

Regional seismic monitoring was upgraded in 1973, three years before the 1976 Guatemala earthquake. The upgraded monitoring showed a cluster of epicenters on what Wunderman and Rose (1984) have inferred to be a resurgent dome within the Amatitlán Caldera (figs. 14.2.2, 14.2.3). The same area remained active during and since the main shock and nearby aftershocks of February 1976. Most epicenters are along west-northwest-trending regional faults, near the center of inferred resurgence. Wunderman and Rose (1984) interpreted this seismicity to indicate that the dome is actively resurging. However, there are many other examples in this compilation of similar earthquake swarms, including some that have demonstrably shown no resurgence during the period of swarm activity, so confirmation of active resurgence would require the geodetic studies recommended by Wunderman and Rose (1984).

An area of the delta of the Rio Villalobos, on the north side of Lake Amatitlán, subsided irregularly in response to the February 1976 earthquake. Fractures up to 2 m wide and 1.5 m deep opened, and a number of houses were destroyed. This subsidence was apparently due to settling of water-saturated sediments and had no obvious relation to Amatitlán Caldera.

Recent eruptions of Pacaya have been preceded by several hours to a day or more of tremor--in some instances by banded tremor. A relatively strong explosion on 14 June 1987 was preceded by 15 hours of an unspecified increase in seismic activity (E. Sanchez, in Smithsonian Institution, 1987).

On 19-24 May 1988, a swarm of earthquakes ($\underline{M}_{max}$=4.5) occurred along the Mixco Fault Zone, slightly north of Amatitlán Caldera (E. Sanchez and D. Harlow, oral commun., 1988).

REFERENCES

Carr, M.J., 1976, Underthrusting and Quaternary faulting in northern Central America: Geol. Soc. Am. Bull, v. 87, p. 825-829.
Eggers, A.A., 1975, Mapa Geologico Amatitlán, Guatemala: map no. 2059-11G, scale 1:50,000, Instituto Geografico Nacional de Guatemala.
Eggers, A.A., and Chavez, D., 1979, Temporal gravity variations at Pacaya Volcano, Guatemala: Jour. Volcanol. Geotherm. Res., v. 6, p. 391-402.

AMATITLAN (continued)

REFERENCES (continued)

Eggers, A.A., Krausse, J., Rusk, H., and Ward, J., 1976, Gravity changes accompanying volcanic activity at Pacaya Volcano, Guatemala: Jour. Volcanol. Geotherm. Res., v. 1, p. 229-236.

Eichelberger, J.C., and McGetchin, T.R., 1976, Petrogenesis of the 1973 Pacaya lavas, Guatemala, in Gonzales-Ferran, O., ed., Proc. Symp. on Andean and Antarctic Volcanological Problems: Naples, IAVCEI, p. 435-449.

Harlow, D.H., 1976, Instrumentally recorded seismic activity prior to the main event, in Espinoza, A.F., ed., The Guatemalan earthquake of February 4, 1976, a preliminary report: U.S. Geol. Surv. Prof. Paper 1002, p. 12-16.

Harlow, D.H., and White, R.A., 1980, Preliminary catalog of seismicity prior to the Guatemala earthquake of February 4, 1976 from the area between Guatemala City and Lake Atitlán (March 1975-February 1976): U.S. Geol. Surv Open-File Rep. 80-60, 27 p.

Koch, A.J., and McLean, H., 1975, Pleistocene tephra and ash-flow deposits in the volcanic highlands of Guatemala: Geol. Soc. Am. Bull., v. 86, p. 529-541.

Mooser, F., Meyer-Abich, H., and McBirney, A.R., 1958, Catalogue of active volcanoes of the world including solfatara fields, Part VI, Central America: Naples, IAVCEI, 146 p.

Sapper, K., 1925, Los volcanes de la América Central: Halle, Max Niemeyer, 116 p.

----- 1927, Vulkankunde: Stuttgart, Engelhorns Nachf, 427 p.

Smithsonian Institution, Scientific Event Alert Network (SEAN), 1976-88, Pacaya Volcano: SEAN Bull., v. 1. nos. 5, 8; v. 2, nos. 8, 10; v. 3. no. 11; v. 5, nos. 2, 12; v. 6, nos. 2, 3; v. 7, nos. 2, 3; v. 8, nos. 1, 9, 11; v. 9, no. 8; v. 10, nos. 3-4; v. 11, nos. 3, 11, 12; v. 12, nos. 1, 5, 7, 8, 12; v. 13, nos. 1, 2 (contributions from A. MacKenney, E. Sanchez, E. Quevec, E. Molina, N. Banks, M. Doukas, and others).

Stoiber, R.E., and Carr, M.J., 1973, Quaternary volcanic and tectonic segmentation of Central America: Bull. Volcanol., v. 37, no. 3, p. 304-325.

White, R.A., and Harlow, D.H., 1979, Preliminary catalog of aftershocks of the Guatemala earthquake of February 4, 1976 from the area between Guatemala City and Lake Atitlán (February-June 1976): U.S. Geol. Surv. Open-File Rep. 79-864, 63 p.

----- 1980, Preliminary catalog of seismicity from south-central Guatemala (July-December 1976): U.S. Geol. Surv. Open-File Rep. 80-83, 39 p.

Wunderman, R.L., and Rose, W.I., 1984, Amatitlán, an actively resurging cauldron 10 km south of Guatemala City: Jour. Geophys. Res., v. 89, no. B10, p. 8525-8539.

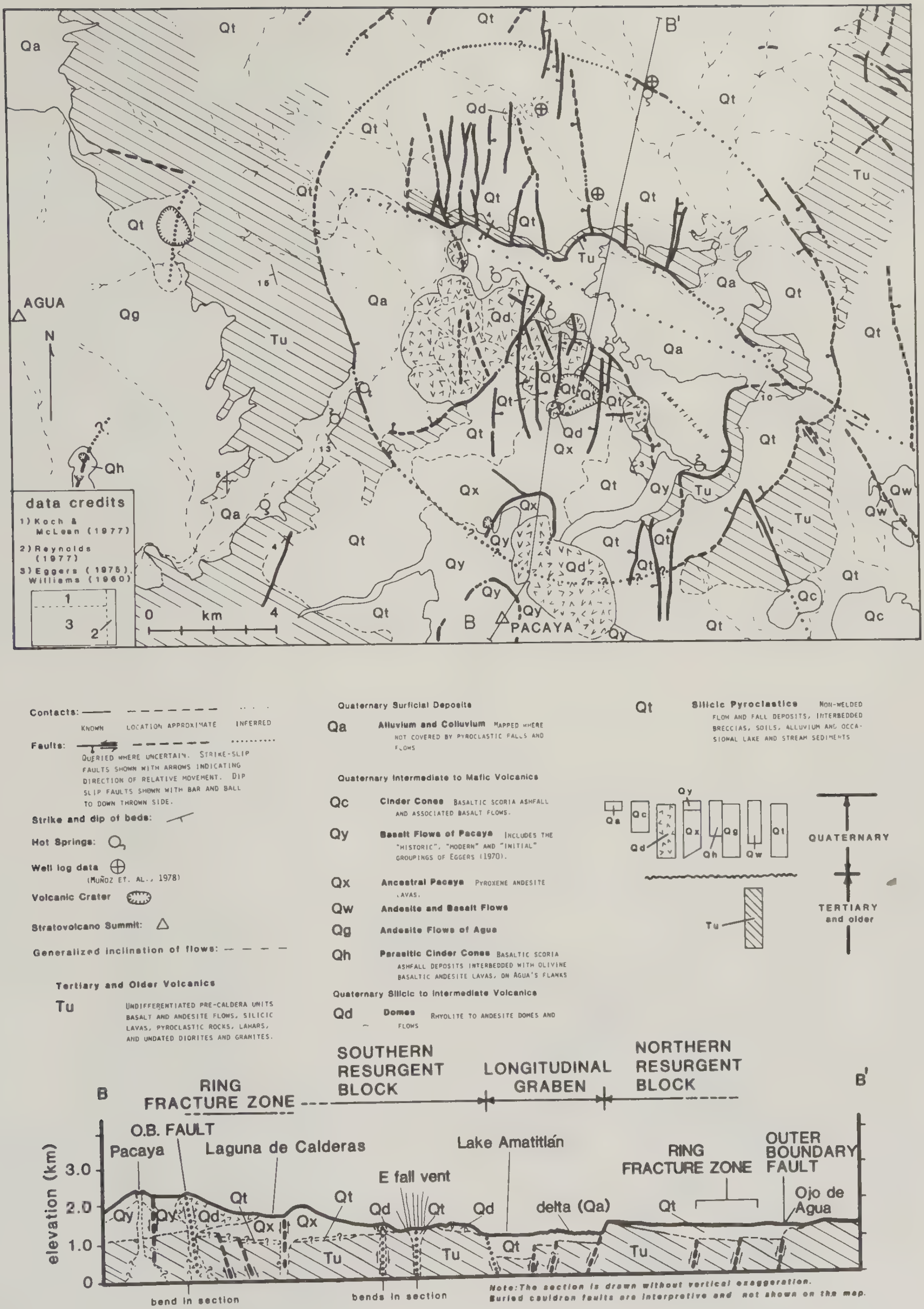

Figure 14.2.1. Generalized geologic map and cross section of Amatitlán Caldera, from Wunderman and Rose (1984). Copyright by the American Geophysical Union.

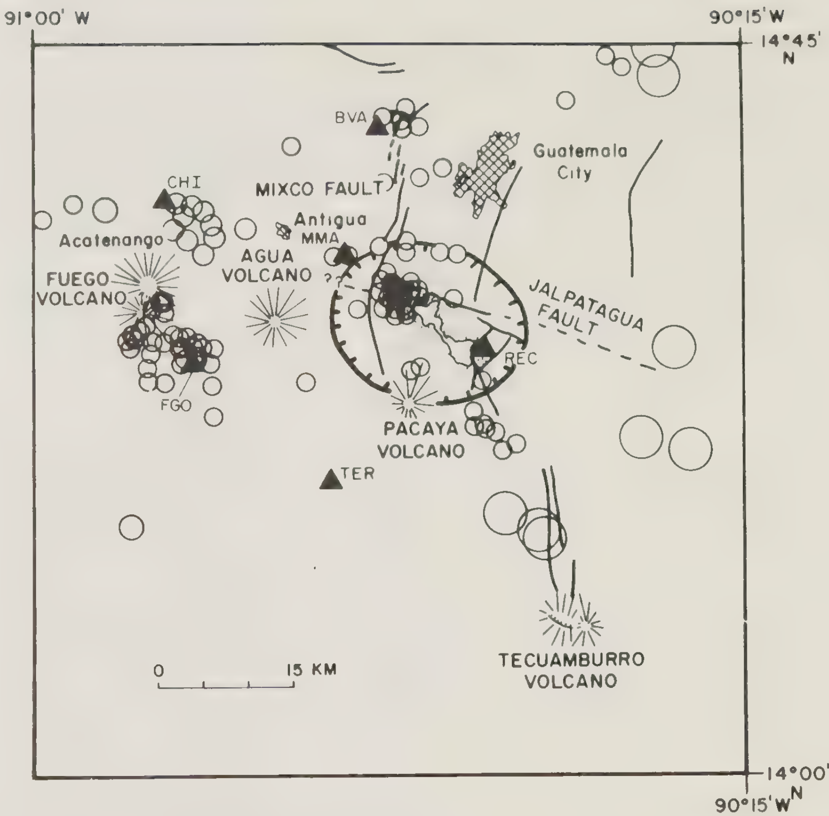

Figure 14.2.2. Epicenter locations (March-September 1975) and known faults in the Amatitlán region, after Harlow (1976). Seismic recording ended before the magnitude 7.5 Guatemalan earthquake of 4 February 1976. Solid triangles indicate seismometers; size of open circles reflects estimated error in epicentral location.

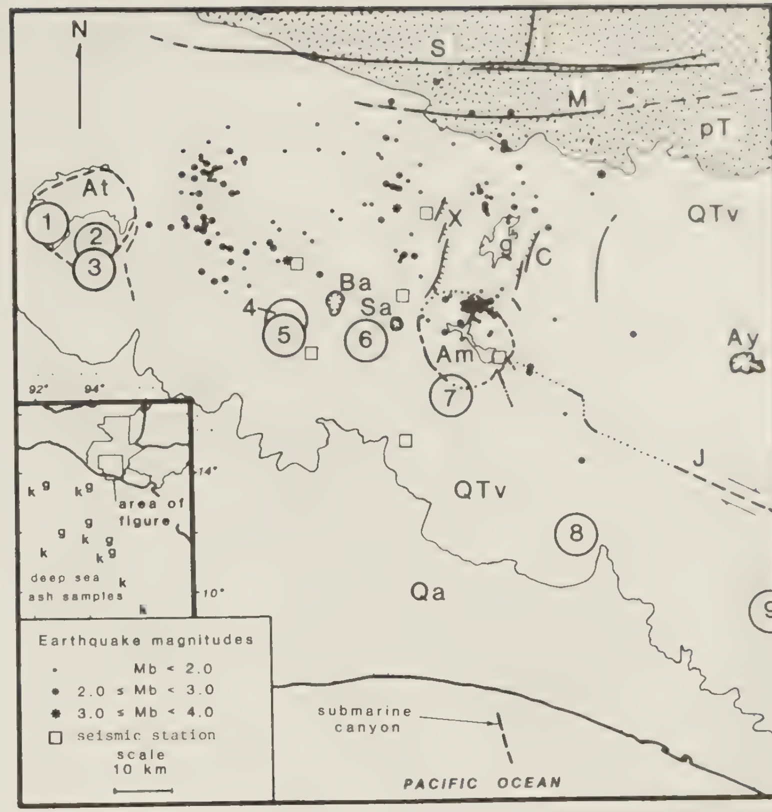

Figure 14.2.3. Regional setting, structure, and seismicity of Amatitlán Caldera, from Wunderman and Rose (1984) after Harlow and White (1980) and White and Harlow (1979, 1980). Qa, Quaternary alluvium; QTv, Quaternary and Tertiary volcanics; pT, pre-Tertiary rocks. Volcanic front composed of following stratovolcanoes: 1, San Pedro; 2, Atitlan; 3, Toliman; 4, Acatenango; 5, Fuego; 6, Agua; 7, Pacaya; 8, Tecuamburro; and 9, Moyuta. Slightly north of these stratovolcanoes are the following silicic centers: At, Atitlan; Ba, Barahona; Sa, Sabana Grande; Am, Amatitlan; and Ay, Ayarza. Major faults include: S, San Agustin; M, Motagua; J, Jalpatagua; X, Mixco; and C, Santa Catarina Pinula. Earthquake epicenters for May 1976 (after M 7.5 Guatemalan earthquake of 4 February 1976) demonstrate recent clustering of epicenters near Amatitlan Caldera. Guatemala City (letter g) is 10 km north-northeast of Amatitlán. Copyright by American Geophysical Union.

PART 3: HISTORICAL UNREST AT LARGE QUATERNARY CALDERAS (continued)

See inside back cover for explanation and abbreviations

COATEPEQUE

CAVW number (active vent)	Latitude Longitude (degrees)	Diameter (km)	Local tectonic setting	Precaldera edifice	SiO_2 content (wt pct)	Age of collapse (yr B.P.)	Date of unrest	Type and duration of unrest ESTU STHF MGTF H Te	Eruption type
14-03-02,	13.87N	7 x 10	Compr,	Strato?	R = 51-62	10,000	1520 (SA)	---- ---- ---- - --	Ex
(Santa Ana=SA)	89.55W		astride		C = 70	to	1524 (SA)	---- ---- ---- - --	Ex
14-03-03			segment			40,000	1570? (SA)	---- ---- ---- - --	Ex
(Izalco=I)			boundary				1576 (SA)	---- ---- ---x - --	Ex
14-03-04							1874 (SA)	---- ---- ---x - --	Ex?
(San Marcelino=SM)							1878 (SA)	---- ---- ---- - --	ex
						Santa	1879 (SA)	---- ---- ---- - --	ex
						Ana	1880 (SA)	---- ---- ---- - --	Ex
							1882? (SA)	---- ---- ---- - --	ex
							1884 (SA)	---- ---- ---- - --	ex
							1904 (SA)	D--- ---- ---- - --	ex
							1920 (SA)	---- ---- ---- - --	ex
							1770-72 (I)	x--x ---- ---x - --	ex,lf
							1783 (I)	x--- ---- ---- - --	lf
							1793+ (I)	---- ---- ---- - --	ex,lf
							1798 (I)	---- ---- ---- - --	ex
							1802-03 (I)	---- ---- ---- - --	ex,lf
							1805-07 (I)	---- ---- ---- - --	ex
							1825? (I)	---- ---- ---- - --	ex
							1836 (I)	---- ---- ---- - --	ex
							1838 (I)	---- ---- ---- - --	ex
							1840 (I)	---- ---- ---- - --	ex
							1842 (I)	---- ---- ---- - --	ex
							1844 (I)	---- ---- ---- - --	ex,lf
						Izalco	1850 (I)	---- ---- ---- - --	ex
							1854 (I)	---- ---- ---- - --	ex,lf
							1856 (I)	---- ---- ---- - --	ex,lf
							1858-60 (I)	---- ---- ---- - --	ex,lf
							1863-70 (I)	---- ---- ---x - --	lf,ex
							1872-73 (I)	---- ---- ---- - --	ex
							1879-85 (I)	---- ---- ---- - --	ex,lf
							1887-1901 (I)	---- ---- ---- - --	ex,lf

COATEPEQUE (continued)

CAVW number (active vent)	Latitude Longitude (degrees)	Diameter (km)	Local tectonic setting	Precaldera edifice	SiO_2 content (wt pct)	Age of collapse (yr B.P.)	Date of unrest	Type and duration of unrest ESTU STHF MGTF H Te	Eruption type
(continued from previous page)							1902 (I)	---- ---- ---- - QU?	ex,lf
							1903-05(I)	D--- ---- ---- - --	ex
							1912-16(I)	x--- ---- ---- - --	ex,lf
							1920-21(I)	N--A A--x ---x - --	ex,lf
							1925-28?(I)	---- ---- ---- - --	ex,lf
							1930-31(I)	---- ---- ---- - --	lf,ex
							1933-34(I)	---- ---- ---- - --	ex,lf
							1937-57(I)	---- ---- ---- - --	ex,Ex,lf
							1966 (I)	---- ---- -NZZ - --	lf
						San Marcelino	1600's(SM)	---- ---- ---- - --	lf
							1722 (SM)	---- ---- ---- - --	lf

TECTONIC SETTING

Coatepeque Caldera is part of the chain of volcanoes resulting from Cocos-Caribbean subduction. Coatepeque lies astride the boundary between the eastern Guatemala and El Salvador segments of that subduction (Stoiber and Carr, 1973).

GEOLOGIC HISTORY

Coatepeque Caldera (figs. 14.3.1, 14.3.2) lies at the eastern foot of Volcán Santa Ana and probably formed after Santa Ana had grown to nearly its current size (Carr and Pontier, 1981). Several rhyolitic and dacitic domes grew within the caldera, and several basaltic and andesitic vents developed just south and west of Coatepeque. V. Santa Ana, V. Izalco, and V. San Marcelino are part of the same volcanic center as Coatepeque Caldera, although they lie just outside the caldera boundary.

HISTORICAL ACTIVITY

Santa Ana was particularly active during the late 1500's and again in the late 1800's. San Marcelino last erupted in 1772. Izalco, presently about 200 m high, began to grow in (or before?) 1770.

1770-1966: After precursory earthquakes and a rise in fumarolic activity, "the land swelled up and...the steam emissions increased amid a violent din" (Montessus de Ballore, 1888). Larde (1925) accepts the 1770 date given above for the birth of Izalco, but Ipiña (in Sapper, 1925, p. 43) places it at 1765. During eruptive periods of Izalco (listed above), explosions commonly occur at intervals of 1 minute to 1 hour. A relatively long period of explosions that began in 1887 stopped abruptly in January 1901, but then resumed on 10 May 1902, three weeks after a $\underline{M}$=7.9 earthquake off the south coast of western Guatemala (18 April) and only two

COATEPEQUE (continued)

HISTORICAL ACTIVITY (continued)

and three days after major eruptions of Mont Pelée and Soufriere St. Vincent, respectively (Sapper, 1925). In 1904, less than two weeks after an earthquake of "sufficient magnitude," both Izalco and Santa Ana again entered into eruption (Sapper, 1925). J. Larde, cited in Sapper (1925), watched the eruptive fissure from a distance of only a few tens of meters in 1920 and noted short-lived, local tumescence of up to 2 m immediately before explosions. The 21-year repose since Izalco's most recent eruption (1966) is slightly longer than any known previous repose of Izalco, but it is not sufficiently long to imply that Izalco's activity is decreasing.

Activity at these three stratovolcanoes is generally not accompanied by felt seismicity, ground deformation, or thermal activity in Coatepeque Caldera; an exception was agitation of Lake Coatepeque during activity of Izalco in mid-January 1925 (Larde, 1925). Records do not specify whether this agitation was of fumarolic or seismic origin.

REFERENCES

Carr, M.J., and Pontier, N.K., 1981, Evolution of a young parasitic cone towards a mature central vent; Izalco and Santa Ana Volcanoes in El Salvador, Central America: Jour. Volcanol. Geotherm. Res., v. 11, p. 277-292.

Larde, Jorge, 1925, El Volcán de Izalco: Bull. Volcanol., Ser. 1, nos. 5-6, p. 209-211.

Meyer, J., 1964, Stratigraphie des Bimskiese und -ashen des Coatepeque-Vulkans im westlichen El Salvador (Mittelamerika): Neues Jahrb. Geol. Palaontol., v. 119, p. 215-246.

Montessus de Ballore, F., 1888, Tremblements de terre et eruptions volcaniques au Centre-Amerique, depuis la conquete espagnole jusqu'a nos jours: Dijon, Soc. Sci. Natur. Saone-et-Loire, 293 p.

Mooser, F., Meyer-Abich, H., and McBirney, A.R., 1958, Catalogue of active volcanoes of the world including solfatara fields, Part VI, Central America: Naples, IAVCEI, 146 p.

Rose, W.I., Jr., Hahn, G.A., Drexler, J.W., Malinconico, M.L., Peterson, P.S., and Wunderman, R.L., 1981, Quaternary tephra of northern Central America, in Self, S., and Sparks, R.S.J., Tephra studies: Dordrecht, D. Reidel Publ. Co., p. 193-211.

Rose, W.I., Jr., and Stoiber, R.E., 1969, The 1966 eruption of Izalco Volcano, El Salvador: Jour. Geophys. Res., v. 74, p. 3119-3130.

Sapper, K., 1925, Los volcanes de la América Central: Halle, Max Niemeyer, 116 p.

Stoiber, R.E., and Carr, M.J., 1973, Quaternary volcanic and tectonic segmentation of Central America: Bull. Volcanol., v. 37, no. 3, p. 304-325.

Williams, H., and Meyer-Abich, H., 1955, Volcanism in the southern part of El Salvador, with particular reference to the collapse basins of Coatepeque and Ilopango: Univ. Calif. Publ. Geol. Sci., v. 32, p. 1-64.

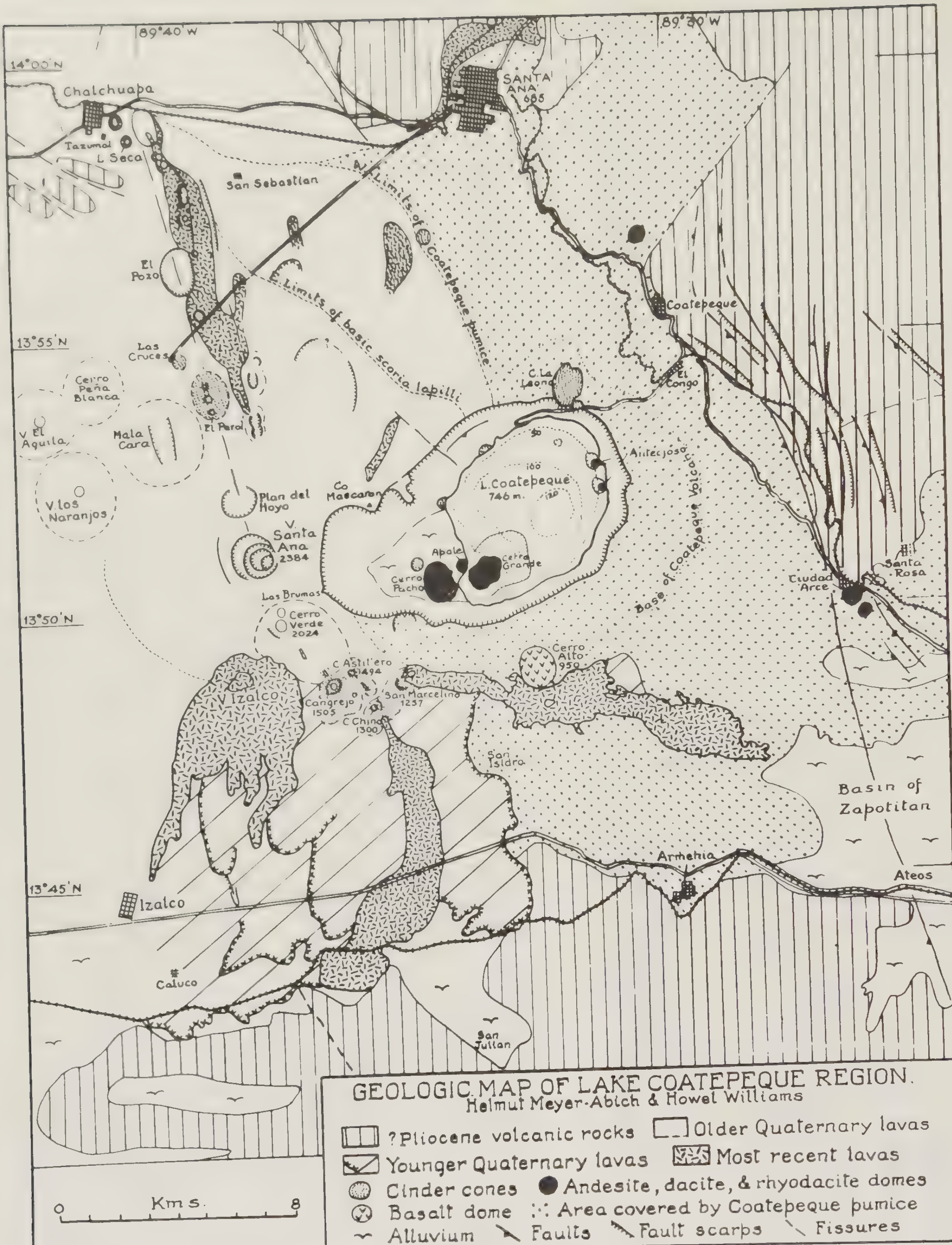

Figure 14.3.1. Geologic map of Lake Coatepeque region, from Williams and Meyer-Abich (1955).

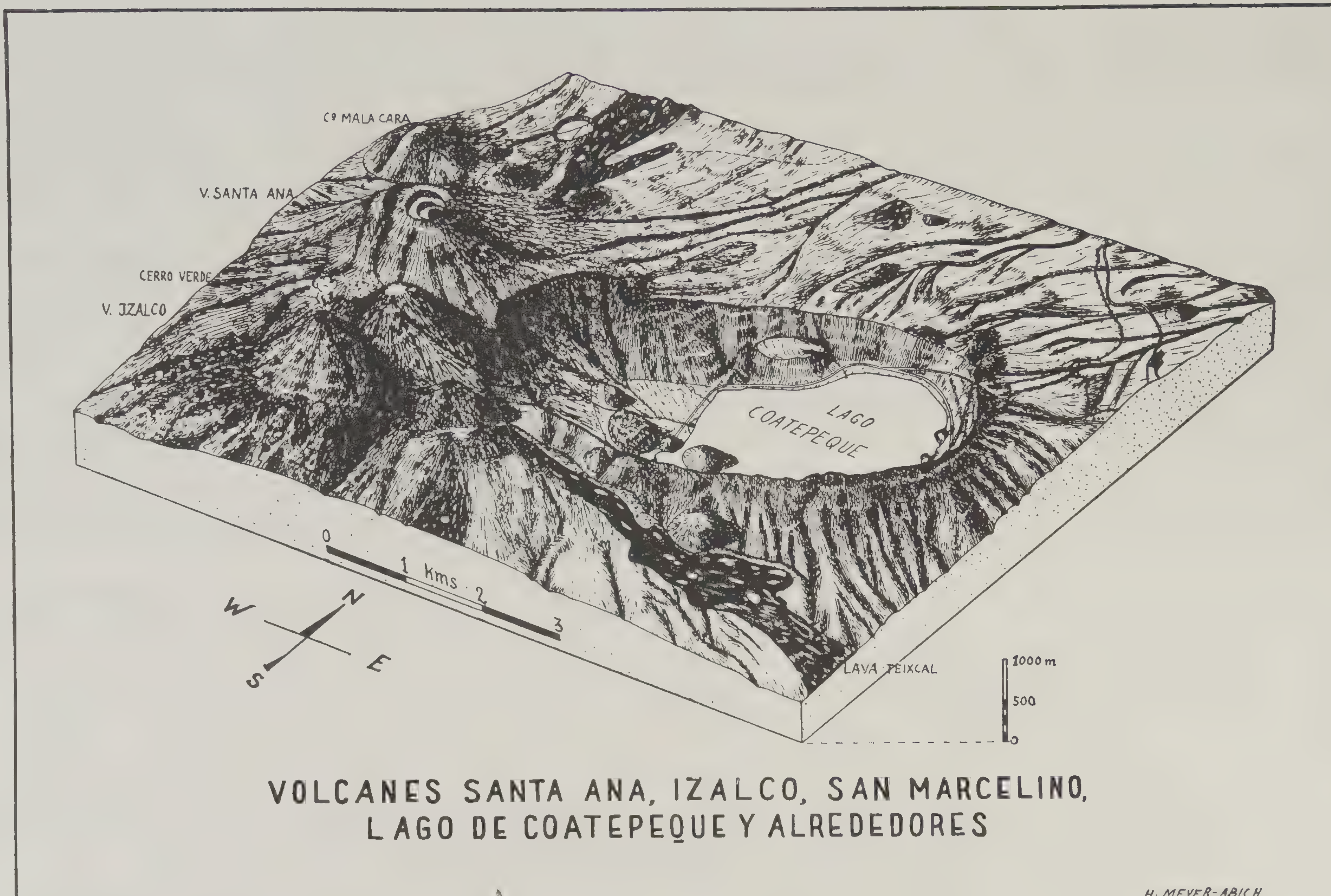

Figure 14.3.2. Perspective drawing of Lake Coatepeque region, from Mooser and others (1958). Note what appears to be a landslide scarp at the west end of caldera.

ILOPANGO

CAVW number (active vent)	Latitude Longitude (degrees)	Diameter (km)	Local tectonic setting	Precaldera edifice	SiO_2 content (wt pct)	Age of collapse (yr B.P.)	Date of unrest	Type and duration of unrest ESTU STHF MGTF H Te	Eruption type
14-03-06 (Islas Quemadas)	13.67N 89.05W	8 x 11	Graben	?	R = 67 C = 63-68	A.D. 260	1765	xx-- ---- ---- - --	none
							1769-70	xx-- ---- ---- - --	none
							1873	---? ---- ---x - QU	none
							1879-80	D--? ?--- ---- - --	dm,ex
							1884	---- ---- ---? - --	unknown

TECTONIC SETTING

Ilopango is an elongate caldera bounded on the north and south by faults of a graben that parallels the volcanic chain throughout El Salvador and parts of Guatemala and Nicaragua.

GEOLOGIC HISTORY

The Ilopango Caldera (figs. 14.4.1, 14.4.2) formed as a result of the Tierra Blanca eruption of 260 A.D. (volume of pyroclastic deposits = 10-20 km^3 DRE) (Williams and Meyer-Abich, 1955; Sheets, 1979; Hart and Steen-McIntyre, 1983). Because Ilopango's shape is strongly controlled by regional faults, Williams and McBirney (1979) cite it as an example of a "volcano-tectonic depression." Islas Quemadas ("burnt islands") is a dacite dome that grew through Lake Ilopango in 1880 (see below).

HISTORICAL ACTIVITY

1765, 1769-70: Earthquakes were felt in the vicinity of Ilopango (Sapper, 1925, p. 54).

1873: At the time of an earthquake that struck nearby San Salvador, water of Lake Ilopango was lifted, bubbling, 2 to 3 ft, but it was not guessed that a volcano might be growing beneath the lake (Sapper, 1925).

1879-80: Severe earthquakes occurred from 20 December 1879 until 31 December 1879, and in January 1880 the Islas Quemadas dome grew up through Lake Ilopango. Sapper (1925) wrote that the lake began to rise on 6 January, and that by 9 January discharge down the Jiboa River was so strong that the entire valley was flooded, the town of Atuscatla was destroyed, and many cattle perished.

ILOPANGO (continued)

HISTORICAL ACTIVITY (continued)

Lake level began to drop on 11 January, and by 12 January emission of sulfur gas from the center of the lake was noted. On 20 January a huge column of ash and incandescent rocks rose from the center of the lake, and by 23 January a group of new islands, Islas Quemadas, had risen above the lake. Explosions and dome growth continued through mid-March (Sapper, 1925).

After the initial earthquakes in December 1879, earthquakes in January were few and rarely strong. However, on 23 February an earthquake (from Ilopango?) was felt throughout El Salvador, and immediately thereafter an unbearable sulfur smell permeated the area. The following day the column of steam increased, but by nightfall both steaming and several small parts of the islands had disappeared. The last of several phases of dome growth and explosions ended on 19 March 1880. Unspecified activity was observed again on 7-9 February and 13 March 1884 (Sapper, 1925), but no activity has been observed since 1884.

Goodyear (1880) calculated that the level of Lake Ilopango rose 1.2 m between 31 December and 11 January; that rise in lake level corresponded to a displacement of 0.13 km^3, or roughly the subaqueous volume of the Islas Quemadas dome, so there is no indication of major uplift of the caldera floor. Between 12 January and 20 January, the lake level fell 9.2 m (volume=0.96 km^3), at a maximum rate of nearly 10 cm/hr. By 8 February the lake level had fallen an additional 2.6 m, for an additional loss of 0.27 km^3, making a total loss of 1.2 km^3. The drop in lake level was due in part or in whole to rapid downcutting of the outlet channel, and towns downstream were flooded. Unfortunately, there is no documentation of the final depth of downcutting to indicate whether some of the decrease in lake level might also have been due to subsidence of the caldera floor.

Golombek and Carr (1978) noted a correlation between the earthquakes preceding the 1879-80 eruption and semidiurnal maxima and minima in earth tides. Five out of six phases of the eruption also showed some correlation with earth tides, with each of these phases beginning near fortnightly minima in tidal amplitude.

A $\underline{M}$=5.4 tectonic earthquake occurred at shallow depth beneath San Salvador in October 1986. Damage in San Salvador was severe, but the quake did not trigger any disturbance at the Ilopango Caldera.

REFERENCES

Anonymous, 1880, A lacustrine volcano: Nature, v. 22, p. 129.

Golombek, M.P., and Carr, M.J., 1978, Tidal triggering of seismic and volcanic phenomena during the 1879-1880 eruption of Islas Quemadas Volcano in El Salvador, Central America: Jour. Volcanol. Geotherm. Res., v. 3, p. 299-307.

Goodyear, W.A., 1880, Earthquake and volcanic phenomena, December 1979 and January 1880 in the Republic of Salvador: Panama, The Star and Herald, 56 p.

Hart, W.E.J., and Steen-McIntyre, V., 1983, Tierra Blanca Joven tephra from the A.D. 260 eruption of Ilopango Caldera, in Sheets, P., ed., Archaeology and volcanism in Central America: The Zapotitán Valley of El Salvador: Austin, Univ. Tex. Press, p. 14-34.

ILOPANGO (continued)

REFERENCES (continued)

Mooser, F., Meyer-Abich, H., and McBirney, A.R., 1958, Catalogue of active volcanoes of the world including solfatara fields, Part VI, Central America: Naples, IAVCEI, 146 p.

Sapper, K., 1925, Los volcanes de la América Central: Halle, Max Niemeyer, 116 p.

Sheets, P.D., 1979, Environmental and cultural effects of the Ilopango eruption in Central America, in Sheets, P.D., and Grayson, D.K., eds., Volcanic activity and human ecology: New York, Academic Press, p. 525-564.

Williams, H., and McBirney, A.R., 1979, Volcanology: San Francisco, Freeman Cooper, 397 p.

Williams, H., and Meyer-Abich, H., 1955, Volcanism in the southern part of El Salvador, with particular reference to the collapse basins of Coatepeque and Ilopango: Univ. Calif. Publ. Geol. Sci., v. 32, p. 1-64.

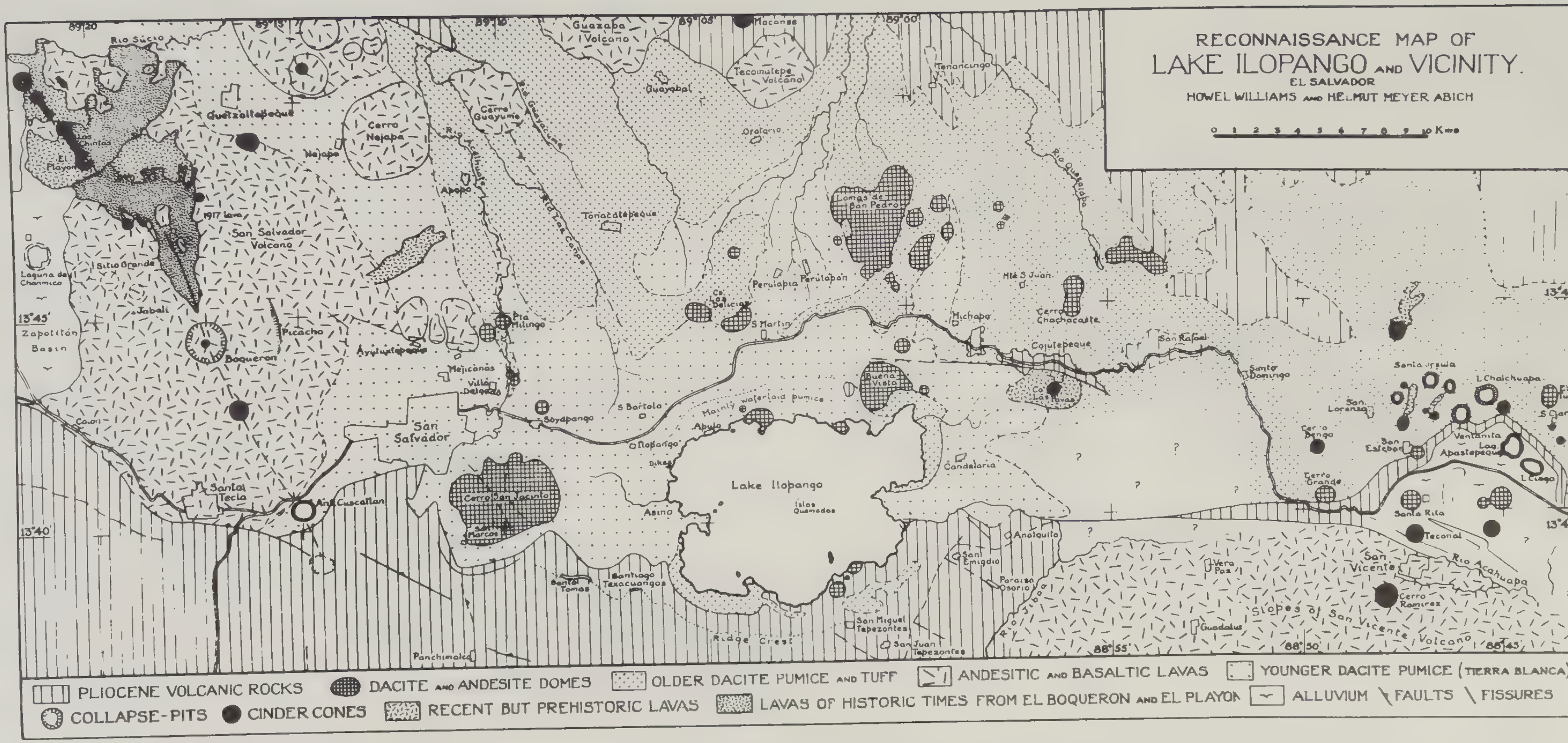

Figure 14.4.1. Geologic map of Ilopango Caldera, from Williams and Meyer-Abich (1955). Topographic rim of caldera is labeled "ridge crest."

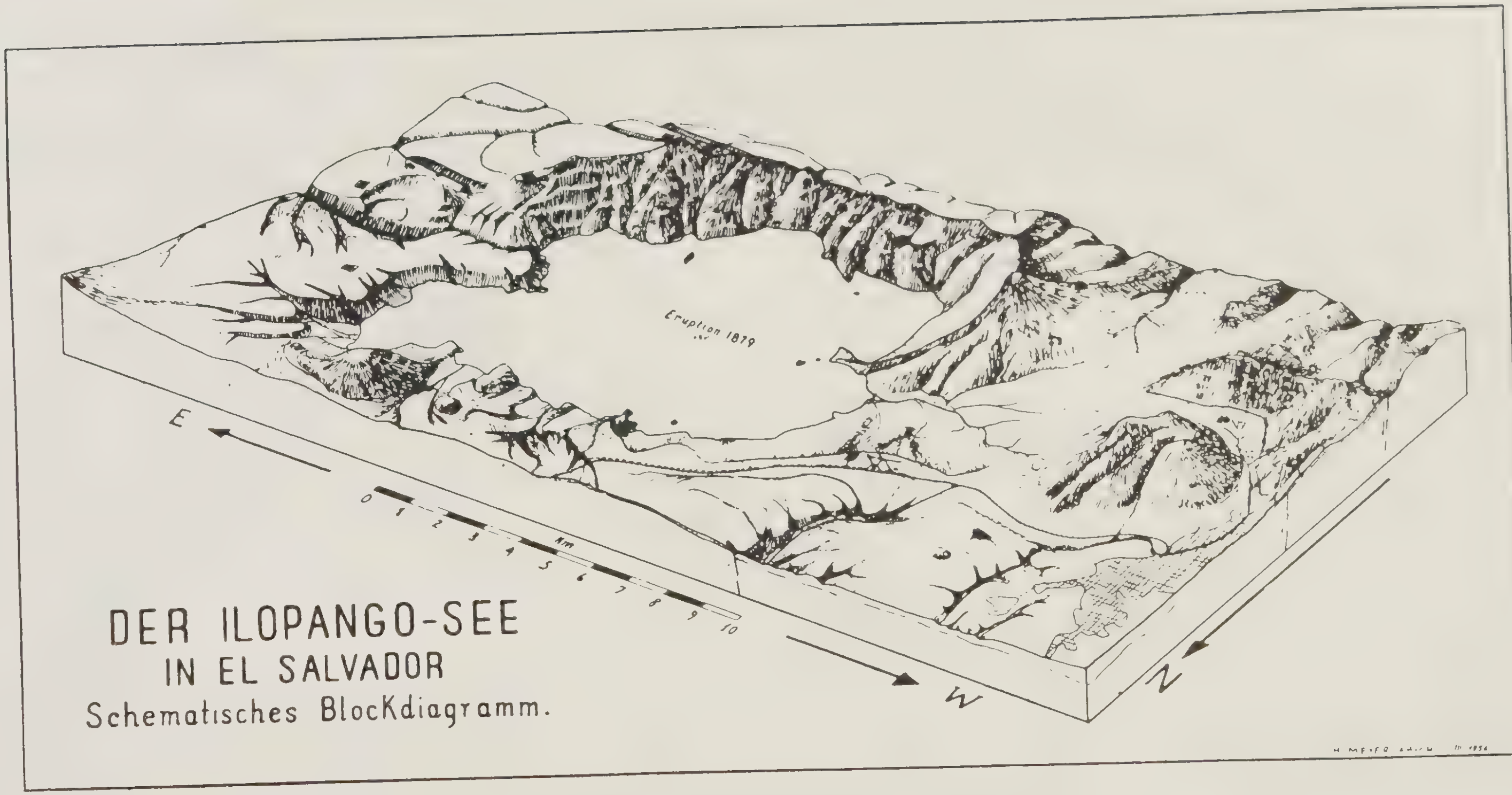

Figure 14.4.2. Perspective drawing of Ilopango Caldera, from Mooser and others (1958).

MASAYA

CAVW number (active vent)	Latitude Longitude (degrees)	Diameter (km)	Local tectonic setting	Precaldera edifice	SiO_2 content (wt pct)	Age of collapse (yr B.P.)	Date of unrest	Type and duration of unrest ESTU STHF MGTF H Te	Eruption type
14-04-10 (Masaya)	11.98N 86.15W	11 x 6	NW-SE-trending fissure	Shield	R = 51 C = 51-53	ca. 6000; ca. 2200	1524	---- ---- ---- - --	unknown
							1529-70	---- ---- ---- - --	ll
							1670	---- ---- ---- - --	Ex,lf
							1772-75	AA-- ---- ---- - --	lf,ex
							1852-59	EE-- ---- ---Y - --	ex,lf
							1902-06	D--- ---- ---Y - --	ex
							1913?	x--- ---- ---- - --	unknown
							1919-24	---- ---- ---Z - --	ex
							1946	---- ---- ---Z - --	lf
							1947-59	---- ---- ---F - --	none
							1965	---- ---- ---- - --	ex,lf
							1970-72+	---- ---- ---- - --	ex,ll
							1974-88+	x--- x--- ---Y - --	ll,ex

TECTONIC SETTING

Masaya is immediately southeast of a zone of transverse faulting that was active in 1972 (M_b 5.6 Managua earthquake on 23 December), and that is thought to be a boundary between western and eastern Nicaragua lithospheric segments (Stoiber and Carr, 1973). Masaya's magma is tholeiitic basalt, and the complex is in a section of Central America where the crust is relatively thin (Carr, 1984).

GEOLOGIC HISTORY

The Masaya Caldera (fig. 14.5.1) formed as a result of plinian eruptions of tholeiitic basalt (Bice, 1980, 1985; Williams, 1983a, b). Masaya is a basaltic shield volcano situated within the caldera and has several striking, steep-walled craters at its summit.

MASAYA (continued)

HISTORICAL ACTIVITY

Strong earthquakes were felt at 1030 hr on 16 March 1772, and at the same time observers saw fire and flying rocks (Sapper, 1925). After a series of earthquakes from 25 April to 11 May 1858, a small eruption occurred on 10 November 1858 (von Wolff (1929) says 10 September). After an earthquake on 25 June 1902, rumbling continued until 6 July, and on 15 July Santiago Crater began to emit steam and ash. Another eruption, on 3 or 5 January 1906, began after a series of earthquakes from 31 December 1905 through 5 January 1906 (Sapper, 1925; von Wolff, 1929). There is an unconfirmed report of an earthquake and activity at Santiago on 12 July 1913.

Episodes of greatly increased SO_2 emissions have occurred at Masaya about every 25 years since at least 1850. Strong outgassing is known to have occurred during 1852-59, 1902-06, 1919-27, 1947-59, and 1979 through the time of this writing (December 1987) (Williams and Stoiber, 1983; Stoiber and others, 1986; Smithsonian Institution, 1985-88). During each episode, crops (and human health?) in the area suffer considerable damage. Gases emerge from a NW-SE trending fissure system. These gas-emission events seem to occur after periods of eruptions and continue until the crater floor collapses and in most instances blocks off further gas emission. Relatively small collapses of the walls of Santiago's inner crater began in November 1986; by December 1987 and January 1988 a continuation of that activity together with collapse of the floor of adjacent Nindiri crater was merging the two craters into a single, larger crater. Gas emission remained vigorous and new magma may have been intruded beneath at least Santiago crater (Smithsonian Institution, 1987, 1988). Seismic swarms in and near the Masaya Caldera are relatively common (D. Harlow, oral commun., 1983).

COMMENTS

By comparing outgassing of SO_2 with the known concentration of sulfur in Masaya magma, Stoiber and others (1986) estimated that approximately 10 km^3 of basaltic magma had been degassed at Masaya since 1875. Comparison of this estimate with the volume of lava erupted since the Spanish Conquest (1524) (ca. 33×10^6 m^3) suggests that >99 percent of Masaya's magma is never erupted. Adding the erupted and intruded products, Stoiber and others (1986) estimated that basaltic magma supply to Masaya has been approximately 0.1 km^3/yr since 1875, a rate comparable to that of Kilauea and Etna.

REFERENCES

Bice, D.C., 1980, Tephra stratigraphy and physical aspects of Recent volcanism near Managua, Nicaragua: Berkeley, Univ. Calif., Ph.D. dissertation, 422 p.

----- 1985, Quaternary volcanic stratigraphy of Managua, Nicaragua: correlation and source assignment for multiple overlapping plinian deposits: Geol. Soc. Am. Bull., v. 96, p. 553-566.

Carr, M.J., 1984, Symmetrical and segmented variation of physical and geochemical characteristics of the Central American volcanic front: Jour. Volcanol. Geotherm. Res., v. 20, p. 231-252.

MASAYA (continued)

REFERENCES (continued)

McBirney, A.R., 1956, The Nicaraguan volcano Masaya and its caldera: Trans. Am. Geophys. Union, v. 37, p. 83-96.

Mooser, F., Meyer-Abich, H., and McBirney, A.R., 1958, Catalogue of active volcanoes of the world including solfatara fields, Part VI, Central America: Naples, IAVCEI, 146 p.

Sapper, K., 1925, Los volcanes de la América Central: Halle, Max Niemeyer, 116 p.

Smithsonian Institution, Scientific Event Alert Network (SEAN), 1985-88, Masaya Volcano: SEAN Bull., v. 10, no. 11, v. 11, no. 11; v. 12, no. 5; v. 13. no. 1 (contributions from D. Fajardo, P. Hradecky, and H. Taleno (INETER), B. van Wyk de Vries, H. Rymer, G. Brown, and others).

Stoiber, R.E., and Carr, M.J., 1973, Quaternary volcanic and tectonic segmentation of Central America: Bull. Volcanol., v. 37, no. 3, p. 304-325.

Stoiber, R.E., Williams, S.N., and Huebert, B.J., 1986, Sulfur and halogen gases at Masaya Caldera Complex, Nicaragua: Total flux and variations with time: Jour. Geophys. Res., v. 91, no. B12, p. 12,215-12,231.

Ui, T., 1972, Recent volcanism in Masaya-Granada area, Nicaragua: Bull. Volcanol., v. 36, p. 174-190.

Williams, S.N., 1983a, Geology and eruption mechanisms of Masaya Caldera complex: Hanover, N.H., Dartmouth Coll., Ph.D. dissertation, 169 p.

----- 1983b, Plinian airfall deposits of basaltic composition: Geology, v. 11, no. 4, p. 211-214.

Williams, S.N., and Stoiber, R.E., 1983, Volcanic hazards at Masaya Caldera complex, Nicaragua [abs.]: Abstracts, 18th Gen. Assembly, IUGG, Hamburg, v. 1, p. 359.

Wolff, F. von, 1929, Der Vulkanismus: Stuttgart, F. Enke, v. 2, p. 449.

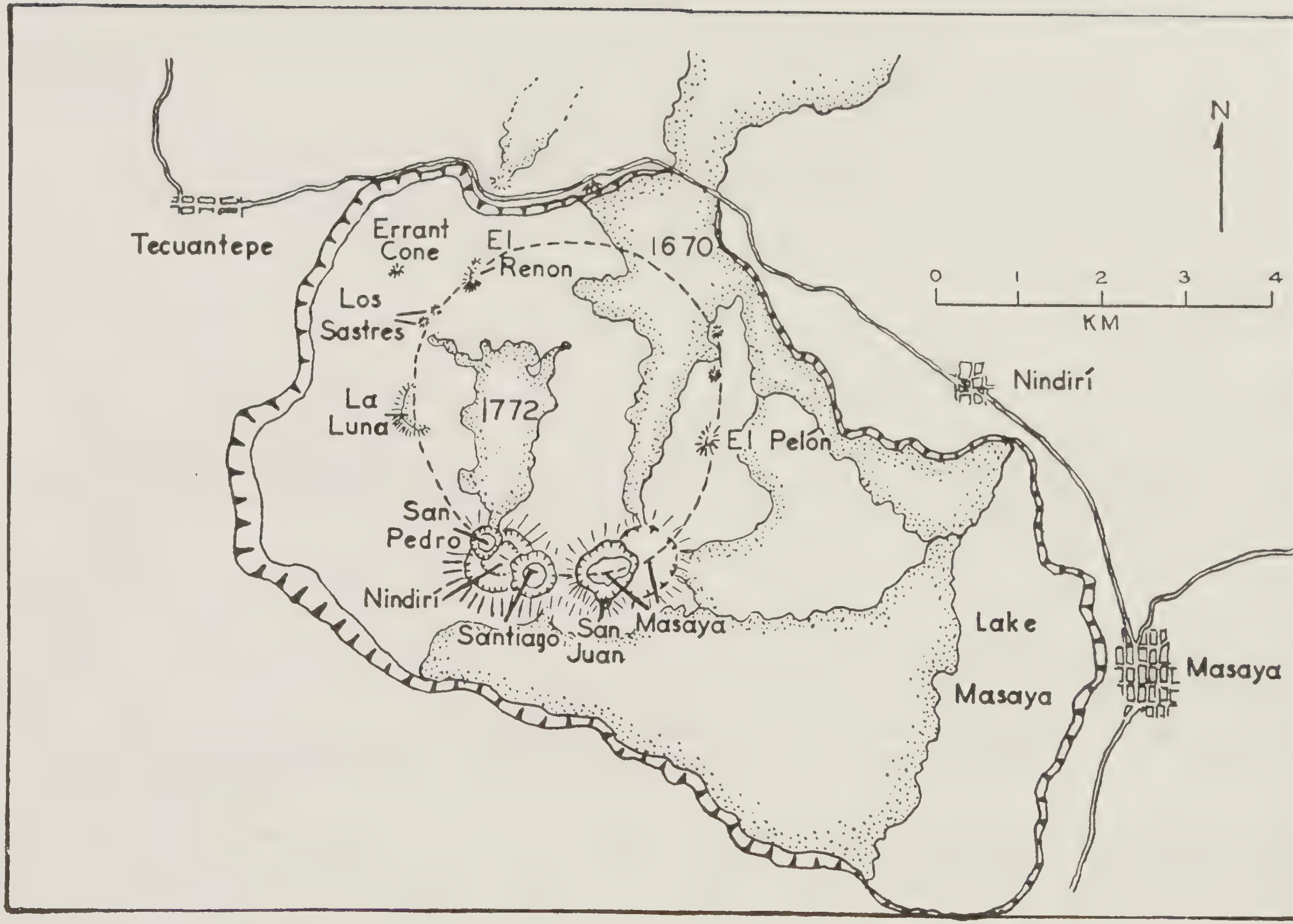

Figure 14.5.1. Sketch map of Masaya Caldera, from Mooser and others (1958). Dashed line shows circular pattern of young postcaldera vents.

APOYO

CAVW number (active vent)	Latitude Longitude (degrees)	Diameter (km)	Local tectonic setting	Precaldera edifice	SiO_2 content (wt pct)	Age of collapse (yr B.P.)	Date of unrest	Type and duration of unrest ESTU STHF MGTF H Te	Eruption type
14-04-101 (Apoyo)	11.92N 86.03W	6.5	Exten	Shield	R = a	23,000	1974	DD-- ---- ---- - QU?	none
					C = 66	21,000	1977	DD-- ---- ---- - --	none
							1978	DD-- ---- ---- - --	none
							1979	DD-- ---- ---- - --	none
							1981	DD-- ---- ---- - --	none
							1986	DD-- ---- ---- - QU?	none

TECTONIC SETTING

Apoyo Caldera (figs. 14.6.1, 14.6.2) lies within the NW-SE Nicaraguan Depression, at its intersection with a N-S graben (Sussman, 1985). Several of the N-S graben faults pass through and just east of Apoyo Caldera, between the caldera and the town of Granada.

GEOLOGIC HISTORY

Basaltic and andesitic lava flows built a broad shield during the Pleistocene, and dacitic domes intruded that pile, one approximately 90,000 yr B.P. Shortly before collapse, tholeiitic basalt lavas and scoria were erupted along N-S fractures cutting the shield and a pyroclastic plateau to the east of Apoyo. From about 23,000 to 21,000 yr B.P., about 11 km^3 of dacite magma was erupted in two Plinian eruptions, resulting in caldera collapse. A small volume of postcaldera andesitic lava was extruded along the ring faults, and the Granada cinder cones grew along a fissure about 2 km east of Apoyo (Walker, 1981, 1982; Sussman, 1985).

HISTORICAL ACTIVITY

Based on a catalog of Nicaraguan earthquakes (D.J. Leeds, cited in Martinez H., 1976), seismic activity occurred in the vicinity of Apoyo Caldera in 1529, 1536, 1570, 1772, 1856-59, 1870, and 1973. Some or even most of this seismicity was probably of regional tectonic origin, in the broader Masaya-Apoyo area. On 23 December 1972, three damaging tectonic earthquakes (largest, $\underline{M}_b$=5.6) struck Managua, 40 km northwest of Apoyo (Brown and others, 1973); no aftershocks occurred in the Apoyo area. However, seismic swarms at Apoyo proper began in or before September 1974 and continued intermittently at least until 1986. At least 100 earthquakes occurred in early September 1974, of which 27 were felt and had $\underline{M}$=3.7 to 4.0; 5 others had similar magnitude but were not felt (Martinez H., 1976).

APOYO (continued)

HISTORICAL ACTIVITY (continued)

Continuous instrumental monitoring began in 1977, and new earthquake swarms were recorded in 1977, 1978, 1979, and 1981 (Shepherd, 1986). Epicentral locations were clustered southeast of the caldera and were probably associated with movement along one of the N-S graben faults noted above (fig. 14.6.3).

A $\underline{M}$=6 earthquake occurred on 16 December 1985, several tens of kilometers south of Apoyo (Shepherd, 1986). Aftershocks were felt in the Apoyo area for a short time, followed by quiet. However, a new local earthquake swarm began in the first few days of January 1986, with many felt shocks and earthquake sounds. Activity may have peaked on 9-10 January, and the Apoyo area returned to relative quiet by mid-February. Felt reports supplemented by locations of some of the later earthquakes in the swarm suggested that the swarm was centered along the earlier-mentioned active fault about 3 km east of the caldera (near the point labeled E in fig. 14.6.2). A UNESCO/UNDP mission to Nicaragua concluded that the earthquakes were of tectonic origin, like those of swarms of the previous decade. A volcanic eruption was deemed not imminent (Shepherd, 1986). The relation of the 1972 Managua earthquake and the December 1985 earthquake to subsequent unrest at Apoyo is not known.

During or before earthquakes in September and October 1974, the temperature of Laguna de Apoyo rose from an unknown value (a warm spring at the lake's west-northwest edge had a temperature of 30.5 °C in 1925) to more than 35 °C. During October and early November 1974, a period between earthquake swarms, the lake temperature dropped by nearly 10 °C, before rising to a stable value of about 32-33 °C that was maintained for at least several months thereafter. The SO_4 content of lake water rose from 19 ppm (1969 baseline) to 180 ppm in September 1974, declined over the October - early November period of decreasing lake temperature, and recovered somewhat thereafter (fig. 14.6.4). The concurrence of temperature and chemical changes with seismicity led Martinez H. (1976) to conclude that the unrest at Apoyo was at least partly of volcanic origin.

As of January 1988, the lake's surface temperature ranged from 28.2-29.1 °C (Smithsonian Institution, 1988).

REFERENCES

Bice, D.C., 1985, Quaternary volcanic stratigraphy of Managua, Nicaragua: correlation and source assignment for multiple overlapping plinian deposits: Geol. Soc. Am. Bull., v. 96, p. 553-566.

Brown, R.D., Jr., Ward, P.L., and Plafker, G., 1973, Geologic and seismologic aspects of the Managua, Nicaragua, earthquakes of December 23, 1972: U.S. Geol. Surv. Prof. Paper 838, 34 p.

Martinez H., M.A., 1976, Riesgos volcanicos en Nicaragua y resultados preliminares sobre una metodologia experimental en la predicción de sismos en la Laguna de Apoyo: Rev. Geofis., no. 5, Mexico, p. 73-82.

Mooser, F., Meyer-Abich, H., and McBirney, A.R., 1958, Catalogue of active volcanoes of the world including solfatara fields, Part VI, Central America: Naples, IAVCEI, 146 p.

APOYO (continued)

REFERENCES (continued)

Sapper, K., 1925, Los volcanes de la América Central: Halle, Max Niemeyer, 116 p.

Shepherd, J.B., 1986, Report on a mission to Nicaragua, Feb 9 to Feb 22, 1986: unpubl. rep. to United Nations Development Programme (UNDP) and United Nations Educational, Scientific, and Cultural Organization (UNESCO), 13 p.

Smithsonian Institution, Scientific Event Alert Network (SEAN), 1988, Apoyo Volcano: SEAN Bull., v. 13, no. 1, p. 12 (information from B. van Wyk de Vries and others).

Sussman, D., 1985, Apoyo Caldera, Nicaragua: a major Quaternary silicic eruptive center: Jour. Volcanol. Geotherm. Res., v. 24, p. 249-282.

Ui, T., 1972, Recent volcanism in Masaya-Granada area, Nicaragua: Bull. Volcanol., v. 36, p. 174-190.

Walker, J.A., 1981, Petrogenesis of lavas from cinder cone fields behind the volcanic front of Central America: Jour. Geol., v. 87, p. 721-739.

----- 1982, Volcanic rocks from the Nejapa and Granada cinder cone alignments, Nicaragua, Central America: New Brunswick, N.J., Rutgers Univ., Ph.D. thesis, 143 p.

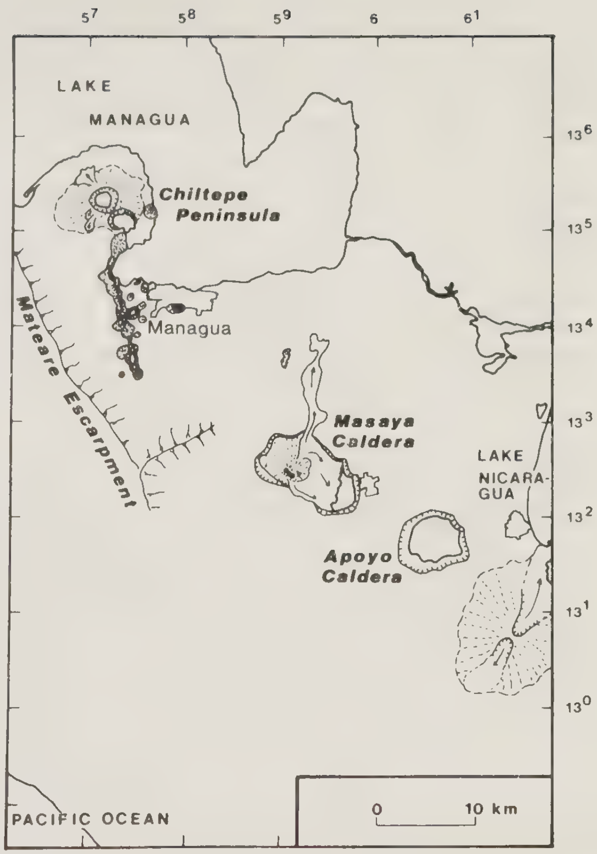

Figure 14.6.1. Principal geographic and volcanic features in central western Nicaragua, including Apoyo Caldera, from Bice (1985).

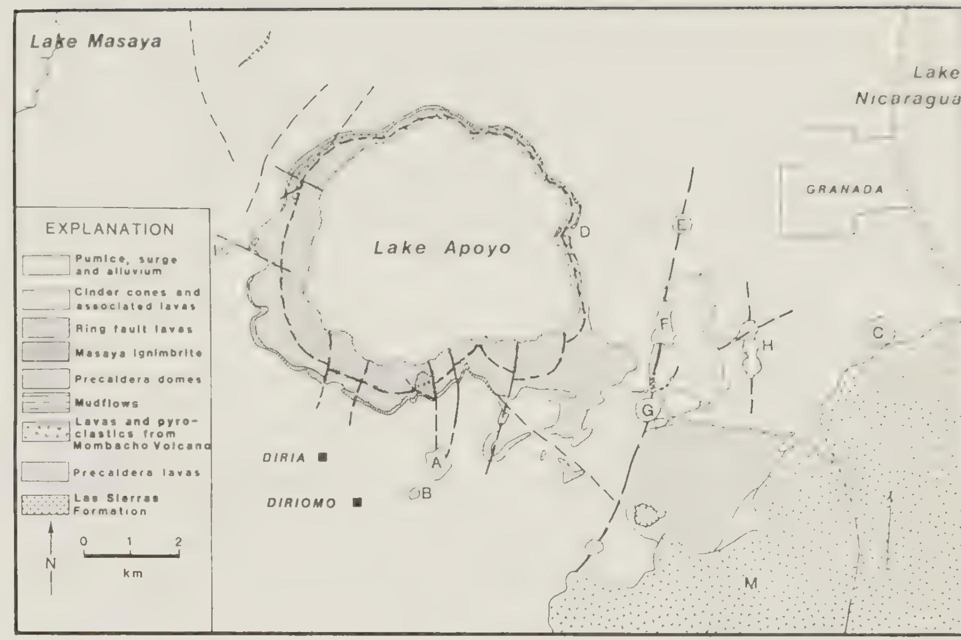

Figure 14.6.2. Simplified geologic map of Apoyo Caldera, from Sussman (1985). Heavy dashed lines denote faults. Patterns for units shown in inset; no pattern, undifferentiated Apoyo pyroclastic deposits (including airfall, ignimbrite, and pyroclastic surge), alluvium, and Masaya surge deposits. Letters refer to names of eruptive centers, as follows: A, El Cerrito dome; B, Cerritito dome; C, Lomo Poisentepe dome; D, Apoyoito dome; E, Granadito cinder cone; F, Cerro el Chanal cinder cone.

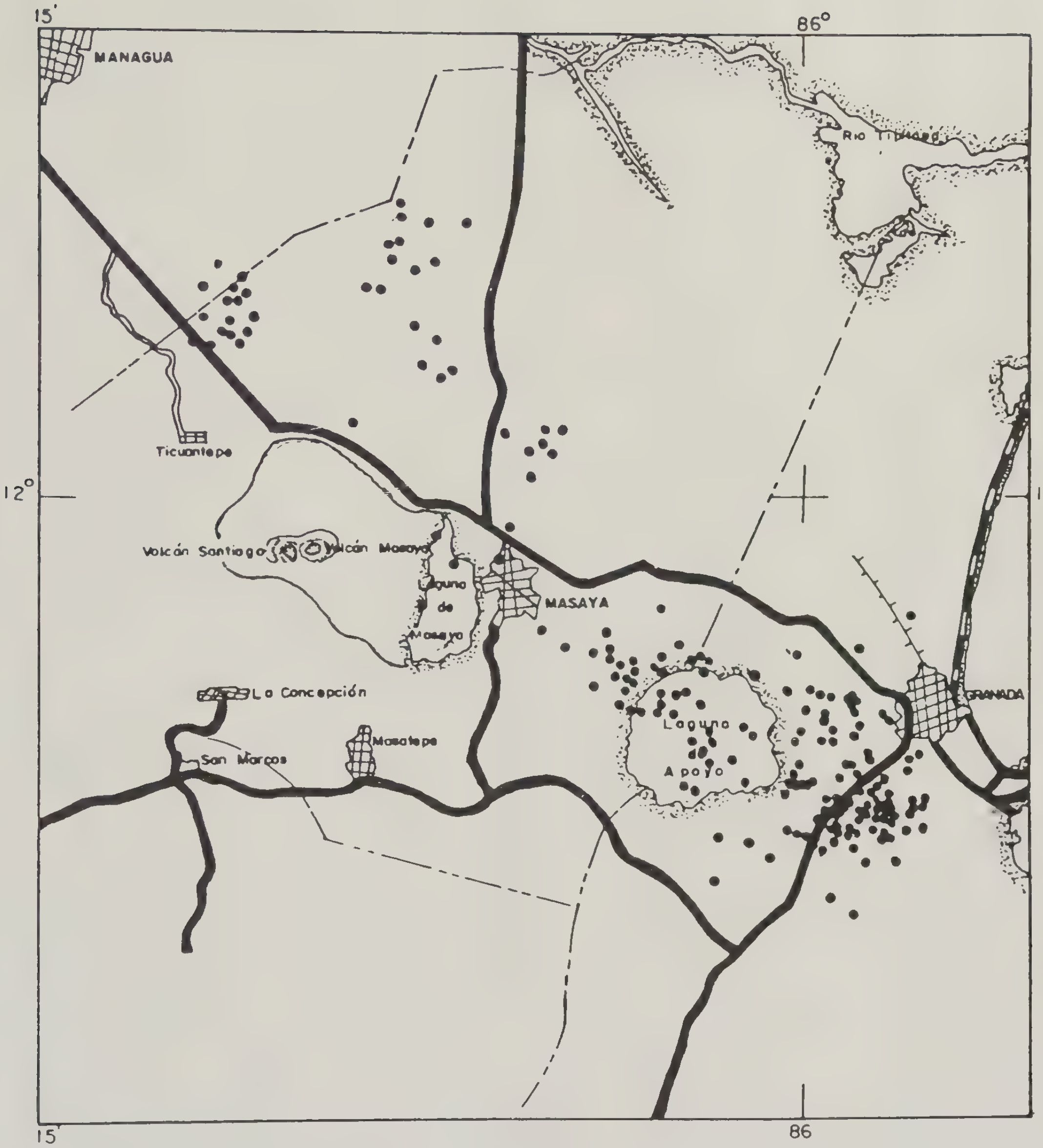

Figure 14.6.3. Location of earthquake epicenters near Apoyo Caldera, 1977 to 1981, after F. Seguro (unpubl. rep., 1982).

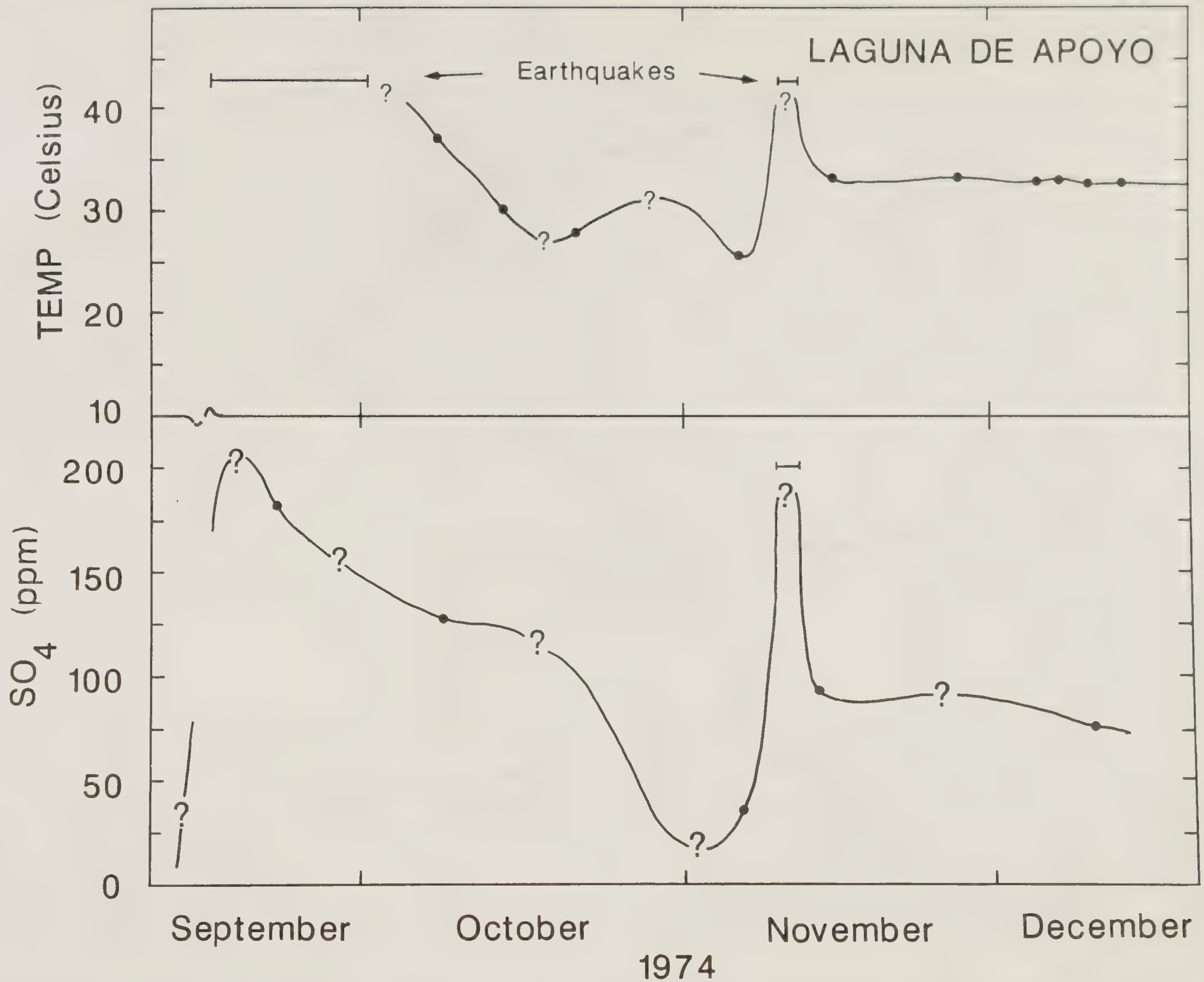

Figure 14.6.4. Temperature and SO_4 content at a sampling site at Lake Apoyo during September-December 1974, from Martinez H. (1976).

RINCON DE LA VIEJA

CAVW number (active vent)	Latitude Longitude (degrees)	Diameter (km)	Local tectonic setting	Precaldera edifice	SiO_2 content (wt pct)	Age of collapse (yr B.P.)	Date of unrest	Type and duration of unrest ESTU STHF MGTF H Te	Eruption type
14-05-02 (Rincón de la Vieja)	10.83N 85.33W	15-20 (outer)	Compr	Strato	R = 57-59		1860-63	---- ---- ---- - --	ex
					C = ?		1922	---- ---- ---C - --	ex
							1963	---- ---- ---x - --	none
		5 (inner)					1965-70	xx-- ---- ---E - --	pex, Ex
							1983-87+	---- ---- ---- - --	p-ex

TECTONIC SETTING

Rincón de la Vieja is situated along the volcanic front of Central America, at or just southeast of a postulated boundary between eastern Nicaragua and Costa Rican segments of the Cocos-Caribbean subduction zone (Stoiber and Carr, 1973).

GEOLOGIC HISTORY

Rincón de la Vieja, the largest volcano in northern Costa Rica, consists of six volcanic centers that form an elongate ridge, built on a shield of ignimbrites (fig. 14.7.1). Healy (1969) outlined a large, 15-20 km diameter caldera within which the present ridge-shaped volcano has grown. Carr and others (1986) concurred with this interpretation and outlined another nested, 5-km-diameter caldera on the Rincón de la Vieja edifice (fig. 14.7.1). A Rincón de la Vieja Caldera is not included in Barquero and Sáenz (1987).

HISTORICAL ACTIVITY

Most historical eruptions of Rincón de la Vieja have been vulcanian, Strombolian, or phreatic explosions from the central crater of the complex (Active Crater, see fig. 14.7.1).

1922: An observer (Don J. Fidel Tristán) found the volcano "active" on 11 April 1922 and with signs of a recent, grand eruption (Sapper, 1925). On 3 June of the same year, Tristán found strong SO_2 emission and a terrible noise from fumaroles; a large eruption occurred on 4 June.

1963: Strong steaming and sulfur gas emission were reported (Barquero, 1964).

RINCON DE LA VIEJA (continued)

HISTORICAL ACTIVITY (continued)

1965-70: Vapor "eruptions" in 1965 and September 1966 were followed by a moderately large ash eruption on 19 December 1966. On 23 February 1967, 28 eruptions occurred within 30 minutes, and nearby villages were evacuated (Thorpe and others, 1985). Bombs that were probably from this eruption have 57-59 percent silica (Carr and others, 1986). Small ash eruptions occurred until 1970.

1983-87+: Small phreatic explosions occurred in 1983 and 1984. Eruptions on 6 and 21 February 1983 produced one or more directed steam blasts that impacted areas up to 2 km south and east of the crater. An eruption on 31 March 1984 produced some blocks that might have been juvenile (Thorpe and others, 1985). Additional eruptions probably occurred between September and November 1985, judging from increased seismicity during that time. A small explosion occurred on 31 December 1986, and yet another on 1 April 1987 (Barquero and Segura, 1983; Thorpe and others, 1985; Smithsonian Institution, 1987).

REFERENCES

Barquero, J., 1964, El volcán Rincón de la Vieja: Inst. Geogr. Nac., Informe Semestral, San Jose, v. 10, p. 11-16.
Barquero H., J., and Sáenz R., R., 1987, Aparatos volcanicos de Costa Rica: Observatorio Vulcanologico y Sismologico de Costa Rica, Universidad Nacional, Heredia, 1 map sheet, scale 1:750,000.
Barquero, J., and Segura, J., 1983, La actividad del volcán Rincón de la Vieja: Bol. Vulcanol., no. 13, p. 5-10.
Carr, M.J., Chesner, C.A., and Gemmell, J.B., 1986, New analyses of lavas and bombs from Rincón de la Vieja volcano, Costa Rica: Bol. Vulcanol., no. 16, p. 23-30.
Healy, J., 1969, Notas sobre los volcanes de la sierra volcanica de Guanacaste, Costa Rica: Inst. Geogr. Nac., Informe Semestral, v. 15, p. 37-47.
Mooser, F., Meyer-Abich, H., and McBirney, A.R., 1958, Catalogue of active volcanoes of the world including solfatara fields, Part VI, Central America: Naples, IAVCEI, 146 p.
Sapper, K., 1925, Los volcanes de la América Central: Halle, Max Niemeyer, 116 p.
Smithsonian Institution, Scientific Event Alert Network (SEAN), 1987, Rincón de la Vieja Volcano: SEAN Bull., v. 12, nos. 2, 4 (information from Jorge Barquero H.).
Stoiber, R.E., and Carr, M.J., 1973, Quaternary volcanic and tectonic segmentation of Central America: Bull. Volcanol., v. 37, no. 3, p. 304-325.
Thorpe, R., Brown, G., Rymer, H., Barritt, S., and Randal, M., 1985, Recent volcano monitoring in Costa Rica: Earthq. Info. Bull., v. 17, no. 2, p. 44-49.

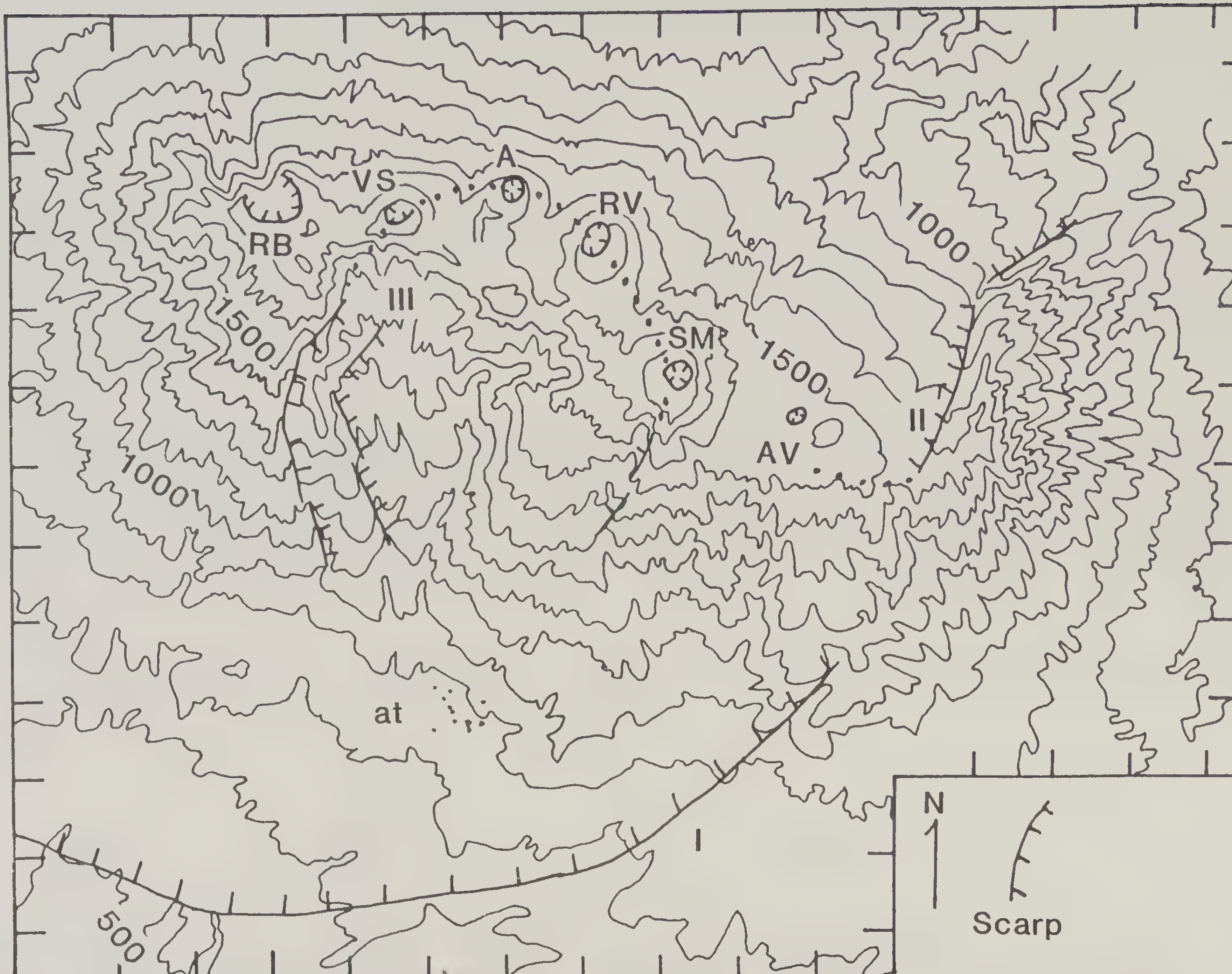

Figure 14.7.1. Topographic map showing outline of a large caldera (I and II) in which Rincón de la Vieja Volcano has grown and a nested caldera (III) on volcanic edifice (Carr and others, 1986). Vents: RB, deeply eroded cone drained by Rio Blanco; VS, Crater von Seebach; A, Active Crater; RV, Rincón de la Vieja; SM, Santa Maria; AV, double cone drained by Rio Aguas Verdes; at, prominent hot-spring area. Spacing between ticks at margins of map is 1 km.

PART 3: HISTORICAL UNREST AT LARGE QUATERNARY CALDERAS (continued)
See inside back cover for explanation and abbreviations

MIRAVALLES

CAVW number (active vent)	Latitude Longitude (degrees)	Diameter (km)	Local tectonic setting	Precaldera edifice	SiO_2 content (wt pct)	Age of collapse (yr B.P.)	Date of unrest	Type and duration of unrest ESTU STHF MGTF H Te	Eruption type
14-05-03	10.75N 85.15W	15 x 20	Compr; local extension, graben	Strato	R = 50-56 C = r	500,000 ±150,000	1946	xx-- ---- --?x - --	"steam eruption"

TECTONIC SETTING

Miravalles is situated along the volcanic front of Central America, just southeast of a postulated boundary between eastern Nicaragua and Costa Rican segments of the Cocos-Caribbean subduction zone (Stoiber and Carr, 1973).

GEOLOGIC HISTORY

Miravalles Caldera formed approximately 0.5 ± 0.15 m.y. ago (Tournon, 1984), after eruption of voluminous silicic ash flows. An andesitic stratovolcano of the same name grew within the caldera (Healy, 1969). At least five cones are recognizable in the summit area, distributed along a northeast-trending line (probable fault). The modern intracaldera cone may be the second of two; a previous postcaldera cone was destroyed (R. Fournier, oral commun., 1987). Melson and others (1986) note a preliminary age of 8,000(?) yr B.P. for a major plinian eruption from Miravalles, and an age of 7,000(?) yr B.P. for a large debris avalanche from Miravalles. A geothermal field is situated between the caldera scarp and Miravalles stratovolcano (fig. 14.8.1).

HISTORICAL ACTIVITY

No significant eruption has occurred at Miravalles in historical time. However, on 14 September 1946, a small steam eruption occurred high on the south flank of the volcano, near the summit crater. Weak earthquakes were felt at the time. An explosion crater 20 m in diameter formed, and steam, mud, and ash were thrown 100 m high (Hantke, 1951, citing a letter from Sigismund von Preussen of the town of La Barranca). The hydrothermal field is a hot-water-dominated system, with a vapor-dominated cap (few tens of meters thick) in some parts of the geothermal field. Changes in the vapor-dominated cap can give rise to surface hydrologic changes and small blowouts. Fumarolic activity has reportedly decreased in recent years (as of late 1987) (R. Fournier, oral commun., 1987).

MIRAVALLES (continued)

REFERENCES

Barquero H., J., and Sáenz R., R., 1987, Aparatos volcanicos de Costa Rica: Observatorio Vulcanologico y Sismologico de Costa Rica, Universidad Nacional, Heredia, 1 map sheet, scale 1:750,000.

Hantke, G., 1951, Uebersicht über die vulkanische tätigkeit, 1941-1947: Bull. Volcanol., v. 11, p. 161-208.

Healy, J., 1969, Notas sobre los volcanes de la sierra volcanica de Guanacaste, Costa Rica: Inst. Geogr. Nac., Informe Semestral, v. 15, p. 37-47.

Melson, W.G., Barquero H., J., Sáenz R., R., and Fernandez, E., 1986, Erupciónes explosivas de importancia en volcanes de Costa Rica: Bol. Vulcanol. (Costa Rica), no. 16, p. 15-19.

Stoiber, R.E., and Carr, M.J., 1973, Quaternary volcanic and tectonic segmentation of Central America: Bull. Volcanol., v. 37, no. 3, p. 304-325.

Tournon, J., 1984, Magmatismes du Mesozoique a l'actuale en Amerique Centrale: L'example de Costa Rica, des ophiolites aux andesites: Paris, Université Pierre et Marie Curie, D.Sc. thesis.

Figure 14.8.1. Miravalles Caldera and nearby volcanoes, from Barquero and Sáenz (1987). The postulated Rincón de la Vieja Caldera is located 5-10 km west-northwest of Miravalles Caldera. 1, El Hacha; 2, Orosi; 3, Cacao; 4, Fortuna; 5, Sn. Roque; 6, Cañas Dulces; 7, Cerro Gorgona; 8, Sn. Vicente; 9, Braun; 10, Von Seebach; 11, Rincón I; 12, Rincón II; 13, Rincón III; 14, Sta. María I; 15, Sta. María II; 16, Sta. María III; 17, Miravalles Caldera; 18, Miravalles I; 19, Miravalles II; 20, Miravalles III; 21, Miravalles IV; 22, Olla de Carne; 23, Bijagua I; 24, Bijagua II; 25, Montezuma; 26, Tenorio I; 27, Tenorio II; 28, C. Barrera; 29, C. Annunciación; 30, C. Tilarán; 31, C. Pelado y Delicias.

POAS

CAVW number (active vent)	Latitude Longitude (degrees)	Diameter (km)	Local tectonic setting	Precaldera edifice	SiO_2 content (wt pct)	Age of collapse (yr B.P.)	Date of unrest	Type and duration of unrest ESTU STHF MGTF H Te	Eruption type
14-05-04	10.20N	7 x 10	Compr	Strato	R = 50-63	<40,000;	1826-28	x--- ---- ---? - --	Pex,Ex?
(Poás)	84.22W	(outer)			C = 52-54	>7,540	1834	---- ---- ---- - --	Ex
		3					1838	---- ---- ---- - --	ex
		(inner)					1880	---- ---- ---- - --	Pex,Ex?
							1884	---- ---- ---- - --	pex
							1888-89	x--- ---- --xx x UQ/QU?	pex,geyser
							1899	---- ---- ---- x --	geyser
							1902-05	---- ---- ---- - --	geyser
							ca. 1907-08	---- ---- ---- - --	pex
							1910	x--- ---- ---- - UQ	Pex,Ex
							1912	?--- ---- ---- - QU	landsl
							1914-15	---- ---- ---- - --	pex,geyser
							1925	---- ---- ---- - --	pex
							1929?	---- ---- ---- - --	geyser?
							1946	---- ---- ---- - --	pex
							1952-57	B--- ---- ---- - --	geyser,pex,Ex
							1961	---- ---- ---- - --	pex
							1963-64	---- ---- ---- - --	pex, ex
							1967	---- ---- ---- - --	pex
							1969	---- ---- ---- - --	pex
							1972-73	---- ---- ---- - --	ex
							1974-75	---- ---- ---- - --	pex
							1976-80	---- ---- ---- - --	pex, ex
							1980-86	---- ---- --FF - --	none
							1987-88	x--- ---E --EE - --	pex

TECTONIC SETTING

Poás is situated near the southeastern end of the Central American arc, above the Cocos-Caribbean subduction zone. Cinder cones are strongly aligned in a N-S direction.

POAS (continued)

GEOLOGIC HISTORY

Two calderas, one nested within the other, developed in the summit area of Poás (fig. 14.9.1) (Thorpe and others, 1981). The younger, smaller collapse occurred less than 40,000 yr B.P. but more than 7,540 yr ago (a ^{14}C date on the postcaldera Botos cone) (Prosser, 1983, 1985; Prosser and Carr, 1987). The modern cone of Poás has grown within and nearly obscured the two calderas; only the flat-topped morphology of Poás belies its calderas. The summit of the modern cone has a main crater that may contain a sulfur-rich lake with a layer of molten sulfur at its base (Bennett and Raccichini, 1978; Francis and others, 1980).

The magma erupted to form the younger caldera has been tentatively identified as basaltic andesite (Prosser and Carr, 1987); magma associated with the earlier caldera-forming eruption is not known. A mafic composition is consistent with the lack of a major gravity low in the area of the caldera and the existence of a local gravity high at Poas's summit. Tournon (1984) presented analyses of basalt, andesite, and low-silica dacite--samples that may span the time(s) of caldera formation.

HISTORICAL ACTIVITY

Most historical eruptions of Poás have been small, phreatic or magmatic, sometimes including molten sulfur. In the 19th century, eruptions of 1828, 1834, and 1880 were relatively large, showering nearby towns with ash (Sapper, 1925). In the 20th century, relatively large eruptions occurred in 1910 and 1953. The eruption of 1910 began as a large geyser eruption on 25 January, when a plume rose to more than 8-km altitude (Sapper, 1925). The entire upper part of the volcano was covered with a thick layer of mud. A period of few observations followed, but by March at least 20 areas of small mud eruptions could be seen in the crater lake. On 13 April, strong earthquakes occurred (at least 23 from 0037 hr to 0815 hr), followed by quiet until additional earthquakes occurred at 1311 hr, 1500 hr, and 2200 hr. Twenty-four earthquakes were reported on 14 April, and 12 on 15 April. Then an especially strong earthquake struck on 4 May, causing severe damage in San Jose and Cartago. During the night of 13-14 May, some observers reported seeing flames from Irazu or Poás (in opposite directions from San Jose!). Two years later, on 6 June 1912, a strong earthquake occurred at shallow depth beneath an old crater, Laguna Vieja, 5 km west of Poás (Sapper, 1925).

During the 1953 eruption, phreatic explosions started at two sublacustrine vents, and the eruption gradually evolved from phreatomagmatic to Strombolian as the crater lake disappeared. The tallest eruption column reached 7 km above the crater and spread ash at least 50 km from the volcano.

An eruption in 1976 sent a column 3 km above the vent; activity in 1978-80 was limited to geyser eruptions. Fumarole temperatures then rose dramatically between September 1980 and March 1981--from about 90 °C to 960 °C (fig. 14.9.2) (Barquero, 1983). Glowing spots were first noted on the small intracrater cone in January 1981. Temperatures dropped only slightly from March 1981 to October 1983 (801 °C), but then cooled to 723 °C by December 1983, to 515 °C by December 1984, to 287 °C by December 1985, and to approximately 300 °C through early 1986 (Barquero and others, 1985; Fernandez and others, 1986; Barquero and Fernandez, 1986). The temperature of another fumarole, near the top of a cone inside the crater, was 530 °C in early 1986, rose to 680 °C by July 1986, declined gradually to 540 °C in January-May 1987, rose to 590 °C before the start of small phreatic eruptions in July 1987, and then

POAS (continued)

HISTORICAL ACTIVITY (continued)

declined to 470 °C or lower by February 1988 (the time of this writing). Small phreatic eruptions continued despite the decrease in temperature (Barquero and Fernandez, 1986; J. Barquero and R. Sáenz, written commun., 1987; Smithsonian Institution, 1988) (fig. 14.9.2).

The crater lake grew hotter in parallel with the subaerial fumarole temperatures, reaching 51 °C in June 1981 and 60 °C in early 1983 (some variability related to seasonal fluctuation in rainfall). Then the lake, too, cooled. Its temperature dropped to 45.5 °C by the end of 1985 and 38 °C in the first half of 1986, but it then rose again to 56 °C by December 1986 (Barquero and Fernandez, 1987). The maximum recorded lake temperature in January 1988 was 61 °C (Smithsonian Institution, 1988). The pH of the lake increased between May and September 1983 from 0.06 to 0.3; by early 1986 the pH of the lake was 0.5 and remained at that level through December 1986 (Barquero and Fernandez, 1986, 1987). SO_2 emission during the period of high fumarole temperatures was about 600 t/day (R.E. Stoiber, cited in Prosser, 1985).

Guendel (1981) showed an inverse correlation between the number of countable seismic events per day (20-140) and the duration of 3-4 Hz harmonic tremor (10^4 to 10^2 sec/day) during March-May 1981. He attributed that relation to rock fracturing (A- and B-type seismic events) under high gas pressure, followed by tremor as magma flows upward and degassing occurs. To better monitor these events, a permanent seismograph was installed in 1984.

Rymer and Brown (1984, 1987) noted fluctuation of gravity values on Poás, with a periodicity of about 30 days. Values changed by about 140 microgals at the crater rim and by 50 microgals on the south flank of Poás. Rymer and Brown interpret these variations as indicating movement of the magma column relative to the edifice or slight vesiculation of the magma--possibly tidally induced.

REFERENCES

Barquero, J., 1983, Termometria de la fumarola del Volcán Poas: Bol. Vulcanol., no. 13, p. 11-12.
Barquero H., J., and Fernandez, E., 1986, Estado de los volcanes de Costa Rica, Enero-Mayo 1986: Bol. Vulcanol., no. 17, p. 5-6.
----- 1987, Estado de los volcanes en Costa Rica, Junio-Diciembre 1986: Bol. Vulcanol., no. 18, p. 5-6.
Barquero H., J., Fernandez, E., and Van der Laat, R., 1985, Estado de los volcanes, Mayo 1983-Diciembre 1984: Bol. Volcanol., no. 15, p. 5-9.
Barquero, J., and Malavassi, E., 1984, Excursion al Volcán Poás, <u>in</u> Seminario vulcanologico conjunto USA-CR: Bol. Vulcanol., no. 14, p. 117-131.
Barquero H., J., Malavassi, E., and Araya, A., 1981, La actividad del volcán Poás en los años 1978-1980: Sumario de tres años del formulario de reporte diario de actividad: Bol. Vulcanol., no. 11, p. 10-12.
Bennett, F.D., and Raccichini, S.M., 1978, Subaqueous sulphur lake in Volcán Poás: Nature, v. 271, p. 342-344.
Boza, M.A., and Mendoza, R., 1981, The National Parks of Costa Rica: San Jose, Costa Rican Inst. of Tourism, 310 p.
Fernandez, E., Barquero, J., and Segura, J., 1986, Estado de los volcanes, Enero-Diciembre 1985: Bol. Vulcanol., no. 16, p. 5-14.

POAS (continued)

REFERENCES (continued)

Francis, P.W., Thorpe, R.S., Brown, G.C., and Glasscock, J., 1980, Pyroclastic sulfur eruption at Poás Volcano, Costa Rica: Nature, v. 283, p. 754-756.

Guendel, F., 1981, Estudio preliminar de las señales sismicas del Volcán Poás I.: Bol. Vulcanol., no. 11, p. 5-9.

Krushensky, R., and Escalante, G., 1967, Activity of Irazú and Poás Volcanoes, Costa Rica, November 1964-July 1965: Bull. Volcanol., v. 31, p. 75-94.

Locke, C.A., Brown, G.C., Thorpe, R.S., Cassidy, J., and Francis, P.W., 1985, Geophysical studies of Poas volcano: Bol. Vulcanol., no. 13, p. 89-94.

Mooser, F., Meyer-Abich, H., and McBirney, A.R., 1958, Catalogue of active volcanoes of the world including solfatara fields, Part VI, Central America: Naples, IAVCEI, 146 p.

Pittier, H., 1910, Costa Rica--Vulcan's Smith: Natl. Geogr., v. 21, p. 494-525.

Prosser, J.T., 1983, The geology of Poás Volcano, Costa Rica: Hanover, N.H., Dartmouth Coll., M.A. thesis, 165 p.

----- 1985, Geology and medium-term temporal magmatic variation found at the summit region of Poás Volcano, Costa Rica: Bol. Vulcanol., no. 15, p. 21-39.

Prosser, J.T., and Carr, M.J., 1987, Poás Volcano, Costa Rica: Geology of the summit region and spatial and temporal variations among the most recent lavas: Jour. Volcanol. Geotherm. Res., v. 33, p. 131-146.

Rymer, H., and Brown, G.C., 1984, Periodic gravity changes at Poás volcano, Costa Rica: Nature, v. 311, p. 243-245.

----- 1987, Causes of microgravity change at Poas volcano, Costa Rica: an active but non-erupting system: Bull. Volcanol., v. 49, p. 389-398.

Sáenz, R., 1982, Edades radiometricas de algunas rocas en Costa Rica: Bol. Vulcanol., no. 12, p. 8-10.

Sapper, K., 1925, Los volcanes de la América Central: Halle, Max Niemeyer, 116 p.

Smithsonian Institution, Scientific Event Alert Network (SEAN), 1987, 1988, Poas Volcano: SEAN Bull., v. 12, nos. 8, 12; v. 13, no. 1 (information from J. Barquero, R. Barquero, G. Alvarado, G. Soto, L.D. Morales, S. Mora, B. van Wyk de Vries, H. Rymer, and G. Brown).

Thorpe, R.S., Locke, C.A., Brown, G.C., Francis, P.W., and Randal, M., 1981, Magma chamber below Poás Volcano, Costa Rica: Jour. Geol. Soc. London, v. 138, pt. 3, p. 367-373.

Tournon, J., 1984, Magmatismes du Mesozoique a l'actuale en Amerique Centrale: L'example de Costa Rica, des ophiolites aux andesites: Paris, Université Pierre et Marie Curie, D. Sc. thesis.

Vargas, C.A., ed., 1979, Antologia: El Volcán Poás: v. 1, San Jose, Ed. Univ. Estatal a Distancia, 162 p.

Williams, H., 1952, Volcanic history of the Meseta Central Occidental, Costa Rica: Univ. Calif. Publ. Geol. Sci., v. 29, p. 145-180.

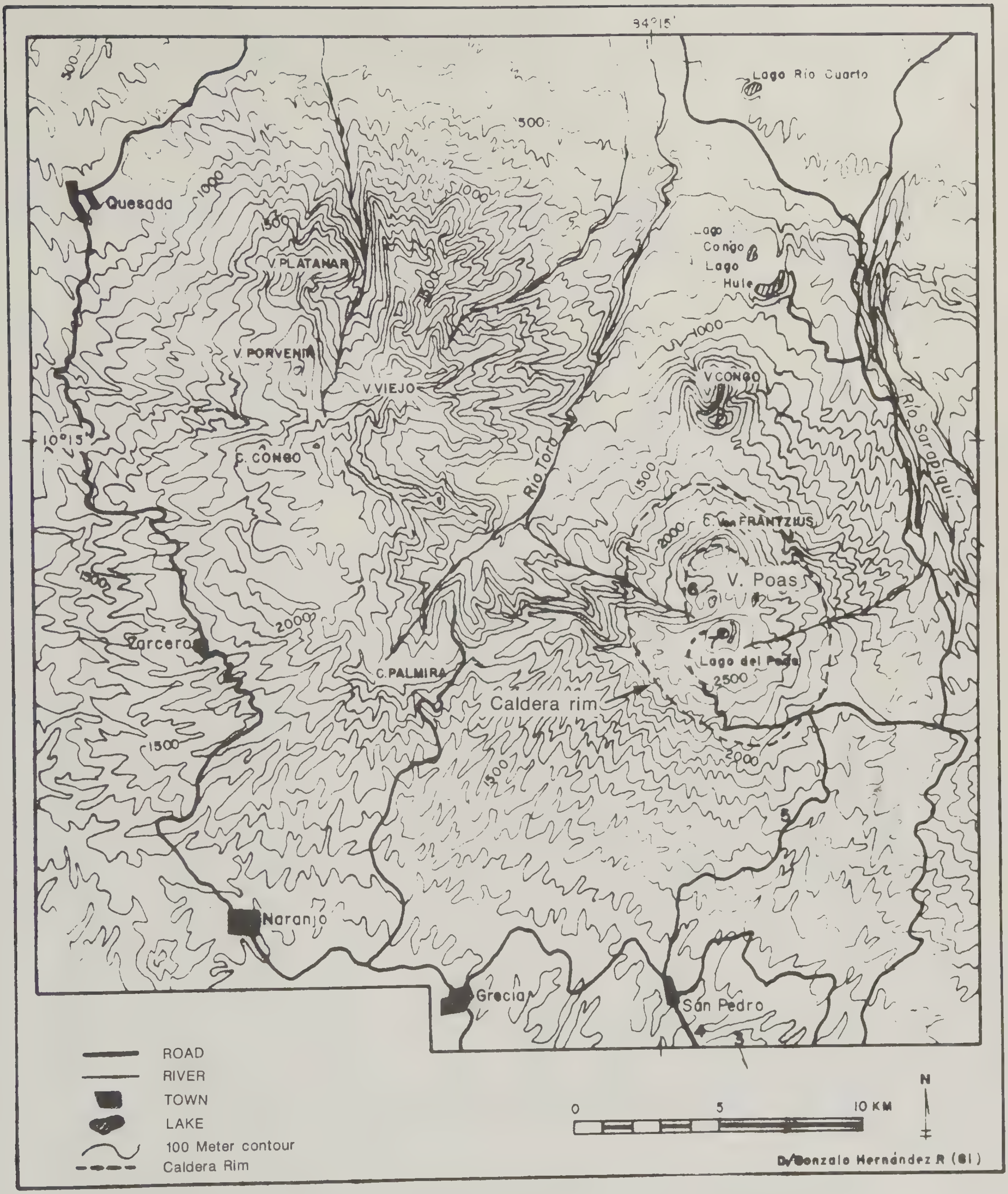

Figure 14.9.1. Location map showing Poás Caldera and V. Poás, after Barquero and Malavassi (1984).

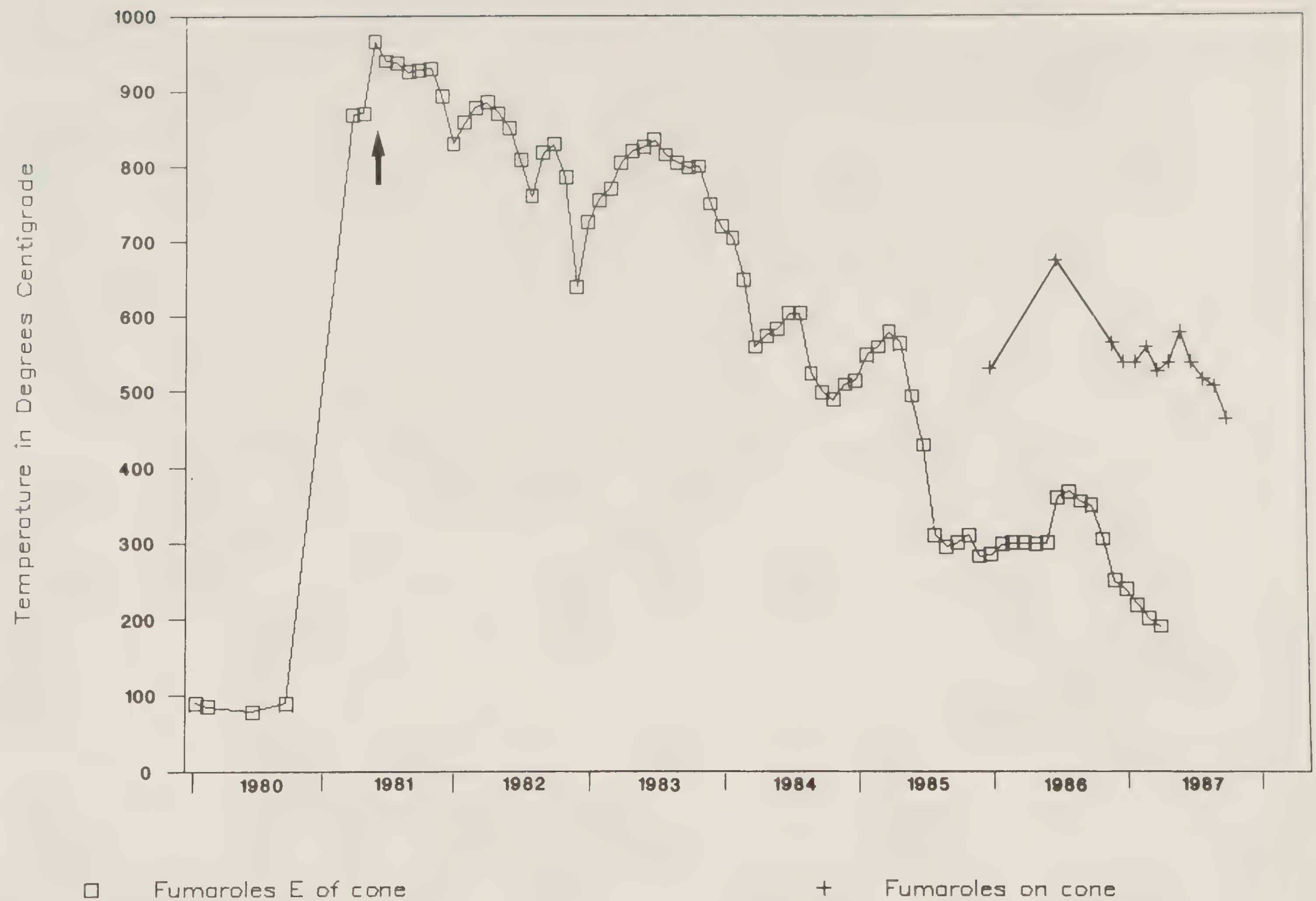

Figure 14.9.2. Changes in fumarole temperatures at V. Poás during 1980-87, from Barquero (1983) with more recent data provided by author. A small steam eruption occurred in May 1981 (arrow).

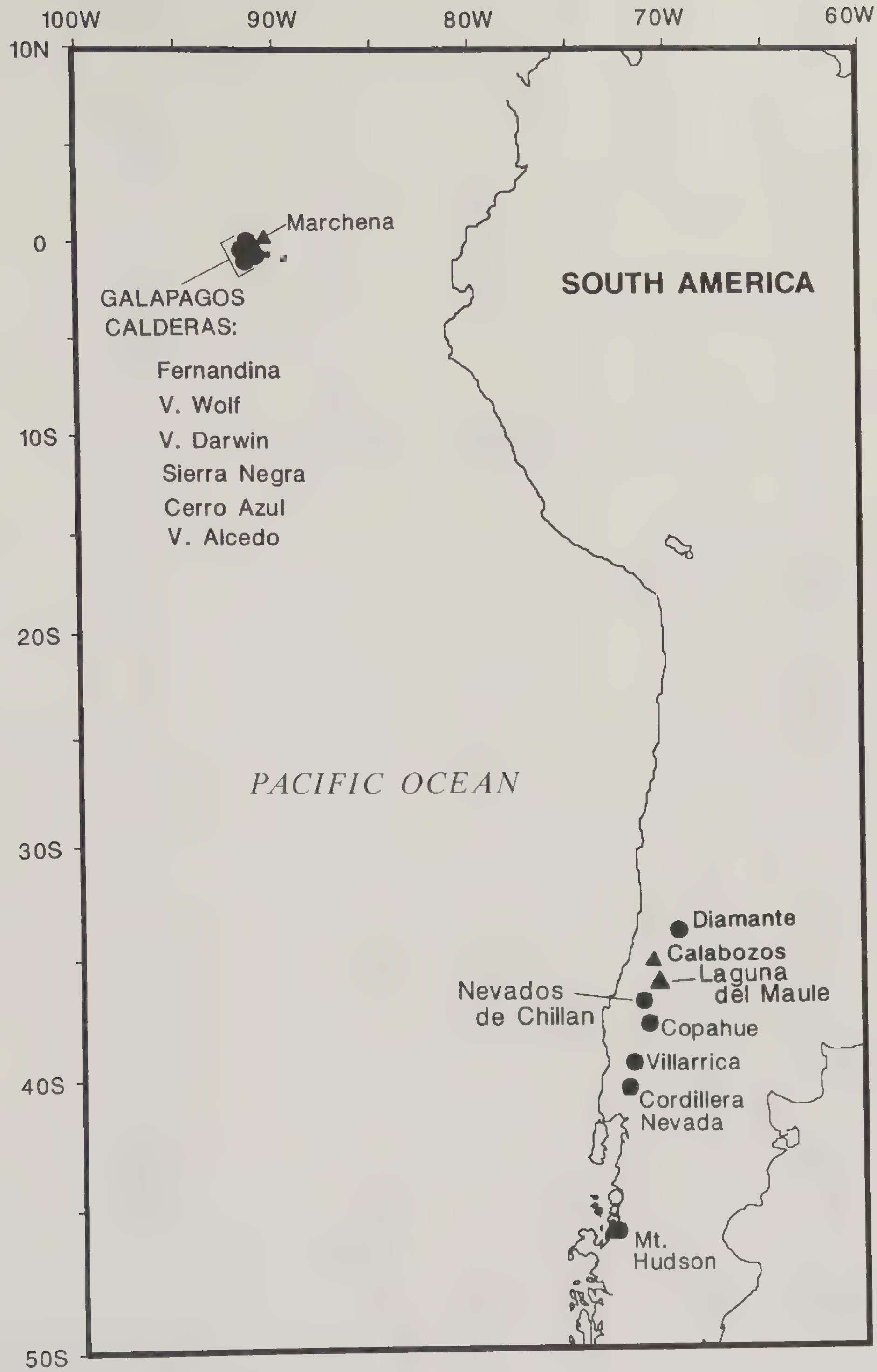

Figure 15. Locations of large, Quaternary restless calderas (solid circles) and nonrestless calderas (triangles) in Region 15.

FERNANDINA

CAVW number (active vent)	Latitude Longitude (degrees)	Diameter (km)	Local tectonic setting	Precaldera edifice	SiO_2 content (wt pct)	Age of collapse (yr B.P.)	Date of unrest	Type and duration of unrest ESTU STHF MGTF H Te	Eruption type
15-03-01 (Fernandina)	0.37S 91.55W	4 x 6.5	Intersection of lineaments over "hotspot"	Shield	R = 49 C = mafic	Renewed collapse in A.D. 1968	1813-14	---- ---- ---- - --	lf,ex
							pre-1817	---- ---- ---- - --	ex,lf
							1819	---- ---- ---- - --	ex,lf
							1825	---- ---- ---- - --	Ex,lf
							1846	---- ---- ---- - --	lf
							1888	---- ---- ---- - --	unknown
							1926-27	---- ---- ---- - --	lf
							1937	---- ---- ---- - --	lf
							1958	---- ---- ---- - --	lf,ll
							1961	---- ---- ---- - --	ex,lf
							1968	C--- Z--Z ---Z Z QU	ex,lf,EX
							1972	---- ---- ---- - --	ex,lf
							1973	---- ---- ---- - --	lf
							1974-76	E--F ---- ---- - --	none?
							1977-78	B--? ---- ---- - QU	ex,lf
							1981	---- ---- ---- - --	lf
							1984	---- ---- ---Y - --	lf,ex

TECTONIC SETTING

The Galápagos Islands (fig. 15.1.1A) lie on the Nazca plate just south of the Galápagos Ridge spreading center. They are also thought to overlie a mantle hotspot, presently beneath the volcanically active western Galápagos Islands (Simkin, 1984, and references therein).

GEOLOGIC HISTORY

Fernandina is a single shield volcano with a well-developed summit caldera (figs. 15.1.1B, 15.1.1C). Benches at both ends of the caldera record prehistoric episodes of collapse. A swarm of arcuate, circumferential fissures occur on the benchlike caldera rim; radial fissures are rare (McBirney and Williams, 1969; Simkin and Howard, 1970).

FERNANDINA (continued)

HISTORICAL ACTIVITY

1968: A M=4.5 earthquake occurred on 15 May 1968, 300 km north of Fernandina. A small flank eruption began 20 May and stopped within a few days. A slight increase in seismicity in the Galápagos region occurred in the last week of May and the first week of June 1968. The area was seismically quiet during 8-10 June; then, a few more earthquakes occurred on 11 June before a major explosive eruption from the caldera proper at 1040 hr on 11 June. Another sharp explosion occurred at 1708 hr on 11 June, and the eruption continued for another day or so. Beginning on 11 June, seismicity increased sharply as the caldera floor began to collapse (fig. 15.1.2). Collapse was asymmetric, like a trapdoor opening down to the southeast, where the maximum subsidence of 350 m was recorded. Seismicity reached its maximum on 19 June and ended on or about 23 June (Filson and others, 1973). The largest earthquake in the collapse event was of M=5.4; several hundred earthquakes were of M=4.0-5.4. Seismic energy release was remarkably constant over a 9-day period, indicating that the collapse took place regularly during this interval (Filson and others, 1973). Epicentral locations seemed to be skewed to the northeast of the caldera, between Fernandina and Isabela Island (fig. 15.1.3). However, Filson and others (1973) suggest that most were beneath the caldera and that their calculated epicenters are skewed to the northeast as an artifact of inaccurate estimates of seismic velocities between the caldera and distant recording stations. The volume of collapse was 1-2 km^3, much greater than the estimated 0.2 km^3 or less of erupted magma.

1974-76: Beginning in mid-1974, earthquakes and presumably concurrent uplift occurred at Punta Espinosa and across the straits at the foot of Darwin Volcano. Cumulative uplift at Punta Espinosa was 30 cm by the time it was first noticed in mid-September 1974, 6 weeks after a local earthquake. Uplift totaled 80-90 cm by February 1976, and no further uplift was noted between then and December 1980 (W.T. Kinoshita, oral commun., 1983; Simkin, 1984). This uplift is similar to but north of uplift that occurred in 1954 at Urvina Bay, at the west foot of V. Alcedo, 30 km south of V. Darwin and 30 km southeast of Punta Espinosa (see further discussion under V. Alcedo, CAVW number 15-03-04).

Another eruption of Fernandina occurred in August 1978, preceded and apparently triggered by a M=4.5 earthquake 1 hour before the eruption. This eruption was from the northwest margin of the caldera, unlike other eruptions since the 1968 collapse that occurred in the southeast end of the caldera (the end that experienced the maximum subsidence in 1968). A small eruption occurred at the rim sometime between 4 December 1980 and 26 March 1982, unnoticed at the time (Simkin, 1984).

1984: Noise and glow from the summit were noted on 30 March 1984, and further activity occurred within the crater at least through 11 April 1984 (Smithsonian Institution, 1984). SO_2 flux as estimated from the TOMS instrument in the NIMBUS 7 satellite peaked on 1 April and dropped below its detection threshold by 3 April (Smithsonian Institution, 1984).

FERNANDINA (continued)

REFERENCES

Filson, J., Simkin, T., and Leu, L., 1973, Seismicity of a caldera collapse: Galápagos Islands 1968: Jour. Geophys. Res., v. 78, p. 8591-8622.

McBirney, A.R., and Williams, H., 1969, Geology and petrology of the Galápagos Islands: Geol. Soc. Am. Memoir 118, 197 p.

Richards, A.F., 1962, Catalogue of active volcanoes of the world including solfatara fields, Pt. XIV, Archipelago de Colon (Galápagos), Isla San Felix, and Islas Juan Fernandez: Rome, IAVCEI, 50 p.

Simkin, T., 1984, Geology of Galápagos, in Perry, R., ed., Galápagos (key environments): Oxford, Pergamon Press, p. 15-41.

Simkin, T., and Howard, K.A., 1970, Caldera collapse in the Galápagos Islands, 1968: Science, v. 169, p. 429-437.

Smithsonian Institution, Scientific Event Alert Network (SEAN), 1978, 1984, Fernandina: SEAN Bull., v. 3, no. 8, p. 4; v. 9, no. 3, p. 15-16.

Volcanological Society of Japan, 1975, Fernandina: Bull. Volcanic Eruptions, no. 13, p. 66-67.

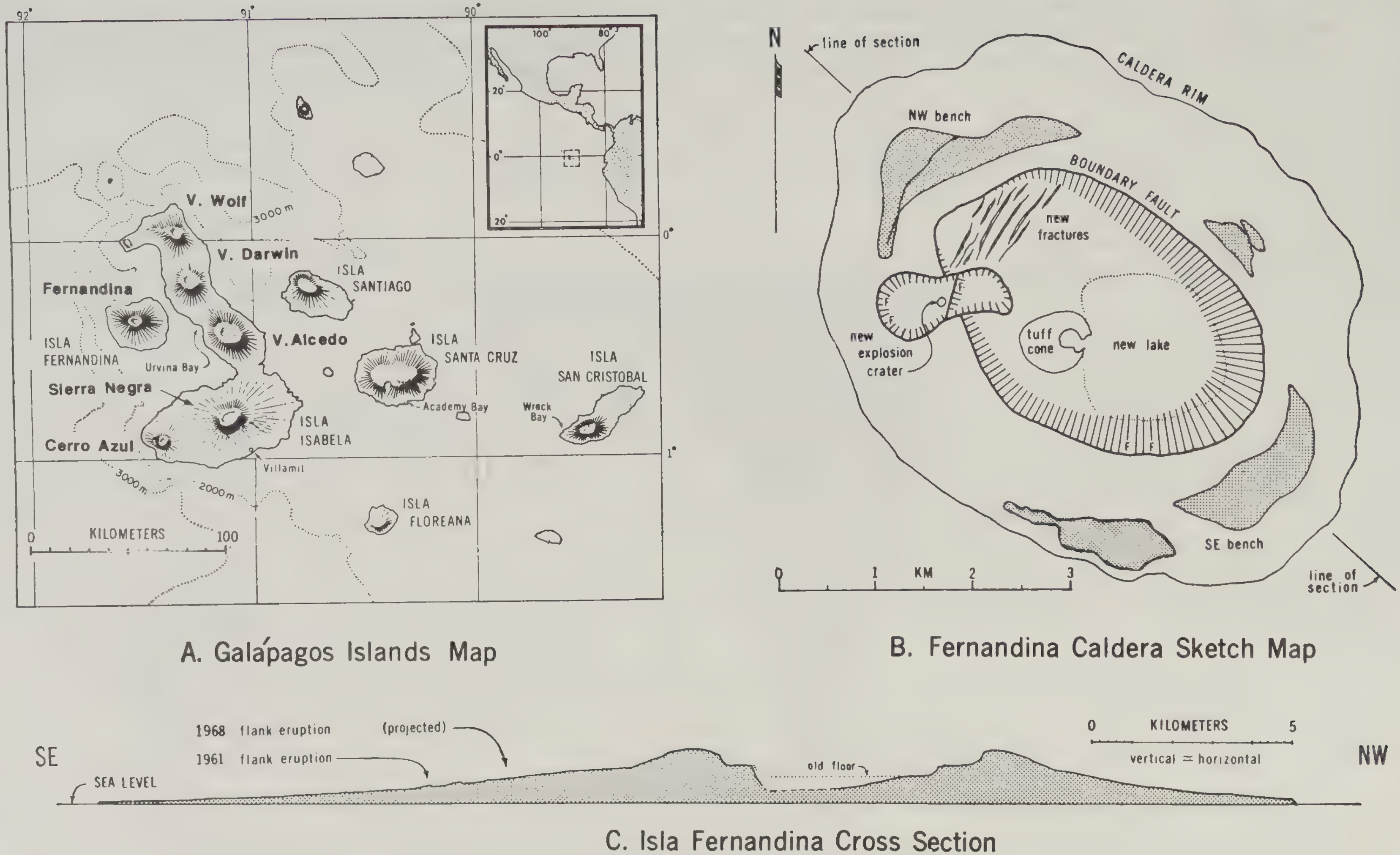

Figure 15.1.1. Location map (A), sketch map (B), and cross section (C) of Fernandina Caldera, from Simkin and Howard (1970). Additional information pertinent to sketch map (B) from Filson and others (1973). Subhorizontal benches are stippled. Prominent northwest and southeast benches, 350 m below the rim at 980-m elevation, mark the floor of an ancient collapse and were in turn isolated by a more recent (but prehistoric) collapse along the same boundary fault as that active in 1968. Copyright by the American Association for the Advancement of Science.

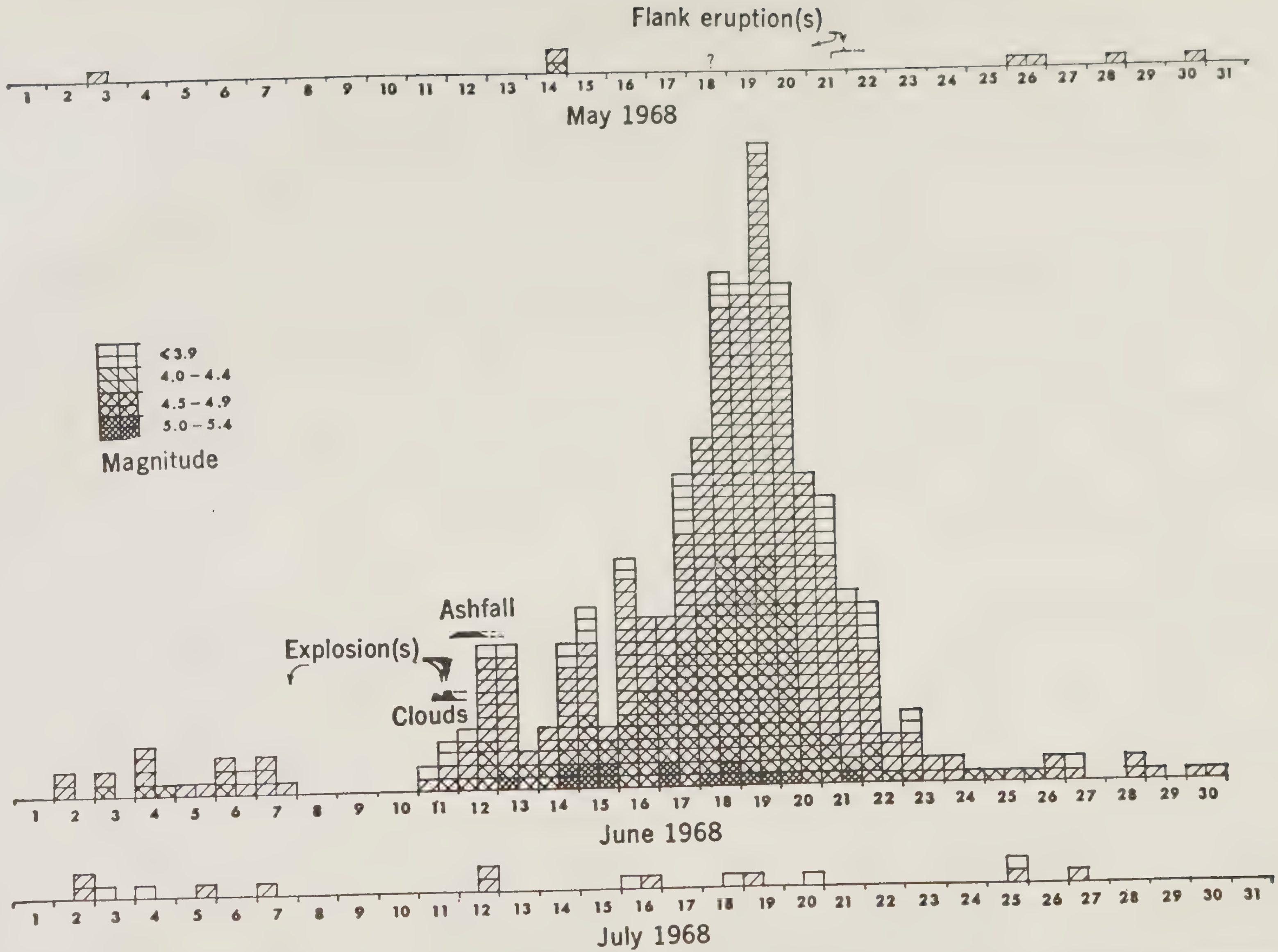

Figure 15.1.2. Earthquakes associated with eruption of Fernandina in June 1968, from Simkin and Howard (1970). Each block represents an earthquake believed to have taken place in Galápagos region during time interval shown. A similar histogram, plus energy release curves, are given in Filson and others (1973). Copyright by the American Association for the Advancement of Science.

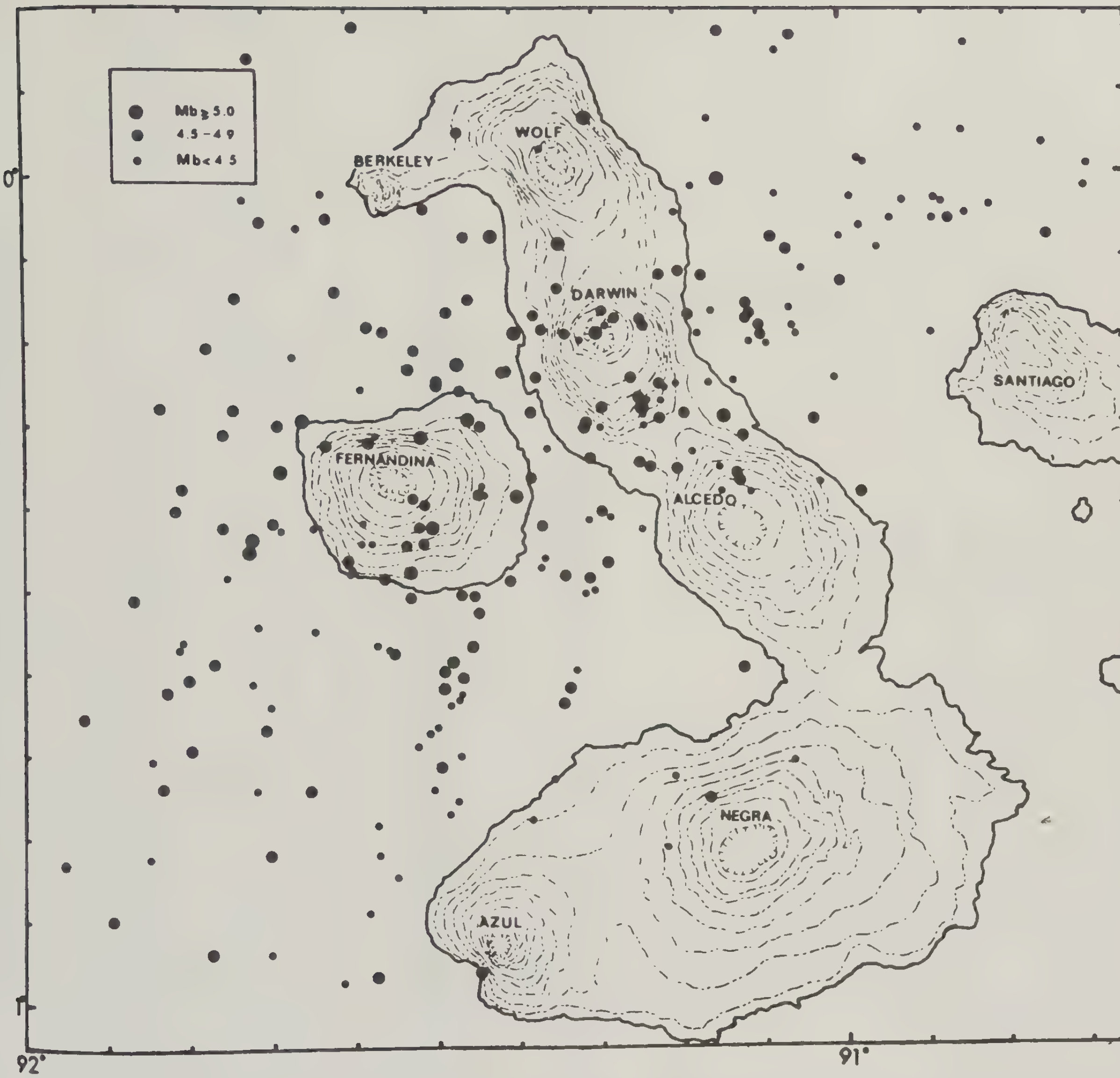

Figure 15.1.3. Epicenter locations of some of the 1968 Galápagos earthquakes, from Filson and others (1973). See text and Filson and others (1973) for discussion of probable errors in epicenters of earthquakes, most of which probably occurred at Fernandina during caldera collapse.

V. WOLF

CAVW number (active vent)	Latitude Longitude (degrees)	Diameter (km)	Local tectonic setting	Precaldera edifice	SiO_2 content (wt pct)	Age of collapse (yr B.P.)	Date of unrest	Type and duration of unrest ESTU STHF MGTF H Te	Eruption type
15-03-02	0.02N	7 x 5.5	Intersection	Shield	R = mafic		1797	---- ---- ---- - --	unknown
(V. Wolf)	91.35W		of lineaments		C = mafic		1800	---- ---- ---- - --	ex
			over "hotspot"				1925-26	---- ---- ---- - --	lf
							1933	---- ---- ---- - --	lf
							1935	---- ---- ---- - --	unknown
							1938	---- ---- ---- - --	unknown
							1948	---- ---- ---- - --	ex,lf
							1963	---- ---- ---- - --	lf
							1973?	EC-- ---- ---- - QU	unknown
							1982	---- ---- ---Z - --	ex,lf

TECTONIC SETTING

The Galápagos Islands lie on the Nazca plate just south of the Galápagos Ridge spreading center. They may also overlie a mantle hotspot, presently beneath the volcanically active, western Galápagos Islands (Simkin, 1984, and references therein).

GEOLOGIC HISTORY

Wolf is a shield volcano at the northern end of Isabela (Albemarle) Island (see fig. 15.1.1A in section on Fernandina). Arcuate fissures occur on the walls of its summit caldera and on and just outside the caldera rim; some radial fissures exist on the west, north, and northeast flanks.

HISTORICAL ACTIVITY

1973: An earthquake swarm on 19 March 1973 included a $\underline{M}$=4.9 event located beneath the southeast flank of Wolf. A small eruption may have occurred in mid-November 1973, when a warden of Galápagos National Park heard strong and constant rumblings from the caldera. No eruption cloud was seen, and a ground party sent to investigate found no evidence of fresh lava or pyroclastic products (Smithsonian Institution, 1973).

1982: An eruption began on 28 August 1982. Lava fountains covered much of the summit caldera floor (in the Northern Hemisphere), and lava issued from the southeast flank (10 km away and in the Southern Hemisphere), making a two-hemisphere eruption (Smithsonian Institution, 1982; T. Simkin, written commun., 1987)!

V. WOLF (continued)

REFERENCES

McBirney, A.R., and Williams, H., 1969, Geology and petrology of the Galápagos Islands: Geol. Soc. Am. Memoir 118, 197 p.

Richards, A.F., 1962, Catalogue of active volcanoes of the world including solfatara fields, Pt. XIV, Archipelago de Colon (Galápagos), Isla San Felix, and Islas Juan Fernandez: Rome, IAVCEI, 50 p.

Simkin, T., 1984, Geology of Galápagos, in Perry, R., ed., Galápagos (key environments): Oxford, Pergamon Press, p. 15-41.

Simkin, T., Siebert, L., McClelland, L., Bridge, D., Newhall, C., and Latter, J.H., 1981, Volcanoes of the world: Stroudsburg, Pa., Hutchinson Ross Publ. Co., 232 p.

Smithsonian Institution, Center for Short-Lived Phenomena (SICSLP), 1973, Volcán Wolf: SICSLP Card 1749.

Smithsonian Institution, Scientific Event Alert Network (SEAN), 1982, Volcán Wolf: SEAN Bull., v. 7, no. 8, p. 4.

Volcanological Society of Japan, 1975, Wolf: Bull. Volcanic Eruptions, no. 13, p. 60.

V. DARWIN

CAVW number (active vent)	Latitude Longitude (degrees)	Diameter (km)	Local tectonic setting	Precaldera edifice	SiO_2 content (wt pct)	Age of collapse (yr B.P.)	Date of unrest	Type and duration of unrest ESTU STHF MGTF H Te	Eruption type
15-03-03 (V. Darwin)	0.18S 91.28W	5	Intersection of lineaments over "hotspot"	Shield	R = 48 C = mafic		1813?	---- ---- ---- - --	ex

TECTONIC SETTING

The Galápagos Islands lie on the Nazca plate just south of the Galápagos Ridge spreading center. They may also overlie a mantle hotspot, presently beneath the volcanically active, western Galápagos Islands (Simkin, 1984, and references therein).

GEOLOGIC HISTORY

Darwin Volcano (see fig. 15.1.1<u>A</u> in section on Fernandina) is a typical Galápagos shield volcano with a caldera in the top of an "upside-down soup bowl" -shaped edifice. Arcuate fissures around the benchlike caldera rim have fed many lava flows, as have radial fissures on the flanks (McBirney and Williams, 1969). Two tuff cones, Tagus and Beagle, formed where one radial fissure extended to the sea.

HISTORICAL ACTIVITY

On 6 June 1813 a sea captain observed "a thick column of smoke rising rapidly", possibly from Darwin (Porter, 1822). "At night the whole atmosphere was illuminated by it, and yet we could perceive neither flames nor sparks thrown out by the centre," probably because activity was confined within the summit caldera.

REFERENCES

McBirney, A.R., and Williams, H., 1969, Geology and petrology of the Galápagos Islands: Geol. Soc. Am.Memoir 118, 197 p.

Porter, D., 1822, Journal of a cruise made to the Pacific Ocean (2nd ed.): New York, Wiley and Halsted, v. 1, 242 p.

Richards, A.F., 1962, Catalogue of active volcanoes of the world including solfatara fields, Pt. XIV, Archipelago de Colon (Galápagos), Isla San Felix, and Islas Juan Fernandez: Rome, IAVCEI, 50 p.

Simkin, T., 1984, Geology of Galápagos, <u>in</u> Perry, R., ed., Galápagos (key environments): Oxford, Pergamon Press, p. 15-41.

V. ALCEDO

CAVW number (active vent)	Latitude Longitude (degrees)	Diameter (km)	Local tectonic setting	Precaldera edifice	SiO_2 content (wt pct)	Age of collapse (yr B.P.)	Date of unrest	Type and duration of unrest ESTU STHF MGTF H Te	Eruption type
15-03-04 (V. Alcedo)	0.43S 91.12W	7	Intersection of lineaments over "hotspot"	Shield	R = mafic C = mafic		between 1945 and 1961	---- ---- ---- - --	lf
							1954	---x ---- ---- - --	none?

TECTONIC SETTING

The Galápagos Islands lie on the Nazca plate just south of the Galápagos Ridge spreading center. They may also overlie a mantle hotspot, presently beneath the volcanically active, western Galápagos Islands (Simkin, 1984, and references therein).

GEOLOGIC HISTORY

Alcedo is the lowest of five shield volcanoes on Isabela (Albemarle) Island (see fig. 15.1.1A in section on Fernandina). Many of the flows on the surface of Alcedo are from radial fissures, and the arcuate, circumferential fissures around the caldera rim are much less evident than at other Galápagos shields (McBirney and Williams, 1969). A bench on the caldera wall indicates at least two episodes of collapse.

HISTORICAL ACTIVITY

By comparing aerial photographs from 1945 and 1961, K. Howard (in Simkin, 1984) found one new lava flow low on the southeast flank of V. Alcedo.

A 6-km length of shoreline including Urvina Bay, at the western foot of V. Alcedo (see fig. 15.1.1A in section on Fernandina), was uplifted by as much as 4.6 m, probably in early 1954 (Couffer, 1956; Richards, 1957). More than 1 km^2 of coral reef was raised above sea level. Richards (1957) attributed the uplift to magma intrusion leading to an eruption of Alcedo in November 1954, but K. Howard (in Simkin, 1984) concluded that Alcedo could not have been the site of the November 1954 activity described by Richards (1957). Sierra Negra (40-50 km south-southeast of Urvina Bay) erupted in late 1953 and in 1954, but there are no reports that uplift of similar or greater magnitude occurred at the foot of that volcano. The cause of the 1954 Urvina Bay uplift is therefore unknown.

V. ALCEDO (continued)

REFERENCES

Couffer, J.C., 1956, The disappearance of Urvina Bay: Nat. Hist., v. 65, p. 378-383.
McBirney, A.R., and Williams, H., 1969, Geology and petrology of the Galápagos Islands: Geol. Soc. Am. Memoir 118, 197 p.
Richards, A.F., 1957, Volcanism in eastern Pacific Ocean basin, 1945-1955: Int. Geol. Congr., 20th, Vulcanologia del Cenozoico, Sect. 1, v. 1, p. 19-31.
----- 1962, Catalogue of active volcanoes of the world including solfatara fields, Pt. XIV, Archipelago de Colon (Galápagos), Isla San Felix, and Islas Juan Fernandez: Rome, IAVCEI, 50 p.
Simkin, T., 1984, Geology of Galápagos, <u>in</u> Perry, R., ed., Galápagos (key environments): Oxford, Pergamon Press, p. 15-41.

SIERRA NEGRA

CAVW number (active vent)	Latitude Longitude (degrees)	Diameter (km)	Local tectonic setting	Precaldera edifice	SiO_2 content (wt pct)	Age of collapse (yr B.P.)	Date of unrest	Type and duration of unrest ESTU STHF MGTF H Te	Eruption type
15-03-05 (Sierra Negra)	0.83S 91.17W	10.5 x 7	Intersection of lineaments over "hotspot"	Shield	R = 47-49 C = mafic		1813	---- ---- ---- - --	ex
							1817	---- ---- ---- - --	unknown
							1844	---- ---- ---- - --	lf
							1860	---- ---- ---- - --	ex
							1911 or 1912	---- ---- ---- - --	unknown
							1948	---- ---- ---- - --	ex,lf
							1953-54	---? ---- ---- - --	Ex,lf
							1957	---- ---- ---- - --	unknown
							1963	---- ---- ---- - --	ex,lf
							1979-80	A--- ---Y ---- - --	Ex,lf

TECTONIC SETTING

The Galápagos Islands lie on the Nazca plate just south of the Galápagos Ridge spreading center. They are thought to overlie a mantle hotspot, presently beneath the volcanically active western Galápagos Islands (Simkin, 1984, and references therein).

GEOLOGIC HISTORY

Sierra Negra is a large shield volcano on Isabela (Albemarle) Island, elongate in an east-northeast direction (see fig. 15.1.1A in section on Fernandina). Its summit caldera is shallower than those of other Albemarle shields. Recent eruptions have been from circumferential fissures just outside the northern rim of the caldera (McBirney and Williams, 1969; Delaney and others, 1973).

HISTORICAL ACTIVITY

Sierra Negra is known to have erupted from August 1953 until January 1954; another eruption in November 1954 has tentatively been attributed to Sierra Negra (Simkin, 1984). Uplift in early 1954 around Urvina Bay, 40-50 km north-northwest of Sierra Negra, bears an uncertain relation, if any, to the eruptions of Sierra Negra (see sections on V. Darwin and V. Alcedo).

A local earthquake was registered at Darwin Station at 0730 hr on 13 November 1979, and two larger, $\underline{M}$=4.4 quakes occurred at 0750 hr and 0817 hr. An explosion was heard at 0845 hr, and during the succeeding days eruption clouds rose as high as 14 km, apparently introducing a globally detectable amount of SO_2 into the stratosphere. Seismicity increased on the second afternoon of the eruption, with $\underline{M}_{max}$ = 4.8. Lava flows issued from an 8-km-long fissure on the north flank (Smithsonian Institution, 1979-80).

SIERRA NEGRA (continued)

REFERENCES

Delaney, J.R., Colony, W.E., Gerlach, T.M., and Nordlie, B.E., 1973, Geology of the Volcán Chico area on Sierra Negra Volcano: Geol. Soc. Am. Bull., v. 84, p. 2455-2470.

McBirney, A.R., and Williams, H., 1969, Geology and petrology of the Galápagos Islands: Geol. Soc. Am. Memoir 118, 197 p.

Richards, A.F., 1962, Catalogue of active volcanoes of the world including solfatara fields, Pt. XIV, Archipelago de Colon (Galápagos), Isla San Felix, and Islas Juan Fernandez: Rome, IAVCEI, 50 p.

Simkin, T., 1984, Geology of Galápagos, in Perry, R., ed., Galápagos (key environments): Oxford, Pergamon Press, p. 15-41.

Smithsonian Institution, Scientific Event Alert Network (SEAN), 1979-80, Sierra Negra: SEAN Bull., v. 4, nos. 11-12; v. 5, no. 1 (with reports from H. Hoeck, A. Tupiza, and National Earthquake Information Service, U.S. Geol. Surv.).

CERRO AZUL

CAVW number (active vent)	Latitude Longitude (degrees)	Diameter (km)	Local tectonic setting	Precaldera edifice	SiO_2 content (wt pct)	Age of collapse (yr B.P.)	Date of unrest	Type and duration of unrest ESTU STHF MGTF H Te	Eruption type
15-03-06 (Cerro Azul)	00.90S 91.42W	4 x 5	Hotspot	Shield	R = mafic C = mafic		1932	---- ---- ---- - --	unknown
							1940	---- ---- ---- - --	lf
							1943	---- ---- ---- - --	Ex, lf
							1948	---- ---- ---- - --	lf
							1949?	---- ---- ---- - --	lf
							1951	---- ---- ---- - --	unknown
							1959	---- ---- ---- - --	lf
							1979	---- ---- ---- - --	ex,lf

TECTONIC SETTING

The Galápagos Islands lie on the Nazca plate just south of the Galápagos Ridge spreading center. They are thought to overlie a mantle hotspot, presently beneath the volcanically active, western Galápagos Islands (Simkin, 1984, and references therein).

GEOLOGIC HISTORY

Cerro Azul is the smallest of the Isabela (Albemarle) Island shield volcanoes (see fig. 15.1.1A in section on Fernandina) and has both circumferential and radial fissures. Benches on caldera walls indicate that several periods of subsidence have occurred.

HISTORICAL ACTIVITY

Historical accounts describe lava flows and eruption columns but nothing about precursors. The eruption in 1959 was from a new crater on the east slopes of Cerro Azul (T. Simkin, written commun., 1985).

REFERENCES

Banfield, A.F., Behre, C.H., Jr., and St. Clair, D., 1956, Geology of Isabela (Albemarle) Island, Archipelago de Colon (Galápagos): Geol. Soc. Am. Bull., v. 67, p. 215-234.

McBirney, A.R., and Williams, H., 1969, Geology and petrology of the Galápagos Islands: Geol. Soc. Am.Memoir 118, 197 p.

Richards, A.F., 1962, Catalogue of active volcanoes of the world including solfatara fields, Pt. XIV, Archipelago de Colon (Galápagos), Isla San Felix, and Islas Juan Fernandez: Rome, IAVCEI, 50 p.

Simkin, T., 1984, Geology of Galápagos, in Perry, R., ed., Galápagos (key environments): Oxford, Pergamon Press, p. 15-41.

Simkin, T., Siebert, L., McClelland, L., Bridge, D., Newhall, C., and Latter, J.H., 1981, Volcanoes of the world: Stroudsburg, Pa., Hutchinson Ross Publ. Co., 232 p.

DIAMANTE

CAVW number (active vent)	Latitude Longitude (degrees)	Diameter (km)	Local tectonic setting	Precaldera edifice	SiO_2 content (wt pct)	Age of collapse (yr B.P.)	Date of unrest	Type and duration of unrest ESTU STHF MGTF H Te	Eruption type
15-07-021 (Maipo)	34.2S 69.8W	15 x 20	Compr		R = 60 C = 74-76	450,000 ±60,000	1822?	---- ---- ---? - --	unknown
							1826?	---- ---- ---? - --	ex?
							1905?	---- ---- ---? - --	unknown
							1912?	---- ---- ---? - --	unknown

TECTONIC SETTING

Diamante Caldera is situated above the gently dipping (25°) subduction zone of south-central Chile, more or less between the loci of great earthquakes that destroyed Mendoza (Argentina) in 1861 and Valparaiso (Chile) in 1906.

GEOLOGIC HISTORY

Diamante Caldera formed approximately 0.45 m.y. ago after eruption of approximately 450 km^3 (bulk volume) of rhyolitic pyroclastic-flow deposits (Polanski, 1962; Stern and others, 1984; Harrington and Stern, 1987). The present surface area of Diamante deposits is 1,300 km^2, but the predissection, preburial area was approximately 15,000 km^2 (Stern and others, 1984) (fig. 15.7.1). Maipo Volcano is an andesitic stratovolcano that partially fills the western part of Diamante Caldera. Precaldera lavas are mostly andesite but include some rhyolite (Harrington and Stern, 1987).

HISTORICAL UNREST

We include Diamante Caldera among historically restless calderas because Maipo has reportedly erupted four times in the 19th and 20th centuries. However, some reported eruptions in this area have been occasional sightings of persistent steam plumes, and we cannot evaluate the accuracy of these particular reports. No deposits are known from any historical eruptions of Maipo.

DIAMANTE (continued)

REFERENCES

Harrington, R., Amini, H., Stern, C.R. and Charrier, R., 1984, The Maipo stratovolcano-caldera complex in the southern Andes of central Chile [abs.]: Eos, Trans. Am. Geophys. Union, v. 65, p. 1136.

Harrington, R., and Stern, C., 1987, The Diamante Caldera and Maipo stratovolcano complex: Acta, X Congr. Geol. Argentino, v. 4, p. 286-288 (Symp. on Andean Volcanism).

Polanski, J., 1962, Estratigrafía, neotectónica y geomorfología del Pleistoceno pedemontano entre los ríos Diamante y Mendoza: Asoc. Geol. Argentina, Rev., v. 27, nos. 3-4, p. 127-149.

Stern, C.R., Amini, H., Charrier, R., Godoy, E., Herve, F., and Varela, J., 1984, Petrochemistry and age of rhyolitic pyroclastic flows which occur along the drainage valleys of the Rio Maipo and Rio Cachapoal (Chile) and the Rio Yaucha and Rio Papagayos (Argentina): Rev. Geol. Chile, no. 23, p. 39-52.

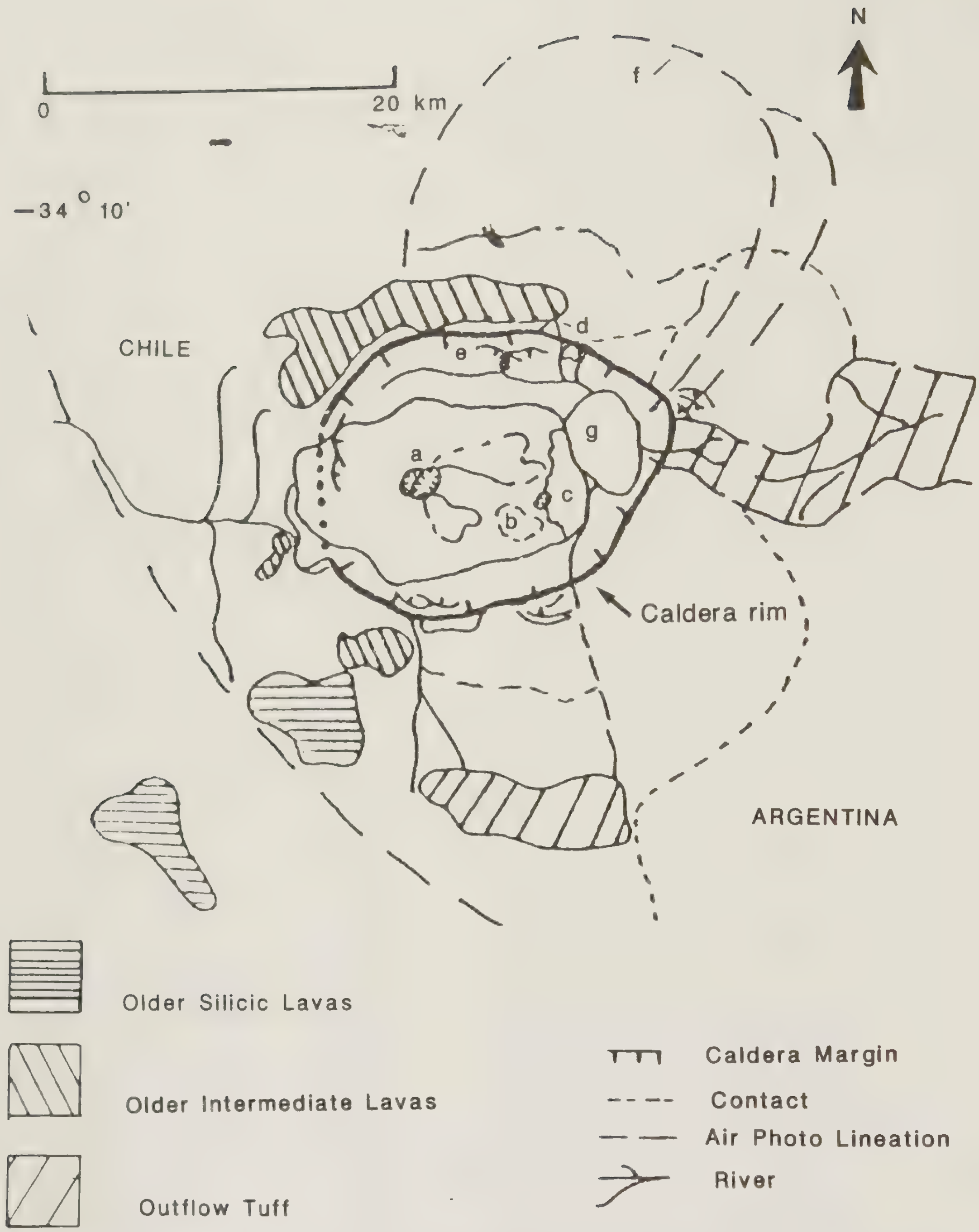

Figure 15.7.1. Geologic sketch map of Diamante Caldera, from Harrington and Stern (1987). Symbols: a, Maipo Volcano; b, mudflow; c, young flows; d, ring dome; e, ring fractures; f, fault; g, Laguna Diamante.

NEVADOS DE CHILLAN

CAVW number (active vent)	Latitude Longitude (degrees)	Diameter (km)	Local tectonic setting	Precaldera edifice	SiO_2 content (wt pct)	Age of collapse (yr B.P.)	Date of unrest	Type and duration of unrest ESTU STHF MGTF H Te	Eruption type
15-07-07 (Nevados de Chillán; V. Nuevo=N)	36.87S 71.38W	7 x 4.5	Compr		R = 60-69 C = ?		1600's	---- ---- ---- - --	Ex
							ca. 1750	---- ---- ---- - --	Ex
							1835	---- ---? ---? ? QU	none
							1861-62	---- ---- ---x - QU	lf,Ex
							1864-65	---- ---- ---- - --	Ex
							1872	---- ---- ---x - --	none
							1877	---- ---- ---x - --	none
							1883	---- ---- ---- - --	ex
							1891	---- ---- ---- - --	ex
							1898	---- ---- ---- - --	ex
							1906 (N)	---- ---- ---x - UQ	ex
							1923 (N)	---- ---- ---x - --	ex
							1929 (N)	---- ---- ---x - --	ex,pex?
							1934 (N)	---- ---- ---x - --	ex
							1945-47(N)	---- ---- ---x - --	ex?
							1965-87+(N)	---- ---- ---F - --	pex,ex,lf,dm

TECTONIC SETTING

In south-central Chile, the Benioff zone dips 25° and has been the site of large, shallow earthquakes. Nevados de Chillán is about 100 km inland from the epicenter of a great earthquake in 1835, and several hundred kilometers south of the epicenters of several more great earthquakes of the 19th and 20th centuries.

GEOLOGIC HISTORY

Voluminous pyroclastic-flow deposits reached from the Nevados de Chillán area to the central valley of south-central Chile, and Deruelle and Deruelle (1975) suggest an 8 km x 10 km caldera at Nevados de Chillán. However, only a 7 km x 4.5 km diameter caldera is clear (fig. 15.8.1) (H. Moreno R., written commun., 1985, 1988). About 10 cones and domes are aligned along a northwest-trending axis through the Nevados de Chillán Caldera, of which Volcán Nuevo is the youngest.

NEVADOS DE CHILLAN (continued)

HISTORICAL ACTIVITY

Shortly after a great earthquake in 1835, centered near Concepción, immense cracks opened near Chillán, 100 km from the coast. Abundant mud and salt water were "erupted", and many new hot springs developed (Perrey, 1854, p. 145-146). Perrey does not indicate whether these changes occurred near the city of Chillán (about 70 km from the coast) or at Nevados de Chillán (about 140 km from the coast). Reiche (1896) described thermal areas of Chillán but did not mention any effect of the 1835 earthquake.

The 1861 eruption commenced a few months after a disastrous earthquake near Mendoza, Argentina, and the simultaneous extinguishing of V. Antuco (each a few hundred kilometers from Nevados de Chillán) (Stone and Ingerson, 1934). The vent for the 1861 eruption was Cerro Negro at the NW foot of Cerro Blanco (Philippi, 1861, 1863).

Stone (1935), Deruelle and Deruelle (1975), and H. Moreno R. (written commun., 1985) report that a small Strombolian eruption at Nevados de Chillán began on 6 August 1906, 10 days before a strong earthquake that destroyed Valparaiso. Volcán Nuevo formed during Strombolian activity of this 1906 eruption. A report by Casertano (1963a, b) of increased fumarolic activity in August and September 1906, <u>after</u> the strong, 16 August Valparaiso earthquake is possibly correct but fails to mention the eruption before the earthquake.

New(?) fumaroles have been observed since 1965, especially on the slopes of V. Nuevo. Remarkable gas emissions occurred in July 1973 along the axis of the caldera, and by December 1973 a new cone (dome) began to form on the slope of V. Nuevo (Deruelle, 1977; Volcanological Society of Japan, 1975, 1976, 1979; H. Moreno R., written commun., 1985). Small, rhythmic phreatomagmatic eruptions ended about June 1983 (H. Moreno R., written commun., 1985), and only a few explosions have been reported from June 1983 to the time of this writing (February 1988) (H. Moreno R., written commun., 1988).

REFERENCES

Casertano, L., 1963a, General characteristics of active Andean volcanoes and a summary of their activities during recent centuries: Bull. Seismol. Soc. Am., v. 53, p. 1415-1433.

----- 1963b, Catalogue of active volcanoes of the world including solfatara fields, Pt. XV, Chilean Continent: Rome, IAVCEI, 55 p.

Deruelle, B., 1977, Sur l'activité récente des Nevados de Chillán (Chili Central): Comptes Rendus Acad. Sci., Paris, Ser. D, v. 284, p. 1651-1654.

Deruelle, B., and Deruelle, J., 1975, Geologie des volcans Quaternaires des Nevados de Chillán (Chili): Bull. Volcanol., v. 38, no. 2, p. 425-444.

Moreno R., H., 1974, Airplane flight over active volcanoes of central-south Chile: Guidebook, Excursion D-3, Symp. on Andean and Antarctic Volcanology Problems: Naples/Santiago, IAVCEI, 56 p.

Perrey, A., 1854, Documents relatifs aux tremblements de terre au Chili: Ann. Soc. Imper. Agric. Hist. Nat. et Arts Utiles, Lyon, 206 p.

NEVADOS DE CHILLAN (continued)

REFERENCES (continued)

Philippi, R.A., 1861, Neuer Vulkan in Chile (Chillán): Petermanns Mitt., v. 8, p. 430.
----- 1862, Viaje a los baños i al nuevo volcán de Chillán: Anal. Univ. Chile, v. 20, p. 279-309.
----- 1863, Exkursion nach den Bädern und dem Neuen Vulkan von Chillán in Chile im Spätsommer 1862: Petermanns Mitt., v. 9, p. 241-257.
Reiche, K., 1896, Die thermen von Chillan in Chile: Globus, v. 69, no. 4, p. 60-62.
Simkin, T., Siebert, L., McClelland, L., Bridge, D., Newhall, C., and Latter, J.H., 1981, Volcanoes of the world: Stroudsburg, Pa., Hutchinson Ross Publ. Co., 232 p.
Smithsonian Institution, Scientific Event Alert Network (SEAN), 1977, Nevados de Chillán: SEAN Bull., v. 4, no. 7, p. 11-12 (information from O. Gonzalez).
Stone, J.B., 1935, The volcanoes of southern Chile: Zeit. Vulkanol., v. 16, p. 81-97.
Stone, J.B., and Ingerson, E., 1934, Some volcanoes of southern Chile: Am. J. Sci., v. 28, no. 166, p. 269-287.
Volcanological Society of Japan, 1975, 1976, 1979, Nevados de Chillán: Bull. Volcanic Eruptions, no. 13, p. 60-61; no. 14, p. 61; no. 15, p. 55; no. 17, p. 77 (information from B. Deruelle, J. Deruelle, and D.C. Shackelford).

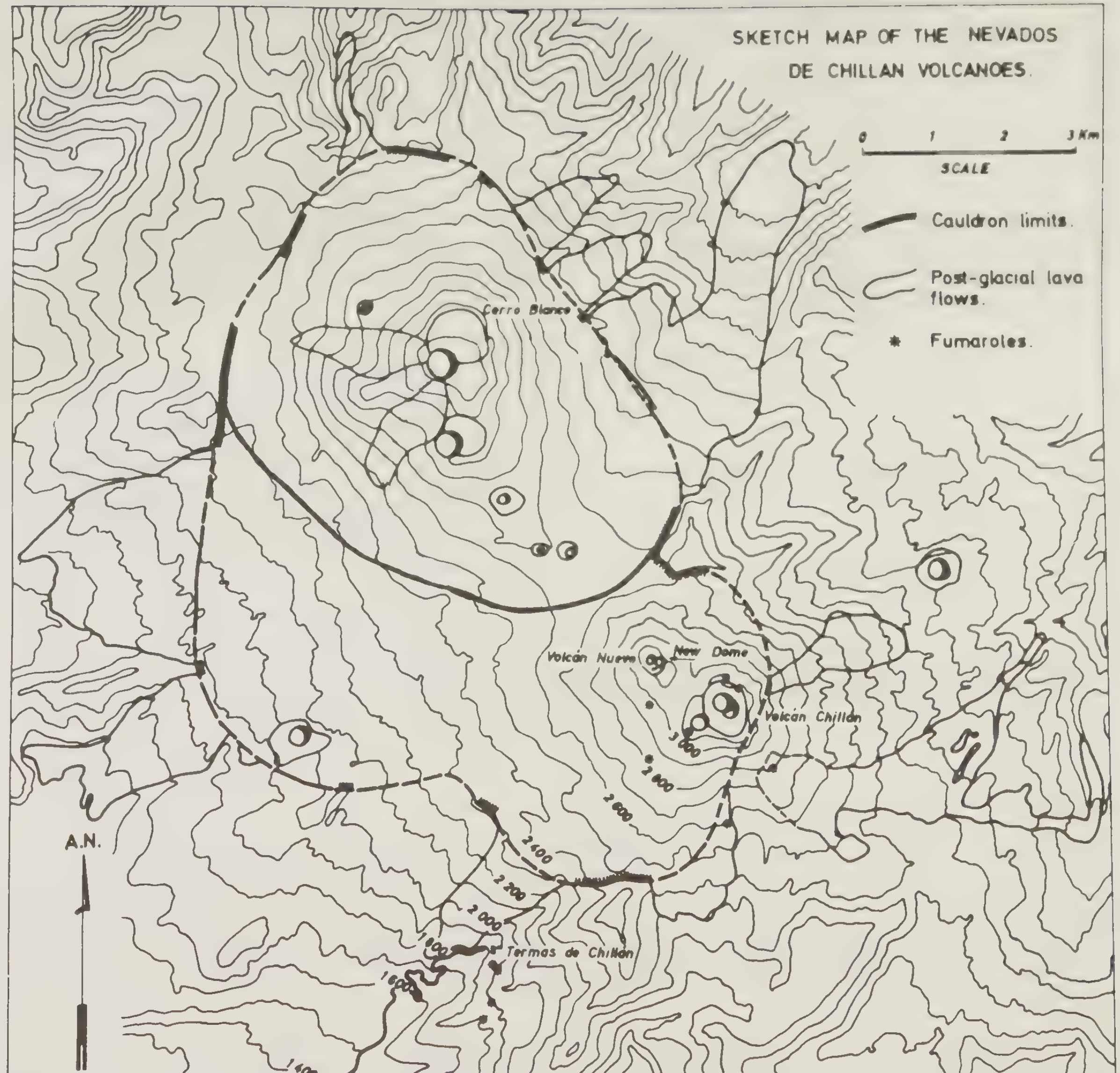

Figure 15.8.1. Approximate outline of Nevados de Chillán Caldera, from a contribution by B. Deruelle and J. Deruelle to Volcanological Society of Japan (1975). These authors propose the existence of an 8 km x 10 km diameter caldera, but Hugo Moreno R. (written commun., 1988) suggests that only a smaller 4.5 x 7 km diameter caldera (inner, solid line) is clear.

COPAHUE

CAVW number (active vent)	Latitude Longitude (degrees)	Diameter (km)	Local tectonic setting	Precaldera edifice	SiO_2 content (wt pct)	Age of collapse (yr B.P.)	Date of unrest	Type and duration of unrest ESTU STHF MGTF H Te	Eruption type
15-07-09 (Copahue)	37.85S 71.17W	ca. 10	Compr	Strato	silicic	Pleistocene	18th or 19th cent.	---- ---- ---- - --	unknown
							1867?	---- ---- ---- - --	unknown
							1937	---- ---- ---- - --	unknown
							1940-45	---- ---- --xx x --	none

TECTONIC SETTING

Copahue is on the Chilean/Argentinian border, at the northern end of the NNE-SSW-trending Liquiñe-Reloncaví fault zone and at or just south of the intersection of that fault zone with a transverse, NW-SE fault zone (Moreno R., 1976; Servicio Nacional de Geologia y Mineria, 1980).

GEOLOGIC HISTORY

Copahue consists of a central cone with several craters, built inside a large caldera (fig. 15.9.1). Intense solfataric activity has occurred in the eastern crater, which is filled with hot briny water.

HISTORICAL ACTIVITY

A notable increase in temperature and total acidity of the lake in Los Copahues crater occurred during 1940-45. A maximum temperature of 90 °C was measured in June 1944. The level of the crater lake dropped as much as 40 m relative to a fixed platform, in an inverse relation to temperature and acidity. Casertano (1964) concluded that drought in the early 1940's caused lake level to drop, and thus temperature and acidity to rise.

COPAHUE (continued)

REFERENCES

Casertano, L., 1964, Some reflections on the fumarolic manifestations of the Los Copahues crater: Bull. Volcanol., v. 27, p. 197-215.

Gonzales-Ferran, O., 1971, Geologia y evolucion del Volcán Copahue: unpubl. rep., Santiago, Chile, Dir. Fronteras y Limites.

Gonzales-Ferran, O., and Vergara, M.M., 1962, Reconocimiento geologico de la Cordillera de los Andes entre los paralelos 35° y 38° Lat. Sur.: Santiago, Dept. Geol., Univ. Chile, Publ. 24, p. 1-121.

Moreno R., H., 1974, Airplane flight over active volcanoes of central-south Chile: Guidebook, Excursion D-3, Symp. on Andean and Antarctic Volcanology Problems: Naples/Santiago, IAVCEI, 56 p.

----- 1976, The Upper Cenozoic volcanism in the Andes of Southern Chile (from 40°00′ to 41°30′S.L.), in Gonzales-Ferran, O., ed., Symp. on Andean and Antarctic volcanology problems: Naples, IAVCEI, p. 143-171.

Servicio Nacional de Geologia y Mineria, 1980, Mapa geologico de Chile: Santiago, Serv. Nac. Geol. Min., scale 1:1,000,000, sheet 4 of 6.

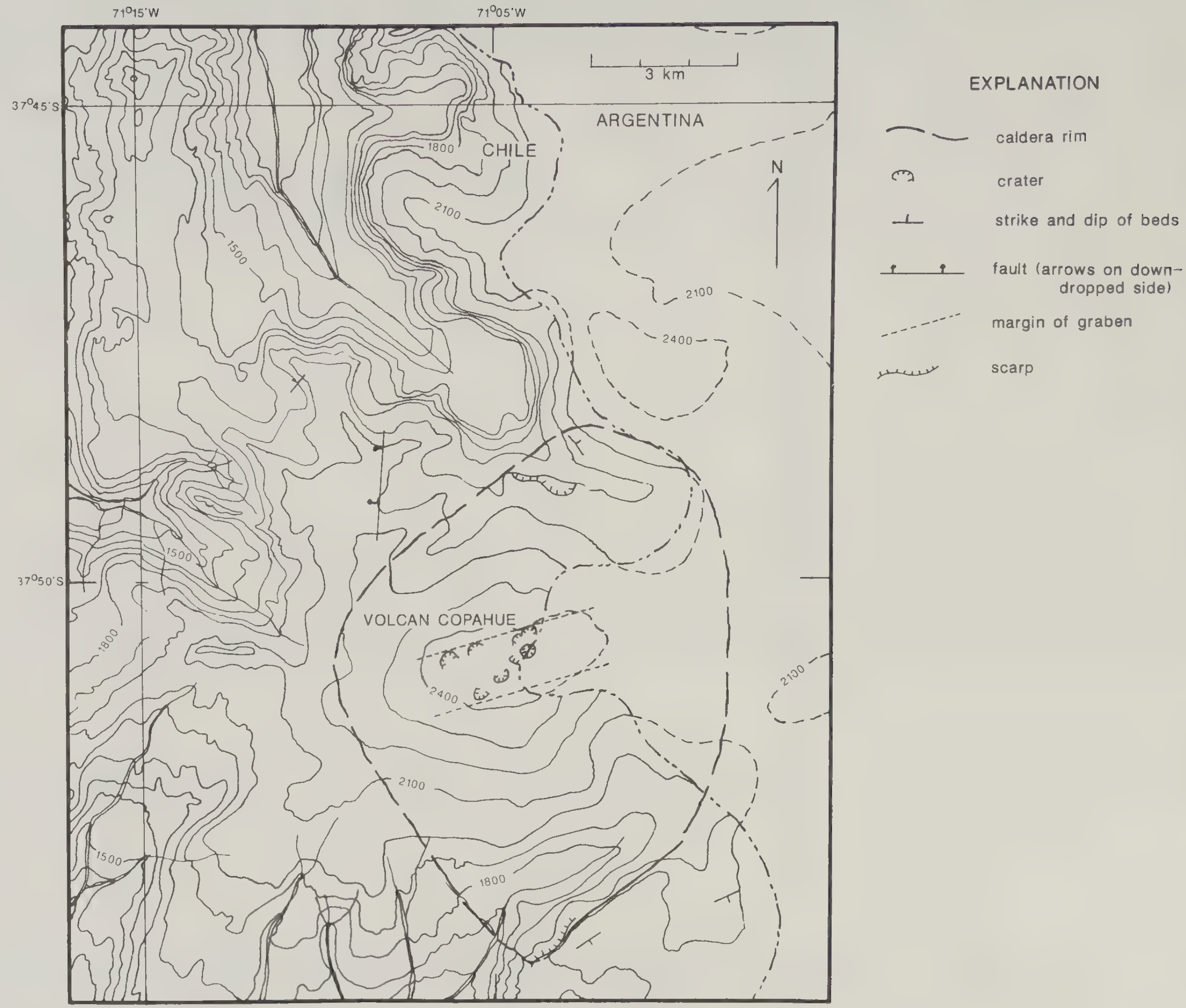

Figure 15.9.1. Volcán Copahue and approximate boundary of Copahue Caldera (Hugo Moreno R., written commun., 1988). Several craters are nested within a summit graben. Contour interval, 100 m within Chile and 300 m within Argentina (latter sketched from aeronautical chart). Topographic contours may not be accurate near border.

See inside back cover for explanation and abbreviations

VILLARRICA

CAVW number (active vent)	Latitude Longitude (degrees)	Diameter (km)	Local tectonic setting	Precaldera edifice	SiO_2 content (wt pct)	Age of collapse (yr B.P.)	Date of unrest	Type and duration of unrest ESTU STHF MGTF H Te	Eruption type
15-07-12	39.42S	9 x 6	Compr	Strato	R = mafic		1558	---- ---- ---- - --	ex
(Villarrica)	71.95W	(outer)			C = 68-71		1575	---- ---- ---- - --	Ex?
							1640	---- ---- ---- - --	ex, lf
		2.2					1647	---- ---- ---- - --	lf, Ex
		(inner)					1657	---- ---- ---- - --	unknown
							1730	---- ---- ---- - --	unknown
							1737	---- ---- ---- - --	unknown
							1777	---- ---- ---- - --	ex
							1787	---- ---- ---- - --	lf
							1790	x--- ---- ---- - --	ex
							1792	x--- ---- ---- - --	ex
							1796	x--- ---- ---- - --	ex
							1799	x--- ---- ---- - --	ex
							1801	x--- ---- ---- - --	ex
							1806	---- ---- ---- - --	ex
							1822*	---- ---- ---- - --	ex
							1832	---- ---- ---- - --	unknown
							1837	---- ---- ---- - --	unknown
							1852*	---- ---- ---- - --	ex
							1860*	---- ---- ---- - --	ex
							1867	---- ---- ---- - --	unknown
							1869*	---- ---- ---- - --	ex
							1874-76*	---- ---- ---- - --	ex
							1879	---- ---- ---- - --	unknown
							1883	---- ---- ---- - --	ex
							1893*	---- ---- ---- - --	ex
							1897-98	---- ---- ---- - --	ex
							1906-09	x--- ---- ---- - --	ex, lf
							1913	---- ---- ---- - --	Ex
							1915-18*	---- ---- ---- - --	ex
							1919	---- ---- ---- - --	unknown
							1920	B--- ---- ---- - --	ex

VILLARRICA, Region 15, CAVW number 15-07-12

VILLARRICA (continued)

CAVW number (active vent)	Latitude Longitude (degrees)	Diameter (km)	Local tectonic setting	Precaldera edifice	SiO_2 content (wt pct)	Age of collapse (yr B.P.)	Date of unrest	Type and duration of unrest ESTU STHF MGTF H Te	Eruption type
(continued from previous page)							1929*	---- ---- ---- - --	ex
							1933*	---- ---- ---- - --	ex
							1935*	---- ---- ---- - --	ex
							1938*	---- ---- ---- - --	ex
							1948-49	---- ---- ---- - --	Ex,lf
							1959-61	---- ---- ---- - --	ex
							1963-64	---- ---- ---- - --	Ex,lf
							1971-72	---- ---- ---- - --	Ex,lf
							1979-80	---- ---- ---E - --	pex,ex
							1983-85	DD-Y ---- ---- - --	lf,ex

* not shown in Riffo and others (1987)

TECTONIC SETTING

Villarrica is situated at the intersection of the major NNE-SSW Liquiñe-Reloncaví transcurrent fault zone and a northwest-trending alignment of volcanoes with Villarrica at its center (Moreno R., 1976; Servicio Nacional de Geologia y Mineria, 1980).

GEOLOGIC HISTORY

Villarrica stratovolcano, a symmetrical, mafic cone, has largely filled a 9 km x 6 km diameter caldera (fig. 15.10.1), which formed during or following eruption of silicic dacite (H. Moreno R., written commun., 1988). The rim of a smaller caldera appears at the 2400-m level on Villarrica stratovolcano as a slight irregularity in that volcano's symmetry (Moreno R. and others, 1980; R. Hickey-Vargas and others, written commun., 1988; H. Moreno R., written commun., 1988).

HISTORICAL ACTIVITY

Villarrica erupts frequently, with a monthly probability of 1.45×10^{-2}, and without regard to the length of time since the previous eruption (Muñoz, 1983, 1984). Typically, eruptions exhibit subterranean noises, loud and repeated bangs from the crater, columns of smoke and vapor, fountains of incandescent debris, ash columns that rise several kilometers above the summit, and lava flows (Flores, 1951).

1558, 1575: The town of Villarrica was destroyed twice; the second time, 350 persons were killed (Riffo and others, 1987).

VILLARRICA (continued)

HISTORICAL ACTIVITY (continued)

1640: Lava reached Lake Villarrica and the valley of the Rio Toltén. The area was visited by the Marquis of Bayde, who, aided by the eruption, negotiated peace with the indigenous Araucanian people (Riffo and others, 1987).

1906-08: In 1906, strong subterranean noises were heard, but little lava emission occurred (Riffo and others, 1987). Then, on 31 October 1908, "there was a great spout of fire that caused an avalanche or flow of rock, snow, and ice from the glacier on the east side of Villarrica...There was no earthquake at this time although there had been one in 1907" (Stone, 1935). A minor eruption occurred on 21 December 1908.

1920: "On December 9, 1920 a severe earthquake threw down the porch on the front of [a house 6 km north of the crater] and moved a large shed three inches off its foundations. Furniture in the house moved from east to west [obliquely down the mountain]. There were three short strong shocks, and slight shakes followed all the night of the ninth at intervals of about five minutes with a stronger shake every half hour. [Nearby] other houses and stables were knocked down. Early in the morning of the tenth began an explosive eruption whose cannonading rattled the windows in the house and lasted for about 36 hours. In the night of the 10th a great fountain of fire was seen..." (Stone, 1935). H. Moreno R. (written commun., 1988) described the 1920 eruption as "small tephra emissions, lava fountain(s), and several explosions."

1948-49: Eruptions occurred between 9 October 1948 and 3 February 1949. Moderately large explosions on 18 October, 1 January, and 31 January generated tephra and large avalanches (pyroclastic flows?) in five river drainages; 60 persons died (H. Moreno R., written commun., 1988). In January 1949 lava flows descended toward Coñaripe. Great forests were burned (Riffo and others, 1987).

1959-61: Weak explosions and minor tephra emission occurred.

1963-64: In 1963, avalanches of unspecified origin were directed to Lake Calafquén, cutting five bridges. Mudflows in March 1964 overwhelmed half of a small village, killing 22 persons (Riffo and others, 1987). H. Moreno R. (written commun., 1988) report tephra emission, lava flows, and lahars.

1971-72: Eruptions beginning on 29 October 1971 intensified in November and December, generating mudflows and tephra and killing 17 persons (H. Moreno R., written commun., 1988). Fluid lava flowed as much as 14 km from the vent (Riffo and others, 1987).

1979-80: Fumarolic activity increased in late September 1979 and small tephra eruptions occurred from 20 June-September 1980.

1983: Weak explosions and minor tephra emission occurred on 14 October (H. Moreno R., written commun., 1988). Reported pyroclastic flows onto ice-covered slopes are doubtful. A red glow was seen at the summit (Smithsonian Institution, 1983).

1984-85: A brief ash eruption, accompanied by an increase in seismicity, occurred on 11 August 1984. Lava extrusion and small explosions began on 30 October, and intense shallow seismicity (mostly B-type earthquakes) was recorded by a seismometer on the

VILLARRICA (continued)

HISTORICAL ACTIVITY (continued)

northwest flank of the volcano during 4-5 November 1984. Then tremor and underground rumbling were reported from Pucon, at a time when no further earthquakes were recorded by the seismometer. Strombolian explosions and lava extrusion occurred during 10-13 November, and weak eruptive activity and tremor continued until 17 November. On 18 November, the southwest slope between 2,200 and 2,800 m above sea level was seen to have bulged visibly, until more lava was extruded from the central crater and the northeast flank (fig. 15.10.2). Most eruptive activity ended in January 1985 (fig. 15.10.3), but minor ash emissions and red glow were observed until 18 April (Smithsonian Institution, 1984; Acevedo and Fuentealba, 1987, H. Moreno R., written commun., 1988). Seismicity in 1983 was dominated by A-type earthquakes, but B-type earthquakes and tremor became dominant in 1984 (Acevedo and Fuentealba, 1987).

Seismicity (B-type earthquakes and harmonic tremor) increased again from June to November 1985 (fig. 15.10.4) (Smithsonian Institution, 1985; H. Moreno R., written commun., 1985; Acevedo and Fuentealba, 1987).

REFERENCES

Acevedo A., P., and Fuentealba C., G., 1987, Antecedentes de la actividad microsismica del Volcán Villarrica relacionada con la erupción de Octubre de 1984: Bol. Vulcanol. (Costa Rica), no. 18, p. 13-17.

Flores S., E., 1951, La ultima erupción del Volcán Villarrica: Informaciones Geograficas, Santiago, v. 1, p. 59-62.

Moreno R., H., 1974, Airplane flight over active volcanoes of central-south Chile, in Gonzales-Ferran, O., ed., Guidebook, Excursion D-3, Symp. on Andean and Antarctic volcanology problems: Naples/Santiago, IAVCEI, 56 p.

----- 1976, The Upper Cenozoic volcanism in the Andes of Southern Chile (from 40°00′ to 41°30′S.L.), in Gonzales-Ferran, O., ed., Symp. on Andean and Antarctic volcanology problems: Naples, IAVCEI, p. 143-171.

Moreno R., H., Marangunic D., C., and Lahsen A., A., 1980, Recopilacion geologica de la zona de Pucon: Santiago, unpubl. rep., 18 p.

Muñoz, M., 1983, Eruption patterns of the Chilean volcanoes Villarrica, Llaima, and Tupungatito: Pure Appl. Geophys., v. 121, p. 835-852.

----- 1984, Probabilidad de erupción en el Volcán Villarrica en los proximos años: Tralka, Dept. Geofis., Univ. Chile, v. 2, no. 3, p. 323-325.

Riffo, P., Fuentealba, G., and Urra, L.H., 1987, Sintesis de las erupciónes del Volcán Villarrica (Chile): Bol. Vulcanol. (Costa Rica), no. 18, p. 8-11.

Servicio Nacional de Geologia y Mineria, 1980, Mapa geologico de Chile: Santiago, Serv. Nac. Geol. Min., scale 1:1,000,000, sheet 4 of 6.

Smithsonian Institution, Scientific Event Alert Network (SEAN), 1983, 1984, 1985, Villarrica: SEAN Bull., v. 8, no. 10, p. 12; v. 9. no. 11, p. 2-4; v. 10, no. 1, p. 3; v. 10, no. 11, p. 6 (information from O. Gonzalez-Ferran, G. Fuentealba C., P. Riffo A., P. Acevedo, and H. Moreno R.).

Stone, J.B., 1935, The volcanoes of Southern Chile: Zeit. Vulkanol., v. 16, p. 81-97.

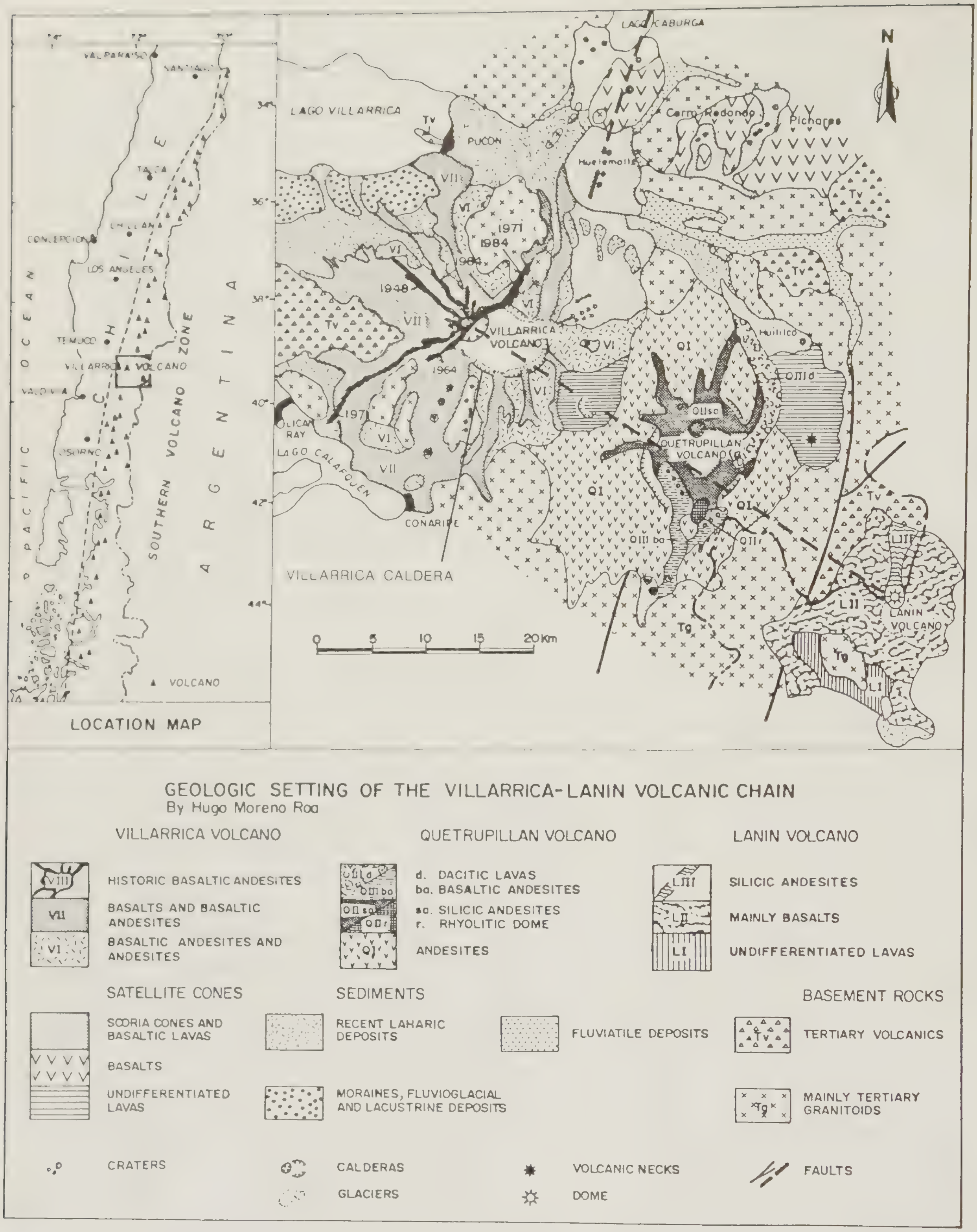

Figure 15.10.1. Geologic map of Villarrica-Lanin volcanic chain, showing locations of Villarrica Volcano and Caldera, from Moreno R. and others (1988).

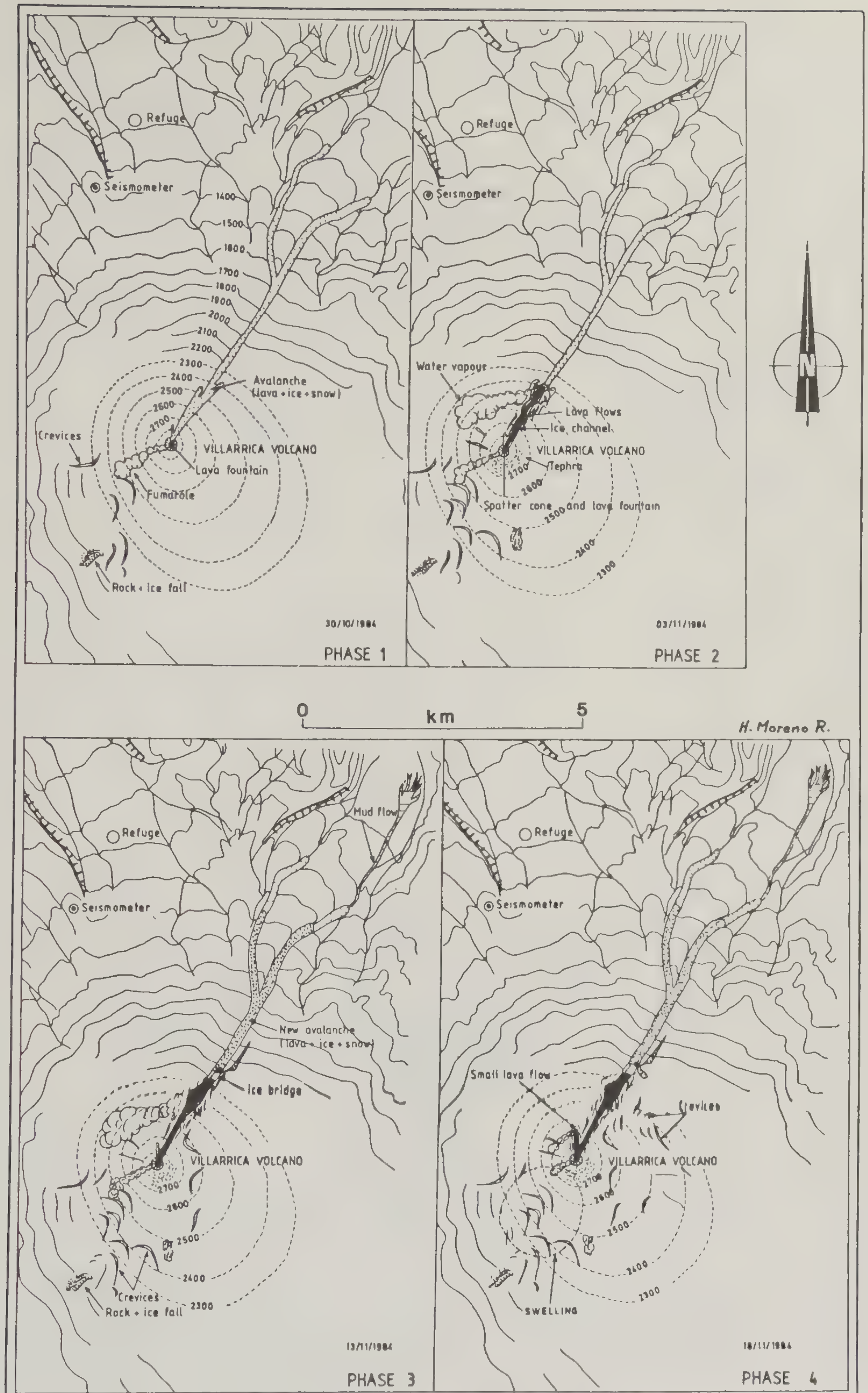

Figure 15.10.2. Sketch maps of Villarrica Volcano showing deposits of phases 1-4 of the 1984 eruption. Eruptive phases occurred on 30 October and 3, 13, and 18 November 1984, respectively (Smithsonian Institution, 1984; courtesy of Hugo Moreno R.). Note swelling of southwest flank during phase 4.

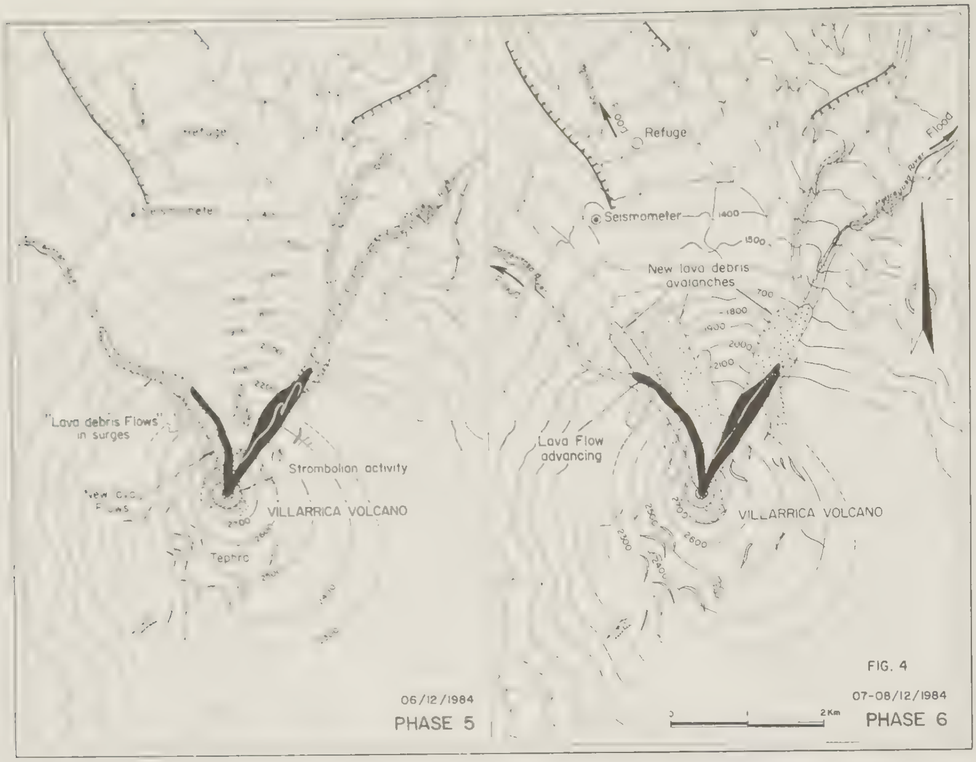

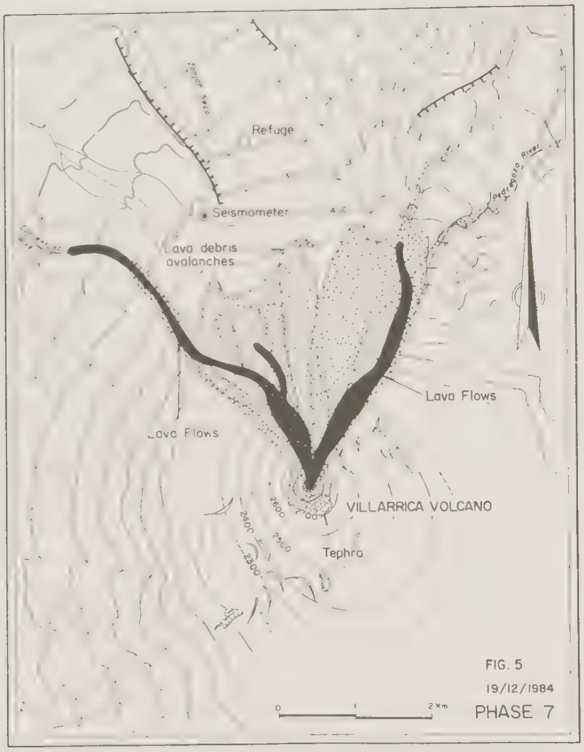

Figure 15.10.3. Sketch maps showing deposits of phases 5-7 of the 1984 eruption of Villarrica Volcano, from Moreno R. and others (1988).

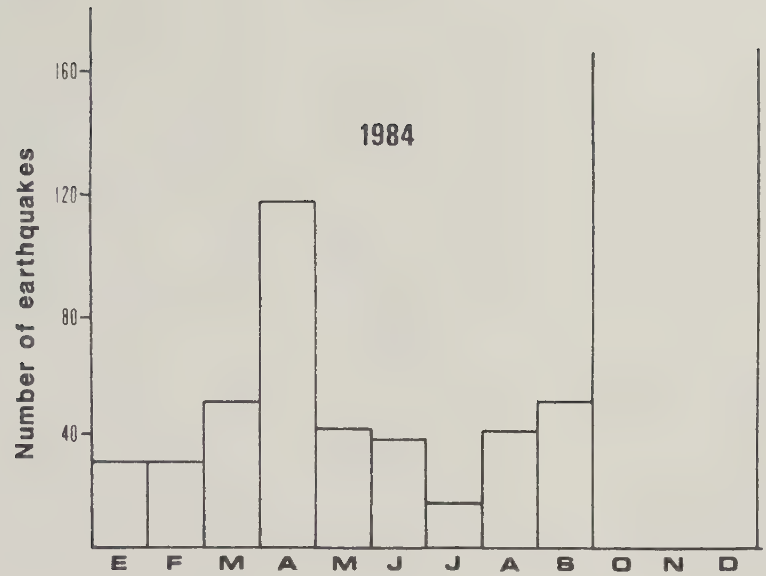

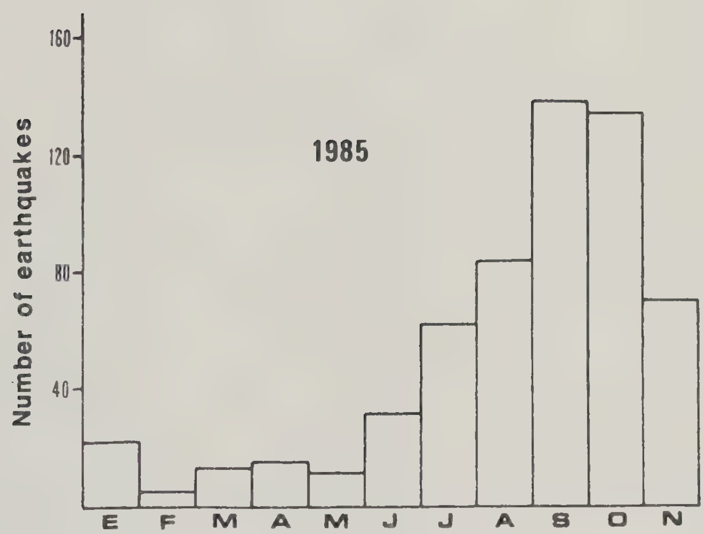

Figure 15.10.4. Monthly number of earthquakes at Villarrica during 1984 (top) and January-November 1985 (bottom), from Acevedo and Fuentealba (1987).

CORDILLERA NEVADA

CAVW number (active vent)	Latitude Longitude (degrees)	Diameter (km)	Local tectonic setting	Precaldera edifice	SiO_2 content (wt pct)	Age of collapse (yr B.P.)	Date of unrest	Type and duration of unrest ESTU STHF MGTF H Te	Eruption type
15-07-141 (Cordón Caulle)	40.46S 72.25W	9	Compr		R = 64-71 C = 62-74	probably 100,000-200,000	1893?	---- ---- ---- - --	lf?
							1921-22	x--- ---- ---- - --	EX,lf
							1929	---- ---- ---- - --	ex
							1934	x--- ---- ---- - --	ex
							1960	C--- ---- ---- - QU	Ex,lf

TECTONIC SETTING

The Cordillera Nevàda Caldera lies just west of the Liquiñe-Reloncaví line, a major N10°E strike-slip fault that spans much of the length of the south-central Chilean volcanic belt. It also lies at the apex of two segments of a conjugate set of N60°E and N50°W faults that are at least in part tension features associated with movement along the Liquiñe-Reloncaví Fault. Many of the volcanoes in this area, including the Cordillera Nevada center, the Cordón Caulle fissures, and Puyehue, have grown along this set of conjugate faults (Moreno R., 1976; Servicio Nacional de Geologia y Mineria, 1980).

GEOLOGIC HISTORY

The Cordillera Nevada Caldera (fig. 15.11.1), mapped by Moreno R. (1977), is the only known source of rhyolitic tuff in the southern Andes (Lopez-Escobar, 1984). The age of the Cordillera Nevada Caldera is unknown; extensive glaciation indicates that it is at least 16,000 years old, and probably 100,000-200,000 yr old (H. Moreno R., written commun., 1988). Cordón Caulle is a group of postcaldera silicic vents along WNW-ESE-trending fissures. The group has been classed with Puyehue Volcano (CAVW number 15-07-15) (Casertano, 1963), but Moreno R. (1977; oral commun., 1985) considers it to be independent of Puyehue. Some of the Cordón Caulle vents occur within the Cordillera Nevada Caldera, while others are outside the caldera--a relation not unlike that of the Inyo domes and the Long Valley Caldera in California, USA. Recent lavas of the Cordón Caulle group are dacitic, but subordinate basalt was erupted in the early development of this group of vents (Moreno R., 1977). It is not known if magma of the Cordón Caulle group is related to any beneath the Cordillera Nevada Caldera. An alternate name for Cordón Caulle, "Los Azufres," refers to solfataric activity that existed before the 1921-22 eruption.

Several maars, including Nilahue, occur in the nearby Carran group but bear no direct relation to the Cordillera Nevada Caldera or the Cordón Caulle group.

CORDILLERA NEVADA (continued)

HISTORICAL ACTIVITY

Simultaneous eruptions of dacite lava from several fissure vents occurred in 1921-22 and 1960, as shown in fig. 15.11.2. The 1921-22 eruption began with explosive activity on 13 December 1921. Ash and pumice were produced in great quantity, after earthquakes and a deafening roar. Further explosions on 19-21 December sent ash 62 km high. Ash fell in La Plata, 3000 km to the northeast, and was seen over Europe and southwest Africa. Lava extrusion began in February 1922 (Krumm, 1923; Hantke, 1940).

A small eruption occurred in 1934, after an earthquake (Hantke, 1940).

The 1960 eruption is one of the best-documented examples of an eruption triggered by a tectonic earthquake. A $\underline{M}$=8.3 earthquake occurred on 22 May 1960, some 300 km northwest of the caldera, and a strong explosive eruption began approximately 48 hours later, followed by extrusion of lava. Dacitic lava was extruded from multiple vents along a 14-km-long set of NW-SE-trending fissures. From the start of the eruption, and continuing for 6 days, ash obscured the sky (Katsui and Katz, 1967; Moreno R., 1977).

COMMENTS

Eruptions of Cordón Caulle are pertinent to unrest at Long Valley Caldera for two reasons. First, multiple, simultaneous dike-fed eruptions of dacitic magma might be a modern analog of the closely spaced eruptions along the Mono Craters - Inyo domes chain, ca. 550 yr B.P. Second, the eruption of Cordón Caulle in 1960 was triggered by a distant tectonic earthquake. Even though the likelihood of an eruption at Long Valley seems relatively low at the time of this writing (December 1987), a large earthquake is still expected in the White Mountains seismic gap. If part of a regional extension event, such an earthquake could conceivably trigger a repetition of the Mono Craters - Inyo domes dike intrusion and eruptions, just as the great 1960 Chilean earthquake apparently triggered the 1960 eruption of Cordón Caulle.

REFERENCES

Casertano, L., 1963, Catalogue of active volcanoes of the world including solfatara fields, Pt. XV, Chilean Continent: Rome, IAVCEI, 55 p.

Gerlach, D.C., Frey, F.A., Hickey, R., Moreno R., H., and Hildreth, W., 1983, Geochemistry of Puyehue Volcano and Cordón Caulle, Southern Andes (40.5°S): Eos, Trans. Am. Geophys. Union, v. 64, p. 326.

Hantke, G., 1940, Das Vulkangebiet zwischen den Seen Ranco und Puyéhue in Süd-Chile: Bull. Volcanol., ser. 2, v. 7, p. 75-83.

Katsui, Y., and Katz, H.R., 1967, Lateral fissure eruptions in the southern Andes of Chile: Jour. Fac. Sci., Hokkaido Univ., ser. IV, v. 13, no. 4, p. 433-448.

Krumm, F., 1923, Topographische und geologische Nachrichten über die Gegend östlich des Ranco-Sees in Süd-Chile, im besondern über den jüngsten Vulkan-Ausbruch "Los Azufres" (Dezember 1922)(sic): Geol. Rundschau, v. 14, p. 146-150.

CORDILLERA NEVADA (continued)

REFERENCES (continued)

Lopez-Escobar, L., 1984, Petrology and chemistry of volcanic rocks of the southern Andes, in Harmon, R.S., and Barreiro, B.A., eds., Andean magmatism--chemical and isotopic constraints: Nantwich, Cheshire, Shiva Publ. Ltd., p. 47-71.

Moreno R., H., 1976, The Upper Cenozoic volcanism in the Andes of Southern Chile (from 40°00′ to 41°30′S.L.), in Gonzales-Ferran, O., ed., Symp. on Andean and Antarctic volcanology problems: Naples, IAVCEI, p. 143-171.

----- 1977, Geologia del area volcanica Puyehue-Carran: Santiago, Univ. Chile, Memoria de Titulo, 181 p.

Philippi, R.S., 1869, Die heissen Quellen am Puyehue--und Llauquihue-See in Chile: Petermanns Mitt., 1869, p. 459-461.

Servicio Nacional de Geologia y Mineria, 1980, Mapa geologico de Chile: Serv. Nac. Geol. Min., scale 1:1,000,000, sheet 4 of 6.

Stone, J.B., 1935, The volcanoes of Southern Chile: Zeit. Vulkanol., v. 16, p. 81-97.

Tazieff, H., 1962, Quelques observations sur la crise séismo-volcanique de mai 1960 au Chili central: Bull. Volcanol., v. 24, p. 83-86.

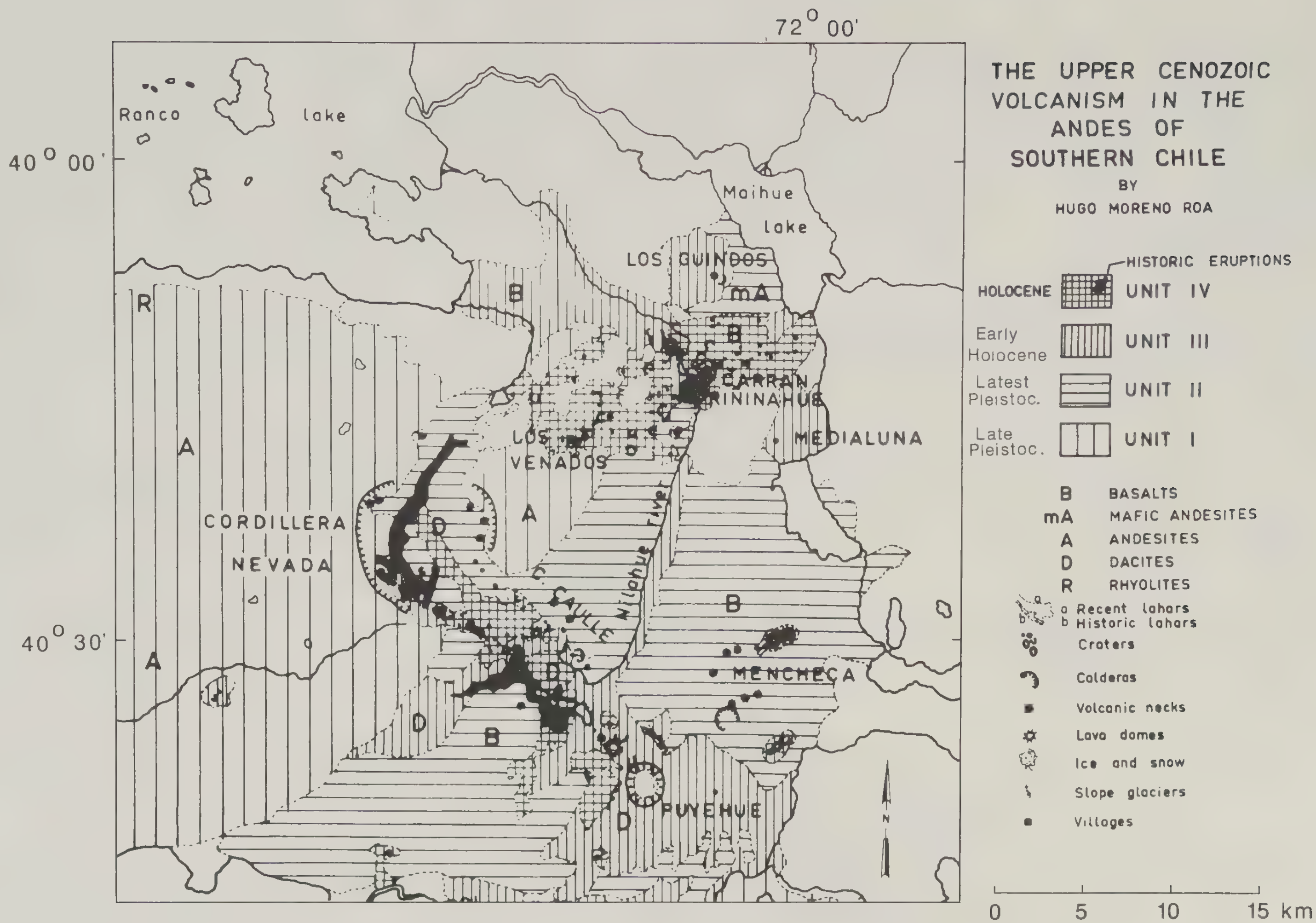

Figure 15.11.1. Geologic map of Cordillera Nevada Caldera, after Moreno R. (1976).

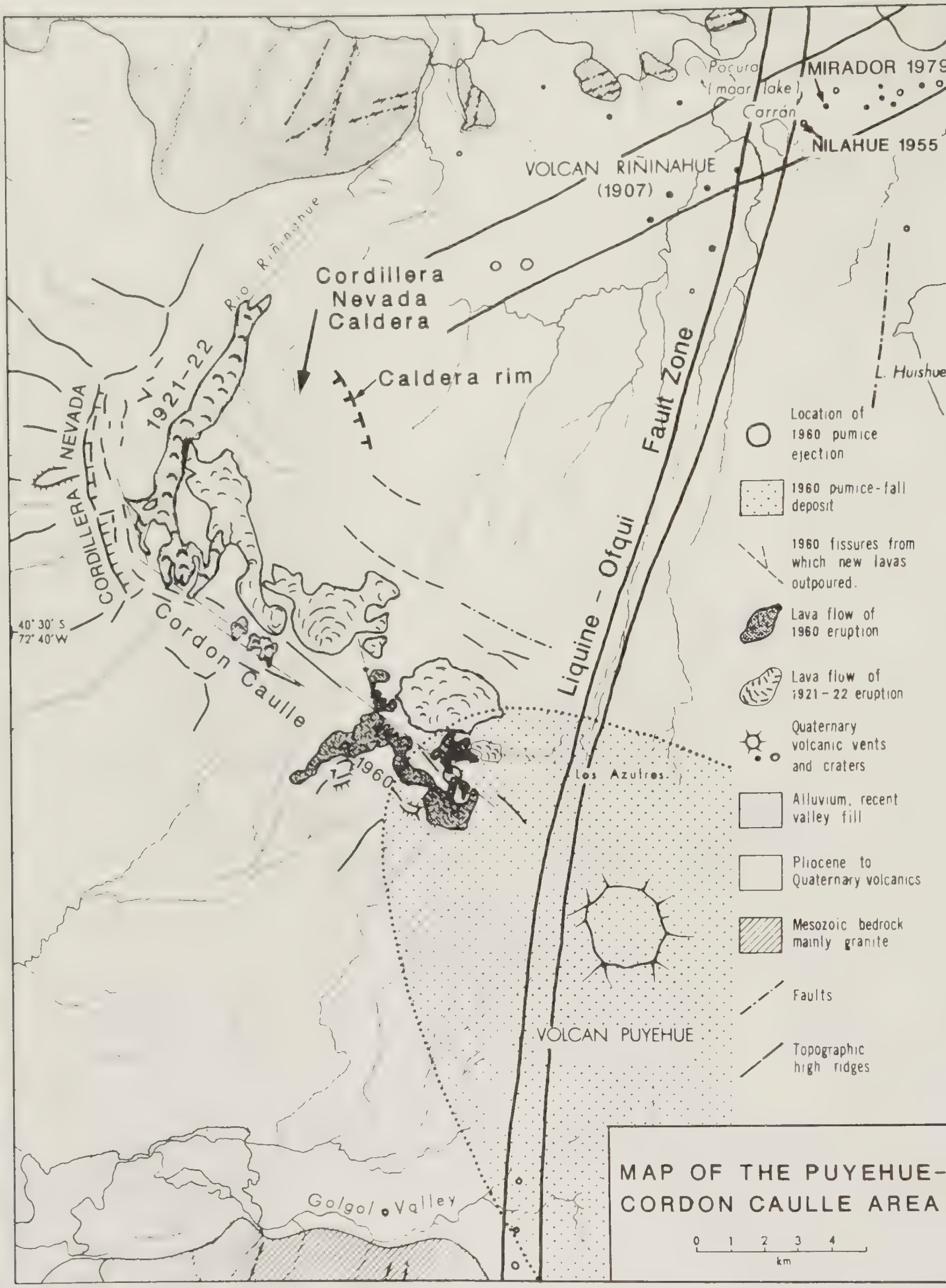

Figure 15.11.2. Vents and lava flows of the 1921-22 and 1960 eruptions of Cordón Caulle, which occurred along northwest-trending fractures that connect Puyehue with the Cordillera Nevada Caldera (see figure 15.11.1). 1955 Nilahue Maar is shown in upper right. Figure from Katsui and Katz (1967), modified by Hugo Moreno Roa (written commun., 1988).

MT. HUDSON

CAVW number (active vent)	Latitude Longitude (degrees)	Diameter (km)	Local tectonic setting	Precaldera edifice	SiO_2 content (wt pct)	Age of collapse (yr B.P.)	Date of unrest	Type and duration of unrest ESTU STHF MGTF H Te	Eruption type
15-08-057 (Mt. Hudson)	45.91S 72.92W	9	Several intersecting fault trends; youngest, E-W	Strato	R = 59-61 C = ?	Preglacial	1970-71	x--- ---- --EE E --	Ex
							1973	---- ---- --D- - --	none?, or subgl

TECTONIC SETTING

Mt. Hudson lies in a stretch of the southern Andes that has relatively few active volcanoes. A N-S fault (one of many extending much of the length of Chile) passes several kilometers west of Mt. Hudson (Servicio Nacional de Geologia y Mineria, 1980).

GEOLOGIC HISTORY

The caldera of Mt. Hudson (fig. 15.12.1) is ice filled and was not known until shortly before the unrest in 1970-71 (Fuenzalida Ponce and Espinosa, 1973).

HISTORICAL ACTIVITY

1970-71: Abnormally high level of a river was observed in April 1970, with marked fluctuations not correlated with rainfall. The caldera is ice filled, and melting of ice presumably was responsible for increased and fluctuating flow. An explosive eruption occurred on 12 August 1971. Shallow local seismicity, with MMI_{max} = 5, was reported, but there was no indication whether it preceded or accompanied the eruption.

1973: Ground temperatures rose suddenly in April, causing 70 percent of the ice cover of Mt. Hudson to melt. No eruption was observed, but it is possible that a small eruption occurred under ice.

REFERENCES

Fuenzalida Ponce, R., 1976, The Hudson Volcano, in Gonzales Ferran, O., ed., Symp. on Andean and Antarctic volcanology problems: Naples, IAVCEI, p. 78-87.
Fuenzalida Ponce, R., and Espinosa N., W., 1973, Hallazgo de una caldera volcanica en la Provincia de Aisen: Rev. Geol. Chile, no. 1, p. 64-66.
Godoy, E., Dobbs, M., and Stern, C., 1981, El volcán Hudson, primeros datos quimicos e isotopicos en coladas interglaciales: Communicaciones Dept. Geol. Univ. Chile, v. 32, p. 1-9.
Servicio Nacional de Geologia y Mineria, 1980, Mapa geologico de Chile: Serv. Nac. Geol. Min., scale 1:1,000,000, sheet 5 of 6.
Volcanological Society of Japan, 1973-75, Mt. Hudson: Bull. Volcanic Eruptions, no. 11, p. 43; no. 13, p. 62.

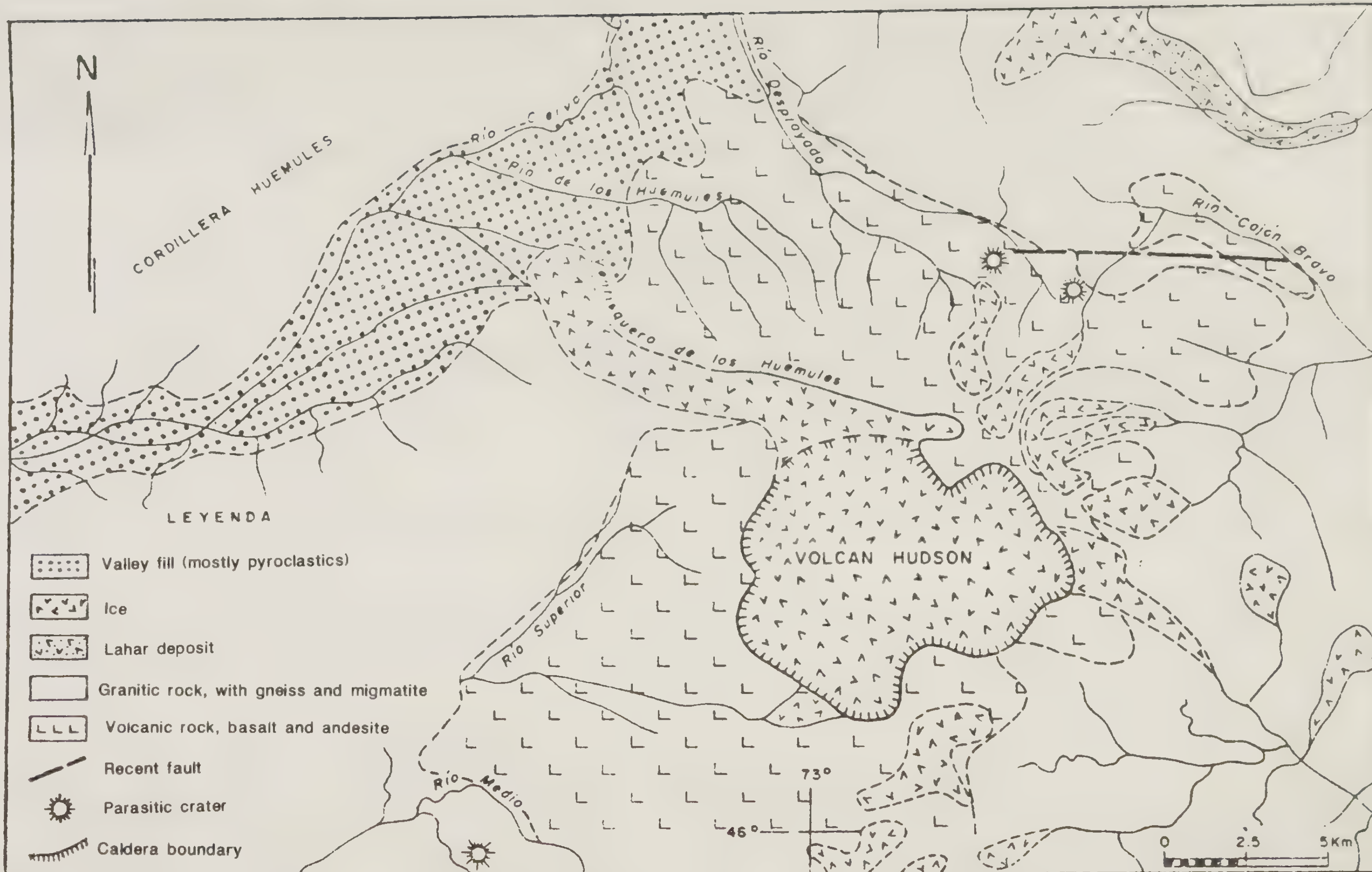

Figure 15.12.1. Geologic sketch map of Mt. Hudson and its caldera, after Fuenzalida Ponce and Espinosa (1973) and Fuenzalida Ponce (1976).

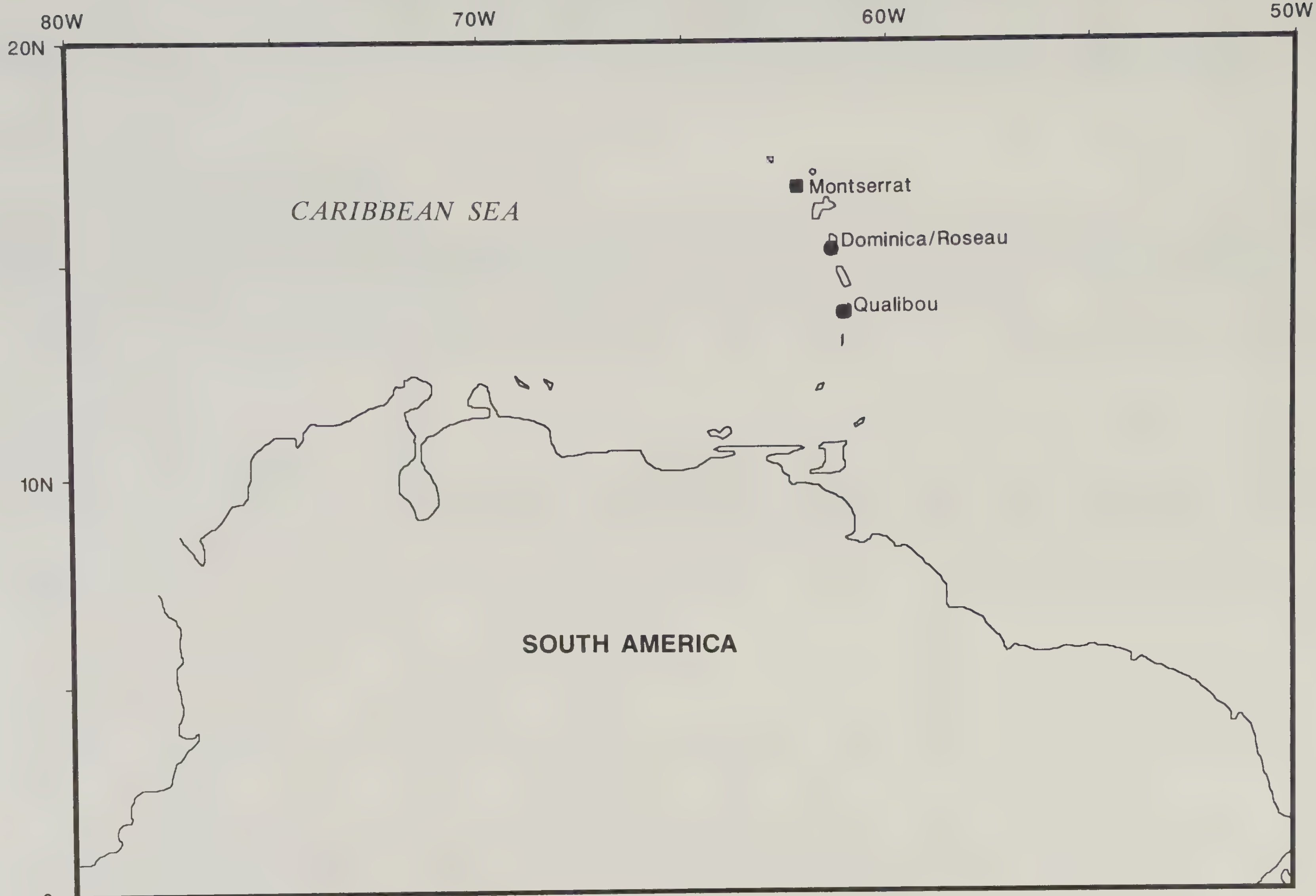

Figure 16. Locations of large, Quaternary restless calderas (solid circles) and a restless noncaldera area (square) in Region 16.

UNNAMED, near Roseau, Dominica

CAVW number (active vent)	Latitude Longitude (degrees)	Diameter (km)	Local tectonic setting	Precaldera edifice	SiO_2 content (wt pct)	Age of collapse (yr B.P.)	Date of unrest	Type and duration of unrest ESTU STHF MGTF H Te	Eruption type
16-00-10 (Valley of Desolation; Micotrin)	15.30N 61.30W	10	Compr	Strato?	R = 59-63 C = silicic	30,000	1673	?--- ---- ---- - --	none
							1765	xx-- ---- ---x - --	none
							1843-49	xx-- ---- ---- - --	none
							1879-80	?--- ---- ---x - --	pex
							1967	CC-- ---- ---- - --	none
							1971	x--- ---- ---N N --	none
							1974	xx-- ---- ---N N --	none
							1976	xx-- ---- ---N N --	none

TECTONIC SETTING

Dominica is at the southern end of the northern Lesser Antilles lithospheric segment (Wadge and Shepherd, 1984). In this northern half of the arc, tectonic earthquakes occur along the Benioff zone and also above it, frequently at shallow depths, and swarms of tectonic earthquakes are relatively common (Shepherd, 1988).

GEOLOGIC HISTORY

A caldera roughly 10 km in diameter (fig. 16.1.1) has been postulated (Robson and Tomblin, 1966, referring to a depression bounded by an arcuate fault), rejected (Wadge, 1984; G. Wadge, written commun., 1984; H. Sigurdsson, written commun., 1984), reinterpreted as the relic of a gravitational collapse (Roobol and others, 1983), and repostulated as a normal collapse caldera (G. Heiken, written commun., 1986; J. Shepherd, 1987, written commun.). Robson and Tomblin (1966) considered Morne Trois Pitons, Morne Macaque (= Micotrin), Grande Soufriere Hills, Watt Mountain, and the Valley of Desolation (a solfatara field between the latter three centers) to be a single volcano, perhaps including two other nearby cones, Morne Anglais and Foundland; Wadge (1984) considers Morne Anglais and Foundland to be petrologically distinct from the earlier-mentioned vents, and Shepherd (1988) considers all of these vents to be closely spaced but independent.

HISTORICAL ACTIVITY

The only historical eruption in this area was a small steam explosion in 1880. Small earthquake swarms occur from time to time beneath the several vents of this center (Shepherd, 1988). Most of what is listed in the table and below is of regional tectonic origin and might not be related to the Roseau center; we include it because the precise epicenters are unknown.

UNNAMED, near Roseau, Dominica, Region 16, CAVW number 16-00-10

UNNAMED, near Roseau, Dominica (continued)

HISTORICAL ACTIVITY (continued)

1673: A strong shock (Perret, 1939), described by Robson (1964) as an earthquake of estimated intensity IV, was centered on or near Dominica.

1765: There was a report of "earthquakes and gas" (Perret, 1939); 150 shocks "more violent than any previously felt" (Robson, 1964), occurred in February and March, and a few more were felt until 30 June. Activity was centered somewhere on Dominica.

1816: Severe shocks on 15 August, with estimated intensity V, were centered on or near Dominica.

1838: During June, several "smart shocks", with maximum intensity V, were centered on or near Dominica.

1843-49: On 8 February, a strong tectonic earthquake occurred north(?) of Dominica. It was felt with intensity VIII in Roseau, and with intensity IX elsewhere in Dominica and on Guadeloupe, Antigua, Montserrat, Nevis, and St. Kitts. A relatively small earthquake in December 1843 was felt only in Roseau, and several more small earthquakes were felt during 1844-45, 1847, and 1849. Those in 1849 occurred in swarms and apparently were centered somewhere in the southern half of Dominica. Shepherd (1988) attributes the 1849 (and forerunning?) swarms to the Morne Patates area, which is south of, and probably unrelated to, the Roseau "caldera."

1879-80: An earthquake occurred beneath or near Dominica, with maximum intensity V, on 10 September 1879. A small phreatic explosion occurred from the Valley of Desolation, a solfataric area on the eastern rim of the caldera. The only reported precursor to this eruption was about 2 minutes of intermittent rumbling sounds before a large black cloud rose from the solfatara area. It is not known if the earthquake was precursory to the eruption.

1967-76: Since seismographs were first installed in Dominica in the 1950's, instrumentally recorded earthquake swarms have occurred in June 1967, January 1971, April-May 1974, September-November 1974, and March-April 1976 (Wadge, 1985). The first, between 19 and 21 June 1967, included 66 shallow earthquakes (Shepherd and others, 1971). The September-November 1974 swarm occurred about 1-2 km southwest of Micotrin, at depths mostly less than 3 km; other shallow earthquakes during the same period coincided with the area of the proposed caldera (J. Shepherd, written commun., 1987) (fig. 16.1.2). Events shown in figure 16.1.2 were shown by Wadge (1985) as being farther to the south but were recently relocated in the Roseau area (J. Shepherd, written commun., 1987).

From 10 February 1976 until May 1976, earthquakes 1-3 km deep occurred in a belt extending beneath the caldera and up to 2 km to the southwest. After the initial swarm on 10 February, fewer than 1 earthquake per day occurred until a $\underline{M}$=5.9 earthquake occurred 170 km north of Dominica on 10 March. The largest event, on 14 March, was felt with a local MMI=VI but was not recorded on the worldwide seismic network. Solfataric activity at the nearby Watten Waven Soufriere did not change (Smithsonian Institution, 1976). The event has been interpreted as a magmatic intrusion (J. Tomblin, cited in Smithsonian Institution, 1976) or slumping in the Roseau delta (H. Sigurdsson, written commun., 1984).

UNNAMED, near Roseau, Dominica (continued)

COMMENTS

We include the Roseau basin here as a possible caldera and source of the voluminous (30 km^3 bulk volume) Roseau ash, because (1) we find it difficult to imagine that an eruption that large would not form a caldera, and (2) earthquake locations coincide with the area of the postulated caldera. The solfatara field and andesite domes noted above also occur within the proposed caldera.

REFERENCES

Carey, S.N., and Sigurdsson, H., 1980, The Roseau ash: deep sea tephra deposits from a major eruption on Dominica, Lesser Antilles: Jour. Volcanol. Geotherm. Res., v. 7, p. 67-86.

Perret, F.A., 1939, The volcano-seismic crisis at Montserrat, 1933-1937: Carnegie Inst. Washington Publ. 512, 76 p.

----- 1950, Volcanological observations: Carnegie Inst. Washington Publ. 549, 153 p.

Robson, G.R., 1964, An earthquake catalogue for the eastern Caribbean: Bull. Seismol. Soc. Am., v. 54, p. 785-832.

Robson, G.R., and Tomblin, J.F., 1966, Catalogue of the active volcanoes of the world including solfatara fields, Pt. XX, West Indies: Rome, IAVCEI, 56 p.

Roobol, M.J., Wright, J.V., and Smith, A.L., 1983, Calderas or gravity-slide structures in the Lesser Antilles Island arc?: Jour. Volcanol. Geotherm. Res., v. 19, p. 121-134.

Shepherd, J.B., 1988, Eruptions, eruption precursors and related phenomena in the Lesser Antilles: Bull. Volcanol. [in press].

Shepherd, J.B., Tomblin, J.F., and Woo, D.A., 1971, Volcano-seismic crisis in Montserrat, West Indies, 1966-1967: Bull. Volcanol., v. 35, p. 143-163.

Sigurdsson, H., 1972, Partly-welded pyroclast flow deposits in Dominica, Lesser Antilles: Bull. Volcanol., v. 36, p. 148-163.

Smithsonian Institution, Scientific Event Alert Network (SEAN), 1976, Micotrin/Dominica, West Indies: SEAN Bull., v. 1, nos. 7, 8, 10 (information from J. Tomblin, W. Person, and W. Aspinall).

Sparks, R.S.J., Sigurdsson, H., and Carey, S.N., 1980, The entrance of pyroclast flows into the sea, pt. 1. Oceanographic and geologic evidence from Dominica, Lesser Antilles: Jour. Volcanol. Geotherm. Res., v. 7, p. 87-96.

Wadge, G., 1984, A preliminary volcanic hazards study of Dominica, West Indies: Spec. Publ. 1984-5, Seismic Res. Unit, Univ. West Indies, Trinidad.

----- 1985, Morne Patates volcano, southern Dominica, Lesser Antilles: Geol. Mag., v. 122, no. 3, p. 253-260.

Wadge, G., and Shepherd, J.B., 1984, Segmentation of the Lesser Antilles subduction zone: Earth Planet. Sci. Lett., v. 71, p. 297-304.

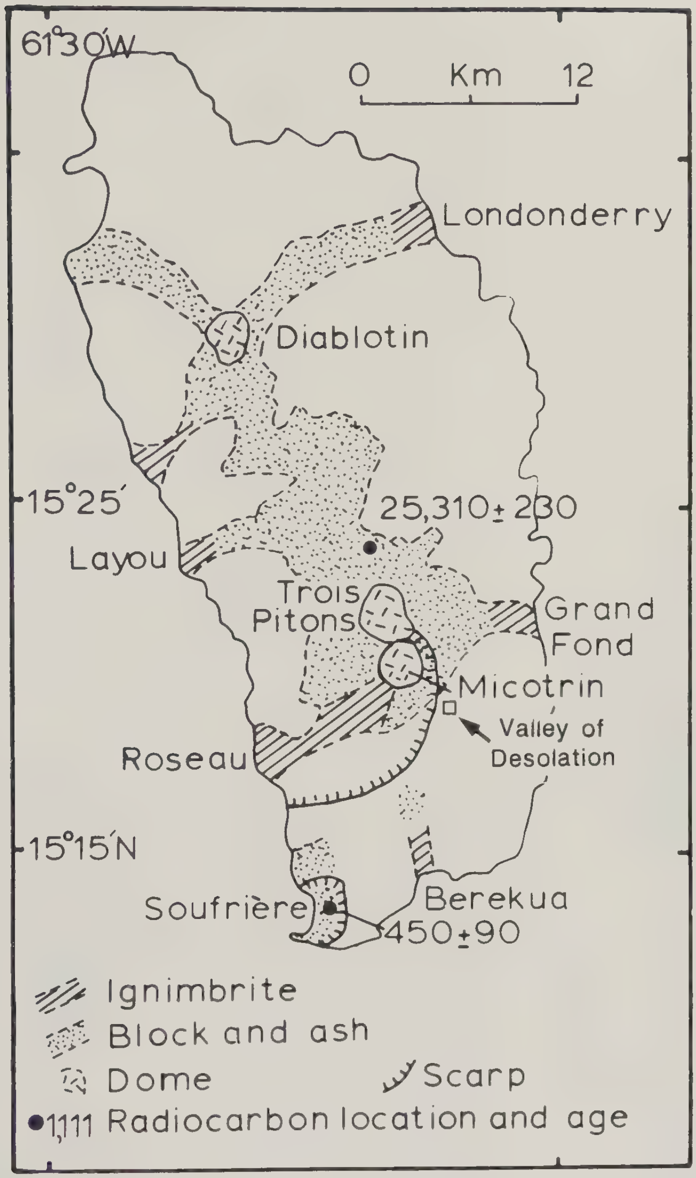

Figure 16.1.1. Unnamed caldera (suggested name, "Roseau") in Dominica, Lesser Antilles. Valley of Desolation is a solfatara field on caldera rim; Micotrin and Trois Pitons are postcaldera domes. Reproduced from Roobol and others (1983), who interpreted the feature as a gravity-slide structure rather than a collapse caldera.

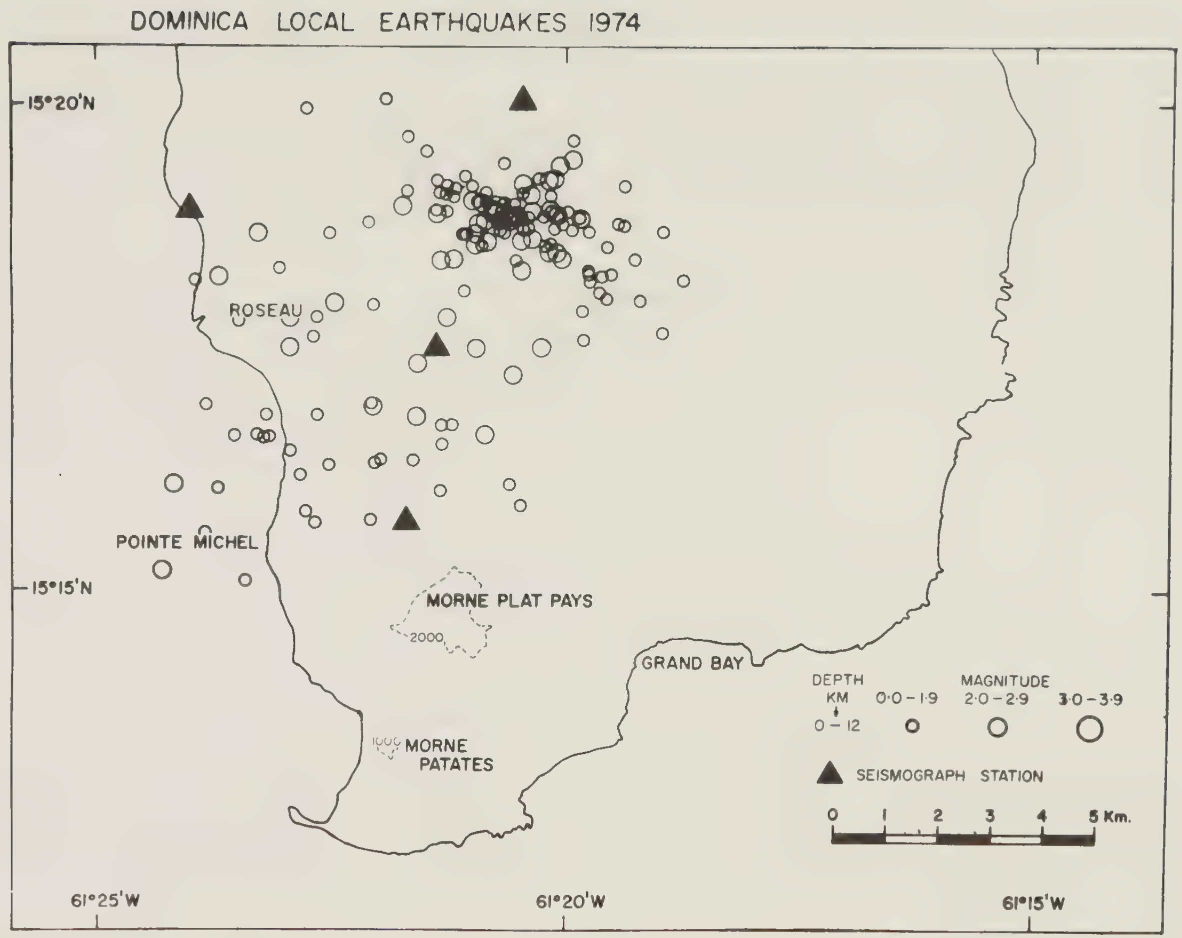

Figure 16.1.2. Locations of earthquakes that occurred during a swarm near Roseau "caldera" in 1974, from John B. Shepherd (written commun., 1987). See figure 16.1.1 for approximate outline of caldera.

QUALIBOU

CAVW number (active vent)	Latitude Longitude (degrees)	Diameter (km)	Local tectonic setting	Precaldera edifice	SiO_2 content (wt pct)	Age of collapse (yr B.P.)	Date of unrest	Type and duration of unrest ESTU STHF MGTF H Te	Eruption type
16-00-14 (Qualibou)	13.83N 61.05W	5 x 7	N60°E-trending faults; compr	Strato-cones	R = d C = silicic	ca. 39,000	1766	---- ---- ---- - --	pex
							1906-08	xx-- ---- ---- - --	none

TECTONIC SETTING

Qualibou is in the southern segment of the Lesser Antilles arc (Wadge and Shepherd, 1984). In this southern half of the arc, tectonic earthquakes are largely restricted to the Benioff zone, and swarms of shallow earthquakes are infrequent (Shepherd, 1988).

GEOLOGIC HISTORY

Qualibou is either a caldera on the west side of Saint Lucia (Tomblin, 1964; Wohletz and others, 1986) or a gravity-slide structure (Roobol and others, 1983) (figs. 16.2.1-16.2.3). The balance of recent work, including drilling and discovery of basalt on the west coast of Saint Lucia, suggests that Qualibou is a caldera that formed after eruption of approximately 6 km^3 (DRE) of silicic magma (Wohletz and others, 1986).

HISTORICAL ACTIVITY

A steam explosion occurred in or about 1766. A main shock - aftershock sequence or an earthquake swarm occurred from February 1906 to June 1908. A tectonic earthquake ($\underline{M}$=6.5, epicenter 13°N, 61.25°W, depth 160 km) shook Saint Lucia on 5 July 1940; numerous other tectonic earthquakes have also been felt on the island.

Occasional shallow earthquakes are detected by a seismometer at Qualibou (Shepherd, 1988). A survey of microseismicity by Aspinall and others (1976) showed repetitive small earthquakes about 2 km deep, which were inferred to reflect the zone of steam generation for this geothermal area (fig. 16.2.4).

QUALIBOU (continued)

REFERENCES

Aspinall, W.P., Michael, M.O., and Tomblin, J.F., 1976, Evidence for fluid bodies beneath the Sulphur Springs Geothermal Region, Saint Lucia, West Indies: Geophys. Res. Lett., v. 3, no. 2, p. 87-90.

Robson, G.R., 1964, An earthquake catalogue for the eastern Caribbean: Bull. Seismol. Soc. Am., v. 54, p. 785-832.

Robson, G.R., and Tomblin, J.F., 1966, Catalogue of the active volcanoes of the world including solfatara fields, Pt. XX, West Indies: Rome, IAVCEI, 56 p.

Roobol, M.J., Wright, J.V., and Smith, A.L., 1983, Calderas or gravity-slide structures in the Lesser Antilles Island arc?: Jour. Volcanol. Geotherm. Res., v. 19, p. 121-134.

Shepherd, J.B., 1988, Eruptions, eruption precursors and related phenomena in the Lesser Antilles: Bull. Volcanol. [in press].

Tomblin, J.F., 1964, The volcanic history and petrology of the Soufriere region, Saint Lucia: Oxford, England, Oxford Univ., Ph.D. thesis, 213 p.

----- 1965, The geology of the Soufriere volcanic centre, Saint Lucia: Trans. 10th Caribb. Geol. Congr., Trinidad, p. 367-376.

Vatin-Perignon, N., Chevallier, L., and Blanc, F., 1981, Les evenements dacitiques recents de la Soufriere de Sainte Lucie, Petite Antilles: PIRPSEV Bull. 90, Paris, 31 p.

Wadge, G., and Shepherd, J.B., 1984, Segmentation of the Lesser Antilles subduction zone: Earth Planet. Sci. Lett., v. 71, p. 297-304.

Westercamp, D., and Tomblin, J., 1980, Le volcanisme recent et les éruptions historiques dan la partie centrale de l'arc insulaire des Petites Antilles: Bull. Bur. Rech. Geol. Min. (BRGM), ser. 2, nos. 3-4, p. 293-319.

Wohletz, K., Heiken, G., Ander, M., Goff, F., Vuataz, F.-D., and Wadge, G., 1986, The Qualibou Caldera, Saint Lucia, West Indies: Jour. Volcanol. Geotherm. Res., v. 27, p. 77-115.

Wright, J.V., Roobol, M.J., Smith, A.L., Sparks, R.S.J., Brazier, S.A., Rose, W.I., Jr., and Sigurdsson, H., 1984, Late Quaternary explosive silicic volcanism on Saint Lucia, West Indies: Geol. Mag., v. 1212, p. 1-15.

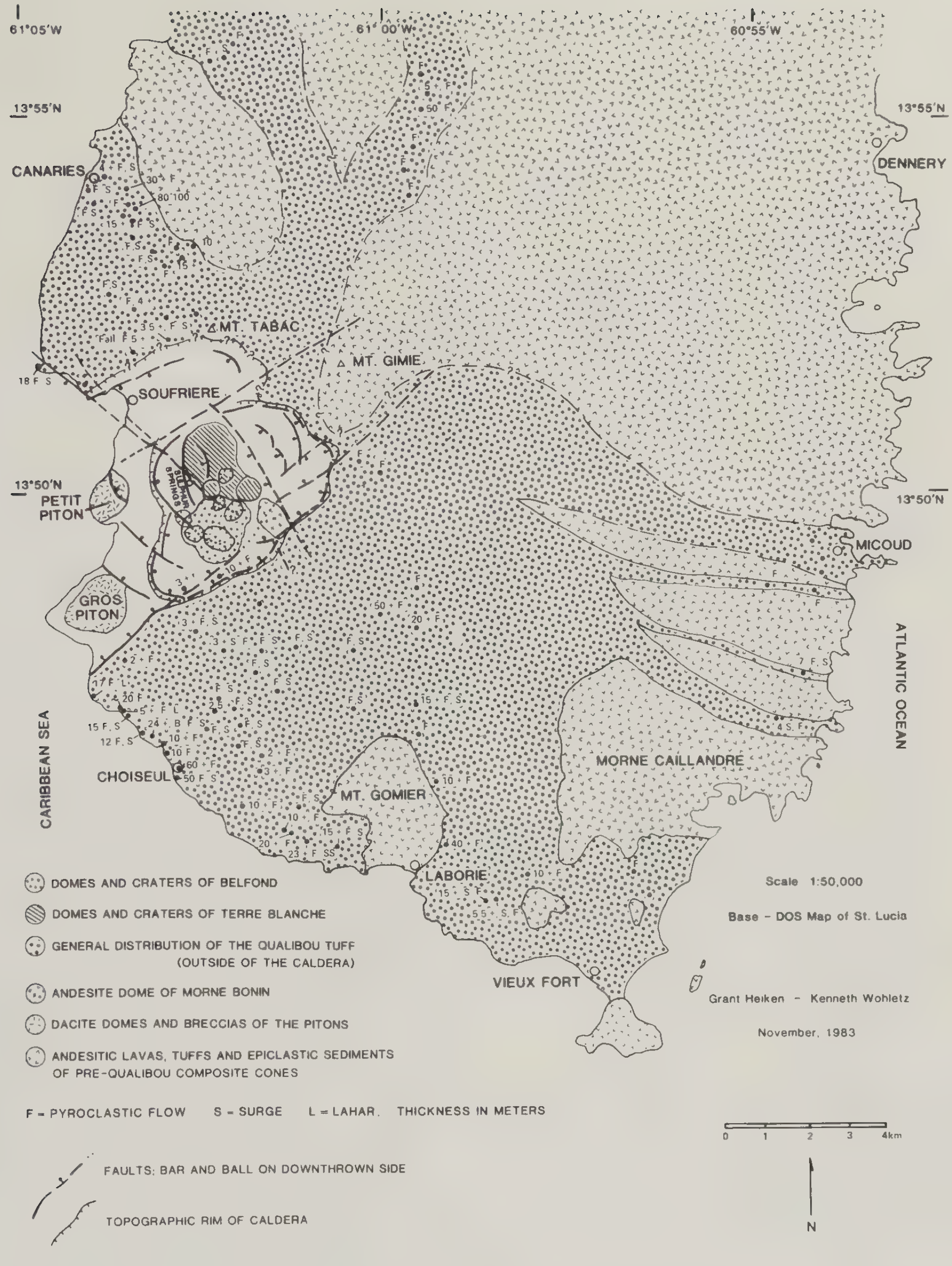

Figure 16.2.1. Reconnaissance geologic map, Qualibou Caldera and tuff, St. Lucia, from Wohletz and others (1986).

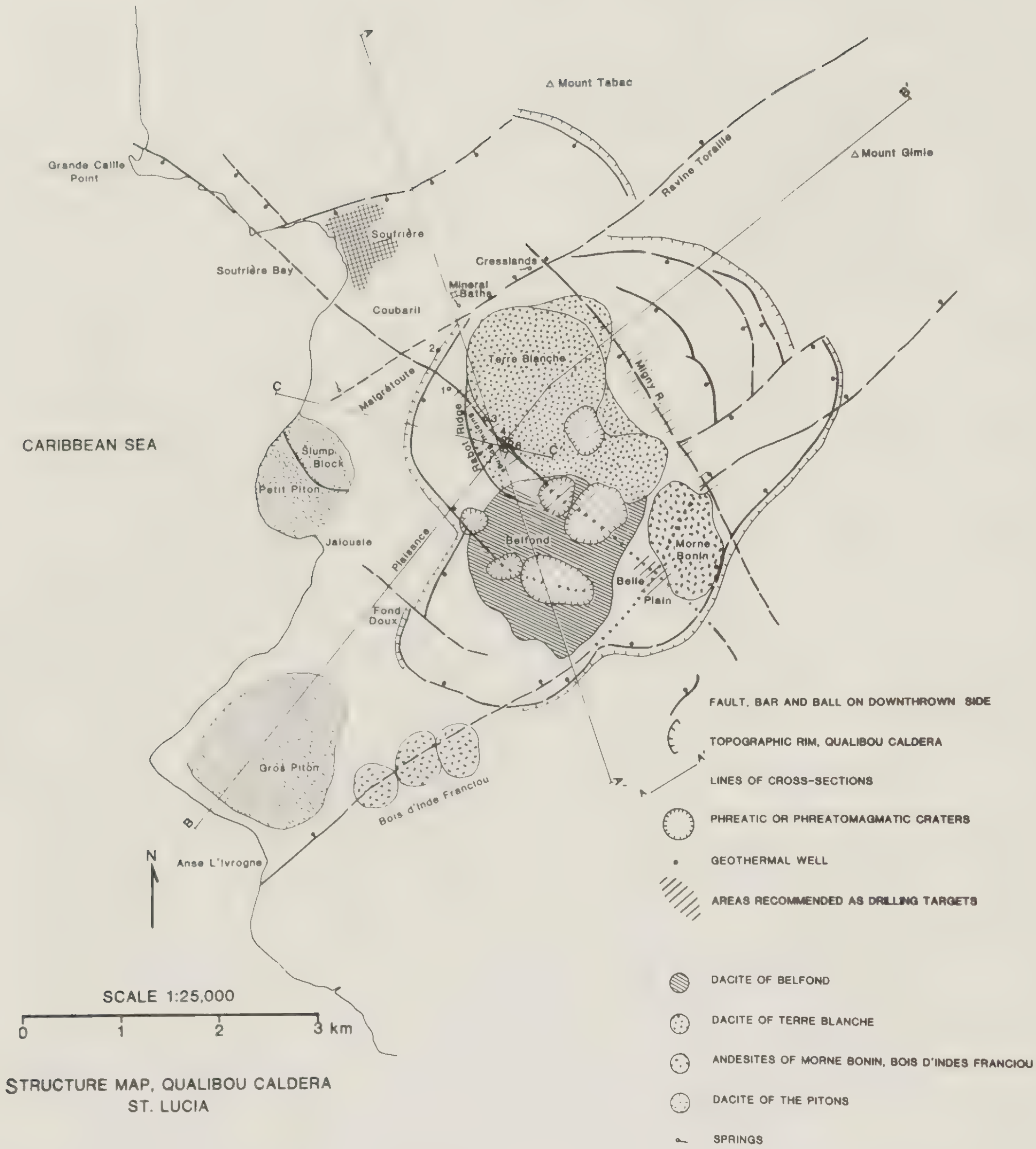

Figure 16.2.2. Structural geologic map of Qualibou Caldera, from Wohletz and others (1986).

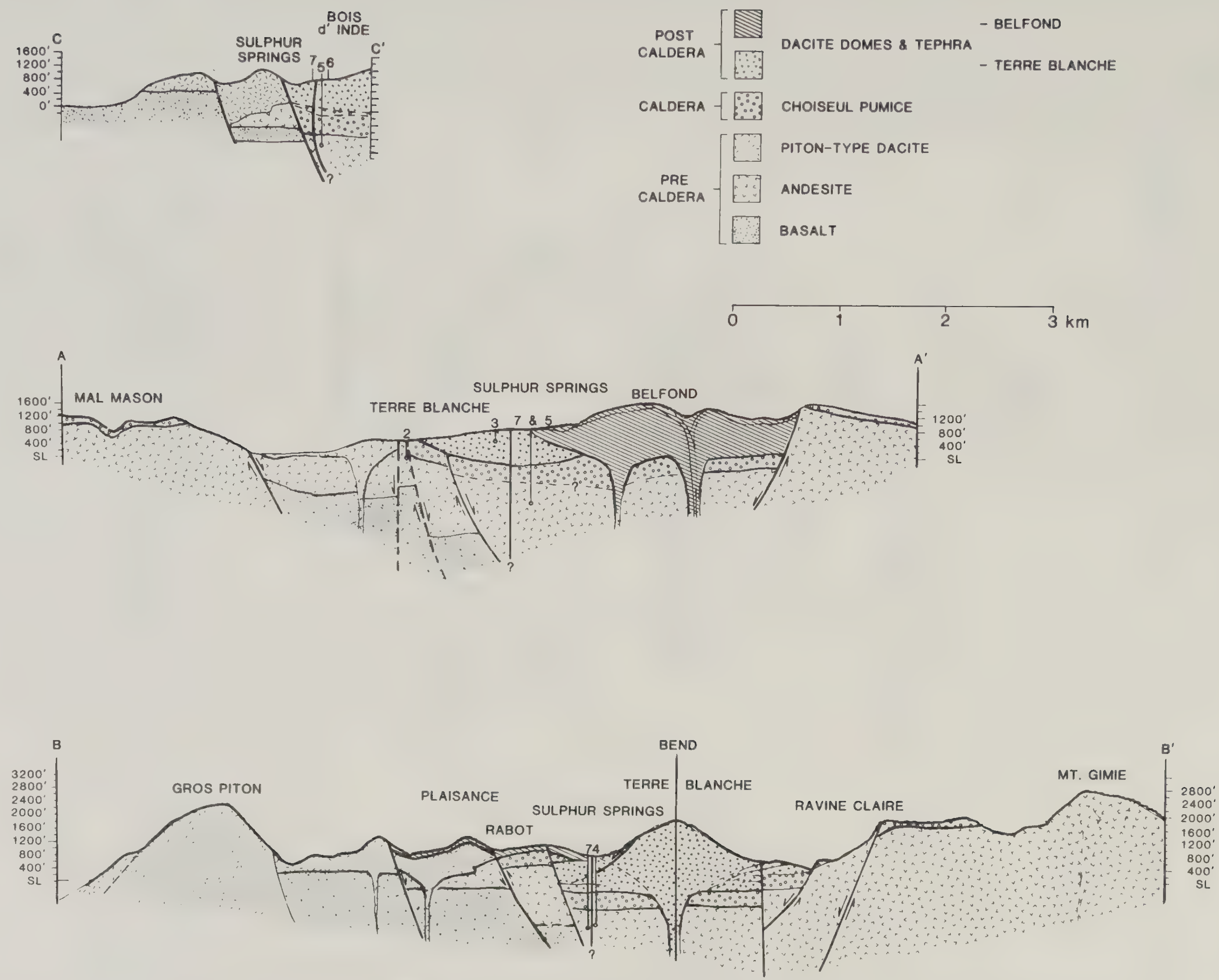

Figure 16.2.3. Cross sections through Qualibou Caldera, from Wohletz and others (1986). A-A': Mal Mason to Belle Vue (azimuth 342°); B-B': Anse L'Ivrogne to Mount Gimie (azimuths 40° and 50°); C-C': Malgretoute through Sulfur Springs (azimuth 282°). See figure 16.2.2 for locations of cross sections.

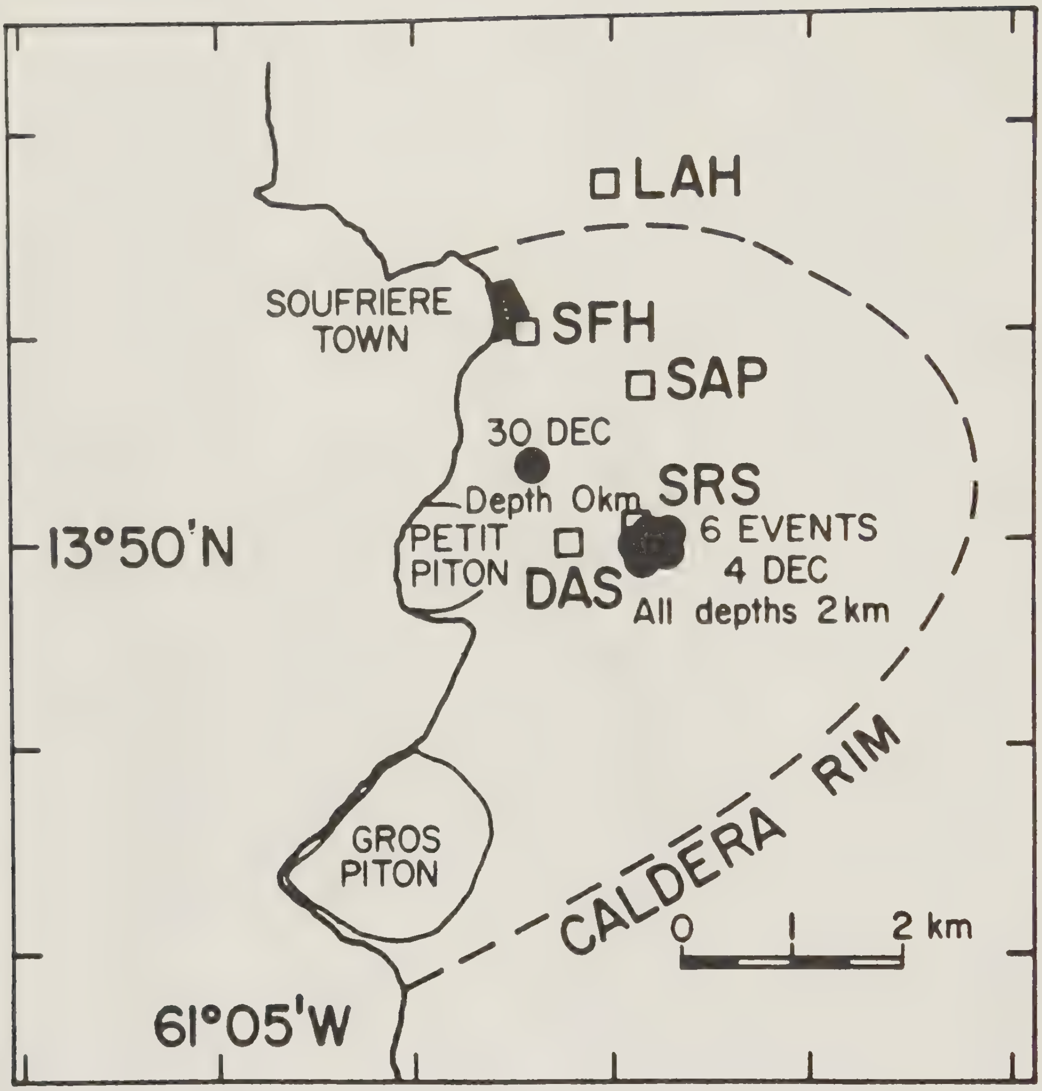

Figure 16.2.4. Location of seismic stations (open squares) and epicenters of local seismic events on 4 December 1974 and 30 December 1974 (solid circles) near Qualibou Caldera, St. Lucia, from Aspinall and others (1976). Copyright by the American Geophysical Union.

Figure 17. Locations of large, Quaternary restless calderas (solid circles) in Region 17.

PART 3: HISTORICAL UNREST AT LARGE QUATERNARY CALDERAS (continued)
See inside back cover for explanation and abbreviations

KATLA

CAVW number (active vent)	Latitude Longitude (degrees)	Diameter (km)	Local tectonic setting	Precaldera edifice	SiO_2 content (wt pct)	Age of collapse (yr B.P.)	Date of unrest	Type and duration of unrest ESTU STHF MGTF H Te	Eruption type
17-02-04 (Katla= K)	63.63N 19.03W	11 x 14	Intraplate	LL-strat (subglacial)	R = 47-49		A.D. 934 (E)	---- ---x ---- - --	Ex, LF
							ca. 950?	---- ---- ---- - --	lf, subgl
including 17-02-14 (Eldgja= E)							ca. 1179	---- ---- ---- - --	ex, subgl
							1245	---- ---- ---- - --	ex, subgl
							1262	---- ---- ---- - --	Ex, subgl
							1311	---- ---- ---- - --	Ex, subgl
							between 1354/1360	---- ---- ---- - --	Ex, subgl
							1416	---- ---- ---- - --	ex, subgl
							ca. 1490	---- ---- ---- - --	Ex, subgl
							1580	---- ---- ---- - --	ex, subgl
							1612	---- ---- ---- - --	ex, subgl
							1625	x--- ---- ---- - --	Ex, subgl
							1660-61	B--- ---- ---- - --	ex, subgl
							1721	x--- ---- ---- - --	EX, subgl
							1755-56	B--- ---- ---Y - --	EX, subgl
							1823	B--- ---- ---- - --	ex, subgl
							1860	B--- ---- ---- - --	ex, subgl
							1918	B--- ---- ---- - --	EX, subgl
							1951-88+	G--- ?--- ---- - --	subgl?

TECTONIC SETTING

The Mid-Atlantic plate boundary passes through Iceland and is reflected in two zones of crustal spreading and volcanism--an eastern zone, the site of most historical eruptions, and a western zone. Katla is situated near the south end of the eastern volcanic zone, south of its junction with the transform zone in South Iceland (fig. 17.1.1). It is thus in an intraplate setting where little or no extension is occurring. Eruptions of Katla are only indirectly linked with episodes of spreading if they are linked at all, in contrast to direct links between eruptions and spreading at Krafla (Gudmundsson and Sæmundsson, 1980).

GEOLOGIC HISTORY

Katla is hidden under the cap of the Myrdalsjökull ice sheet--on average about 400 m thick (fig. 17.1.2) (Thorarinsson, 1960; Rist, 1967; Sigbjarnarson, 1973). The only products of Katla that have been studied are distal tephra and glacial outburst flood (jökulhlaup) deposits (Thorarinsson, 1957; Einarsson and others, 1980; Jonsson, 1982). The Eldgja fissure swarm northeast of Katla, active in A.D. 934, is part of the Katla volcanic system (Thorarinsson and Sæmundsson, 1979).

KATLA (continued)

HISTORICAL ACTIVITY

Eruptions of Katla are known from as early as the 10th century, and since 1580 they have occurred on average every 42 years.

934: A fissure eruption from Eldgja was one of the largest in recorded history, comparable to that from Laki in 1783.

1625, 2 September and following: Small earthquakes were felt in Alftaver, ca. 35 km southeast of Katla, on the early morning of 2 September and were followed by an eruption and a jökulhlaup later the same morning. Earthquakes were reported to have occurred intermittently during the 12 days the eruption lasted.

1660, 3 November: Earthquakes were felt in Myrdalur ca. 20 km south of Katla for about 1 hour before an eruption cloud was observed.

1721: An earthquake was felt in Myrdalur at about 0900 hr on 11 May, followed at about 1300 hr by an eruption and a jökulhlaup. Earthquakes were reported to have occurred intermittently for several weeks.

1755: Earthquakes began to be felt at noon on 17 October in Myrdalur and continued for some hours before lightning (commonly reported in eruption clouds during Katla eruptions) and a jökulhlaup indicated that eruption had begun. Earthquakes were felt occasionally during the next few weeks.

1823: Earthquakes began to be felt at about 1800 hr on 26 June in Myrdalur, followed by an eruption about three hours later. Earthquakes were reported intermittently during the following two to three weeks.

1860: Earthquakes began to be felt in Myrdalur at 600-800 hr on 8 May. A jökulhlaup followed at 1730 hr that day, and an eruption cloud was observed early next morning.

1918: Earthquakes began to be felt in Myrdalur at about 1300 hr on 12 October. Shortly thereafter an eruption cloud was seen, and a jökulhlaup followed at about 1500 hr (Jonsson, 1982). Earthquakes continued to be felt at least until 28 October.

1951-88+: Earthquake activity at Katla apparently increased around 1951 (Tryggvason 1973b), and since then it has been moderately high. The seismicity has a pronounced annual cycle. The activity culminated in 1967 and 1976-77 with a few earthquakes approaching and exceeding magnitude 5. A small jökulhlaup, possibly caused by a small subglacial eruption, occurred on 25 June 1955. Because of the regular occurrence of Katla eruptions since 1580, another large eruption was expected about 1960, but none has yet occurred. Einarsson (1987) interprets the present seismicity as the result of deflation of the volcano, and speculates that the 1963-67 Surtsey eruptions and the 1973 Heimaey eruption might have relieved pressure in a deep zone of partial melt, thereby delaying the expected Katla eruption.

KATLA (continued)

HISTORICAL ACTIVITY (continued)

Ground tilt measurements made each year near the Myrdalsjökull ice cap (fig. 17.1.3) showed responses to variable snow load, and thus a relatively low ($<10^{13}$ poises) viscosity of the underlying crust and mantle (Tryggvason, 1973a).

The only two historical eruptions of Eyjafjallajökull, a stratovolcano that lies about 30 km west of Katla, coincided approximately with eruptions of Katla in 1612 and 1821-23 (G. Larsen and P. Einarsson, written commun., 1988).

REFERENCES

Einarsson, E.H., Thorarinsson, S., and Larsen, G., 1980, The Solheimar tephra layer and the Katla eruption of 1357: Acta Nat. Islandica, v. 28, p. 3-20.

Einarsson, P., 1987, The anomalous mantle beneath Iceland and possible magma pressure connection between volcanoes [abs.]: Abstracts, Hawaii Symp. on How Volcanoes Work, Hilo, January 1987, p. 61.

Einarsson, P., and Sæmundsson, K., 1987, Earthquake epicenters 1982-1985 and volcanic systems in Iceland: map accompanying the festschrift "I Hlutarins Edli", Reykjavík, Menningarsjóour, 1 sheet, scale 1:750,000.

Gudmundsson, G., and Sæmundsson, K., 1980, Statistical analysis of damaging earthquakes and volcanic eruptions in Iceland from 1550-1978: Jour. Geophys., v. 47, p. 99-109.

Hid islenzka bokmentafelag, 1907-1915, Safn til sogu Islands, v. IV: Reykjavik, Kaupmannahofn, 1025 p.

Jakobsson, S.P., 1979, Petrology of Recent basalts of the Eastern Volcanic Zone, Iceland: Acta Nat. Islandica, v. 26, p. 1-103.

Johannesson, H., Jakobsson, S.P. and Sæmundsson, K., 1982, Geological map of Iceland, sheet 6, S-Iceland, second ed.: Reykjavik, Icelandic Museum of Nat. History/Iceland Geodetic Survey.

Jonsson, J., 1982, Notes on the Katla volcanoglacial debris flows: Jökull, v. 32, p. 61-68.

Kjartansson, G., 1962, Geological map of Iceland, sheet 6, South-Central Iceland: Reykjavik, Museum of Natural History, 1 sheet, scale 1:250,000.

Rist, S., 1967, The thickness of the ice cover of Mýrdalsjökull, southern Iceland: Jökull, v. 17, p. 237-242.

Sæmundsson, K., 1982, Oskjur a virkum eldfjallasvaedum a Islandi (Calderas in active volcanic areas in Iceland), in Thorarinsdóttir, H., Oskarsson, O.H., Steinthorsson, S., and Einarsson, Th., (eds.), Eldur er i nordri: Reykjavik, Sogufelag, p. 221-240.

Sigbjarnarson, G., 1973, Katla and Askja: Jökull, v. 23, p. 45-51.

Thorarinsson, S., 1957, The jökulhlaup from the Katla area 1955, compared with other jökulhlaups in Iceland: Jökull, v. 7, p. 20-25.

----- 1960, On the predicting of volcanic eruptions in Iceland: Bull. Volcanol., v. 23, p. 45-52.

----- 1973, Data sheets of the post-Miocene volcanoes of the world, Sheet II, Iceland: Rome, IAVCEI, 10 p.

Thorarinsson, S., and Sæmundsson, K., 1979, Volcanic activity in historical time: Jökull, v. 29, p. 29-32.

Thoroddsen, Th., 1925, Die Geschichte der Islandischen Vulkane: D. Kgl. Dansk Vidensk. Selsk. Skrifter, Naturvidensk. og Mathem. Afd. Copenhagen, 8th ser., v. 9, 458 p.

Tryggvason, E., 1973a, Surface deformation and crustal structure in the Myrdalsjökull area of south Iceland: Jour. Geophys. Res., v. 78, no. 14, p. 2488-2497.

Tryggvason, E., 1973b, Seismicity, earthquake swarms and plate boundaries in the Iceland region: Bull. Seismol. Soc. Am., v. 63, p. 1327-1348.

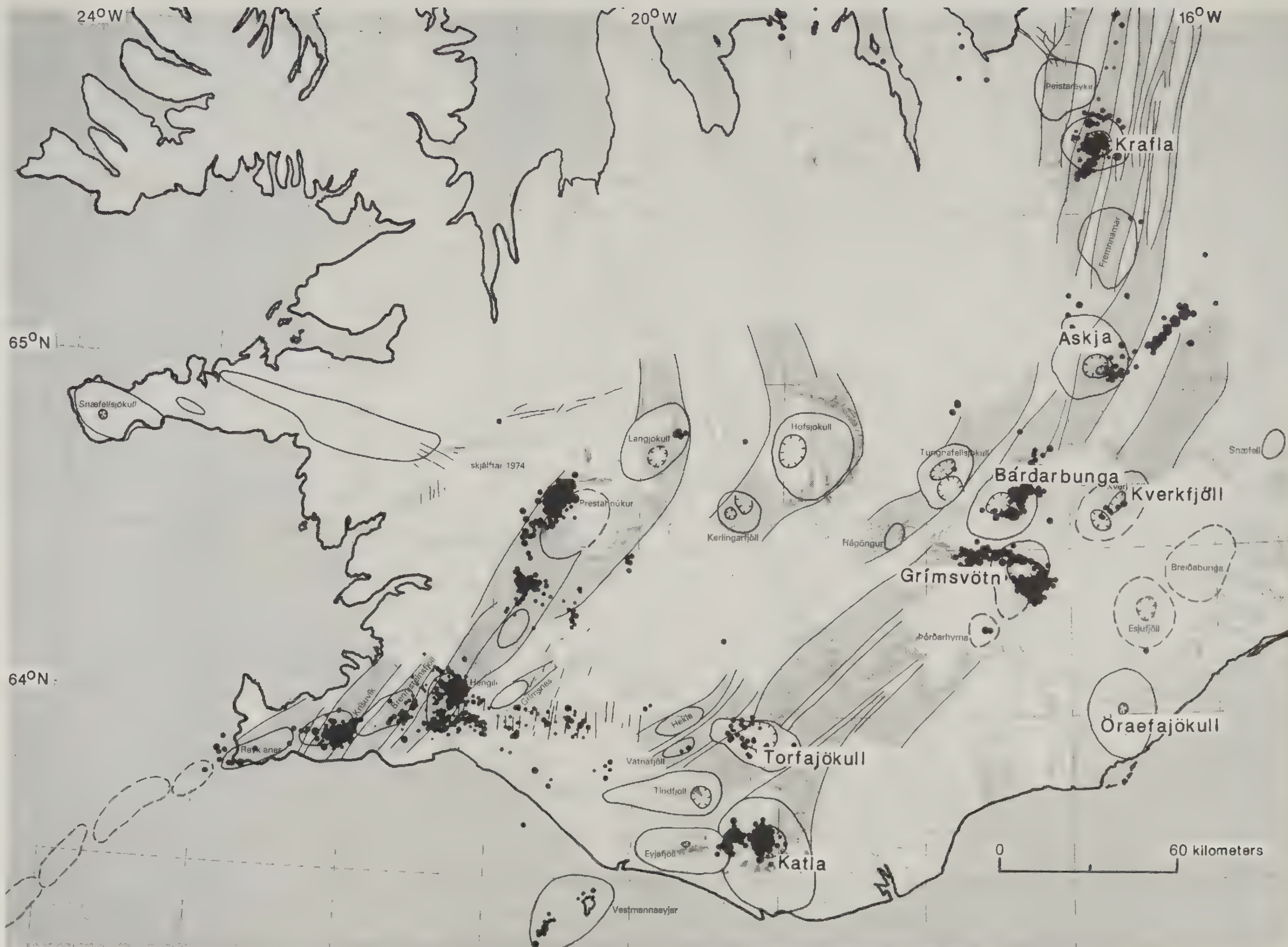

Figure 17.1.1. Volcanic centers and earthquake epicenters (1982-85) in Iceland, from Einarsson and Sæmundsson (1987). Restless calderas are labeled prominently.

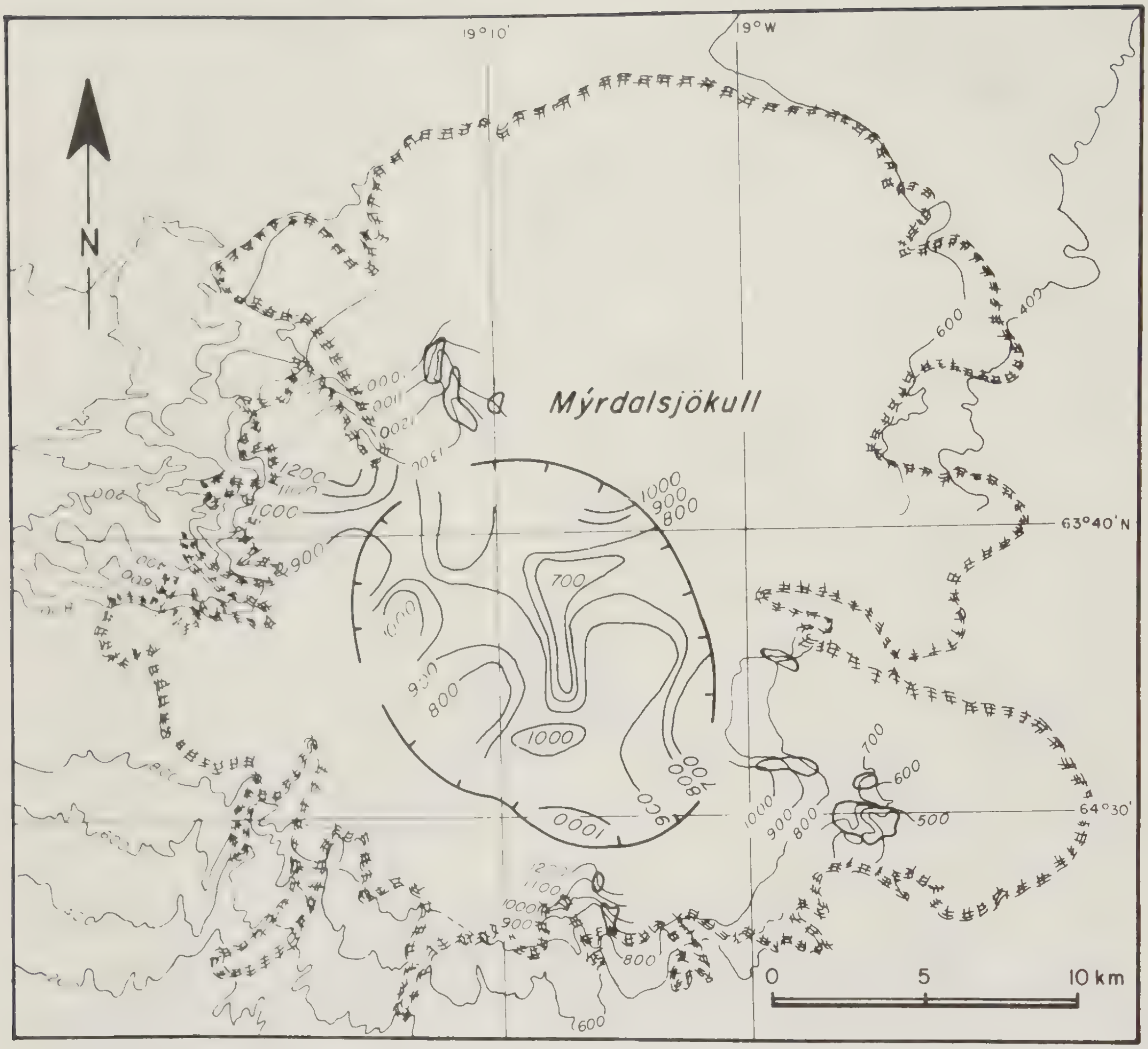

Figure 17.1.2. Katla Volcano and Caldera (both under the Myrdalsjökull ice sheet), from Sæmundsson (1982). Contour interval for subglacial topography,. 100 m.

Figure 17.1.3. Southeast part of Myrdalsjökull ice field showing locations of Katla Volcano and bench-mark arrays for tilt measurements (Tryggvason, 1973a). Insets show location of map area and configurations of arrays.

ORÆFAJÖKULL

CAVW number (active vent)	Latitude Longitude (degrees)	Diameter (km)	Local tectonic setting	Precaldera edifice	SiO_2 content (wt pct)	Age of collapse (yr B.P.)	Date of unrest	Type and duration of unrest ESTU STHF MGTF H Te	Eruption type
17-02-21	64.00N	5 x 4	Intraplate	Strato	R = 70(1362)	<700,000	1362	?--- ---- ---- - --	EX,subgl
(Oræfajökull)	16.65W				R = 56(1727)		1727-28	C--- ---- ---- - --	Ex,subgl

TECTONIC SETTING

The Mid-Atlantic plate boundary passes beneath Iceland and is reflected in two zones of spreading and volcanism--an eastern zone, the site of most historical eruptions, and a western zone. Oræfajökull is situated east of the eastern volcanic zone, in an intraplate setting (see fig. 17.1.1 in section on Katla). Eruptions of Oræfajökull are only indirectly linked with episodes of spreading, in contrast to direct links between eruptions and spreading at Krafla (Gudmundsson and Sæmundsson, 1980).

GEOLOGIC HISTORY

Oræfajökull is the highest central volcano in Iceland, 2119 m above sea level, and has a glacial cap (fig. 17.2.1). Most of its rocks are basaltic lava flows, palagonitic tuffs, and glacial deposits, but the high northwestern caldera rim (Hvannadalshnúkur) is a flow-banded rhyolite (liparite) (Thorarinsson, 1958). Most eruptions in the Holocene have been explosive summit eruptions; however, some Holocene lava flows from flank eruptions are also known (Thorarinsson, 1958).

HISTORICAL ACTIVITY

1362: At least 2 km^3 of rhyolitic magma (DRE) were erupted in 1362. Several settlements were destroyed by jökulhlaups and tephra fall. Because pumice fall penetrated farmhouses from nearly the beginning of the eruption, Thorarinsson (1958) inferred that strong earthquakes had occurred shortly before the eruption, damaging those houses.

1727: The second eruption during historical time, of intermediate composition magma, occurred in 1727. Earthquakes were felt at the Sandfell vicarage 9 km southwest of the center of the caldera approximately 1 day before the 1727 eruption began, but there is no historical record or archaeological evidence that the 1727 earthquakes caused damage (Thorarinsson, 1958).

ORÆFAJÖKULL (continued)

REFERENCES

Gudmundsson, G., and Sæmundsson, K., 1980, Statistical analysis of damaging earthquakes and volcanic eruptions in Iceland from 1550-1978: Jour. Geophys., v. 47, p. 99-109.

Perrey, A., 1845, Sur les tremblements de terre de la Peninsule Scandinave: Paris, Arthus Bertrand, 63 p.

Prestvik, T., 1980, Petrology of hybrid intermediate and silicic rocks from Oræfajökull, southeast Iceland: Geol. Foren. Stockh. Forh., v. 101, p. 299-307.

Thorarinsson, S., 1958, The Oræfajökull eruption of 1362: Acta Nat. Islandica, v. 2, no. 2, p. 1-99.

----- 1960, On the predicting of volcanic eruptions in Iceland: Bull. Volcanol., v. 23, p. 45-52.

----- 1973, Data sheets of the post-Miocene volcanoes of the world, Sheet II, Iceland: Rome, IAVCEI, 10 p.

Thoroddsen, Th., 1925, Die Geschichte der Islandischen Vulkane: D. Kgl. Dansk Vidensk. Selsk. Skrifter, Naturvidensk. og Mathem. Afd. Copenhagen, 8th ser., v. 9, 458 p.

Torfason, H., 1985, Geological map of Iceland, sheet 9, SA-Iceland: Reykjavik, Icelandic Museum of Natural History and Iceland Geodetic Survey, 1 sheet, scale 1:250,000.

Figure 17.2.1. Location of Oræfajökull Volcano and Caldera on east border of eastern volcanic zone of Iceland, from Thoroddsen (1925). Caldera rim added from Torfason (1985).

BARDARBUNGA

CAVW number (active vent)	Latitude Longitude (degrees)	Diameter (km)	Local tectonic setting	Precaldera edifice	SiO_2 content (wt pct)	Age of collapse (yr B.P.)	Date of unrest	Type and duration of unrest ESTU STHF MGTF H Te	Eruption type
no CAVW number (Bárdarbunga)	64.62N 17.50W	7 x 11	Exten	LL-strat (subglacial)	R = b C = b		1477-ca.1480	---- --xx ---- - =?	EX
							1717	---- ---- ---- - --	EX
							1974-87	xx-- ---- ---- - --	none
17-02-18 (Trollagigar =Trollahraun)	64.43N 18.13W						1862-64	---- --xx ---- - --	1f,ex
within 17-02-11 (Vatnaöldur)	63.95N 19.28W						ca. 900	---- --xx ---- - --	EX,1f
17-02-11 (Veidivötn)	63.95N 19.28W						ca. 1480	---- --xx ---- - --	EX,1f

TECTONIC SETTING

The Mid-Atlantic plate boundary passes through Iceland and is reflected in two zones of spreading and volcanism--an eastern zone, the site of most historical eruptions, and a western zone. Bárdarbunga is situated in the central part of the eastern volcanic zone. A 150-km-long fissure swarm extends 40 km to the northeast and 110 km to the southwest of Bárdarbunga (figs. 17.1.1 in section on Katla, 17.3.1). As at Krafla, magma from a shallow magma chamber beneath Bárdarbunga has moved laterally into the fissure swarm during rifting episodes (Larsen, 1984). Alternatively, Jakobsson (1979) and Blake (1984) have suggested that a central feeder lies in the Klofnafell-Mani area, 70-80 km southwest of Bárdarbunga.

GEOLOGIC HISTORY

Bárdarbunga lies beneath the northwest corner of the Vatnajökull ice cap. It is the second highest central volcano in Iceland, with rocks exposed up to 1800 m above sea level. On the basis of historical accounts of eruptions and glacial outbursts, and distinctive chemical characteristics of tephra layers, at least ten tephra-producing eruptions are thought to have taken place beneath the northwest corner of the Vatnajökull ice cap during the last 1200 years (Thorarinsson, 1974; Larsen, 1982, 1984; Gudmundsson, 1986). Three eruptions took place on the fissure swarm southwest of Bárdarbunga during the same period. There is no direct evidence that eruptions have taken place within the Bárdarbunga caldera itself during historical time.

BARDARBUNGA (continued)

HISTORICAL ACTIVITY

1477 and 1717: Two large basaltic tephra layers have been correlated with historical accounts of tephra falls in 1477 and 1717. The 1477 tephra (tephra layer "a", formerly attributed to Kverkfjöll by Thorarinsson, 1958) was formed during a large event that included the Veidivötn eruption on the fissure swarm 40-110 km southwest of Bárdarbunga (Larsen, 1984). The 1717 tephra layer was formed by one of several eruptions reported during the first three decades of the eighteenth century, now attributed to the fissure swarm northeast of Bárdarbunga (Gudmundsson, 1986).

ca. 900 and ca. 1480: The two largest eruptions on the fissure swarm southwest of Bárdarbunga in historical time are the Vatnaöldur eruption, ca. 900 A.D., and the Veidivötn eruption, 1480 A.D.±11 yr (Larsen, 1984, 1987). The eruption fissures are up to 70 km long and each produced >1 km^3 of basalt (DRE) that was mostly erupted as tephra. In 1480, at least 1.6 km^3 of basalt was erupted from simultaneously active vents along the full 70-km length of the fissure (Larsen, 1987). Production was strongly controlled by elevation: Vents between 500- and 600-m elevation erupted 5 times as much magma per kilometer as did vents between 600- and 700-m elevation, and vents from 700- to 900-m elevation erupted very small volumes of magma (Larsen, 1987). The fissures continue into the Torfajökull caldera (see section on Torfajökull), where rhyolites were erupted simultaneously with the basalts elsewhere on the fissures. No historical accounts mention eruptions in this area, and they were identified through tephrochronological studies (Larsen, 1984, 1987).

1862-64: An eruption on the Trollahraun fissure, 30-45 km southwest of Bárdarbunga, produced 0.3 km^3 of lava and a minor amount of tephra (Thorarinsson and Sigvaldason, 1972). Contemporary documents do not mention earthquakes.

1974-88 and continuing: The seismic activity of Bárdarbunga increased markedly in 1974, and in the period 1974-86 nine earthquakes of magnitude 5 and larger occurred. No earthquakes of comparable magnitude occurred in the previous 50 years. Fault-plane solutions show reverse faulting that Einarsson (1986, 1987) suggested is the result of deflation of a shallow magma chamber beneath Bárdarbunga.

COMMENTS

Einarsson (1987) suggested that deflation at Bárdarbunga might be a pressure-drop response to concurrent inflation at Krafla, 110 km to the north, and speculated that the pressure changes were transmitted through a partially molten layer beneath the crust that has been inferred from seismic and magnetotelluric measurements.

BARDARBUNGA (continued)

REFERENCES

Blake, S., 1984, Magma mixing and hybridization processes at the alkalic, silicic, Torfajökull central volcano triggered by tholeiitic Veidivötn fissuring, South Iceland: Jour. Volcanol. Geotherm. Res., v. 22, p. 1-31.

Brandsdóttir, B., 1984, Seismic activity in Vatnajökull in 1900-1982, with special reference to Skeidararhlaups, Skaflarhlaups, and Vatnajökull eruptions: Jökull, v. 34, p. 141-150.

Einarsson, P., 1986, Seismicity along the eastern margin of the North American Plate, in Vogt, P.R. and Tucholke, B.E., eds., The geology of North America, v. 14, The western North Atlantic region: Boulder, Geol. Soc. Am., p. 99-116.

----- 1987, The anomalous mantle beneath Iceland and possible magma pressure connection between volcanoes [abs.]: Abstracts, Hawaii Symp. on How Volcanoes Work, Hilo, January 1987, p. 61.

Einarsson, P., and Bjornsson, S., 1979, Earthquakes in Iceland: Jökull, v. 29, p. 37-43.

Einarsson, P., and Brandsdóttir, B., 1984, Seismic activity preceding and during the 1983 volcanic eruption in Grímsvötn, Iceland: Jökull, v. 34, p. 13-23.

Gudmundsson, A., 1986, Eldgos a Dyngjuhalsi a 18. old (Eruptions in the Dyngjuhals area in the 18th century): Náttúrufrædingurinn, v. 56, p. 43-48.

Jakobsson, S.P., 1979, Petrology of Recent basalts of the Eastern Volcanic Zone, Iceland: Acta Nat. Islandica, v. 26, p. 1-103.

Larsen, G., 1982, Gjoskutimatal Jökuldals og nagrennis (Tephrochronology of the Jökuldalur area), in Thorarinsdóttir, H., Oskarsson, O.H., Steinthorsson, S. and Einarsson, Th., eds., Eldur er i nordri: Reykjavik, Sogufelag, p. 51-65.

----- 1984, Recent volcanic history of the Veidivötn fissure swarm, southern Iceland--an approach to volcanic risk assessment: Jour. Volcanol. Geotherm. Res., v. 22, p. 33-58.

----- 1987, The dike of the 1480 A.D. Veidivötn eruption, S-Iceland [abs.]: IUGG XIX Gen. Assembly, Vancouver, B.C., Abstracts, v. 2, p. 396.

Sæmundsson, K., 1972, Jardfraediglefsur um Torfajökulssvaedid: Náttúrufrædingurinn, v. 42, p. 81-99.

----- 1982, Oskjur a virkum eldfjallasvaedum a Islandi (Calderas in active volcanic areas in Iceland), in Thorarinsdóttir, H., Oskarsson, O.H., Steinthorsson, S. and Einarsson, Th., eds., Eldur er i nordri: Reykjavik, Sogufelag, p. 221-240.

Thorarinsson, S., 1958, The Oræfajökull eruption of 1362: Acta Nat. Islandica, v. II, 2, p. 1-99.

----- 1974, Votnin strid. Saga Skeidararhlaupa og Grimsvatnagosa (The swift flowing rivers. The history of Grímsvötn eruptions and jökulhlaups in Skeidara river): Reykjavik, Menningarsjodur, 254 p.

Thorarinsson, S., and Sigvaldason, G.E., 1972, The Trollagigar eruption 1862-64: Jökull, v. 22, p. 12-26.

Figure 17.3.1. Veidivötn fissure swarm (ruled area) on eastern volcanic zone of southern Iceland, from Larsen (1984). B, Bárdarbunga central volcano; T, Torfajökull central volcano; KL, Klofnafell area; H, Hekla central volcano; K, Katla central volcano; Ö, Oræfajökull central volcano.

TORFAJÖKULL

CAVW number (active vent)	Latitude Longitude (degrees)	Diameter (km)	Local tectonic setting	Precaldera edifice	SiO_2 content (wt pct)	Age of collapse (yr B.P.)	Date of unrest	Type and duration of unrest ESTU STHF MGTF H Te	Eruption type
no CAVW number (Torfajökull)	63.93N 19.15W	13 x 18	Intraplate		R = 70-72 C = silicic		ca. 900 A.D.	---- --xx ---- - --	lf,Ex
							ca. 1480 A.D.	---- --xx ---- - --	lf,Ex
							1986-88+	CC-- ---- ---- - --	none

TECTONIC SETTING

The Mid-Atlantic plate boundary passes through Iceland and is reflected in two zones of spreading and volcanism -- an eastern zone, the site of most historical eruptions, and a western zone. The Torfajökull Central Volcano is located at the intersection where the eastern volcanic zone (a divergent plate boundary) joins with the south Iceland seismic zone (a transform plate boundary) (fig. 17.1.1 in section on Katla). Little or no extension is occurring south of this intersection.

GEOLOGIC HISTORY

Torfajökull Volcano is a feature of relatively low relief, and is an area of predominantly rhyolite volcanism and intense geothermal activity (fig. 17.4.1). Most of the rhyolite has been subglacially emplaced as domes or flows. A few postglacial flows of rhyolite exist in the western part of the caldera (Sæmundsson, 1972; Ivarsson, 1983; Blake, 1984; McGarvie, 1984).

HISTORICAL ACTIVITY

ca. 900 A.D.: Rhyolitic tephra and lava was erupted at Hrafntinnuhraun, inside the Torfajökull caldera, during a rifting episode on the Veidivötn fissure swarm. Basaltic tephra was erupted at the same time on the Vatnaöldur fissure (see section on Bárdarbunga).

ca. 1480 A.D.: Rhyolitic lava and tephra was erupted at Laugahraun and Namshraun, near the north rim of the Torfajökull caldera, during a rifting episode on the Veidivötn fissure swarm. These lavas lie on the southwesternmost 3-4 km of the ca. 70-km-long Veidivötn fissure (see section on Bárdarbunga), which produced basaltic tephra and lava (Larsen, 1984; McGarvie, 1984; Mörk, 1984).

The Torfajökull caldera is an area of moderate, persistent seismicity. A few earthquakes in the magnitude range 3-4 occur every year. The epicenters are mainly in the western part of the caldera, where the high temperature geothermal activity and postglacial volcanism is also concentrated. Since 1985, when a local seismograph was installed, low frequency earthquakes have been detected that appear to originate in the northern or eastern part of the caldera. Bursts of more than 40 low-frequency earthquakes per day occurred in August 1986, November 1986, March 1988, and April 1988 (Brandsdóttir and Einarsson, 1988).

TORFAJÖKULL (continued)

REFERENCES

Blake, S., 1984, Magma mixing and hybridization processes at the alkalic, silicic, Torfajökull central volcano triggered by tholeiitic Veidivötn fissuring, South Iceland: Jour. Volcanol. Geotherm. Res., v. 22, p. 1-31.

Brandsdóttir, B. and Einarsson, P., 1988, On low frequency earthquakes in the volcanic zones of Iceland [abs.]: Eos, Trans. Am. Geophys. Union, v. 69 [in press].

Einarsson, P., and Bjornsson, S., 1979, Earthquakes in Iceland: Jökull, v. 29, p. 37-43.

Ivarsson, G., 1983, The Torfajökull volcano, central south Iceland - chemical evolution and magma-mixing processes [abs.]: Eos, Trans. Am. Geophys. Union, v. 64, no. 45, p. 887.

Jakobsson, S.P., 1979, Petrology of Recent basalts of the Eastern Volcanic Zone, Iceland: Acta Nat. Islandica, v. 26, p. 1-103.

Larsen, G., 1984, Recent volcanic history of the Veidivötn fissure swarm, southern Iceland--an approach to volcanic risk assessment: Jour. Volcanol. Geotherm. Res., v. 22, p. 33-58.

McGarvie, D.W., 1984, Torfajökull - A volcano dominated by magma mixing: Geology, v. 12, p. 685-688.

Mörk, M.B.E., 1984, Magma mixing in the post-glacial Veidivötn fissure eruption, South Iceland: Lithos, v. 17, p. 55-75.

Sæmundsson, K., 1972, Jardfraediglefsur um Torfajökulssvaedid: Náttúrufrædingurinn, v. 42, p. 81-99.

----- 1982, Oskjur a virkum eldfjallasvaedum a Islandi (Calderas in active volcanic areas in Iceland), in Thorarinsdóttir, H., Oskarsson, O.H., Steinthorsson, S. and Einarsson, Th., eds., Eldur er i nordri: Reykjavik, Sogufelag, p. 221-240.

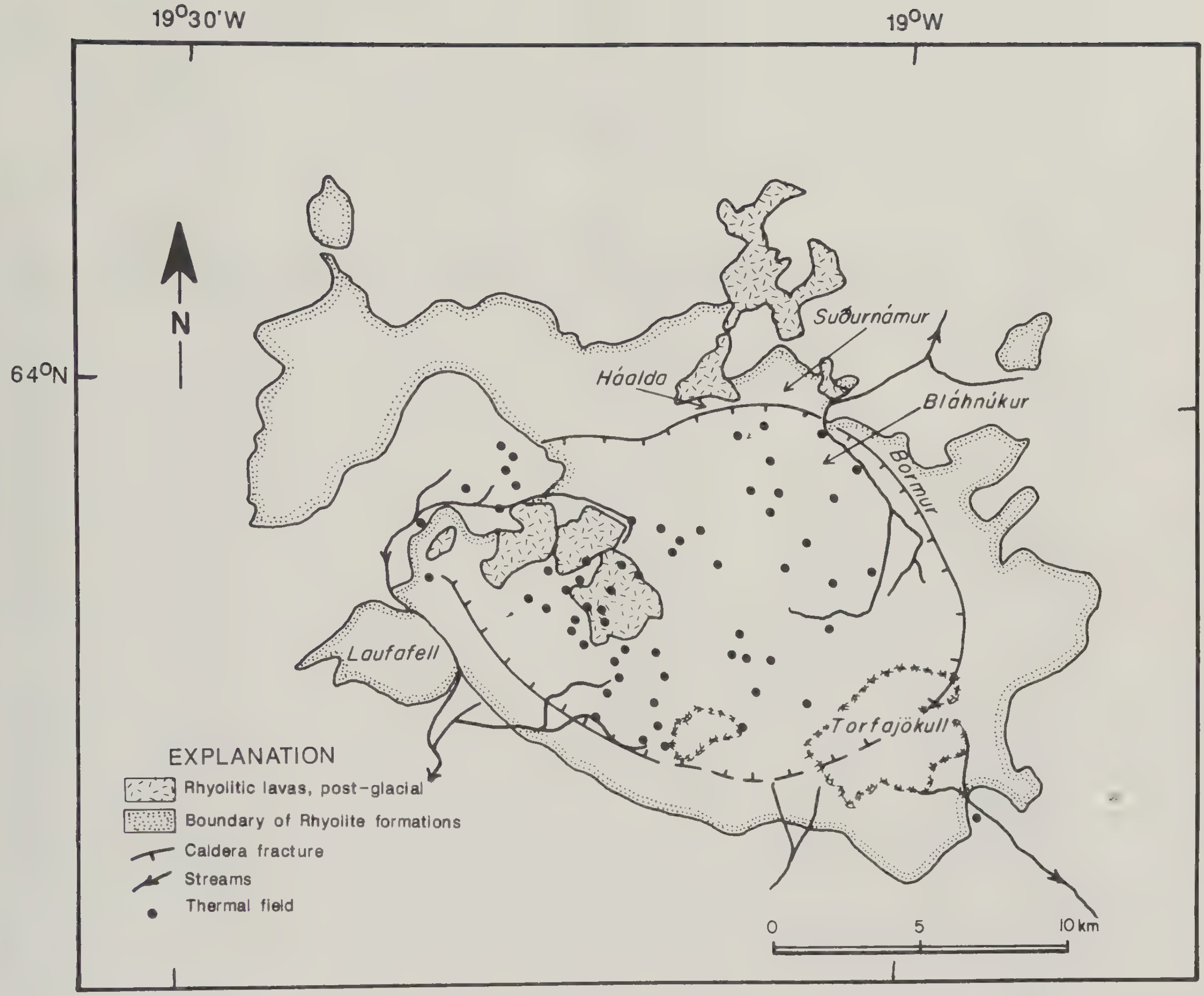

Figure 17.4.1. Outline map of Torfajökull central volcano and caldera, from Sæmundsson (1982). See figures 17.1.1 and 17.3.1 for location of Torfajökull at southwest end of Veidivötn fissure swarm.

PART 3: HISTORICAL UNREST AT LARGE QUATERNARY CALDERAS (continued)
See inside back cover for explanation and abbreviations

GRIMSVÖTN

CAVW number (active vent)	Latitude Longitude (degrees)	Diameter (km)	Local tectonic setting	Precaldera edifice	SiO_2 content (wt pct)	Age of collapse (yr B.P.)	Date of unrest	Type and duration of unrest ESTU STHF MGTF H Te	Eruption type
17-02-22	64.42N	6-8	Exten	LL-strat	R = mafic		1332	---- ---- ---- - --	ex, subgl
(Grimsvötn= G)	17.33W			(subglacial)			1341	---- ---- ---- - --	ex, subgl
17-02-15							1598	---- ---- ---- - --	Ex, subgl
(Lakagigar= L)							1603?	---- ---- ---- - --	ex, subgl
17-02-16							1619	---- ---- ---- - --	ex, subgl
(Sidhjökull= S)							1629	---- ---- ---- - --	ex, subgl
17-02-17							1638	---- ---- ---- - --	ex, subgl
(Hagongur= H)							1659	---- ---- ---- - --	ex, subgl
17-02-19							1681?	---- ---- ---- - --	subgl?
(Thordarhyrna= T)							1684-85	---- ---- ---- - --	ex, subgl
							1706	---- ---- ---- - --	ex, subgl
							1716	---- ---- ---- - --	ex, subgl
							1725-26	---- ---- ---- - --	subgl
							1753 (S)	---- ---- ---- - --	ex
							1766	---- ---- ---- - --	ex, subgl
							1774	---- ---- ---- - --	ex, subgl
							1783-84(L)	DD-- --xx ---- - --	EX, LF
							1783-85	---- ---- ---- - --	ex, subgl
							1797	---- ---- ---- - --	ex, subgl
							1816	---- ---- ---- - --	ex, subgl
							1823?(G,T)	---- ---- ---- - --	ex, subgl
							1838	---- ---- ---- - --	ex, subgl
							1854?	---- ---- ---- - --	ex, subgl
							1861?	---- ---- ---- - --	ex, subgl
							1867	---- ---- ---- - --	ex, subgl
							1873	Y--- ---- ---- - --	Ex, subgl
							1883	---- ---- ---- - --	ex, subgl
							1887? (T)	---- ---- ---- - --	ex, subgl
							1891-92?	---- ---- ---- - --	ex, subgl
							1902-4(G,T)	x--- ---- ---- - --	ex, subgl
							1910?	---- ---- ---- - --	ex, subgl

GRIMSVÖTN (continued)

CAVW number (active vent)	Latitude Longitude (degrees)	Diameter (km)	Local tectonic setting	Precaldera edifice	SiO_2 content (wt pct)	Age of collapse (yr B.P.)	Date of unrest	Type and duration of unrest ESTU STHF MGTF H Te	Eruption type
(continued from previous page)							1922	---- ---- ---- - --	ex, subgl
							1933-34	Y--- ---- ---- - --	ex, subgl
							1938	---- ---- ---- - --	subgl
							1939	---- ---- ---- - --	subgl
							1941	---- ---- ---- - --	subgl
							1945	---- ---- --x- - --	pex, subgl
							1948	---- ---- --x- - --	none?
							1954	---- ---- ---- - --	pex, subgl
							1982-83	EBA- ---- ---- - --	subgl, ex

TECTONIC SETTING

The Mid-Atlantic plate boundary passes through Iceland and is reflected in two zones of spreading and volcanism -- an eastern zone, the site of most historical eruptions, and a western zone. Grímsvötn is situated in the central part of the eastern volcanic zone (fig. 17.1.1 in section on Katla). A fissure swarm extends 70 km to the southwest. By analogy with Krafla it has been suggested that magma from a shallow magma chamber beneath Grímsvötn has moved laterally into the fissure swarm during rifting episodes (Sigurdsson and Sparks, 1978).

GEOLOGIC SETTING

Grímsvötn, together with Bárdarbunga and Kverkfjöll, lie beneath the vast Vatnajökull icecap in east-central Iceland (fig. 17.5.1). Due to its subglacial setting and remoteness, the geology of Grímsvötn is poorly known. The volcano has a composite central caldera, of which the southern rim is the only exposed part of the volcano. Only basaltic material is known to have erupted from Grímsvötn. Most known eruptions of Grímsvötn have occurred within the caldera, but the Laki eruption (12 km^3 of basaltic lava) from the fissure swarm 40-70 km southwest of the volcano may also have been fed from a shallow chamber beneath the caldera (Sigurdsson and Sparks, 1978; Sigurdsson, 1983). A large geothermal area in the caldera, with an estimated heat output of 5000 MW (Bjornsson, 1974, 1983), continually supplies meltwater to an ice-covered caldera lake. Approximately every 4-10 years the accumulated water is released in glacial outburst floods (jökulhlaups) when the water level is high enough to lift its ice dam (Thorarinsson, 1953; Björnsson, 1974, 1975; Björnsson and Kristmannsdóttir, 1984). Some jökulhlaups are associated with eruptions. In some instances it can be argued that the extra meltwater generated by a subglacial eruption triggered the draining of the caldera lake (for example, during the 1938 eruption). In other cases the sudden pressure release associated with draining may trigger an eruption (Thorarinsson, 1974).

GRIMSVÖTN (continued)

HISTORICAL ACTIVITY

Many of the eruptions listed in the table may be mislocated. They may have occurred in other volcanoes, known or unknown, beneath the northwest part of the Vatnajökull ice sheet.

1783-84: The largest basaltic fissure eruption in historical time began on 8 June 1783 on the Lakagigar fissure, 40-70 km southwest of Grímsvötn, after three weeks of earthquake activity. The eruption produced 11.9 km^3 of lava, 0.2 km^3 (DRE) of tephra, and a gas plume ("haze") that drifted across Europe. Beginning on about 8 June 1783, vigorous fountaining occurred from 135 craters along 10 en echelon segments of a 27-km-long rift (Thordarson and others, 1987). Eruptions began at the distal (southwest) end of the rift and migrated systematically uprift from 8 June until October 1783 (Thordarson and others, 1987). The eruption ended in February 1784. Eruptions also occurred at or near Grímsvötn on 26 September 1783 and possibly as early as on 18 July 1783, and continued into 1785 (Thorarinsson, 1969, 1984; Einarsson and Sveinsdóttir, 1984; Sigurdsson, 1982; Thordarson and others, 1987).

1873: During an eruption of Grímsvötn, an earthquake was felt in South Iceland, about 150 km away (Thorarinsson, 1974); it is uncertain whether the earthquake was associated with Grímsvötn.

1902-04: Jökulhlaups occurred north of Grímsvötn in December 1902 and May 1903. Another jökulhlaup began on 25 May 1903, southeast of Grímsvötn, during which earthquakes were felt in the Oræfi district on two (unspecified) days (Brandsdóttir, 1984). Earthquakes, rumbling, and crashing noises reached their maximum on 28-29 May 1903. Eruptions are thought to have occurred at Thordarhyrna (20 km south-southwest of Grímsvötn) and at Grímsvötn itself. The eruption(s?) continued until January 1904, but there are no further reports of felt earthquakes (Brandsdóttir, 1984).

1933-34: From 30 November to 10 December 1933, red glow and "fires" were reported at Grímsvötn, but no earthquakes were recorded at Reykjavik. Then, in 1934, a jökulhlaup occurred on 22 March. Five earthquakes of $\underline{M}$=3.5 or greater occurred on 30 March--one of $\underline{M}$=4.5 at 2004 hr and four of $\underline{M}$=3.5-3.75 within 2 hours after the start of an eruption at 2030 hr. Eruptions continued until 7 April, and a felt earthquake was reported on 30 April. Another eruption, possibly in Grímsvötn, occurred in December 1934 without any recorded earthquakes.

1938, 1941: Subglacial eruptions occurred, but there were no earthquakes large enough to be recorded (that is, none larger than $\underline{M}$=3.5).

1945: Increased geothermal activity was discovered in the south part of the caldera on 26-27 July. Jökulhlaups began on 16 September and lasted 11 days. A small eruption probably occurred, but no earthquakes were recorded or felt.

1948: The rate of ice melting at Grímsvötn was 50 percent higher than average in 1948, but no eruption or earthquakes were recorded.

GRIMSVÖTN (continued)

HISTORICAL ACTIVITY (continued)

1954 - mid-1982: Generally higher seismicity beneath the Vatnajökull ice sheet was associated with an increase in geothermal activity in the cauldron areas northwest of Grímsvötn. This and other short periods of heating contrast with a generally declining heat output during 1900-80 (Björnsson, 1983). Over the same period, a comparable increase in heat output has occurred in an area 10 km northwest of Grímsvötn, about halfway between Grímsvötn and Bárdarbunga (Björnsson, 1977, 1983).

1982-83: Earthquakes began in December 1982 and gradually increased during April-May 1983, centered under the southeast rim of Grímsvötn caldera (fig. 17.5.2). Intense seismicity began at 0400 hr on 28 May 1983, with $\underline{M}_{max}$ about 4. Earthquake activity declined at approximately 1000 hr, and bursts of tremor began at approximately 1200 hr. Tremor increased in intensity (amplitude) at about 1500 hr on 28 May and continued at a high level for about 1 day before decreasing. The eruption was first visible on the morning of 29 May, by which time it had broken and melted its way through the icecap (fig. 17.5.3) (Einarsson and Brandsdóttir, 1984; Grönvold and Jóhannesson, 1984).

REFERENCES

Björnsson, H., 1974, Explanation of Jökulhlaups from Grímsvötn, Vatnajökull, Iceland: Jökull, v. 24, p. 1-26.

----- 1975, Subglacial water reservoirs, Jökulhlaups and volcanic eruptions: Jökull, v. 25, p. 1-14.

----- 1977, The cause of Jökulhlaups in the Skaftá River, Vatnajökull: Jökull, v. 27, p. 71-78.

----- 1983, A natural calorimeter at Grímsvötn: an indicator of geothermal and volcanic activity: Jökull, v. 33, p. 13-18.

Björnsson, H., and Kristmannsdóttir, H., 1984, The Grímsvötn geothermal area, Vatnajökull, Iceland: Jökull, v. 34, p. 25-50.

Brandsdóttir, B., 1984, Seismic activity in Vatnajökull in 1900-1982, with special reference to Skeidararhlaups, Skaflarhlaups, and Vatnajökull eruptions: Jökull, v. 34, p. 141-150.

Einarsson, P., and Brandsdóttir, B., 1984, Seismic activity preceding and during the 1983 volcanic eruption in Grímsvötn, Iceland: Jökull, v. 34, p. 13-23.

Einarsson, Th., and Sveinsdóttir, E.L., 1984, in Gunnlaugsson, G.A., Gudbergsson, G.M., Thorarinsson, S., Rafnsson, S., and Einarsson, Th., eds., Skaftareldar 1783-1784: Reykjavik, Mal og Menning, p. 37-48.

Grönvold, K., and Johannesson, H., 1984, Eruption in Grímsvötn 1983, course of events and chemical studies of the tephra: Jökull, v. 34, p. 1-12.

Gudmundsson, G., and Sæmundsson, K., 1980, Statistical analysis of damaging earthquakes and volcanic eruptions in Iceland from 1550-1978: Jour. Geophys., v. 47, p. 99-109.

Johannesson, H., 1983, Gossaga Grimsvatna 1900-1983 i stuttu mali (A brief review of the volcanic activity of the Grímsvötn volcanic system 1900-1983): Jökull, v. 33, p. 146-147.

----- 1987, Grimsvatnagos 1816 (Evidence of an eruption in Grímsvötn in 1816): Náttúrufrædingurinn, v. 57, p. 157-159.

GRIMSVÖTN (continued)

REFERENCES (continued)

Kjartansson, G., 1962, Geological map of Iceland, sheet 6, South-Central Iceland: Reykjavik, Museum of Natural History, 1 sheet, scale 1:250,000.

Sigurdsson, H., 1982, Volcanic pollution and climate: the 1783 Laki eruption: Eos, Trans. Am. Geophys. Union, v. 63, p. 601-602.

----- 1983, The 1783 Lakagigar fissure eruption [abs.]: Eos, Trans. Am. Geophys. Union, v. 64, p. 887.

Sigurdsson, H., and Sparks, R.S.J., 1978, Lateral magma flow within rifted Icelandic crust: Nature, v. 274, p. 126-130.

Smithsonian Institution, Scientific Event Alert Network (SEAN), 1982-83, Grímsvötn: SEAN Bull., v. 7, no. 2; v. 8, no. 5.

Steinthorsson, S., 1977, Tephra layers in a drill core from the Vatnajökull ice cap: Jökull, v. 27, 27 p.

Thorarinsson, S., 1953, Some new aspects of the Grímsvötn problem: Jour. Glaciol., v. 2, no. 14, p. 267-274.

----- 1960, On the predicting of volcanic eruptions in Iceland: Bull. Volcanol., v. 23, p. 45-52.

----- 1969, The Lakagigar eruption of 1783: Bull. Volcanol., v. 33, no. 3, p. 910-929.

----- 1973, Data sheets of the post-Miocene volcanoes of the world, Sheet II, Iceland: Rome, IAVCEI, 10 p.

----- 1974, Votnin strid. Saga Skeidararhlaupa og Grimsvatnagosa (The swift flowing rivers. The history of Grímsvötn eruptions and jökulhlaups in Skeidara river): Reykjavik, Menningarsjodur, 254 p.

----- 1984, Annall Skaftarelda (The Laki Fires), in Gunnlaugsson, G.A., Gudbergsson, G.M., Thorarinsson, S., Rafnsson, S., and Einarsson, Th., eds., Skaftareldar 1783-1784: Reykjavik, Mal og Menning, p. 11-36.

Thordarson, Th., Self, S., Larsen, G., and Steinthorsson, S., 1987, Eruption sequence of the Skaftar Fires 1783-1785, Iceland [abs.]: Eos, Trans. Am. Geophys. Union, v. 68, p. 1550.

Thoroddsen, Th., 1925, Die Geschichte der Islandischen Vulkane: D. Kgl. Dansk Vidensk. Selsk. Skrifter, Naturvidensk. og Mathem. Afd. Copenhagen, 8th ser., v. 9, 458 p.

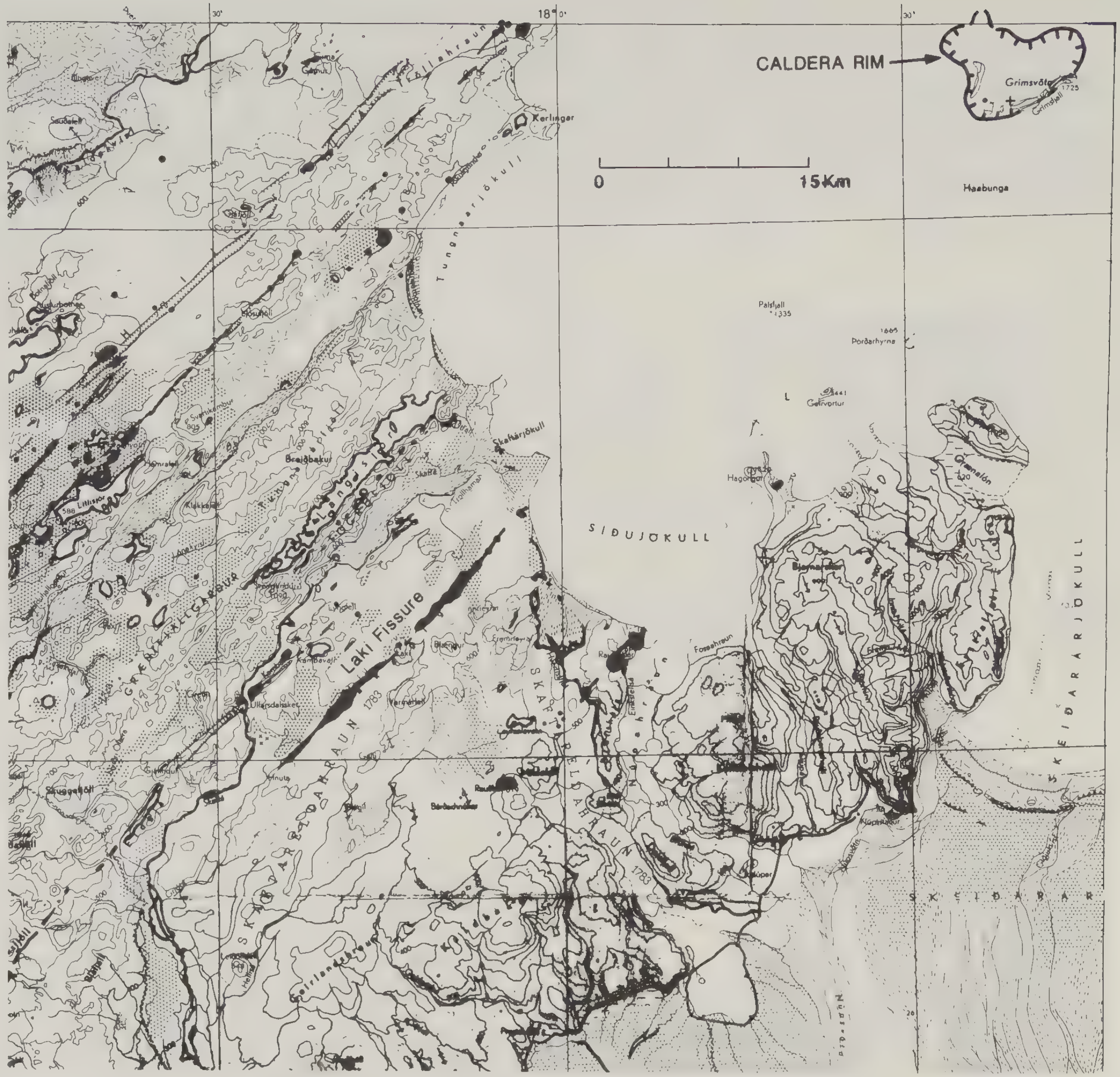

Figure 17.5.1. Grímsvötn Caldera, located under Vatnajökull icecap, from Kjartansson (1962). Voluminous basaltic lava flows were erupted from Lakagigar (Laki), southwest of Grímsvötn, in 1783.

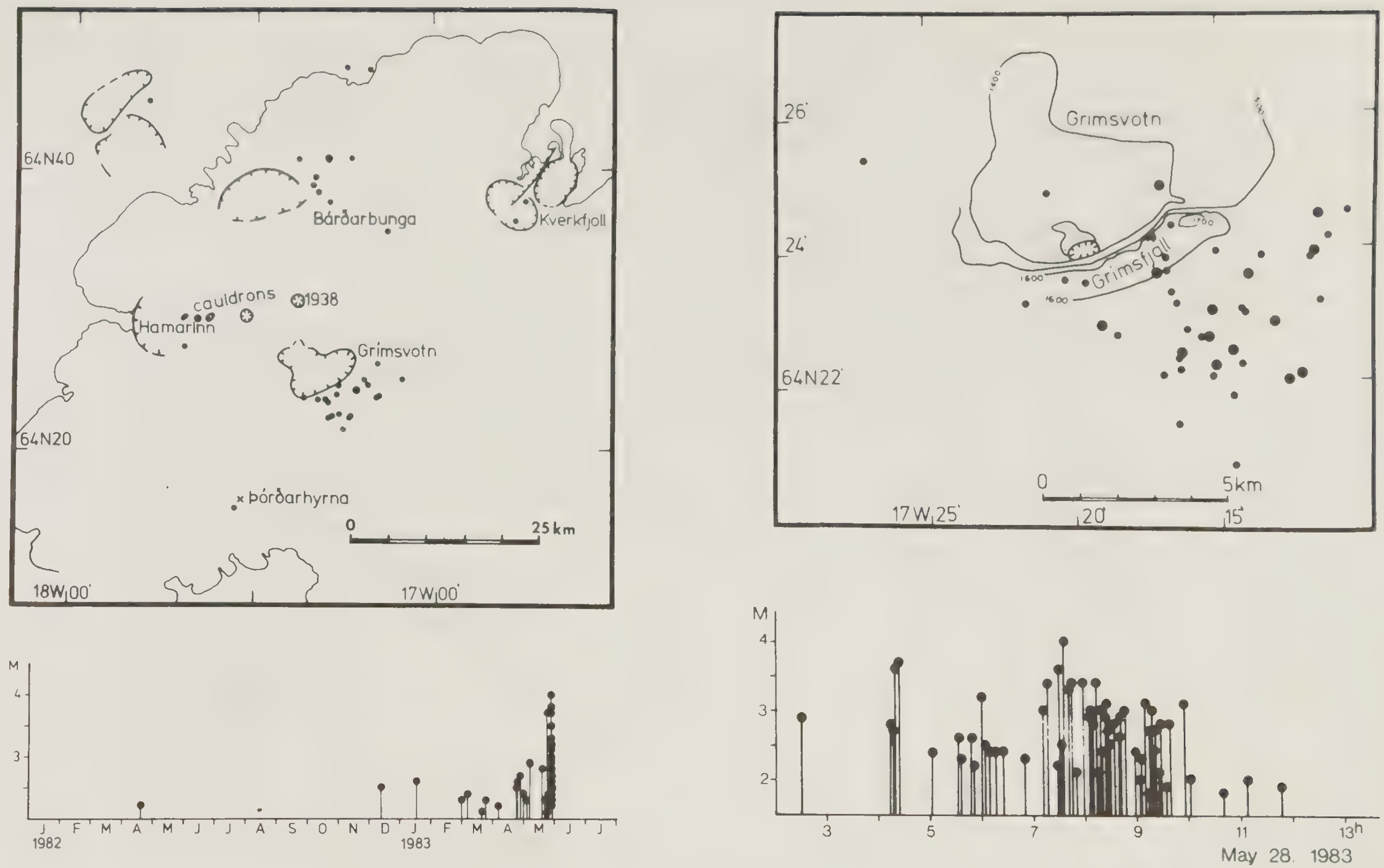

Figure 17.5.2. Epicentral map (left) of western Vatnajökull area for the period 1 January 1982 to 27 May 1983, from Einarsson and Brandsdóttir (1984). Small dots mark epicenters of earthquakes smaller than magnitude 3; larger dots denote events larger than magnitude 3. Calderas and inferred subglacial calderas are shown, as are ice cauldrons associated with jökulhlaups in Skafta River and presumed subglacial eruption of 1938. Almost all earthquakes southeast of Grímsvötn occurred in early 1983. Enlarged view (right) of Grímsvötn epicentral area and plot of earthquake magnitude versus time during May 1983.

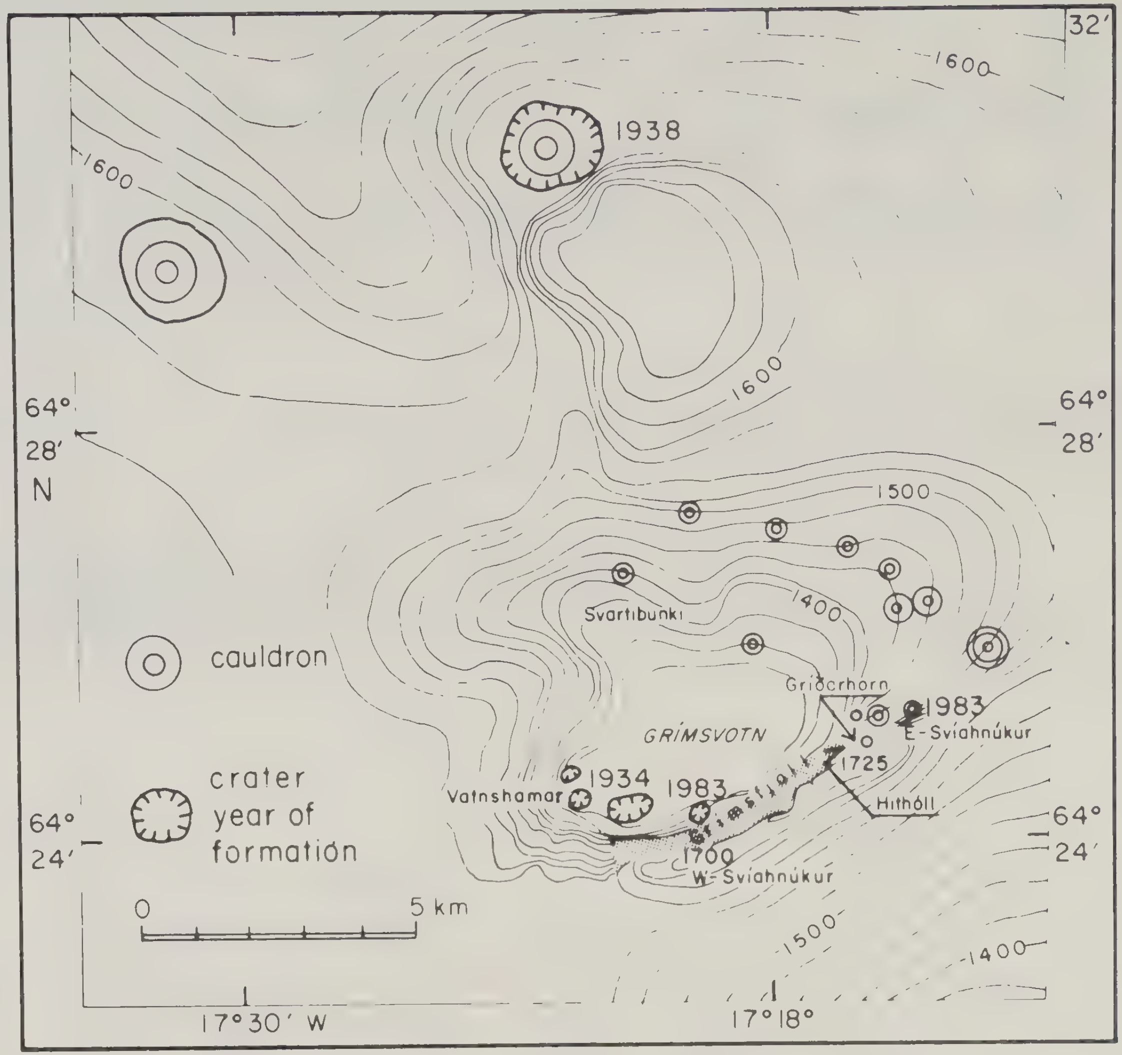

Figure 17.5.3. Grímsvötn area, from Björnsson and Kristmannsdóttir (1984). Shown are craters of 1934 and 1983, depression north of Svartibunki from 1938, and ice cauldrons. Cauldron that formed during jökulhlaup in 1983 is also marked. Cauldron northwest of Grímsvötn drains to Skafta River.

PART 3: HISTORICAL UNREST AT LARGE QUATERNARY CALDERAS (continued)
See inside back cover for explanation and abbreviations

KVERKFJÖLL

CAVW number (active vent)	Latitude Longitude (degrees)	Diameter (km)	Local tectonic setting	Precaldera edifice	SiO_2 content (wt pct)	Age of collapse (yr B.P.)	Date of unrest	Type and duration of unrest ESTU STHF MGTF H Te	Eruption type
17-02-23 (Kverkfjöll)	64.65N 16.70W	7.5 x 5.5 8 x 5	Exten	LL-strat, partly subglacial	R = mafic		1655	---- ---- ---- - --	subgl
							1684	---- ---- ---- - --	subgl, ex
							1711	---- ---- ---- - --	subgl
							1716?-17	---- ---- ---- - --	subgl, ex?
							1726	---- ---- ---- - --	subgl
							1726	---- ---- ---- - --	subgl
							1729	---- ---- ---- - --	subgl
							1874-75?	---- ---- ---- - --	subgl, ex

TECTONIC SETTING

The Mid-Atlantic plate boundary passes beneath Iceland and is reflected in two zones of spreading and volcanism--an eastern zone, the site of most historical eruptions, and a western zone. Kverkfjöll is situated in the central part of the eastern volcanic zone, just northeast of Grímsvötn (fig. 17.1.1 in section on Katla).

GEOLOGIC HISTORY

Kverkfjöll is a central stratovolcano on the northeast edge of the Vatnajökull ice sheet (fig. 17.6.1). Two ice-filled calderas have been inferred.

HISTORICAL ACTIVITY

No historical eruptions are known with certainty to have occurred at Kverkfjöll. Most possible eruptions of Kverkfjöll have been inferred from glacial outburst floods. The location of the 17th century eruptions is uncertain. The 18th century eruptions listed above have been attributed to Bárdarbunga as well as to Kverkfjöll (Gudmundsson, 1986; Larsen, 1982).

1874-75: An eruption column south of Askja may have originated at Kverkfjöll (Sigurdsson and Sparks, 1978; G. Larsen and P. Einarsson, written commun., 1988). This inferred eruption of Kverkfjöll occurred during major rifting in the Askja area (see section on Askja).

Small earthquakes have been recorded in Kverkfjöll in recent years.

KVERKFJÖLL (continued)

REFERENCES

Einarsson, P., and Brandsdóttir, B., 1984, Seismic activity preceding and during the 1983 volcanic eruption in Grímsvötn, Iceland: Jökull, v. 34, p. 13-23.
Gudmundsson, A., 1986, Eldgos a Dyngjuhalsi a 18. old (Eruptions in the Dyngjuhals area in the 18th century): Náttúrufrædingurinn, v. 56, p. 43-48.
Gudmundsson, G., and Sæmundsson, K., 1980, Statistical analysis of damaging earthquakes and volcanic eruptions in Iceland from 1550-1978: Jour. Geophys., v. 47, p. 99-109.
Larsen, G., 1982, Gjoskutimatal Jökuldals og nagrennis (Tephrochronology of the Jökuldalur area), in Thorarinsdóttir, H., Oskarsson, O.H., Steinthorsson, S. and Einarsson, Th., eds., Eldur er i nordri: Reykjavik, Sogufelag, p. 51-65.
Sæmundsson, K., 1982, Oskjur a virkum eldfjallasvaedum a Islandi (Calderas in active volcanic areas in Iceland), in Thorarinsdóttir, H., Oskarsson, O.H., Steinthorsson, S. and Einarsson, Th., eds., Eldur er i nordri: Reykjavik, Sogufelag, p. 221-240.
Sigurdsson, H., and Sparks, R.S.J., 1978, Rifting episode in North Iceland in 1874-1875 and the eruption of Askja and Sveinagja: Bull. Volcanol., v. 41, p. 149-167.
Thorarinsson, S., 1960, On the predicting of volcanic eruptions in Iceland: Bull. Volcanol., v. 23, p. 45-52.
----- 1973, Data sheets of the post-Miocene volcanoes of the world, Sheet II, Iceland: Rome, IAVCEI, 10 p.
Thorarinsson, S., and Sæmundsson, K., 1979, Volcanic activity in historical time: Jökull, v. 29, p. 29-32.
Thoroddsen, Th., 1925, Die Geschichte der Islandischen Vulkane: D. Kgl. Dansk Vidensk. Selsk. Skrifter, Naturvidensk. og Mathem. Afd. Copenhagen, 8th ser., v. 9, 458 p.

Figure 17.6.1. Inferred outlines of Kverkfjoll Calderas, located under Vatnajökull ice sheet. Outlines of calderas from Einarsson and Brandsdóttir (1984). See also figures 17.1.1 and 17.5.2.

ASKJA, OSKJUVATN

CAVW number (active vent)	Latitude Longitude (degrees)	Diameter (km)	Local tectonic setting	Precaldera edifice	SiO_2 content (wt pct)	Age of collapse (yr B.P.)	Date of unrest	Type and duration of unrest ESTU STHF MGTF H Te	Eruption type
17-03-03 (Askja)	65.03N 16.75W	9 (Askja) 4 (Oskju-vatn)	Exten	LL-strat	R = 50-51 C = 51-75	A.D. 1875	1874-75	EE-- E--E --EE E QU	EX,lf
							1919?	---- ---- ---- - --	ex
17-03-09 (Sveinagja)							1921-26	---- ---- ---- - --	lf,ex
							1929	---- ---- ---- - --	lf,ex
							1961	D--Z Z--D --DD D --	lf,ex
							late 1960's-present	---F FF-- ---- - --	none

TECTONIC SETTING

Askja is in the central part of the volcanic rift zone that marks the Mid-Atlantic plate boundary through Iceland. The 100-km-long Askja fissure swarm extends 25 km south-southwest and 75 km north-northeast of Askja (fig. 17.7.1). Two episodes of rifting are known historically (see below). Sveinagja, an area of venting during the 1874-75 unrest, is near the northern end of the Askja fissure swarm. The Tjornes Fracture Zone is an E-W-trending ridge-ridge transform zone, about 100 km north of Askja, connecting the eastern volcanic zone of Iceland and the Kolbeinsey Ridge.

GEOLOGIC HISTORY

Askja is a caldera in Dyngjufjoll, a central stratovolcano built mainly of palagonite tuff and pillow lavas. The Askja Caldera formed in prehistoric time; the Oskjuvatn Caldera formed in early 1875 (see below). The Askja Caldera apparently formed in response to migration of basaltic magma into the Askja fissure swarm; the Oskjuvatn Caldera formed in response to similar migration of basaltic magma and a late-stage explosive eruption of mixed basalt-rhyolite magma (Sigurdsson and Sparks, 1978; Sparks and others, 1981).

HISTORICAL ACTIVITY

1874-75: A rifting episode and large volcanic eruption occurred during this period (fig. 17.7.1). Severe earthquakes, including one with an estimated magnitude of 6 to 7, occurred on 17-18 April 1872 along the Tjornes Fracture Zone roughly 100 km north-northwest of Askja. A causal relationship with the Askja events is uncertain. Intense steam emission from Askja was reported in February 1874, and increased seismic activity and ground cracking occurred in the Sveinagja area, 50-70 km north of Askja in the fall of 1874. In mid-December 1874, seismic activity increased in the northern rift zone, and between Christmas and New Year's Day

ASKJA, OSKJUVATN (continued)

HISTORICAL ACTIVITY (continued)

earthquakes were felt continuously all over northeast Iceland (Sparks and others, 1981). Small explosive and effusive eruptions (of both basalt and rhyolite) began at Askja on 1 January 1875 and were soon joined by basaltic fissure eruptions at Sveinagja on 18 February. A paroxysmal, dominantly rhyolitic eruption of Askja occurred on 28-29 March. Eruptions continued until May 1875 at Askja and until October 1875 at Sveinagja.

The Oskjuvatn Caldera formed by collapse, principally as basaltic magma migrated into the fissures north of Askja. Collapse had begun by mid-February 1875, before the main explosion (28 March), and most collapse had occurred by July 1875. The volume of collapse was 2 km^3, compared with only 0.5 km^3 of magma erupted at Askja and Sveinagja combined; the balance was presumably intruded as dikes between Askja and Sveinagja (Sigurdsson and Sparks, 1978).

1919: A small eruption, for which the only evidence is a tephra layer in the Bárdarbunga ice core (Steinthorsson, 1977). Askja is a possible but uncertain source for this tephra.

1921-26: Lava flows issued from vents around Oskjuvatn's rim (fig. 17.7.2), but no regional rifting was observed.

1929: A basaltic fissure eruption occurred south of Askja about this time but the year is uncertain.

1961: An eruption occurred from vents in the northeast part of the Askja Caldera, but no regional rifting occurred. Small earthquakes began on 6 October 1961; large solfataras and geysers began to form on or about 9 October, together with many fissures on the caldera floor. The principal fissure was a N-S line in the eastern part of Askja Caldera, marked by a number of fumaroles in figure 17.7.2. This fissure opened from before 10 October until 15-17 October, accompanied by discharges of hot water. Violent geyser activity occurred from 17 October until 19 October or shortly thereafter, and this activity shifted to rhythmic fuming (without water discharge) until an eruption began on 26 October (Sigvaldason, 1964). About 0.1 km^3 of basaltic lava was erupted from an E-W trending fissure on the floor of Askja Caldera. After the eruption, the level of the caldera lake dropped 2-3 m and fissures formed along the caldera wall.

Late 1960's-present: Measurements of ground deformation in Askja were initiated in 1966. Precision leveling, lake-level measurements, and electronic distance measurements (EDM) show three periods of deflation (1966-67, 1968-70, and after 1972) and two periods of inflation (1967-68 and 1970-72) with a poorly defined center of uplift or subsidence in the central region of the Askja caldera. The rate of subsidence during deflation is about 8-9 cm/yr; the rate of inflation in 1970-72 was two or three times faster (20-30 cm/yr) in the central part of the caldera. Slow deflation occurred from 1972 until at least 1987 (Tryggvason, 1987).

ASKJA, OSKJUVATN (continued)

COMMENTS

Oskjuvatn is the only caldera in this compilation to have formed in conjunction with a major rifting episode in historical time, in 1874-75. Rifting and basaltic dike intrusion preceded and presumably triggered the eruption of silicic magma from the Askja central volcano.

REFERENCES

Björnsson, A., Sæmundsson, K, Einarsson, P., Tryggvason, E., and Grönvold, K., 1977, Current rifting episode in North Iceland: Nature, v. 266, p. 318-323.

Gudmundsson, G., and Sæmundsson, K., 1980, Statistical analysis of damaging earthquakes and volcanic eruptions in Iceland from 1550-1978: Jour. Geophys., v. 47, p. 99-109.

Sæmundsson, K., 1982, Oskjur a virkum eldfjallasvaedum a Islandi (Calderas in active volcanic areas in Iceland), in Thorarinsdóttir, H., Oskarsson, O.H., Steinthorsson, S., and Einarsson, Th., eds., Eldur er i nordri: Reykjavik, Sogufelag, p. 221-240.

Sigurdsson, H., and Sparks, R.S.J., 1978, Rifting episode in North Iceland in 1874-1875 and the eruption of Askja and Sveinagja: Bull. Volcanol., v. 41, p. 149-167.

Sigvaldason, G.E., 1964, Some geochemical and hydrothermal aspects of the 1961 Askja eruption: Beitrage Mineral. Petrog., v. 10, p. 263-274.

----- 1968, Structure and products of subaquatic volcanoes in Iceland: Contrib. Mineral. Petrol., v. 18, p. 1-16.

Sparks, R.S.J., Wilson, L., and Sigurdsson, H., 1981, The pyroclastic deposits of the 1875 eruption of Askja, Iceland: Phil. Trans. Roy. Soc. London, v. 299, Ser. A, p. 241-273.

Steinthorsson, S., 1977, Tephra layers in a drill core from the Vatnajökull ice cap: Jökull, v. 27, p. 2-27.

Thorarinsson, S., 1973, Data sheets of the post-Miocene volcanoes of the world, Sheet II, Iceland: Rome, IAVCEI, 10 p.

Thorarinsson, S., and Sigvaldason, G.E., 1962, The eruption of Askja in 1961, a preliminary report: Am. Jour. Sci., v. 260, p. 641-651.

Thoroddsen, Th., 1925, Die Geschichte der Islandischen Vulkane: D. Kgl. Dansk Vidensk. Selsk. Skrifter, Naturvidensk. og Mathem. Afd. Copenhagen, 8th ser., v. 9, 458 p.

Tryggvason, E., 1973, Seismicity, earthquake swarms and plate boundaries in the Iceland region: Bull. Seismol. Soc. Am., v. 63, p. 1327-1348.

Tryggvason, E., 1987, Surface deformation of the volcano Askja [abs.]: Abstracts, Hawaii Symposium on How Volcanoes Work, Hilo, January 1987, p. 257.

Volcanological Society of Japan, 1963, Askja: Bull. Volcanic Eruptions, no. 3, p. 7.

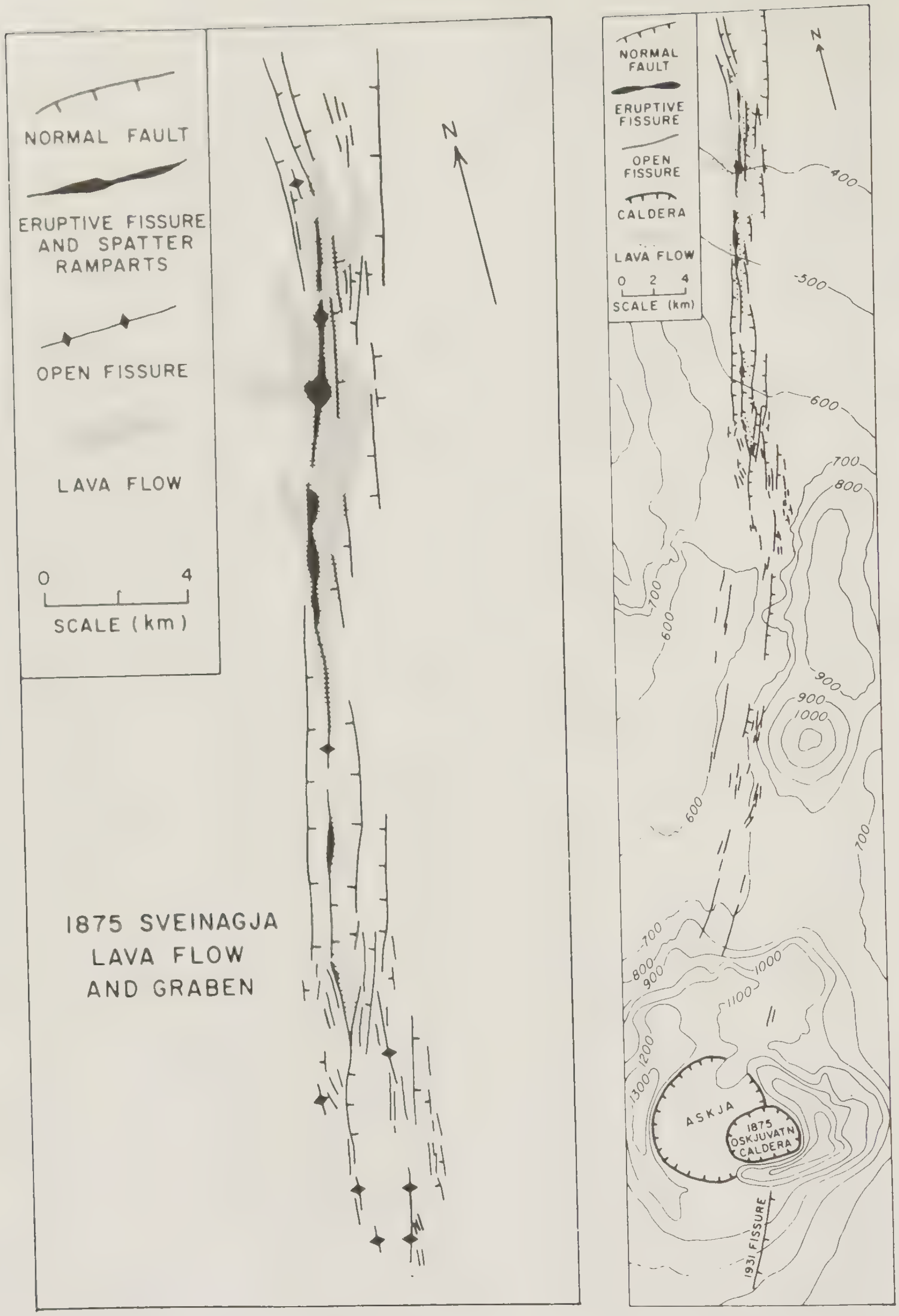

Figure 17.7.1. Askja-Sveinagja fissure swarm, active in the 1874-75 rifting episode, and location of Askja and Oskjuvatn Calderas (Sigurdsson and Sparks, 1978). Left, detailed faulting and distribution of 1875 lava in Sveinagja graben; right, position of graben and lava flow in relation to Askja and Oskjuvatn Calderas.

Figure 17.7.2. Askja Caldera, showing locations of recent lava flows, hot springs, craters, and major faults (Sigvaldason, 1964). I, 1961 lava flow; II, lava flows with indicated year of formation; III, preeruption hot springs; IV, lava craters; V, major tectonic fault escarpments.

KRAFLA

CAVW number (active vent)	Latitude Longitude (degrees)	Diameter (km)	Local tectonic setting	Precaldera edifice	SiO_2 content (wt pct)	Age of collapse (yr B.P.)	Date of unrest	Type and duration of unrest ESTU STHF MGTF H Te	Eruption type
17-03-11 (Krafla)	65.73N 16.68W	10, 8	Exten	Shield	R = b + minor r,d,a	<70,000	1724-29	BB-Y Y--Y --YY Y UQ	P-ex,ex,lf
							1746	Y--Y ---- ---- Y --	lf?
							1975-88+	EEBE BEEE -Exx Y UQ	lf,pex

TECTONIC SETTING

The Mid-Atlantic plate boundary passes through Iceland and is reflected in two zones of spreading and volcanism -- an eastern zone, the site of most historical eruptions, and a western zone. The axial rift zone of northeastern Iceland consists of five fissure swarms, each associated with and named after a central volcano (fig. 17.1.1 in section on Katla). These fissure swarms reflect spreading of the Eurasian and North American plates at a half-rate of about 1 cm/yr, and also updoming and spreading around an Icelandic hotspot. Rifting is episodic, occurring about once every hundred years; two of four historically recorded episodes have been along the Krafla swarm (figs. 17.8.1-17.8.3), in 1724-29 and 1975-present (Sæmundsson, 1974; Björnsson, 1985). Detailed observations of rifting in the Krafla area from 1975-1988+ have provided important insights into the processes of rifting and crustal accretion at ridges (see below).

GEOLOGIC HISTORY

Like most of the central volcanoes within the rift zones of Iceland, the Krafla Central Volcano is an indistinct structure. The weak, divergent crust does not support high volcanic edifices and subsidence plays a major role in the development of these volcanoes. Some of them have caldera structures and all have an associated fissure swarm running through them. The Krafla Central Volcano has produced mostly basaltic material in the form of interglacial or postglacial lavas, or subglacial formations of pillow lavas and palagonite tuffs and breccias. A few domes and ridges of rhyolite exist, and at least one catastrophic event has produced dacitic tephra. Krafla Caldera is marked by poorly defined arcuate structures where the dacite tephra is exposed. On the basis of S-wave shadows a crustal magma chamber is inferred to underlie the central part of the caldera. This chamber is thought to derive its magma from a subcrustal, partially molten layer indicated by seismic and magnetotelluric measurements.

The following is a conceptual model of Krafla activity from P. Einarsson and G. Larsen (written commun., 1988):

The activity of Krafla is primarily influenced by two processes, namely, inflow of magma into the crustal chamber and rifting of the plate boundary, as regulated by the magma pressure in the chamber and tectonic stress at the plate boundary. Tectonic stress

KRAFLA (continued)

GEOLOGIC HISTORY (continued)

presumably builds up slowly with time due to plate movements. When magma begins flowing into the magma chamber it can trigger the release of tectonic stress and thus initiate rifting. Fissures propagate away from the magma chamber near the center of the volcano, and magma flows laterally along the fissure swarm to the north and south of the volcano for tens of kilometers and forms a dike. Typical dike propagation velocities are 0.5-2.5 m/s. During emplacement of dikes the pressure in the magma chamber drops and the volcano deflates. This process can last hours to a few weeks depending on the length of the dike, and the deflation amounts to centimeters to a few meters in the center of the caldera. Extensive fissuring and normal faulting occurs above the dike, the central part of the swarm subsides, and the flanks are uplifted (figs. 17.8.16, 17.8.17). Horizontal and vertical displacements are of the order of tens of centimeters to meters. If magma inflow continues after a deflation event, the volcano reinflates at about 1-10 mm per day for weeks or months. Many such inflation - deflation cycles may occur during a rifting episode that may last several years to over a decade (figs. 17.8.10, 17.8.12, 17.8.15, 17.8.18). In the beginning of an episode the tectonic stress is high and most of the magma is emplaced in dikes in the crust. As the tectonic stress is released, the crust supports higher magma pressures, and an increasing proportion of the mobilized magma reaches the surface in eruptions.

Each phase of the activity is accompanied by its characteristic type of seismic activity:

Inflation earthquakes: During inflation periods earthquakes with magnitudes up to 4 occur in the magma chamber roof beneath the caldera. After stress in the roof exceeds a threshold level these earthquakes are well correlated with the rate of inflation. Inflation earthquakes stop immediately when inflation stops or deflation begins.

Deflation earthquakes: During large deflation events the deviatoric stress in the chamber roof is first relaxed, but then increases in the opposite sense. This can lead to earthquakes if deflation exceeds about 1 m. Deflation earthquakes occupy the same hypocentral volume as the inflation earthquakes, but have been as large as magnitude 5 at Krafla.

Rifting earthquakes: Intense swarms of earthquakes accompany rifting and dike intrusions in the fissure swarm of Krafla. The earthquakes begin near the caldera shortly after deflation sets in, and propagate along the fissure swarm away from the caldera, presumably marking the propagating edge of a dike (for example, figs. 17.8.4, 17.8.6). Both high and low frequency events occur--the latter apparently associated with surface faulting. Rifting earthquakes only seldom exceed magnitude 4, in spite of extensive surface faulting (fig. 17.8.5).

Intrusion tremor: Continuous tremor accompanies deflation and dike intrusion (fig. 17.8.13). The tremor begins as soon as deflation starts and its amplitude is roughly correlated with the rate of deflation. Amplitudes are uneven and spasmodic, and the frequency spectrum is broad. The tremor is mixed with rifting earthquakes.

Eruption tremor: When a dike reaches the surface and an eruption begins, a new type of tremor becomes the dominant seismicity. Eruption tremor has an even amplitude and a narrow frequency spectrum, with predominant frequency below 3 Hz. Its amplitude appears to be correlated with the height of lava fountains.

KRAFLA (continued)

GEOLOGIC HISTORY (continued)

During inflation periods almost all measured changes occur within the caldera or in its immediate vicinity. The inflation is centered beneath the caldera, as shown by elevation changes, tilt measurements, distance measurements and gravimetry (figs. 17.8.8, 17.8.9, 17.8.11, 17.8.17). These data fit well to a Mogi-type model of an inflating magma chamber at a depth of 2.6-3.0 km. Inflation is also reflected in a gradual widening of fissures within the caldera. Sometimes changes in geothermal activity and the composition of gases are detected during inflation, particularly if the previous deflation event was accompanied by intrusion into the magma chamber roof within the caldera.

During deflation events measurable changes occur both within the caldera and outside it. The onset of deflation is usually abrupt (figs. 17.8.12-17.8.14). Recording tiltmeters show a reversal in tilt within minutes or tens of minutes, and intrusion tremor appears simultaneously on the seismographs (figs 17.8.14, 17.8.15). The inflation bulge subsides and rifting earthquakes appear outside the caldera. The deflation rate reaches a maximum within hours and then slowly decreases as the dike lengthens. Eruptions in the current rifting episode have begun 1-7 hours after the onset of deflation, and have lasted 4-14 days. The lava is highly fluid basalt, erupted through 1-9-km-long fissures. Some very small phreatic eruptions have occurred, each lasting a few hours, and some small steam fields have developed in the fissure swarm days or weeks after an intrusion.

HISTORICAL ACTIVITY

The following is a summary of events of the current rifting episode, from P. Einarsson and G. Larsen (written commun., 1988) and references cited below (see also figs. 17.8.3-17.8.18):

1975: Seismic activity increased in the caldera region in the early part of the year. Each day 10-20 events were recorded, some reaching magnitude 4.

1975, 20 December: A major deflation event began, accompanied by a small fissure eruption in the caldera, and intrusion 10-15 km to the south and 60 km to the north (fig. 17.8.3). The northern intrusion extended all the way to the transform fault offshore and triggered a large earthquake swarm that culminated with a transform event of magnitude 6.5 on 13 January 1976. Both deflation of the caldera and rifting near the northern end of the fissure swarm continued until the middle of February with considerable seismicity in both areas. Total deflation in the caldera exceeded 2 m.

1976, 28 September: Small and slow deflation event lasted about 6 days. The intrusion was to the north, as shown by a swarm of very small earthquakes 10 km north of the caldera.
31 October: A rapid deflation was accompanied by intrusion and an intense earthquake swarm to the north of the volcano.

KRAFLA (continued)

HISTORICAL ACTIVITY (continued)

1977, 20 January: A deflation and intrusion event similar to, but shorter than, the last event.

27 April: A rapid deflation event was accompanied by a small eruption near the northern caldera rim and an intrusion to the south of the volcano (fig. 17.8.7).

8 September: A deflation event that was similar to that of April, except that the eruption near the caldera rim was larger and the dike to the south shorter. A small volume of basalt was erupted through a geothermal drill hole when the intrusion entered a producing geothermal area 10 km south of the caldera.

2 November: A very small deflation event occurred. The intrusion probably went a short distance to the north.

1978, 7 January: The second largest deflation event started off slowly but continued for 3 weeks. Earthquakes were initially small, as activity migrated to the north. After 20 hours the seismicity increased and culminated on 10-11 January with events of magnitude 4.6. Large scale rifting occurred 30-40 km north of the volcano, and the total deflation within the caldera exceeded 1 m.

10 July: A large deflation event was accompanied by a 30-km-long intrusion to the north (figs. 17.8.4-17.8.6).

10 November: A deflation event that was similar to the last one, but with a slightly shorter intrusion.

1979, 13 May: A deflation similar to the last two events was accompanied by a yet shorter intrusion to the north.

6 December: A small and slow deflation event was accompanied by small earthquakes slightly south of the caldera.

1980, 10 February: A relatively slow deflation was accompanied by a 5-7-km-deep intrusion into the southern fissure swarm. Very little surface rifting was observed.

16 March: A fast deflation was accompanied by a small lava eruption from a 5-km-long fissure extending northward from the center of the caldera. A larger volume of magma was intruded into the northern and southern fissure swarm. Significant rifting occurred along a 20-km-long segment of the swarm. This event marked the transition from the primarily intrusive phase to the eruption phase of the rifting episode.

10 July: A lava eruption followed the onset of deflation by 4 hours. The eruptive fissure zone was 4 km long, located about 9 km north of the caldera. A good part of the erupted lava flowed into open fissures within the fissure swarm, causing secondary rifting and intrusion from above. The eruption lasted 8 days and the lava volume is estimated to be 23 million m^3. Most of the mobilized magma is thought to have reached the surface in this event.

18 October: An eruption lasting 5 days followed the beginning of rapid deflation by about an hour. The eruptive fissure was 7 km long and extended northward from the center of the caldera. The volume of erupted lava is estimated to be 3.5 million m^3.

22 December: A small and slow deflation event was accompanied by small earthquakes about 13 km north of the center of the caldera, indicating intrusion.

KRAFLA (continued)

HISTORICAL ACTIVITY (continued)

1981, 30 January: A slow deflation began about 7 hours before the outbreak of a lava eruption. The eruptive fissure was 2 km long, located about 8 km north of the caldera center. The eruption lasted 6 days and the erupted volume is estimated to be 32 million m^3. A significant amount of lava is thought to have flowed into fissures during this eruption.

18 November: A lava eruption broke out a little over an hour after the onset of rapid deflation. The fissure was about 8 km long and extended from the caldera center to the north. The eruption lasted 5 days.

1982-84: The volcano reinflated after the November 1981 eruption but then stopped. A few periods of intermittent inflation occurred during the following two years, accompanied by moderate seismic activity within the caldera, demonstrating that the volcano was still alive.

1984: 4 September. An inflation period ended with deflation and lava eruption. The eruption began 3 hours after the onset of deflation. The fissure was 8.5 km long, extending from the center of the caldera to the north. After the initial outbreak the eruptive part of the fissure shortened and the flow rate decreased as in previous eruptions. After the second day, however, the eruption rate and the vigor of the eruption slowly increased, until the eruption suddenly came to an end on 18 September. The eruption was by volume significantly larger than the previous eruptions, and much lava flowed into fissures from above. Details of the surface deformation during this eruption led Tryggvason (1986) to suggest that magma was supplied from four reservoirs at depths between 2.6 and 20 km.

1984-88: The volcano reinflated after the 1984 eruption, and in early 1985 the inflation had nearly reached the highest previous level. Since then inflation has been intermittent, with long periods of no detectable movements. The most important periods of inflation were October 1986 - April 1987 and February - March 1988. A few small tilt events have suggested minor magma movements within the caldera. This unrest shows that the current episode of magmatism and rifting is not over yet, and the magma pressure in the shallow chamber is sufficient to bring magma to the surface.

The current unrest at Krafla has now lasted more than 12 years. Rifting during this episode has affected nearly 80 km of the Krafla fissure swarm. In the caldera region and immediately to the north the cumulative rifting exceeds 8 m, and in other areas the rifting amounts to at least 2-3 m. The total volume of erupted lava is about 0.25 km^3, and a minimum of 0.6 km^3 has been intruded into the fissure swarm.

The only significant historical activity before the current rifting episode occurred in the eighteenth century, mostly in the period 1724-29. Large scale crustal deformation was reported, and an estimated 0.45 km^3 of basaltic lava was erupted from fissures, mainly within the caldera. Two small eruptions occurred in the southern fissure swarm, and it appears that intrusive activity and rifting was mostly directed southward, to a distance of at least 30 km. As in the current episode, the first years were characterized by earthquakes and rifting, and most of the lava was erupted in the last two years of the episode.

KRAFLA (continued)

HISTORICAL ACTIVITY (continued)

The most prominent events in the 1724-29 unrest were:

1724, 17 May: A phreatomagmatic eruption in the caldera was preceded by strong earthquakes. The seismicity began a few hours before the eruption, which produced basaltic scoria mixed with silicic pumice. Changes in the water level of Lake Myvatn indicated that magma was intruded to the south.

1725, 11 January: Volcanic activity and changes in geothermal areas occurred within the caldera. Earthquakes were felt for several days prior to this event.
19 April: An eruption broke out on a short fissure 6 km south of the caldera, preceded by considerable seismic activity. Fissuring and vertical movements were observed in the fissure swarms as far as 30 km south of the volcano.
8 September: Strong earthquakes and changes in lake level indicate an intrusion to the south.

1727, 21 August: A lava eruption began in the caldera and lava flowed to the north and south.

1728, 18 April: A lava eruption began in the caldera after several hours of earthquake activity. A few hours later another eruption broke out 4 km south of the caldera. Changes in the level of Lake Myvatn indicated an intrusion to the south.
18 December: A lava eruption began in the caldera.

1729: 30 January: An intense lava eruption began in the caldera. Lava flows were reported several times during the following months, but it is unclear whether activity was continuous or intermittent. No activity was reported after September.

1746: 10 July: Volcanic activity of unspecified nature occurred in the caldera. It was accompanied by earthquakes and changes in the level of Lake Myvatn, indicating that an intrusion may have occurred.

COMMENTS

Recent unrest at Krafla is a superbly documented example of rifting and crustal accretion at a spreading ridge. Magma is supplied from depth to one or more central reservoirs (one atop another), and from those reservoirs the magma spreads laterally into rifts. Tectonic extension and magma intrusion are intimately linked; neither causes the other, but rather both are processes of spreading and crustal accretion.

KRAFLA (continued)

REFERENCES

Björnsson, A., 1985, Dynamics of crustal rifting in NE Iceland: Jour. Geophys. Res., v. 90, no. B12, p. 10,151-10,162.

Björnsson, A., Johnsen, G., Sigurdsson, S., Thorbergsson, G., and Tryggvason, E., 1979, Rifting of the plate boundary in North Iceland 1975-1978: Jour. Geophys. Res., v. 84, no. B6, p. 3029-3038.

Björnsson, A., Sæmundsson, K., Einarsson, P., Tryggvason, E., and Grönvold, K., 1977, Current rifting episode in North Iceland: Nature, v. 266, p. 318-323.

Brandsdóttir, B., and Einarsson, P., 1979, Seismic activity associated with the September 1977 deflation of the Krafla central volcano in NE Iceland: Jour. Volcanol. Geotherm. Res., v. 6, p. 197-212.

Einarsson, P., 1978, S-wave shadows in the Krafla caldera in NE-Iceland: evidence for a magma chamber in the crust: Bull. Volcanol., v. 41, p. 187-195.

Einarsson, P., and Björnsson, S., 1979, Earthquakes in Iceland: Jökull, v. 29, p. 37-43.

Einarsson, P., and Brandsdóttir, B., 1980, Seismological evidence for lateral magma intrusion during the July 1978 deflation of the Krafla volcano in NE-Iceland; Jour. Geophys., v. 47, p. 160-165.

Gudmundsson, G., and Sæmundsson, K., 1980, Statistical analysis of damaging earthquakes and volcanic eruptions in Iceland from 1550-1978: Jour. Geophys., v. 47, p. 99-109.

Hauksson, F., 1981, Episodic rifting and volcanism at Krafla in North Iceland; radon (222) emission from fumaroles near Leirhnjukur: Jour. Geophys. Res., v. 86(B), p. 11,806-11,814.

----- 1983, Episodic rifting and volcanism at Krafla in North Iceland: Growth of large ground fissures along the plate boundary: Jour. Geophys. Res., v. 88, no. B1, p. 625-636.

Johnsen, G.V., Björnsson, A., and Sigurdsson, S., 1980, Gravity and elevation changes caused by magma movement beneath the Krafla caldera: Jour. Geophys., v. 47, p. 132-140.

Larsen, G., Grönvold, K., and Thorarinsson, S., 1979, Volcanic eruption through a geothermal borehole at Námafjall, Iceland: Nature, v. 278, p. 707-710.

Marquart, G., and Jacoby, W., 1985, On the mechanism of magma injection and plate divergence during the Krafla rifting episode in NE Iceland: Jour. Geophys. Res., v. 90, no. B12, p. 10,178-10,192.

Oskarsson, N., 1984, Monitoring of fumarole discharge during the 1975-1982 rifting in Krafla Volcanic Center, North Iceland: Jour. Volcanol. Geotherm. Res., v. 22, p. 97-121.

Sæmundsson, K., 1974, Evolution of the axial rifting zone in northern Iceland and the Tjornes Fracture Zone: Geol. Soc. Am. Bull., v. 85, p. 495-504.

----- 1978, Fissure swarms and central volcanoes of the neovolcanic zones of Iceland: Geol. Jour., Spec. Iss. 10, p. 415-432.

Science Institute, University of Iceland, and the Icelandic Meteorologic Office, 1975-88, Skjalftabref (Seismological bulletin): v. 1-64, (various short articles on Krafla by Einarsson, P., Brandsdóttir, B., Grönvold, K., Tryggvason, E., Sæmundsson, K., and others).

Sigurdsson, H., 1980, Myvatn volcanism: Volcano News, no. 3, p. 1-8.

Sigurdsson, S., 1980, Surface deformation of the Krafla fissure swarm: two rifting events: Jour. Geophys., v. 47, p. 154-159.

KRAFLA (continued)

REFERENCES (continued)

Smithsonian Institution, Scientific Event Alert Network (SEAN), 1975-85, 1987, Krafla: SEAN Bull., v. 1-10, 12 (information from P. Einarsson, K. Grönvold, H. Sigtryggsson, G. Sigvaldason, E. Trygvasson, and others).

Thorarinsson, S., 1960, On the predicting of volcanic eruptions in Iceland: Bull. Volcanol., v. 23, p. 45-52.

----- 1973, Data sheets of the post-Miocene volcanoes of the world, Sheet II, Iceland: Rome, IAVCEI, 10 p.

Thoroddsen, Th., 1925, Die Geschichte der Islandischen Vulkane: D. Kgl. Dansk Vidensk. Selsk. Skrifter, Naturvidensk. og Mathem. Afd Copenhagen, 8th ser., v. 9, 458 p.

Torge, W., and Kanngieser, E., 1980, Gravity and height variations during the present rifting episode in northern Iceland: Jour. Geophys., v. 47, p. 125-131.

----- 1985, Regional and local vertical crustal movements in Northern Iceland, 1965-1980: Jour. Geophys. Res., v. 90, no. B12, p. 10,173-10,177.

Tryggvason, E., 1980, Subsidence events in the Krafla area, North Iceland, 1975-1979: Jour. Geophys., v. 47, p. 141-153.

----- 1984, Widening of the Krafla Fissure Swarm during the 1975-1981 volcano-tectonic episode: Bull. Volcanol., v. 47, no. 1, p. 47-69.

----- 1986, Multiple magma reservoirs in a rift zone volcano: ground deformation and magma transport during the September 1984 eruption of Krafla, Iceland: Jour. Volcanol. Geotherm. Res., v. 28, p. 1-44.

----- 1987, Myvatn lake level observations 1984-1986 and ground deformation during a Krafla eruption: Jour. Volcanol. Geotherm. Res., v. 31, p. 131-138.

Volcanological Society of Japan, 1977-86, Krafla: Bull. Volcanic Eruptions, nos. 15-23 (information from S. Thorarinsson, P. Einarsson, K. Grönvold, G. Sigvaldason, and others).

Wendt, K., Moller, D., and Ritter, B., 1985, Geodetic measurements of surface deformations during the present rifting episode in NE Iceland: Jour. Geophys. Res., v. 90, no. B12, p. 10,163-10,172.

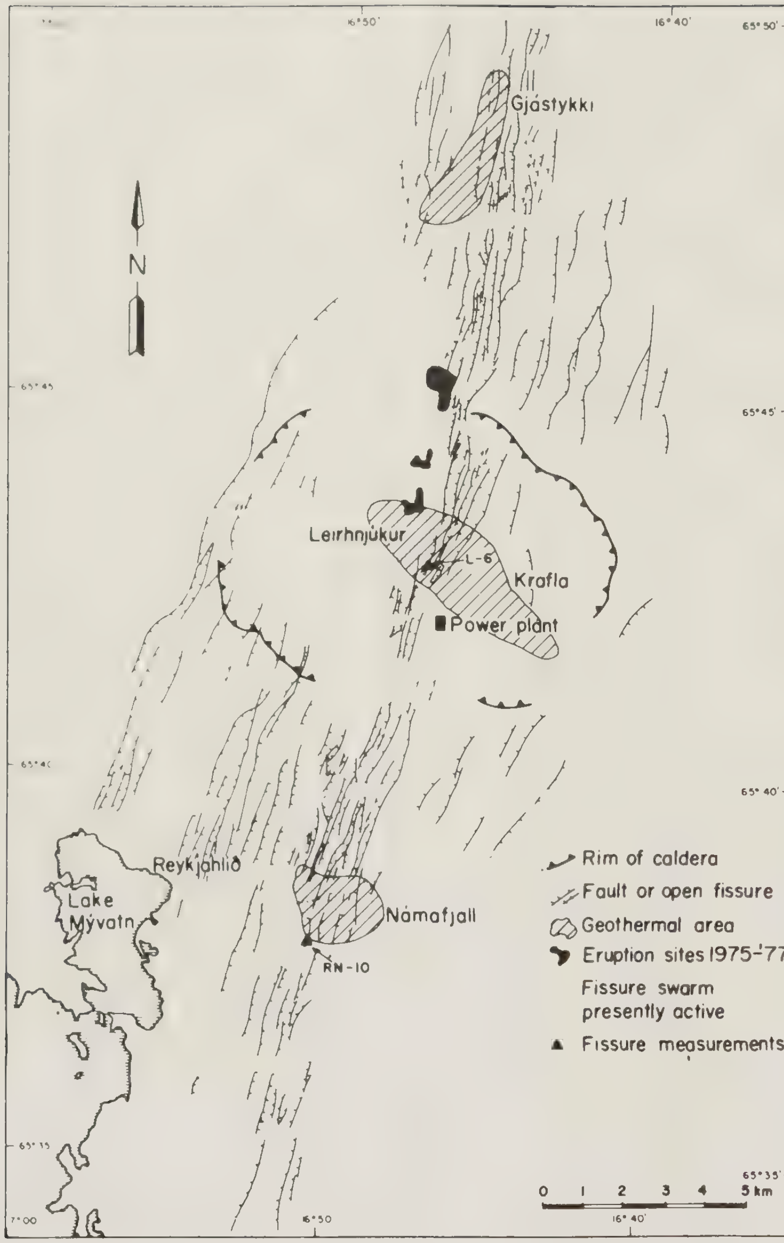

Figure 17.8.1. Outline geologic map of Krafla Caldera and associated fissure swarm. Mapped by K. Sæmundsson, from Björnsson and others (1979). Copyright by the American Geophysical Union.

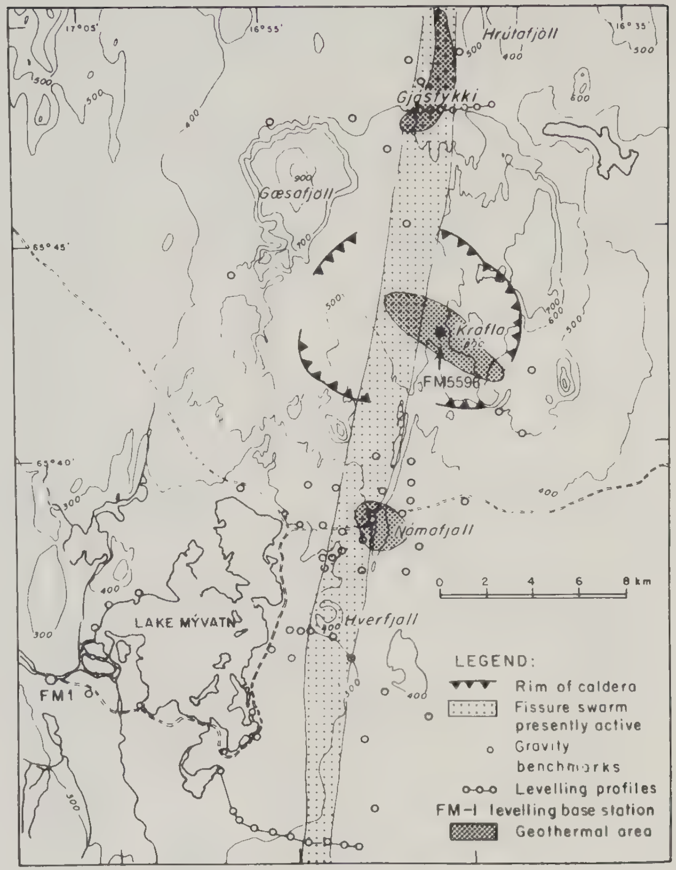

Figure 17.8.2. Krafla central volcano and its surroundings, from Johnsen and others (1980). Caldera and central part of active fissure swarm are shown. Open circles show gravity and leveling bench marks outside caldera.

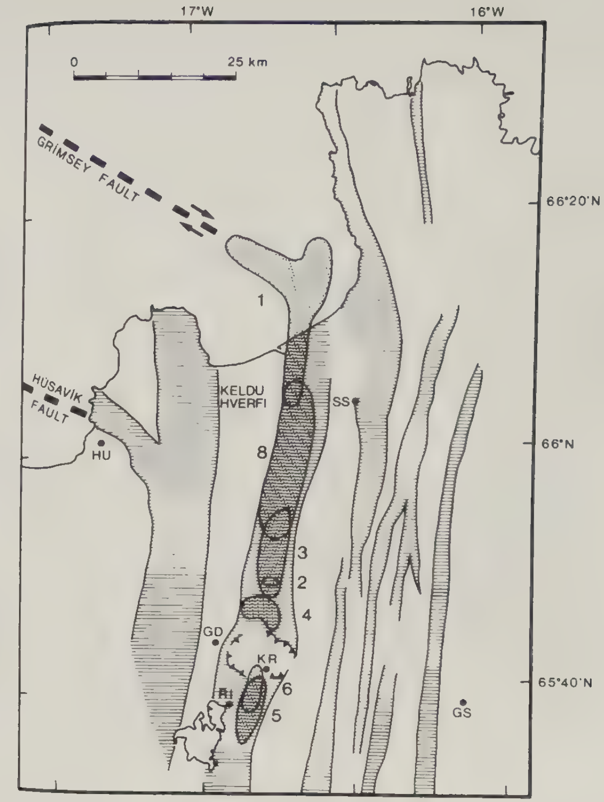

Figure 17.8.3. Index map of northern part of volcanic rift zone in northeast Iceland, from Einarsson and Brandsdóttir (1980). Dots, permanent seismograph stations. Hachured areas, fault swarms (from Björnsson and others (1977)). Krafla Caldera is located within Krafla fault swarm. Stippling, areas of maximum earthquake activity during different deflation events at Krafla. Area 1, epicentral area of first swarm of December 1975 - February 1976; 2, 1-2 October 1976; 3, 31 October - 1 November 1976; 4, January 1977; 5, April 1977; 6, September 1977; small swarm in November 1977 could not be located and is not shown; 8, January 1978.

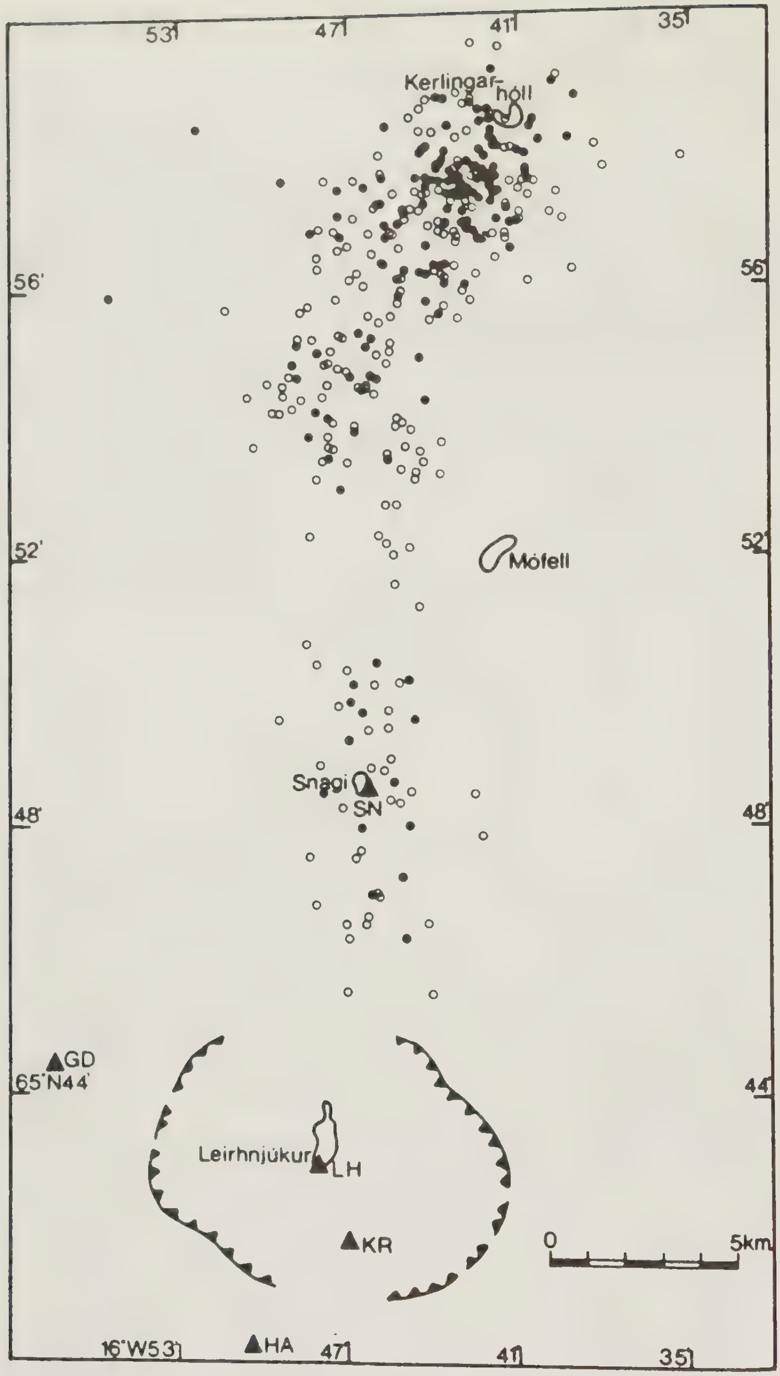

Figure 17.8.4. Epicentral map of July 1978 earthquake swarm, from Einarsson and Brandsdóttir (1980). Dots mark epicenters located with horizontal standard error of 1 km or less; circles denote epicenters with errors between 1 and 2 km. Seismograph stations are shown with triangles.

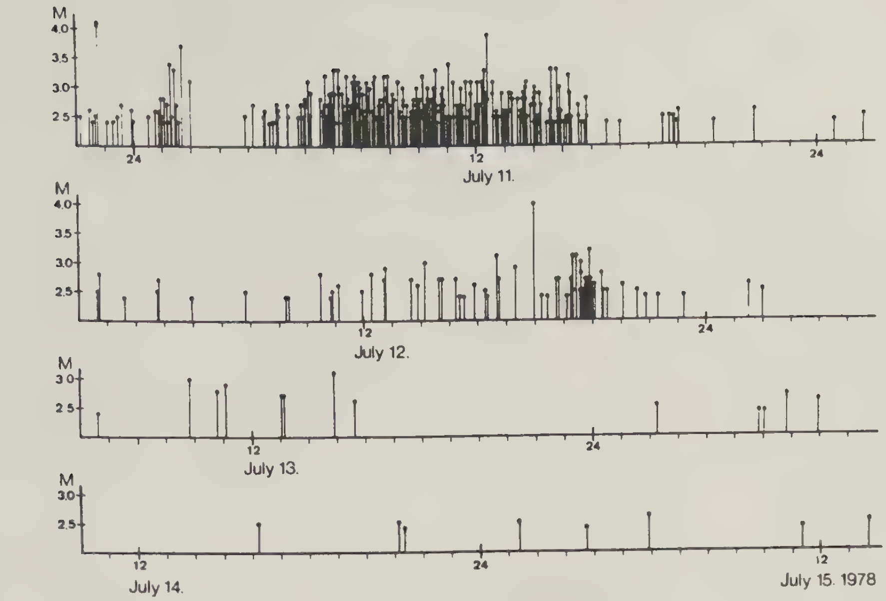

Figure 17.8.5. Time sequence of earthquakes during the July 1978 swarm at Krafla, from Einarsson and Brandsdóttir (1980). Magnitude is plotted as a function of time. Deflation began about 5 hours before start of plot.

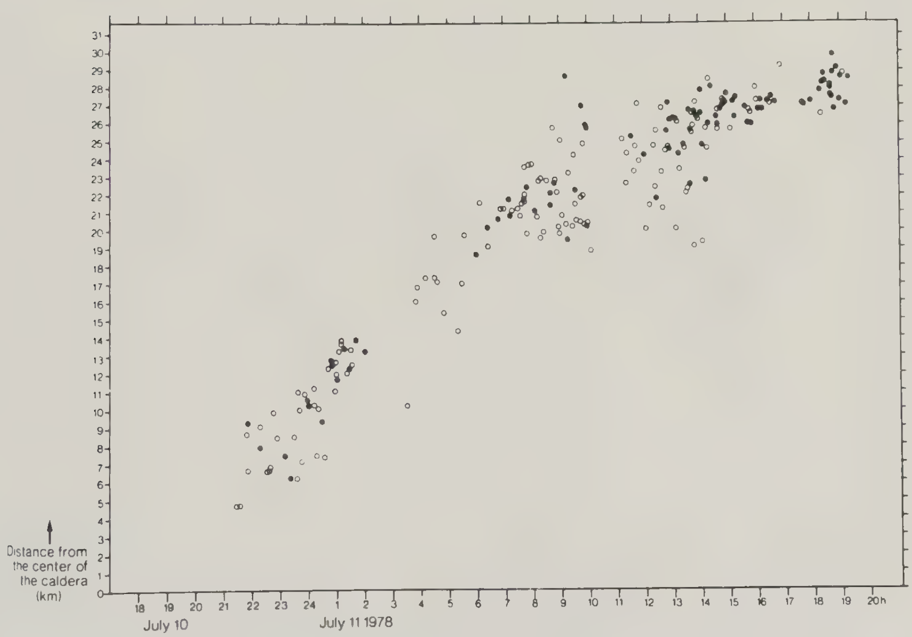

Figure 17.8.6. Migration of seismic activity during the July 1978 swarm, from Einarsson and Brandsdóttir (1980). Distance of epicenters from center of Krafla Caldera is plotted as a function of time. Dots and circles have the same meaning as in figure 17.8.4. Apparent gap in activity between 1000 hr and 1100 hr on 11 July was caused by a time signal failure. Tremor and deflation started at about 1700 hr.

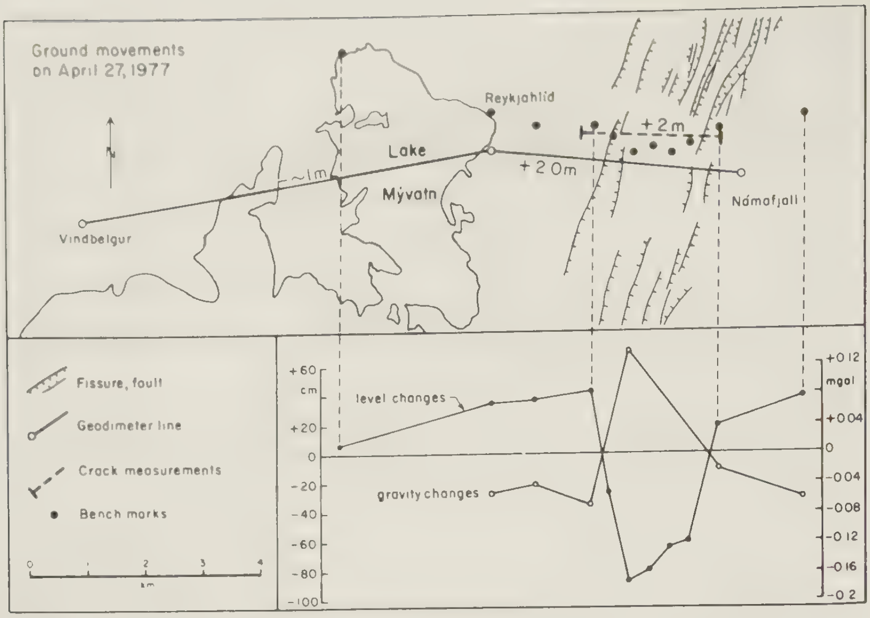

Figure 17.8.7. Horizontal and vertical ground movements across Krafla fissure swarm near Namafjall during subsidence event of 27 April 1977, from Björnsson and others (1979). Expansion was measured on individual cracks and also across swarms of cracks with an electronic distance meter (EDM). Elevation and gravity changes are shown in lower part of figure. Copyright by the American Geophysical Union.

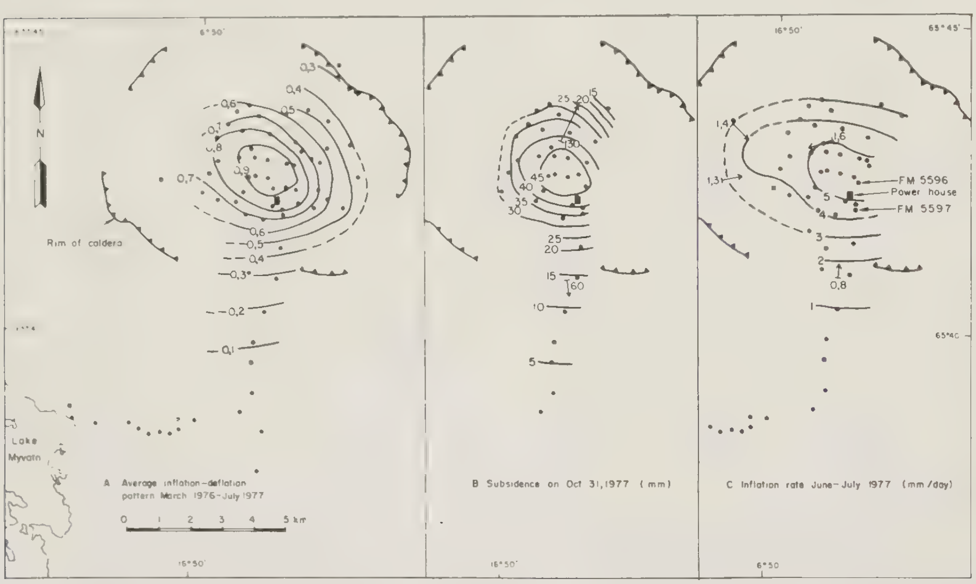

Figure 17.8.8. Patterns of uplift and subsidence in the Krafla area, from Björnsson and others (1979). Average vertical ground movement (left) throughout the period March 1976 to July 1977 in fractions of maximum movements. Total subsidence (middle) in centimeters during subsidence event of 31 October to 1 November 1976. Rate of uplift (right) in millimeters per day during a period of 1 month (June-July 1977). Arrows show tilt changes in microradians at four stations. Copyright by the American Geophysical Union.

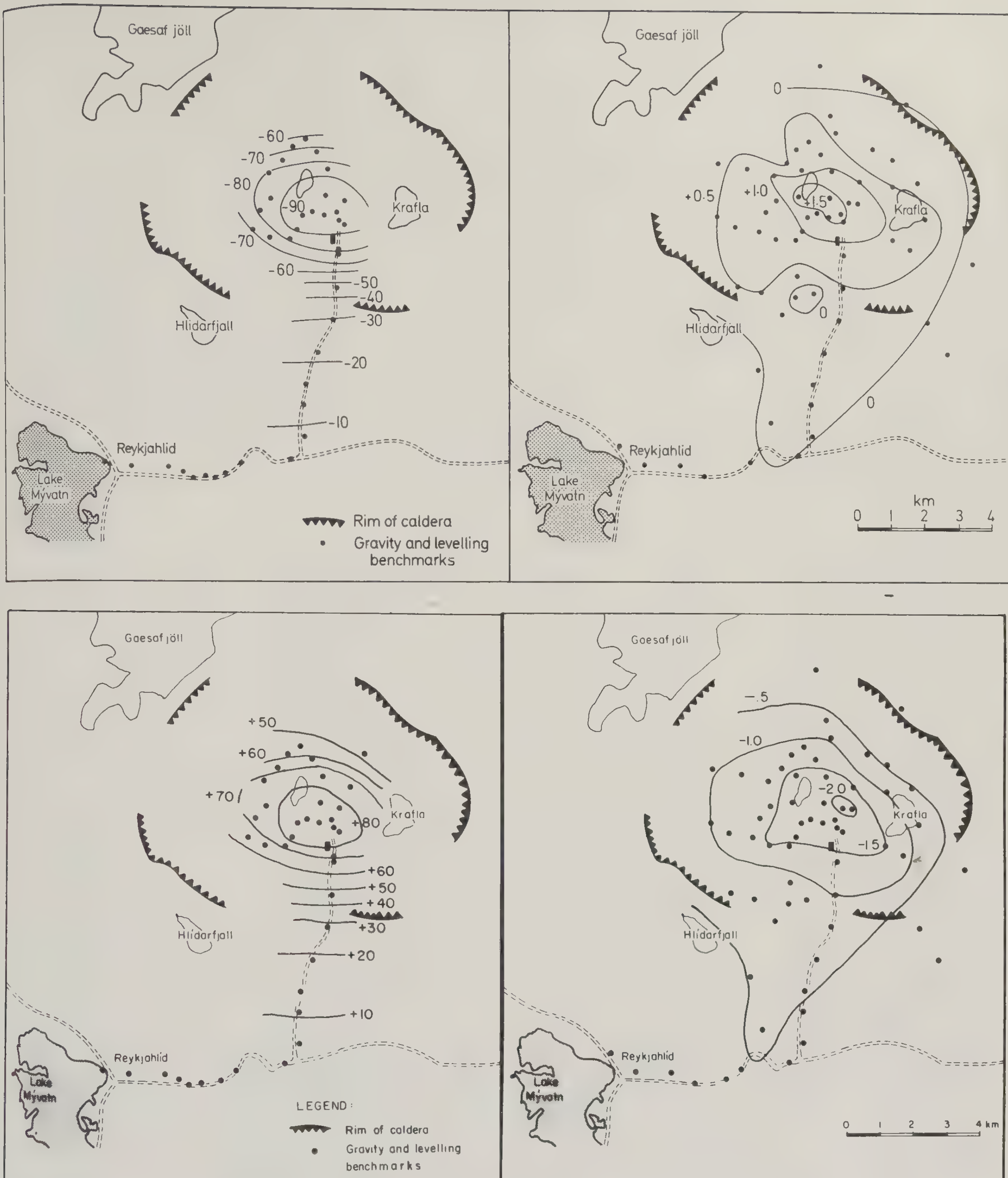

Figure 17.8.9. Measured elevation changes in centimeters (left) and gravity changes in milligals (right), from Johnsen and others (1980). Filled circles show bench marks occupied at the time. Subsidence event (top) in January 1978; inflation period (bottom) from January to June 1978.

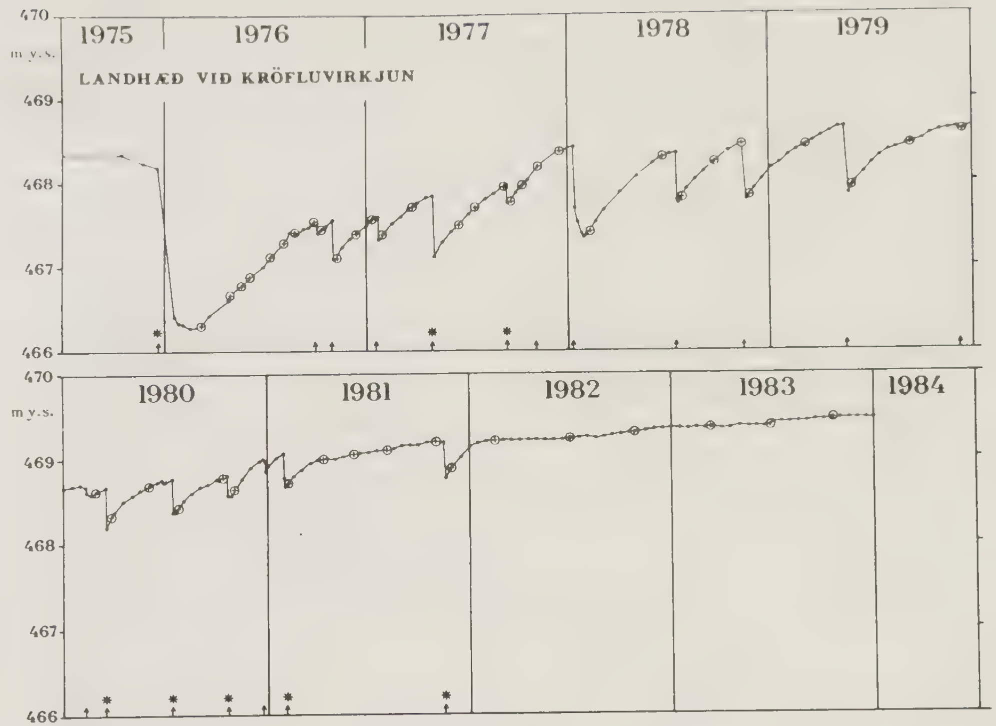

Figure 17.8.10. Land elevation changes at bench mark FM5596 about 1 km southeast of center of Krafla Caldera (see figure 17.8.2 for location), from Björnsson (1985). Reference bench mark (FM6414) is 20 km away, at southern end of Lake Myvatn. Crosses, leveling data; dots, interpolated values based on tilt measurements at Krafla power plant; arrows, rifting-deflation events; stars, volcanic eruptions. Copyright by the American Geophysical Union.

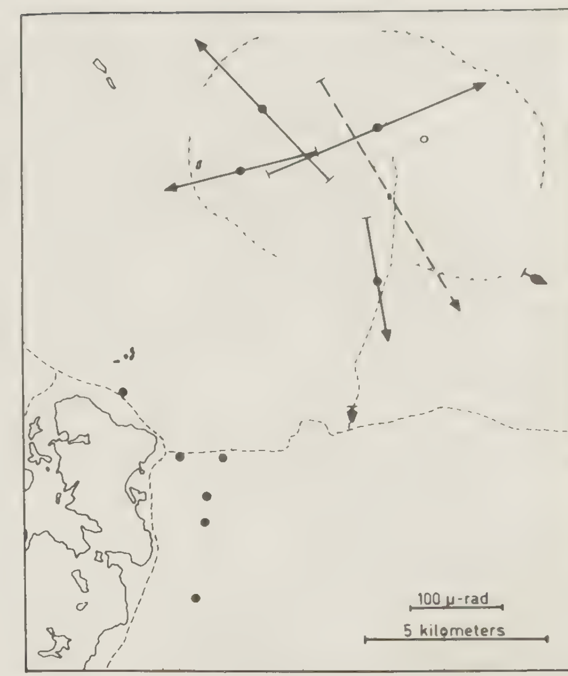

Figure 17.8.11. Observed ground tilt during inflation period 29 April to 8 September 1977, from Björnsson and others (1979). Arrows show direction and magnitude of observed tilt; if no arrow was drawn, tilt was less than error of the observations. Solid dots are dry-tilt stations. Direction of tilt at power station (dashed arrow) is based on an electronic tiltmeter that was operated for a few weeks during this period. Dotted lines outline most active part of Krafla fissure swarm. Copyright by the American Geophysical Union.

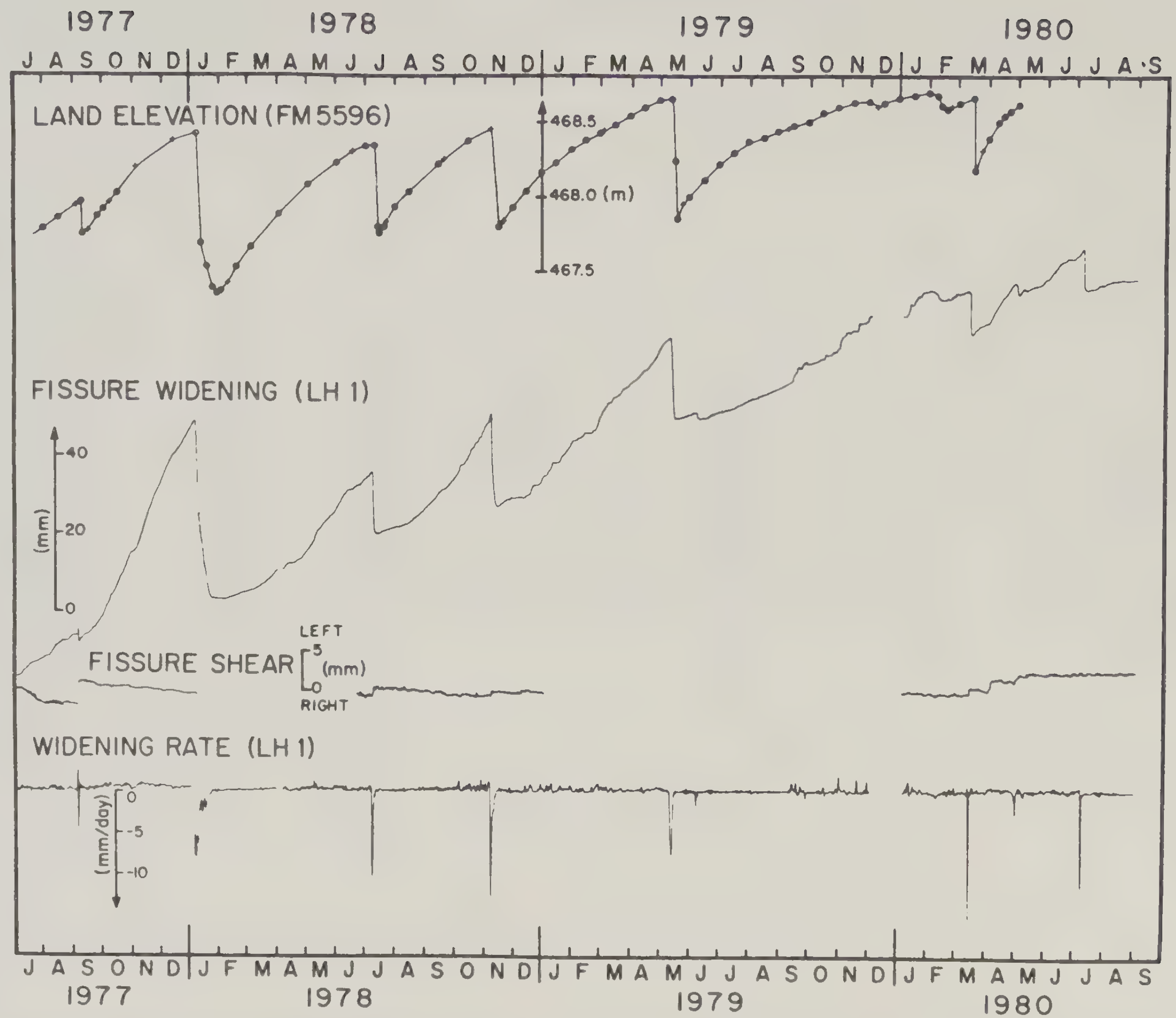

Figure 17.8.12. Time series of fissure width (LH1), fissure shear (LH2), and fissure widening rate at a site in Krafla Caldera, from Hauksson (1983). Land elevation at bench mark FM5596 (see figure 17.8.2 for location) is shown for comparison. Copyright by the American Geophysical Union.

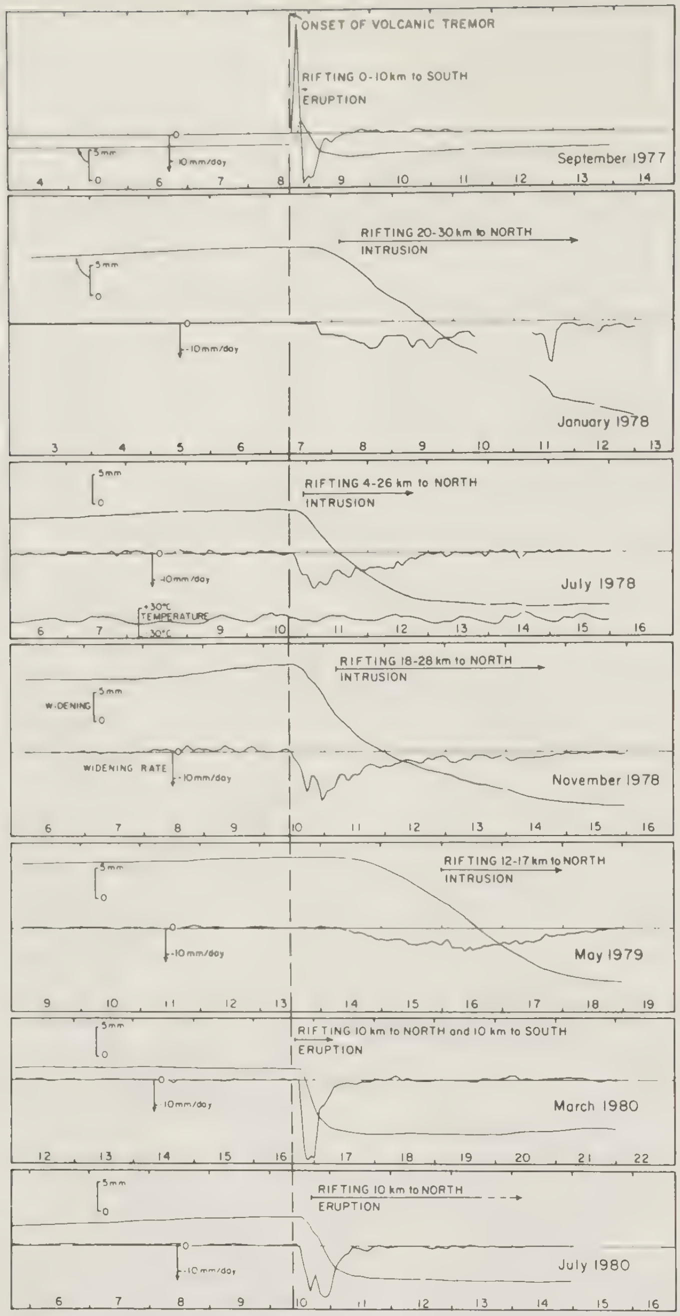

Figure 17.8.13. Rifting and tremor during subsidence episodes at Krafla, from Hauksson (1983). Rifting data from site LH1 (see figure 17.8.12). Different episodes are aligned so that onset of volcanic tremor coincides. Long horizontal arrow indicates direction and extent of rifting, and accompanying notes indicate whether subsidence was associated with an intrusion or an eruption. Rapid fluctuations in closure rate are real. Copyright by the American Geophysical Union.

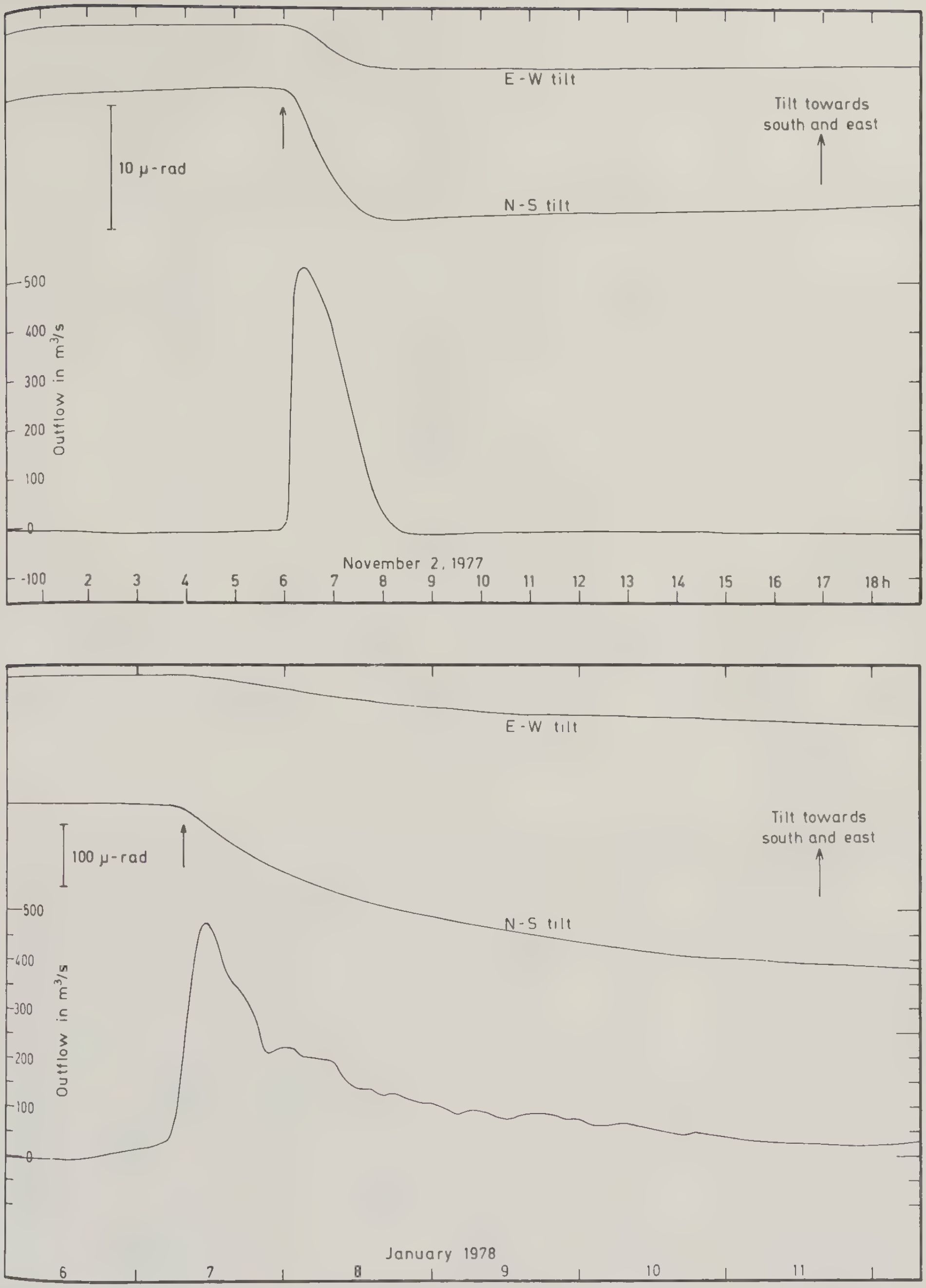

Figure 17.8.14. Tilt in Krafla power station as measured by an electronic tiltmeter, and rate of outflow from Krafla magma chamber during subsidence event of 2 November 1977 (top) and first days of subsidence event of January 1978 (bottom), from Tryggvason (1980).

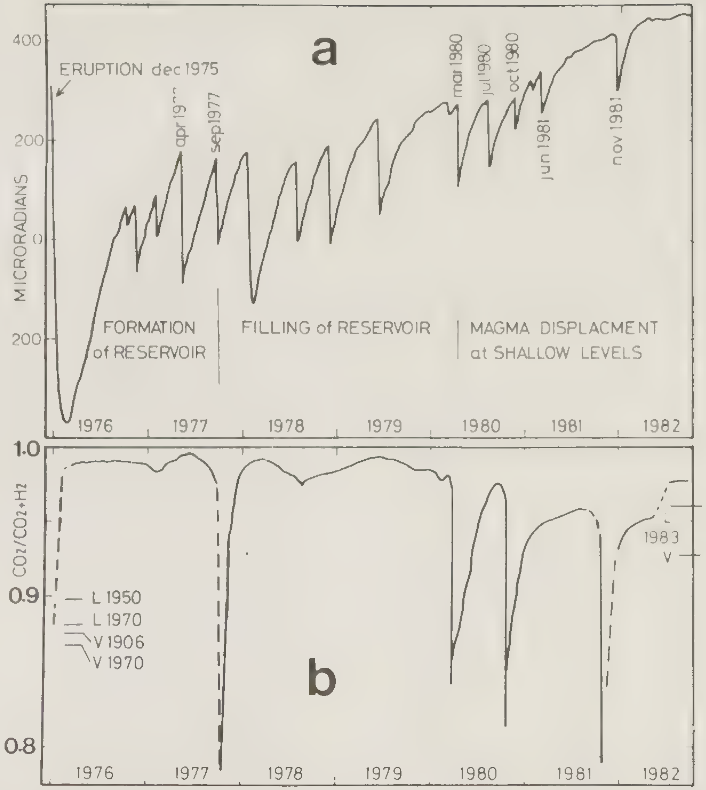

Figure 17.8.15. Ground tilt in Krafla power station (top), and carbon dioxide/hydrogen gas ratio at a monitoring station 1.2 km northwest of power station (bottom), both as a function of time (Oskarsson, 1984). Vertical scale at top shows relative tilt variation. Initial deflation, to left in figure, was estimated at about 2.5 m at center of caldera. Deflation events associated with volcanic eruptions are labeled with their dates. Bottom diagram shows $CO_2/(CO_2+H_2)$ ratio; dashed lines indicate missing data and are thus to be taken as inferred behavior of ratio. On left-vertical axis ratio for some older data is indicated by horizontal bars. Ratios for September 1983 are shown on right-vertical axis. Pulses of H_2 in conjunction with shallow intrusions and eruptions are evident in lower figure.

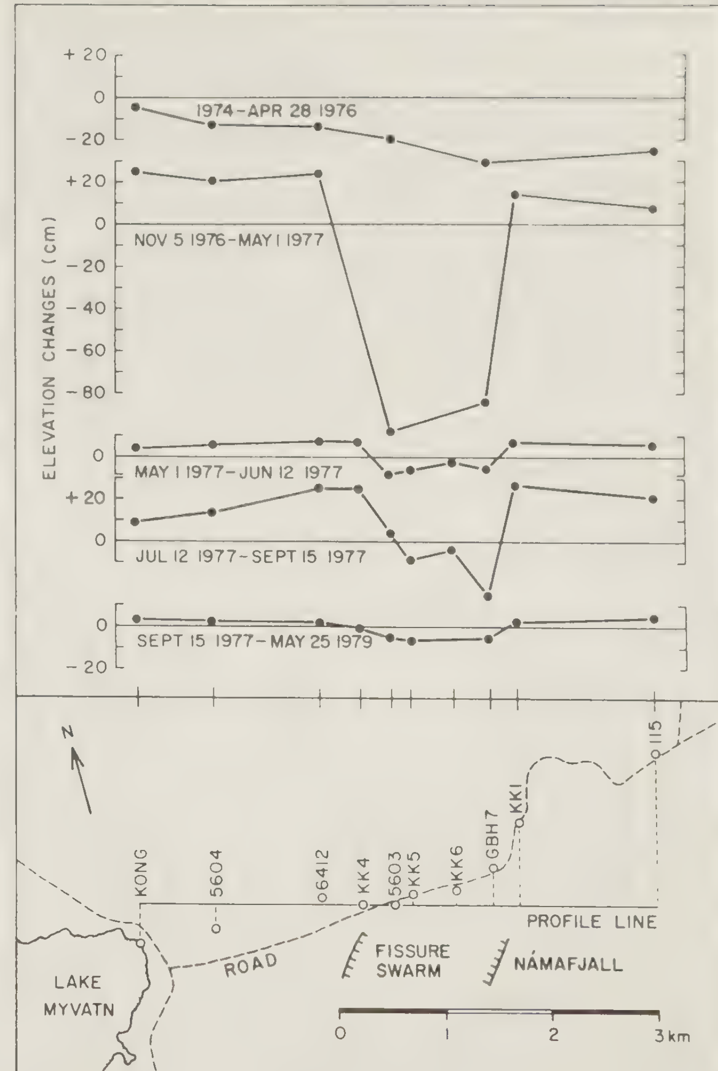

Figure 17.8.16. Elevation changes during 1974-79 on a profile across the Krafla fissure swarm at Namafjall, 10 km south of Krafla Caldera, from Björnsson (1985). Copyright by the American Geophysical Union.

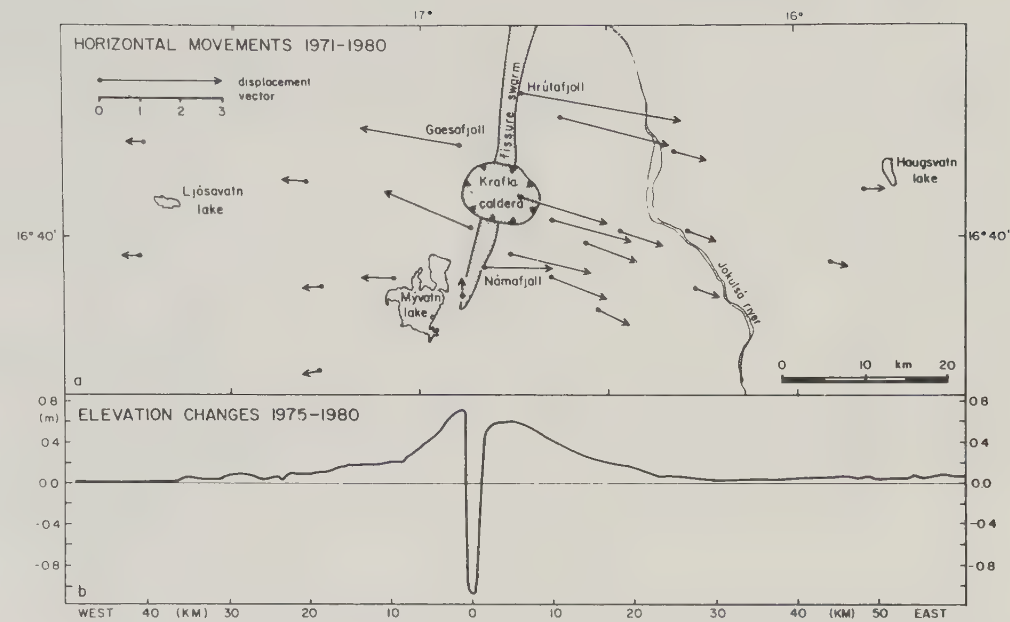

Figure 17.8.17. Horizontal movements (top), 1971-80, on a profile across axial rift zone in Krafla area. Elevation changes (bottom), 1975-80, on an E-W profile, projected onto latitude 16°40' (Björnsson, 1985). Copyright by the American Geophysical Union.

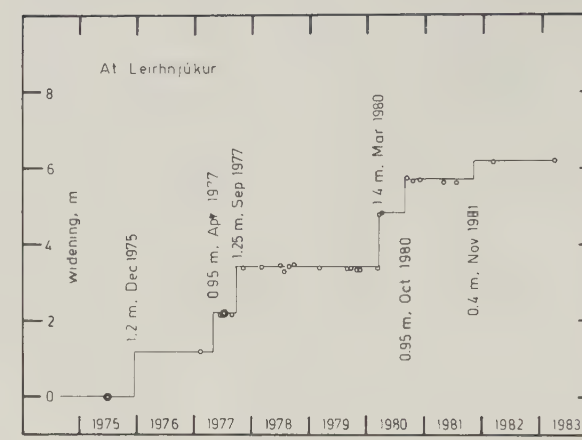

Figure 17.8.18. Accumulated widening of Krafla fissure swarm at Leirhnjukur (center of Krafla Caldera, see fig. 17.8.4) as a function of time, from Tryggvason (1984).

Figure 18. Locations of large, Quaternary restless calderas (solid circles) and nonrestless caldera (triangle) in Region 18.

SETE CIDADES

CAVW number (active vent)	Latitude Longitude (degrees)	Diameter (km)	Local tectonic setting	Precaldera edifice	SiO_2 content (wt pct)	Age of collapse (yr B.P.)	Date of unrest	Type and duration of unrest ESTU STHF MGTF H Te	Eruption type
18-02-08	37.87N 25.78W	5	Spreading center exten	LP-LL strat	R = 44-48 C = 65	ca. 22,000	ca. 1444	---- ---- ---- - --	P-ex
							1638	EE-- ---- ---- - --	ex, sub
							1682	xx-- ---- ---- - --	ex, sub
							1713	xx-- ---- ---- - --	sub?
							1810-11	EE-E ---E ---- - --	Ex, sub
							1861	---- ---- ---- - --	sub
							1880	---- ---- ---- - --	sub

TECTONIC SETTING

The Azores mark a possible hotspot along a spreading center, the WNW-ESE-trending Azores Fracture Zone. This fracture zone is responsible for the location and in part the caldera-bounding faults of Sete Cidades Caldera (Laughton and Whitmarsh, 1975; Moore, 1983, 1988).

GEOLOGIC HISTORY

The Sete Cidades Caldera (fig. 18.1.1) formed approximately 22,000 yr B.P., after eruption of about 6 km^3 of trachytic pumice (Moore, 1983, 1988). At least 22 postcaldera eruptions have occurred, and 12 postcaldera tephras have been identified by Booth and others (1978); these range in volume from 0.06 to 0.16 km^3 (DRE), and together they represent slightly over 1 km^3 of magma.

HISTORICAL ACTIVITY

ca. 1444: An eruption of trachyte occurred from a vent on the southwestern caldera floor.

1638: Strong earthquakes began on 26 May and continued for eight days. These were so strong that many persons abandoned their homes (Zbyszewski, 1963). A submarine basaltic eruption began on 3 July, from an offshore vent just west of Sete Cidades.

1682: Earthquakes on 16 December alarmed the populace, especially in the south part of the island, and a submarine eruption occurred 4 leagues (ca 15 km) from Ferraria (Zbyszewski, 1963).

SETE CIDADES (continued)

HISTORICAL ACTIVITY (continued)

1713: A seismic swarm and possible submarine eruption west of Sete Cidades were reported by Agostinho (1936).

1810-11: An earthquake on 17 June 1810 was followed by progressively more frequent and stronger earthquakes until 24 June. At 1400 hr on the latter date a very strong earthquake destroyed grand houses of the towns around Sete Cidades. In the town of Mosteiros, a crack opened that stretched from the caldera to the west. The crack was (on average) 1 large palm wide (22 cm), and at points was 20 to 30 palms (4.5-6.75 m) wide. Additional earthquakes occurred in August and October, and these were especially intense near Ponta Delgada. Residents noted that the land had been uplifted. During 29-30 January 1811, earthquakes intensified and began to occur at shorter and shorter intervals. On 31 January, there were 30 earthquakes or more within a few hours, and on 1 February a submarine eruption began several (2?) km offshore from the village of Ginetes, forming the ephemeral island of Sabrina. The volcano was quiet from 8 February to 13 June, when strong earthquakes were felt every 15-20 minutes on the western part of Ile São Miguel. Sulfur odor was unpleasant in Ponta Delgada, 35 km from Sabrina. On the night of the 14th, a new submarine eruption commenced from a point 1.8 km northwest of Pic de Camarinhas and 4-5 km west of the February eruption site (Zbyszewski, 1963).

1861, 1880: Submarine eruptions occurred off São Miguel (Mitchell-Thome, 1981). No details are available.

REFERENCES

Agostinho, J., 1936, The volcanoes of the Azores: Bull. Volcanol., v. 8, p. 123-138.
Booth, B., Croasdale, R., and Walker, G.P.L., 1978, A quantitative study of five thousand years of volcanism on São Miguel, Azores: Phil. Trans. Roy. Soc. London, Ser. A, v. 288, p. 271-319.
Laughton, A.S., and Whitmarsh, R.B., 1975, The Azores-Gibraltar plate boundary, in Kristjansson, L., ed., Geodynamics of Iceland and the North Atlantic area: Dordrecht, D. Reidel Publ. Co., p. 63-81.
Mitchell-Thome, R.C., 1981, Vulcanicity of historic times in the Middle Atlantic Islands: Bull. Volcanol., v. 44, no. 1, p. 57-69.
Moore, R.B., 1983, Preliminary geologic map of Sete Cidades Volcano, São Miguel, Azores: U.S. Geol. Surv. Open-File Rep. 83-742, 1 sheet, scale 1:18,000.
----- 1988, Geology of three late Quaternary stratovolcanoes on São Miguel, Azores: Bull. Volcanol. [in press].
Neumann van Padang, M., Richards, A.F., Machado, F., Bravo, T., Baker, P.E., and LeMaitre, R.W., 1967, Catalogue of active volcanoes of the world including solfatara fields, Pt. XXI, Atlantic Ocean: Rome, IAVCEI, 128 p.
Zbyszewski, G., 1963, Les phénomènes volcaniques modernes dan l'Archipel des Açores: Serv. Geol. Portugal, v. 47, p. 5-277.

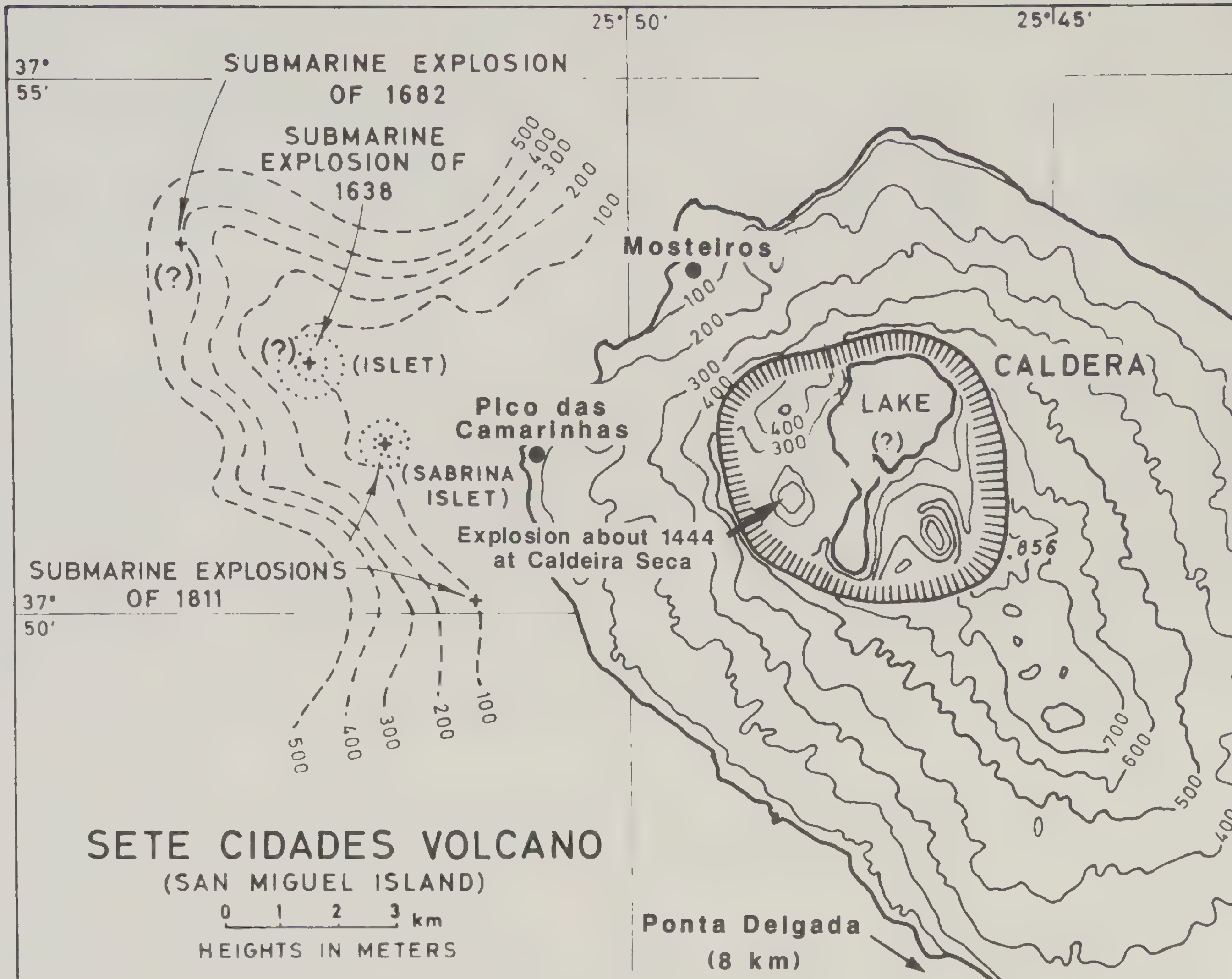

Figure 18.1.1. Topographic map of Sete Cidades Volcano, including submarine adventive vents, from Neumann van Padang and others (1967). Revised location of 1444 explosion from R.B. Moore (written commun., 1987)

AGUA DE PAU

CAVW number (active vent)	Latitude Longitude (degrees)	Diameter (km)	Local tectonic setting	Precaldera edifice	SiO_2 content (wt pct)	Age of collapse (yr B.P.)	Date of unrest	Type and duration of unrest ESTU STHF MGTF H Te	Eruption type
18-02-09	37.77N 25.47W	4 x 7 (outer) 2.5 x 3 (inner)	Spreading center exten	LL-LP strat	R= 45-65 C= ca. 65	15,200 and between 30,000 and 45,000	1563-64	CC-- ---x ---- - --	EX, pex, lf
							1652	DD-- ---B ---Y - --	ex, lf
							1980's	xx-- ---- ---- - --	none

TECTONIC SETTING

The Azores mark a possible hotspot along a spreading center, the WNW-ESE-trending Azores Fracture Zone (Laughton and Whitmarsh, 1975).

GEOLOGIC HISTORY

Agua de Pau stratovolcano (fig. 18.2.1) consists of trachytic lava flows, domes, and pyroclastic deposits, built on a base of older volcanic rocks (Moore, 1986, 1988). Mafic eruptions have occurred on the flanks of the volcano but not within the caldera. An outer, 4 km x 7 km diameter caldera formed when at least 5 km^3 of trachyte was erupted sometime between 30,000 and 45,000 yr B.P. An inner, 2.5 km x 3 km caldera formed about 15,200 yr B.P., after a smaller eruption of trachyte (Moore, 1988). Several hot springs and fumaroles with temperatures near boiling occur on Agua de Pau, mainly on its northwest flank (Zbyszewski and others, 1958; Zbyszewski and Ferreira, 1959), and some of these are being explored for geothermal power potential (Moore, 1988).

HISTORICAL ACTIVITY

1563-64: A plinian eruption of trachyte pumice (on-land volume, 0.15 km^3) blanketed most of the island of São Miguel east of Agua de Pau (Walker and Croasdale, 1971). Earthquakes began on 24 June and became more frequent and more intense over the succeeding four days, until the eruption began on 28 June. On 29 June, strong earthquakes damaged houses of Ribeira Grande (8 km northwest of the caldera), and by 1 July most houses of that town were ruined. On 2 July, eruption from the main vent subsided, but extrusion of alkali olivine basalt began from the Cerro Queimado vent, 5.5 km northwest of the caldera vent and 5 km from Ribeira Grande (Zbyszewski, 1963; Moore, 1986, 1988). An additional, small phreatic(?) eruption occurred in the caldera on 10 February 1564 (Zbyszewski, 1963, p. 43). An intrusion of basalt into trachytic magma may have triggered the 1563 eruption (Moore, 1988).

AGUA DE PAU (continued)

HISTORICAL ACTIVITY (continued)

1652: Earthquakes beginning on 10 October 1652 continued until 16 October, causing some damage in the region of Lagoa. On 17-18 October the earthquakes became weaker, reintensifying for an hour and a half on 18 October. On the afternoon of 19 October, fissures opened at a vent at the west foot of Agua de Pau, about 10 km west of Lagoa de Fogo. A 1-week Strombolian eruption of alkali olivine basalt built a small cone and extruded a short lava flow (Zbyszewski, 1963; Moore, 1988).

1980's: Bursts of microearthquakes occur from time to time under the northeast flank of Agua de Pau (R.B. Moore, written commun., 1987)

REFERENCES

Booth, B., Croasdale, R., and Walker, G.P.L., 1978, A quantitative study of five thousand years of volcanism on São Miguel, Azores: Phil. Trans. Roy. Soc. London, Ser. A, v. 288, p. 271-319.

Laughton, A.S., and Whitmarsh, R.B., 1975, The Azores-Gibraltar plate boundary, in Kristjansson, L., ed., Geodynamics of Iceland and the North Atlantic area: Dordrecht, D. Reidel Publ. Co., p. 63-81.

Moore, R.B., 1986, Preliminary geologic map of Agua de Pau Volcano, São Miguel, Azores: U.S. Geol. Surv. Open-File Rep. 86-192, 1 sheet, scale 1:18,000.

----- 1988, Geology of three late Quaternary stratovolcanoes on São Miguel, Azores: Bull. Volcanol. [in press].

Neumann van Padang, M., Richards, A.F., Machado, F., Bravo, T., Baker, P.E., and LeMaitre, R.W., 1967, Catalogue of active volcanoes of the world including solfatara fields, Pt. XXI, Atlantic Ocean: Rome, IAVCEI, 128 p.

Walker, G.P.L., and Croasdale, R., 1971, Two plinian-type eruptions in the Azores: Jour. Geol. Soc. London, v. 127, p. 17-55.

Weston, F.S., 1964, List of recorded volcanic eruptions in the Azores with brief reports: Bol. Mus. Lab. Miner. Geol. Fac. Ciencas Lisboa, v. 10, p. 3-18.

Zbyszewski, G., 1963, Les phénomènes volcaniques modernes dan l'Archipel des Açores: Serv. Geol. Portugal, v. 47, p. 5-277.

Zbyszewski, G., Almeida, F.M. de, Ferreira, O. da V., and Assuncao, C.T. de, 1958, Carta geologica de Portugal na escala de 1/50,000; et Noticia explicativa da folia B, S. Miguel (Açores): Lisboa, Serv. Geol. Portugal.

Zbyszewski, G., and Ferreira, O. da V., 1959, Carta geologica de Portugal na escala de 1/50,000; et Noticia explicativa de folia A, S. Miguel (Açores): Lisboa, Serv. Geol. Portugal.

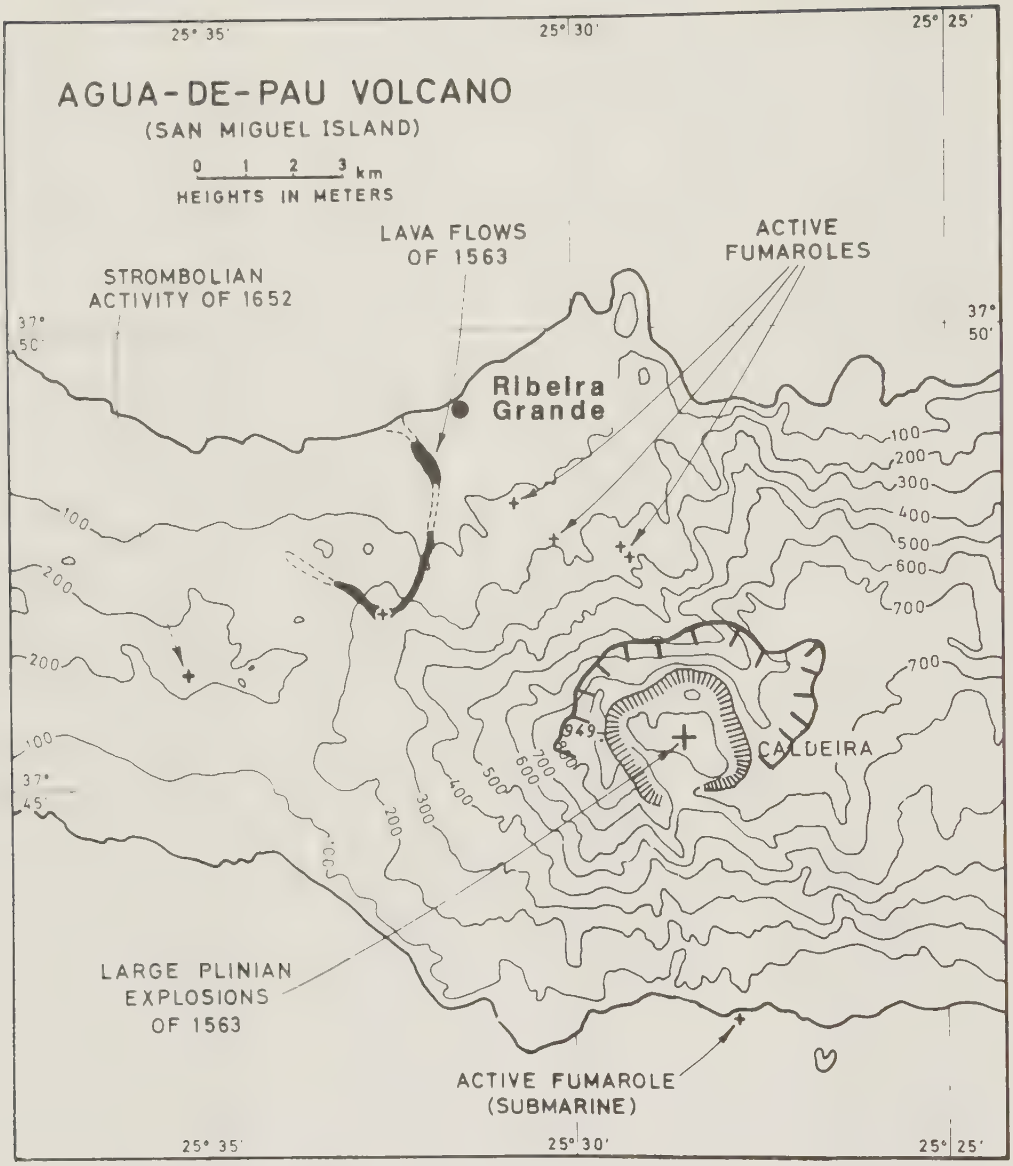

Figure 18.2.1. Activity of Agua de Pau during historical times, from Neumann van Padang and others (1967). Outline of outer caldera rim is after Moore (1986).

FURNAS

CAVW number (active vent)	Latitude Longitude (degrees)	Diameter (km)	Local tectonic setting	Precaldera edifice	SiO_2 content (wt pct)	Age of collapse (yr B.P.)	Date of unrest	Type and duration of unrest ESTU STHF MGTF H Te	Eruption type
18-02-10	37.77N 25.32W	6	Spreading center; exten	LP-strat	R = ca. 65 C = 65	ca. 12,000	1630	B--- ---B ---B B --	EX, dm

TECTONIC HISTORY

The Azores mark a possible hotspot along a spreading center, the WNW-ESE-trending Azores Fracture Zone (Laughton and Whitmarsh, 1975).

GEOLOGIC HISTORY

The modern caldera (fig. 18.3.1) formed about 12,000 yr B.P. after eruption of at least 7 km^3 of trachytic pumice (Moore, 1983, 1988). At least 11 layers of trachytic pumice, 4 with associated domes, postdate the caldera. All 11 eruptions occurred within the past 5,000 years (Booth and others, 1978), and 5 occurred within the past 1,000 years (Moore, 1988), most recently in A.D. 1630. Minor postcaldera eruptions have also produced lava flows and built cinder cones of hawaiite, west and south of the caldera (Moore, 1983, 1988). The older, 6-km diameter Povoaçao Caldera is contiguous with the east rim of Furnas Caldera.

HISTORICAL ACTIVITY

Earthquakes began on 2 September 1630, between 2100 hr and 2200 hr. The next morning, at 0800 hr, strong earthquakes were felt in the region of Furnas. Two small lakes dried out (or were emptied?) on account of the eruption. At 1100 hr, the earth continued to shake, and two fiery clouds arose from a vent on the southern caldera (Zbyszewski, 1963; Moore, 1988). Approximately 0.1 km^3 of magma (DRE) was erupted (Booth and others, 1978). At least 200 people were killed, most of them probably by mudflows in Ribeira Quente on the south coast (Zbyszewski, 1963; R.B. Moore, written commun., 1987).

REFERENCES

Booth, B., Croasdale, R., and Walker, G.P.L., 1978, A quantitative study of five thousand years of volcanism on São Miguel, Azores: Phil. Trans. Roy. Soc. London, Ser. A, v. 288, p. 271-319.

Laughton, A.S., and Whitmarsh, R.B., 1975, The Azores-Gibraltar plate boundary, in Kristjansson, L., ed., Geodynamics of Iceland and the North Atlantic area: Dordrecht, D. Reidel Publ. Co., p. 63-81.

FURNAS (continued)

REFERENCES (continued)

Moore, R.B., 1983, Preliminary geologic map of Furnas Volcano, São Miguel, Azores: U.S. Geol. Surv. Open-File Report 83-395, 1 sheet, scale 1:15,000.

----- 1988, Geology of three late Quaternary stratovolcanoes on São Miguel, Azores: Bull. Volcanol. [in press].

Neumann van Padang, M., Richards, A.F., Machado, F., Bravo, T., Baker, P.E., and LeMaitre, R.W., 1967, Catalogue of active volcanoes of the world including solfatara fields, Pt. XXI, Atlantic Ocean: Rome, IAVCEI, 128 p.

Zbyszewski, G., 1963, Les phénomènes volcaniques modernes dan l'Archipel des Açores: Serv. Geol. Portugal, v. 47, p. 5-277.

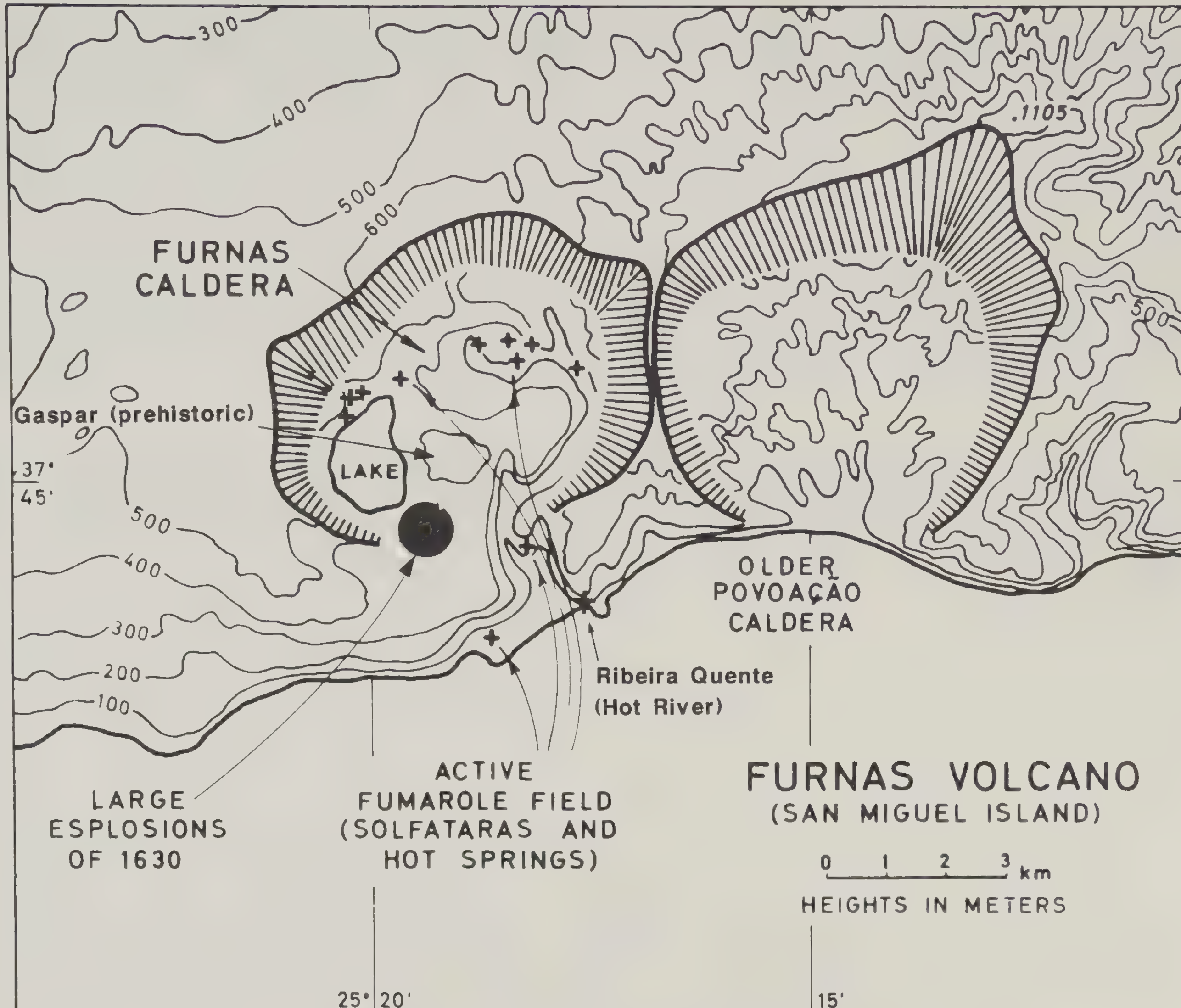

Figure 18.3.1. Furnas Volcano and extinct volcano of Povoacao, from Neumann van Padang and others (1967).

PART 3: HISTORICAL UNREST AT LARGE QUATERNARY CALDERAS (continued)

See inside back cover for explanation and abbreviations

LAS CAÑADAS

CAVW number (active vent)	Latitude Longitude (degrees)	Diameter (km)	Local tectonic setting	Precaldera edifice	SiO_2 content (wt pct)	Age of collapse (yr B.P.)	Date of unrest	Type and duration of unrest ESTU STHF MGTF H Te	Eruption type
18-03-03	28.30N	10 x 17	Hotspot?	LL-strat	R = 44-52	ca.	1341?	---- ---- ---- - --	unknown
(Pico de Teide,	16.63W				C = 60-61	150,000	1393/99?	---- ---- ---- - --	unknown
Chinyero,							1444?	---- ---- ---? - --	none?
and others)							1492	---- ---- ---- - --	lf
							1704-06	CC-- ---- ---- - --	ex,lf
							1798	---- ---- ---- - --	ex,lf
							1909	FF-- ---- ---- - --	ex,lf

TECTONIC SETTING

The Canary Islands lie in an intraplate setting, on the African continental shelf. Volcanism may result from a mantle hotspot beneath the islands. The alignment of vents and fissures in the Canary Islands suggests northeast-, northwest-, and north-south-trending faults; Las Cañadas Caldera is situated at the intersection of three such fissures or rift zones, called dorsals, of which the northwest- and northeast-trending ones have been dominant in recent geologic and historical time (Carracedo, 1985).

GEOLOGIC HISTORY

The Las Cañadas Caldera (figs. 18.4.1, 18.4.2) formed initially by collapse following a large plinian eruption that produced the Granadilla pumice (Booth, 1973), perhaps around 150,000 yr B.P. (Arana and others, 1985). Thick plinian and phreatoplinian pumice deposits occur on Tenerife (Fuster and others, 1968; Ridley, 1972; Booth, 1973; Arana and Carracedo, 1978). Subsequent gravitational failure of part of the north wall left the caldera open to the north (Booth, 1979). Pico Viejo and Teide Volcanoes have grown within the area of collapse, north of the escarpment.

HISTORICAL ACTIVITY

1492: The eruption of 1492 was probably from the Teide vent (Soler and others, 1984) (figs. 18.4.1, 18.4.2).

1704-06: An eruption of Siete Fuentes on 31 January 1704 (volume 0.4×10^6 m^3) was preceded by 7 days of premonitory seismicity; eruptions of Volcán Fasnia on 5 January 1705 (volume 2.5×10^6 m^3) and of Montana Arenas on 2 February 1705 (volume 24×10^6 m^3) were preceded by several days of seismicity, and an eruption of Montana Negra on 5 May 1706 (volume 66×10^6 m^3) was preceded by one evening of seismicity (data from F. Machado and A. Hernandez Pacheco, cited in Carracedo, 1985).

LAS CAÑADAS (continued)

HISTORICAL ACTIVITY (continued)

1909: A flank eruption along the northwest dorsal in 1909 was preceded by 18 months of seismicity, including earthquake swarms in July, August, and especially November 1908 (figs. 18.4.3-18.4.6). Maximum activity was 14 shocks in two hours, as felt in Orotava. "The top of a tall araucaria tree, seen reflected in a pool of water, was constantly agitated.... On 18 November 1909 detonations were heard, and these increased in violence until they were audible at Santa Cruz, 40 km from the scene of the outbreak, which was initiated on that date" (Perret, 1950, p. 149-151). Monge Montano (1983) also describes an increase in the intensity of earthquakes in November and December 1909, corresponding to an increase in the intensity of eruption (fig. 18.4.6). A short-term, very local precursor was noted by a farmer from Los Llanos who was "working 100 m away from the place of eruption when the earth began to tremble, and there was a sound like that of a flock of pigeons fluttering up... and then the earth burst forth amid a great noise" (von Wolff, 1929, v. 1, p. 520).

Geodetic and gravity networks have recently been established in the caldera (MacFarlane and Ridley, 1968; Sevilla and Martin, 1986; Sevilla and others, 1986; Viera and others, 1986), and a telemetered seismometer at the base of Teide has been operated by the Estacion Vulcanologica de Canarias since November 1987 (J. Carracedo, written commun., 1987).

REFERENCES

Arana, V., Barberi, F., and Ferrara, G., 1985, Petrology and geochemistry of Teide-Pico Viejo volcanic complex [abs.]: IAVCEI Symp., Catania, September 1985 (unpaginated).

Arana, V., and Carracedo, J.C., 1978, Los volcánes de las Islas Canarias: v. 1, Tenerife: Madrid, Ed. Rueda.

Booth, B., 1973, The Granadilla Pumice deposit of southern Tenerife, Canary Islands: Proc. Geol. Assoc., v. 84, no. 3, p. 353-370.

----- 1979, Assessing volcanic risk: Jour. Geol. Soc. London, v. 136, p. 331-340.

Carracedo, J.C., 1985, Geology of the Canary Islands, in Geografia de Canarias, Edit. Interinsular, Sta. Cruz de Tenerife, Canary Islands, 104 p.

Fernandez Navarro, L., 1924, Datos sobre el volcanismo canario: Bull. Volcanol., ser. I, no. 2, p. 129-155.

Fuster, J.M., Arana, V., Brandle, J.L., Navarro, M., Alonso, U., and Aparicio, A., 1968, Geologia y vulcanologia de las Islas Canarias--Tenerife: Madrid, Inst. "Lucas Mallada," 218 p.

MacFarlane, D.J., and Ridley, W.I., 1968, An interpretation of gravity data for Tenerife, Canary Islands: Earth Planet. Sci. Lett., v. 4, p. 481-486.

Monge Montano, F., 1983, Sismicidad en el Archipelago Canario, relacion con las erupciónes: Cuarta asamblea nacional de geodesia y geofisica, v. 1: Madrid, Inst. Geogr. Nac., p. 457-471.

Neumann van Padang, M., Richards, A.F., Machado, F., Bravo, T., Baker, P.E., and LeMaitre, R.W., 1967, Catalogue of active volcanoes of the world including solfatara fields, Pt. XXI, Atlantic Ocean: Rome, IAVCEI, 128 p.

Perret, F.A., 1950, Volcanological observations: Carnegie Inst. Washington Publ. 549, 153 p.

Ridley, W.I., 1972, The field relations of the Las Cañadas Volcanoes, Tenerife, Canary Islands: Bull. Volcanol., v. 35, p. 318-334.

LAS CAÑADAS (continued)

REFERENCES (continued)

Sevilla, M.J., and Martin, M.D., 1986, Geodetic network design for crustal deformation studies in the Caldera of Teide area: Tectonophysics, v. 130, p. 235-248.

Sevilla, M.J., Martin, M.D., and Camacho, A.G., 1986, Data analysis and adjustment of the first geodetic surveys in the Caldera of Teide, Tenerife, Canary Islands: Tectonophysics, v. 130, p. 213-234.

Soler, V., Carracedo, J.C., and Heller, F., 1984, Geomagnetic secular variation in historical lavas from the Canary Islands: Geophys. Jour. Roy. Astron. Soc., v. 78, p. 313-318.

Viera, R., Toro, C., and Arana, V., 1986, Microgravimetric survey in the Caldera of Teide, Tenerife, Canary Islands: Tectonophysics, v. 130, p. 249-257.

Wolff, F. von, 1929, Der Vulkanismus: Stuttgart: Ferdinand Enke, v. 1, no. 2, p. 520.

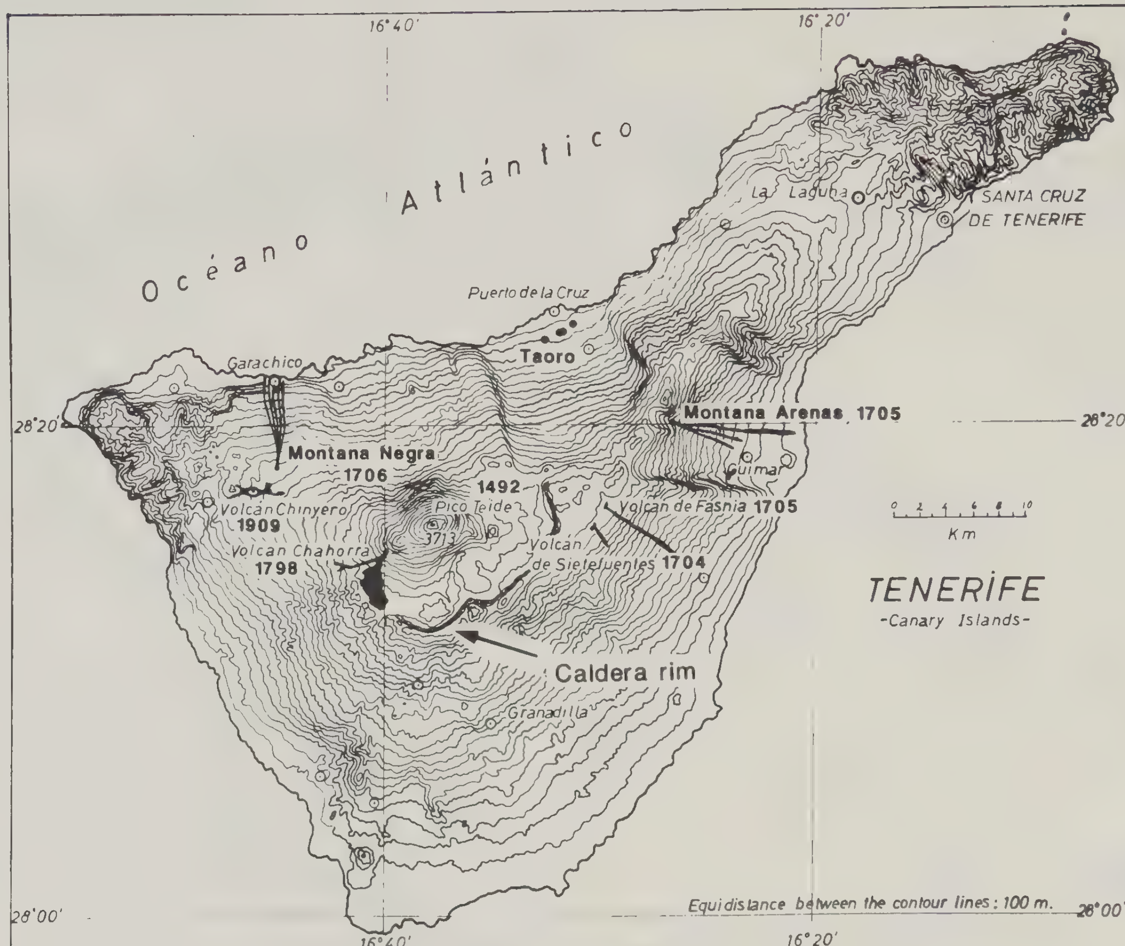

Figure 18.4.1. Island of Tenerife and Las Cañadas Caldera, with Pico de Teide at its center, from Neumann van Padang and others (1967), with eruption dates from Soler and others (1984).

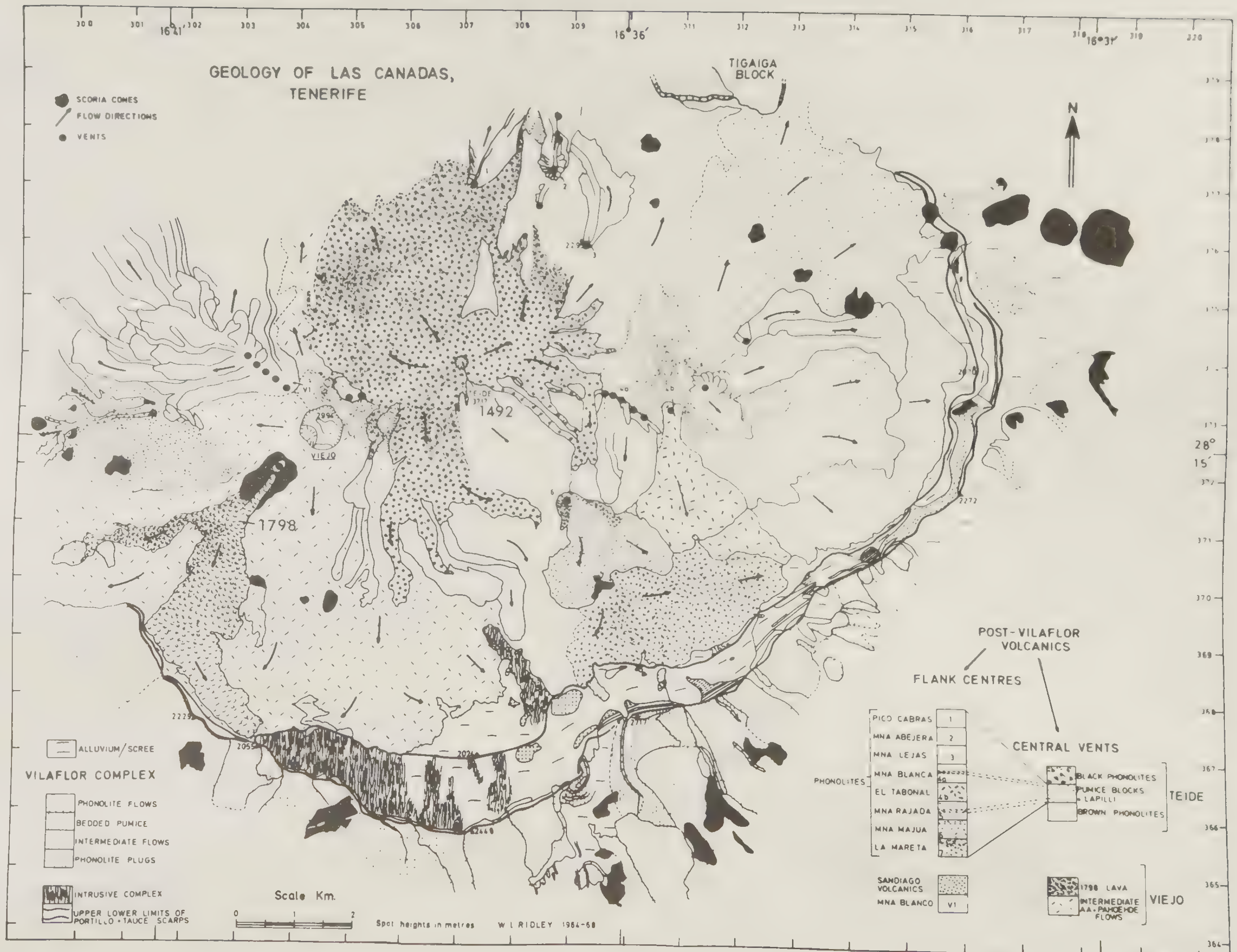

Figure 18.4.2. Geologic map of Las Cañadas volcanoes, including locations of the 1492 and 1798 vents, from Ridley (1972).

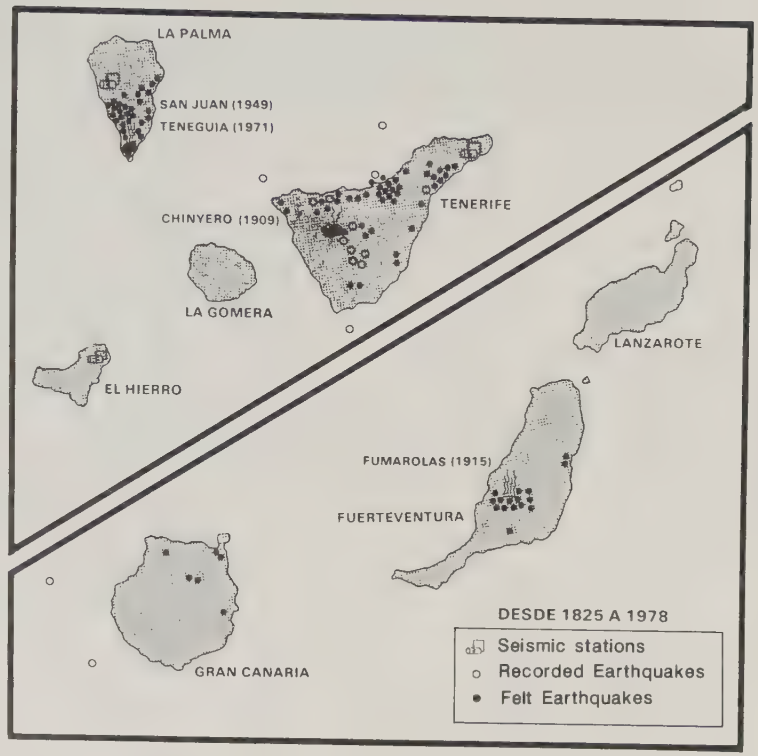

Figure 18.4.3. Seismic activity associated with volcanism in Canary Islands from 1825 to 1978, from Carracedo (1985). Note epicenters at Las Cañadas Caldera, Tenerife.

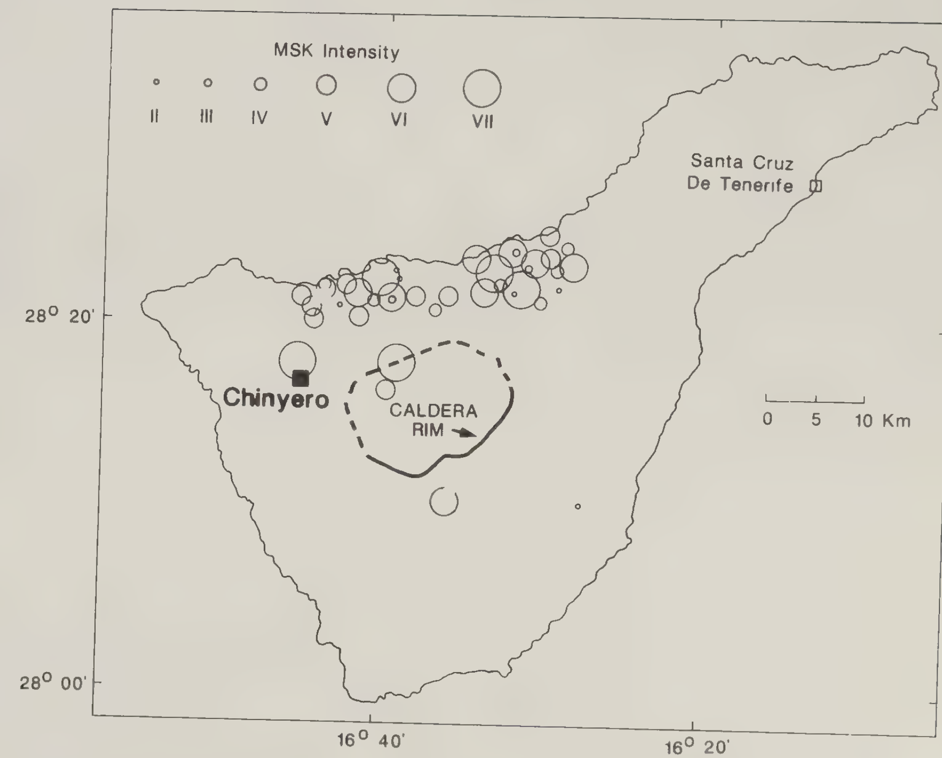

Figure 18.4.4. Distribution and intensity of earthquakes near Las Cañadas Caldera in 1909, from Monge Montano (1983). Caldera outline dashed where inferred.

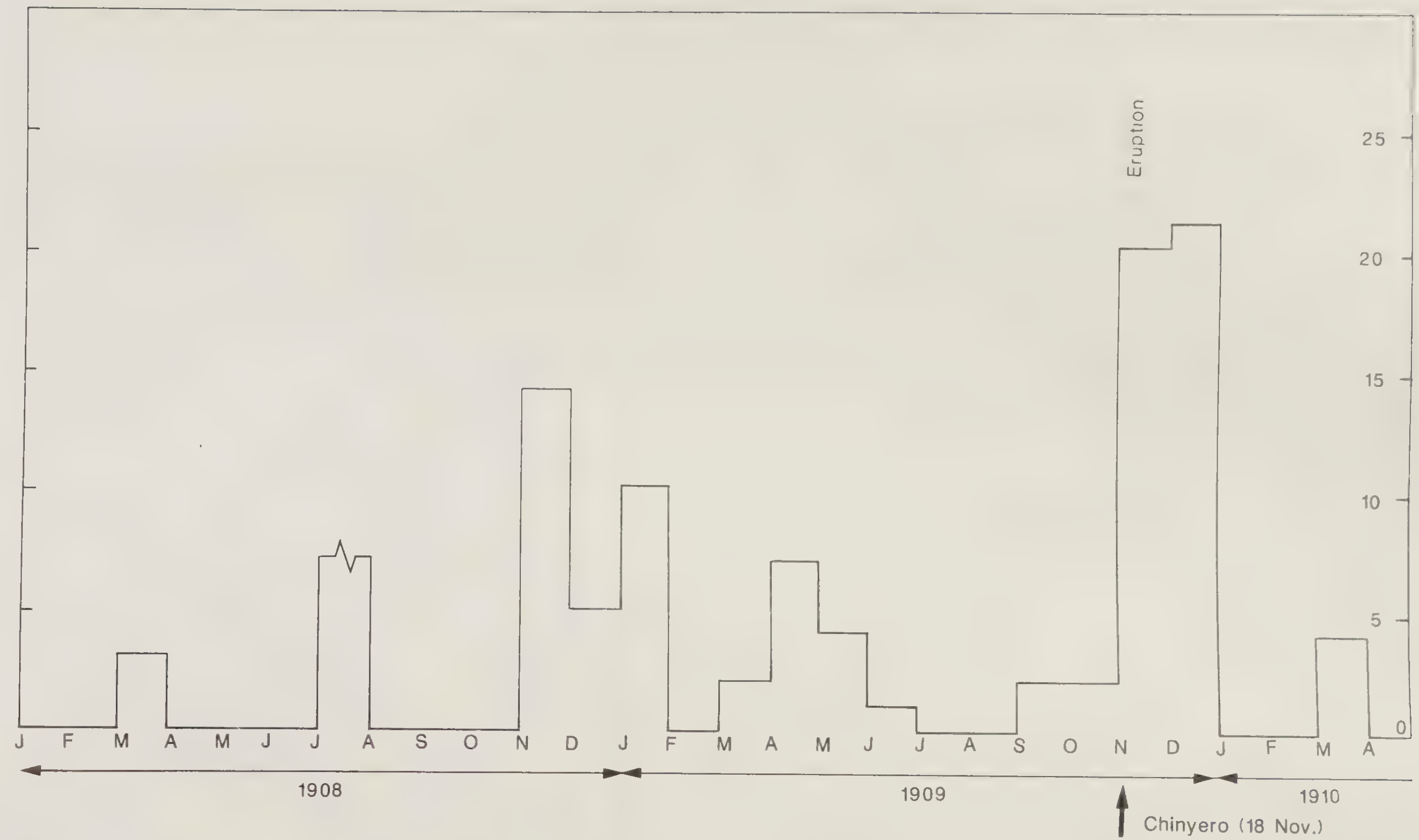

Figure 18.4.5. Temporal distribution of felt earthquakes associated with the 1909 Chinyero eruption (arrow) northwest of Las Cañadas Caldera, from Monge Montano (1983).

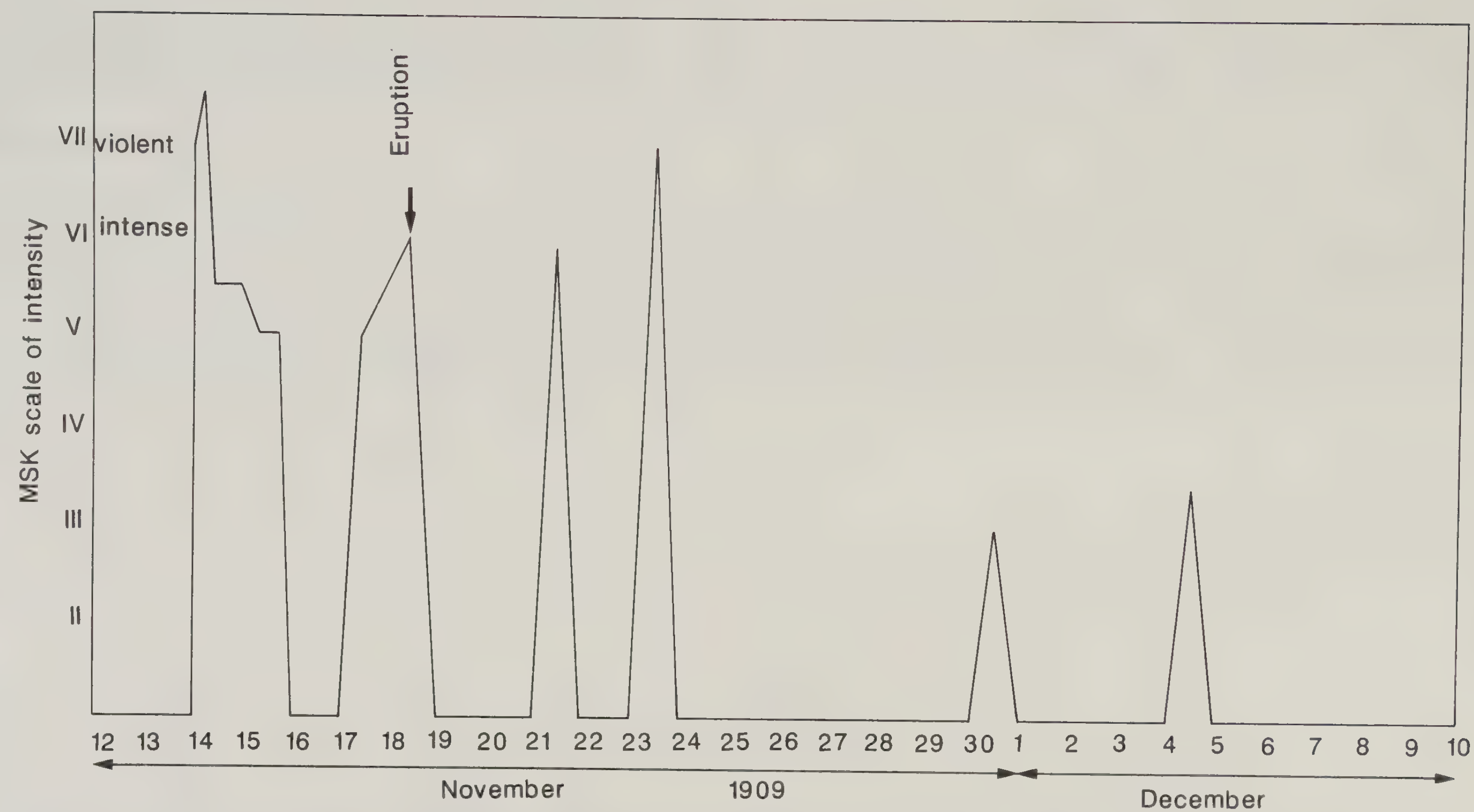

Figure 18.4.6. Temporal variation in intensity of earthquakes felt during an eruption of Volcano Chinyero, Las Cañadas Caldera, in 1909 (Monge Montano, 1983).

PART 3: HISTORICAL UNREST AT LARGE QUATERNARY CALDERAS (continued)
See inside back cover for explanation and abbreviations

CHA

CAVW number (active vent)	Latitude Longitude (degrees)	Diameter (km)	Local tectonic setting	Precaldera edifice	SiO_2 content (wt pct)	Age of collapse (yr B.P.)	Date of unrest	Type and duration of unrest ESTU STHF MGTF H Te	Eruption type
18-04-01 (Fogo)	14.95N 24.35W	8	Intra-plate	Shield	R = 40-50 C = mafic		<1500-1761	---- ---- ---- - --	ex,lf
							1769	---- ---- ---- - --	ex
							1785	---- ---- ---- - --	pex,lf
							1799	---- ---- ---- - --	ex,lf
							1817	---- ---- ---- - --	unknown
							1847	x--- ---- ---- - --	ex,lf
							1852	---- ---- ---- - --	ex,lf
							1857	---- ---- ---- - --	ex,lf
							1951	x--- ---- ---- - --	ex,lf

TECTONIC SETTING

Fogo Island (fig. 18.5.1) and the rest of the Cape Verde Islands are intraplate volcanic islands situated west of the margin of the African continent (Dash and others, 1971).

GEOLOGIC HISTORY

The Cape Verde Islands are known geologically for a strongly alkaline suite of volcanic and plutonic rocks (Mitchell-Thome, 1970; Gunn and Watkins, 1976).

HISTORICAL ACTIVITY

17th and 18th centuries: von Humboldt (1861-63) reports that Fogo was in continuous eruption from 1680 to 1713 and then in repose until 1798. Neumann van Padang and others (1967) and Mitchell-Thome (1981) cite different dates, which we adopt here, including continuous eruption from before 1500 until 1761, intermittent eruptions until 1857, and a subsequent period of repose until 1951.

1847: Fatalities occurred as a result of an earthquake.

1951: The eruption of 12 June was preceded by strong earthquakes and volcanic tremors (Ribeiro, 1954).

CHA (continued)

REFERENCES

Dash, B.P., Ball, M.M., Kings, G.A., Butler, L.W., and Rona, P.A., 1971, Geophysical measurements in the Cape Verde archipelago [abs.]: Eos, Trans. Am. Geophys. Union, v. 52, p. 235.

Gunn, B.M., and Watkins, N.D., 1976, Geochemistry of the Cape Verde Islands and Fernando de Noroñha: Geol. Soc. Am. Bull., v. 87, p. 1089-1100.

Humboldt, A. von, 1861-63, Cosmos: (transl. from the German by E.C. Otté and W.S. Dallas): New York, Harper and Brothers, v. 5, p. 243.

Mitchell-Thome, R.C., 1970, Geology of the South Atlantic islands: Beitr. Regionalen Geol. Erde, v. 10, 367 p.

----- 1981, Vulcanicity of historic times in the middle Atlantic islands: Bull. Volcanol., v. 44, p. 57-70.

Neumann van Padang, M., Richards, A.F., Machado, F., Bravo, T., Baker, P.E., and LeMaitre, R.W., 1967, Catalogue of active volcanoes of the world including solfatara fields, Pt. XXI, Atlantic Ocean: Rome, IAVCEI, 128 p.

Ribeiro, O., 1954, A ilha do Fogo e as suas erupções: Lisbon, Ministério do Ultramar, Memórias, Série Geográfica, no. 1, 319 p.

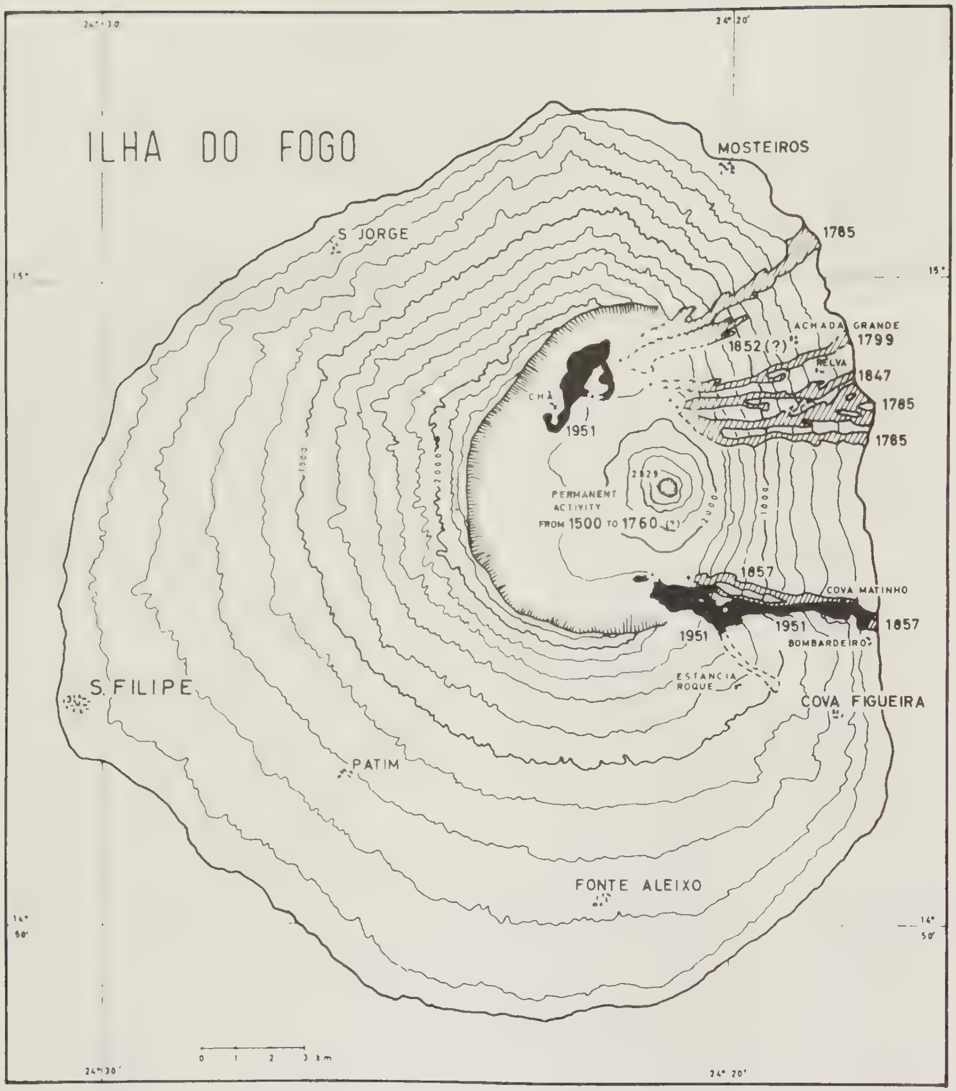

Figure 18.5.1. Island of Fogo, showing Cha Caldera and recent lava flows, from Neumann van Padang and others (1967).

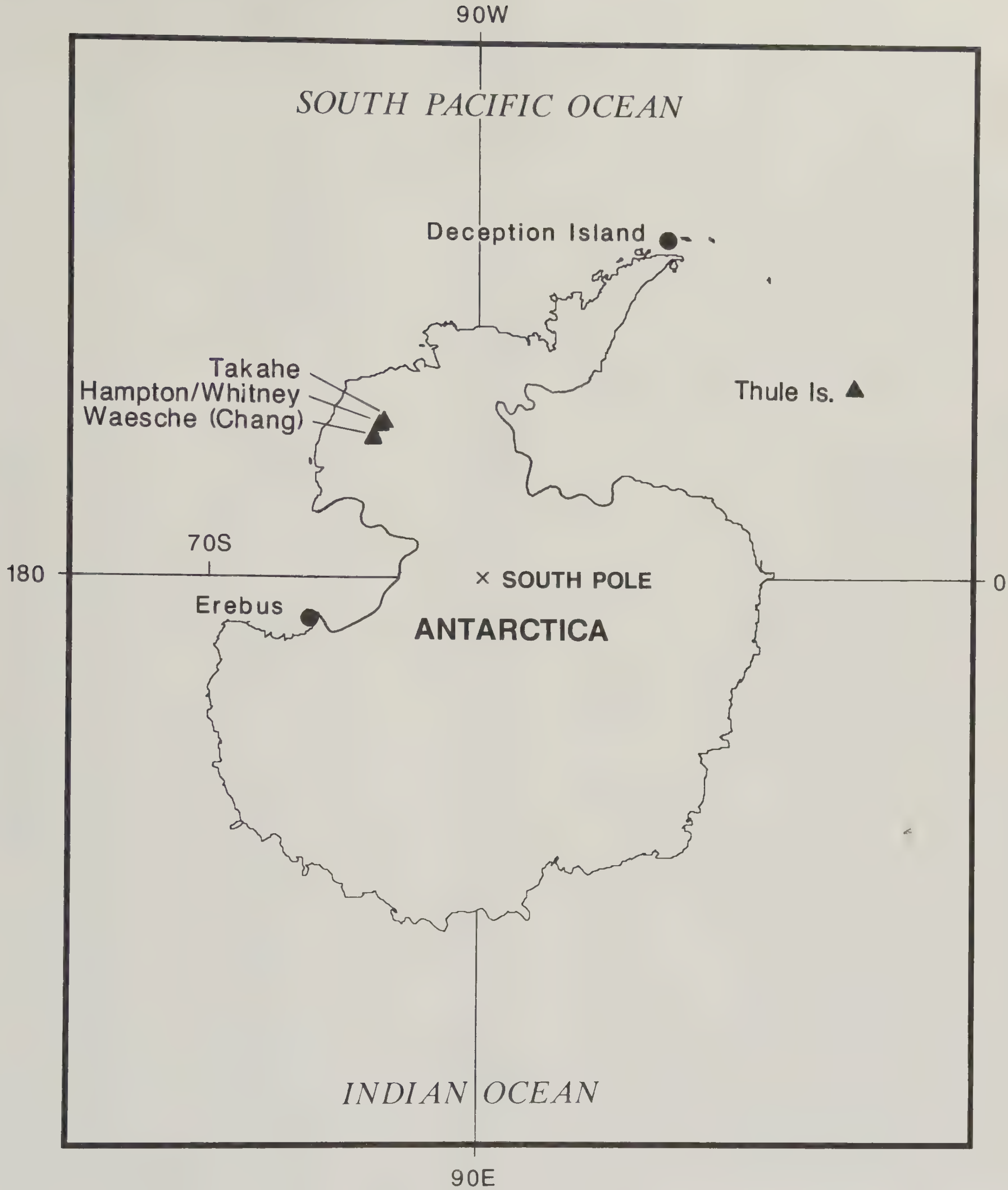

Figure 19. Locations of large, Quaternary restless calderas (solid circles) and nonrestless calderas (triangles) in Region 19.

EREBUS

CAVW number (active vent)	Latitude Longitude (degrees)	Diameter (km)	Local tectonic setting	Precaldera edifice	SiO_2 content (wt pct)	Age of collapse (yr B.P.)	Date of unrest	Type and duration of unrest ESTU STHF MGTF H Te	Eruption type
19-00-02 (Erebus)	77.58S 167.17E	6 (older) 5 (younger)	Intra-plate	Strato	R = 56 (anorthoclase phonolite)		1841	---- ---- ---- - --	ex,lf
							1900?	---- ---- ---- - --	ex
							1908	---- ---- ---E - --	ll
							1911-12	---- ---- ---- - --	ex
							1915	---- ---- ---- - --	ex
							1947	---- ---- ---- - --	ex,lf(?)
							1955	---- ---- ---- - --	ex
							1963	---- ---- ---- - --	ll
							1972-87+	YYY- Y--- Y--- - --	ex,lf,ll

TECTONIC SETTING

Mt. Erebus is an intraplate volcano, situated at the southern end of the Terror Rift within the Victoria Land basin, a major sedimentary basin with over 12 km of fill and underlain by 21-km-thick crust. The basin is bounded to the west by the Transantarctic Mountains, with 40-km-thick crust (Cooper and Davey, 1985; Fitzgerald and others, 1986).

GEOLOGIC HISTORY

An older cone of Mt. Erebus (Fang Volcano), composed largely of benmoreite, was partly destroyed by an unknown event, leaving a caldera of ca. 6-km diameter (fig. 19.1.1). The modern cone of Mt. Erebus, composed largely of anorthoclase phonolite (Kyle, 1977), has largely filled the older caldera, leaving only Fang Ridge (north of Mt. Erebus) as a relic of the older cone. A roughly 5-km-diameter caldera developed at the top of the modern cone, and it too has been largely filled (Berninghausen and Neumann van Padang, 1960; P. Kyle, written commun., 1987).

HISTORICAL ACTIVITY

Most historical activity has been confined to the younger caldera. A reported exception was increased fumarolic activity in April-September 1908 and on 17 June 1908, near Abbott Peak, 10 km north-northeast of the summit of Mt. Erebus (cited in Berninghausen and Neumann van Padang, 1960). A seismic swarm in roughly the same area was recorded in October 1982 (Ueki and others, 1984; Kaminuma and others, 1985) (figs. 19.1.2-19.1.4).

EREBUS (continued)

HISTORICAL ACTIVITY (continued)

A lava lake discovered in 1972 grew slowly until 1976, when it was circular, about 60 m in diameter. It remained relatively constant until September 1984. Larger-than-usual Strombolian explosions occurred in September to December 1984. Earthquakes were felt, and glow and increased steaming were observed from McMurdo Sound (37 km southwest of the volcano) (P. Kyle and others, in Smithsonian Institution, 1984). The summit crater lava lake was buried by ejecta between 13 September 1984 and October 1984. When the lake was exhumed in December 1985 it was 15 m in diameter, and it grew to 20 m in diameter by December 1986 (P. Kyle, written commun., 1987).

SO_2 emission was 230 tonnes/day in December 1983, but less than 30 tonnes/day since then (P. Kyle, written commun., 1987); no remarkable deformation occurred during the same time period.

Dibble and others (1984) report that numerous small volcanic earthquakes occur in conjunction with volcanic activity (figs. 19.1.2, 19.1.3). Most events above 1 kJ in energy (ca. $\underline{M}$=0) are explosion earthquakes, with emergent rather than impulsive onsets. Numerous B-type earthquakes have energy greater than 10 kJ. Volcanic tremor is rare. Hypocenters shown in figures 19.1.2 and 19.1.3 are currently being reexamined and are shallower than shown (P. Kyle, written commun., 1987).

REFERENCES

Berninghausen, W.H., and Neumann van Padang, M., 1960, Catalogue of Active Volcanoes of the World including solfatara fields, Pt. X, Antarctica: Naples, IAVCEI, 32 p.

Cooper, A.K., and Davey, F.J., 1985, Episodic rifting of Phanerozoic rocks in the Victoria Land basin, western Ross Sea, Antarctica: Science, v. 229, p. 1085-1087.

Dibble, R.R., and Barrett, S.I.D., 1987, Time comparisons between video and seismic signals from explosions in the lava lake of Erebus Volcano, Antarctica [abs.]: Abstracts, 19th Gen. Assem. IUGG, Vancouver, Canada, v. 2, p. 397.

Dibble, R.R., Kienle, J., Kyle, P.R., and Shibuya, H., 1984, Geophysical studies of Erebus Volcano, Antarctica, for 1974 December to 1982 January: New Zealand Jour. Geol. Geophys., v. 27, no. 4, p. 425-455.

Fitzgerald, P.G., Sanford, M., Barnett, P.J., and Gleadow, A.J.W., 1986, Asymmetric extension associated with uplift and subsidence in the Transantarctic Mountains and Ross Embayments: Earth Planet. Sci. Lett., v. 81, p. 67-78.

Giggenbach, W.F., Kyle, P.R., and Lyon, G.L., 1973, Present volcanic activity on Mount Erebus, Ross Island, Antarctica: Geology, v. 1, no. 3, p. 135-136.

Kaminuma, K., Ueki, S., and Kienle, J., 1985, Volcanic earthquake swarms at Mt. Erebus, Antarctica: Tectonophysics, v. 114, p. 357-369.

Kienle, J., Rowe, C.A., Marshall, D.L., and Estes, S.A., 1984, Volcanic seismic studies of Mt. Erebus, Antarctica: Biennial Rep., Univ. Alaska Geophys. Inst., p. 147-149.

EREBUS (continued)

REFERENCES (continued)

Kyle, P.R., 1977, Mineralogy and glass chemistry of recent volcanic ejecta from Mt. Erebus, Ross Island, Antarctica: New Zealand Jour. Geol. Geophys., v. 20, no. 6, p. 1123-1146.

Kyle, P.R., and Cole, J.W., 1974, Structural control of volcanism in the McMurdo Volcanic group, Antarctica: Bull. Volcanol., v. 38, no. 1, p. 16-25.

Kyle, P.R., Dibble, R.R., Giggenbach, W.F., and Keys, J., 1982, Volcanic activity associated with the anorthoclase phonolite lava lake, Mount Erebus, Antarctica, in Craddock, C., ed., Antarctic geoscience, Madison, Univ. Wisconsin, p. 735-745.

Rose, W.I., Chuan, R.L., and Kyle, P.R., 1985, Rate of sulphur dioxide emission from Erebus volcano, Antarctica, December, 1983: Nature, v. 316, p. 710-712.

Rowe, C.A., and Kienle, J., 1986, Seismicity in the vicinity of Ross Island, Antarctica: Jour. Geodynam., v. 6, p. 375-385.

Shibuya, K., Baba, M., Kienle, J., Dibble, R.R., and Kyle, P.R., 1982, A study of the seismic and volcanic activity of Mount Erebus, Antarctica, 1981-1982, in Nagata, T., ed., Proc. 3rd Symp. on Antarctic geosciences, 1982, Tokyo, Nat. Inst. Polar Research, p. 54-66.

Smith, W.C., 1954, The volcanic rocks of the Ross archipelago: Brit. Antarct. Exped., 1910, Nat. Hist. Rep., Geology, v. 2, no. 1, p. 1-107.

Smithsonian Institution, Scientific Event Alert Network (SEAN), 1976-85, Erebus: SEAN Bull., v. 1-10 (contributions from P. Kyle and others).

Ueki, S., Kaminuma, K., Baba, M., Koyama, E., and Kienle, J., 1984, Seismic activity of Mount Erebus, Antarctica in 1982-1983: Memoirs Nat. Inst. Polar Research (Tokyo), p. 29-40.

U. S. Geological Survey, 1970, Ross Island topographic sheet, Antarctica 1:250,000 Reconnaissance Series, ST 57-60/6*(162°E-170°E), 1960, revised 1970.

Volcanological Society of Japan, 1974-83, Erebus: Bull. Volcanic Eruptions, nos. 12-20.

Figure 19.1.1. Topographic map showing outlines of Erebus Caldera and an older caldera (Proto-Erebus Caldera or Fang Volcano Caldera; dotted where inferred), which is now buried by Erebus except at Fang Ridge (U.S. Geological Survey, 1970; outlines courtesy of P.R. Kyle, 1987; dashed where inferred).

Figure 19.1.2. Epicenter map, 20 December 1980 to 6 January 1981, and projection of hypocenters onto a N-S section (left); epicenter map and projection of hypocenters during the 1981-82 field season onto a NE-SW section (right). Hypocenters below sea level are shown bold. Both diagrams from Dibble and others (1984).

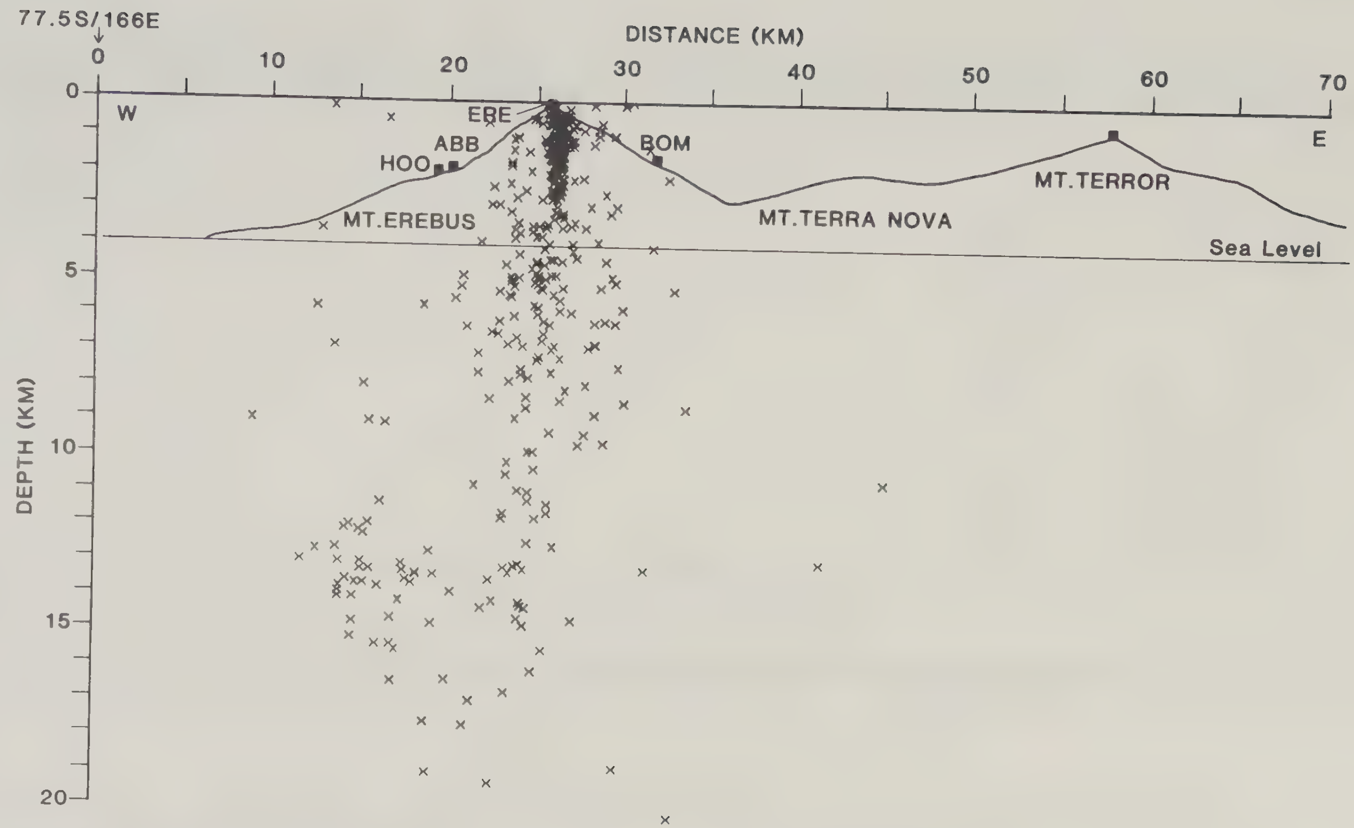

Figure 19.1.3. West-east hypocentral cross section through Mount Erebus and Mount Terror, Ross Island, Antarctica, showing 403 best-located events, December 1980 to February 1984 (Kienle and others, 1984). More recent data from video experiments suggest that most earthquakes plotted here at less that 5-km depth actually occurred at lava surface during Strombolian eruptions. Discrepancy probably reflects errors in seismic velocity models used to locate earthquakes in this area (Dibble, 1987; P. Kyle, written commun., 1987).

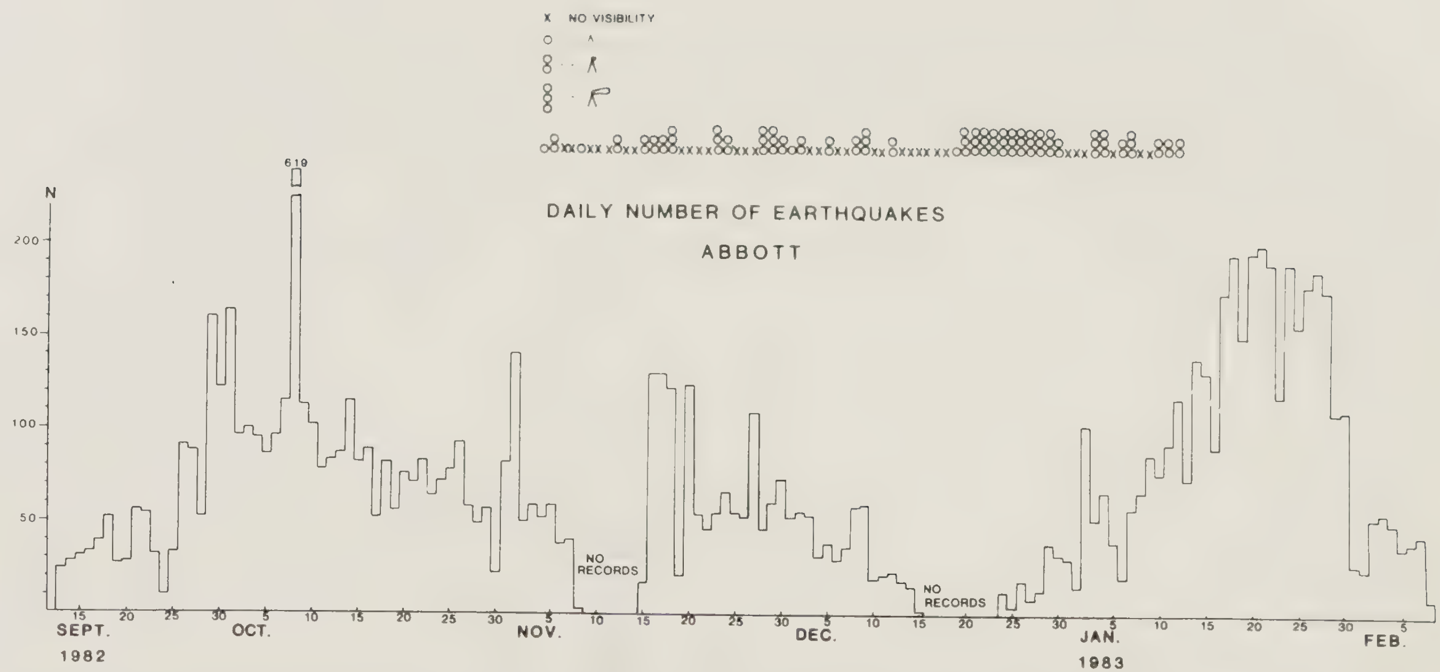

Figure 19.1.4. Plume observations of Erebus Volcano from McMurdo Station (top). Daily counts of earthquakes at Abbott Peak station (see fig. 19.1.2) from September 1982 to February 1983 (bottom; from Kaminuma and others, 1985).

DECEPTION ISLAND

CAVW number (active vent)	Latitude Longitude (degrees)	Diameter (km)	Local tectonic setting	Precaldera edifice	SiO_2 content (wt pct)	Age of collapse (yr B.P.)	Date of unrest	Type and duration of unrest ESTU STHF MGTF H Te	Eruption type
19-00-03 (Deception Island)	62.93S 60.57W	7	Exten	Strato	R = 50-70 C = 51-54		1820/29	---- ---- ---- - --	ex
							1829	x--- ---- ---x x --	none?
							1839-42	---- ---- ---F F --	ex, lf
							ca. 1912	---- ---- ---- - --	ex, Ex
							ca. 1917	---- ---- ---- - --	ex, Ex
							1923-27	x--- x--- --xx - --	none?
							1930	x--- x--- ---- - --	none
							before 1956	---- ---- ---- - --	ex
							1967	FF-x ---x ---- - --	pex,Ex
							1969	x--? ---Y ---E - --	Ex,ex,pex
							1970	x--x Z--x ---- - --	Ex,ex,pex
							1972	---- ---- ---- - --	sub
							1987	x--- ---- ---- - --	Ex?

TECTONIC SETTING

Deception Island is in the South Shetland Islands, on the Bransfield Rift where the rift is offset by a short ridge-ridge transform fault (Circum-Pacific Map Project, 1981).

GEOLOGIC HISTORY

A 7-km-diameter caldera in the center of Deception Island is largely flooded by the sea (figs. 19.2.1-19.2.3). The caldera apparently formed as a result of voluminous eruptions of sodic andesite or basaltic andesite (Baker and others, 1975). Numerous active vents are situated along the ring fractures, near the shoreline of the natural harbor. Slight chemical differences between magma erupted from various locations along the ring fracture in 1967, 1969, and 1970 were interpreted by Baker and others (1975) and Roobol (1979) as evidence of isolated intrusive pods of magma along the ring fracture.

HISTORICAL ACTIVITY

Deception Island has no permanent inhabitants, so apparent episodicity of eruption reports probably reflects episodic visits by sealing, whaling, and exploring expeditions.

DECEPTION ISLAND (continued)

HISTORICAL ACTIVITY (continued)

1829: The HMS Chanticleer visited Deception Island for 2 months to conduct pendulum experiments among other tasks. The captain wrote (reproduced in Roobol, 1979): "Subterranean sounds, as of mountain torrents, were frequently heard and on one occasion were so loud as to create some apprehension for the safety of the instruments, and accordingly the pendulums that had been experimented with were immediately taken (back) on board." Numerous fumaroles were observed throughout the caldera.

1842: The whole south side of Deception Island (13 vents) appeared "as if on fire." Hawkes (1961) correlated this report with young lavas in the Mount Kirkwood area; Roobol (1979) agrees with the location but interprets some of the 13 vents and "fire" to have been fumaroles and steam.

1912±5 yr, 1917±3 yr: Eruptions are inferred from pyroclastic deposits interbedded with ice. Vents were in or near "Lake Crater," south of Fumarole Bay (Klay and Orheim, 1969; Orheim, 1972).

1923: The shore of Deception Island subsided near a whaling station. Waters of the bay "boiled" and stripped paint from ship hulls (erroneously reported by some as 1921; Roobol, 1979).

1930: During or after an earthquake, the bottom of the harbor (caldera floor) dropped about 4.5 m.

1967: An eruption was preceded by 2-3 weeks of precursory seismicity (fig. 19.2.4); from the data of Lorca (1976), it appears that this seismicity was only slightly more than previous swarms in early, mid-, and late 1966 ($\underline{M}_{max}$ = 4.7; $\underline{d}_{max}$ ~ 20 km). The starting date for increased seismicity is not known; monitoring was begun on 16 January 1966. Eruption was from four vents along the northwest part of the ring fracture. A new island was built (Yelcho Island, or "New Island 1967" of fig. 19.2.3). In addition, Baker and others (1975, p. 25-26) report that a small area immediately south of the "Land Center" (fig. 19.2.3) was 55 m higher after the eruption than before and was intensely fractured and rifted, suggesting uplift. An alternate explanation--that 55 m of tephra was deposited at the site--was not supported by field observations.

1969: Almost 2 months of precursory seismicity greatly intensified 6 hours before eruptions on 21 February 1969. The temperature of Kroner Lake also increased from January to February. Eruptions were from 20-30 vents along a 5-km-long section of the caldera's east ring fracture (Baker, 1969; Baker and others, 1975).

1970: Shultz (1972) showed new land in the vicinity of the 1967 and 1970 craters (northwestern ring fracture; fig. 19.2.3). Some of this land was uplifted so much that the shoreline was displaced more than 500 m and Yelcho Island was rejoined to land, reducing the surface of Telefon Bay by nearly half (Gonzales-Ferran and others, 1971). Eleven or more 1970 vents developed along a 5-km-long arcuate graben, within and slightly outside the area of uplift.

DECEPTION ISLAND (continued)

HISTORICAL ACTIVITY (continued)

Roobol (1979) proposed five intrusive episodes culminating in eruptions since 1820, based on the historical record and particularly on information about areas of heat escape and eruption vents. These episodes were: 1. Mount Pond, 1829 (possible Pendulum Cove eruption); 2. Mount Kirkwood, 1839-42 (Mount Kirkwood fissure eruptions); 3. Pendulum Cove - Mount Pond - Whalers Bay sector, 1908-60 (1969 fissure eruption); 4. Telefon Bay, ca. 1956-70 (1967 and 1970 eruptions); and 5. Wensleydale Beacon, post-1962 to 1970 (1970 eruptions). Each of these intrusions emplaced a pod of magma at shallow depth, each in a slightly different state of chemical evolution.

1987: A plume was seen on satellite images on 23 July, and "recent, local" seismic activity was recorded at a station on King George Island, 100 km southeast of Deception Island (Smithsonian Institution, 1987).

COMMENTS

Deception Island is of special interest because on at least three occasions, eruptions have occurred simultaneously from multiple vents around a ring fracture. Because leaks of magma along ring structures are known to have preceded some large, prehistoric caldera-forming eruptions (see Bacon, 1985), we might expect that simultaneous eruptions from multiple vents like those at Deception Island could also lead to larger eruptions and caldera collapse, but so far that has not been the case.

REFERENCES

Bacon, C.R., 1985, Implications of silicic vent patterns for the presence of large crustal magma chambers: Jour. Geophys. Res., v. 90, no. B13, p. 11,243-11,252.
Baker, P.E., 1968, Comparative volcanology and petrology of the Atlantic island arcs: Bull. Volcanol., v. 32, p. 189-206.
----- 1969, A volcano erupts beneath the Antarctic ice: Geogr. Mag., v. 41, p. 115-126.
Baker, P.E., Davies, T.G., and Roobol, M.J., 1969, Volcanic activity at Deception Island in 1967 and 1969: Nature, v. 224, p. 553-560.
Baker, P.E., and McReath, I., 1971, Volcanic eruption of Deception Island: Nature, Phys. Sci., v. 231, p. 5-9.
Baker, P.E., McReath, I., Harvey, M.R., Roobol, M.J., and Davies, T.G., 1975, The geology of the South Shetland Islands: V. The volcanic evolution of Deception Island: Brit. Antarctic Surv. Sci. Reps., no. 78, 81 p.
Berninghausen, W.H., and Neumann van Padang, M., 1960, Catalogue of active volcanoes of the world including solfatara fields, Pt. X, Antarctica: Naples, IAVCEI, 32 p.
Circum-Pacific Map Project, Antarctic Panel, 1981, Plate-tectonic map of the Circum-Pacific region, Antarctica sheet, scale 1,10,000,000: Tulsa, Circum-Pacific Council for Energy and Mineral Resources/Am. Assoc. Pet. Geol., 1 sheet.
Clapperton, C., 1969, The volcanic eruption at Deception Island, December 1967: Brit. Ant. Surv. Bull. 22, p. 83-90.

DECEPTION ISLAND (continued)

REFERENCES (continued)

Gonzales-Ferran, O., Munizaga V., F., and Moreno R., H., 1971, Sintesis de la evolucion volcánica de isla Decepcion y la erupción de 1970: Univ. Chile, INACH Ser. Cient., v. 2, no. 1, p. 1-14.

Hawkes, D.D., 1961, The geology of the South Shetland Islands: II, The geology and petrology of Deception Island: Falkland Islands Dependencies Surv. Sci. Reps., no. 27, 43 p.

Klay, J.R., and Orheim, O., 1969, Glaciology and glacial geology on Deception Island: Antarctic Jour., v. 4, no. 4, p. 125-126.

Lorca, E., 1976, Deception Island: Seismic activity prior to the eruption of 1967, <u>in</u> Gonzales-Ferran, O., ed., Proc. Symp. Andean and Antarctic volcanology problems: Naples, IAVCEI, p. 632-645.

Orheim, O., 1972, Volcanic activity on Deception Island, South Shetland Islands, <u>in</u> Adie, R.J., ed., Antarctic geology and geophysics: Oslo, Universsitesforlaget, p. 117-120.

Roobol, M.J., 1973, Historic volcanic activity at Deception Island: Brit. Antarctic Surv. Bull., v. 32, p. 23-30.

----- 1979, A model for the eruptive mechanism of Deception Island from 1820-1970: Brit. Antarctic Surv. Bull., no. 49, p. 137-156.

Shultz, C.H., 1972, Eruption at Deception Island, Antarctica, August 1970: Geol. Soc. Am. Bull. v. 83, p. 2837-2842.

----- 1976, Petrology and petrochemistry of Deception Island, Antarctica, <u>in</u> Gonzales-Ferran, O., ed., Proc. Symp. Andean and Antarctic volcanology problems: Naples, IAVCEI, p. 498-517.

Smithsonian Institution, Scientific Event Alert Network (SEAN), 1987, Deception Island Volcano: SEAN Bull., v. 12, no. 8, p. 18 (information from W. Gould and G. Gutheridge).

Wilkes, C., 1845, Narrative on the United States Exploring Expedition, during the years 1838, 1839, 1840, 1841, and 1842: Philadelphia, Lea and Blanchard, 5 vols.

Williams, H., and McBirney, A.R., 1968, Geologic and geophysical features of calderas: Progress Rep., NASA Grant NGR-38-033-012, 87 p.

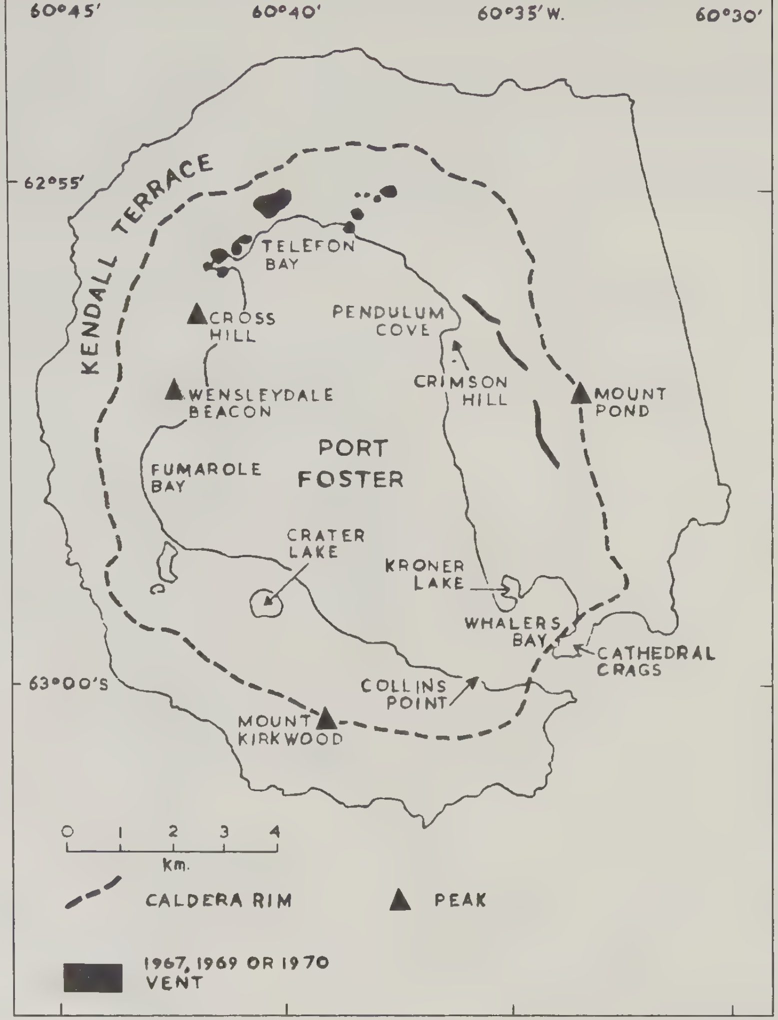

Figure 19.2.1. Location map of Deception Island, showing coastline after the 1970 eruption, from Roobol (1979).

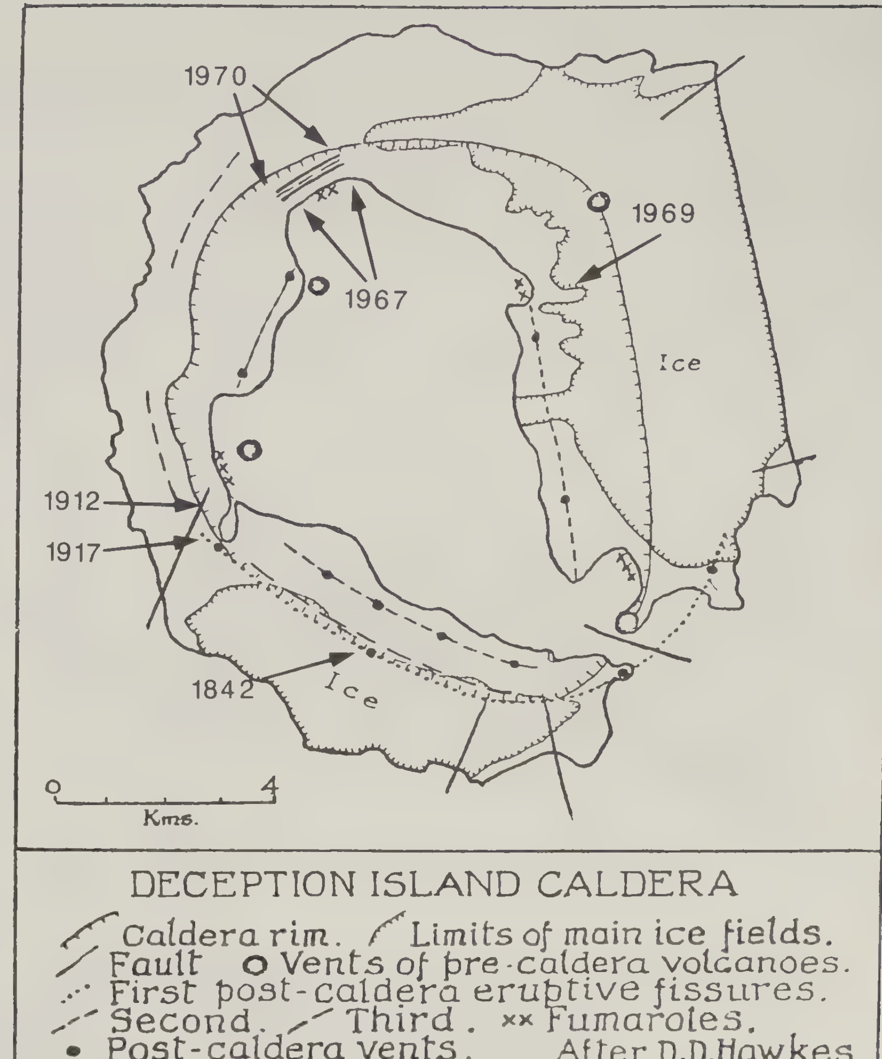

Figure 19.2.2. Sketch map of Deception Island Caldera, from Williams and McBirney (1968), with dates of historical eruptions from Gonzales-Ferran and others (1971).

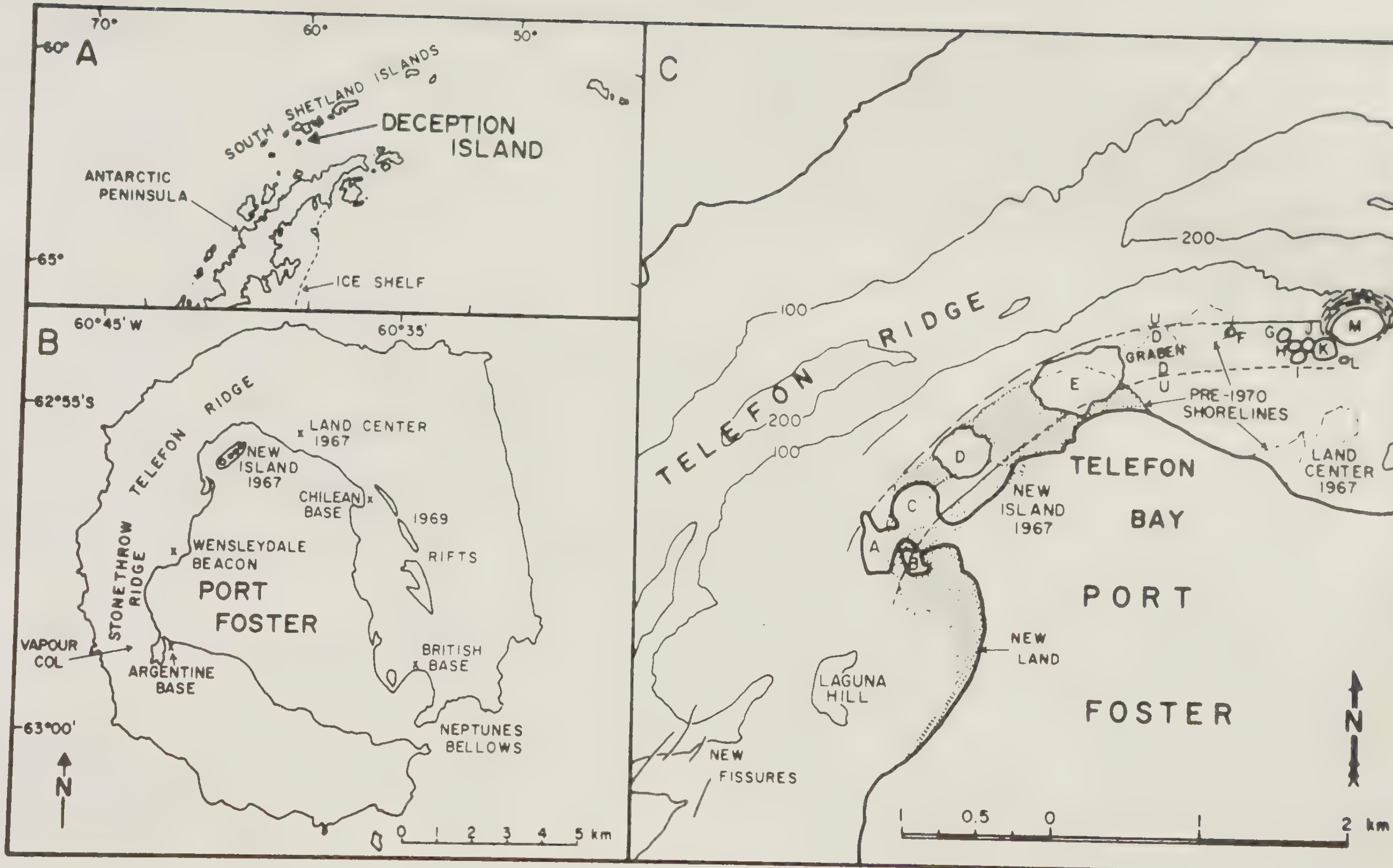

Figure 19.2.3. Deception Island showing recent eruption sites, from Schultz (1972). A-M are craters.

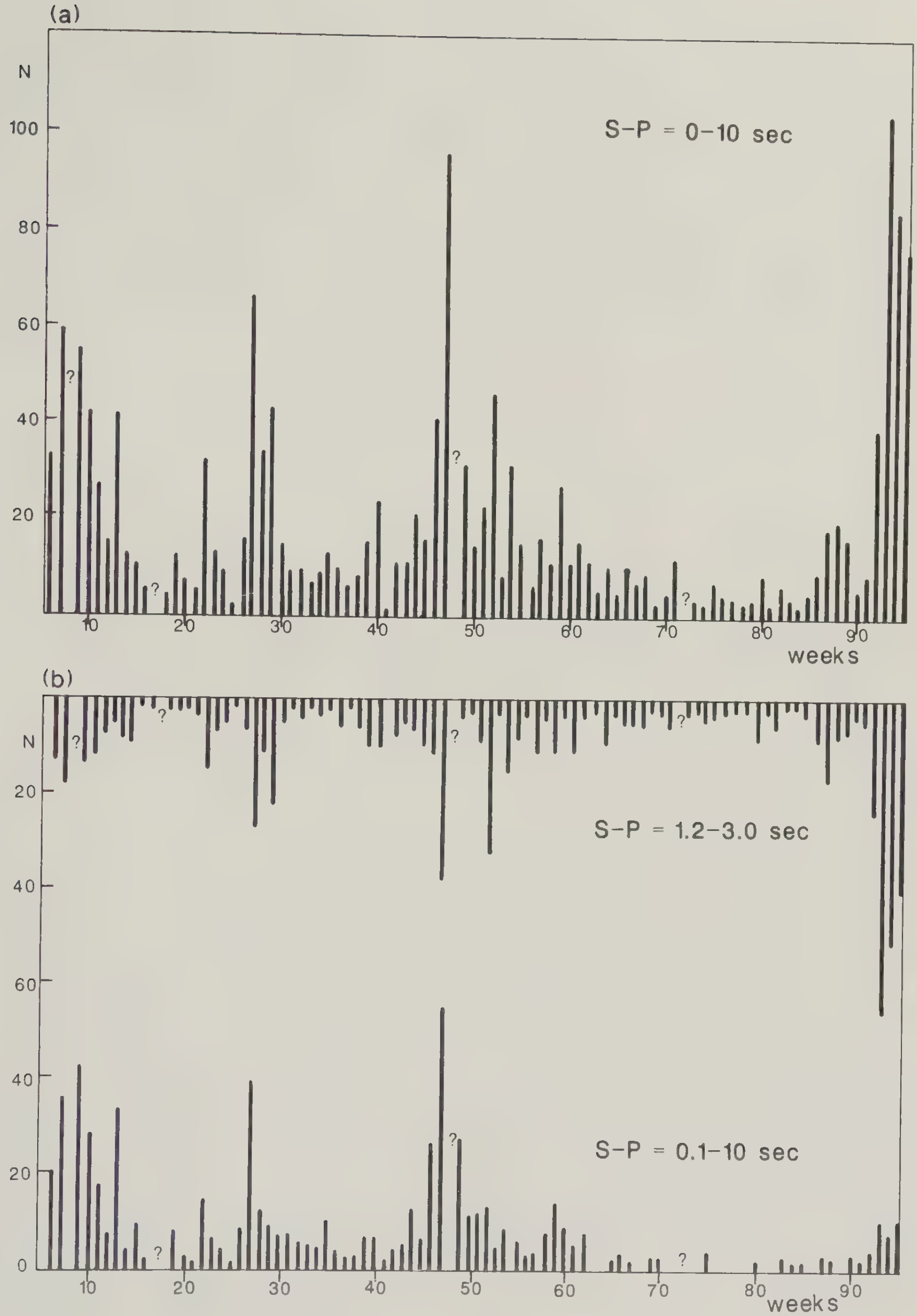

Figure 19.2.4. Seismic precursors to the 1967 eruption of Deception Island, from Lorca (1976). Number of events per week from 16 January 1966 to 30 November 1967 in each of three categories is shown: (a) events with S - P up to 10 s; (b) events with S - P of 0.1-1.0 s (bottom) and 1.2-3.0 s (top). Horizontal axes show number of weeks since the start of recording on 16 January 1966.

PART 4: Historical Unrest in Selected Noncaldera Settings

In Part 4 we demonstrate that unrest resembling that at calderas also occurs in noncaldera (and even nonvolcanic) settings. Several of these episodes have generated lively debate about the processes of unrest. We are persuaded by arguments that unrest at the first four of these locales (Chijiwa, Izu Peninsula, Kii Peninsula, and Matsushiro, all in Japan) has been fundamentally tectonic in origin, but we acknowledge and cite arguments for some involvement of magma in this unrest. Unrest at Socorro, New Mexico, is generally believed to be related to a large, deep magma reservoir in a tectonically active rift, and unrest at Montserrat is included as an example of unrest caused by episodic magma intrusion into a noncaldera volcano.

CHIJIWA

Latitude Longitude (degrees)	Tectonic setting	Age of latest volcanism	Youngest volcanic rock types	Restless years	Type and duration of unrest ESTU STHF MGTF H Te	Associated eruption?
32.7N 130.1E	East-west graben	A.D. 1791-92 1835?	a, d	860	---- ---- ---- - --	Ex?
				1657	---- ---- ---- - --	lf, ex?
				1663-64	---- ---- ---- - --	ex
				1791-92	EE-- ---Y ---Y Y --	ex,lf,LANDSL
				1835?	---- ---- ---- - --	ex?
				1922	CC-- ---- ---- - --	none
				1929-40	FF-- ---- ---- - --	none
				1951-66	FF-- ---- ---- - --	none
				1968-74	FF-- G-G- --F- F --	none
				1977-82	EE-- ---- ---- - --	none
				1984	EE-- ---- ---- - --	none

TECTONIC SETTING

An 8-km-wide E-W graben joins Chijiwa Bay and the central part of Unzen Volcano; recent volcanism in the area has occurred mainly within this graben. A largely submarine caldera has been postulated at the western foot of Unzen Volcano, about 90 km west of Aso Caldera (Ota, 1984) (figs. 20.1.1, 20.1.2). However, no products of a caldera-forming eruption are known, and most workers refer to the graben but not to a caldera. Sugiyama and others (1986) infer that the graben formed between 170,000 and 70,000 yr B.P.

GEOLOGIC HISTORY

Unzen Volcano (CAVW number 08-02-10) consists of a central, active cone (Fugen-dake) and eroded remnants of several older cones including Mayu-yama, a biotite-hornblende andesite dome.

CHIJIWA (continued)

HISTORICAL ACTIVITY

1657: In 1657 an olivine-bearing biotite-hornblende andesite lava flow (the Hato-ana or Koyake flow, formerly called the Furu-yake flow) was extruded from the Fugen-dake central cone of Unzen Volcano (Ogawa and Homma, 1926; Sendo and others, 1967). In the following year, thermal water and a lahar caused approximately 30 fatalities.

1663-64: Small explosions occurred in March 1663 and January 1664, and perhaps for as many as 10 to 12 years thereafter (Ogawa and Homma, 1926).

1791-92: Earthquakes that were precursory to the 1792 eruption of Unzen began on 2 November 1791 and were felt most strongly around the western coast of the Shimabara Peninsula (in the vicinity of Obama and Chijiwa). Shocks were felt 3-4 times daily, and increased in intensity about 6 December. Even though earthquakes were most intense on the west side of the Shimabara Peninsula, landslides occurred on the southeast flank of Mayu-yama. Detonation sounds, described as sounding like the firing of artillery, were heard in late January. Small explosions at the Fugen-dake vent of Unzen began on 9 or 11 February 1792, accompanied by strong earthquakes. Then, on 25 February, the ground at Biwa-no-bachi (1 km from the top of Fugen-dake and 4 km from Shimabara) began to tremble and "shook off earth and rocks" (Ogawa and Homma, 1926). The unrest at Biwa-no-bachi quickly led to extrusion of the Shinyake lava from a nearby flank vent (29 February or 1 March 1792; hypersthene biotite-hornblende dacite, 4-km-long flow, volume=0.11 km^3). On 21 March, another vent opened near the top of Fugen-dake, followed on 24 March by opening of seven more vents about 200 m northwest of the first. All were connected underground with the crater on Anasako-dani, and for this reason the top of Hando-iwa developed a rift 1-5 m wide (Ogawa and Homma, 1926, p. 13).

All the while that lava was flowing from vents on Fugen-dake, earthquakes continued. The strongest shock yet occurred on 21 April, with roaring and echoing noises from Mayu-yama "like the sound of guns on a Dutch frigate" (Ogawa and Homma, 1926). At least 300 earthquakes occurred on 21-22 April; $\underline{M}_{max}$ for 1792 (exact date unspecified) was 6.4. "Shaken by the shocks, masses of rocks and debris fell down from Mayu-yama and set the trees below on fire through the heat of their friction. The shocks were very severe and frequent for three days, more than 300 being counted during the night and more than 100 in each of the next two days. They were most intense from midnight to the morning of the second day... however, the earthquakes subsided gradually after the third day, although another severe shock occurred on the 29th of April" (Ogawa and Homma, 1926, p. 14). These earthquakes of late April caused a landslide near the village of Nakakoba, destroyed 61 houses and structures and 288 stables, and damaged the stone walls of Shimabara castle. Crevices formed in several places between Shimabara and Antoku, including two trending NW-SE and about 1 km long that crossed the castle ground. These crevices were at first only a few centimeters wide, but they later widened with increasing intensity of the shocks to more than 30 cm. The ground on the south side of these sank, and "springs gushed forth on the east of the castle close to the shore, while on the west up the hill beyond the castle, the fountain-heads dried up for a time" (Ogawa and Homma, 1926, p. 14). A larger crack, at least 1 m wide, opened from Iwomi-dake on the southern slope of Azuma-dake to the northern flank of Fugen-dake. This and parallel cracks trended E-W along the old Chijiwa fault scarp, south of Azuma-dake.

CHIJIWA (continued)

HISTORICAL ACTIVITY (continued)

On 29 April, a block from near the east foot of Mayu-yama reportedly slid about 200 m eastward (Katayama, 1974). Toward the middle of May, lava extrusion from Fugen-dake and earthquakes diminished, and people returned to their houses in Shimabara. But at about 2000 hr on 21 May, severe shocks resumed, accompanied or followed shortly by eastward collapse of a large portion of Mayu-yama (volume, 0.34 km^3). The resulting debris avalanche swept through two small villages and into the sea, causing a devastating tsunami. More than 14,000 people died, most from the tsunami. Kuno (1962) reports some difference of opinion as to whether the avalanche resulted from an explosion or was triggered by earthquakes; most workers have concluded that there were no major explosions, and that earthquakes were the immediate trigger of the avalanche. Katayama (1974), adapting a hydrologic model of Ota (1973), suggested that an influx of hydrothermal water from Chijiwa into Mayu-yama made the edifice unstable (related discussion below).

Two more eruptions followed from Fugen-dake--explosions on 19 July and 15 August--with lesser activity continuing until at least April 1793.

1922: A major earthquake swarm in December 1922 (fig. 20.1.3) caused 27 deaths, most on 8 December 1922. The largest event of this swarm, estimated to be $\underline{M}$=6.0, was preceded by a smaller event on 3 October and by several on 7 December in the 9.5 hours before the largest event (Ogawa and Homma, 1926). At least 1798 microseisms and 110 macroseisms were recorded at Nagasaki up to 13 January 1923. Omori (1928) considered these earthquakes to be volcanic, whereas Imamura (1928a, b) and others considered them to be tectonic. All workers agreed that they were centered beneath Chijiwa Bay.

1968-74: Several earthquake swarms occurred from 1968 to 1974, especially during 1970 and 1973-74 (figs. 20.1.4-20.1.8). New fumaroles appeared at the end of 1974(?). The $\underline{b}$-values for various swarms of this period ranged from 0.6 to 1.3. Hypocenters were approximately 10 km deep beneath the postulated caldera and progressively shallower to the east, reaching depths of 0-2 km beneath Unzen Volcano. Ota (1973) concluded that epicenters migrated upward and eastward, from 8 km to less than 5 km (possibly less than 1 km), during a swarm in June 1970, over a period of 3 weeks and a horizontal distance of 10-15 km. The sequence was not perfect, however, because the last earthquakes in the swarm were about 10 km deep at the western end of the supposed eastward migration (figs. 20.1.6, 20.1.7). A relocation of those hypocenters and a study of their first motions (Yamashina and Mitsunami, 1977) suggests movement along an E-W-trending, south-dipping normal fault (fig. 20.1.8).

The temperature and composition of hot springs change eastward toward Unzen and Shimabara Hot Springs (on the eastern flank of Unzen). Ota (1973) correlated these changes with the inferred eastward shallowing of earthquake hypocenters and suggested that the earthquakes were caused at least in part by migration of hydrothermal fluids from the postulated caldera eastward and upward to Unzen and Shimabara Hot Springs. Observation of this migration suggested to Katayama (1974) and Ota (1974) that the large 1792 debris avalanche from Mayu-yama occurred after a similar migration of hydrothermal fluids destabilized the east flank of Unzen.

1977-82: Earthquake swarms occurred in November 1977, January and December 1978, June and September 1979, and August and November 1980 (figs. 20.1.9-20.1.12). One shock in 1980 was felt nearby with JMA intensity 4.

CHIJIWA, Latitude 32.7N, Longitude 130.1E

CHIJIWA (continued)

HISTORICAL ACTIVITY (continued)

1984: Seismicity started increasing in May 1984 and climaxed in August with a swarm of 6,307 events, 409 of which were felt ($\underline{M}_{max}$=5.7, depth ca. 7 km, deepening from east to west; figs. 20.1.13-20.1.16) (Smithsonian Institution, 1984).

The east coast of the Shimabara Peninsula subsided 10-15 cm between leveling surveys in 1894 and 1958 (fig. 20.1.17). The net(?) horizontal strain across the Chijiwa area between 1890 and 1958 was approximately 10^{-5} (N-S extension--consistent with historical seismicity and mapped faults; fig. 20.1.18) (Yamashina and Mitsunami, 1977).

COMMENTS

Historical unrest at Chijiwa is a manifestation of active graben development superimposed on related volcanic activity at Unzen. The collapse of Mayu-yama in 1792 is probably an example of a large and devastating debris avalanche caused by graben faulting in conjunction with an eruption at a nearby vent.

REFERENCES

Homma, F., 1936, Unzen-dake: Bull. Volcanol. Soc. Japan, v. 3, p. 71-124.
Imamura, A., 1928a, Report on the changes in the land-level in connection with the Simabara earthquake of 1922: Bull. Imperial Earthq. Invest. Comm., v. 10, no. 2, p. 63-64.
----- 1928b, Seismographic study of the Simabara earthquake: Bull. Imperial Earthq. Invest. Comm., v. 10, no. 2, p. 66-70.
Katayama, N., 1974, Old records of natural phenomena concerning the "Shimabara catastrophe": Sci. Rep. Shimabara Volcano Obs., Kyushu Univ., no. 9, p. 1-45.
Komada, I., 1916, Report on geology of Onsendake (Unzen) Volcano: Rep. Imperial Earthq. Invest. Comm., v. 84, p. 1-102.
----- 1924, Geological considerations of the Shimabara earthquakes of December 8, 1922: Japanese Jour. Geol. Geogr., v. 3, p. 91-100.
Kubotera, A., 1975, Relation among earthquake swarm, gravity anomalies, and geothermal activities at Shimabara Peninsula: Jour. Japan Geotherm. Assoc., v. 12, no. 2, p. 9-13.
Kubotera, A., and Kikuchi, S., 1967, Seismic observation in Shimabara Peninsula--on the activity of Volcano Unzen: Spec. Contrib., Geophys. Inst., Kyoto Univ., no. 7, p. 161-168.
Kuno, H., 1962, Catalogue of active volcanoes of the world including solfatara fields, Pt. XI, Japan, Taiwan, and Marianas: Rome, IAVCEI, 332 p.
Matsuwo, N., 1979, Seismicity in and near the Shimabara Peninsula, April 1977-June 1978: Sci. Rep. Shimabara Volcano Obs., Kyushu Univ., no. 12, p. 17-28.
Mogi, K., 1963, Some discussion on aftershocks, foreshocks and earthquake swarms--the fracture of a semi-infinite body caused by an inner stress origin and its relation to the earthquake phenomena (Third paper): Bull. Earthq. Res. Inst., v. 41, p. 615-658.

CHIJIWA (continued)

REFERENCES (continued)

Ogawa, T., and Homma, F., 1926, Unzen Volcano: Guidebook for Excursion E-1,3,4, 3rd Pan-Pacific Sci. Congr., Tokyo, p. 1-30.

Omori, F., 1907, Note on the eruptions of the Unsen-dake in the 4th year of Kansei (1792): Bull. Tokyo Imperial Earthq. Invest. Comm., v. 1, p. 142-144.

----- 1928, On the Shimabara Earthquake of Dec. 8, 1922: Bull. Imperial Earthq. Invest. Comm., v. 10, no. 2, p. 43-62.

Ota, K., 1969, Study on the collapses in the Mayu-yama: 1. On the mechanism of collapse: Sci. Rep. Shimabara Volcano Obs., Kyushu Univ., p. 6-35.

----- 1970, On the ground water in the northern coast area of the Shimabara Peninsula: Sci. Rep. Shimabara Volcano Obs., Kyushu Univ., p. 14 ff.

----- 1971, Ground water in Chijiwa town and its adjacent area, the Shimabara Peninsula: Sci. Rep. Shimabara Volcano Obs., Kyushu Univ., p. 19 ff.

----- 1973, A study of hot springs on the Shimabara Peninsula: Sci. Rep. Shimabara Volcano Obs., Kyushu Univ., no. 8., p. 1-33.

----- 1974, Observation of volcanic hot-spring waters in the Unzen Volcano (I)-- An attempt for the prediction of volcanic eruption by monitoring the water qualities of volcanic hot-springs and the observation well of the Shimabara Volcano Observatory: Sci. Rep. Shimabara Volcano Obs., Kyushu Univ., no. 10, p. 21-33.

----- 1984, Unzen Volcano, geomorphology, geology and volcanic phenomena: Nagasaki Prefecture, 98 p.

Sawada, Yosihiro, 1978, Seismic activity at Unzen-dake Volcano and the unusual number of its occurrence frequency: Pap. Meteorol. Geophys., v. 29, no. 2, p. 83-96.

Sendo, T., Matsumoto, H., and Imamura, R., 1967, Geology and petrography of Unzen Volcano: Kumamoto Jour. Sci., ser. B, sec. 1, v. 7, p. 31-89.

Shimabara Earthquake and Volcano Observatory, Kyushu University, 1985, On the earthquakes (that) occurred on 6 August 1984 at Unzen Volcano, Shimabara Peninsula: Rep. Coord. Comm. for Prediction of Volcanic Eruptions, no. 32, p. 37-41.

Shimabara Volcano Observatory, Kyushu University, 1983, Seismic activity of Unzen Volcano in 1981 and 1982: Rep. Coord. Comm. for Prediction of Volcanic Eruptions, no. 28, p. 42-43.

Siebert, L., Glicken, H., and Ui, T., 1987, Volcanic hazards from Bezymianny- and Bandai-type eruptions: Bull. Volcanol., v. 49, p. 435-459.

Smithsonian Institution, Scientific Event Alert Network (SEAN), 1984, Unzen Volcano: SEAN Bull., v. 9, no. 9, p. 6-7.

Sugiyama, H., Hayashi, M., and Fujino, T., 1986, Fission track ages of the Unzen volcanic rocks in Western Kyushu, Japan: Bull. Volcanol. Soc. Japan, v. 31, no. 2, p. 85-94.

Volcanological Society of Japan, 1982, Unzen: Bull. Volcanic Eruptions, no. 20, p. 95.

Yamashina, K., and Mitsunami, T., 1977, Stress field in the Unzen volcanic area, Kyushu, Japan; Bull. Volcanol. Soc. Japan, v. 22, p. 13-25.

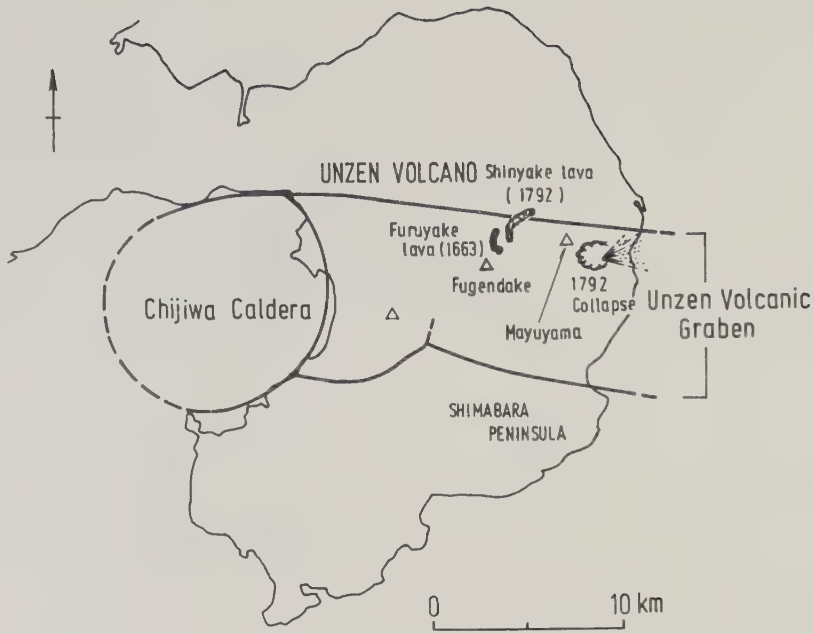

Figure 20.1.1. Locations of postulated Chijiwa Caldera and Unzen Volcano, courtesy of an anonymous reviewer. Most authors refer to Chijiwa graben but not to Chijiwa Caldera.

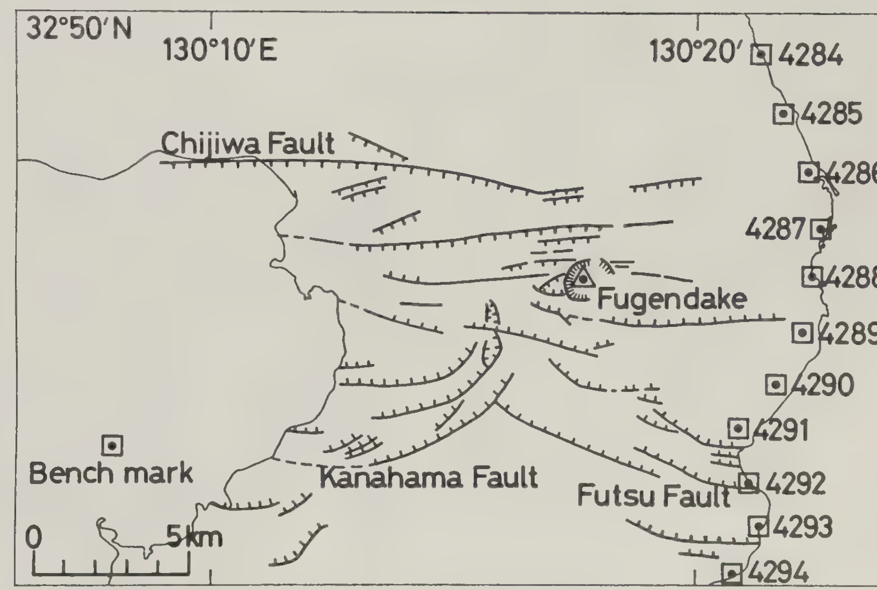

Figure 20.1.2. Active faults in Chijiwa area, from Yamashina and Mitsunami (1977). Numbers at right indicate bench marks (see figure 20.1.17).

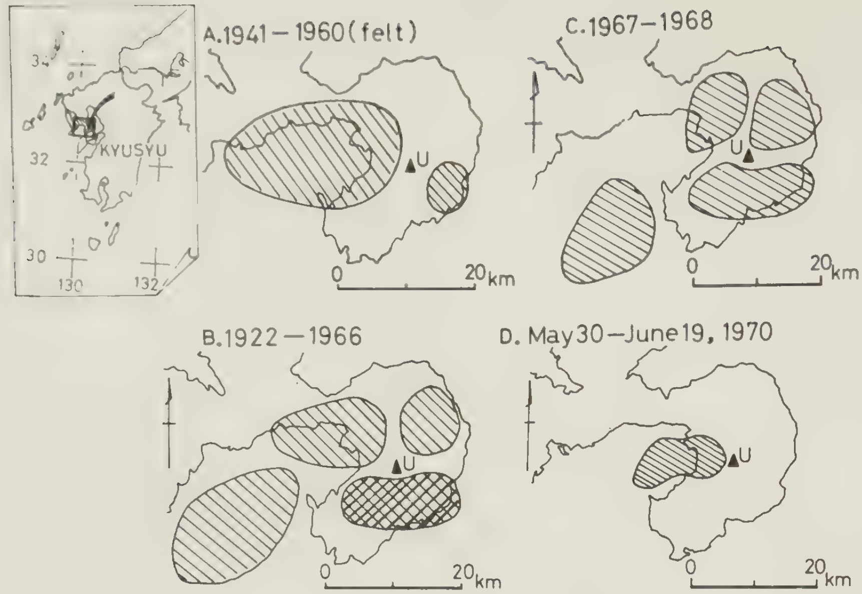

Figure 20.1.3. Epicentral areas near Unzen Volcano, from Sawada (1978). A, Felt earthquakes from 1941 through 1960. B, 1922 through 1966. C, 1967 through 1968. D, May-June 1970. U, Unzen Volcano. Cross hatching in B represents epicentral area of 1922 swarm, according to Omori (1928); Imamura (1928a,b) concluded that largest quakes of the 1922 swarm were centered northwest of area shown by Omori (1928), near head of Chijiwa Bay.

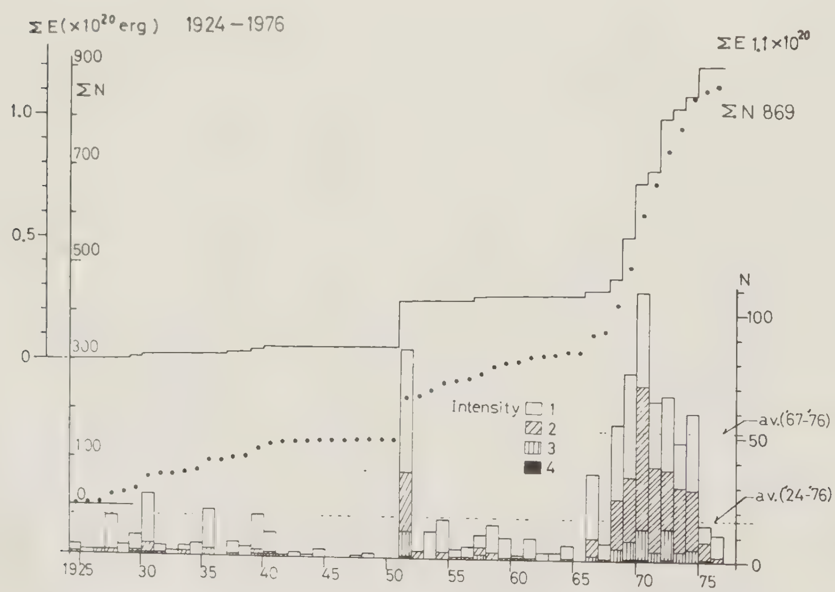

Figure 20.1.4. Seismicity in Chijiwa-Unzen area during 1924-76, from Sawada (1978). Bars, yearly number of felt earthquakes of indicated seismic intensities; dotted line, cumulative number of earthquakes; solid line, cumulative seismic energy release.

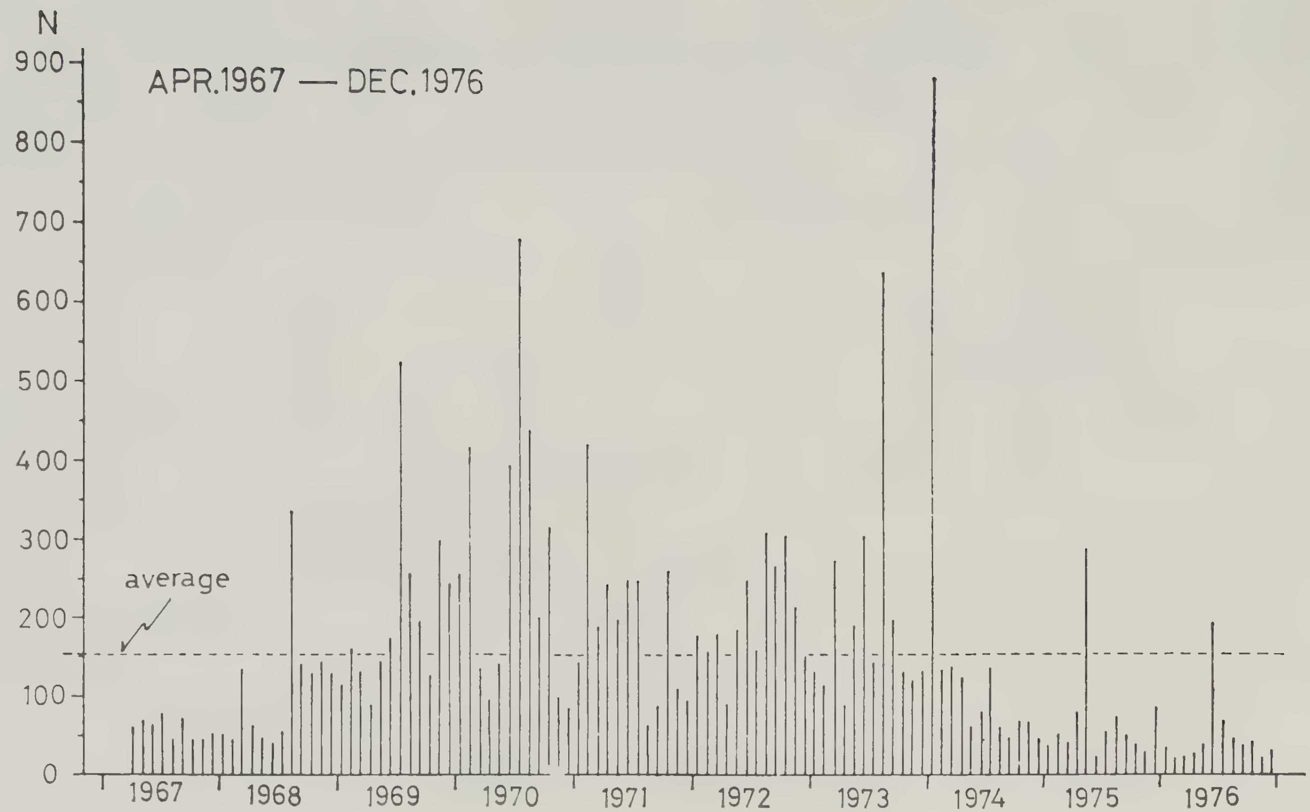

Figure 20.1.5. Monthly number of earthquakes near Unzen Volcano from April 1967 through December 1976, from Sawada (1978).

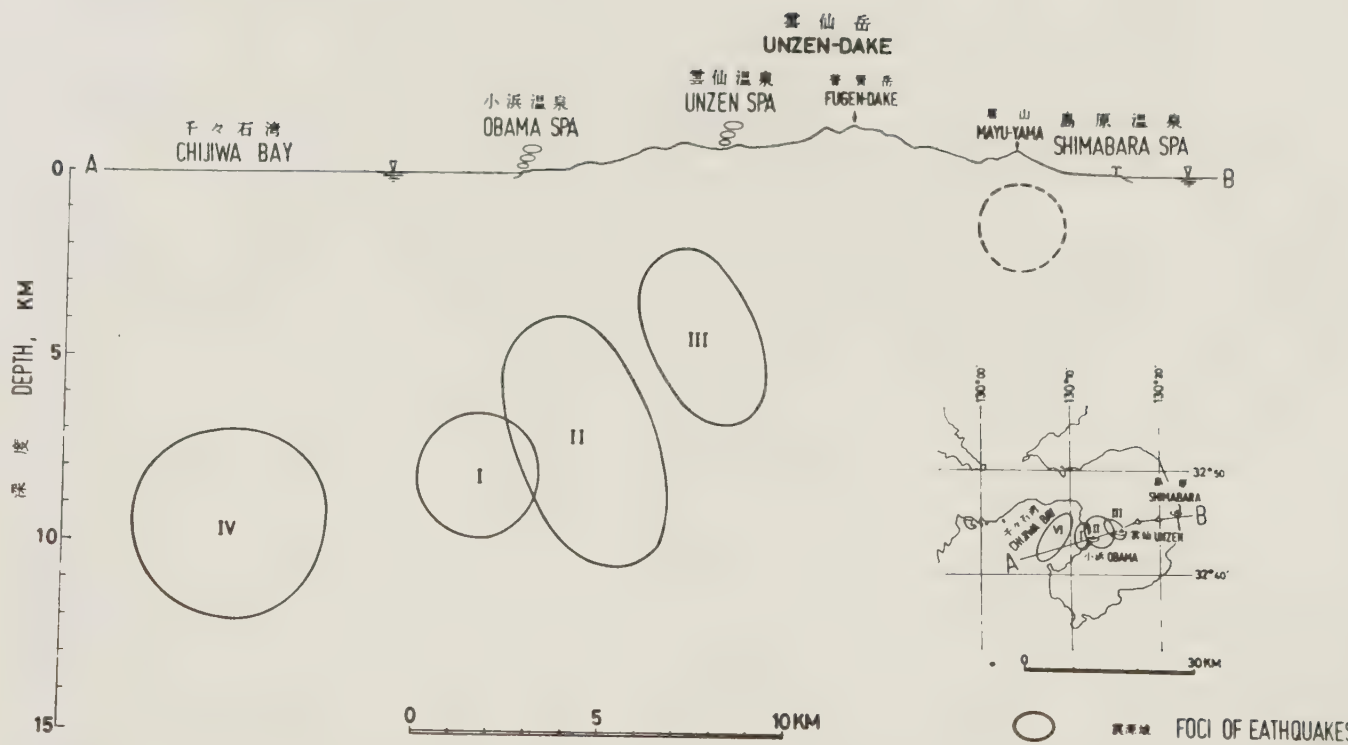

Figure 20.1.6. Distribution of hypocenters during an earthquake swarm in Chijiwa region during June 1970, from Ota (1973). Hypocenters initially migrated upward and eastward (from beneath Chijiwa Caldera toward Unzen Volcano), but last hypocenters were again beneath Chijiwa. Note revised locations shown in figure 20.1.8.

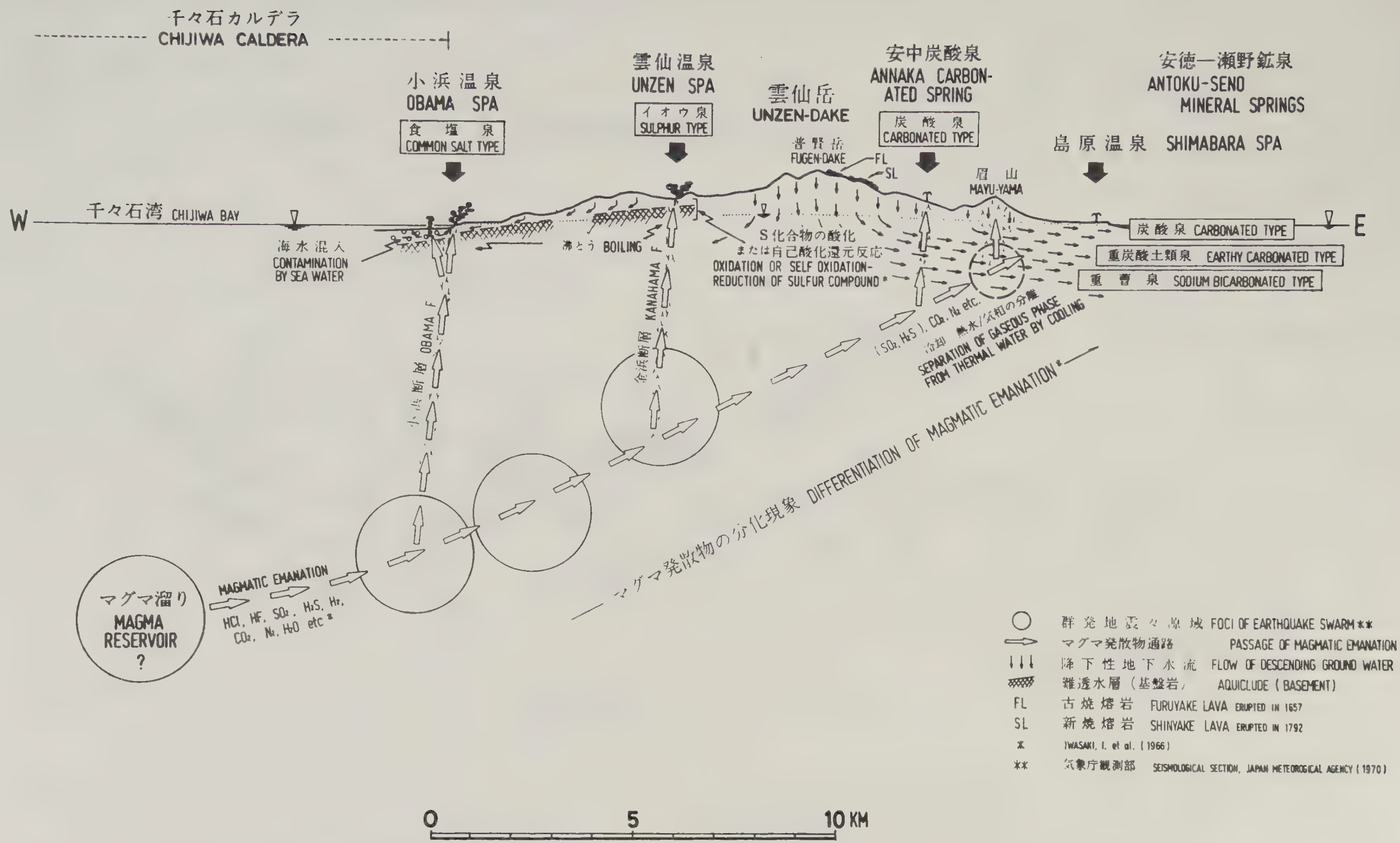

Figure 20.1.7. Schematic diagram showing a mechanism for earthquake migration resulting from fluid migration, from Ota (1973).

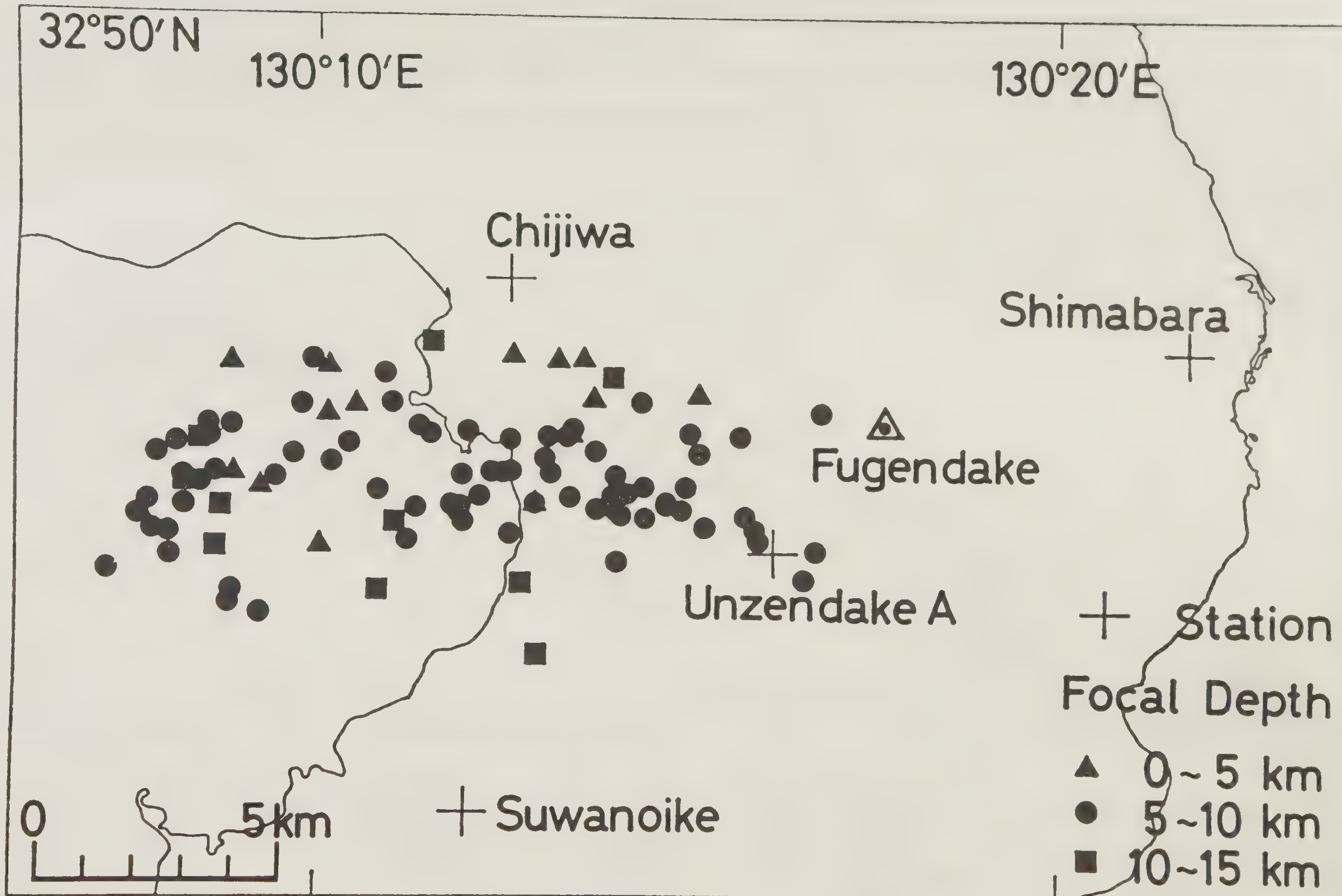

Figure 20.1.8. Relocated epicenters for same earthquakes as shown in figure 20.1.6, from Yamashina and Mitsunami (1977). No systematic migration pattern is obvious here.

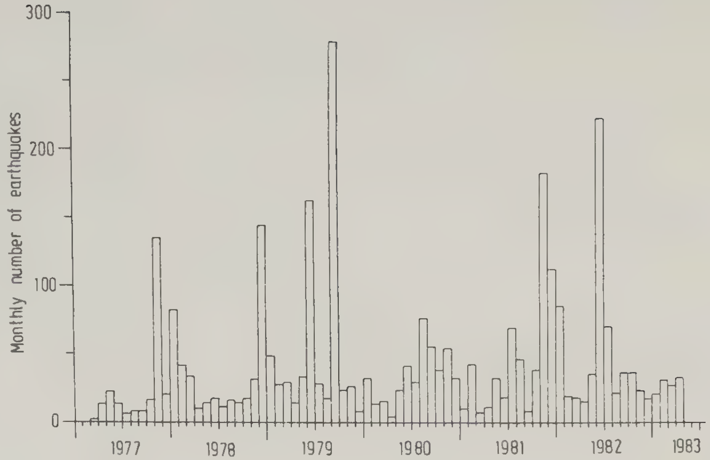

Figure 20.1.9. Monthly number of earthquakes at Unzen Volcano from March 1977 to April 1983, from Shimabara Earthquake and Volcano Observatory (1985).

Figure 20.1.10. Epicentral zones for earthquakes in Chijiwa area from April 1977 to June 1978, from Matsuwo (1979).

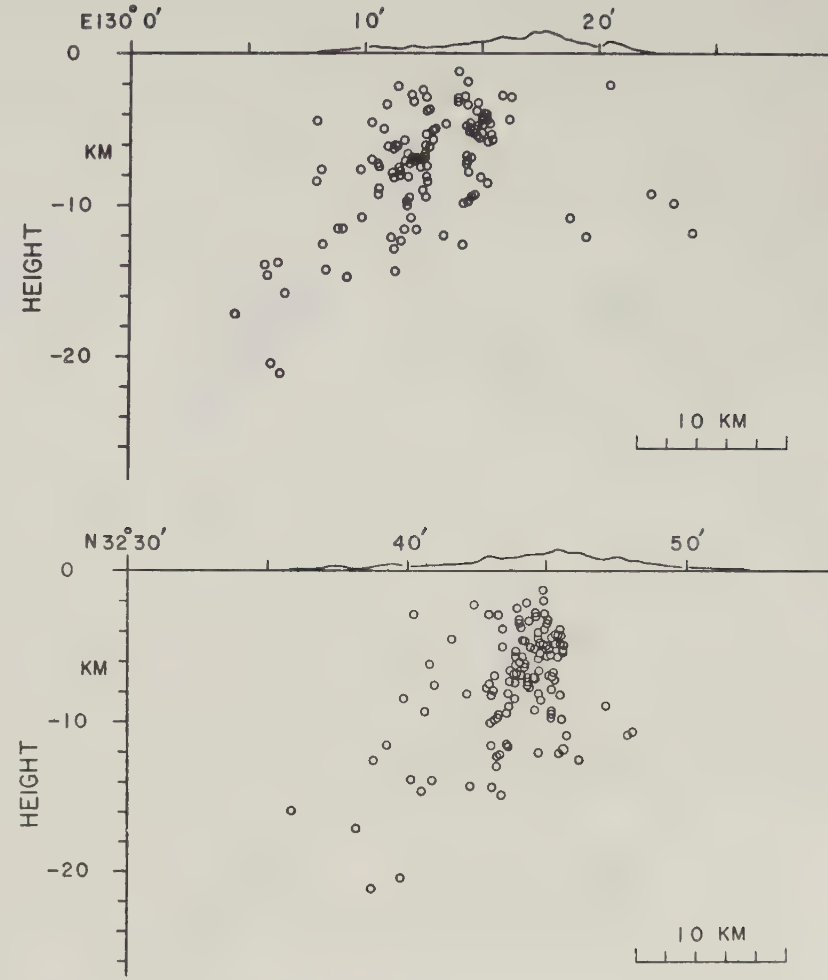

Figure 20.1.11. North-south (top) and east-west (bottom) vertical cross sections showing hypocenters of earthquakes in Chijiwa area from April 1977 to June 1978, from Matsuwo (1979).

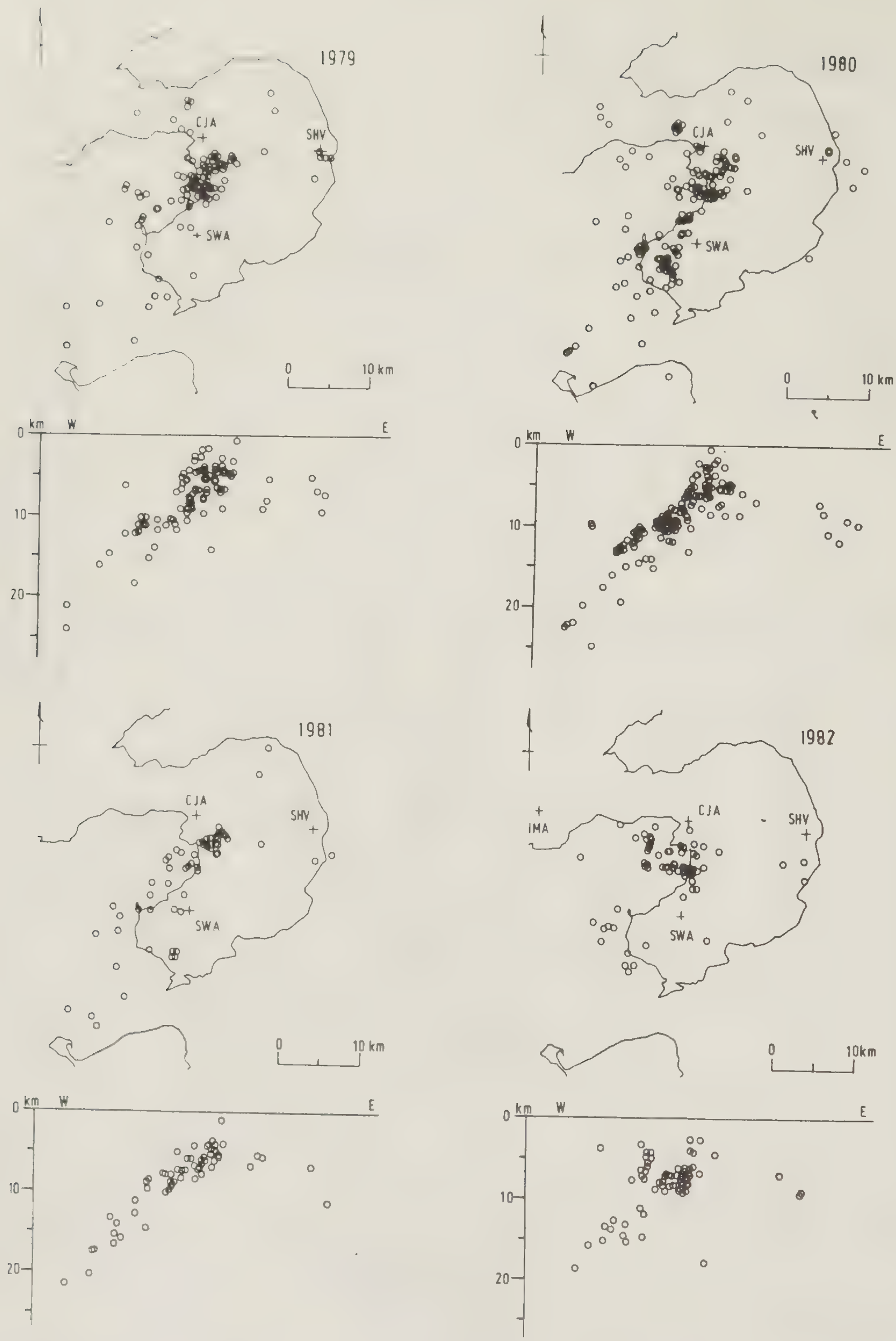

Figure 20.1.12. Epicentral distributions and vertical sections showing earthquakes in Chijiwa area from 1979 to 1982, from Ota (1984).

Figure 20.1.13. Epicenters of a series of foreshocks from 29 April to 11 July 1984 that preceded a swarm at Unzen Volcano in August 1984 (Shimabara Earthquake and Volcano Observatory, 1985). +, seismometer station; SHV, Shimbara; CJA, Chijiwa; SWA, Obama; IMA, Iimori.

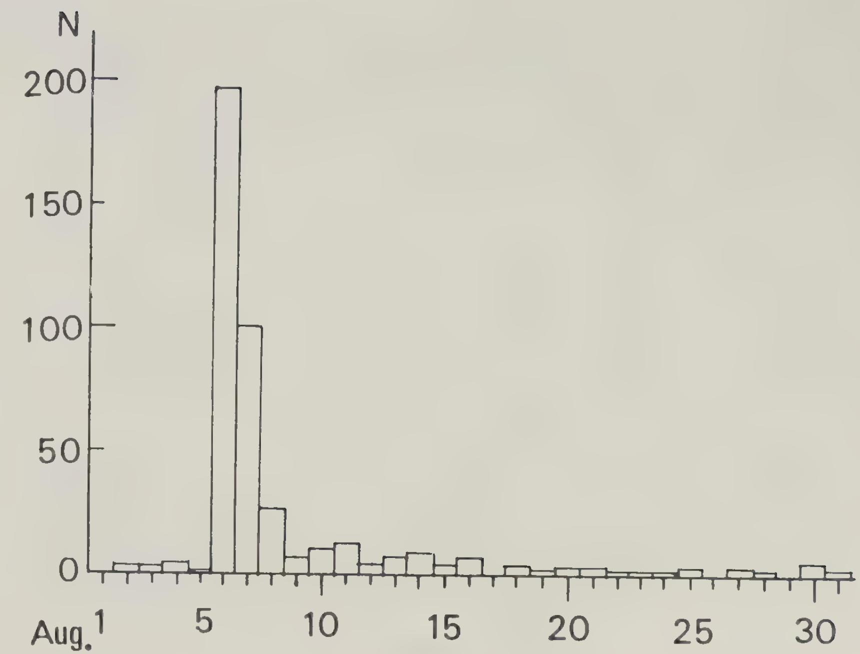

Figure 20.1.14. Daily number of felt earthquakes during a swarm at Unzen Volcano in August 1984, from Smithsonian Institution (1984).

Figure 20.1.15. Epicenters and vertical section showing earthquakes at Unzen Volcano in August 1984, from Smithsonian Institution (1984).

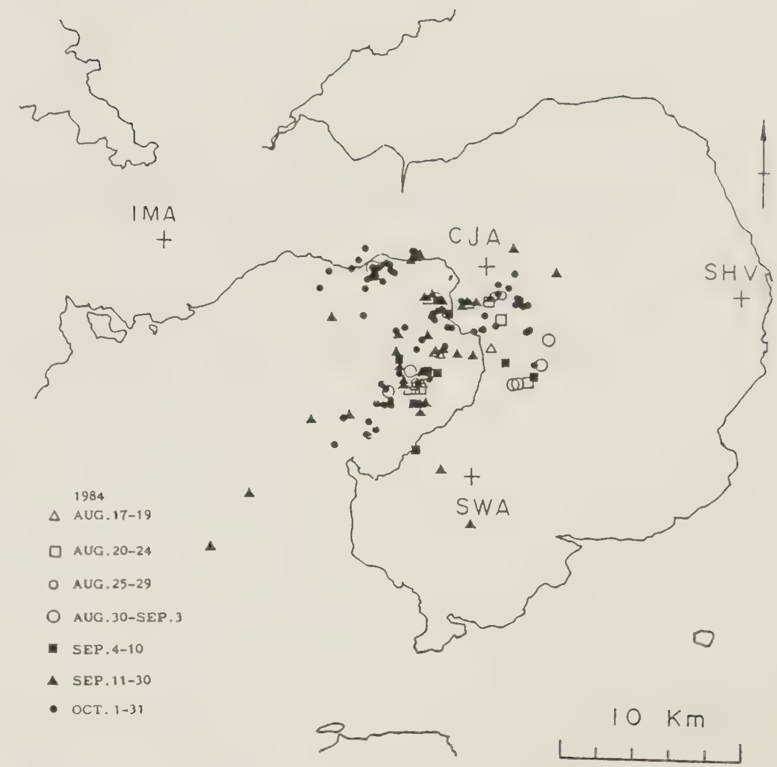

Figure 20.1.16. Epicenters of aftershocks near Unzen Volcano from 17 August 1984 to 31 October 1984, from Shimabara Earthquake and Volcano Observatory (1985).

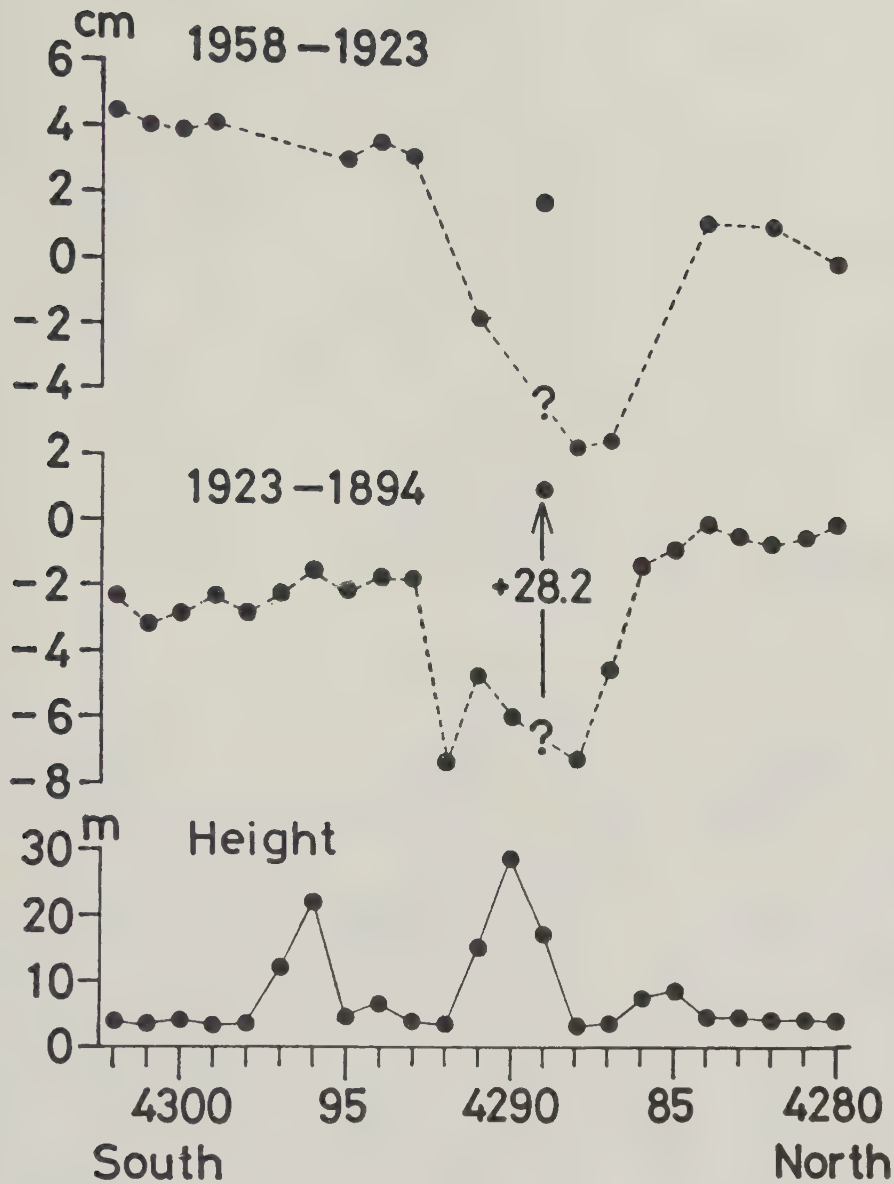

Figure 20.1.17. Leveling data showing subsidence in E-W-trending graben that crosses Shimabara Peninsula, from Yamashina and Mitsunami (1977). Bench-mark locations are shown in figure 20.1.2.

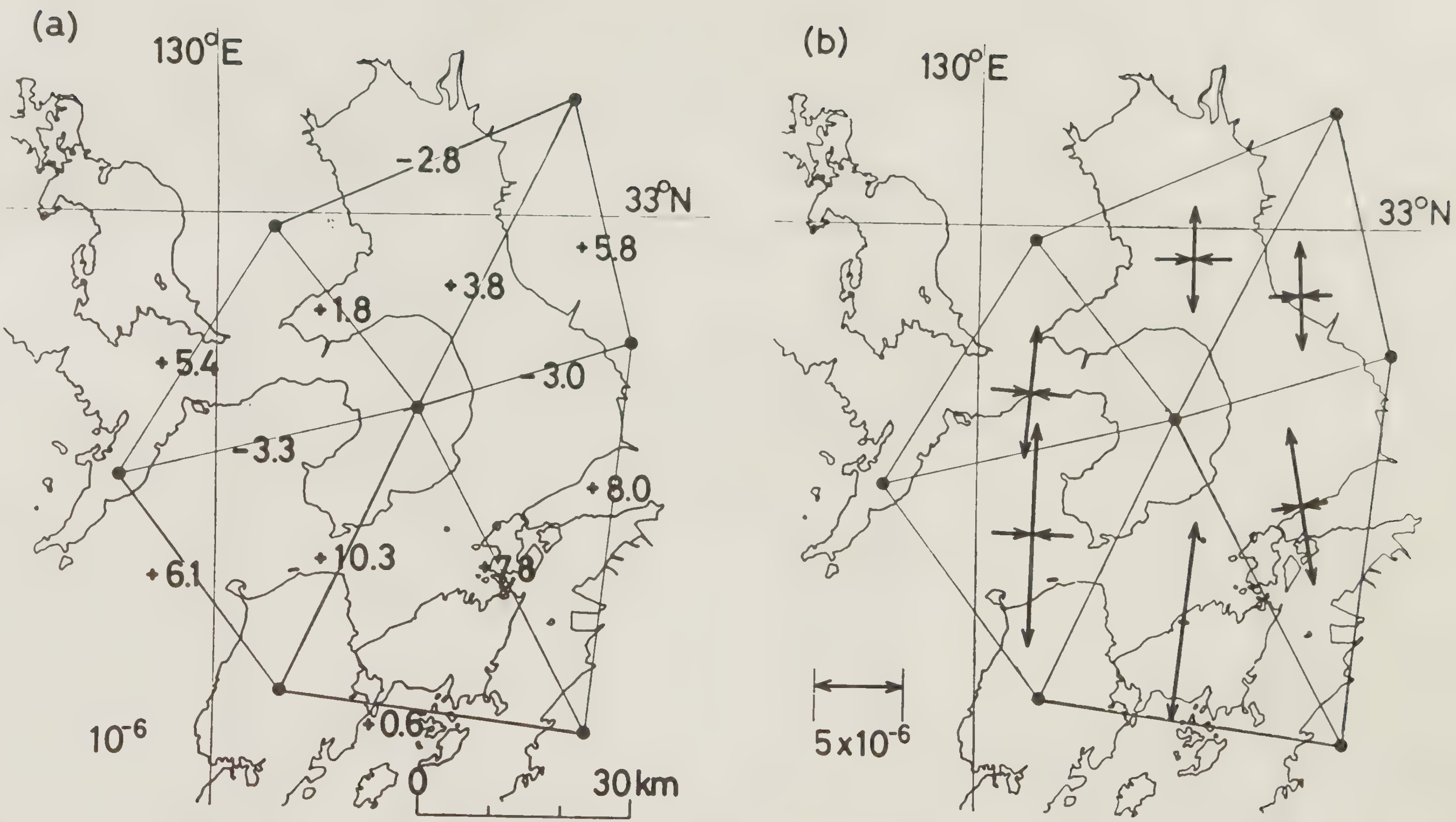

Figure 20.1.18. Horizontal strain (left, in units of 10^{-6}) and principal axes of horizontal strain (right) in Shimabara Peninsula from 1890 to 1958, from Yamashina and Mitsunami (1977). Positive values, extension; negative values, contraction. North-south extension shown here and subsidence in graben (from figure 20.1.17) suggest that dominant cause of repeated earthquake swarms in area is rifting (that is, graben formation).

IZU PENINSULA

Latitude Longitude (degrees)	Tectonic setting	Age of latest volcanism	Youngest volcanic rock types	Restless years	Type and duration of unrest ESTU STHF MGTF H Te	Associated eruption?
34-35N 139E	Compr	Late Pleistocene	b, a, d	1905	xx-- ---- ---- - =?	none
				1930	EE-G ---x ---- - =?	none
				1967-80+	FF-G --Gx x--- F =?	none

TECTONIC/GEOLOGIC SETTING

The Izu Peninsula lies at the northern tip of the Philippine Sea plate, where that plate is overriding the Pacific plate and being subducted beneath the Eurasian plate (Fujita and Tada, 1983) (see also section on Izu-Oshima Caldera, CAVW number 08-04-01). The Izu Peninsula has numerous volcanic vents, ranging from a small vent on the southern tip of the peninsula (Nanzaki) and Amagi Volcano in the south-central part of the peninsula to Hakone at its northern end (figs. 20.2.1, 20.2.2). Many small vents of the Higashi-Izu monogenetic volcano group, including 63 basaltic cinder cones, 4 dacite domes, and 9 phreatic craters (maars), lie in the general vicinity of a series of historical earthquake swarms (discussed below). Dacitic domes have grown as recently as 3,000 years ago, but most basaltic eruptions in the area occurred before about 40,000 years ago (Oki and others, 1978).

HISTORICAL ACTIVITY

Seismicity:

In 1905, an earthquake with estimated $\underline{M}$=6.5 occurred slightly north of the 1978 epicenter (see below). It was preceded by swarm activity.

The great Kanto earthquake of 1923 occurred about 40 km northeast of the center of unrest on the Izu Peninsula (fig. 20.2.5).

Swarms occurred again in February-April 1930 and continued at a lower level until August 1930. From February to August 1930, 4,880 earthquakes were felt. New, intense swarms began on 7 November 1930, reached 690 earthquakes/day on 25 November, and culminated in the $\underline{M}$=7.0 Kita-Izu earthquake on 26 November 1930, centered near the November swarm but 30-40 km from swarms of February-May 1930 (figs. 20.2.3, 20.2.5). The Kita-Izu earthquake had left-lateral slip on the N-S-trending Tanna Fault, indicating NW-SE compression. Earthquakes migrated upward immediately before the strong earthquake, from an average of about 6 km to an average of between 4 and 5 km. Most aftershocks were less than 5 km deep. Nasu (1935) interpreted this upward migration to indicate

IZU PENINSULA (continued)

HISTORICAL ACTIVITY (continued)

Seismicity (continued):

magmatic intrusion into a zone approximately 5 km deep, 2 hours before the strong earthquake. The final earthquake of this sequence was the M=5.5 Minami-Izu earthquake in March 1934, followed by 40 years of relative seismic quiet.

The Izu-Hanto-Oki earthquake of 1974 (M=6.9) at the southern tip of the Izu Peninsula involved right-lateral motion along a NW-SE-trending fault (figs. 20.2.3-20.2.5). Seismicity after the 1974 Izu-Hanto-Oki earthquake was high, with numerous swarms and a few shocks up to M=5, including the Amagi earthquake (M=4.9; 9 July 1974) and the Kawazu earthquake (M=5.4; 17 August 1976). The locus of swarms has shifted over a broad area, about 30-40 km in an E-W direction by about 20 km in a N-S direction, between Mt. Amagi on the west and Oshima Volcano on the east. All are generally 10-30 km south of the area of the 1930 swarms, and 5-15 km south of the center of the 1967-76 uplift (see below and figs. 20.2.3-20.2.7, 20.2.12).

A M=7.0 earthquake on 14 January 1978 was located between the Izu Peninsula and Oshima Island (figs. 20.2.3, 20.2.5, 20.2.8). The earthquake relieved strain on the east coast but not in the northern part of the area.

Another earthquake on 28 June 1980 (M=6.7, depth 16 km), was located near the east coast of the Izu Peninsula, between the 1978 epicenter and those of the 1975-76 swarms (fig. 20.2.7), and 10-20 km southeast of the center of recent uplift (figs. 20.2.3, 20.2.5, 20.2.6).

Fault-plane solutions for six earthquakes in this region (1930, 1934, 1974(2), 1976, and 1980) all show nearly vertical strike-slip faulting. The solution for the 1930 earthquake and observations of surface rupture indicate NW-SE compression; solutions for the subsequent earthquakes show N-S compression and movement along conjugate NW-SE- and NE-SW-trending faults (Abe, 1978).

Ground Deformation:

Releveling in April 1930 of a line previously leveled in 1923-24 showed a bulge of approximately 3 cm, with its center 2-4 km north of Ito-cho (Tsuboi, 1931a, 1933). Releveling in November-December 1930 showed that the bulge had grown to 10 cm just before and to 22 cm just after the 26 November earthquake, and that the growth from March 1930 until November 1930 was at a rate of 19 cm/yr (Tsuboi, 1931b). The maximum uplift was closer to the February-May swarms rather than to the November "main shock." Uplift continued after the November 1930 earthquake, and by 1933 the maximum uplift measured was 35 cm (Tsuboi, 1933; figs. 20.2.9-20.2.11).

From 1967 to 1980, maximum uplift was about 20 cm centered about 10 km west-southwest of Ito, in about the same place as the 1930 uplift (fig. 20.2.12). The half-width of the uplift was about 15 km, and its maximum extent was about 40 km. About 1 cm of subsidence occurred from 1967 to 1974, followed by 1 cm of uplift from 1974 to 1976, about 7 cm of additional uplift in the months before the 1978 earthquake, and about 8 cm of additional uplift before the 1980 earthquake (data reproduced in Thatcher and Savage,

IZU PENINSULA (continued)

HISTORICAL ACTIVITY (continued)

Ground deformation (continued):

1982). Viewed in a different way, about 8 cm of uplift followed the 1974 earthquake, and another 8 cm of uplift followed the 1978 earthquake. One interpretation of the uplift invokes inflation of a magma body 4 km in diameter at 10-km depth (Hagiwara, 1978) or, alternatively, by a volume increase of 0.15 km^3 in a magma body at 11-km depth (Thatcher and Savage, 1982).

In general, ground deformation on the Izu Peninsula is characterized by periods of subsidence lasting several decades alternating with intermittent uplift lasting about one decade. Strain energy in the northeast part of the Izu Peninsula has been released mainly in intermittent aseismic crustal uplift (Fujita and Tada, 1983). The gravitational potential associated with the uplift from 1974 to 1981 is equivalent to a $\underline{M}$=7.5 earthquake, slightly larger than the actual seismic energy release (equivalent to a $\underline{M}$=7.2 earthquake). Tada and Asano (1983) note that, as at Matsushiro, seismicity and uplift are centered where a "granitic layer" with a relatively high P-wave velocity ($\underline{V}_p$=5.7 km/sec) lies at anomalously shallow depth (about 1 km).

Fujii (1977a, b) inferred a systematic migration in the locus of uplift, from east-northeast to west-southwest across the head of Sagami Bay, from 1923 to 1930 and from 1971 to 1974. By 1976, the locus of uplift had shifted back slightly to the north, between the loci of 1972 and 1974. Fujii interprets this migration as evidence for creep dislocation at depth, along a postulated "East-off-Izu subduction zone." The activity from 1923 to 1930 followed major right-lateral slip during the 1923 Kanto earthquake.

Hydrologic Changes:

Water-well levels rose in quadrants of contraction (compression) after the Izu-Hanto-Oki earthquake of 9 May 1974 and fell in quadrants of dilatation, thereby serving as a useful indicator of tectonic strain (Wakita, 1975). The water level in a well in Omaezaki, Shizuoka (95 km west-southwest of Ito) dropped by approximately 20 cm beginning on 28 December 1977, then returned to normal by 14 January 1978, at which time a large earthquake occurred just east of Ito (Wakita, 1982). The water temperature of one well and the Cl-content of water in another well, both near the center of uplift on the Izu Peninsula, decreased slightly several days before the same 1978 earthquake (Takahashi and Tsuneishi, 1978). A 0.2 °C decrease in the temperature of a thermal artesian well and a 1-2 cm increase in water levels in several wells were reported as much as 6 days before a $\underline{M}$=6.7 earthquake on 29 June 1980 (Oki and Hiraga, 1980).

IZU PENINSULA (continued)

COMMENTS

Five general explanations have been advanced for recent unrest on the Izu Peninsula (figs. 20.2.13-20.2.15):

(1) Dilatancy before earthquakes (general concept of Scholz and others, 1973; Kaidzu and Tada, 1980);

(2) Aseismic creep dislocation (slow, aseismic thrust faulting at depth along the "East-off-Izu Line" (Ishibashi, 1977; Fujii, 1977a, b);

(3) Inflation or upward intrusion of a body of magma (Nasu and others, 1931; Hagiwara, 1978; Thatcher and Savage, 1982);

(4) NW-SE compression of a plastic volume, such as magma (Somerville, 1978); and

(5) Bending of the northern tip of the Philippine plate between the Sagami Trough and the Suruga Trough, compensatory movement of material at depth toward the axis of bending, and uplift caused by the resulting mass excess at depth (Nakamura and others, 1984; K. Nakamura, written commun., 1984).

REFERENCES

Abe, K., 1978, Dislocations, source dimensions and stress associated with earthquakes in the Izu Peninsula, Japan: Jour. Phys. Earth, v. 26, p. 253-274.

Fujii, Y., 1977a, Creep dislocation model of crustal upheaval in Izu Peninsula: Rep. Coord. Comm. Earthq. Prediction, v. 17, p. 68-70.

----- 1977b, Creep dislocation propagation along the East-off-Izu Tectonic Line, Japan, around the year of 1930 and 1976: Zisin, v. 30, p. 389-400.

Fujita, N., and Tada, T., 1983, Anomalous crustal uplift in the northeastern part of the Izu Peninsula, Central Honshu, Japan: Tectonophysics, v. 97, p. 147-152.

Hagiwara, Y., 1978, Gravity changes associated with seismic activities, in Kisslinger, C., and Suzuki, K., eds., Earthquake precursors: Tokyo, Japan Scientific Societies Press, p. 137-146.

Hiraga, S., Ito, H., Odaka, S., and Hakamata, K., 1982, Seismometrical observations in Hakone Volcano, 1980: Bull. Hot Springs Res. Inst., Kanazawa Prefecture, v. 13, no. 5, p. 111-125.

Ishibashi, K., 1977, Creep dislocation model of the Izu Peninsula uplift--significance of the East-off-Izu Tectonic Line: Rep. Coord. Comm. Earthq. Prediction, v. 17, p. 65-67.

Kaidzu, M., and Tada, T., 1980, Recent crustal uplift in the northeastern part of the Izu Peninsula: The Earth Monthly, v. 2, p. 132-136.

IZU PENINSULA

REFERENCES (continued)

Kimura, M., 1976, Major magmatic activity as a key to predicting large earthquakes along the Sagami through, Japan: Nature, v. 260, p. 131-133.

----- 1978, Significant eruptive activities related to large interplate earthquakes in the northwestern Pacific margin, _in_ Uyeda, S., Murphy, R.W., and Kobayashi, K., eds., Geodynamics of the western Pacific: Jour. Phys. Earth, v. 26 supp., p. S557-S570.

Kimura, M., and Toyoda, J., 1975, Recent level change in the bottom-floor in the summit crater of Mihara-yama, Oshima Island, Japan: Bull. Volcanol. Soc. Japan, v. 20, p. 65-78.

Mogi, K., 1985, Earthquake prediction: Tokyo, Academic Press, 355 p.

Murai, I., and Kaneko, S., 1974, The Izu-Hanto-oki earthquake of 1974 and the earthquake faults, especially, the relationships between the earthquake faults, the active faults, and the fracture systems in the earthquake area: Spec. Bull. Earthq. Res. Inst., no. 14, p. 159-203.

Nakamura, K., 1971, Volcano as a possible indicator of crustal strain: Bull. Earthq. Res. Inst., v. 16, p. 63-71.

Nakamura, K., Shimazaki, K., and Yonekura, N., 1984, Subduction, bending and eduction. Present and Quaternary tectonics of the northern border of the Philippine Sea plate: Bull. Soc. Geol. France, v. 26, no. 2, p. 221-243.

Nakamura, K., and Tazawa, K., 1975, A physical interpretation for correlation between 1974 Izu-Hanto-oki earthquake and a minor eruption of Mihara-yama, Izu-Oshima: Bull. Volcanol. Soc. Japan, v. 19, p. 159-160.

Nasu, N., 1935, Recent seismic activities in the Izu Peninsula (Part II): Bull. Earthq. Res. Inst., v. 13, p. 400-416.

Nasu, N., Kishinouye, F. and Kodaira, T., 1931, Recent seismic activities in the Izu Peninsula, Part I: Bull. Earthq. Res. Inst., v. 9, p. 22-35.

Oki, Y., Aramaki, S., Nakamura, K., and Hakamata, K., 1978, Volcanoes of Hakone, Izu and Oshima: Hakone, Hakone Town Office, 88 p.

Oki, Y., and Hiraga, S., 1980, Water level anomalies prior to the magnitude 6.7 East-Off-Izu Peninsula earthquake, June 29, 1980: Bull. Hot. Springs Res. Inst., Kanazawa Prefecture, v. 12, no. 1, p. 9.

Scholz, C.H., Sykes, L.R., and Aggarwal, Y.P., 1973, Earthquake prediction: a physical basis: Science, v. 181, p. 803-809.

Shimazaki, K., and Somerville, P., 1979, Static and dynamic parameters of the Izu-Oshima, Japan earthquake of January 14, 1978: Bull. Seismol. Soc. Am., v. 69, p. 1343-1378.

Smithsonian Institution, Scientific Event Alert Network (SEAN), 1980, Earthquakes, Izu Peninsula: SEAN Bull., v. 5, no. 6.

Somerville, P., 1978, The accommodation of plate collision by deformation in the Izu block, Japan: Bull. Earthq. Res. Inst., v. 53, p. 629-648.

Tada, T., and Asano, S., 1983, Anomalous crustal uplift and crustal structure in the Matsushiro and the Izu Peninsula earthquake swarm regions: Tectonophysics, v. 97, p. 241-250.

Takahashi, H., and Tsuneishi, Y., 1978, Variations in chemical composition of thermal water before and after the 1978 Izu-Oshima-kinkai earthquake, at Tokunaga-minami and Tsukigase in the Izu Peninsula: Bull. Earthq. Res. Inst., v. 53, p. 987-994.

Thatcher, W., and Savage, J.C., 1982, Triggering of large earthquakes by magma chamber inflation, Izu Peninsula, Japan: Geology, v. 10, p. 637-640.

IZU PENINSULA

REFERENCES (continued)

Tsuboi, C., 1931a, A note on the results of the repeated precise levellings across the Ito earthquake area: Bull. Earthq. Res. Inst., v. 9, p. 151-158.

----- 1931b, On the results of repeated precise levellings around Idu Peninsula: Bull. Earthq. Res. Inst., v. 9, p. 271-289.

----- 1932, Investigation on the deformation of the earth's crust in Idu Peninsula connected with the Idu earthquake of November 26, 1930: Bull. Earthq. Res. Inst., v. 10, no. 2, p. 435-448.

----- 1933, Vertical crustal displacement in the seismic region of Ito, on the East coast of the Idu Peninsula: Bull. Earthq. Res. Inst., v. 11, p. 488-499.

Tsumura, K., 1977, Anomalous crustal activity in the Izu Peninsula, Central Honshu: Jour. Phys. Earth, v. 25 supp., p. S51-S68.

Tsumura, K., Karakama, I., Ogino, I., and Takahashi, M., 1978, Seismic activities before and after the Izu-Oshima-Kinkai earthquake of 1978: Bull. Earthq. Res. Inst., v. 53, p. 675-706.

Wakita, H., 1975, Water wells as possible indicators of tectonic strain: Science, v. 189, p. 553-555.

----- 1982, Changes in groundwater level and chemical composition, in Asada, T., and Ohnuki, M., eds., Earthquake prediction techniques: Tokyo, Univ. Tokyo Press, p. 175-216.

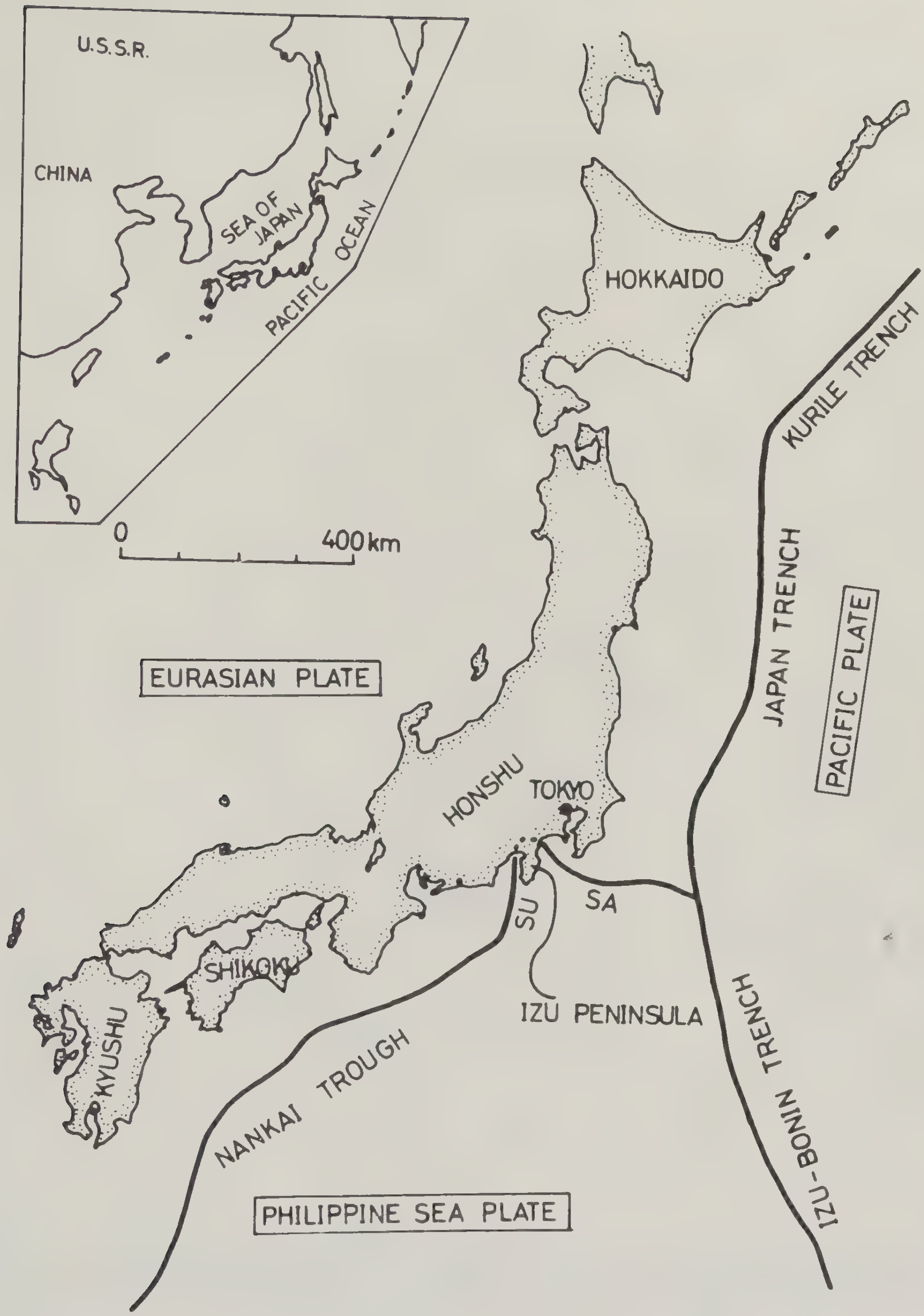

Figure 20.2.1. Location of Izu Peninsula and plate boundary around Japanese Islands, from Fujita and Tada (1983). SA and SU denote Sagami and Suruga Troughs, respectively.

Figure 20.2.2. Index map showing distribution of Quaternary volcanoes in Izu Peninsula, from Oki and others (1978). Area of Higashi-Izu monogenetic volcanoes is outlined; individual vents are indicated by solid circles.

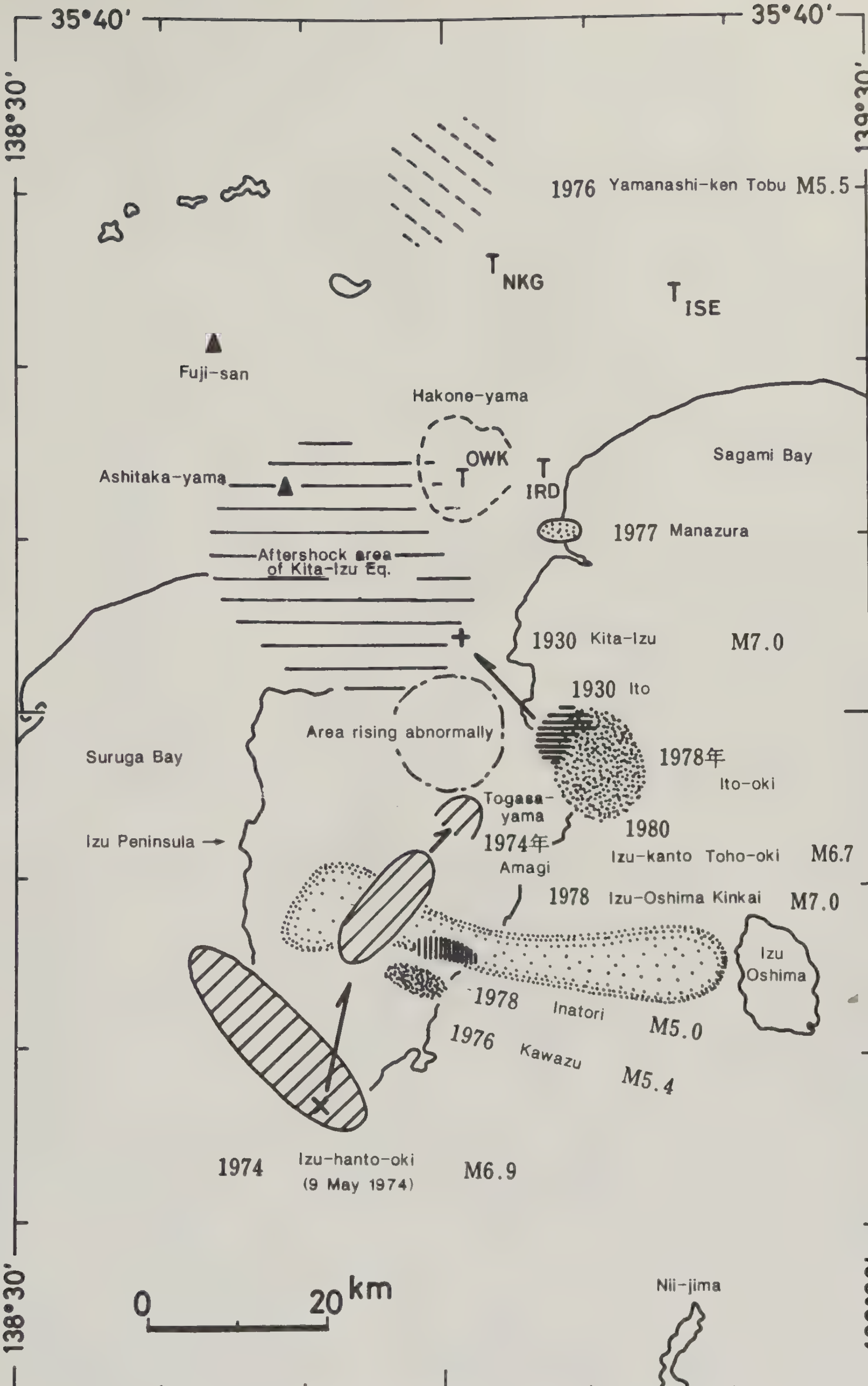

Figure 20.2.3. Locations of large earthquakes and aftershocks on Izu Peninsula, 1930-80, from Hiraga and others (1982). Note migration of activity during February-November 1930 (swarm culminating in main shock) and during May-June 1974 (main shock followed by swarms). Seismic stations are indicated by letter T.

Figure 20.2.4. Active faults and lineaments in Izu Peninsula, from Tsumura (1977) after Murai and Kaneko (1974). 1, right-lateral fault; 2, scarplet; 3, lava flow; 4, volcanic cone; 5, explosion crater.

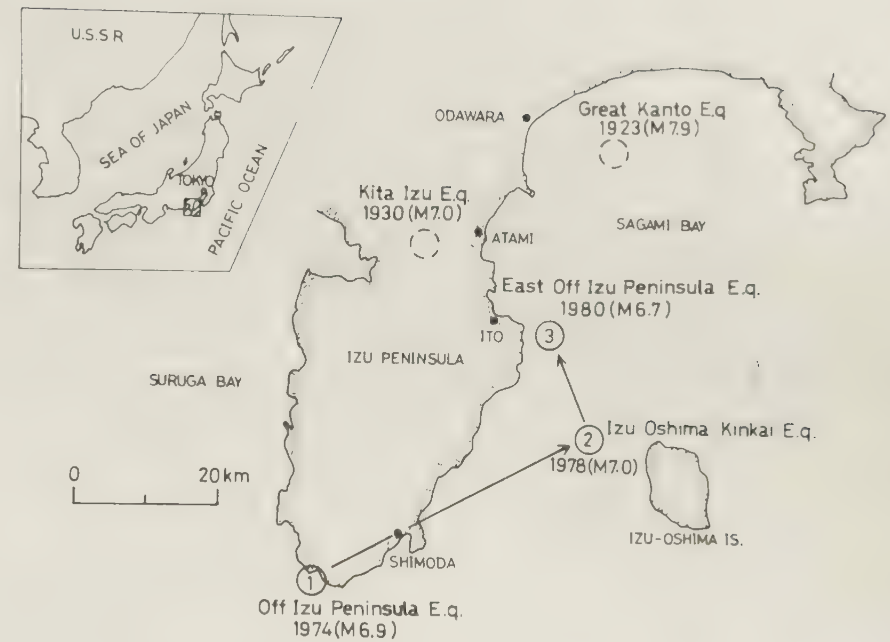

Figure 20.2.5. Epicenters of destructive earthquakes ($\underline{M} > 6.5$) in and around the Izu Peninsula since 1974, from Fujita and Tada (1983). Note that epicenters generally have migrated northward.

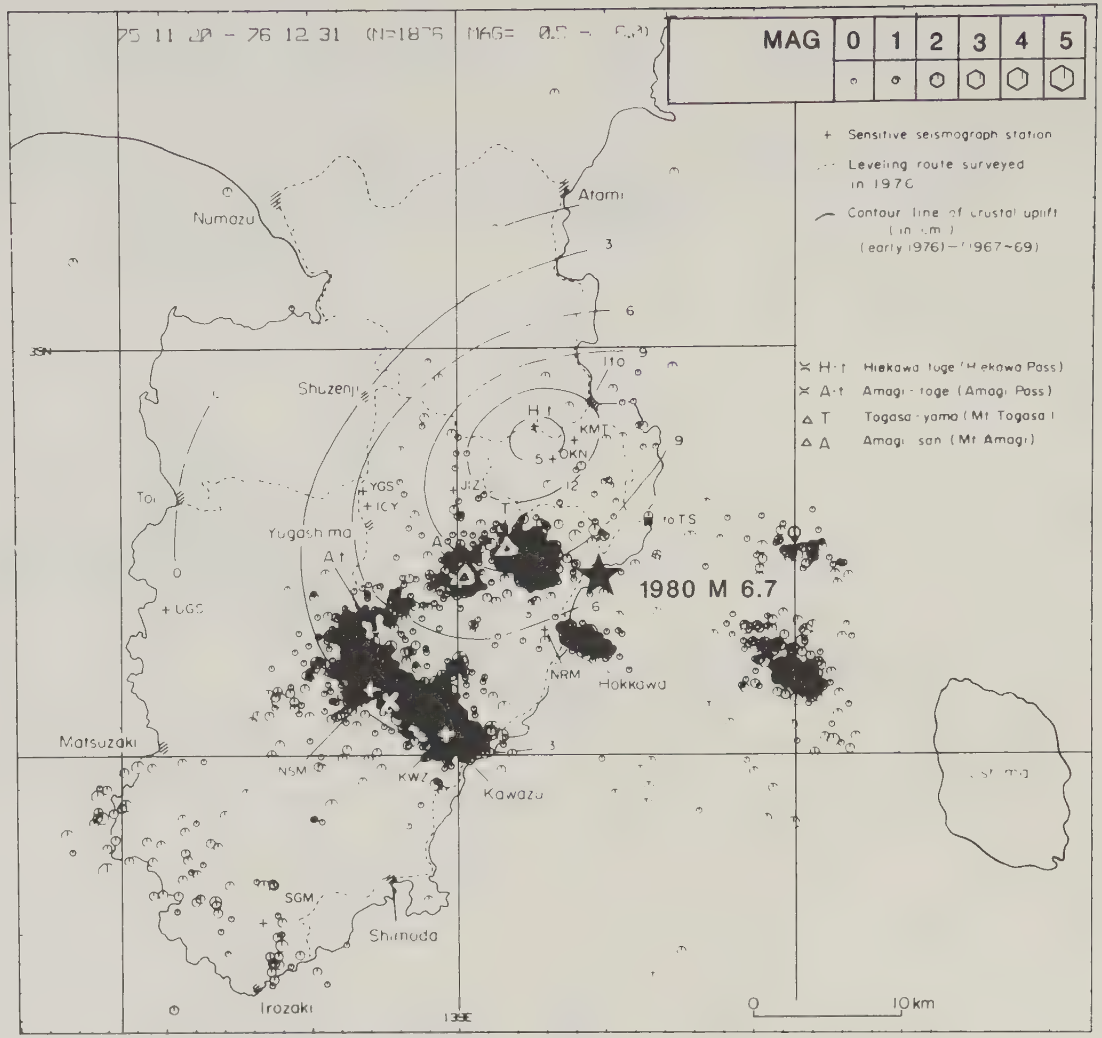

Figure 20.2.6. Distributions of crustal uplift (in centimeters) and epicenters of microearthquakes in Izu Peninsula, from Tsumura (1977). Contour lines are for interval from 1967-69 surveys to January-April 1976 surveys. Broken lines indicate leveling route along which surveys were carried out in 1976. Epicenters were determined by Earthquake Research Institute temporary seismographic network (stations OKN, ICY, NRM, and KWZ) from November 1975 to December 1976.

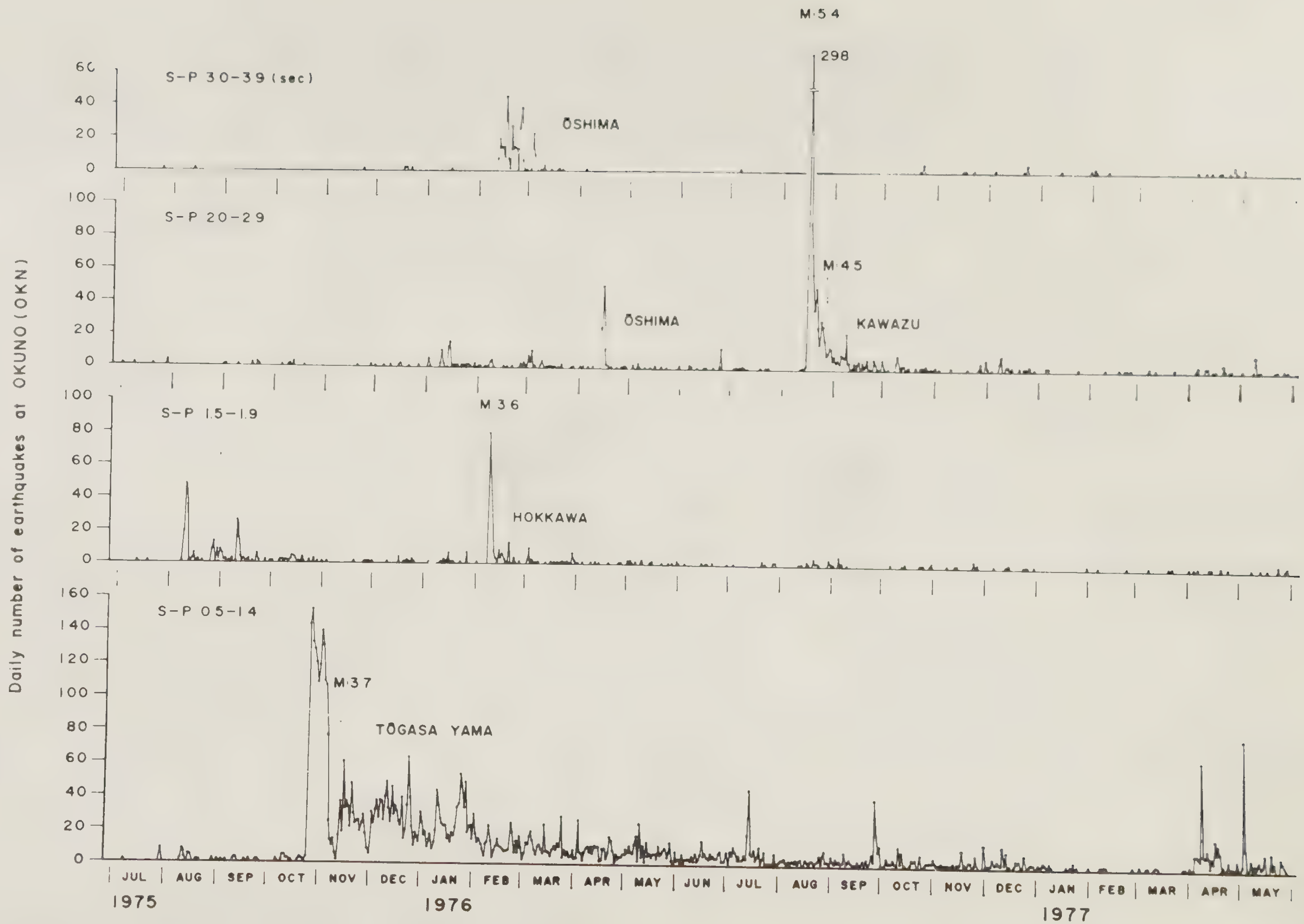

Figure 20.2.7. Number of microearthquakes recorded at Okuno station (OKN) during 1975-77 for different ranges of S - P time, from Tsumura (1977).

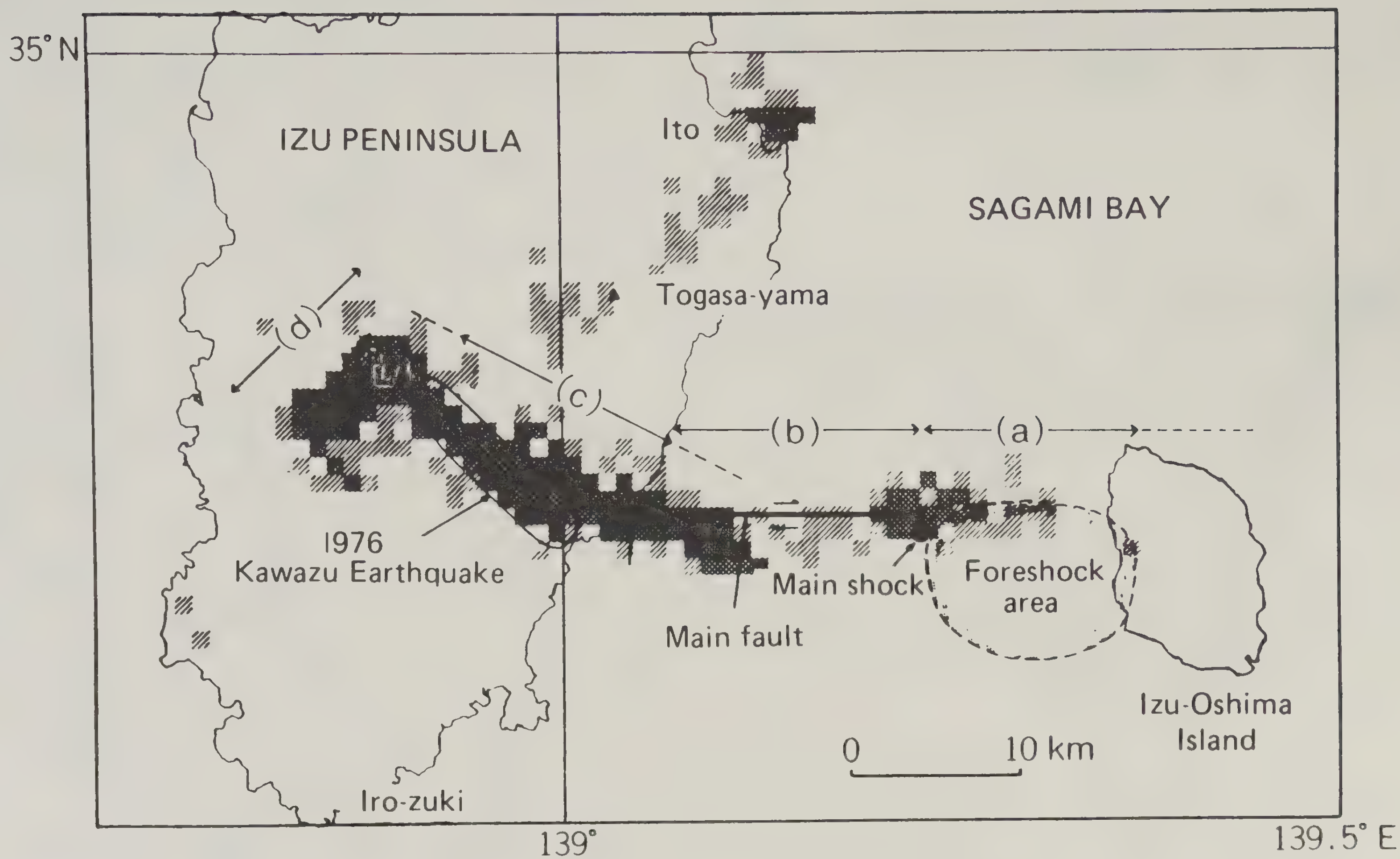

Figure 20.2.8. Main shock, principal fault, foreshock region, and aftershock region of the 1978 Izu-Oshima-kinkai earthquake ($\underline{M}$ 7.0), from Tsumura and others (1978).

Figure 20.2.9. Leveling route around and across Izu Peninsula, from Tsuboi (1931b).

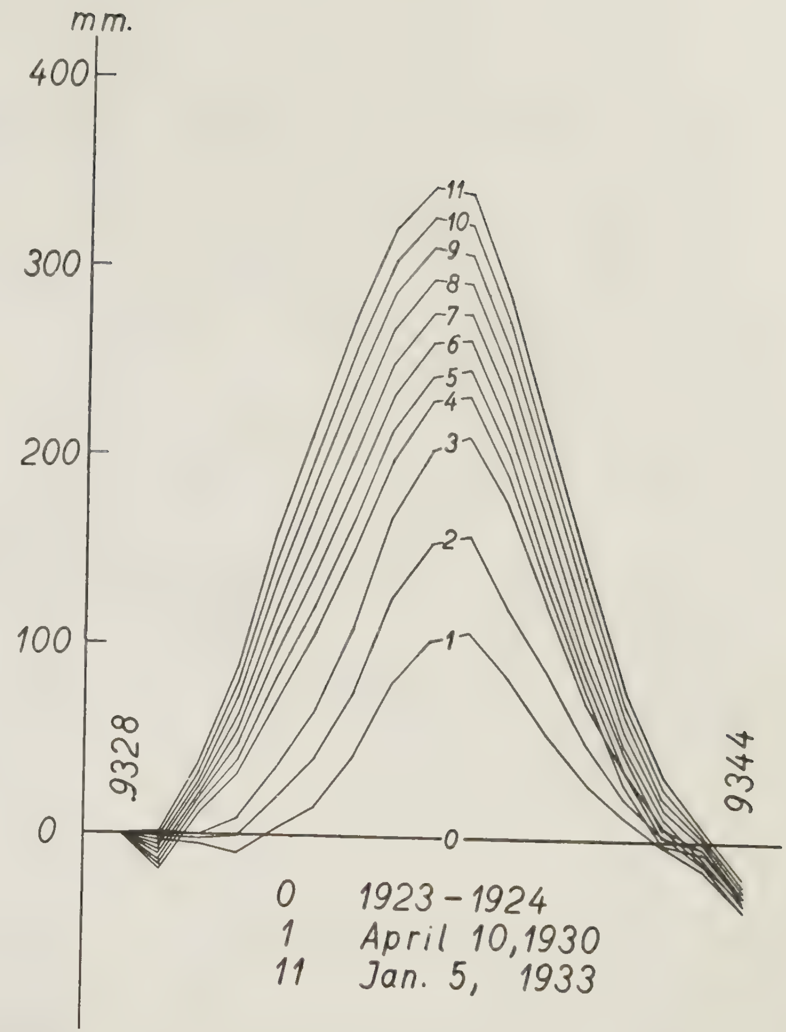

Figure 20.2.10. Successive heights of bench marks around Izu Peninsula at 100-day intervals starting on 10 April 1930 (Tsumura, 1977). Locations of bench marks 9328 and 9344 are indicated in figure 20.2.9.

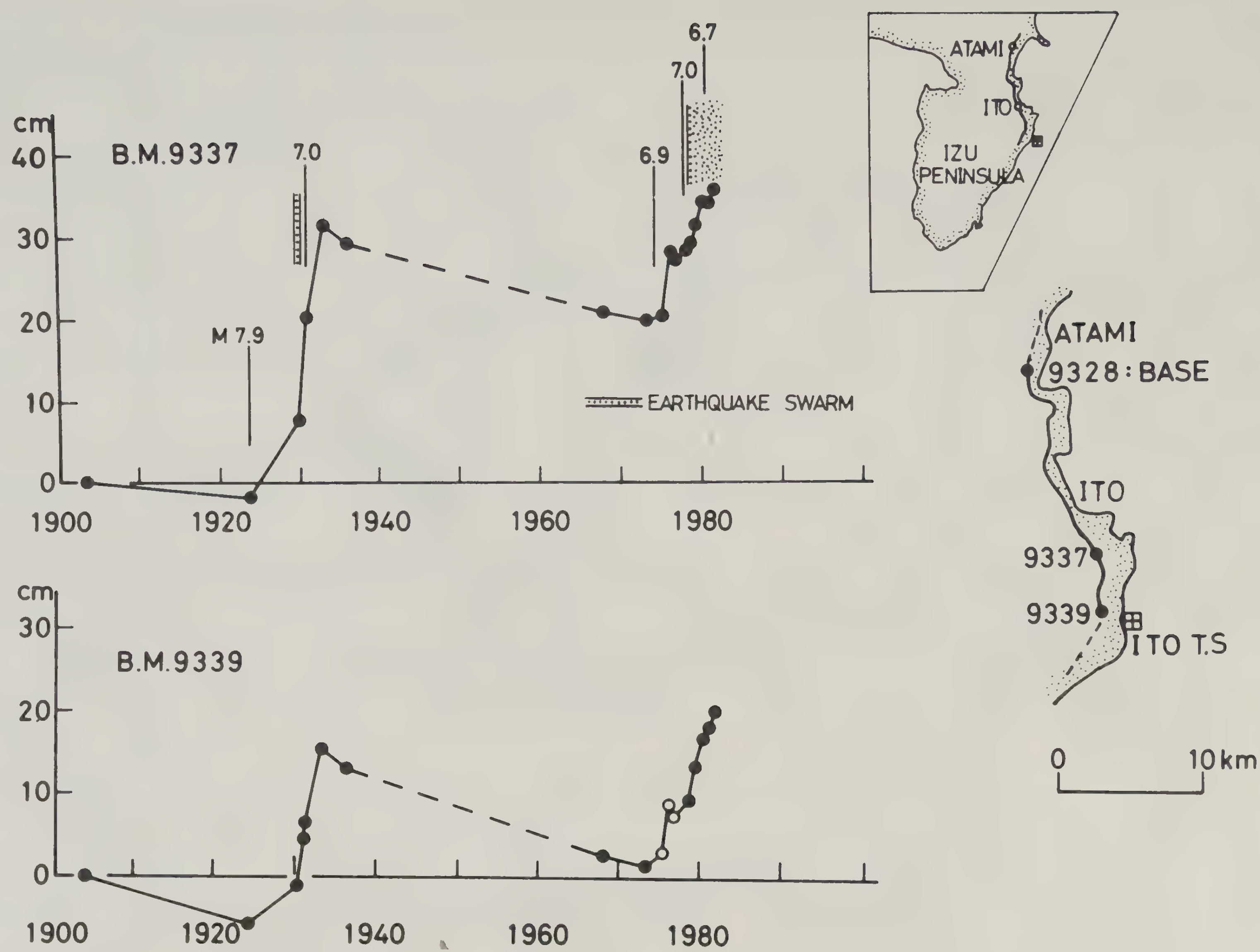

Figure 20.2.11. History of vertical crustal movement at bench mark 9339 near Ito (inset), from Fujita and Tada (1983). Note association of uplift and seismic activity during periods from 1924 to 1933 and from 1975 to 1983.

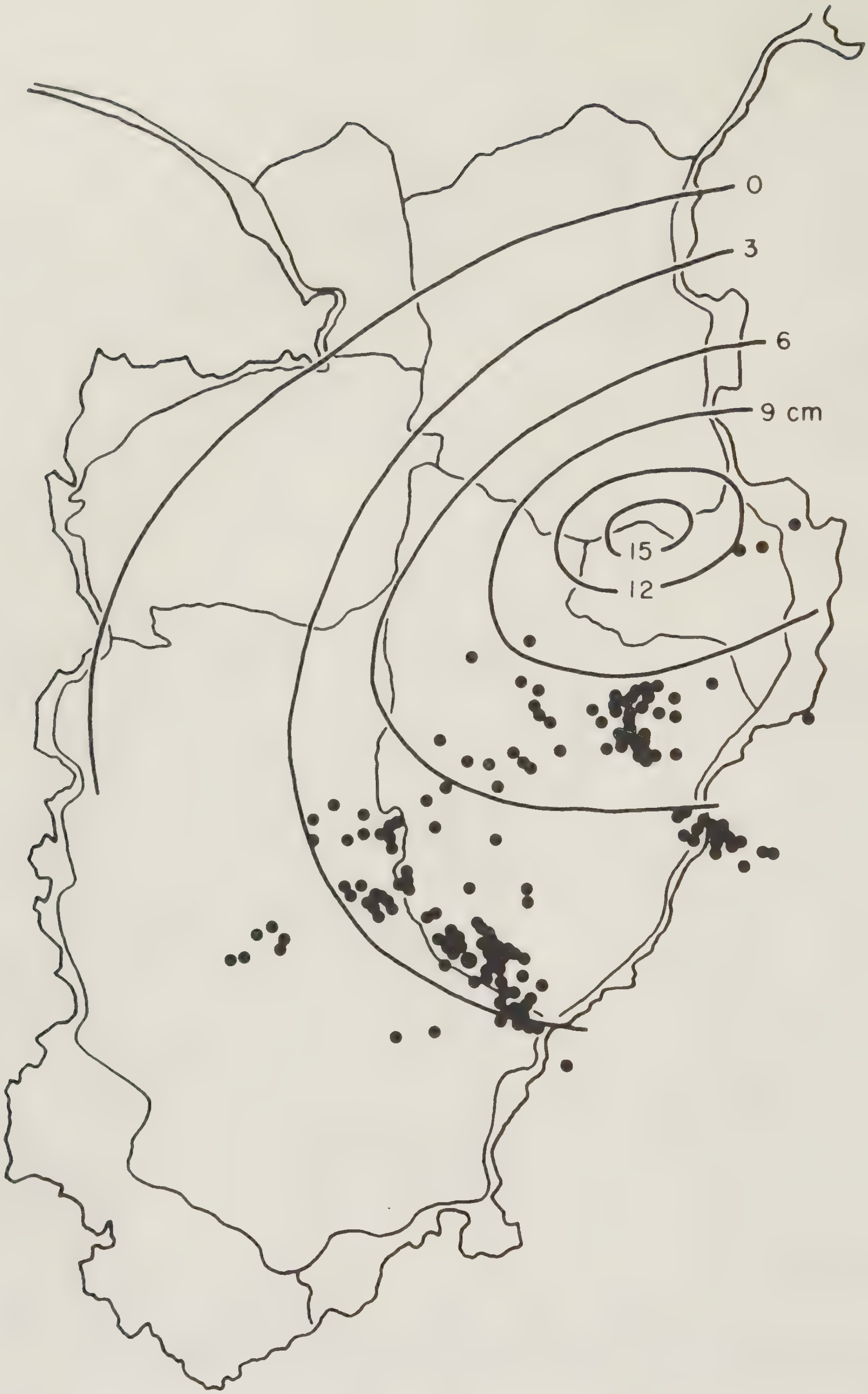

Figure 20.2.12. Ground uplift in eastern Izu Peninsula between 1967 and 1976, and earthquake swarms between 1975 and 1976 (Tsumura, 1977).

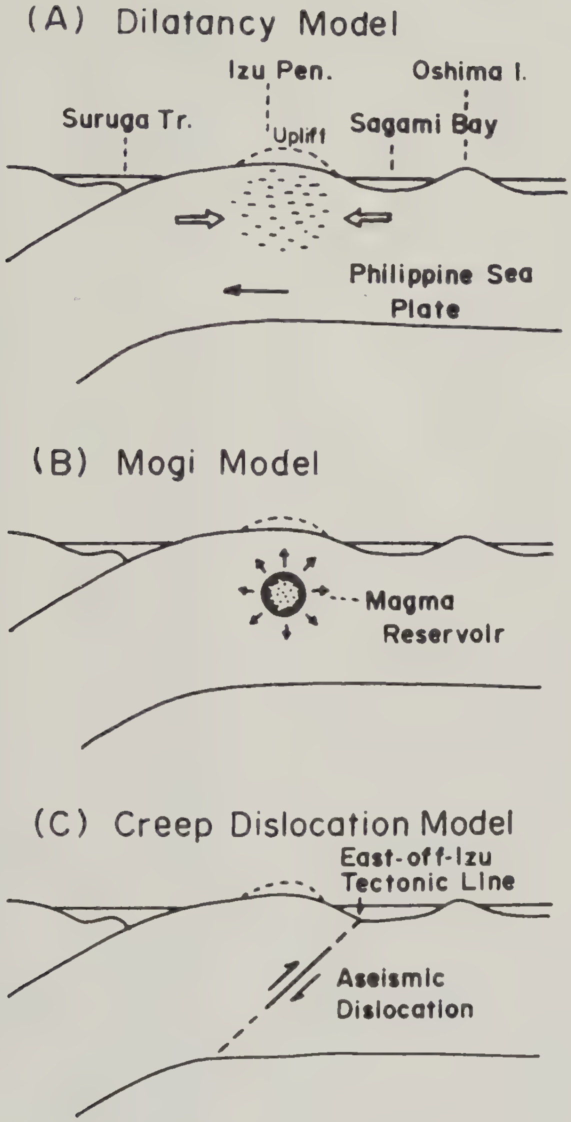

Figure 20.2.13. Three models for historical uplift of Izu Peninsula, from Tsumura (1977).

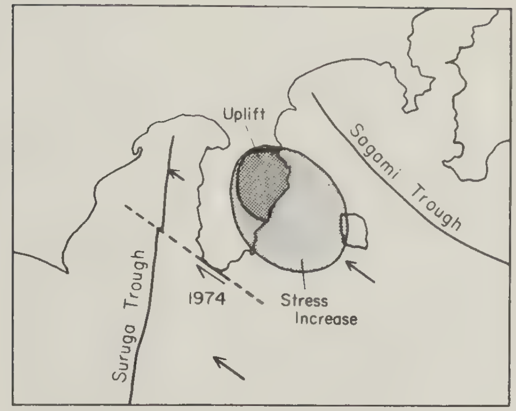

Figure 20.2.14. Illustration of hypothesis explaining increased crustal activity in eastern Izu Peninsula following the 1974 Izu-Hanto-oki earthquake (Mogi, 1985). Thick arrows, direction of movement of Philippine Sea plate. Compression of a plastic volume (magma?) is thought to focus uplift above that volume.

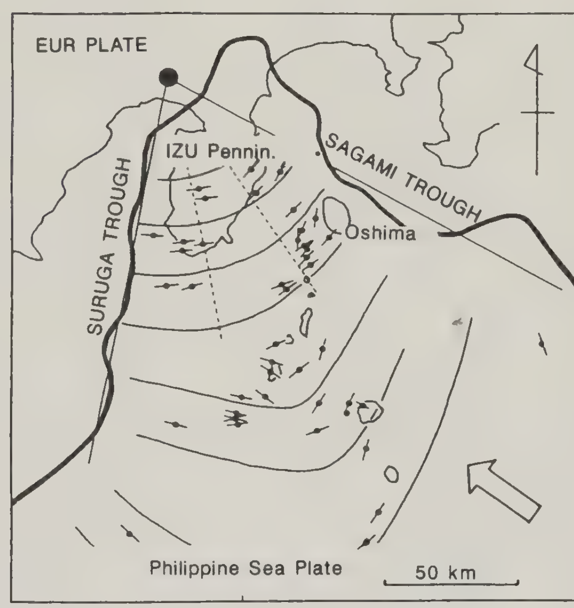

Figure 20.2.15. Concentric trajectories of T-axes of focal-mechanism solutions of shallow earthquakes in northern tip of Philippine Sea plate, from Nakamura and others (1984). Radial broken and solid lines show P-axis trajectories and general trend of troughs, respectively. Open arrow indicates direction of convergence between Philippine Sea and Eurasian plates.

KII PENINSULA

Latitude Longitude (degrees)	Tectonic setting	Age of latest volcanism	Youngest volcanic rock types	Restless years	Type and duration of unrest ESTU STHF MGTF H Te	Associated eruption?
34N 135-136E	Compr	Cretaceous?	?	1899	x--- ---- ---- - --	none
				1920-30+	xx-x xx-- ---- - --	none
				1944	x--- ---- ---- - --	none
				1946	x--x ---- ---- - --	none
				1948	x--- ---- ---- - --	none
				1952-53	xx-x xx-- ---- - --	none

TECTONIC/GEOLOGIC SETTING

The Kii Peninsula, about 350 km west-southwest of the Izu Peninsula (fig. 20.3.1), has outcrops of serpentinite and other high-pressure, low-temperature metamorphic rocks in its central and southern parts, and Cretaceous(?) plutons and higher temperature metamorphic rocks in its northern part. No Quaternary volcanism is known, but hot springs are common. The tectonic setting is similar to that of the Izu Peninsula, with NW-SE compression at the interface between the Philippine Sea plate and the continental lithosphere. The Median Tectonic Line, a major structure with recent right-lateral strike-slip motion, passes ENE-WSW through the peninsula and separates the serpentinites and related rocks in the south from the plutons and related rocks in the north.

Kanamori and Tsumura (1971) distinguished two types of earthquakes on the Kii Peninsula: shallow earthquakes (less than 10 km deep) on the west coast near Wakayama, and deep mantle earthquakes (30-70 km deep) that define a NE-SW line across the central part of the peninsula (figs. 20.3.2, 20.3.3).

HISTORICAL ACTIVITY

At least three large earthquakes have occurred on the peninsula in the past 100 years: $\underline{M}$=7.6 in 1899, and $\underline{M}$=7.0 in 1948 and 1952. In addition, great earthquakes occurred just offshore from the Kii Peninsula in 1944 (the Tonankai earthquake, $\underline{M}$=8.3) and in 1946 (the Nankaido earthquake, $\underline{M}$=8.4) (figs. 20.3.1, 20.3.4, 20.3.5). Notable seismic swarms occurred in the vicinity of Wakayama, on the west coast of the peninsula and south of the Median Tectonic Line, in the early 1920's and 1952-53 (fig. 20.3.4). Interestingly, this swarm activity was greatest just before the Kanto earthquake (1923, $\underline{M}$=8.3, near Tokyo), and the Boso-Oki earthquake (1953, $\underline{M}$=8.3(?), 250 km southeast of Tokyo) (Kanamori, 1972).

KII PENINSULA (continued)

HISTORICAL ACTIVITY (continued)

Swarm activity on the peninsula increased from 1920 to 1923 and then declined (after the Kanto earthquake) for about 7 years. The shocks were shallow, less than 4 km deep, and scarcely felt beyond a radius of 20 km. "The worst do no more than cause cracks in plaster walls, overturn unstable objects, and only rarely throw down stone fencings, so that they could hardly arouse the interest of investigators in Japan, much less of those abroad" (Imamura and others, 1932). The increase in swarm earthquakes was accompanied by uplift of 9 cm at the midpoint of a 10-km-long N-S leveling line between Wakayama and Siotu/Kainan; the center of uplift was broadly coincident with the earthquake epicenters (figs. 20.3.6, 20.3.7). Although the line was established in 1898 and not remeasured until 1928, most of the uplift probably occurred after 1920 (Imamura and others, 1932).

After the peak swarm activity in 1923, the number of earthquakes felt at Wakayama did not return to the pre-1920 background level of about 10/yr but instead remained at approximately 100/year until the 1944 Tonankai earthquake. The number of felt earthquakes did decrease to about 20/yr in 1945 but rose again before the 1946 Nankaido earthquake, and then increased sharply to more than 300/yr in 1952-53 (Kanamori, 1972). Then, after the $\underline{M}$=8.3 Boso-Oki earthquake in 1953 the number declined again so that by 1958 (and until at least 1969), the number of earthquakes felt at Wakayama was again about 100/yr. Within each year, earthquakes were concentrated in discrete swarms separated by a month or more of inactivity.

While the area near Wakayama was being uplifted in the early 1920's, the southern tip of the Kii Peninsula was subsiding. A leveling line around the southern tip of the peninsula, roughly 60 km south-southeast of the swarm area, was measured in 1899 and 1931; at least 7 cm and probably 20-30 cm of subsidence of the southern tip of the peninsula occurred during that interval. Then the bench mark of maximum subsidence was uplifted suddenly by 72 cm at the time of the 1946 Nankaido earthquake. The time of uplift relative to the earthquake is not known from leveling, but tide gauges suggest that it occurred during or just after the earthquake. After the earthquake, slow subsidence of the southern tip of the peninsula resumed at a few millimeters per year, with a slight interruption in 1950-51 before the 1952-53 swarms (see below). Corresponding tilts were 12 microradians (down to the south) from 1900 until the 1946 earthquake, 24 microradians (up to the south) during the earthquake, and 4.8 microradians (back down to the south) from 1946 to 1958 (Okada, 1960) (fig. 20.3.8).

The N-S leveling line between Wakayama and Siotu/Kainan was releveled eight times between 1948 and 1967, following the Nankaido earthquake (figs. 20.3.6, 20.3.9, 20.3.10). The point of maximum uplift for the period 1898-1928 showed further uplift except during 1954-55, just after the 1952-53 swarms. Net uplift was 7 cm from 1948 to 1967; unfortunately, the shape of the uplift is not well known.

Wakita and others (1987) report anomalously high $^{3}He/^{4}He$ ratios in gases from hot springs on the Kii Peninsula (fig. 20.3.11). Because high ratios are associated with He from upper-mantle sources, Wakita and others interpret those high ratios to indicate a magmatic intrusion beneath the Kii Peninsula.

KII PENINSULA (continued)

COMMENTS

Most studies have concluded that the Kii swarms are of tectonic origin, in a region of NW-SE compression. Kanamori and Tsumura (1971) and Kanamori (1972) suggested that earthquakes occur in swarms where there is serpentinite and other rock that has been extensively fractured. The weak rocks cannot sustain enough stress to produce a large earthquake; rather, they fail in many small increments, as represented by the swarm earthquakes. As an alternative interpretation, Wakita and others (1987) suggested deep magmatic intrusion, as they did also for Matsushiro (see discussion in section on Matsushiro).

REFERENCES

Imamura, A., Kodaira, T., and Imamura, H., 1932, The earthquake swarms of Nagusa and vicinity: Bull. Earthq. Res. Inst., v. 10, p. 636-648.

Kanamori, H., 1972, Relation between tectonic stress, great earthquakes and earthquake swarms: Tectonophysics, v. 14, p. 1-12.

Kanamori, H., and Tsumura, K., 1971, Spatial distribution of earthquakes in the Kii Peninsula, Japan, south of the Median Tectonic Line: Tectonophysics, v. 12, p. 327-342.

Miyamura, S., 1960, Local earthquakes in Kii peninsula, central Japan: Bull. Earthq. Res. Inst., pts. 1-3 in v. 37, p. 347-358, 593-608, 609-635; pt. 4 in v. 38, p. 71-112.

Miyamura, S., Hori, M., and Matumoto, H., 1966, Local earthquakes in Kii Peninsula: Bull. Earthq. Res. Inst., pt. 5. in v. 44, p. 709-729.

Okada, A., 1960, Land deformation of the southern part of the Kii peninsula, southwestern Japan: Bull. Earthq. Res. Inst., v. 38, p. 125-143.

Okada, A., Izutuya, S., Ito, Y., and Kadono, K., 1968, Results of levelling resurvey between Wakayama and Kainan, Wakayama prefecture: Bull. Earthq. Res. Inst., v. 46, p. 413-416.

Sano, Y., and Wakita, H., 1985, Geographical distribution of $^3He/^4He$ ratios in Japan: Implications for arc tectonics and incipient magmatism: Jour. Geophys. Res., v. 90, no. B10, p. 8729-8742.

Wakita, H., Sano, Y., and Mizoue, M., 1987, High ^3He emanation and seismic swarms observed in a nonvolcanic, forearc region: Jour. Geophys. Res., v. 92, no. B12, p. 12,539-12,546.

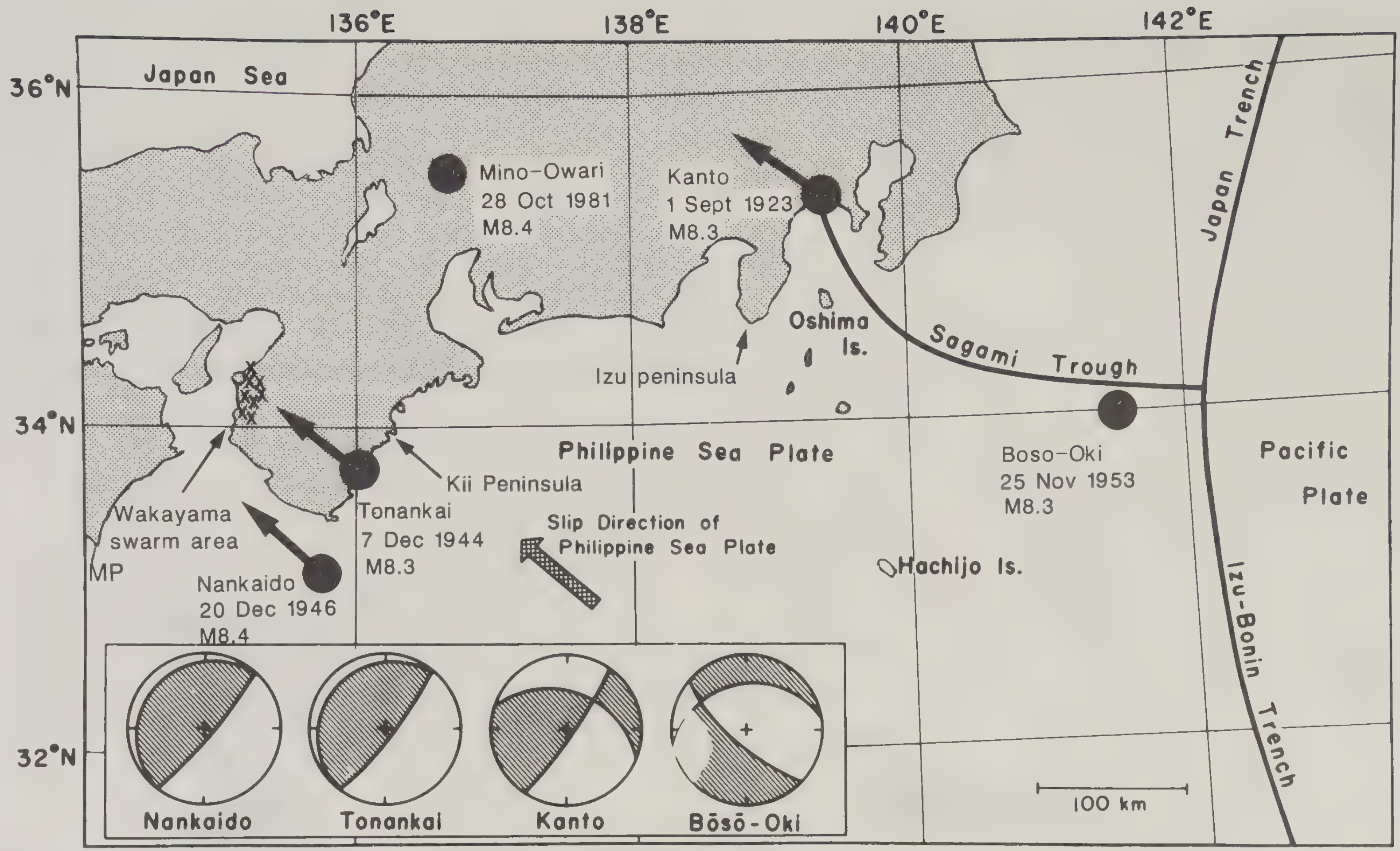

Figure 20.3.1. Locations of Kii Peninsula, Izu Peninsula, and great earthquakes ($\underline{M} > 8$) of southwestern and central Honshu since 1880, from Kanamori (1972). Arrows show direction of slip of footwall side for Kanto, Tonankai, and Nankaido earthquakes. Note location of Muroto Point (MP) on Shikoku Island for later reference in figure 20.3.8.

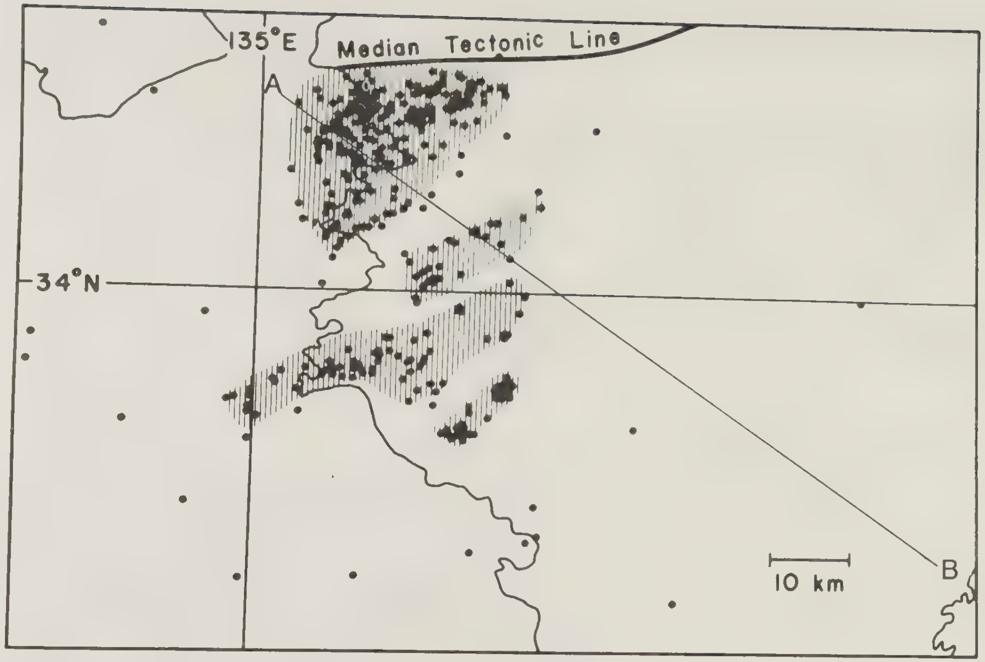

Figure 20.3.2. Epicenters of shallow earthquakes in vicinity of Wakayama, Kii Peninsula, from January to June 1975 (Kanamori and Tsumura, 1971). Note abrupt termination at Median Tectonic Line (see text).

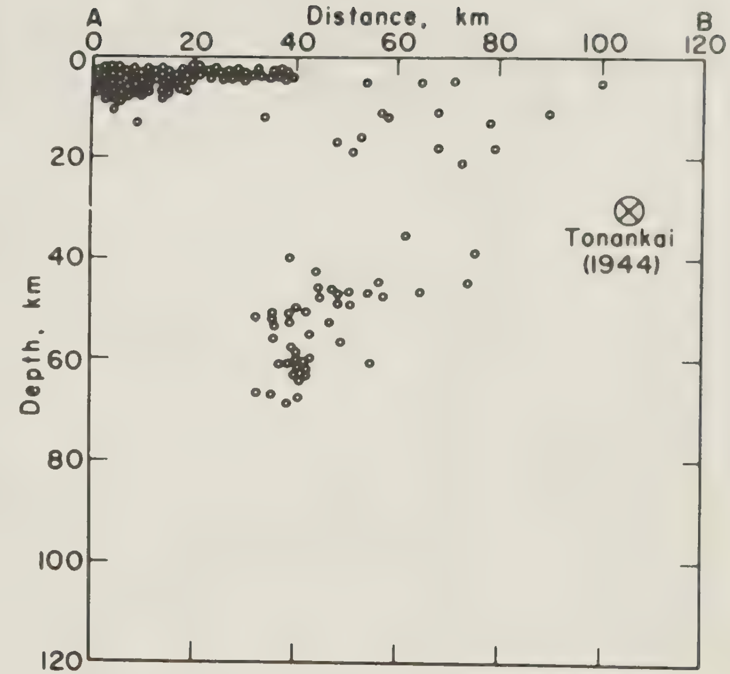

Figure 20.3.3. Hypocenters of earthquakes in vicinity of Wakayama, Kii Peninsula, from January to June 1975, projected onto a northwest-trending plane (Kanamori and Tsumura, 1971). Endpoint A is near Wakayama, and B is near epicenter of the 1944 Tonakai earthquake at southeast tip of Kii Peninsula. Note shallow swarm earthquakes near Wakayama and deep subduction earthquakes to southeast.

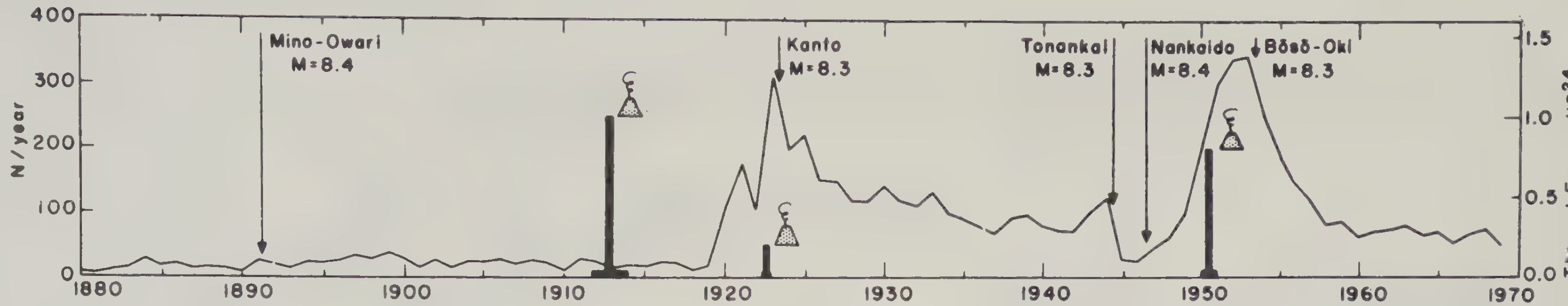

Figure 20.3.4. Annual number of felt earthquakes at Wakayama, 1880-1970 (Kanamori, 1972). Peaks represent swarms in Wakayama area (see figure 20.3.1). Arrows mark times of great earthquakes ($\underline{M} > 8$) in region. Vertical bars indicate thermal energy from eruptions of Oshima Island.

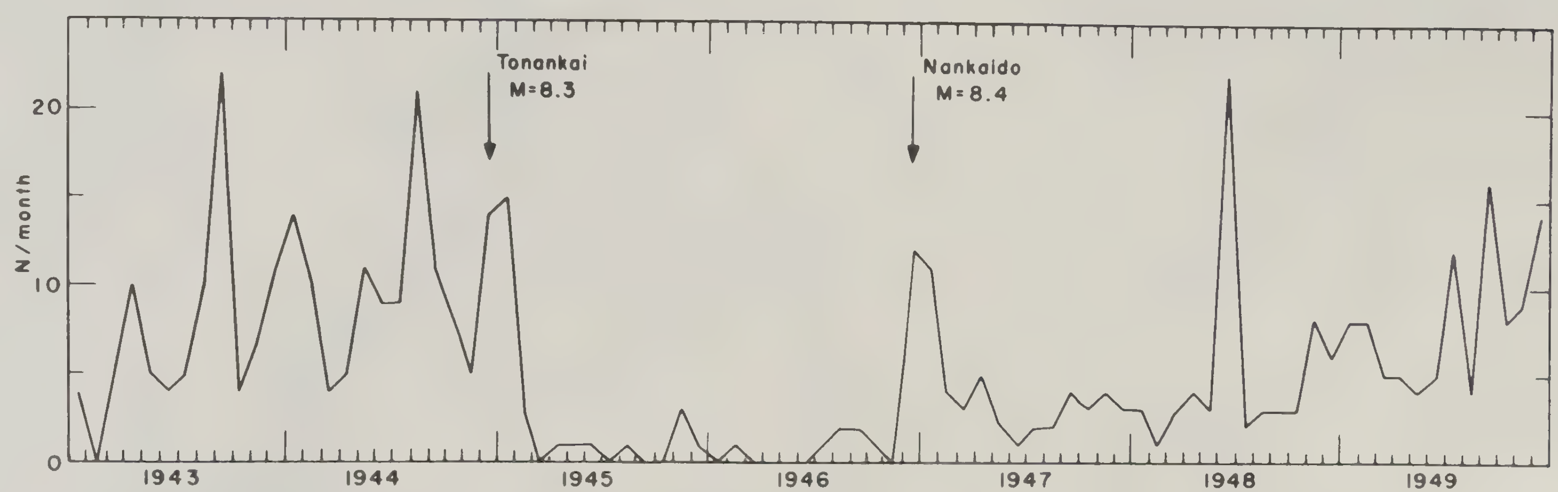

Figure 20.3.5. Monthly number of felt earthquakes at Wakayama, 1943-49 (Kanamori, 1972). Peaks represent swarms in Wakayama area.

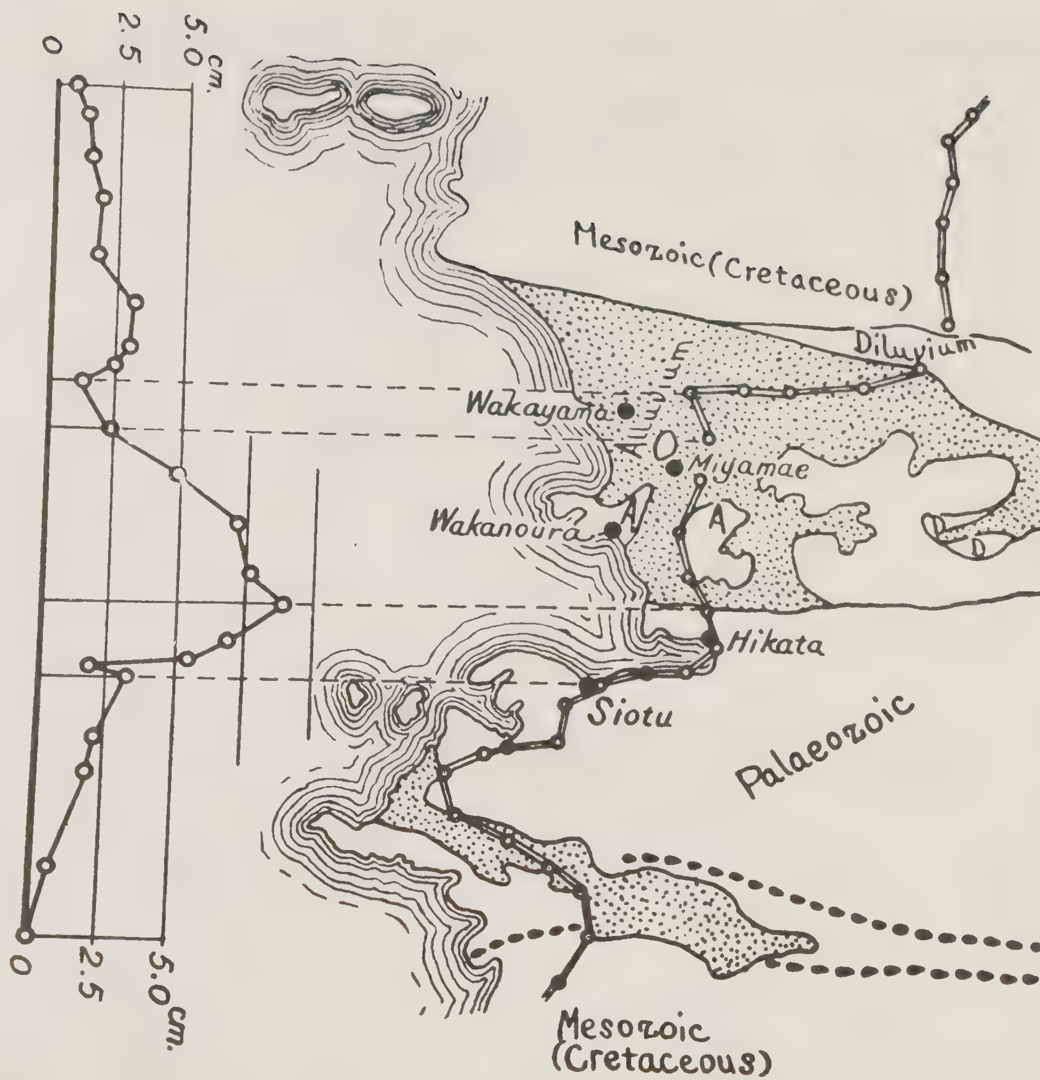

Figure 20.3.6. Location of leveling line along west coast of Kii Peninsula near Wakayama and uplift profile, 1895-1928 (Imamura and others, 1932).

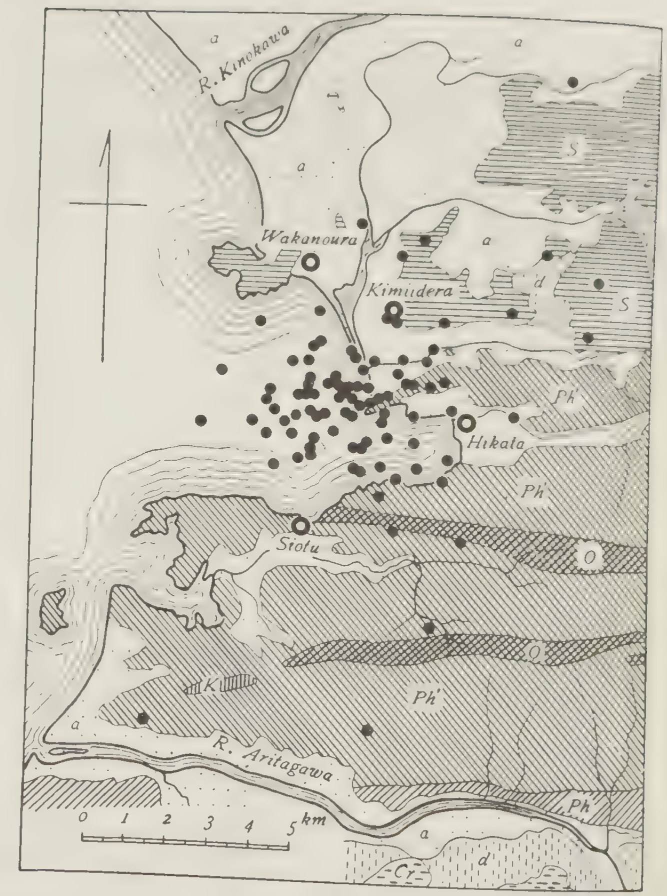

Figure 20.3.7. Earthquake epicenters along west coast of Kii Peninsula south of Wakayama, 1929-31 (Imamura and others, 1932). Bold open circles are towns; patterns show geologic units.

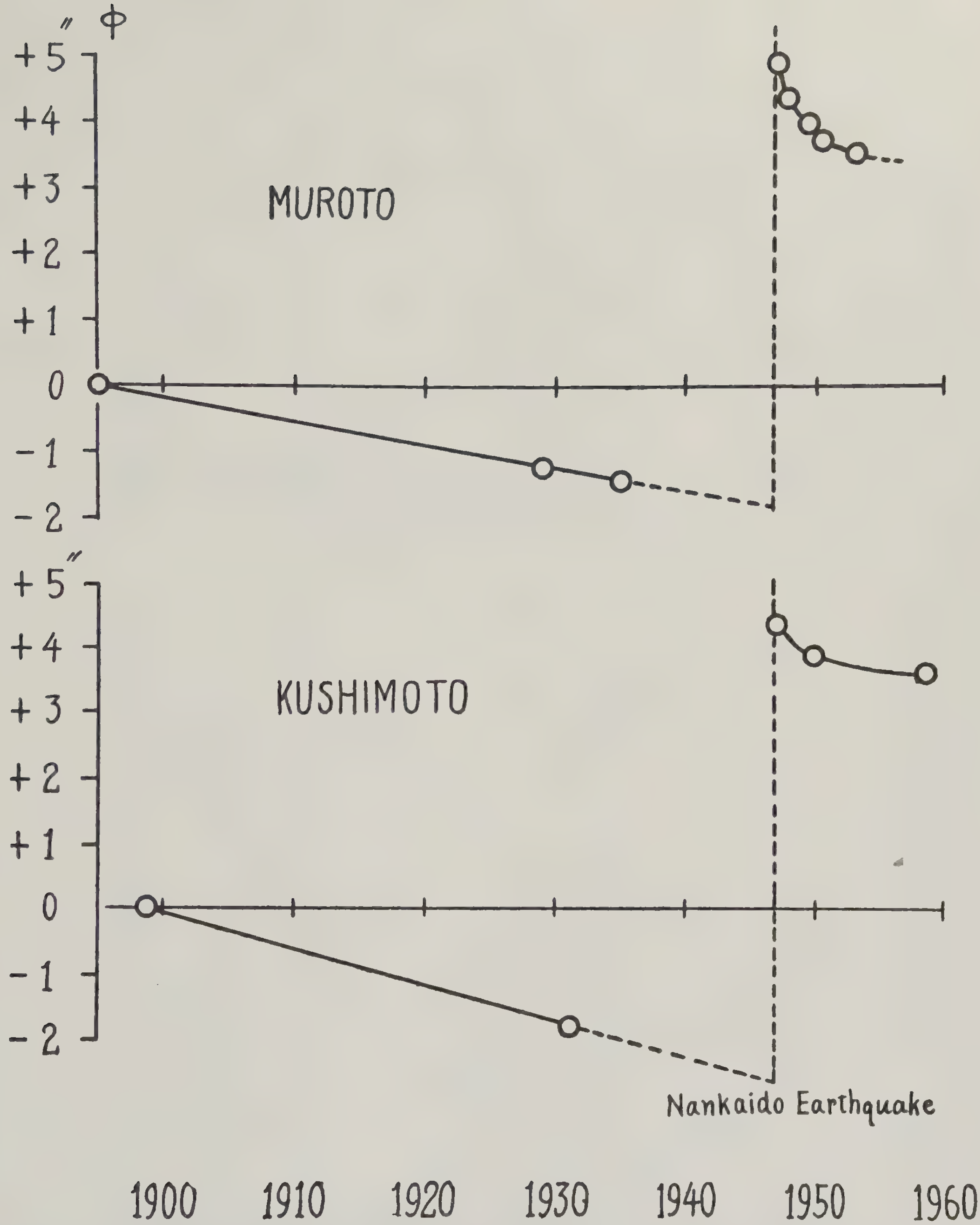

Figure 20.3.8. Southerly tilt in arcseconds (1 arcsecond is about 5 microradians) at Muroto Point, Shikoku Island (see figure 20.3.1) and Kushimoto (south tip of Kii Peninsula), 1928-50 (Okada, 1960). Tilting preceded the Tonakai (1944) and Nankaido (1946) earthquakes by at least two decades.

Figure 20.3.9. Results of leveling surveys around southern tip of Kii Peninsula, 1928-50 (Okada, 1960). Note uplift and northerly tilt shortly after great earthquakes of 1944 and 1946.

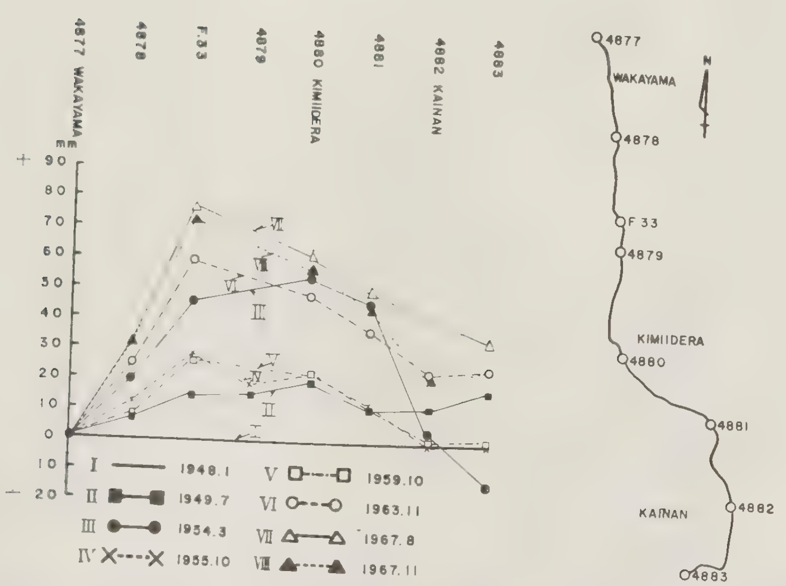

Figure 20.3.10. Profiles of elevation changes along west coast of Kii Peninsula, showing uplift and subsidence, 1948-67 (Okada and others, 1968). Bench mark 4877 at north end of leveling line was assumed stable.

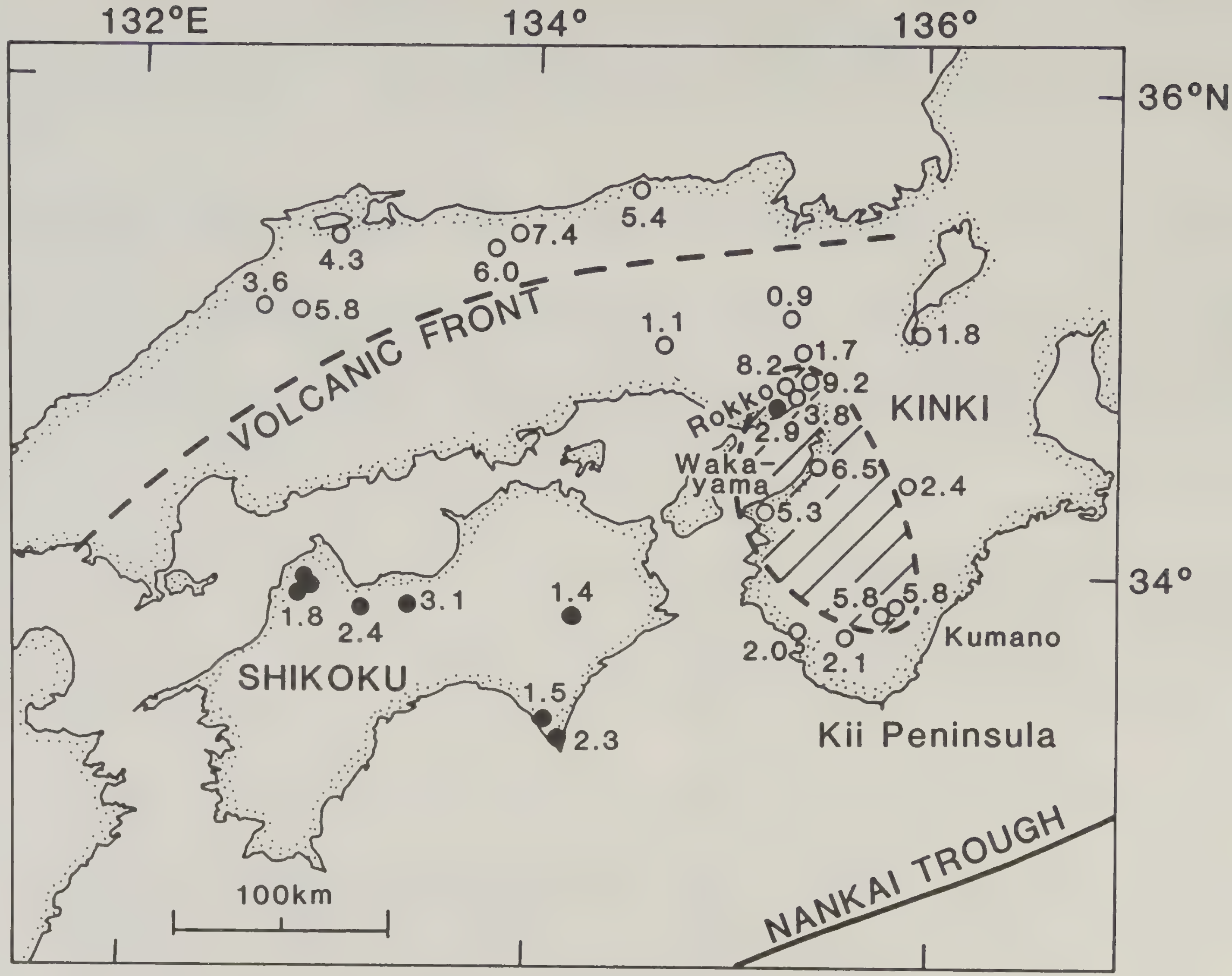

Figure 20.3.11. Locations of sampling sites and measured $^3He/^4He$ ratios (x 10^{-6}), Kii Peninsula (Wakita and others, 1987). Shown are volcanic front and outline of an area (hachured region) where $^3He/^4He$ ratios are higher than 2.8 x 10^{-6}, twice the atmospheric value. Closed and open circles represent data from studies by Wakita and others (1987) and Sano and Wakita (1985), respectively. Copyright by the American Geophysical Union.

MATSUSHIRO

Latitude Longitude (degrees)	Tectonic setting	Age of latest volcanism	Youngest volcanic rock types	Restless years	Type and duration of unrest ESTU STHF MGTF H Te	Associated eruption?
36.55N 138.20E	Compr	350,000 yr B.P.	d	887	x--- ---- ---- - --	none
				1718	x--- ---- ---- - --	none
				1847	x--- ---- ---- - --	none
				1853	x--- ---- ---- - --	none
				1858	x--- ---- ---- - --	none
				1897	EE-- ---- ---- - --	none
				1912	x--- ---- ---- - --	none
				1941-44	FF-- ---- ---- - --	none
				1952	x--- ---- ---- - --	none
				1958	x--- ---- ---- - --	none
				1965-68	FF-E EFFx FFF? F =?	none

TECTONIC/GEOLOGIC SETTING

An area around Matsushiro in northwest Honshu has experienced earthquakes, earthquake swarms, and other crustal unrest many times in recorded history (fig. 20.4.1). Earthquake swarms during 1965-68 are the best known and probably the strongest in the recent history of this area, but they are just the latest of at least three swarms in the past 100 years. The maximum compressional stress (regional) is WNW-ESE or E-W, and a number of NW-SE-trending left-lateral faults and NE-SW-trending right-lateral faults have been mapped. Nakamura (1983, 1984) inferred that Matsushiro, Niigata, and several other nearby areas prone to frequent seismic swarms lie near a nascent (newly forming) convergent boundary between the Eurasian and North American plates--a boundary that includes the Fossa Magna and passes along the northwest coast of Honshu.

No volcanic activity is known within historical time; one of the youngest volcanic vents in the area is Mt. Minakami, a dacite dome that last erupted about 350,000 yr B.P. (Matsuda, 1967; I. Yokoyama, written commun., 1983).

HISTORICAL ACTIVITY

An earthquake swarm occurred near Matsushiro in 1897 ($\underline{M}_{max}$=6.3) and another occurred in 1941-44 ($\underline{M}_{max}$=6.2) (fig. 20.4.2). In addition, earthquakes with magnitudes estimated to be greater than 5 occurred in the Matsushiro-Nagano area in 887, 1718, 1847, 1853,

MATSUSHIRO (continued)

HISTORICAL ACTIVITY (continued)

1858, 1912(?), 1952, 1958, and 1963 (Ichikawa, 1969). The largest earthquake in 1941 (July) had a $\underline{M}$=5.0 foreshock in March 1941 and many small foreshocks 1 hour before the main shock.

Unrest from 1965 to 1968, centered about 2 km north-northeast of Mt. Minakami, included increased seismicity, uplift, surface ruptures of local origin (landslides), and en echelon fractures with 50 cm of observable left-lateral strike-slip displacement and 30 cm of opening along a vertical fault trending N55°W (figs. 20.4.3-20.4.10). An inferred fault passes through the center of uplift, with about 20-30 cm of uplift on the southwest side of the fault relative to the northeast side (Nakamura and Tsuneishi, 1967). More than 700,000 earthquakes were recorded, with a total seismic energy release equivalent to a $\underline{M}$=6.3 earthquake (approximately 10^{23} ergs) (Tada and Asano, 1983). Hagiwara and Iwata (1968) described five periods of seismicity:

(1) August 1965 - February 1966, including a peak in November 1965 (relatively small epicentral area, less than 10-km diameter; mean depth about 4 km, 2-3 km during November 1965 - February 1966; first motion suggesting strike-slip(?), maximum compression N80-90°E) (fig. 20.4.3);

(2) March 1966 - July 1966, including a peak in March-April 1966 (still a relatively small epicentral area, just slightly expanded in a NE-SW direction; mean focal depth=4 km; included the strongest earthquakes of the entire swarm);

(3) August 1966 - December 1966, including a peak in August - September 1966 (noticeable extension of epicentral area NE-SW; perhaps a few more deeper earthquakes, mean depth about 5 km; earthquakes decreased on northeast side of Mt. Minakami, near the inferred fault; earthquakes were accompanied by landslides, ground fracturing, and new, gushing springs);

(4) January 1967 - May 1967 (earthquake epicenters became much more scattered along the same NE-SW zone, now measuring about 18 km x 34 km; a significant number of earthquakes occurred at depths of 8-14 km in the southwest part of the area) (fig. 20.4.4); and

(5) June 1967 - May 1968 (sparse number of earthquakes, with very few near Matsushiro; a few earthquakes at 2-8 km depths in the southwest end of the expanded epicentral area).

Fault-plane solutions for events until March 1966 indicated a consistent maximum horizontal stress direction, N80°W. Solutions for April 1966 to July 1966 gave more variable directions, averaging N87°W, and solutions from August 1966 onward indicated even more variable directions, averaging S88°W in the northern and central parts of the area and N74°W in the southern part of the epicentral area (Ichikawa, 1969). The source region, 15 km x 30 km and 0-10 km deep, is also an area of high seismic velocities at anomalously shallow depth ($\underline{V}_p$=6 km/sec, "granitic") surrounded by an area of anomalously low velocities and high attenuation ("weak country rock") (Okada and others, 1970; Tada and Asano, 1983; Nakamura, 1984). The "granitic layer" was more subject to brittle fracture

MATSUSHIRO (continued)

HISTORICAL ACTIVITY (continued)

than were the relatively weak rocks surrounding it. The area of uplift at the surface corresponded to the area in which this "granitic layer" lies at a shallow depth.

Anomalous rapid tilts of approximately 5 microradians magnitude, just south of Matsushiro town and just southwest of Mt. Minakami, occurred a few days prior to the relatively large earthquakes on 22 November 1965 and 10 March 1966 (Hagiwara and others, 1966). Maximum observed tilt between October 1965 and March 1966 was about 15 arcseconds (45-50 microradians), east and south up.

Uplift was especially rapid during periods 2 and 3. Maximum uplift (70-80 cm) was attained in October 1966. Subsidence from October 1966 onward reduced the net uplift to about 40 cm by the end of the swarms.

Maximum horizontal deformation (from electronic distance measurements) in the epicentral area was 116 cm of extension along a 3.1-km-long, N-S line (Sorobeku line), and 22 cm of compression on a 2.4-km-long, E-W line (Zozan line). Together, these data indicate between 1.5 and 2 m of left-lateral offset on the 10-km-long fault zone. Kasahara and others (1968) showed a change in the direction of contractional strain, from N70-80°W in late 1965 and early 1966 to S70-90°W in May-October 1966; this change correlates with the change in strain axes inferred from fault-plane solutions (Ichikawa, 1969).

The total magnetic intensity at Matsushiro relative to that at Kanozan (a control site, 180 km from Matsushiro) increased by 15 nT from November 1965 to September 1966. In October and November it declined by about 10 nT, and upon remeasurement 3 years later, it had declined by an additional 10 nT (fig. 20.4.13). Yamazaki and Rikitake (1970) infer that the increase in 1965-66 was a piezomagnetic effect due to stress of an unspecified origin, and that the subsequent decrease was due to a relaxation of that stress. Stuart and Johnston (1975) inferred that the initial increase was caused by "inflation of a shallow magma reservoir within a crust containing pre-existing horizontal shear stresses," and that the subsequent decrease was caused by "thermal demagnetization of host rocks." Johnston and others (1983) retained their interpretation of the increase at Matsushiro, but suggested that the decrease was due to stress relaxation.

Earthquakes triggered artesian activity at one or more hot-water wells. On two occasions, in March and August 1966, discharge at the Kagai thermal springs declined for several days, then increased on the day before principal earthquake swarms, with net increases of up to 10 percent of normal discharge (Kasuga, 1967) (figs. 20.4.11, 20.4.12). A remarkable peak in flow from both new and old springs--termed a "water eruption"--occurred during September-October 1966, just before the time of maximum uplift (October 1966) and just prior to expansion of the epicentral area. On two occasions, in July and mid-September 1966, strong flow from Well A of Kagai thermal springs carried sludge and rock fragments--in small hydrothermal eruptions. The temperature of discharged waters at Kagai rose 2 °C from November 1965 to April 1966, then rose another 1.5 °C by January 1967. These temperature changes bore an inverse relation to the discharge--higher rates of discharge corresponded to slightly lower temperatures, as would be expected if the ground water was of shallow, cool origin and was being heated in proportion to the time it convected through hotter rock at depth before being discharged, or if the normally hot water was being augmented by cool ground water from new sources.

MATSUSHIRO, Latitude 36.55N, Longitude 138.20E

MATSUSHIRO (continued)

HISTORICAL ACTIVITY (continued)

Centers of uplift, earthquakes, and unusual spring flow were all more or less coincident. The volume of subsidence following the peak uplift in October 1966 corresponds roughly to the total volume of anomalous spring discharge in the Matsushiro area (10^7 m^3, according to Iijima (1969) and Kisslinger (1975)).

COMMENTS

A lively debate on Matsushiro activity has included the following interpretations:

(a) magma intrusion into a region with preexisting horizontal shear stresses (modeled as a 1-km-diameter source at 3.5-km depth or as a 1-km-diameter cylinder at 2-km depth) (Stuart and Johnston, 1975; Wakita and others, 1978);

(b) dilatancy associated with formation of a new NW-SE-trending left-lateral fault, and conjugate right-lateral motion on one or more NE-SW-trending faults (Kasahara, 1970; Nur, 1974; Kisslinger, 1975);

(c) a combination of tectonic and hydrologic processes in which formation of the above-mentioned fault increased ground water pore pressures causing uplift until the "eruption" of ground water in September 1966 reduced pore pressures and permitted subsidence (Tsuneishi and Nakamura, 1970; Nakamura, 1971; Ohtake, 1974, 1976);

(d) a dominantly hydrothermal process, in which an influx of hot water caused increased ground water pore pressures or hydration of clay minerals and thereby caused uplift (Kasuga, 1967; Matsushima, 1967).

REFERENCES

Asano, S., Kubota, H., Okada, H., Nogoshi, M., Suzuki, H., Ichikawa, K., and Watanabe, H., 1969, Explosion seismic studies of the underground structure of the Matsushiro swarm area: Jour. Phys. Earth, v. 17, p. 77-90.

Hagiwara, T., and Iwata, T., 1968, Summary of the seismographic observation of Matsushiro swarm earthquakes: Bull. Earthq. Res. Inst., v. 46, p. 485-515.

Hagiwara, T., Yamada, J., and Hirai, M., 1966, Observation of tilting of the earth's surface due to Matsushiro earthquakes (I): Bull. Earthq. Res. Inst., v. 44, p. 351-361.

Healy, J.H., Rubey, W.W., Griggs, D.T., and Raleigh, C.B., 1968, The Denver earthquakes: Science, v. 161, p. 1301-1310.

Ichikawa, M., 1969, Matsushiro earthquake swarm: Geophys. Mag., v. 34, p. 307-331.

Iijima, H., 1969, Surface geology of Matsushiro area and disasters by the Matsushiro swarms, in Studies on the Matsushiro earthquake swarm: Tokyo, National Research Center for Disaster Prevention, p. 103-115.

Johnston, M.J.S., Mueller, R.J., Silverman, S.A., and Keller, V.G., 1983, Magnetic measurements across the Long Valley caldera, 1972-1983: A comparison with observations and mechanisms during the Matsushiro earthquake swarm [abs.]: Earthq. Notes, v. 54, no. 1, p. 90.

MATSUSHIRO (continued)

REFERENCES (continued)

Kasahara, K., 1970, The source region of the Matsushiro swarm earthquakes: Bull. Earthq. Res. Inst., v. 48, p. 581-602.

Kasahara, K., Okada, A., Shibano, M., Sasaki, K., Matsumoto, S., and Hirai, M., 1968, Electro-optical measurement of horizontal strains accumulating in the swarm earthquake area (4): Bull. Earthq. Res. Inst., v. 46, p. 651-661.

Kasuga, I., 1967, Aspect on the relation of thermal water and Matsushiro earthquakes in Kagai Hotspring area, Nagano Prefecture: Jour. Geogr. (Chigaku Zasshi), v. 76, p. 16-26.

Kisslinger, C., 1968, Energy density and the development of the source region of the Matsushiro earthquake swarm: Bull. Earthq. Res. Inst., v. 46, p. 1207-1223.

----- 1975, Processes during the Matsushiro, Japan, earthquakes as revealed by leveling, gravity, and spring-flow observations: Geology, v. 3, p. 57-62.

Matsuda, T., 1967, Geological aspect of the Matsushiro earthquake fault: Bull. Earthq. Res. Inst., v. 45, p. 537-550.

Matsushima, S., 1967, Water content in the crust and the hydrothermal reaction as a possible cause for the swarm type earthquake: Kyoto Univ. Geophys. Inst. Spec. Contrib., no. 7, p. 201-210.

Nakamura, K., 1971, A lesson from the Matsushiro earthquake swarm: Kagaku Asahi, no. 10, p. 127-133.

----- 1983, Possible nascent trench along the eastern Japan Sea as the convergent boundary between Eurasian and North American Plates: Bull. Earthq. Res. Inst., v. 58, p. 711-722.

----- 1984, On the hypothesis that the East Japan Sea - Fossa Magna represent a convergent boundary between the Eurasian and North American plates: Earth Monthly, v. 6, p. 25-28.

Nakamura, K., and Tsuneishi, Y., 1967, Ground cracks at Matsushiro probably of underlying strike-slip fault origin (II)--The Matsushiro earthquake fault: Bull. Earthq. Res. Inst., v. 45, p. 417-471.

Nur, A., 1974, Matsushiro, Japan, earthquake swarm: confirmation of the dilatancy-fluid diffusion model: Geology, v. 2, p. 217-221.

Ohtake, M., 1974, Seismic activity induced by water injection at Matsushiro, Japan: Jour. Phys. Earth, v. 22, p. 163-176.

----- 1976, The Matsushiro earthquakes, after 10 years: Kagaku (Science), v. 46, p. 306-313.

Okada, H., Suzuki, S., and Asano, S., 1970, Anomalous underground structure in the Matsushiro earthquake swarm area as derived from a fan-shooting technique: Bull. Earthq. Res. Inst., v. 48, p. 811-833.

Rikitake, T., Yamazaki, Y., Sawada, M., Sasai, Y., Yoshino, T., Uzawa, S., and Shimomura, T., 1967, Geomagnetic and geoelectric studies of the Matsushiro earthquake swarm (5): Bull. Earthq. Res. Inst., v. 45, p. 395-416.

Stuart, W.D., and Johnston, M.J.S., 1975, Intrusive origin of the Matsushiro earthquake swarm: Geology, v. 3, p. 63-67.

Tada, T., and Asano, S., 1983, Anomalous crustal uplift and crustal structure in the Matsushiro and the Izu Peninsula earthquake swarm regions: Tectonophysics, v. 97, p. 241-250.

Tsubokawa, I., Okada, A., Izutuya, S., Ito, Y., and Kadono, K., 1968, Levelling resurvey associated with the area of Matsushiro earthquake swarm (2): Bull. Earthq. Res. Inst., v. 46, p. 417-429.

Tsuneishi, Y., and Nakamura, K., 1970, Faulting associated with the Matsushiro swarm earthquakes: Bull. Earthq. Res. Inst., v. 48, p. 29-51.

Wakita, H., Fujii, N., Matsuo, S., Notsu, K., Nagao, K., and Takaoka, N., 1978, "Helium spots": Caused by diapiric magma from the upper mantle: Science, v. 200, p. 430-432.

Yamazaki, Y., and Rikitake, T., 1970, Local anomalous changes in the geomagnetic field at Matsushiro: Bull. Earthq. Res. Inst., v. 48, p. 637-643.

MATSUSHIRO, Latitude 36.55N, Longitude 138.20E

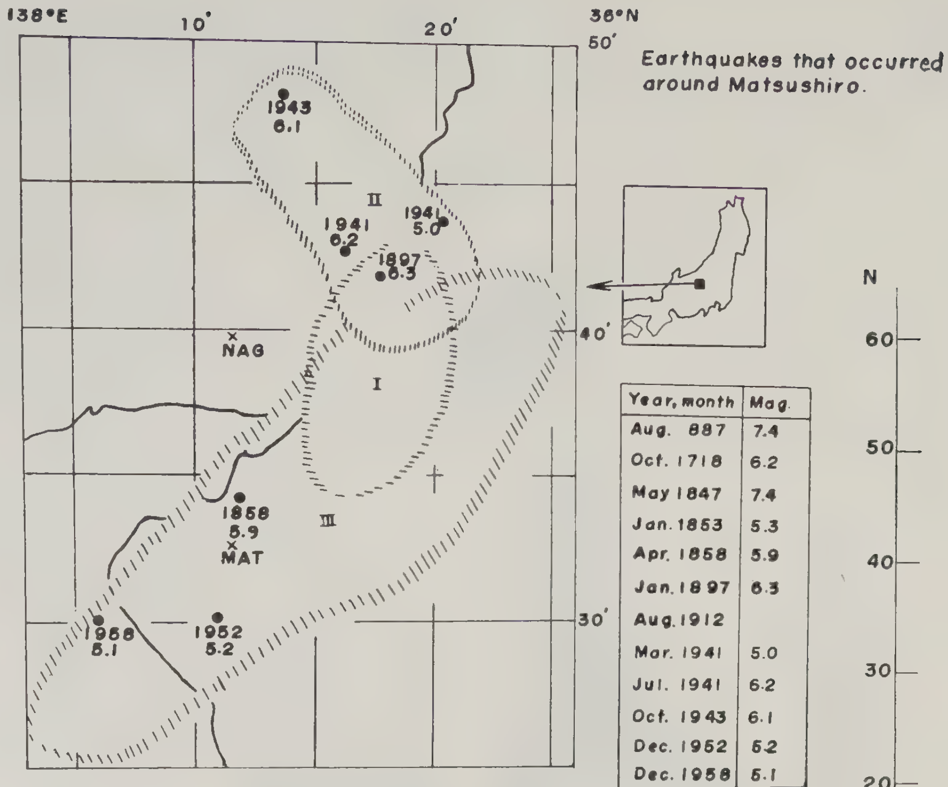

Year, month	Mag.
Aug. 887	7.4
Oct. 1718	6.2
May 1847	7.4
Jan. 1853	5.3
Apr. 1858	5.9
Jan. 1897	6.3
Aug. 1912	
Mar. 1941	5.0
Jul. 1941	6.2
Oct. 1943	6.1
Dec. 1952	5.2
Dec. 1958	5.1

Figure 20.4.1. Major earthquakes in Matsushiro area, A.D. 887-1958 (Ichikawa, 1969). NAG, Nagano Meteorological Observatory; MAT, Matsushiro Seismological Observatory; I, area of 1897 earthquake swarm; II, area of 1941-43 earthquake swarm; III, area of 1965-68 earthquake swarm.

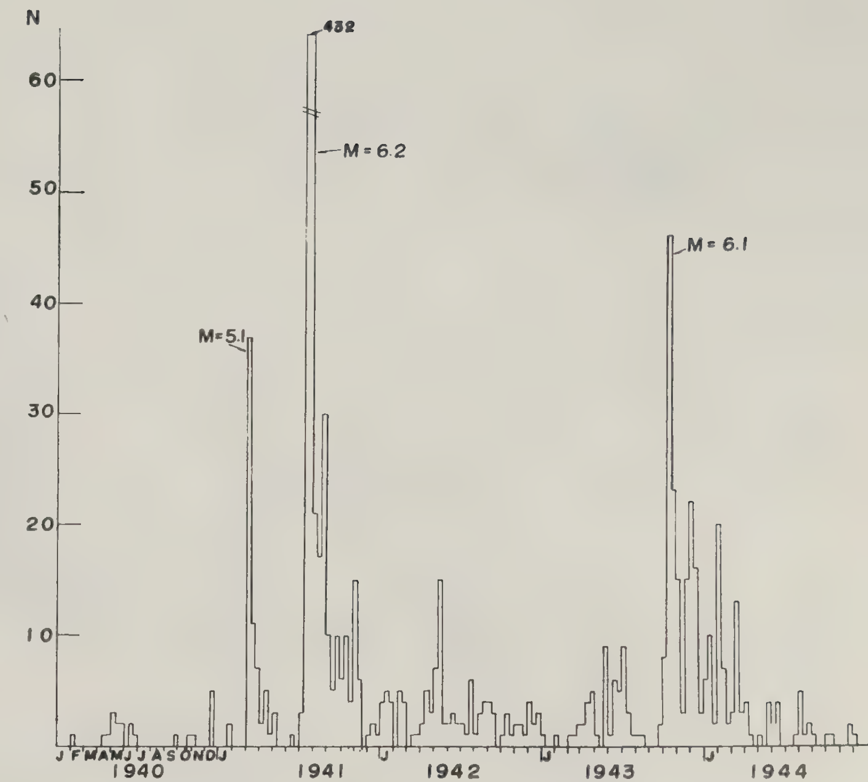

Figure 20.4.2. Number of earthquakes at Matsushiro per 10-day interval, 1940-44 (Ichikawa, 1969). Plotted is number of earthquakes with P - S intervals > 3 s on seismograms of Nagano Meteorological Observatory (see figure 20.4.1).

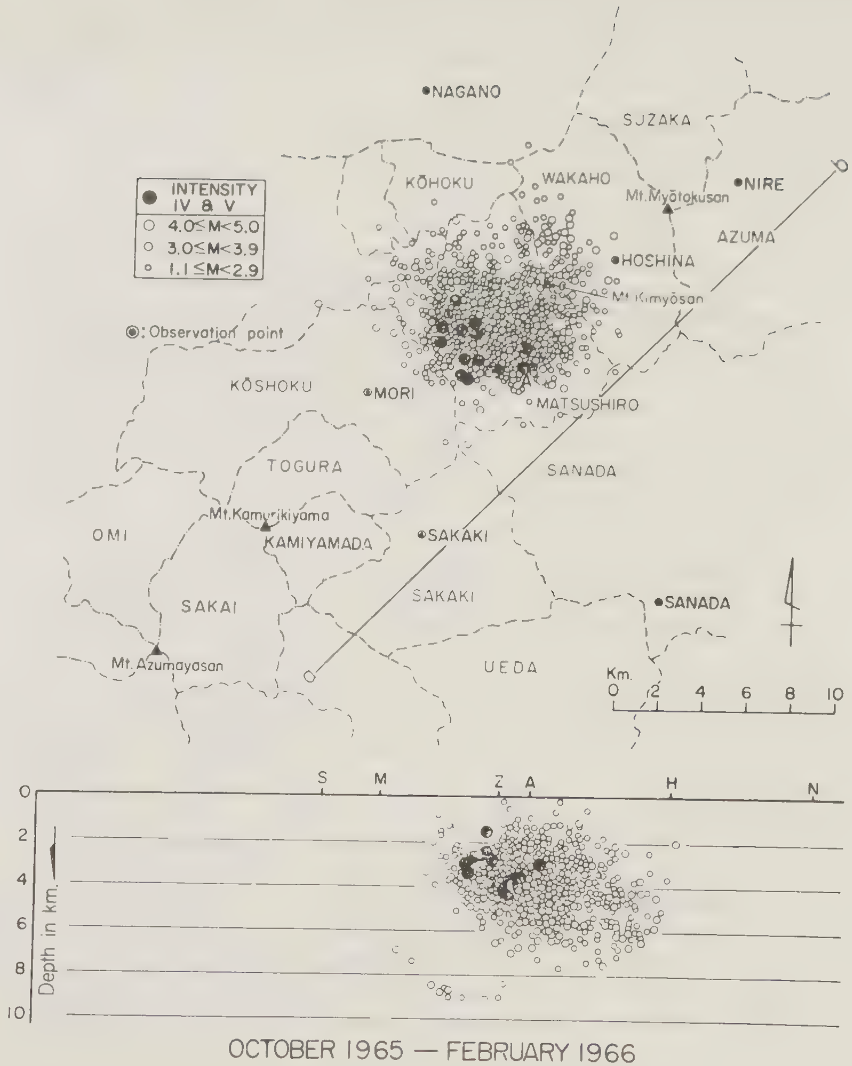

Figure 20.4.3. Epicenters and hypocenters during period 1 (see text), tightly clustered and relatively shallow, near Matsushiro and Mt. Minami-dake (Hagiwara and Iwata, 1968).

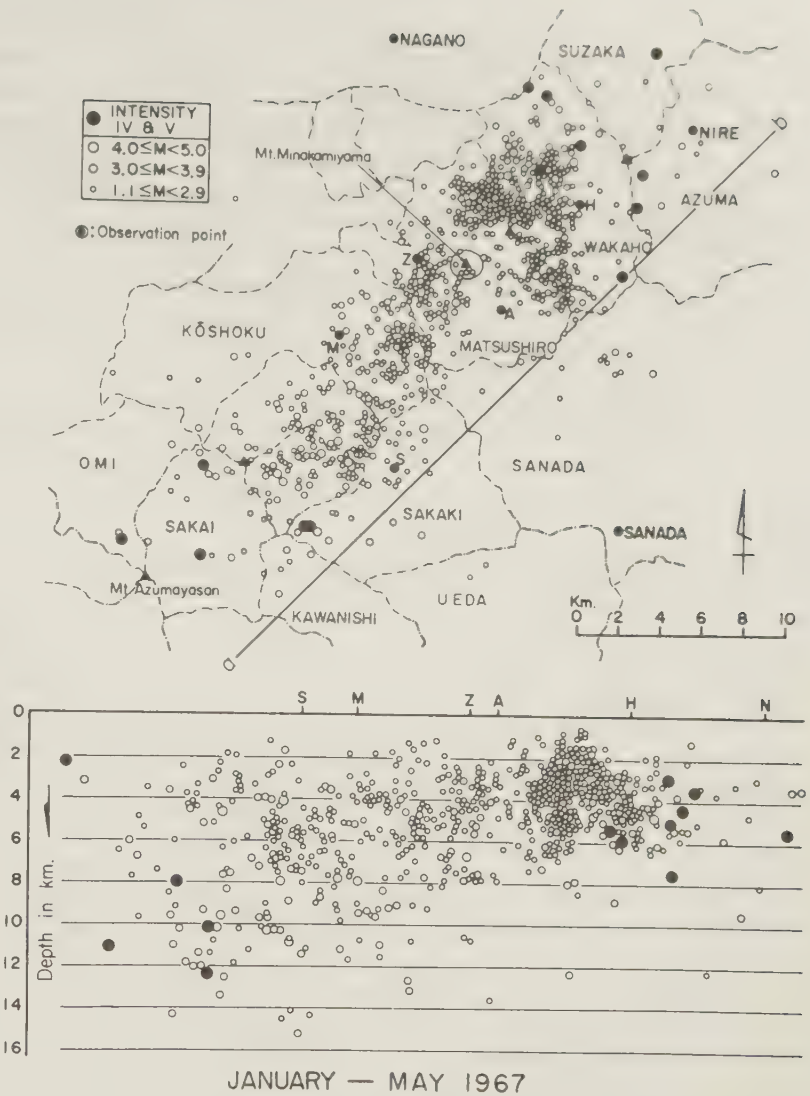

Figure 20.4.4. Epicenters and hypocenters during period 4 (see text), dispersed along a NE-SW trend and spanning a greater depth range in southwest part of swarm area (Hagiwara and Iwata, 1968).

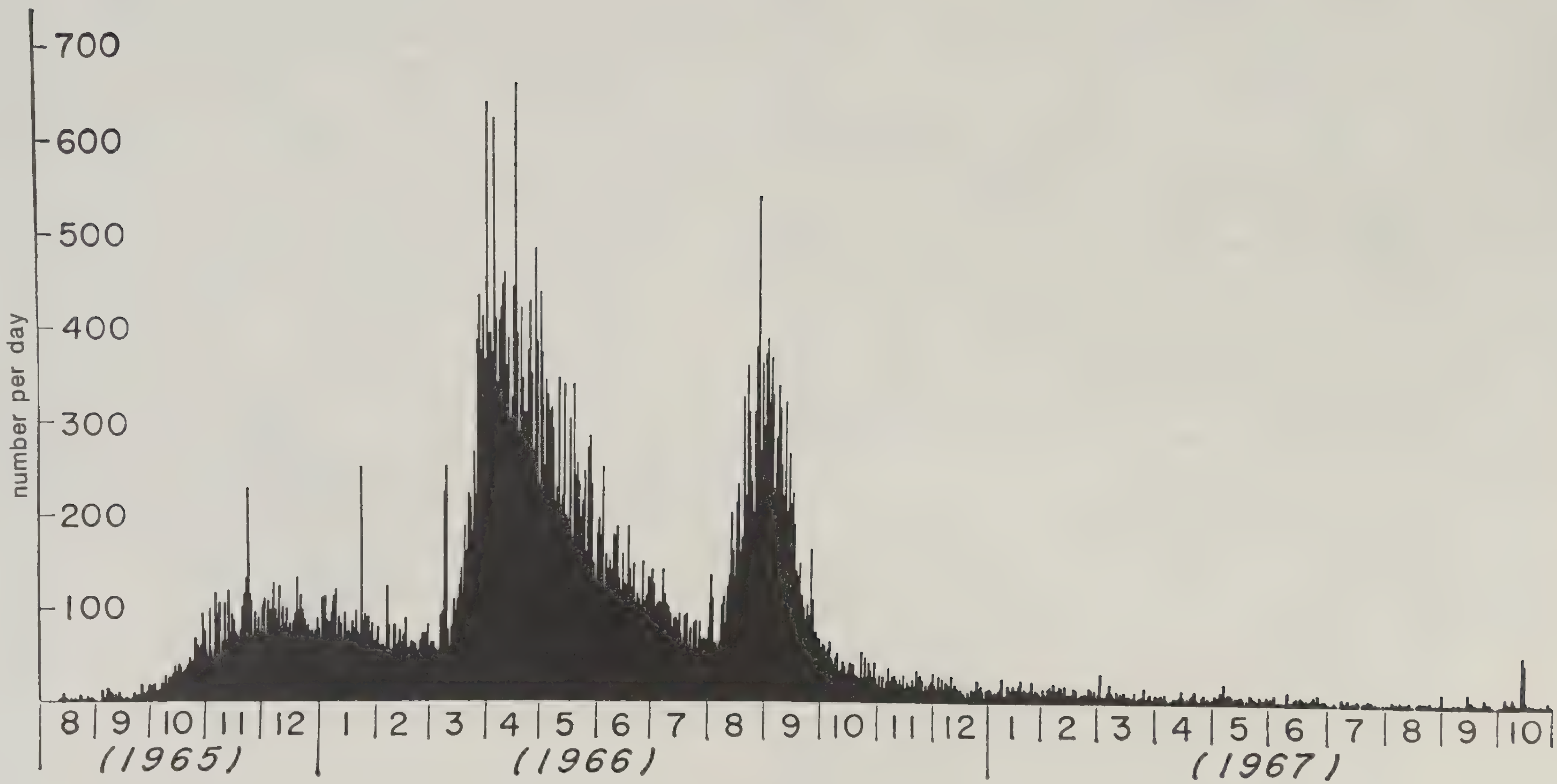

Figure 20.4.5. Daily frequency of felt earthquakes registered at Matsushiro Seismological Observatory, 1965-67, from Tsuneishi and Nakamura (1970).

Figure 20.4.6. Contours of vertical land movements over a broad area around Matsushiro, late 1965 to mid-1966, from Kasahara (1970).

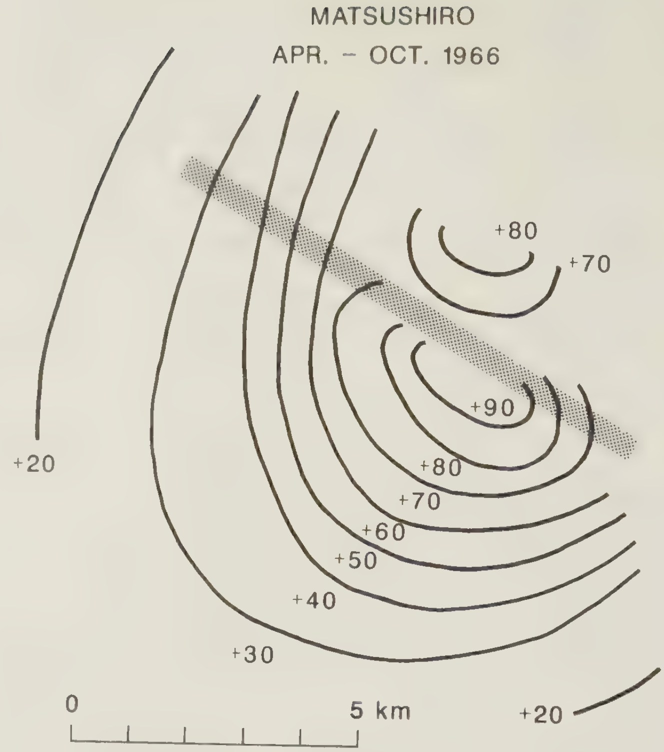

Figure 20.4.7. Contours of local uplift near Matsushiro town, April-October 1966, from Kasahara (1970).

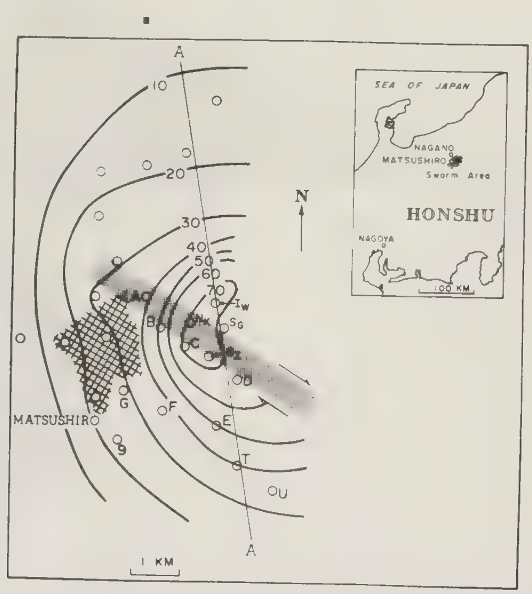

Figure 20.4.8. Contours of local uplift near Matsushiro, October 1965 - September 1966, from Stuart and Johnston (1975).

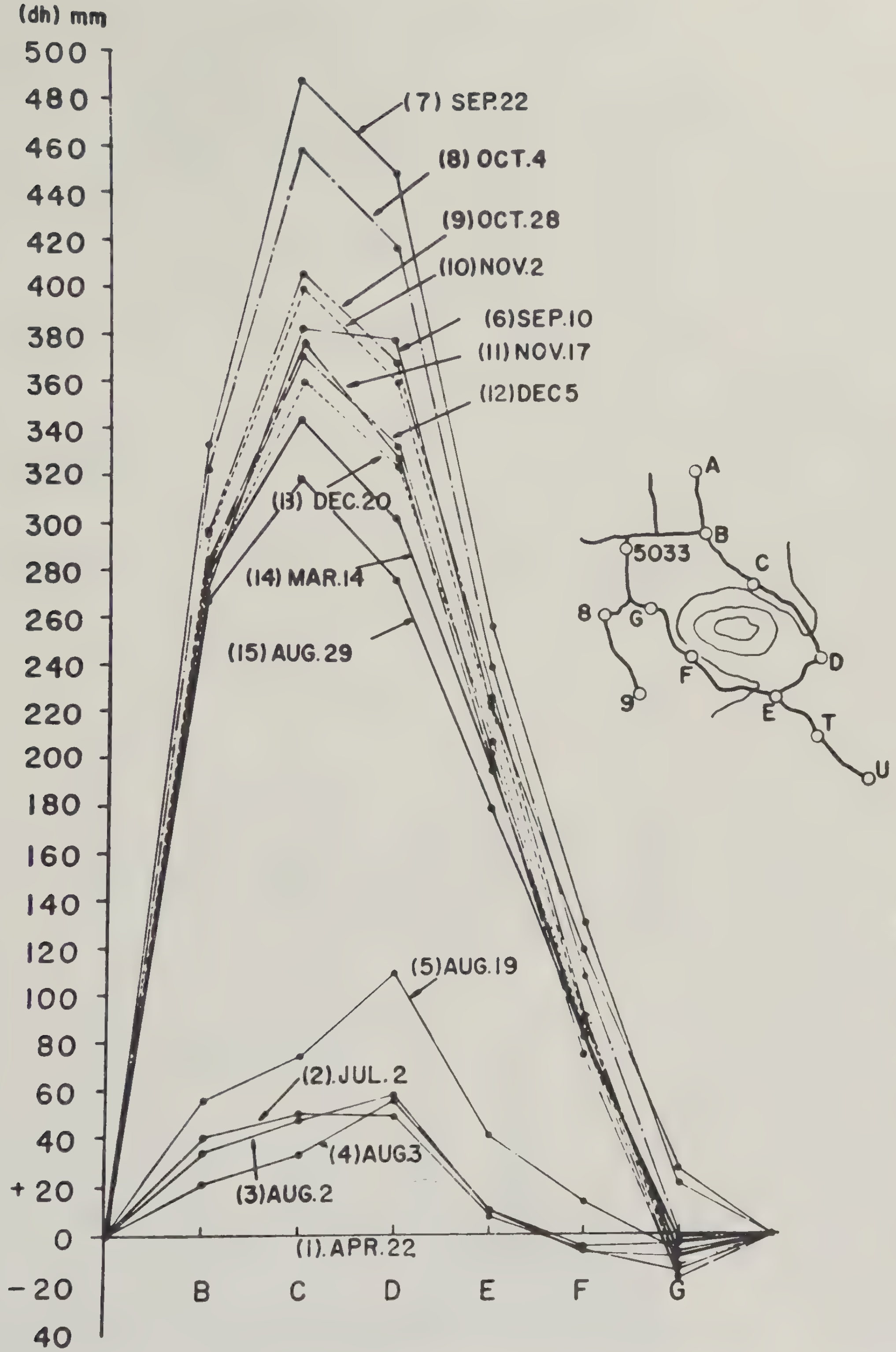

Figure 20.4.9. Sequential profiles of vertical ground displacements along a leveling route just east of Matsushiro, around Mt. Minakami, from 22 April 1966 to 29 August 1967. Numbers in parentheses indicate chronological order of leveling surveys. Reproduced from Tsubokawa and others (1968).

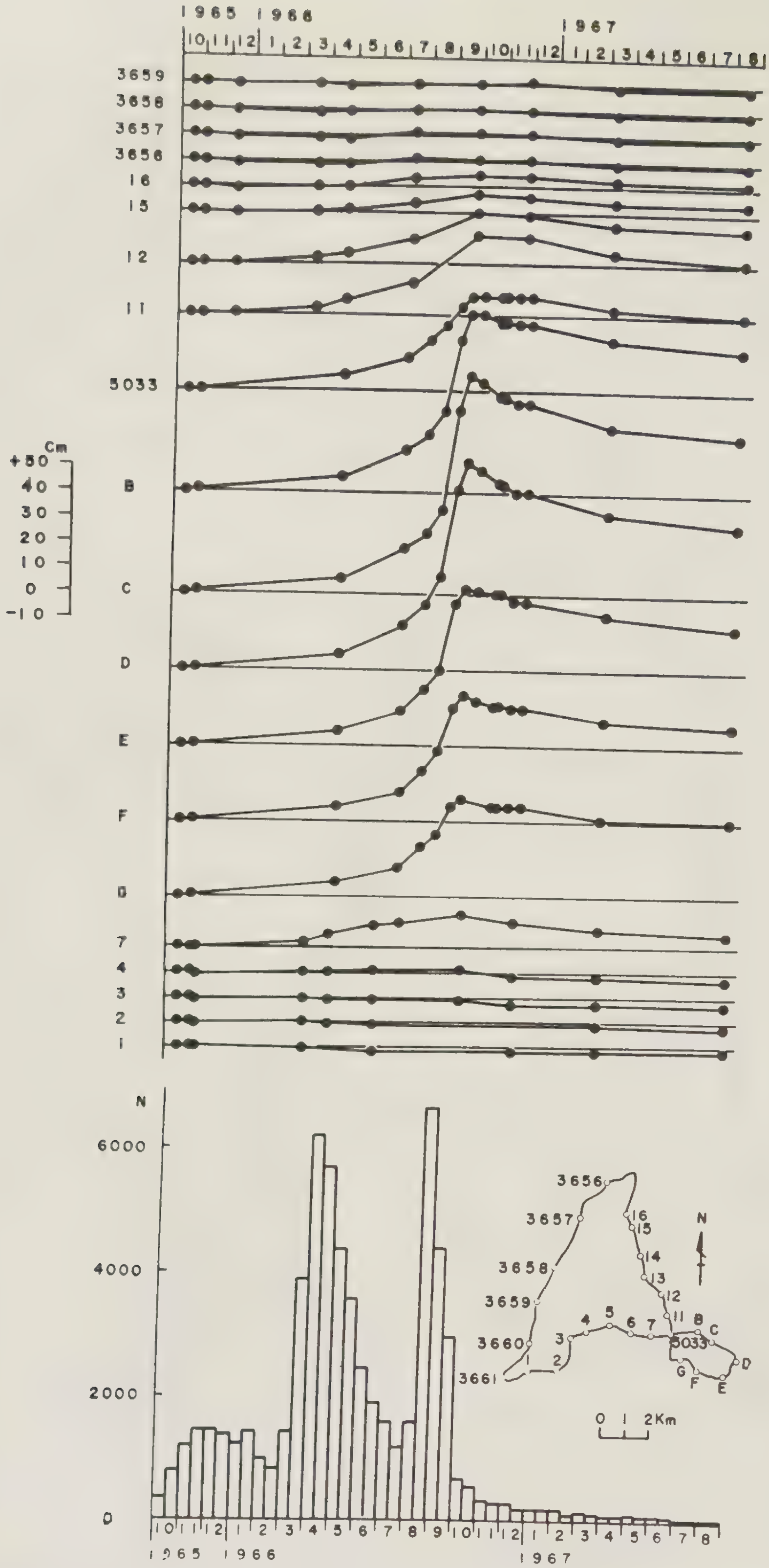

Figure 20.4.10. Top, history of vertical ground displacements at various numbered or lettered bench marks (inset). Bottom, biweekly numbers of earthquakes from October 1965 to August 1967. Both figures from Tsubokawa and others (1968). See figure 20.4.9 for profiles of vertical ground displacements through time.

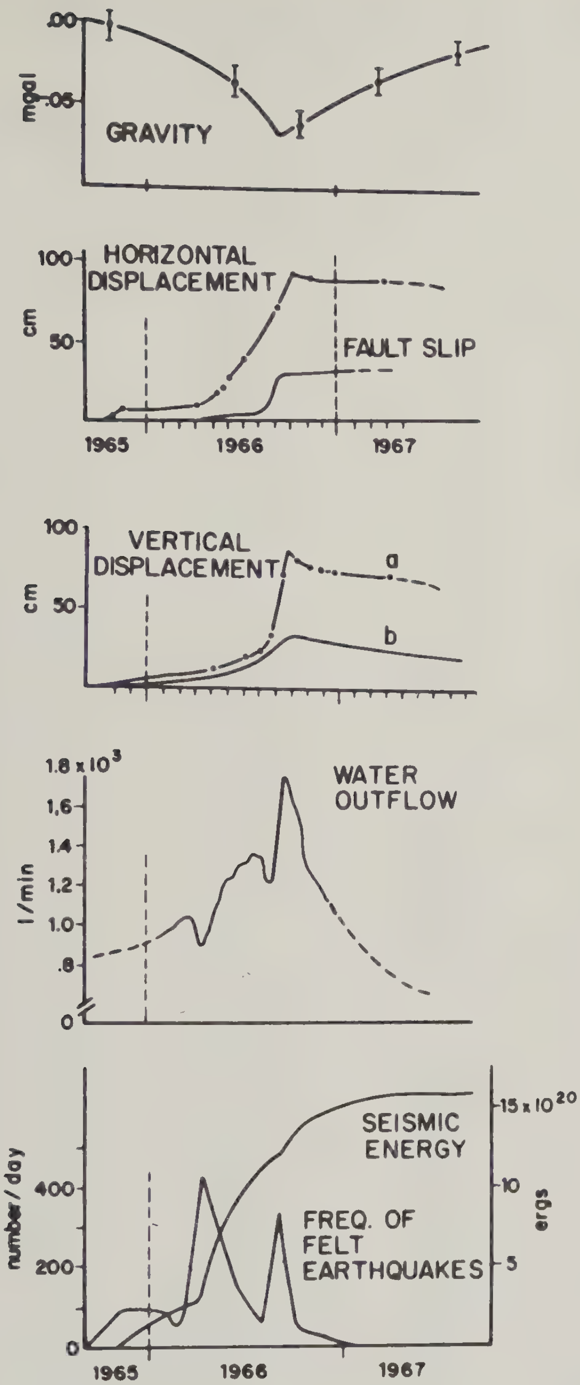

Figure 20.4.11. Temporal variations of deformation, water outflow, seismicity, and gravity at Matsushiro, 1965-68, from Nur (1974). Note that each seismic episode is preceded by declining outflow of ground water and followed by increased outflow. By the end of 1967, ground subsidence was 10-35 percent of peak uplift, whereas gravity had recovered almost completely, indicating net increase of mass.

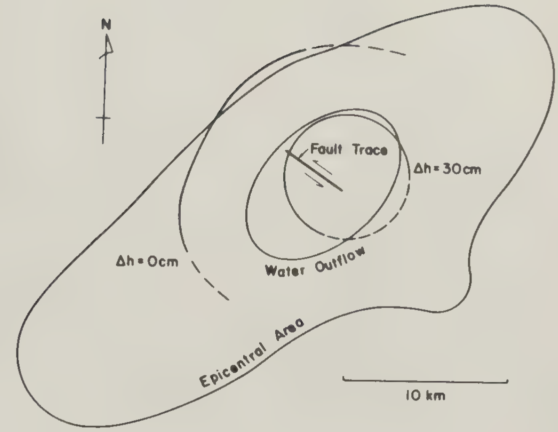

Figure 20.4.12. Spatial distribution of seismicity, water outflow, upheaval, and faulting around Matsushiro during the 1965-68 unrest (Nur, 1974).

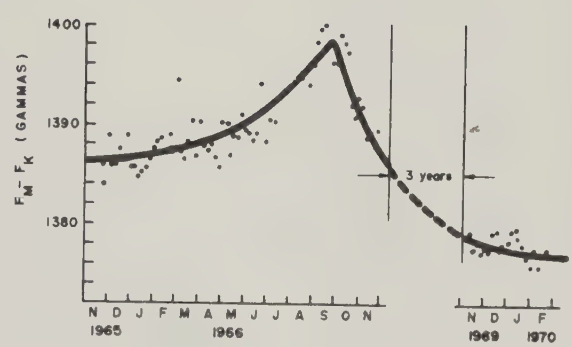

Figure 20.4.13. Five-day means of local magnetic-field differences between stations at Matsushiro and Kanozan, 1965-70 (Stuart and Johnston, 1975).

PART 4: SELECTED EPISODES OF HISTORICAL UNREST IN NONCALDERA SETTINGS (continued)
See inside back cover for explanation and abbreviations

SOCORRO

Latitude Longitude (degrees)	Tectonic setting	Age of latest volcanism	Youngest volcanic rock types	Restless years	Type and duration of unrest ESTU STHF MGTF H Te	Associated eruption?
34.00N 107.00W	Extension, with left-lateral shear on ENE-trending fault(?)	Pliocene	b	1849-50	xx-- ---- ---- - --	none
				1904	xx-- ---- ---- - --	none
				1906-07	xx-- ---- ---- - --	none
				1960's-87+	GG-G ---- --?- ? --	none

TECTONIC/GEOLOGIC SETTING

At least seven overlapping and nested cauldrons of Oligocene to Miocene age lie immediately west of Socorro, New Mexico (fig. 20.5.1) (Chapin and others, 1978). The easternmost and next to the youngest of these, the Socorro cauldron, formed approximately 27 m.y. B.P. It lies wholly within the Rio Grande rift and also lies atop the Morenci lineament, an inferred ENE-WSW-trending transverse shear zone (Chapin and others, 1978). The caldera also lies at the southern tip of an inferred, large, midcrustal magma body (Rinehart and others, 1979; Brocher, 1981). Neotectonic activity in the Rio Grande rift has been summarized by Riecker (1979).

According to Chapin and others (1978), "caldera collapse was followed by resurgent doming and accumulation of moat volcanics and sediments. After a long lull in magmatism...renewed rhyolitic magmatism occurred during the interval 12 to 7 m.y. ago. After another quiet spell, basaltic lava flows were emplaced at approximately 4 m.y. ago."

HISTORICAL ACTIVITY

Anomalous seismicity and uplift have occurred in an area approximately 85 km in diameter extending northward from Socorro (figs. 20.5.1-20.5.4). Swarms are known to have occurred in 1849-50, 1904, 1906-07, and from the early 1960's to the present. Microearthquake swarms have been persistent since a seismometer network was established in 1962. Since then, all earthquakes have been less than 13.5 km deep, mostly 5-10 km deep. Seismic activity at Socorro is significantly greater than in adjacent parts of the rift.

The center of uplift is approximately 25 km north of Socorro, within the Rio Grande rift but outside the Socorro cauldron (Reilinger and Oliver, 1976; Reilinger and others, 1980) (figs. 20.5.2-20.5.6). Maximum observed uplift is 20 cm relative to points outside the rift. The average rate of uplift was approximately 0.23 cm/yr from 1912 to 1951 and 0.18 cm/yr from 1951 to 1980 (Larsen

SOCORRO (continued)

HISTORICAL ACTIVITY (continued)

and others, 1986). Uplift in the nearby Belen-Albuquerque basin may be an extension of the Socorro uplift, or it may be a similar, related uplift in an adjacent segment of the rift.

No significant strain accumulation in the Socorro area was detected by precise trilateration measurements across the Rio Grande rift during 1972-84 (Savage and others, 1985) (figs. 20.5.7-20.5.9). The absence of detectable strain accumulation places an upper limit (2 standard deviations) of 3 mm/yr on east-west spreading across the 100-km-wide rift.

A roughly twofold increase in specific conductance and hardness of water from two wells near Socorro from 1951 to 1962 was tentatively interpreted by Bushman (1963) as related to pumping in the area.

COMMENTS

The seismicity and uplift occur directly above a crustal discontinuity inferred to be a sill-shaped magma body at a depth of 18-20 km, with a minimum areal extent of 1700 km^2 (Rinehart and others, 1979; Sanford and others, 1979; Brocher, 1981). Uplift and seismicity could be explained by an inflation of the inferred magma body at a rate of 0.01-0.02 km^3/yr. However, at this inflation rate, the crustal thickness would double in 10 m.y., which is not observed. Therefore, Reilinger and others (1980) infer that inflation of the magma body must be "oscillatory or episodic on the longer time scale."

Although the relation between historical activity and the Socorro cauldron is not entirely clear, recent activity is much more extensive than the old cauldron and seems to be more closely related to regional rifting and a larger magma reservoir than to any residual magma of the Socorro cauldron.

REFERENCES

Brocher, T.M., 1981, Geometry and physical properties of the Socorro, New Mexico, magma bodies: Jour. Geophys. Res., v. 86, no. B10, p. 9420-9432.

Bushman, F.X., 1963, Ground water in the Socorro Valley, in Kuellmer, F.J., ed., Guidebook of the Socorro region: New Mexico Geol. Soc., 14th Field Conf., p. 155-159.

Chapin, C.E., Chamberlin, R.M., Osburn, G.R., White, D.W., and Sanford, A.R., 1978, Exploration framework of the Socorro geothermal area, New Mexico: New Mexico Geol. Soc. Spec. Publ. 7, p. 115-129.

Hall, F.R., 1963, Springs in the vicinity of Socorro, in Kuellmer, F.J., ed., Guidebook of the Socorro region: New Mexico Geol. Soc. 14th Field Conf., p. 160-170.

SOCORRO (continued)

REFERENCES (continued)

Larsen, S., Reilinger, R., and Brown, L., 1986, Evidence of ongoing crustal deformation related to magmatic activity near Socorro, New Mexico: Jour. Geophys. Res., v. 91, no. B6, p. 6283-6292.

Reilinger, R., and Oliver, J., 1976, Modern uplift associated with a proposed magma body in the vicinity of Socorro, New Mexico: Geology, v. 4, p. 583-586.

Reilinger, R., Oliver, J., Brown, L., Sanford, A., and Balazs, E., 1980, New measurements of crustal doming over the Socorro magma body, New Mexico: Geology, v. 8, p. 291-295.

Riecker, R.E., ed., 1979, Rio Grande rift: Tectonics and magmatism: Washington, D.C., Am. Geophys. Union, 438 p.

Rinehart, E.J., Sanford, A.R., and Ward, R.M., 1979, Geographic extent and shape of an extensive magma body at mid-crustal depths in the Rio Grande rift near Socorro, New Mexico, _in_ Riecker, R.E., ed., Rio Grande rift: Tectonics and magmatism: Washington, D.C., Am. Geophys. Union, p. 237-251.

Sanford, A.R., 1963, Seismic activity near Socorro, _in_ Kuellmer, F.J., ed., Guidebook of the Socorro region: New Mexico Geol. Soc. 14th Field Conf., p. 146-151.

Sanford, A.R., Olsen, K.H., and Jaksha, L.H., 1979, Seismicity of the Rio Grande rift, _in_ Riecker, R.E., ed., Rio Grande rift: Tectonics and magmatism: Washington, D.C., Am. Geophys. Union, p. 145-168.

Savage, J. C., Lisowski, M., and Prescott, W. H., 1985, Strain accumulation in the Rocky Mountain states: Jour. Geophys. Res., v. 90, no. B12, p. 10,310-10,320.

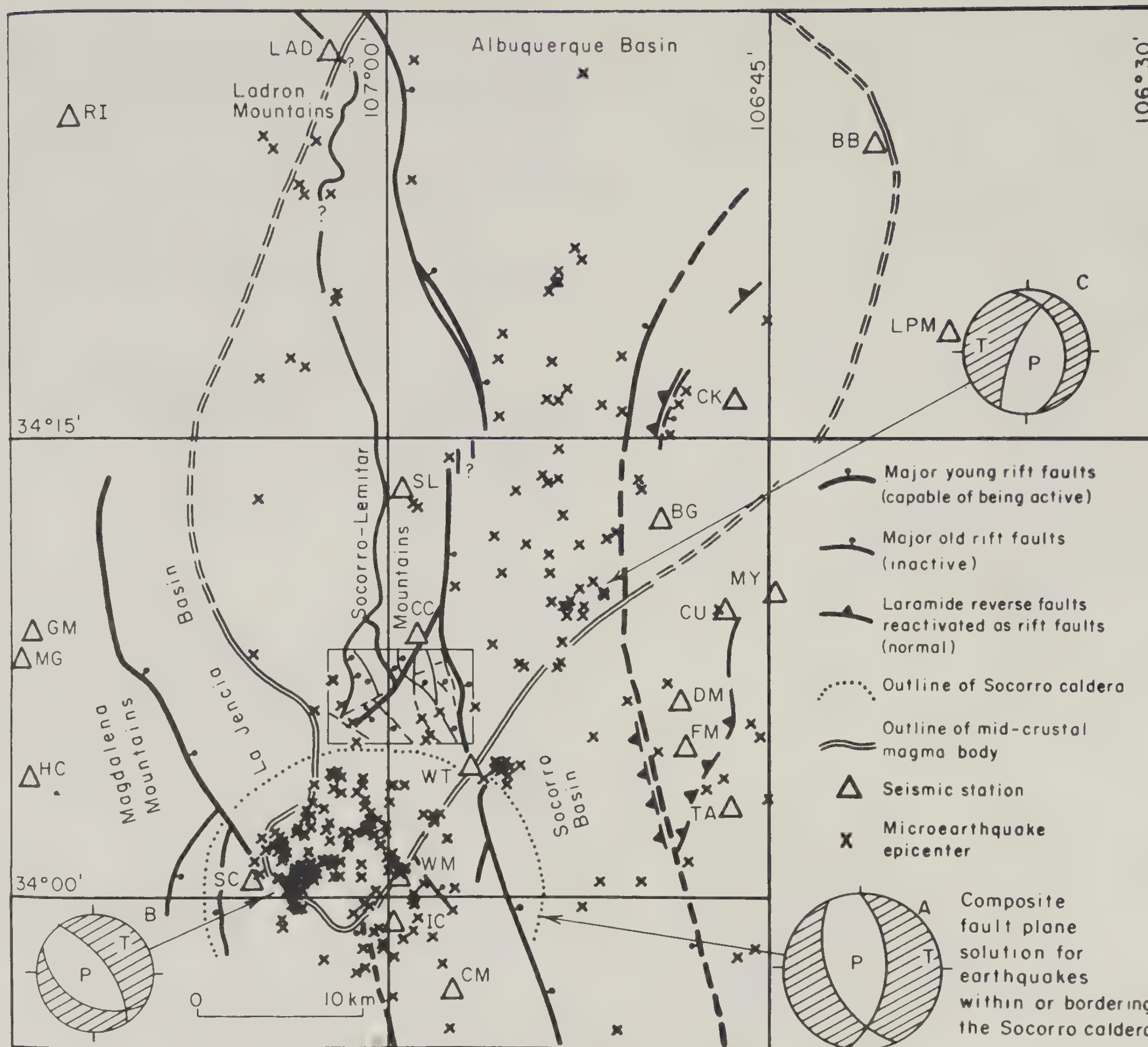

Figure 20.5.1. Rio Grande rift in vicinity of Socorro, New Mexico, showing epicenters of microearthquakes in relation to major faults, margins of a midcrustal layer of magma, and Tertiary Socorro Caldera (Sanford and others, 1979). Copyright by the American Geophysical Union.

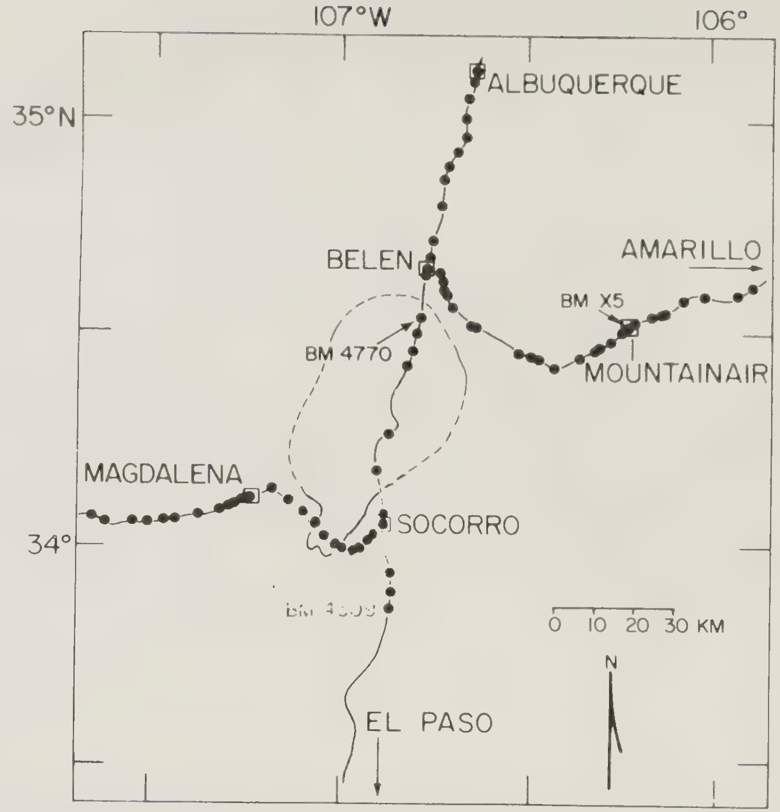

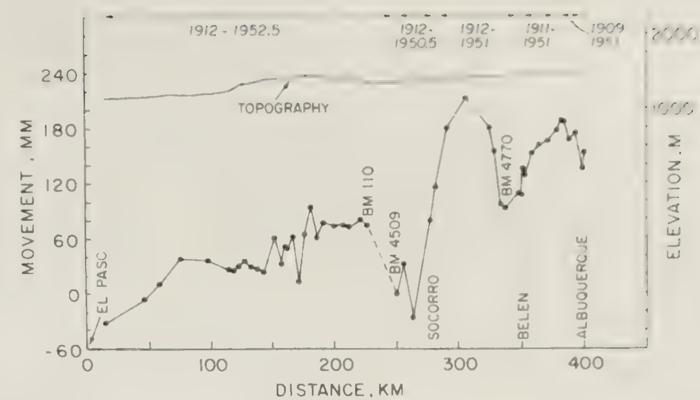

Figure 20.5.2. Top left, Locations of leveling routes and bench marks (dots) near Socorro, New Mexico, from Reilinger and others (1980). Outline of an inferred midcrustal magma body also is shown.

Figure 20.5.3. Top right, Elevation-change profiles and topography from El Paso, Texas, to Albuquerque, New Mexico, along route shown in figure 20.5.2 (Reilinger and others, 1980). Dates of leveling at top.

Figure 20.5.4. Bottom right, Contour map of vertical crustal movement in Socorro-Albuquerque area, from Reilinger and others (1980). Contours represent deformation that accumulated during a 40-year period or total movement between 1934 and 1958 (see text). Contour interval is 40 mm. Ruled area shows location of magma body; leveling routes and bench marks (dots) also shown.

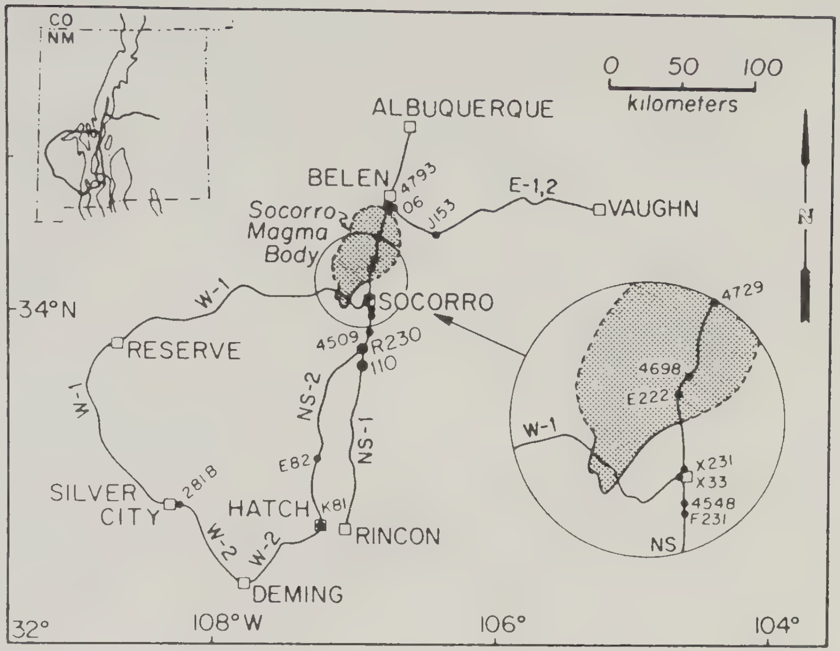

Figure 20.5.5. Leveling routes in Socorro area, from Larsen and others (1986). Inset at top left shows leveling lines relative to New Mexico and Rio Grande rift. Midcrustal Socorro magma body is shown by hachured pattern. Bench marks shown as solid dots. Copyright by the American Geophysical Union.

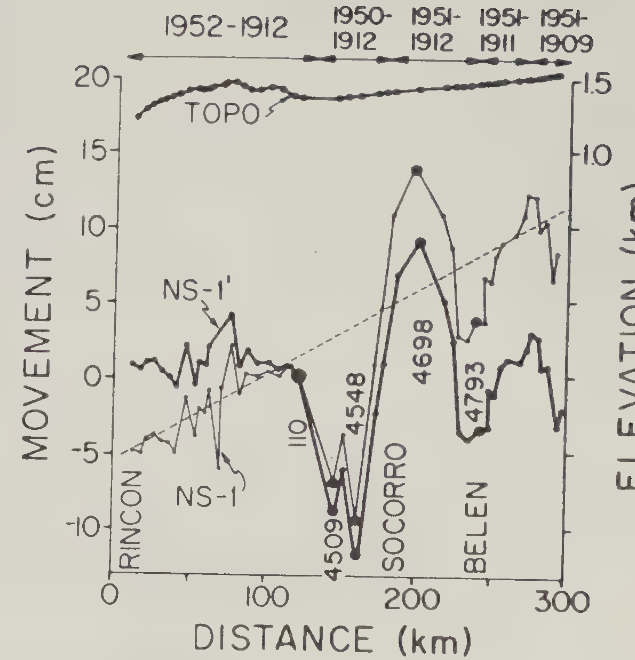

Figure 20.5.6. Elevation-change profiles and topography from Rincon to Albuquerque along the leveling route shown in figure 20.5.5 (Larsen and others, 1986). Dates of leveling are indicated at top of plot. Bench marks are shown as solid dots. Dashed line represents regional trend, possibly due to systematic error or long-wavelength tectonic tilt. Copyright by the American Geophysical Union.

Figure 20.5.7. Socorro strain network, from Savage and others (1985). Extent of Rio Grande rift is indicated by dotted lines. Copyright by the American Geophysical Union.

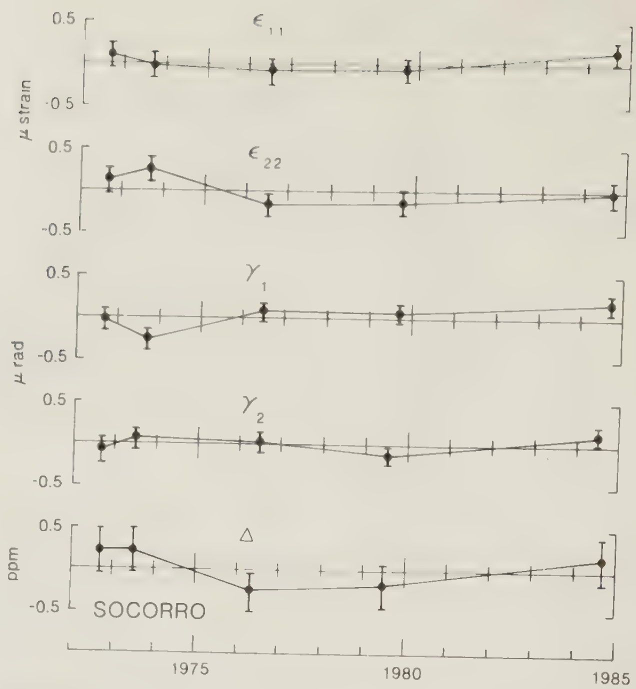

Figure 20.5.8. Line-length changes as a function of time for each of the lines in Socorro strain network (see figure 20.5.7), 1972-84 (Savage and others, 1985). Error bars, 1 standard deviation on either side of points. Copyright by American Geophysical Union.

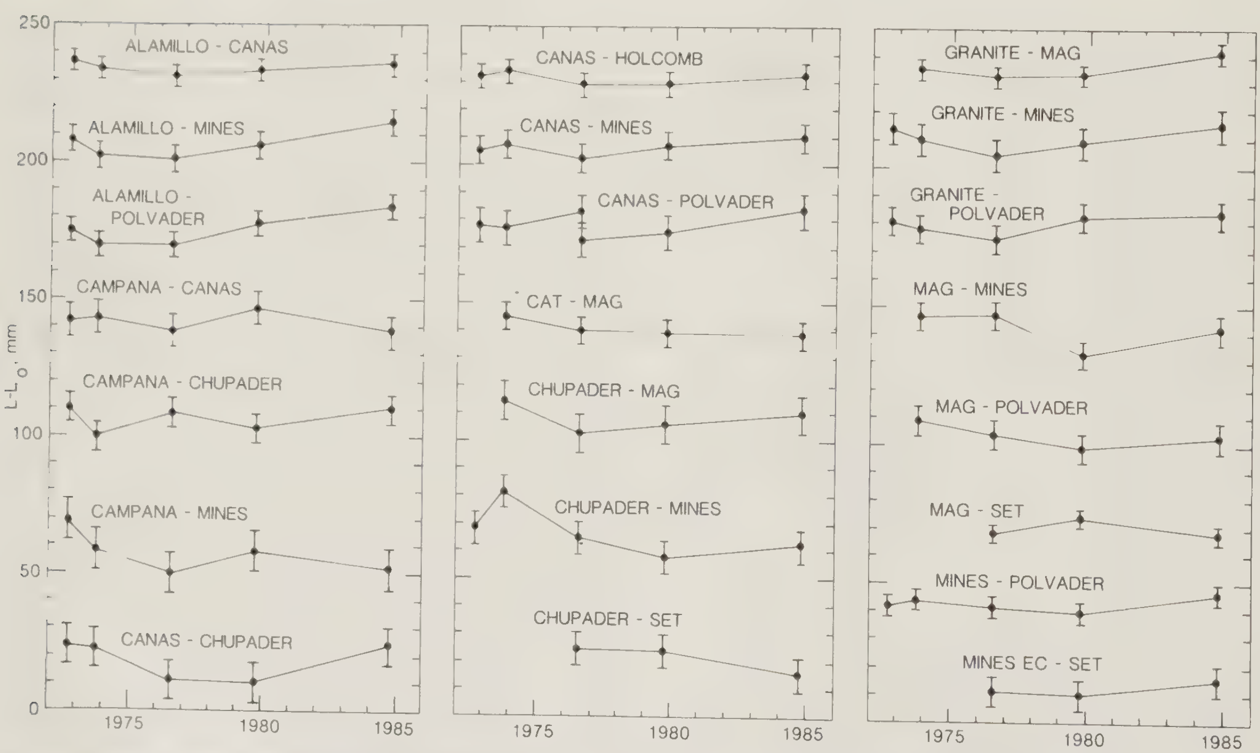

Figure 20.5.9. Strain accumulation in Socorro network, 1972-84 (Savage and others, 1985). Strains are referred to a geographic coordinate system (the 1-axis directed east and the 2-axis directed north). Error bars represent 1 standard deviation on either side of plotted points. Copyright by the American Geophysical Union.

MONTSERRAT
(Soufriere Hills)
CAVW # 16-00-05

Latitude Longitude (degrees)	Tectonic setting	Age of latest volcanism	Youngest volcanic rock types	Restless years	Type and duration of unrest ESTU STHF MGTF H Te	Associated eruption?
16.72N 62.18W	Compr	300 yr B.P.	58-63 pct SiO_2	1897-1900	FF-- ---- ---x x --	none
				1933-1937	FF-- ---- ---C x UQ	none
				1966-1967	FF-- -F-- ---F F --	none

TECTONIC/GEOLOGIC SETTING

Historical unrest on Montserrat has been in the vicinity of the Soufriere Hills, the youngest of many volcanic centers on this small island. The Soufriere Hills are a complex of andesitic domes; older andesitic domes and andesitic to basaltic lavas form nearby hills (fig. 20.6.1). In mapping to date (MacGregor, 1938; Rea, 1974), no evidence has been found that the Soufriere Hills lie within a caldera. Similarly, there is no suggestion from either mapping or geophysical studies that the Soufriere Hills are underlain by any large magma reservoir. A strong NW-SE lineament connects several vents, including the Soufriere Hills.

Lavas on Montserrat in general contain 50-63 percent SiO_2; three samples from the Soufriere Hills proper had 58-63 percent SiO_2. A few blocks of lava and pumice show compositional banding, 58 percent versus 62 percent SiO_2 (Rea, 1974).

HISTORICAL ACTIVITY

The southern half of Montserrat, in the vicinity of the Soufriere Hills Volcano, has experienced three volcano-seismic crises within the past century. A series of earthquakes occurred during 23-27 April 1897; one particularly strong event (MMI= 8) occurred on 25 April 1897. Even stronger earthquakes of this episode occurred in October 1900, near the end of the unrest. Houses, churches, and windmills were heavily damaged on and near the northern and western flanks of the volcano, and solfataric activity intensified about the time of the earthquakes. Another strong earthquake occurred near Guadeloupe on 29 April 1897, suggesting that the Montserrat activity was related to regional tectonic strain. Perhaps coincidentally, the 1897-1900 earthquakes followed the heaviest rains and flooding in recent years, in 1896.

MONTSERRAT (continued)

HISTORICAL ACTIVITY (continued)

Beginning in March 1933, solfataras on the lower slope of the Soufriere Hills began to show intensified activity. Earthquake swarms began in July 1933, and increased in frequency and intensity to a peak in November 1935 (figs. 20.6.2-20.6.4). Several thousand shocks were felt on the island during 1933-37. Those measured were shallow (1-2 km; Perret, 1939). At least 28 were of "the seventh or eighth magnitudes of the seismic scale" (Perret, 1939); the two strongest earthquakes of the series (12 December 1934 and 6 May 1935) had modified Mercalli intensities of 8 (Robson, 1964). Earthquake damage and solfataric activity were in essentially the same zone, north and northwest of the Soufriere Hills, as they had been in the 1897-1900 episode. The frequency of earthquakes varied seasonally, with maxima in May and November-December of each year. Increased H_2S emission often preceded the 1933-37 earthquake swarms by a few days, but it also intensified after the larger earthquakes. On 10 November 1935, a strong tectonic earthquake occurred 100 km north of Montserrat; activity at Montserrat decreased thereafter, although it did not fully return to background levels until late 1937.

Earthquakes were felt in January and February 1966 ($\underline{M}_{max}$=4.0), and a seismic array was installed in March and April 1966. The epicentral region was broad and crudely elongate in a NW-SE direction, coincident with the lineament connecting the Soufriere Hills and several other vents (figs. 20.6.5-20.6.8). It is not certain whether this represents a slight southward shift relative to the activity of 1933-37, because the latter activity was not precisely located. In the 1966-67 swarm, earthquake depths varied systematically, averaging 5.2 km in April and May 1966, rising to a minimum of 2.8 km (average) in July-September, deepening to an average of 13.1 km in April 1967, and ending at an average of 9.7 km in November 1967. The total seismic energy release was 3×10^{16} ergs, equivalent to a $\underline{M}$=4.5 earthquake. The $\underline{b}$-value of the earthquakes was 0.8 throughout the entire series. Seismic energy release reached seasonal maxima in May 1966, November-December 1966, and October-November 1967 (similar to the seasonality observed during 1933-37).

Three water-tube tiltmeters, located on the lower flanks of the Soufriere Hills about 3-4 km from the summit, indicated inflation centered just south of the summit area, coincident with the center of seismicity (figs. 20.6.9, 20.6.10). Inflation was greatest in July-October 1966 (maximum recorded rate of tilt=12 microradians/month). Inflation continued at a lower rate from October 1966 until January 1967, deflation occurred during January-March 1967, and inflation occurred again during March-September 1967. The net change was inflationary. Fumarolic activity increased sympathetically with inflation.

COMMENTS

The Royal Society mission (Powell, 1937, 1938), Perret (1939), and Shepherd and others (1971) have unanimously inferred that the unrest has been due to episodic, small magmatic intrusions beneath the Soufriere Hills. Perret thought a (phreatic) explosion from one of the solfataras would be the most likely outcome, whereas Shepherd and others considered an eruption from the summit of the Soufriere Hills to be more likely.

MONTSERRAT, Latitude 16.72N, Longitude 62.18W, CAVW # 16-00-05

MONTSERRAT (continued)

REFERENCES

MacGregor, A.G., 1938, The volcanic history and petrology of Montserrat, with observations on Mt. Pelee, in Martinique: Trans. Roy. Soc. (London), v. B229, p. 1-90.

Perret, F.A., 1939, The volcano-seismic crisis at Montserrat, 1933-1937: Carnegie Inst. Washington Publ. 512, 76 p.

Powell, C.F., 1937, Royal Society expedition to Montserrat, B.W.I.: Preliminary report on seismic observations: Proc. Roy. Soc. (London), v. A158, p. 479-494.

----- 1938, Royal Society expedition to Montserrat, B.W.I.: Final report: Trans. Roy. Soc. (London), v. A237, p. 1-34.

Rea, W.J., 1974, The volcanic geology and petrology of Montserrat, West Indies. Jour. Geol. Soc. London, v. 130, p. 341-366.

Robson, G.R., 1964, An earthquake catalogue for the eastern Caribbean, 1530-1960: Bull. Seismol. Soc. Am., v. 54, no. 2, p. 785-832.

Shepherd, J.B., Tomblin, J.F., and Woo, D.A., 1971, Volcano seismic crisis in Montserrat, West Indies, 1966-1967: Bull. Volcanol., v 35, p. 143-163.

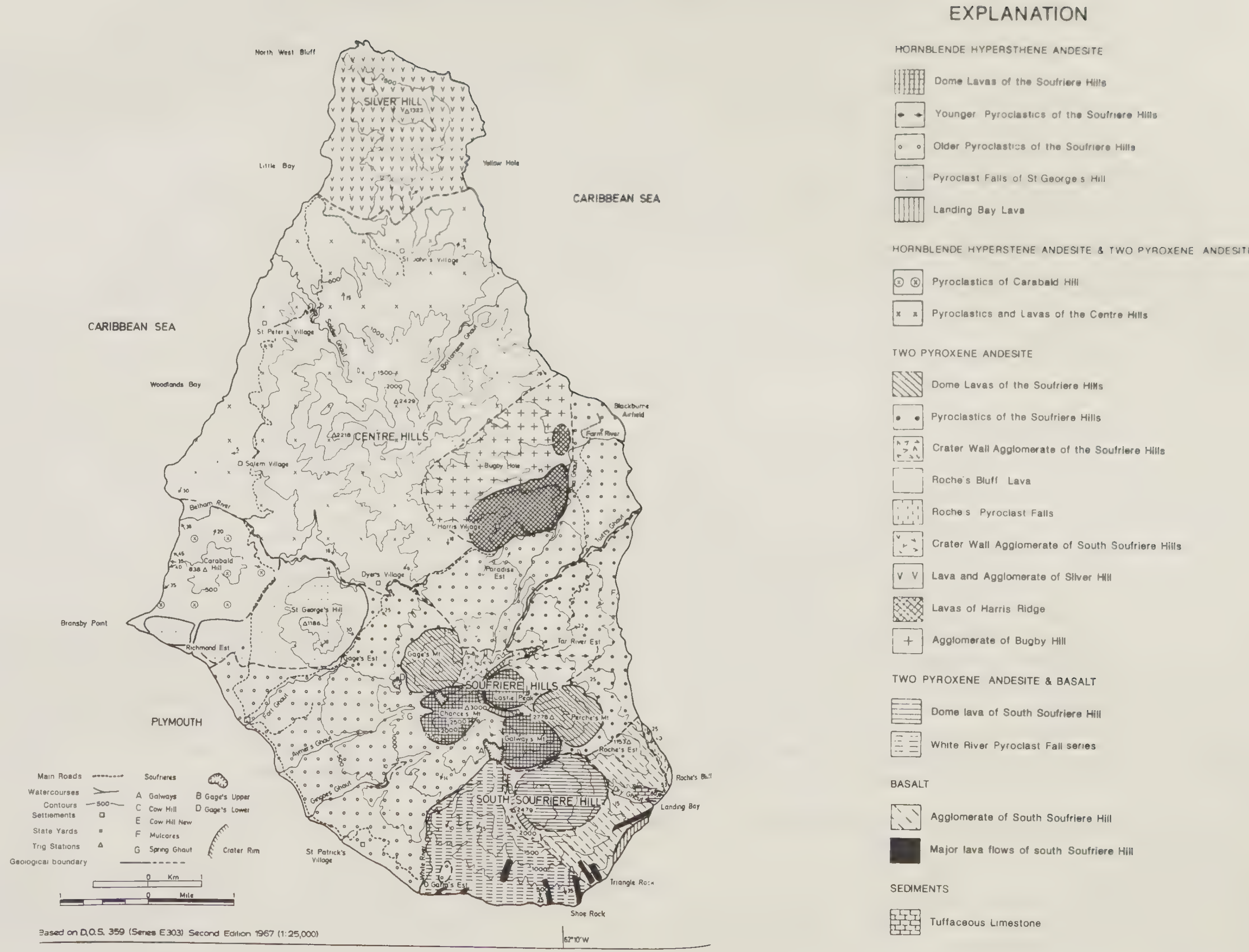

Figure 20.6.1. Geologic sketch map of Montserrat, Lesser Antilles, from Rea (1974). Most recent eruptions have been from Soufriere Hills. Reproduced by permission of the Geological Society of London.

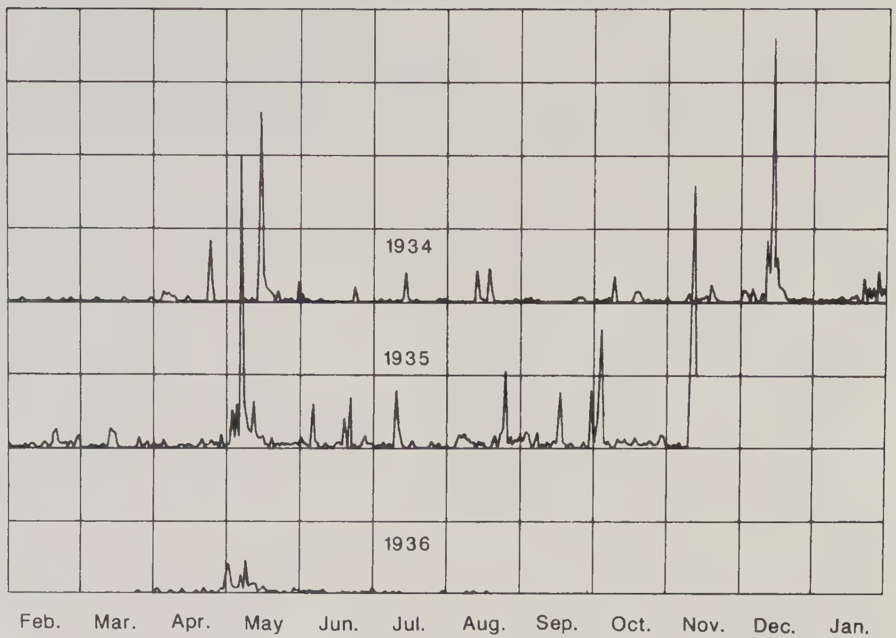

Figure 20.6.2. Daily number of earthquakes at Montserrat during 1934-36, from Powell (1937). Data for the period from 12 November 1935 to 24 March 1936 were unavailable, but seismic activity was minor.

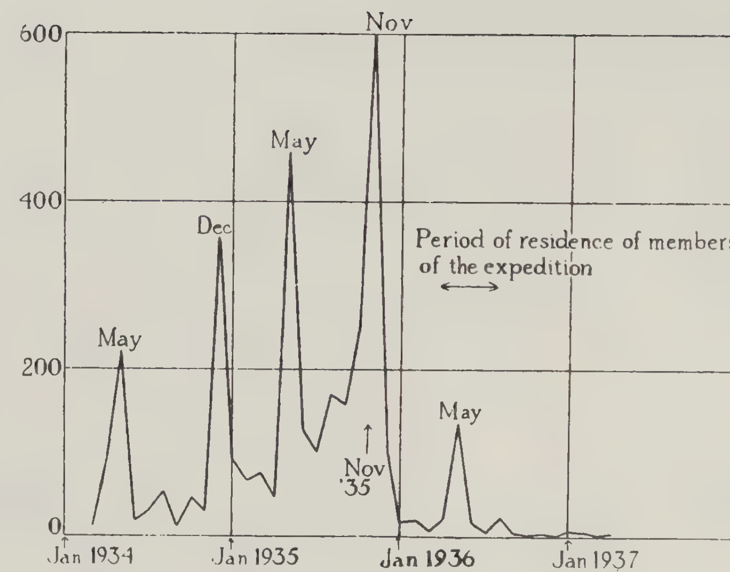

Figure 20.6.3. Monthly number of earthquakes at Montserrat during 1934-37, from Powell (1938).

Figure 20.6.4. Epicenters for earthquakes at Montserrat during 1934-37, from Powell (1938).

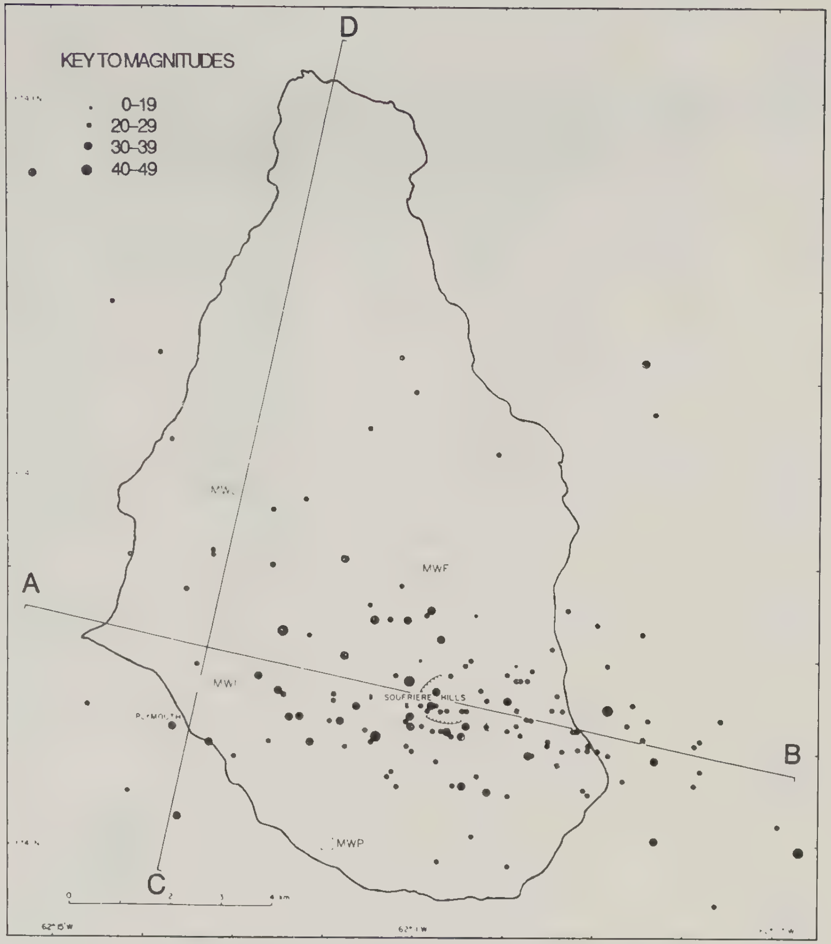

Figure 20.6.5. Distribution of epicenters during the 1966-67 seismic crisis at Montserrat, from Shepherd and others (1971). Solid circles, epicenters; squares, seismograph stations; MWI, Grove; MWL, Salem; MWF, Farrels; MWP, St. Patrick's.

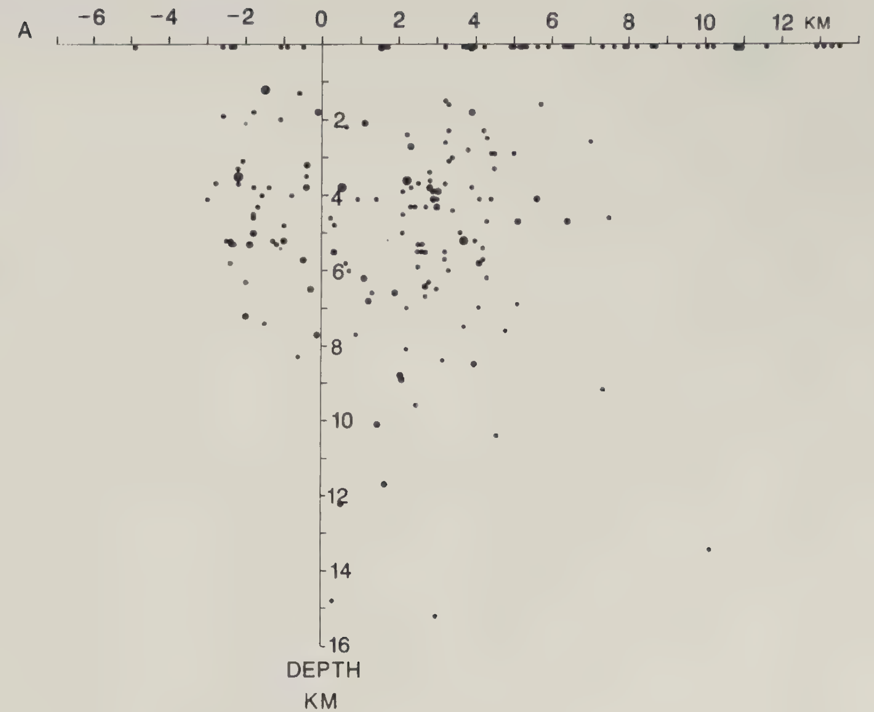

Figure 20.6.6. Cross section along line A-B in figure 20.6.5, showing all hypocenters projected onto a vertical plane (Shepherd and others, 1971). Earthquake magnitude is indicated by size of dot, as in figure 20.6.5.

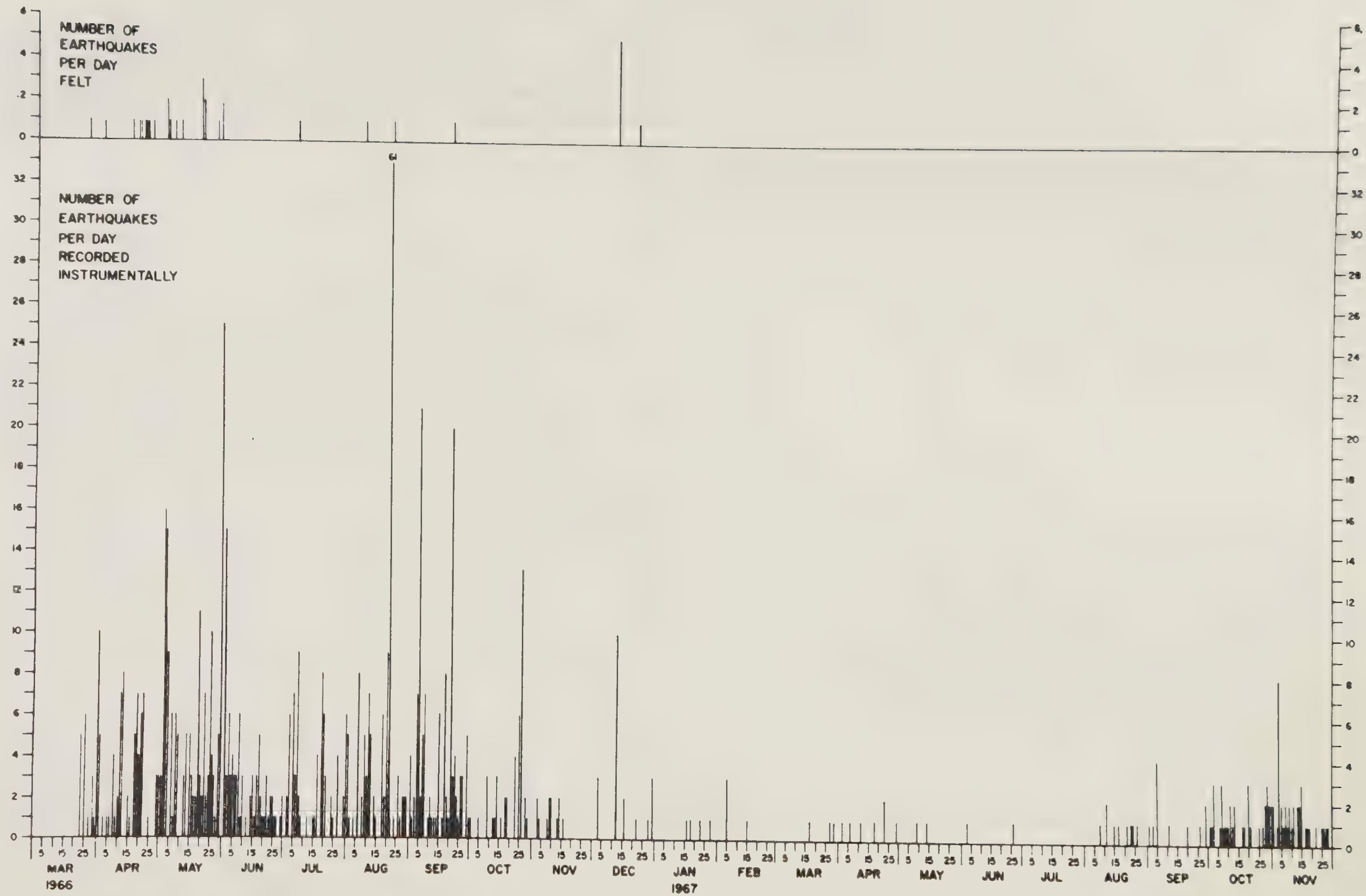

Figure 20.6.7. Daily number of local earthquakes during the 1966-67 seismic crisis at Montserrat, from Shepherd and others (1971).

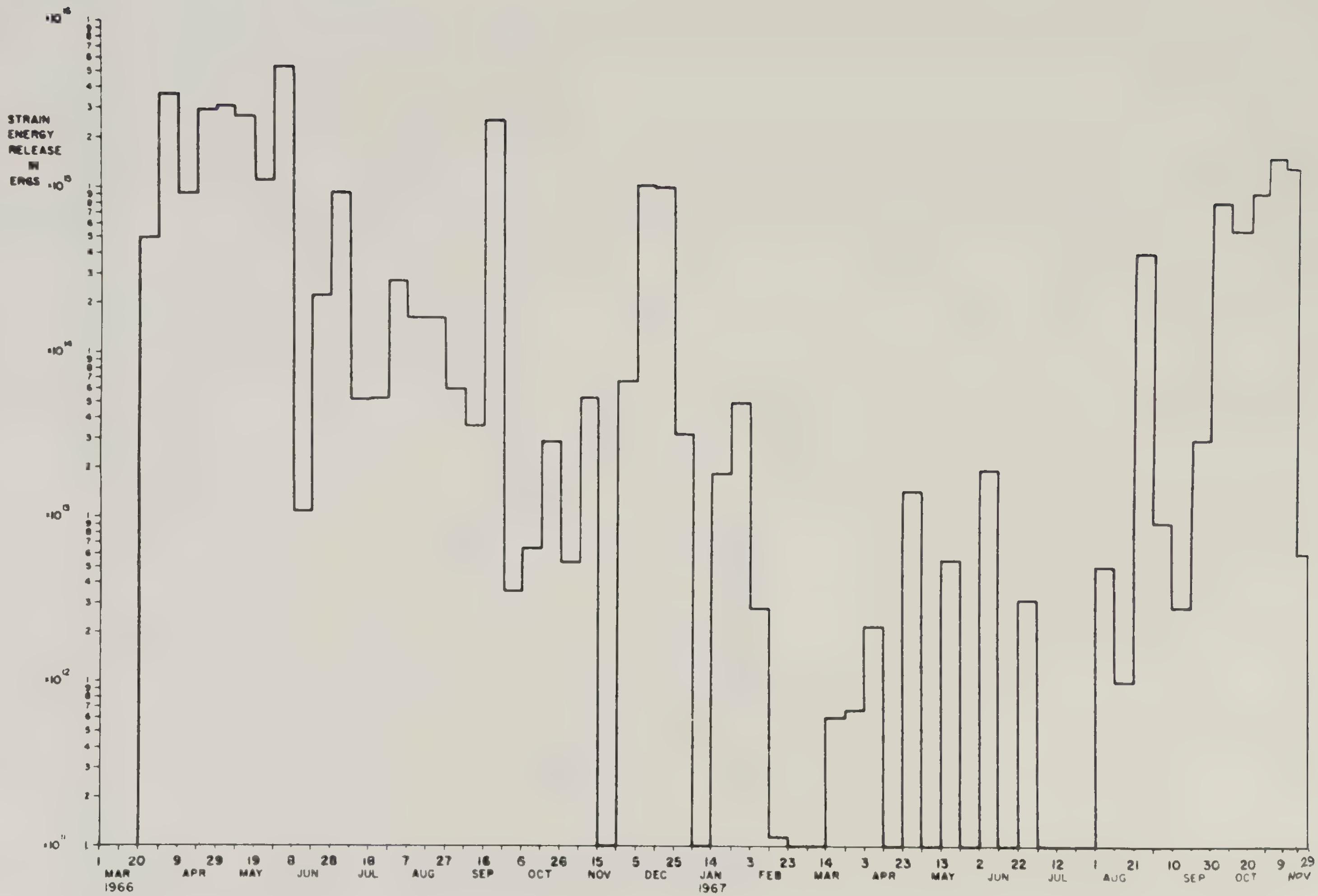

Figure 20.6.8. Earthquake strain energy release during the 1966-67 seismic crisis at Montserrat, from Shepherd and others (1971).

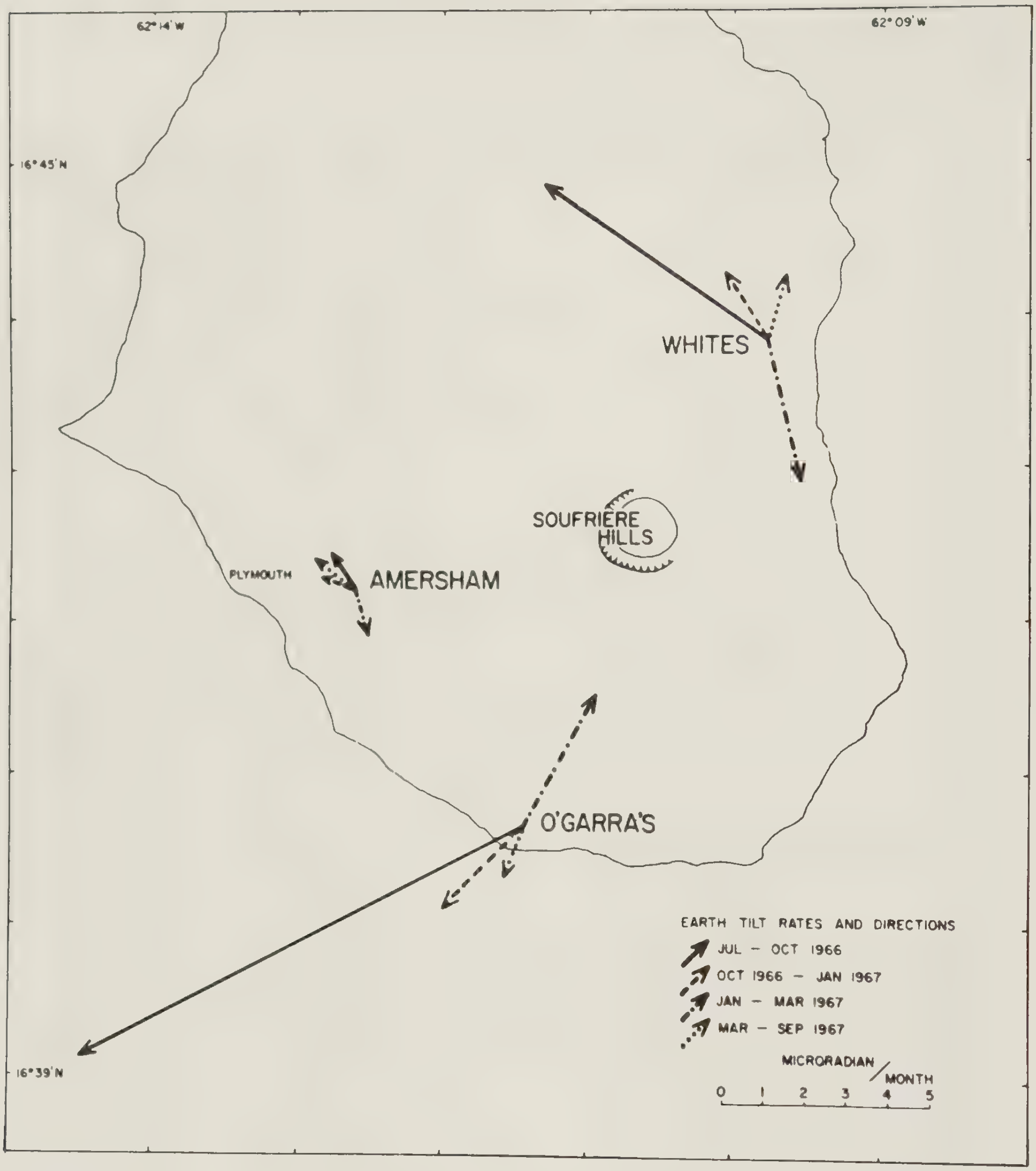

Figure 20.6.9. Earth-tilt rates and directions during the 1966-67 seismic crisis at Montserrat, from Shepherd and others (1971). Tilts were measured with a long-base water-tube tiltmeter.

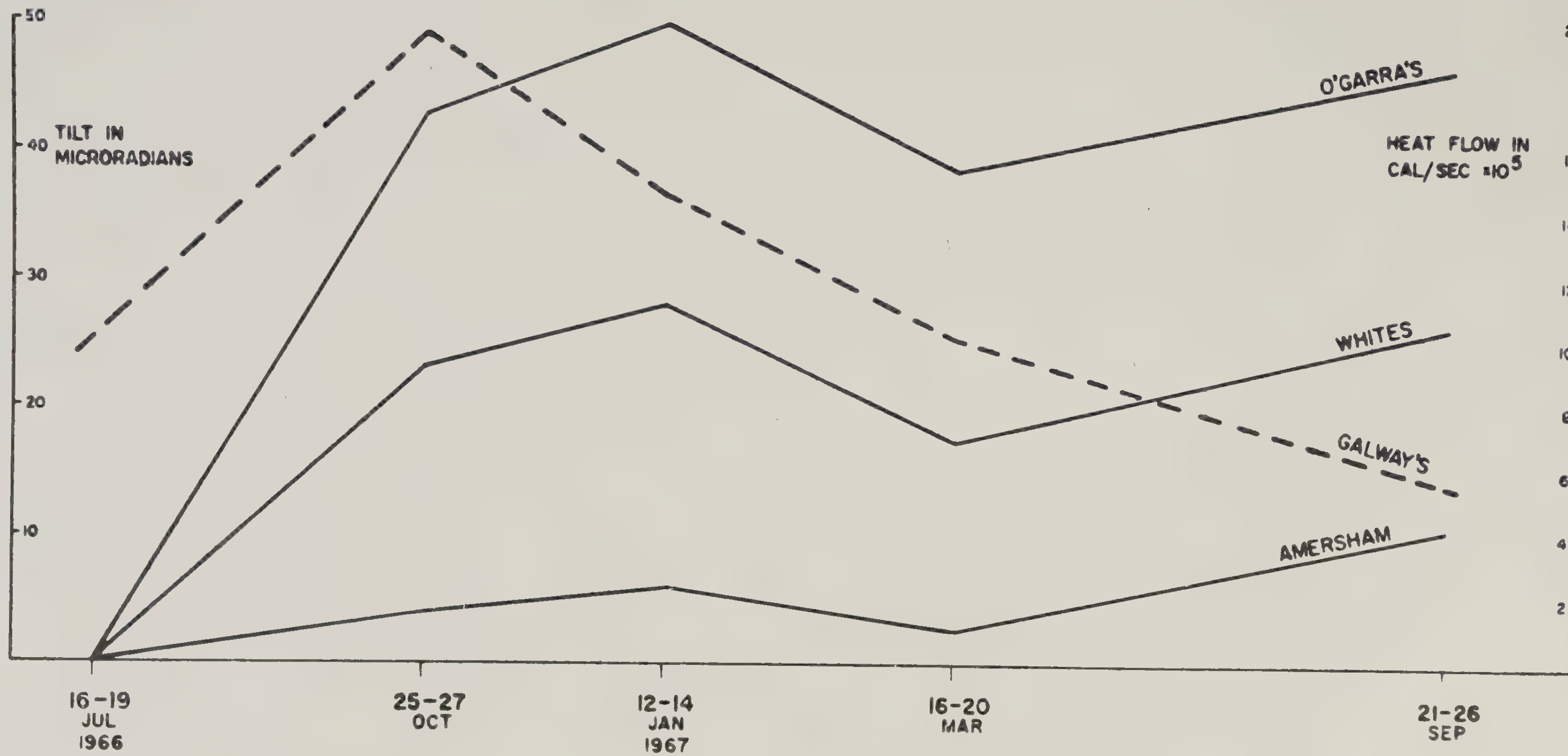

Figure 20.6.10. Comparison of rates of earth tilt (solid lines) with total heat flow at Galway's soufriere (dashed line) during the 1966-67 seismic crisis at Montserrat, from Shepherd and others (1971).

PART 5: Large Quaternary Calderas Not Known to Have Shown Historical Unrest

This section has two purposes:

(1) to provide a basis for comparing numbers of restless vs. quiet calderas of similar size and age;

(2) to elicit information from readers about unrest at some of the calderas listed, or about additional, quiet calderas. The list of calderas in this section is certainly incomplete, and your corrections and additions are welcome.

PART 5: LARGE QUATERNARY CALDERAS NOT KNOWN TO HAVE SHOWN HISTORICAL UNREST

Caldera	CAVW number	Latitude	Longitude	Diameter	Age of latest collapse	Dominant magma composition	References
Vico	None	42.3N	12.3E	7	ca. 0.15 Ma	tephrite, tephrite phonolite	Sollevanti (1983)
Sacrofano -Baccano	None	42.1 N	12.4E	25 x 13?	0.4-0.3 Ma	leucite tephrite, phonolite	de Rita and others (1983)
Nabro	02-01-101	13.35N	41.68E	8		rhyolite	IAVCEI (1973)
Mallahle	02-01-102	13.27N	41.65E	5		silicic	Mohr and Wood (1976)
Sorkale	02-01-103	13.27N	41.65E			rhyolite	IAVCEI (1973); CNR-CNRS Afar Team (1975)
Asavyo	02-01-104	13.07N	41.60E	8		silicic	Mohr and Wood (1976)
Oyma	02-01-104A	12.88N	41.62E	5		silicic	Mohr and Wood (1976)
Dabbahu (Moina)	02-01-113	12.63N	40.45E			basalt, trachyte, rhyolite	CNR-CNRS Afar Team (1973, 1975)
Groppo	02-01-116	11.73N	40.25E			silicic	IAVCEI (1973)
Afdem	02-01-17A	9.50N	40.85E			rhyolite	IAVCEI (1973)
Chana (Arussi)	02-01-19A	8.90N	40.22E			rhyolite	IAVCEI (1973)
Gadamsa	02-01-23	8.35N	39.18E	ca. 10			Di Paola (1972)
Bora-Bericcio (Bericha)	02-01-24	8.18N	38.98E			silicic	Di Paola (1972)
Gademota	None	7.9N	38.6E	ca. 20		silicic	G. Gabriel (written commun., 1987)
Aluto	02-01-27	7.77N	38.78E	ca. 8		silicic	Di Paola (1972)

PART 5: LARGE QUATERNARY CALDERAS NOT KNOWN TO HAVE SHOWN HISTORICAL UNREST (continued)

Caldera	CAVW number	Latitude	Longitude	Diameter	Age of latest collapse	Dominant magma composition	References
Shalla(=O'A)	02-01-28	7.50N	38.50E	17	0.24 Ma	rhyolite	IAVCEI (1973);Mohr and Wood (1976)
Duguna	None	7.1 N	37.9	ca. 10		silicic	G. Gabriel (written commun., 1987)
Emuruangogolak	02-02-051	1.50N	36.33E	outer, 7x9 inner, 3x4	ca. 0.5 Ma	trachyte	Weaver (1976-77); Williams and others (1984)
Silali	02-02-052	1.15N	36.23E	5 x 7.5		trachyte	McCall (1968); Williams and others (1984)
Menengai	02-02-06	0.23S	36.10E	8 x 12	29 ka	trachyte	Leat and others (1984)
Longonot	02-02-10	0.92S	36.45E	ca. 7.5	<0.5 Ma	trachyte, hawaiite	Williams and others (1984)
Suswa	02-02-11	1.18S	36.35E	outer, 8x12 inner, 5	ca. 0.24 Ma	phonolite, trachyte	Johnson (1969); Williams and others (1984)
Embagai	02-02-12A	2.92S	35.83E			alkali basalt, trachyte, nephelinite	IAVCEI (1973)
Olmoti	02-02-12D	3.00S	35.65E			alkali basalt, trachyte, nephelinite	IAVCEI (1973)
Ngorongoro	02-02-12H	3.17S	35.57E	16		alkali basalt, trachyte, nephelinite	Williams (1970); Searle (1972)
Ngurdoto	02-02-15A	3.30S	36.92E			nephelinite	IAVCEI (1973)
Ngozi	02-02-172	9.00S	33.55E			trachyte, phonolite, basalt	Harkin (1960); IAVCEI (1973)
Emi Koussi	02-05-021	19.70N	18.57E	14			Geze and others (1959)

PART 5: LARGE QUATERNARY CALDERAS NOT KNOWN TO HAVE SHOWN HISTORICAL UNREST (continued)

Caldera	CAVW number	Latitude	Longitude	Diameter	Age of latest collapse	Dominant magma composition	References
Tarso Yega	None			22			Geze and others (1959)
Tarso Tieroko	None	20.72N	17.86E	8		trachyte?	Geze and others (1959)
Tarso Voon	02-05-02	20.97N	17.17E	12 x 15		trachyte, andesite, rhyolite	Geze and others (1959)
Tarso Toon	None	21.05N	17.66E	12		trachyte?	Geze and others (1959)
Tousside	02-05-01	21.05N	16.42E	6			Geze and others (1959)
Maroa/ Whakamaru	04-01-24A	38.55S	176.05E	ca. 50	1.1-0.5 Ma	rhyolite	Wilson and others (1984, 1986)
Umboi (Talo)	05-01-06	5.59S	147.88E	13		silicic?	Johnson and others (1972)
Gallosuelo	05-02-10	5.33S	151.12E	13 x 10.5		andesite, dacite	Cooke and others (1976)
Bur ni Geureudong	06-01-04	4.82N	96.80E	30		andesite	Neumann van Padang (1951)
Singkarak	None	0.50S	100.50E	8 x 21		silicic	Verstappen (1973)
Hutapanjang	06-01-171	2.27S	101.60E	10 x 18		silicic	Posavec and others (1973) Rock and others (1982)
Gedongsurian	None	5.04S	104.23E	10 x 20		silicic	van Bemmelen (1949a)
Hulubelu	06-01-28	5.35S	104.60E	large		dacite, andesite	van Bemmelen (1931, 1949a, b) Neumann van Padang (1951)
Dano (Banten)	None	ca. 6.3S	106.0E	7 x 15		dacite	Katili (1983)
Buyan-Bratan	06-04-014	8.28S	115.13E	7 x 11		silicic	Purbo-Hadiwidjojo (1971)

PART 5: LARGE QUATERNARY CALDERAS NOT KNOWN TO HAVE SHOWN HISTORICAL UNREST (continued)

Caldera	CAVW number	Latitude	Longitude	Diameter	Age of latest collapse	Dominant magma composition	References
Poco Leok	06-04-07	8.41S	120.29E	6 x 6.75			Neumann van Padang (1972) Kusumadinata (1979)
Natib	07-03-082	14.72N	120.37E	7.5 x 4.5	ca. 70 ka	andesite, dacite	EBASCO (1978-79)
Sambe	08-03-001	35.15N	132.32E	6 x 8	16 ka	dacite	Ono and others (1981) Japan Assoc. Quat. Res. (1987)
Daisen	08-03-001B	35.37N	133.55E		46 ka	dacite	IAVCEI (1973)
Tateyama (Midagahara)	08-03-08	36.57N	137.60E	6 x 4	ca. 60 ka	andesite, dacite	Yamasaki and others (1966) Machida (1980) Kusakabe and others (1983)
Myoko	08-03-10	36.88N	138.12E		> 2 ka	andesite	Hayatsu (1976); Hayatsu and Arai (1980)
Tazawa	08-03-22B	39.75N	140.67E	ca. 6		dacite	IAVCEI (1973)
Hakkoda	08-03-28	40.65N	140.88E	8	2.1 Ma	andesite	Kuno (1962)
Akaigawa	08-05-04E	43.08N	140.82E	ca. 8	2.1 Ma	andesite, dacite	IAVCEI (1973); Ono and others (1981)
Kuttara	08-05-033	42.50N	141.18E	5?	11 ka	andesite-dacite	Katsui and others (1981)
L'vinaya Past	09-00-041	44.60N	147.00E	8	9.5 ka		Erlich and Melekestsev (1972) Erlich and others (1972)
Uratman	09-00-191	47.12N	152.23E	7.5		andesite	Gorshkov (1970)
Prizrak	10-00-041	51.6N	157.3E	5+			Luchitsky (1974)
Khodutka	10-00-051	52.07N	157.70E				Tomkeieff (1949) Vlasov (1967)
Beliankin	10-00-121	53.97N	159.42E				Sviatlovsky (1959)

PART 5: LARGE QUATERNARY CALDERAS NOT KNOWN TO HAVE SHOWN HISTORICAL UNREST (continued)

Caldera	CAVW number	Latitude	Longitude	Diameter	Age of latest collapse	Dominant magma composition	References
Sobolinyy	10-00-131	54.15N	159.60E				Vlasov (1967)
Bolshoy Semiachik	10-00-15A,B	54.3N	160.0E	25 x 30(?)			Erlich (1986)
Unana	10-00-161	54.62N	159.70E				Krijanovsky (1934); Tomkeieff (1949); Vlasov (1967)
Zimina	10-00-242	56.03N	160.72E				IAVCEI (1973); Vlasov (1967)
Dalnaya Ploskaya (Plosky)	10-00-261	56.20N	160.63E	5.6		basalt?	Erlich (1986)
Hangar	10-00-271	54.85N	157.53E	12 x 16 (?)	6.4 ka	basalt-dacite	Erlich (1986)
Ichinsky	10-00-28	55.77N	157.92E	inner, 6 outer,60		basalt, rhyolite	Erlich (1986)
Uksichan	10-00-30	55.92N	158.63E	ca. 10		basalt-rhyolite	Erlich (1986)
Newberry	12-02-11	43.68N	121.25W	6 x 8		basalt-dacite	MacLeod and others (1981)
Crater Lake	12-02-16	42.93N	122.12W	10	6.8 ka	andesite-dacite	Bacon (1983)
Medicine Lake	12-03-05	41.53N	121.53W	6 x 8	0.21 Ma(?)	andesite?	Donnelly-Nolan and others (1981) Mertzman (1981)
Island Park	12-04-05A	44.28N	111.40W	18 x 22	2, 1.3 Ma	rhyolite, basalt	Hamilton (1965); Christiansen (1984)
Valles	12-10-03	35.87N	106.57W	ca. 20	0.3 Ma	rhyolite	Smith and others (1961)

PART 5: LARGE QUATERNARY CALDERAS NOT KNOWN TO HAVE SHOWN HISTORICAL UNREST (continued)

Caldera	CAVW number	Latitude	Longitude	Diameter	Age of latest collapse	Dominant magma composition	References
Haleakala[1] (East Maui)	13-01-01	20.71N	156.25W	12 x 4		basalt	Stearns (1966); Macdonald (1972); Macdonald and others (1983); Clague and Dalrymple (1987)
Koolau (Oahu)	13-02-07	21.37N	157.80W	13 x 16	> 1.8 Ma	basalt	Clague and Dalrymple (1987)
Palawai (Lanai)	None	20.79N	156.91W	6 x 5	> 1 Ma	basalt	Stearns (1966); Clague and Dalrymple (1987)
E. Molokai (Molokai)	None	21.15N	156.85W	7 x 3	> 1 Ma	basalt	Stearns (1966); Clague and Dalrymple (1987)
Kahoolawe	None	20.55N	156.55W	5 x 4	> 1 Ma	basalt	Stearns (1966); Clague and Dalrymple (1987)
Los Humeros (including Los Potreros)	14-01-09B	19.68N	97.42W	15 x 21 (LH) 10 (LP)	0.46 Ma (LH) 0.1 Ma (LP)	rhyolite-rhyodacite	Ferriz and Mahood (1984)
Ayarza	14-02-113A	14.42N	90.12W	4 x 6	23 ka	rhyolite	Peterson and Rose (1985)
Las Lajas	14-04-17	12.30N	85.73W	7		basalt	McBirney and Williams (1965)
La Primavera	14-01-032C	20.7 N	103.53W	12	95 ka	rhyolite	Mahood (1980)
Marchena	15-03-08	0.33N	90.47W	6 x 4		tholeiitic + alkali basalt	McBirney and Williams (1969)
Calabozos	15-07-043	35.5 S	70.5 W	14 x 26	0.8 Ma 0.3 Ma 0.15 Ma	dacite, rhyolite	Hildreth and others (1984), Grunder and others (1987)

[1]Haleakala is thought by some to be primarily an erosional feature (Macdonald, 1972; Macdonald and others, 1983; Stearns, 1966, p. 43); others believe that the caldera formed initially by subsidence and was subsequently eroded. The most recent eruption of Haleakala occurred ca. A.D. 1790, from two vents along the southwest rift zone.

PART 5: **LARGE QUATERNARY CALDERAS NOT KNOWN TO HAVE SHOWN HISTORICAL UNREST** (continued)

Caldera	CAVW number	Latitude	Longitude	Diameter	Age of latest collapse	Dominant magma composition	References
Laguna del Maule	15-07-061	36.08S	70.52W	ca. 10?	postglacial	rhyolite	Lopez and Munizaga (1983), Frey and others (1984), W. Hildreth, written commun., 1987)
Terceira (Cinco Picos)	18-02-05=	38.70N	27.15W	7	>> 23 ka	alkali basalt, trachyte	Self and Gunn (1976)
Waesche (Chang)	19-00-026	77.17S	126.88W	6 x 8		silicic	Gonzales-Ferran and Gonzales-Bonorino (1972)
Hampton/ Whitney	19-00-027	76.48S	125.80W	Hamp: 6 Whit: 5?		silicic?	Gonzales-Ferran and Gonzales-Bonorino (1972)
Takahe	19-00-028	76.28S	122.08W	8		mafic?	Gonzales-Ferran and Gonzales-Bonorino (1972)
Thule Island	19-00-07	59.45S	27.32W	6-7		silicic?	Baker (1968)

REFERENCES

Bacon, C.R., 1983, Eruptive history of Mount Mazama and Crater Lake Caldera, Cascade Range, U.S.A.: Jour. Volcanol. Geotherm. Res., v. 18, nos. 1-4, p. 57-116.

Baker, P.E., 1968, Comparative volcanology and petrology of the Atlantic island arcs: Bull. Volcanol., v. 32, p. 189-206.

Bemmelen, R.W. van, 1931, Is de Oeloebeloe een vulkaan?: De Mijningenieur, v. 12, no. 3, p. 30-32.

----- 1949a, The geology of Indonesia, v. 1A+B, General geology of Indonesia and adjacent archipelagoes (w/ map folio): The Hague, Government Printing Office, 732 p. + maps.

----- 1949b, Report on the volcanic activity and volcanological research in Indonesia during the period 1936-1948: Bull. Volcanol., v. 9, p. 3-30.

Christiansen, R.L., 1984, Yellowstone magmatic evolution: its bearing on understanding large-volume explosive volcanism, in Explosive volcanism, Inception, evolution, and hazards: Washington, D.C., National Research Council, p. 84-95.

Clague, D.A., and Dalrymple, G.B., 1987, The Hawaiian-Emperor volcanic chain: Part I, Geologic evolution, in Decker, R.W., Wright, T.L., and Stauffer, P.H., eds., Volcanism in Hawaii: U.S. Geol. Surv. Prof. Paper 1350, p. 5-54.

CNR-CNRS Afar Team, 1973, Geology of northern Afar (Ethiopia): Rev. Geogr. Phys. Geol. Dynamics, v. 15, p. 443-490.

----- 1975, Geological maps of Afar: 1, Northern Afar (1971); 2, Central and Southern Afar (1975): La Celle St. Cloud, France, Geotechnip.

REFERENCES (continued)

Cooke, R.J.S., Baldwin, J.T., and Sprod, T.J., 1976, Recent volcanoes and mineralization in Papua New Guinea: Int. Geol. Congr., 25th, Excursion Guide no. 53, 30 p.

de Rita, D., Funiciello, R., Rossi, U., and Sposato, A., 1983, Structure and evolution of the Sacrofano-Baccano caldera, Sabatini volcanic complex, Rome: Jour. Volcanol. Geotherm. Res., v. 17, p. 219-236.

Di Paola, G.M., 1972, The Ethiopian Rift Valley (between 7 Deg 00 Min and 8 Deg 40 Min Lat. North): Bull. Volcanol., v. 36, p. 517-560.

Donnelly-Nolan, J., Ciamcanelli, E.V., Eichelberger, J., Fink, J.H., and Heiken, G., 1981, Roadlog for field trip to Medicine Lake Highland, in Johnston, D.A., and Donnelly-Nolan, J., eds, Guides to some volcanic terranes in Washington, Idaho, Oregon, and northern California: U.S. Geol. Surv. Circular 838, p. 141-150.

EBASCO, 1978-79, Volcanism and volcanic hazards [in association with the Philippine Nuclear Power Plant #1]: unpublished documents for the International Atomic Energy Agency, p. 56-86.

Erlich, E., 1986, Geology of the calderas of Kamchatka and Kurile Islands with comparison to calderas of Japan and the Aleutians, Alaska: U.S. Geol. Surv. Open-File Rep. 86-291, 300 p.

Erlich, E.N., and Melekestsev, I.V., 1972, Evolution of Quaternary volcanism and tectonics in the western part of the Pacific rim: Pacific Geol., v. 4, p. 1-22.

Erlich, E.N., Melekestsev, I.V., Tarakanovsky, A.S., and Zubin, M.I., 1972, Quaternary calderas of Kamchatka: Bull. Volcanol., v. 36, p. 222-237.

Ferriz, H., and Mahood, G.A., 1984, Eruption rates and compositional trends at Los Humeros Volcanic Center, Puebla, Mexico: Jour. Geophys. Res., v. 89, no. B10, p. 8511-8524.

Frey, F.A., Gerlach, D.C., Hickey, R.L., Lopez-Escobar, L., and Munizaga-Villavicencio, F., 1984, Petrogenesis of the Laguna del Maule volcanic complex, Chile (36°S): Contrib. Mineral. Petrol., v. 88, p. 133-149.

Geze, B., Hudeley, H., Vincent, P., and Wacrenier, Ph., 1959, Les volcans du Tibesti (Sahara du Tchad): Bull. Volcanol., v. 22, p. 135-172.

Gonzalez-Ferran, O., and Gonzalez-Bonorino, F., 1972, The volcanic ranges of Marie Byrd Land between long 100° and 140° W, in Adie, R.J., ed., Antarctic geology and geophysics: IUGS series-B no. 1, p. 261-275 (Andrus Caldera).

Gorshkov, G.S., 1970, Volcanism and the upper mantle: Investigations in the Kurile volcanic arc: New York, Plenum Press, 385 p.

Grunder, A., Thompson, J.M., and Hildreth, W., 1987, The hydrothermal system of the Calabozos Caldera, Central Chilean Andes: Jour. Volcanol. Geotherm. Res., v. 32, p. 287-298.

Hamilton, W., 1965, Geology and petrogenesis of the Island Park Caldera of rhyolite and basalt, eastern Idaho: U.S. Geol. Surv. Prof. Paper 504-C, p. C1-C37.

Harkin, D.A., 1960, The Rungwe Volcanics at the northern end of Lake Nyasa: Geol. Surv. Tanganyika, Memoir II, 172 p.

Hayatsu, K., 1976, Geologic study on the Myoko Volcanoes, Central Japan - Part 1. Stratigraphy: Kyoto Univ., ser. Geol. Min., v. 42, no. 2, p. 131-170.

Hayatsu, K., and Arai, F., 1980, Tephrochronological study on the Myoko Volcano tephra layers and their relation to activity of the volcano: Jour. Geol. Soc. Japan, v. 86, p. 243-263.

Hildreth, W., Grunder, A., and Drake, R.E., 1984, The Loma Seca Tuff and the Calabozos caldera: a major ash-flow and caldera complex in the southern Andes of central Chile: Geol. Soc. Am. Bull., v. 95, p. 45-54.

IAVCEI (International Association of Volcanology and Chemistry of the Earth's Interior), 1973-present, Data sheets on post-Miocene volcanoes of the world: Rome, IAVCEI.

REFERENCES (continued)

Japan Association of Quaternary Research, 1987, Quaternary maps of Japan: Tokyo, Univ. Tokyo Press, 119 p. + 4 map sheets.

Johnson, R.W., 1969, Volcanic geology of Mount Suswa, Kenya: Phil. Trans. Roy. Soc. London, v. 265, p. 383-412.

Johnson, R.W., Taylor, G.A.M., and Davies, R.A., 1972, Geology and petrology of Quaternary volcanic islands off the north coast of New Guinea: Aust. Bur. Min. Res. Record 1972/21, 127 p.

Katili, J.A., 1983, On the relation between tectonics and the formation of caldera with special reference to Krakatau: paper read at the 100th Centennial of Krakatau, Jakarta, August 1983.

Katsui, Y., Yokoyama, I., Murozumi, M., 1981, Noboribetsu Spa, in Katsui, Y., ed., Symposium on Arc Volcanism, Field Excursion Guide to Usu and Tarumai Volcanoes and Noboribetsu Spa, Pt. 3: Tokyo, Volcanological Society of Japan, p. 55-64.

Krijanovsky, N., 1934, Volcanoes of Kamchatka: Bull. Geol. Soc. Am., v. 45, p. 529-550.

Kuno, H., 1962, Catalogue of the active volcanoes of the world including solfatara fields, Pt. XI, Japan, Taiwan and Marianas: Rome, IAVCEI, 332 p.

Kusakabe, H., Hayashi, N., and Kobayashi, T., 1983, Genesis of banded sulfur sediments at the Jigokudani valley, Tateyama volcano, Japan: Bull. Volcanol. Soc. Japan, v. 28, no. 3, p. 245-261.

Kusumadinata, K., ed., 1979, Data Dasar Gunungapi Indonesia: Bandung, Volcanol. Surv. Indonesia, 820 p.

Leat, P.T., Macdonald, R., and Smith, R.L., 1984, Geochemical evolution of the Menengai caldera volcano, Kenya: Jour. Geophys. Res. v. 89, no. B10, p. 8571-8592.

Lopez E., L., and Munizaga V., F., 1983, Caracteristicas geoquimicas y petrogenesis del complejo volcanico Laguna del Maule, Andes del Sur, 36°00'S: Rev. Geol. Chile, no. 19-20, p. 3-24.

Luchitsky, I.V., ed., 1974, Development of Rugged Relief of Siberia: Far East: Kamchatka, Kurile, and Komandor Islands: Moscow, Nauka Press, 430 p.

Macdonald, G.A., 1972, Volcanoes: Englewood Cliffs, N.J., Prentice-Hall, Inc., 510 p.

Macdonald, G.A., Abbott, A.T., and Peterson, F.L., 1983, Volcanoes in the Sea (2nd ed.): Honolulu, Univ. Hawaii Press, 517 p.

Machida, H., 1980, Tephra and its implications with regard to the Japanese Quaternary period, in Association of Japanese Geographers, eds., Geography of Japan: Special Publ. 4, Assoc. Japanese Geographers, Tokyo, Teikoku-Shoin Co., p. 29-53.

MacLeod, N.M., Sherrod, D.R., Chitwood, L.A., and McKee, E.H., 1981, Newberry Volcano, Oregon: U.S. Geol. Surv. Circular 838, p. 85-103.

Mahood, G.A., 1980, Geological evolution of a Pleistocene rhyolite center--Sierra La Primavera, Jalisco, Mexico: Jour. Volcanol. Geotherm. Res., v. 8, p. 199-230.

McBirney, A.R., and Williams, H., 1965, Volcanic history of Nicaragua: Univ. Calif. Publ. Geol. Sci., v. 55, p. 1-65.

----- 1969, Geology and petrology of the Galapagos Islands: Geol. Soc. Am. Memoir 118, 197 p.

McCall, G.J.H., 1968, The five caldera volcanoes of the central rift valley in Kenya: Geol. Soc. London, Proc., no. 1647, p. 54-59.

Mertzman, S.A., 1981, Pre-Holocene silicic volcanism on the northern and western margins of the Medicine Lake Highland, California, in Johnston, D.A., and Donnelly-Nolan, J., eds., Guides to some volcanic terranes in Washington, Idaho, Oregon, and northern California: U.S. Geol. Surv. Circular 838, p. 163-169.

Mohr, P.A., and Wood, C.A., 1976, Volcano spacings and lithospheric attenuation in the eastern rift of Africa: Earth Planet. Sci. Lett., v. 33, p. 126-144.

REFERENCES (continued)

Neumann van Padang, M., 1951, Catalogue of the active volcanoes of the world including solfatara fields, Pt. I, Indonesia: Rome, IAVCEI, 271 p.

----- 1972, Catalogue of terrestrial crateriform structures: Part 2, Indonesia: Int. Astronom. Union, European Space Res. Organisation Publ. SP-93, 65 p.

Ono, K., Soya, T., and Mimura, K., 1981, Volcanoes of Japan (2nd ed.): Geol. Surv. Japan Map Series, no. 11, scale 1:2,000,000, 1 sheet.

Peterson, P., and Rose, W.I., Jr., 1985, Explosive eruptions of the Ayarza calderas, southeastern Guatemala: Jour. Volcanol. Geotherm. Res., v. 25, p. 289-307.

Posavec, M., Taylor, D., van Leeuwen, T., and Spector, A., 1973, Tectonic controls of volcanism and complex movements along the Sumatran Fault System: Geol. Soc. Malaysia, Bull. 6, p. 43-60.

Purbo-Hadiwidjojo, M.M., 1971, Geologic map of Bali: Bandung, Geol. Surv. of Indonesia, scale 1:250,000, 1 sheet.

Richards, A.F., 1962, Catalogue of active volcanoes of the world including solfatara fields, Pt. XIV, Archipelago de Colon (Galápagos), Isla San Felix, and Islas Juan Fernandez: Rome, IAVCEI, 50 p.

Rock, N.M.S., Syah, H., Davis, A.E., Hutchison, D., Styles, M.T., and Lena, R., 1982, Permian to Recent volcanism in Northern Sumatra, Indonesia: A preliminary study of its distribution, chemistry, and peculiarities: Bull. Volcanol., v. 45, p. 127-152.

Searle, R.C., 1972, A gravity survey of Ngorongoro Caldera, Tanzania: Bull. Volcanol., v. 35, p. 350-357.

Self, S., and Gunn, B.M., 1976, Petrology, volume and age relations of alkaline and saturated peralkaline volcanics from Terceira, Azores: Contrib. Mineral. Petrol., v. 54, p. 293-313.

Smith, R.L., and Bailey, R.A., 1968, Resurgent cauldrons: Geol. Soc. Am. Memoir 116 (Howel Williams Volume), p. 613-662.

Smith, R.L., Bailey, R.A., and Ross, C.S., 1961, Structural evolution of the Valles Caldera, New Mexico, and its bearing on the emplacement of ring dikes: U.S. Geol. Surv. Prof. Paper 424-D, p. D145-D149.

Sollevanti, F., 1983, Geologic, volcanologic, and tectonic setting of the Vico-Cimino area, Italy: Jour. Volcanol. Geotherm. Res., v. 17, p. 203-217.

Stearns, H.T., 1966, Geology of the State of Hawaii: Palo Alto, Calif., Pacific Books, 266 p.

Sviatlovsky, A.E., 1959, Atlas of the volcanoes of the Soviet Union: Moscow, Akad. Nauk Press, 172 p.

Tomkeieff, S.I., 1949, The volcanoes of Kamchatka: Bull. Volcanol., ser. 2, v. 8, p. 87-112.

Varekamp, J.C., 1980, The geology of the Vulsinian area, Lazio, Italy: Bull. Volcanol., v. 43, no. 3, p. 487-503.

Verstappen, H. Th., 1973, A geomorphological reconnaissance of Sumatra and adjacent islands (Indonesia): Verh. Roy. Dutch. Geogr. Soc., Gröningen, Wolters-Noordhoff Publ., 182 p.

Vlasov, G.M., 1967, Kamchatka, Kuril, and Komandorskiye Islands: Geological description: Geol. of the USSR, v. 31, Moscow, Izd.-vo Nedra, 827 p.

Weaver, S.D., 1976-77, The Quaternary caldera volcano Emuruangogolak, Kenya Rift, and the petrology of a bimodal ferrobasalt-pantelleritic trachyte association: Bull. Volcanol., v. 40, p. 209-230.

Williams, L.A.J., 1970, The volcanics of the Gregory Rift Valley, East Africa: Bull. Volcanol., v. 34, p. 439-465.

Williams, L.A.J., Macdonald, R., and Chapman, G.R., 1984, Late Quaternary caldera volcanoes of the Kenya Rift Valley: Jour. Geophys. Res., v. 89, no. B10, p. 8553-8570.

Wilson, C.J.N., Houghton, B.F., and Lloyd, E.F., 1986, Volcanic history and evolution of the Maroa-Taupo area, Central North Island, in Smith, I.E.M., ed., Late Cenozoic volcanism in New Zealand: Roy. Soc. New Zealand Bull. 23, p. 194-223.

REFERENCES (continued)

Wilson, C.J.N., Rogan, A.M, Smith, I.E.M., Northey, D.J., Nairn, I.A., and Houghton, B.F., 1984, Caldera volcanoes of the Taupo volcanic zone, New Zealand: Jour. Geophys. Res., v. 89, no. B10, p. 8463-8484.

Yamasaki, M., Nakanishi, N., and Miyata, K., 1966, History of Tateyama Volcano: Sci. Rep. Kanazawa Univ., v. 11, p. 73-92.

ABBREVIATIONS USED IN PARTS 2, 3, 4, AND 5

CAVW number= Number assigned to active vent(s) in "Catalogue of Active Volcanoes of the World Including Solfatara Fields" (IAVCEI, 1951–present) or Simkin and others (1981). Calderas are listed geographically, according to CAVW number. Order of presentation, by region, is Europe, Africa, southwestern Pacific, Indonesia, northwestern Pacific, Alaska, western North America, Hawaii, Central America, South America, the Caribbean, Iceland, other Atlantic islands, and Antarctica.

Local tectonic setting: exten, extension; compr, compressional

Precaldera edifice: Strato, stratovolcano; shield, shield; LL-strat, low, lava flow-dominated stratovolcano; LP-strat, low, pyroclastic-dominated stratovolcano.

Compositions of recent and caldera-forming eruptions, expressed as whole-rock SiO_2 (water free) or, if no analysis is available, as mafic, intermediate, or silicic. b, basalt; a, andesite; d, dacite; r, rhyolite; ol, olivine; px, pyroxene; hb, hornblende. R, compositions of recently erupted magma (historical if known); C, composition of magma of latest caldera-forming eruption.

Nature and duration of unrest:

Column headers:

ESTU: E, earthquakes; S, earthquakes explicitly reported in swarms; T, tremor (harmonic or spasmodic); U, uplift

STHF: S, subsidence; T, tilt; H, horizontal strain (in most cases measured with electronic distance measuring instrument); F, ground fractures and fissures

MGTF: M, changes in magnetic field; G, changes in gravitational field; T, change, usually increase, in temperature of ground water, soil, or fumaroles; F, change in intensity, area, or composition of fumarolic activity

H, change in discharge or composition of ground water or springs, or change in level of water in wells or lakes

Te, temporal relation with large tectonic earthquakes:

QU, earthquake followed by unrest at caldera; UQ, earthquake after unrest at caldera; UU, unrest followed by earthquake, then by further unrest; QQ, earthquake followed by unrest, then by another large earthquake. No causal relations are implied.

Letters in each column:

Letters indicate preeruption duration of each type of activity--for example, the duration of elevated seismicity before eruption. If no eruption ensued, letter indicates total duration of that particular type of unrest. A, minutes; B, hours; C, days; D, weeks; E, months; F, years; G, decades; x, occurred, no other information; Y, occurred during eruption; Z, occurred after eruption; N, did not occur; -, no information.

Eruption type: pex, phreatic explosion; ex, magmatic or unspecified type of explosion; p-ex, phreatomagmatic explosion; subgl, subglacial eruption; sub, submarine eruption; pf, pyroclastic flow; mf, mudflow (debris flow); lf, lava flow; ll, lava lake; cc, cinder cone formation; dm, dome; cdm, cryptodome; da, debris avalanche; landsl, landslide. Scale of explosive activity shown by upper and lower case: EX, major explosion (VEI 4 and above); Ex, moderate explosion (VEI 3); ex, small to moderate explosion (VEI 1 or 2). Similar abbreviations used for phreatic explosions (PEX, Pex, pex), phreatomagmatic explosions (P-EX, P-Ex, and p-ex), and lava flows (LF, Lf, and lf).

U. S. DEPARTMENT OF THE INTERIOR

March 3, 1849